# Laboratory-Directed Research and Development

## FY-2003 Annual Report

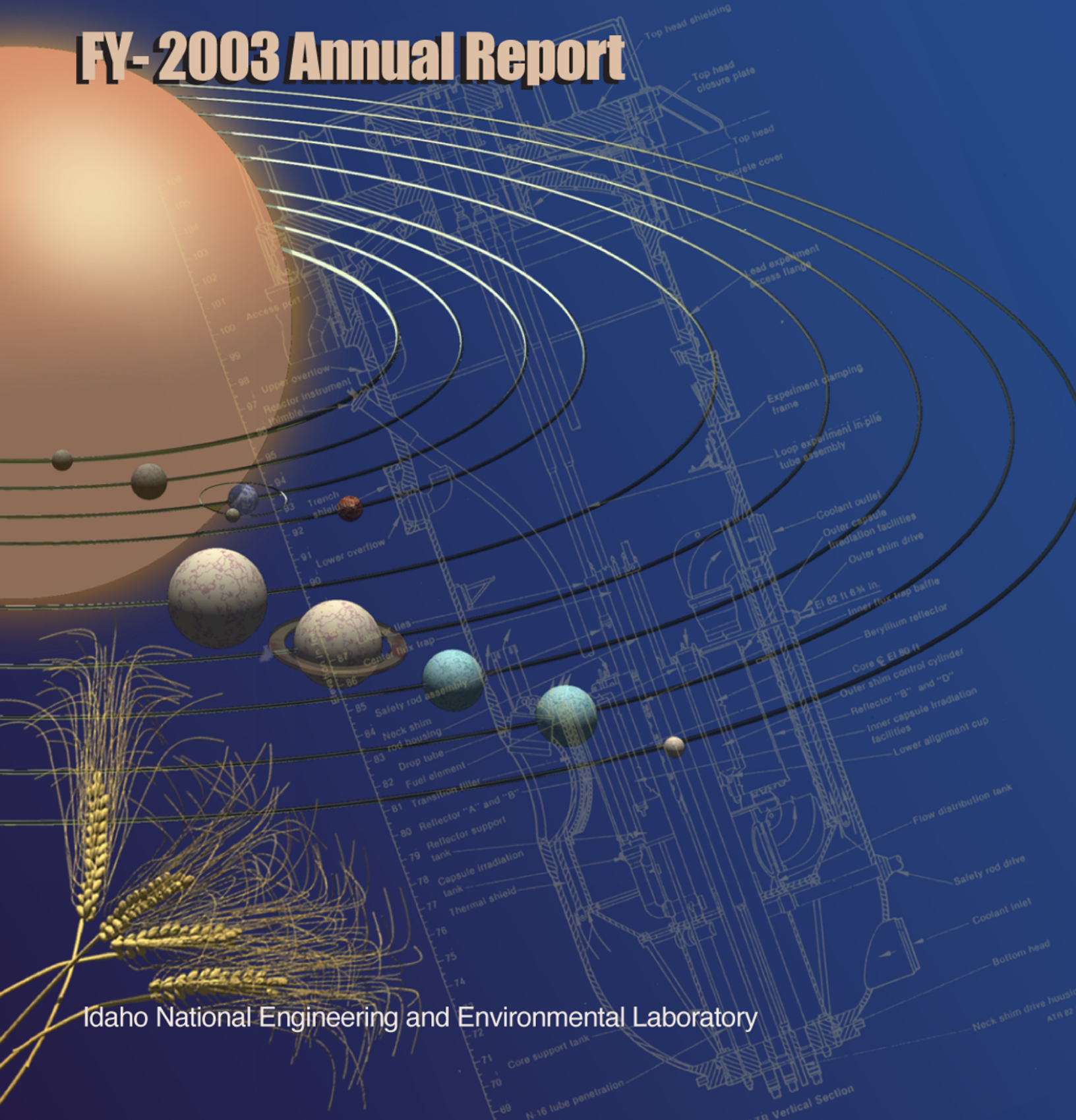


Idaho National Engineering and Environmental Laboratory

It is my pleasure to submit the fiscal year 2003 Annual Report for the Laboratory Directed Research and Development (LDRD) Program at the Idaho National Engineering and Environmental Laboratory (INEEL). This has been a year of change for the INEEL. Becoming the nation's leading center for nuclear energy research required us to adjust our LDRD portfolio and focus more on nuclear energy and energy security. In addition, the upcoming creation of the Idaho National Laboratory and spin-out of our environmental clean-up mission into a separate contract led to additional redirection in our science and engineering research.

In spite of these changes, our researchers have risen to the challenge. This report provides an overview of the research that was conducted with LDRD dollars in FY03, and the resulting successes. Some of these successes are highlighted in the 'Research Highlights' section of this report. For example, two different teams of researchers have taken on the challenge of developing methods of making reactors safer and more cost effective. Another researcher has developed a method for covert tracking of equipment in the field, making it easier to secure military assets. Finally one of our robotics researchers won the AAAI Robot Rescue Competition using a family of sensor-rich robots he developed with LDRD dollars.

The INEEL continues to be a multi-program laboratory and our expertise in environmental science and technology is evidenced in projects under both the Environmental, Subsurface Science Initiative and Advanced Mixed Waste Management Solutions Initiative sections of this report. LDRD is also a pivotal component of collaborations with universities, other national laboratories and private industry. Through these collaborations, relationships are built that help stimulate intellectual vitality, and provide us the opportunity to hire young, upcoming scientists and engineers to fuel our future. I believe these collaborations are a key to strengthening and growing this laboratory into the future.

I am proud of the accomplishments achieved in FY03, and hope you share my enthusiasm as you read this report. I also look forward to continued success as the INEEL moves forward into FY04.

Paul K. Kearns

**Paul K. Kearns, Ph.D.**

**Vice President and Deputy Laboratory Director**

# Acknowledgments

This annual report provides an overview of the Laboratory Directed Research and Development (LDRD) Program at the Idaho National Engineering and Environmental Laboratory (INEEL). Summarized in this report are 121 technical research projects conducted in fiscal year 2003. The LDRD Program at the INEEL is managed for the laboratory by Dr. Paul Kearns, Vice President and Deputy Laboratory Director, Dr. Ray S. Enge, Director for Strategic Planning, and Dr. Debonny Shoaf, LDRD Program Manager.

Many people contributed to this report; particular thanks go to the principal investigators who conduct the cutting-edge research so important to this laboratory.

**Managing Editor:** Mary Catherine Thelen
**Associate Editor:** Lonnie Martinell
**Science Writer:** Diane Salisbury
**Designer:** Shaun Eames

Prepared for the U.S. Department of Energy
Assistant Secretary for Energy
Under DOE Idaho Operations Office
Contract DE-AC07-99ID13727

# Table of Contents

Acknowledgments ..... 3

Table of Contents ..... 5

Overview ..... 11

*Highlights*

Intelligent Behavior Makes Robot a Team Player ..... 14

Tiny Antennas Track and Identify Important Assets ..... 16

Cooling Reactors with Molten Lead ..... 18

Reactor's Unique Attributes Require Rethinking of Modeling Tools ..... 20

Building the Foundation for Energy-Wise Homes ..... 22

*Energy*

Hydrogen Production from High Temperature Nuclear Reactors ..... 27

Hydrogen Technologies R&D ..... 30

Stable Enzymes for Hemicellulose Hydrolysis ..... 32

93mNb, A Portable Excitation Source for Elemental Analysis ..... 34

Contaminants and Improved Energy Production: Laboratory Studies ..... 36

Two-Phase Mass Flow Measurement for Geothermal Wells ..... 37

Advanced Test Reactor Three Dimensional Neutronics Modeling ..... 39

Computational Fluid Dynamics Model Based Control of Two-Phase Flow ..... 42

Active Neutron Spectrometry for Neutron Capture Beam Characterization ..... 44

Development of Analytical Decision-Making Tools for Energy Efficient Agricultural Biomass Production ..... 47

Flow Characterization of Complex Biomass Flows for Bioenergy Feedstock Development ..... 49

Radiation Chemistry of Supercritical Water ..... 52

Estimation of Neutron Irradiation-Induced Displacements-Per-Atom ..... 54

Energy Efficient Building Simulation and Technologies ..... 57

Friction Stir Welding of Lightweight Materials ..... 60

Genetic Control of Straw Stem Ultrastructure that Affects the Biomechanics of Stem Separation ..... 62

Laser Ultrasonic Corrosion Monitor ..... 65

Hollow Waveguide Laser Ultrasonics ..... 68

Pretreatment Technologies for Cellulosic Biomass ..... 72

## *Environmental*

Elemental Tracers and Multi-Variate Receptor Modeling Methods in Assessing Air Pollution ..... 79

Improving Stakeholder Interactions: A Stakeholder-Based Research Methodology for Reaching Decisions on Polarized Issues ..... 81

Biologically Based Catalysts for Processing and Detection in Harsh Service Environments ..... 84

Atmospheric Pressure Surface Analysis Mass Spectrometry ..... 86

Long-Term Record Storage for Long-Term Stewardship ..... 88

Development of the Scientific Basis for Landscape Management of Federal Lands ..... 89

Advanced Multi-Operation Control Architectures for Human-Robot Synergy in Complex Domains ..... 90

Intelligent Control of Multi-Nodal Systems ..... 93

Characterization of Legacy Risk ..... 94

Use of Engineered Nano-Particles for Nutrient Delivery and Bioremediation in Subsurface Environments ..... 97

Supercritical Fluid Catalyst Regeneration Chemistry ..... 100

Human Factors for Management of High Consequence Events ..... 102

Model-Based Decision Making ..... 103

Designing Advanced Emergency Response Planning Support Systems ..... 105

Nanostructure Characterization for Sensing ..... 107

Surface-Sensitive Laser Acoustic Studies of Heterogeneous Catalysis ..... 109

DOE Complex-Wide Long-term Stewardship Options Analysis System ..... 111

Developing a Predictive Decision Network for Long-Term Stewardship ..... 113

Enhanced Transport in Nano-Crystalline Ceramic Films ..... 114

Development of Microelectrode Arrays for In Situ Detection of Localized Corrosion ..... 116

Understanding Societal Issues Associated with Acceptance of Bioremediation Strategies ..... 118

The Controlled Synthesis, Structural, Electrical, and Optical Properties of One-Dimensional Metals ..... 121

Making Sustainable Decisions Using the KONVERGENCE Framework ..... 123

Dependence of Coal Bed Permeability on Pore Pressure and Adsorbed Gas Composition ..... 126

Nucleation and Growth of Nanoparticle Materials in Supercritical Fluid Processes ..... 129

Development of an Integrated Watershed Information Management Tool for Long-Term Facilities Stewardship ..... 131

Elucidating the Photo-Physics of Complex Metal Ions Trapped in a Fourier Transform Mass Spectrometer ..... 134

Recombinant Adhesive Protein Production and Investigation into Alternate Natural Adhesive Systems in Marine Mussels ..... 137

Novel Maerials for Evaluation of Generation IV Materials ..... 140

Mechanical and Flow Properties of Dry Granular Media ..... 142
Developing Collaborative Approaches to Long-Term Environmental Stewardship ..... 144

## *National Security*

Enhanced Isotope Ratio Measurement Sensitivity ..... 149
Security of Cyber Systems ..... 151
Wireless Security Research ..... 152
Novel Threat-Risk Index Using Probabilistic Risk Assessment and Human Reliability Analysis ..... 155
Smart Antenna Systems in a Wireless Local Area Network ..... 157
Automated Control and Electronic Signal Acquisition/Processing Systems for Sprayed Distributed Sensors ..... 160
Thermomechanical Processing of Titanium 10V-2A1-3Fe ..... 162
Client/Server Architecture for High-Performance Computing ..... 165
Development of Enzyme-Activity-Based Assays for Potential Bioterrorist Agents Designed for Use With Current Detection Platforms ..... 167
Cermet Filters for Hazardous Material, Chemical and Biological Weapon Agent Destruction ..... 169
Microantenna Infrared Tags ..... 172
Novel Fabrication of Blast and Penetration Resistant Materials ..... 174
Novel Selective Matrix for Collection and Identification of Priority Pathogens ..... 178
Imaging of Heavy Metals and Nuclear Materials ..... 181

## *Advanced Computing Initiative*

Development and Validation of Advanced Simulation and Collaboration Capability ..... 187
Parallel Computing with Cluster Technology ..... 190
Aerospace Situation Awareness and Risk Monitor Tool ..... 194
Improving Numerical Model Efficiency of an Existing, In-House Simulation Model ..... 197

## *Advanced Waste Management Solutions Initiative*

Thermally Hot Offgas Cleanup Sorbent Technology Development ..... 203
Direct Dissolution of Plutonium and Neptunium Species Using Chelated Agents in Supercritical Fluid Carbon Dioxide ..... 205
Cold Crucible Design Parameters for Next Generation High Level Waste Melters ..... 207
Novel Abrasion Resistant Enhanced Flux UF Membranes ..... 210
Development of Advanced Aqueous Processing to Support the Nuclear Fuel Cycle ..... 212
Investigation and Modeling of Dynamic Strain Rate Effects on Structural Material Response ..... 214
Thermodynamic Modeling of High-Ionic Non-Ideal Solutions ..... 216

Electrochemical Recovery of Mercury from Nuclear Industry Process Solutions ..... 218

Highly Selective Sorbents for the Removal of Arsenic from Drinking Water ..... 221

## *Critical Infrastructure Protection Initiative*

Critical Infrastructure Critical Sub-network ..... 225

Development of a Compact Laser-Compton X-ray Source ..... 228

Advanced Automated Ion Mobility Spectrometer for Explosives Detection ..... 230

## *Generation IV Nuclear Reactor Initiative*

Advanced Fission Product Detection Systems for Generation IV Fuel Testing ..... 235

Advanced Transient Analysis Capabilities for Generation IV Reactors ..... 238

Advanced Nuclear Fuels for Enhanced Proliferation Resistance ..... 240

Design of an Actinide Burning, Lead or Lead-Bismuth Reactor That Produces Low Cost Electricity ..... 242

Modular Pebble Bed Reactor ..... 244

Generation IV Gas-Cooled Reactor System Analysis Tools ..... 247

An Innovative Gas-Cooled Fast Reactor ..... 249

## *Subsurface Science Initiative*

Use of Molecular Markers for Detection and Tracking of Environmental Bacteria ..... 255

A New Hydrogeophysical Method for Characterizing and Monitoring Preferential Flow Paths in Complex Layered and Fractured Basalt ..... 257

Characterizing Microbial Population Shifts in Response to Alternative Electron Donors and Their Effect on TCE-Dechlorination Efficiency ..... 259

Uptake and Translocation Patterns of Strontium by Sagebrush Steppe Ecosystem Plants ..... 262

Hybrid Nanocomposite Materials as Subsurface Permeable Reactive Barriers ..... 265

Advanced Technology for Mapping Subsurface Water Conductivity ..... 268

Electrical Resistivity Imaging to Define Preferred Flow Paths in a Heterogeneous, Layered Vadose Zone ..... 271

Application of New Borehole Geophysical Methods for Stratigraphic Correlation and Identification of Non-Aqueous-Phase Contaminants ..... 273

Fundamental Studies on Gas Contaminant Mobility in the Vadose Zone from Atmospheric Pressure Fluctuations ..... 276

Estimating Soil Water Flux in the Deep Vadose Zone ..... 279

Modeling Solute Partitioning at Interfaces ..... 281

Investigation of the Movement and Fate of Chlorinated Hydrocarbons ..... 282

Regional Setting and Flow Dynamics of the Snake River Plain Aquifer ..... 284

Modeling of Flow and Colloid Behavior in Subsurface Fractures ..... 287
Multiscale Modeling of Multiphase Flow (Unsaturated) ..... 290
Natural and Synthetic Subsurface Colloids ..... 292
Modeling an Earth-Borehole System for Physical Property Determination in Shallow Subsurface Environments ..... 295
Development of Techniques for In situ Measurement of Groundwater Contaminant Source Strength ..... 297
Enhanced Techniques for Evaluating Colloidal Transport Processes ..... 300
Evaluating Microelectrodes and Fiber-Optic Probes for Use in Mesoscale Experiments ..... 303
Estimating the Climatic Sensitivity of Vadose Zone Infiltration Rates Through Paleohydrologic Analyses ..... 306
In Situ Degradation of Explosives in the Vadose Zone ..... 308
Kinetics of Inter-Surface Transfer of Surface-Complexed Metals by Surface-Surface Contact ..... 311
Organic Co-Solvent and Co-Contaminant Effects on Sorption of Uranyl and Cesium to Metal Oxide Surfaces ..... 314
Computational Experiments of Hysteretic Chemical and Moisture Migration ..... 317
Development of Imaging Fourier Transform Mass Spectrometer Capabilities for Analyses of Complex & Heterogeneous Samples ..... 320
Dual Electrodes and Defining the Electrically Disturbed Region in Induced Polarization Measurements ..... 322
Development and Application of Custom Flow Models for Understanding Flow in Porous and Fractured Matrices with Biological Components ..... 324
Use of Genetic Markers as a Screening Tool for Ecological Risk Assessment ..... 326
Characterization of Nonlinear Complex Resistivity Spectra During Biochemical Reduction of Cr+6 to Cr+3 ..... 329
Development of Enzymatic Biosensors for Environmental Applications ..... 332
Calibration and Enhancement of Geophysical Imaging Tools in Mesoscale Experiments ..... 334
Advanced Borehole Seismic Sources for High-Resolution Subsurface Imaging and Characterization for Environmental Applications ..... 337

## *Appendices*

Appendix A Author Index ..... 344
Appendix B Refereed Publications ..... 348
Appendix C Key Terms ..... 354
Appendix D Project Performance ..... 362
Appendix E Relevance to Major DOE Missions ..... 370
Appendix F Relevance to Major National Programs ..... 376

INEEL

# Overview

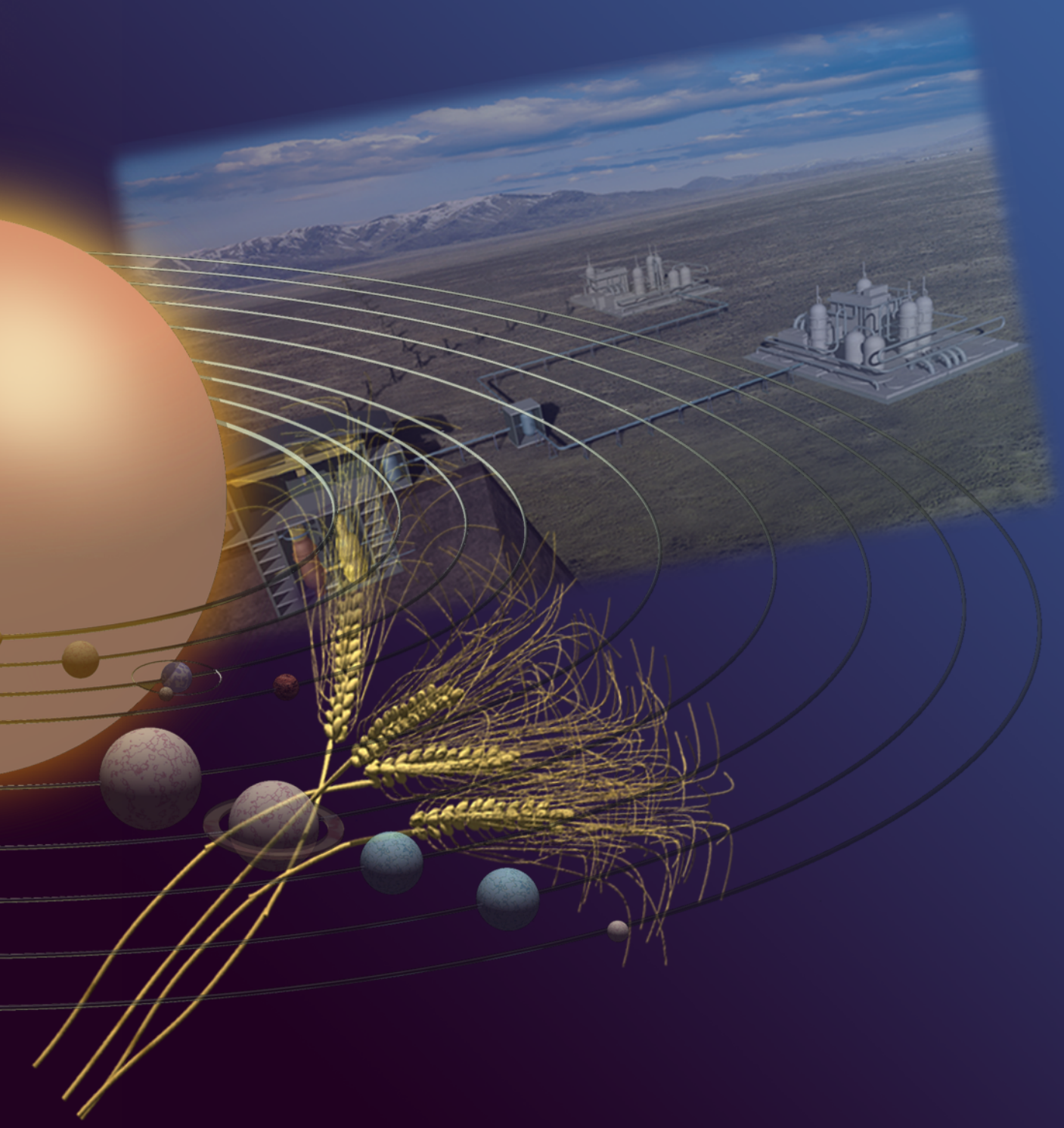

# Overview and Highlights

*INEEL – the leading U.S. research laboratory in nuclear science and engineering – providing the next generation technology for the United States and the world – recognized for providing solutions to energy, security, and scientific challenges.*

National laboratories and their Laboratory Directed Research and Development (LDRD) programs are a crucial part of this nation's ability to rapidly solve ever-changing research needs. Because of the flexibility of LDRD, each national laboratory has the ability to redirect research to address these new and important needs with speed and agility.

The LDRD program was instituted by Congress to provide DOE laboratories the flexibility to perform cutting edge research that addresses DOE missions and national needs. LDRD is managed by DOE under Order 413.2A which describes the purpose, limitations and guidelines for the program. This annual report fulfills one of the program requirements specified in that Order.

At the INEEL, LDRD research provides a number of benefits including:

1) development of new and innovative scientific and technological ideas;
2) enhances the scientific and technological vitality of the laboratory;
3) assists in development of strategic direction; and
4) development and retention of new workforce capabilities.

LDRD plays a seminal role in attracting and retaining the most qualified scientists and engineers to meet the long-term, evolving needs of the DOE and the nation. LDRD is considered a unique resource for scientists newly hired by the laboratory. In FY03, LDRD supported over 100 postdoctoral fellows, graduate students, and university faculty. Approximately 78% of all the postdoctoral fellows at the laboratory were sponsored by LDRD research.

LDRD is used to initiate research programs and build technical capabilities. Veteran researchers at the laboratory value LDRD for enabling the exploration of ideas believed to be of importance, but not yet sufficiently developed to attract programmatic support. The program also enables researchers to establish important partnerships with universities and industrial research groups that enliven and diversify the intellectual approaches to the research. LDRD is responsible for some of the highest quality research conducted at the laboratory. A significant number of the technical publications, presentations, invention disclosures and patents are derived from LDRD. In 2004 INEEL honored three inventors who generated more than ten inventions each over the span of their research careers at the laboratory. The inventors attributed more than 95% of their successes to having had access to LDRD to explore novel ideas. Likewise, many of the national awards and recognition of INEEL researchers occurred because of accomplishments on LDRD projects. Tables 1 and 2 provide statistical information about project performance and portfolio composition for fiscal year 2003.

*Table 1. FY03 Performance Statistics*

| | |
|---|---|
| Refereed Publications | 89 |
| Symposia Chaired or Organized | 10 |
| Invited Presentations | 58 |
| Invention Disclosures | 23 |
| Patents Awarded | 2 |
| University Personnel | 112 |

*Table 2. FY03 Program Statistics*

| | |
|---|---|
| Total Projects | 121 |
| Smallest Project | $41.6 |
| Largest Project | $553 |

This Annual Report contains progress summaries of all the research sponsored by the INEEL LDRD Program in fiscal year 2003. It represents some of the most exciting research conducted at the INEEL that addresses complex technical problems facing DOE and the nation. Some notable examples that are found in this report are:

- Development of cost-effective sorbents to remove sulfur and chlorine pollutants, and toxic metals from coal combustion, gasifier offgas, and other thermal conversion.
- Modeling of programs for modern 3-D ion optics to design a more efficient ion source and lens.
- Evaluation of the design, optimization and field-testing of an in situ vadose zone explosives remediation system.
- Development of a unique, multipurpose instrument capable of providing both mass spectral, and optical imaging of complex, heterogeneous sample surfaces.
- Investigation into whether thorium-based fuels can be used to further increase the proliferation resistance of light water reactor fuels.

The Appendices of this report provide a portrait of the INEEL LDRD research portfolio. Appendix A provides a cross-reference of authors with progress reports. Appendix B is a list of refereed publications. Appendix C is a cross reference of key terms to individual projects. Appendix D lists performance indicators such as number of publications, patents, national awards, students and postdoctoral fellows supported. Appendix E identifies the relevance of each project to DOE missions. Appendix F identifies the relevance to major national programs.

An Annual Report focuses on achievements in a single fiscal year, and does not illustrate the impact of a 10 or 20-year retrospective. Nevertheless, even from a 12-month perspective, it is evident that LDRD makes a unique contribution to the laboratory's ability to serve all of DOE's missions and the nation. LDRD provides the ability to invest in long-term, higher risk research that has a potentially high payoff. It is essential to INEEL's ability to attract and retain the best researchers. By its exploratory nature, LDRD allows researchers to anticipate technological needs and envision and test the potential value of novel ideas. The INEEL LDRD Program will continue to evolve to support emerging national needs and future DOE missions.

# Highlights

# Intelligent Behavior Makes Robot a Team Player

*David Bruemmer*

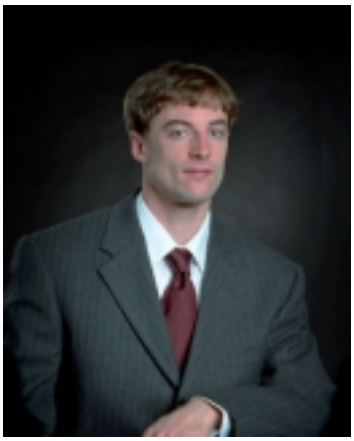

*"In the near future, human-robot teams will be deployed that complement each other's strengths and exceed the limitations of fully autonomous or remote-controlled systems."*

***David Bruemmer***

About a decade ago, a shift in robotic design occurred that rejuvenated the industry. It was the shift from designing robotic systems that could *think* intelligently to systems that could *act* intelligently. This focus on engineering *behavior* rather than *cognition* has led to a new class of robotic systems that can leverage their intrinsic intelligence and the level of user control to accomplish real-world tasks without being told exactly how to do them.

"The systems we're developing in this project promote true teamwork between humans and robots," says principle investigator David Bruemmer. "They're not meant to be fully autonomous, super-intelligent robots that never need human assistance. However, they have decision-making capabilities and can adjust to changing environments and revised task goals. They can even say 'no' to the user if they perceive themselves to be in danger."

Intelligence and adaptation begin with situational awareness. To this end, Bruemmer has developed four sensor-rich robots that are equipped with infrared, scanning laser, sonar, video, thermal imaging, bump sensors, tilt sensors, a compass, and temperature sensors. The sensors not only provide information that is relayed back to the user, they enable the robot to understand and respond to its environment.

Users can switch between four basic levels of control over the robot system. In "teleoperation," the robot is passive and all control comes from the user. "Safe mode" keeps the lion's share of control with the user, but the robot can take initiative to protect itself; for example, if the user is operating the robot rapidly through a cluttered environment, the robot will stop if confronted by an obstacle that could cause it harm. "Shared mode" enables the robot to take greater initiative in driving. If the robot comes to an obstacle, it won't just stop; it will figure out how to get around the object and continue on with its task. The fourth user level is "autonomous mode," where the robot makes all the decisions on how to accomplish a high-level task it has been given such as searching an area, monitoring a perimeter, or following a user-designated path.

Unlike most robotic systems, which share raw data, the INEEL robots are designed to dialogue intelligently with humans and other robots. They can use information from external sources, but are not dependent on it. This trait enables the system to cope with communication interruptions, component failures, and changes in operator instructions.

"It's peer-to-peer communication," says Bruemmer. "By sharing knowledge, goals and intentions on the fly, missions will be carried out more efficiently and with greater trust and reliability."

Proving this claim is the INEEL robotic system's 2003 win at the AAAI Robot Rescue Competition in Acapulco, Mexico. During the allotted five runs, the robot found 18 "victims" within a collapsed building, reliably identifying victims' ID tags, their location, and whether or not they were still alive.

Of all the accomplishments during this last project year, one of the most significant has been making the advanced control architecture "universal" and porting it to the four robotic platforms that ranged in size from 35 to 300 lbs. Recent demonstrations before the U.S. Armed Forces showed that the technology can be transferred to a variety of existing vehicle platforms in just days. The software quickly adapts to its new sensors and geometry through a process of self-discovery and from reading a parameter file, opening up applications as diverse as space exploration, waste management and agriculture.

"Junior, an all-terrain robot, was recently used to deploy a gamma-locating device within a radioactive environment."

*INEEL Robot Family*

# Tiny Antennas Track and Identify Important Assets

*Dale Kotter*

*"Infrared emissions are more directional than radio signals, which are easy to intercept. Microantenna tags that operate in the infrared frequency range will enable selective, line-of-site monitoring, and identification without detection."*

***Dale Kotter***

There are many needs to track "assets" from remote or standoff distances in military and national security applications. An evacuation helicopter might need to be tracked, a missing tank located, or a covert operator monitored. If tagging and tracking an object could be accomplished with the assurance of positive identification and without enemy detection, current tracking technologies would be greatly enhanced.

Tiny antennas that work in the infrared (IR) frequency range could provide an important enhancement to our ability to tag and track important assets. They can be configured to operate at very narrow-band discrete frequencies, making them almost impossible to be defeated.

"According to electromagnetic theory, an antenna's frequency of operation is partly a function of its physical dimensions," says investigator Dale Kotter. "For example, a cell phone utilizes a stubby antenna. To receive a slower AM/FM signal in your car requires a larger whip antenna."

In comparison, infrared is six orders of magnitude faster in frequency. To effectively detect an IR emission requires antennas smaller than the naked eye can see.

To that end, this LDRD has led to the design of antenna microstructures with the ability to transmit and receive IR emissions. For practical application, thousands of these microantennas are assembled together to form a postage-stamp size antenna array that can be applied to the surface of existing assets. When illuminated by infrared energy, the array's surface reflects a unique pattern, providing a positive ID of the tagged item that is immune to deception.

The IR tags have a flexible substrate that allows them to adapt to the contours of the asset to which they are applied. The tags are completely passive and covert until interrogated. In addition, no modifications to the asset are required to support the technology. The new microantennas can be configured to enhance an asset's emission in the portion of the infrared band that existing thermal imagers, such as night vision goggles, can typically detect. The thermal IR emissions result in improved detection and are less susceptible to distortion from background noise (e.g., sandstorms) or purposeful interference that can result in deadly tagging errors.

The project to-date has focused on static tags with embedded permanent codes and information. Future research will develop electronic, tunable antennas capable of being reprogrammed and providing encrypted, optical data communication.

Right now, the tags operate at a certain frequency," says Kotter. "But by applying a small voltage to the antenna structure, it can be tuned to different frequencies, giving it the ability to communicate."

These future tags may work in tandem with other field-deployed sensors, such as chemical and biological detectors. Through remote interrogation, they could be used to relay

information about hazards ahead of troops. At command, the tags would go into a covert sleep mode and remain undetectable.

"Infrared surveillance methods in current use with night vision and other thermal detection systems are state-of-the-art and are why our military 'owns the nighttime skies,'" says Kotter. "But we know there are ways to confuse our detection systems, and they don't always operate well under non-ideal conditions. With the microantenna infrared tag, we will be able to enhance thermal signatures, and more accurately identify assets."

# Cooling Reactors with Molten Lead

*Eric Loewen*

*"Using the waste products from one system to fuel another is an attractive path to sustainable, low-cost electricity production."*

***Eric Loewen***

In the early 1950s, the Soviet Union discovered how to use molten lead as a cooling agent for nuclear reactors. The technology was unknown to the western world until nearly 40 years later when east-west relations thawed, and small, compact lead-cooled reactors were found to be powering some Russian nuclear submarines. As the Generation IV initiative began taking shape, six design paths were selected, including a lead-cooled fast reactor concept.

"A lead-cooled fast reactor seems promising as a design that might produce cheap electricity while burning radioactive wastes from our current reactors," says Eric Loewen, one of the project investigators. "Our team, which included researchers from MIT, looked at what other scientists were proposing in this area, and we came up with our own medium-powered reactor concepts for cost-efficient electricity production using old reactor waste."

Key safety and operational issues were identified and analyzed such as core neutronics, materials, thermal-hydraulic, fuels, and the economics of production. Ultimately four designs with the same physical configuration were studied. Three designs focused on waste management by recycling spent fuel. The fourth design was a once-through concept for producing low-cost electricity.

One of the challenges the investigators encountered in trying to build upon the previous research was the availability of materials. "We had the recipe for the Russian alloys that were used to prevent corrosion, but they're no longer made," says Eric. "To keep the cost of the final reactor down, we searched out and evaluated commercially available U.S. steels."

That evaluation came partially with the help of a research team of four undergraduate students from around the nation. Joining the project through a 10-week fellowship grant, the students conducted a focused study on circulation corrosion of the metals in four major areas: interaction layer, tensile strength, analytical techniques using ultrasound, and coolant chemistry. Through this multidisciplinary approach the students found an acceptable substitution to the Russian alloy — iron-silicon-chrome (Fe-Si-Cr). Their investigation resulted in technical papers, a presentation at a conference in Washington D.C., a poster presentation at a technical conference in Japan, and an Invention Disclosure.

"Part of what LDRD supports is developing our nation's technical talent, the scientists of tomorrow," says Eric who was named DOE Mentor of the Year by Secretary Abrams for his work with the fellowship undergraduate students.

It's also about enabling the exploration of ideas believed to be important. "The design we ended up proposing has a seven-year-life core for burning waste from spent light water reactor fuel," says Eric. "It offers a nuclear waste destruction rate nearly as high as more complex accelerator-driven systems, and a passive shutdown if coolant is lost."

Though the INEEL lead-cooled fast reactor concept was not ultimately selected for further development, research results were widely

disseminated. A major accomplishment during the last year of this LDRD was completion of a special issue of *Nuclear Technology* with nine integrated papers providing the technical information. These archives will provide researchers and evaluators with an invaluable starting point for future work.

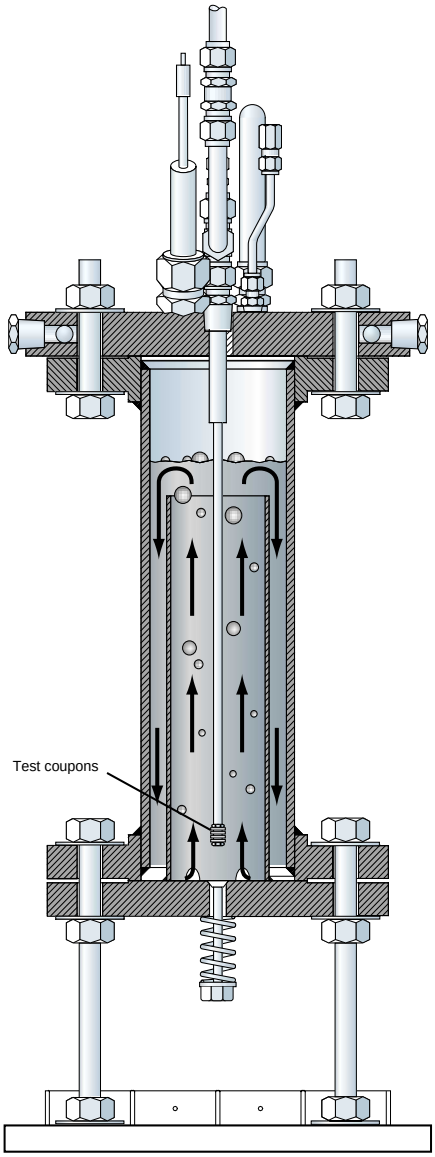


*Experimental Apparatus (zirconium pipe)*

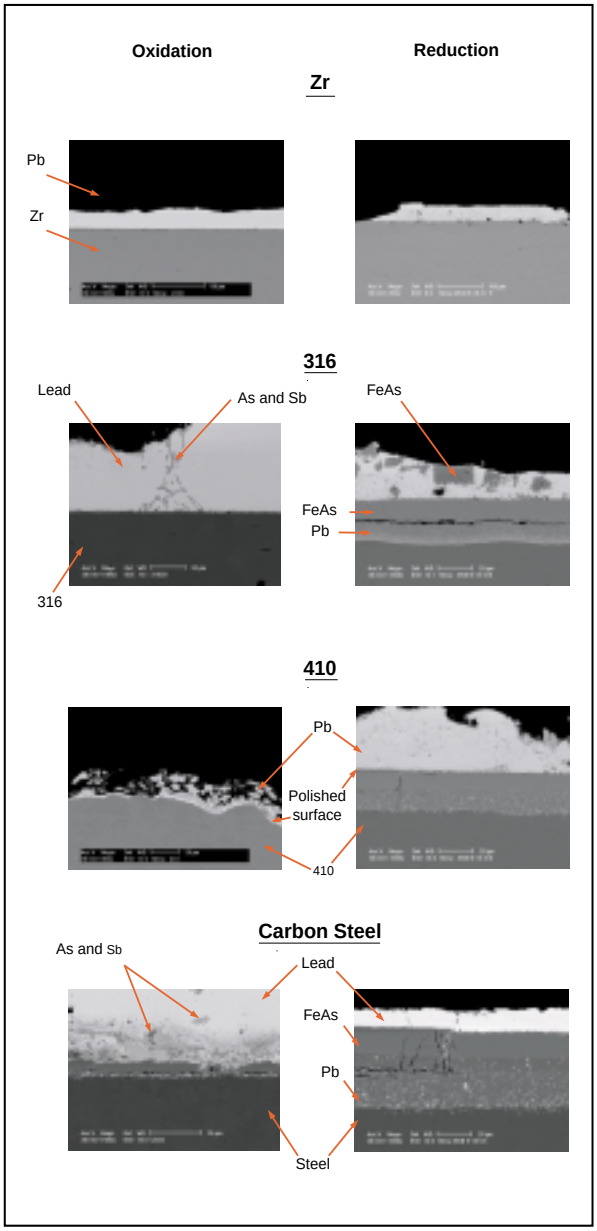


*Coupon Cross Sections*

# Reactor's Unique Attributes Require Rethinking of Modeling Tools

*David Petti, Greg K. Miller, Hans Gougar, Richard C. Moore*
*(photo: left to right)*

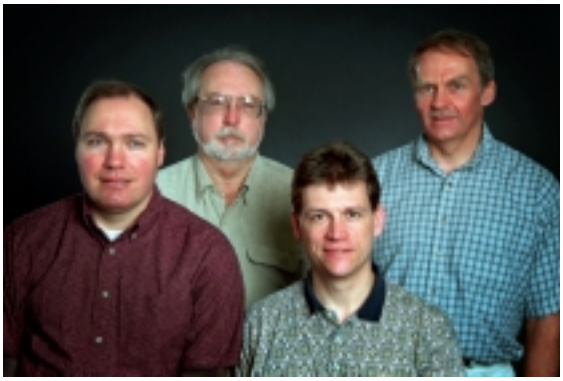

*"The modular design of these reactors might help developing countries economically and safely produce electricity, and enable them to add power with additional units as their needs grow."*

***Hans Gougar***

Several decades ago, as light water reactors (LWRs) became the design choice in the U.S., German and American scientists were pursuing an approach that used helium gas, instead of water, to cool a reactor core. A German gas-cooled reactor design that showed particular promise, but was only implemented as a low-power demo at the time, was a pebble bed reactor (PBR). This earlier research has been re-invigorated by scientists at the INEEL as part of the Generation IV Roadmap for future nuclear power plant design.

"The pebble-bed offers a number of advantages over light water reactors and even other gas-cooled reactor designs," says Hans Gougar, a co-investigator on the project. "But because it operates so differently, current modeling tools for understanding and predicting performance don't apply."

The most unique attribute of the PBR is that the fuel is able to move around within the core as opposed to being stacked and stationary as with other reactors. The coated uranium oxide fuel is locked up in thousands of pebble-shaped containers and then loaded into the reactor — like filling a gumball machine. The fluidity of the fuel allows for better heat dissipation and enables on-line refueling. Theoretically, the reactor would never have to be shut down to replenish, shuffle, or remove the fuel. In an ongoing process, the fuel would be loaded from the top, shuffled in the core, and dropped out the bottom for removal when spent.

"The three modeling needs we're looking at in this LDRD are predicting fuel performance, computing core attributes, and evaluating safety characteristics," says Hans Gougar, one of the investigators for this project. Current modeling tools for LWRs look at these same issues, but from a completely different perspective. For example, a safety model for an LWR will address potential loss-of-coolant (water) events that can cause core meltdown. Water doesn't even come into play for a PBR. However, exposure of high-temperature fuel to oxygen does need to be considered.

To answer these and other questions, the investigators have written the first new code in 20 years for this type of reactor. Named PEBBED, the code has already successfully been used to help develop a fuel-testing program and determine the proliferation risks associated with this reactor concept.

Currently, the DOE is considering which of two helium-cooled reactor designs — the pebble-bed or prismatic core – will be built in the near future at the INEEL. Whether the PBR

is selected or not, this research will be available to other utilities around the world that choose to pursue this design. In fact, the investigators on this project are already in collaboration with a South African company, PBMR (PTY), Ltd., planning to build a PBR.

"The PBR design won't be for every application," says Gougar. "It's a large reactor for the amount of power it produces. However, it's very safe and proliferation resistant. For lower power applications where safety might be a concern, the PBR could offer one of Gen IV's best solutions."

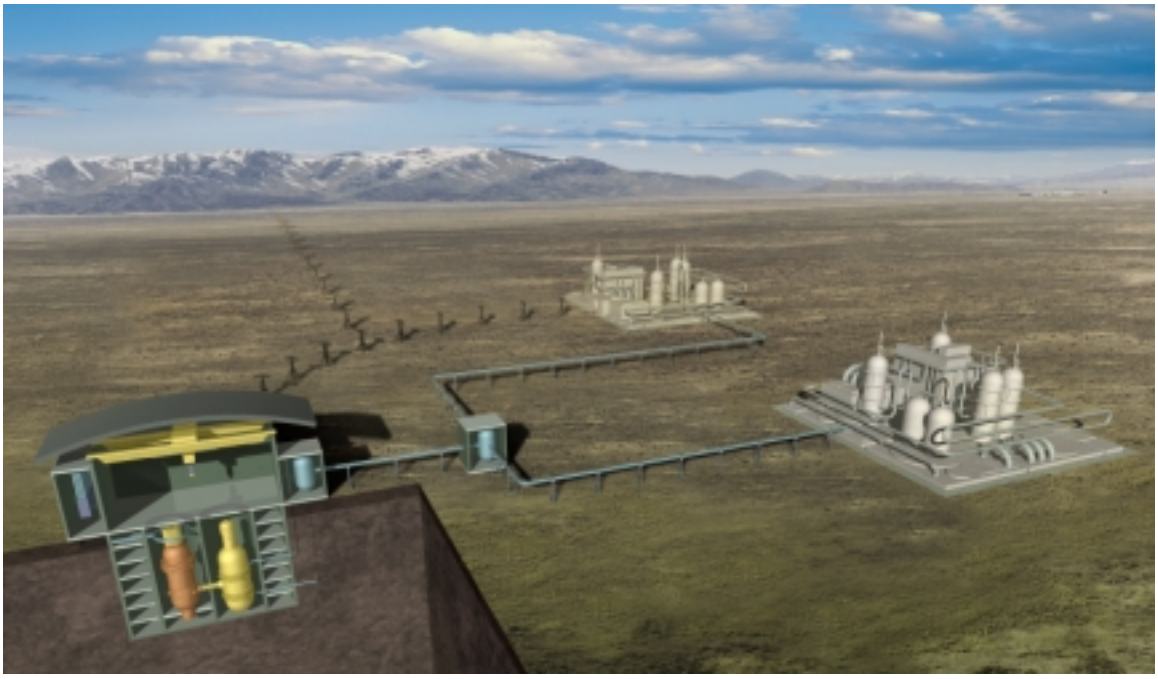

*Next-generation nuclear power plant.*

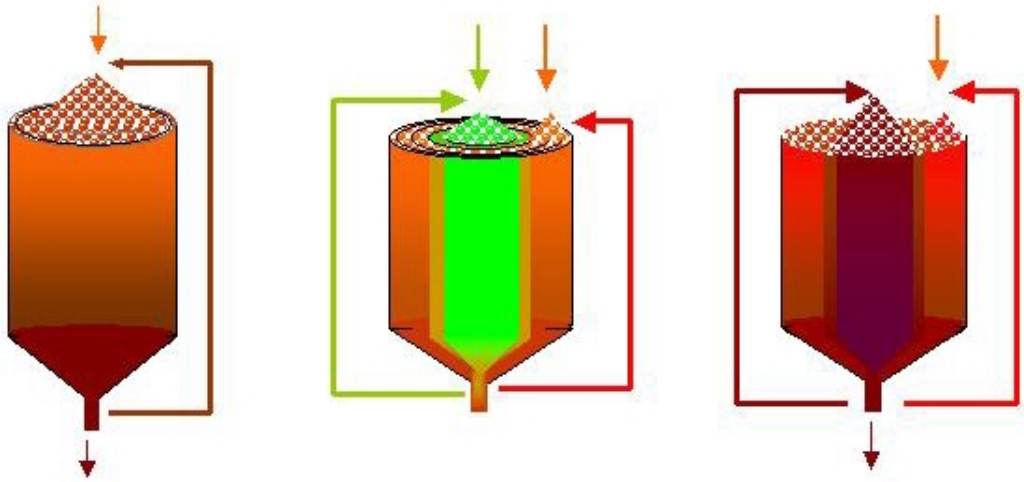

*Modeling Fuel Management: Develop a method for efficient and accurate core design and fuel management for recirculating pebble-bed reactors.*

# Building the Foundation for Energy-Wise Homes

*William Richins, Thomas Larson*

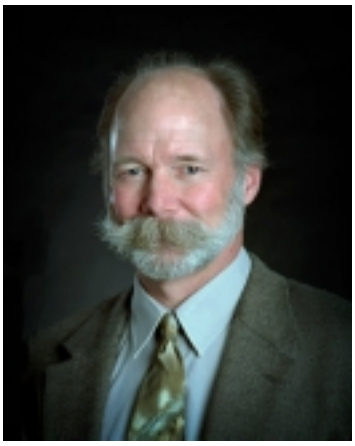

*"Homes of the future could have HVAC control systems that automatically open and close window shutters, adjust solar panels, and regulate air flow to create optimally healthy, comfortable, energy-efficient environments."*

***William Richins***

Hurricane Andrew left a path of devastation when it hit the U.S. Eastern shore a decade ago. Hardest hit of all were manufactured homes. To better understand the structural impact of such harsh conditions, HUD requested a study of manufactured housing. This research, conducted by the INEEL in 1999, led to a smorgasbord of energy efficiency ideas that had wide applicability to not only manufactured homes but to office buildings and standard residences as well. Those ideas were the genesis of this LDRD.

"As a result of previous research, we had a site, a structure, the experience, and the test equipment in place," said co-principal investigator Tom Larson. "It occurred to us this was an ideal test bed to conduct complete energy usage monitoring."

The test site was a forsaken piece of ranch land 8,000 ft. above sea level near Arlington, Wyoming. Wind conditions peak at 90 mph and are typically strong enough (~35 mph) to support a nearby wind "farm." Temperatures range from lows of -30ºF to summer highs of 100ºF.

With these extreme conditions as a backdrop, the investigators embarked upon this three-year project to evaluate air infiltration, air leakage, and temperature control, and to deploy and test innovative heating and cooling methods. These methods included structural transpired air solar panels (TSP) that would be applicable for residential retrofit and new construction and ground-source heating/cooling that could be integrated with optimized control systems into a whole house heating, ventilation, and air-conditioning (HVAC) system.

Among the tests conducted were tracer gas monitoring, pressurized leakage, and infrared video scans. Extensive arrays of instrumentation for measuring thermal performance of the homes were designed and installed. Thermocouple arrays were placed to measure vertical temperature profiles – i.e., in the crawl space, belly pan, near-floor, room center, ceiling, and attic — in various household locations. Measured data were used to validate a model created by the investigators for use in the DOE EnergyPlus code so that adjustments such as increased insulation or changing out a window could be simulated.

What did they learn?

"There were a few surprises," recalls principal investigator Bill Richins. "Energy-wise, the double-section manufactured home was tighter than we'd expected, even with single-pane windows. And the solar system was very efficient, providing up to 40% of the household

heating in sunny weather, even in very cold outside temperatures."

Another important finding was that air infiltration has a linear relationship with wind speed. This discovery led to the development of parameters that can be used by future HVAC control systems to automatically adjust airflow in homes. For example, based on wind speed measurements, airflow might be adjusted to prevent stale air and mold formation ("sick home syndrome") while balancing energy efficiency.

A ground-source cooling loop (installed at an off-grid home in Cedar City, UT) was another innovation that showed promise as a cost-effective way of cooling air during summer months. Installed five feet underground where the temperature is constant, the loop naturally cools water that passes through it. The cooled water is then incorporated into the home's air conditioning system.

"The Arlington site will continue to be used as a testbed for sustainable products that can be used in mainstream construction," says Larson.

There is a growing need. As more and more of our population moves to warmer climates, manufactured homes are expected to account for 30-60% of all homes purchased in the next decade. Implementation of the products and methods investigated in this research could result in significant energy savings over existing technology and reduced greenhouse gas emissions for these future homeowners.

*Singlewide test home installation near Arlington, Wy.*

*Interior of doublewide home showing instrumentation and data acquisition system.*

INEEL

# Energy

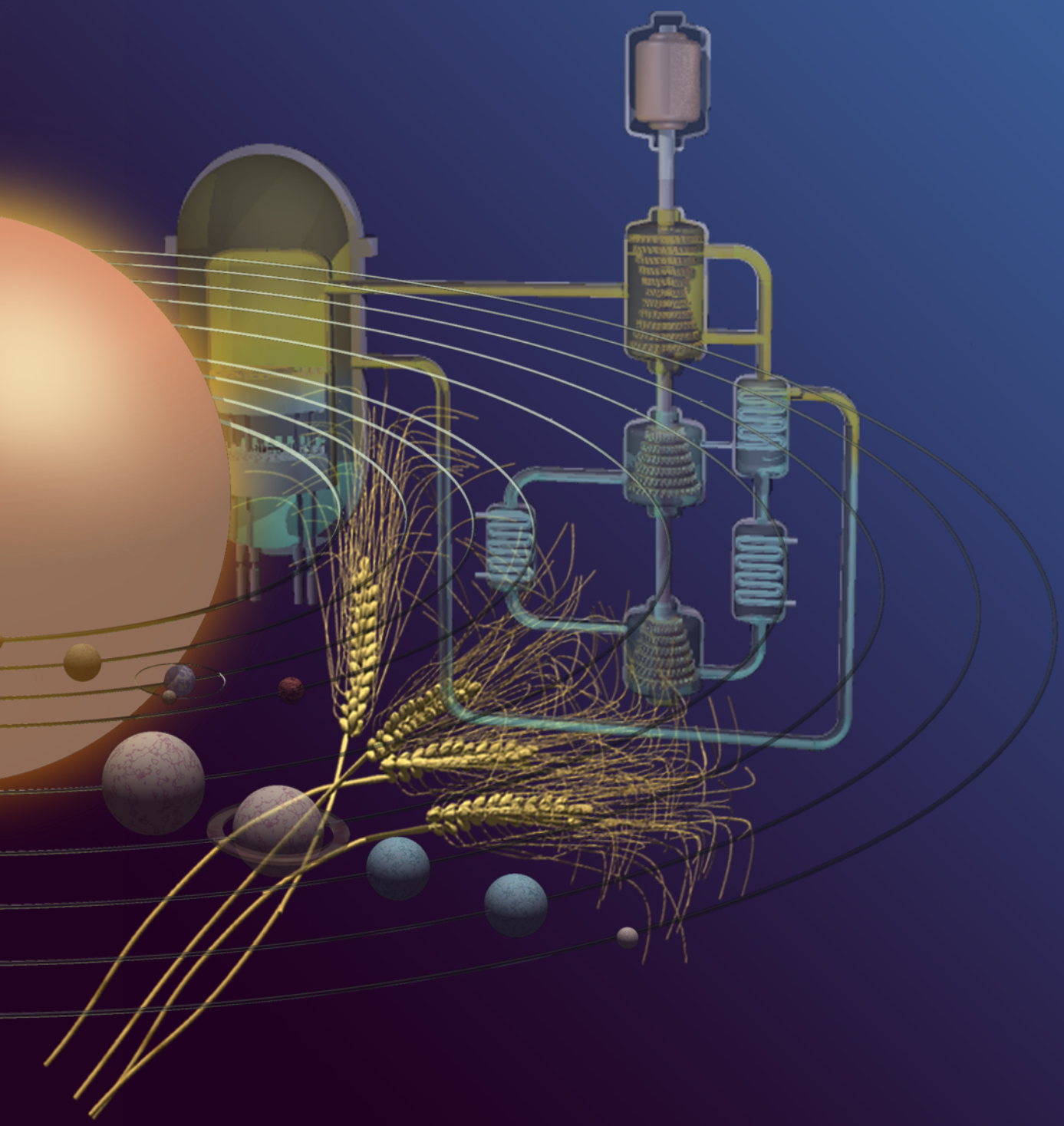

# Hydrogen Production from High Temperature Nuclear Reactors

*Raymond P. Anderson, Daniel M. Ginosar, J. Stephen Herring, Thomas M. Lillo, Frederick F. Stewart, David F. Glenn*

***Removing barriers to hydrogen energy production***

NE120

Drivers for using hydrogen as an energy carrier, especially for transportation, are improved energy efficiency, energy security, and environmental constraints. However, carbon dioxide, a greenhouse gas, is liberated when hydrogen is produced from fossil fuels. Domestically, most hydrogen is made by the steam reforming of natural gas. Compelling reasons for using nuclear energy for hydrogen production are that it relies only on domestic resources, does not consume our finite supply of fossil fuels, and does not release greenhouse gases.

A number of thermochemical cycles have been proposed that may be used for splitting water to oxygen and hydrogen using nuclear heat or heat/electricity as the energy source. These thermochemical cycles generally use very high temperatures and highly corrosive materials, involve separations of complex chemical mixtures, and sometimes include electrochemical steps that suffer from lower than desirable efficiencies. Thus there are a number of obstacles that must be overcome to allow the engineering demonstration of these cycles.

This LDRD addresses some of these obstacles to assist in the ambitious target of having a Very High Temperature (Nuclear) Reactor (VHTR) operating on the Idaho desert and supplying energy to a prototype hydrogen production unit (50 MW thermal) by 2015. Tasks include studies of kinetics/catalysis of the decomposition of sulfuric acid (a step included in several of the leading thermochemical cycles), materials, separations, and the electrolysis step of the Westinghouse process.

Technical objectives for fiscal year 2003:

- Develop enabling technologies in the following key areas that are applicable to the front-runner thermochemical cycles for production of hydrogen by water splitting:
- Kinetics/catalysis of sulfuric acid decomposition
- Materials
- Separations
- Electrolysis step of the Westinghouse process

*Sulfuric acid decomposition*. Common to three of the four top-ranked thermochemical cycles is the high-temperature catalytic sulfuric acid decomposition reaction.

$$2H_2SO_4 \rightarrow 2SO_2 + 2H_2O + O_2$$

The reaction takes place at 850°-900°C and is promoted by a heterogeneous catalyst. This is the highest temperature component of the General Atomics (GA) Sulfur Iodine (SI) cycle. To accommodate the corrosive environment, specialized materials of construction will be required. A catalyst is necessary to improve process economics as well as plant safety. Catalysts are well known to increase reaction kinetics by orders-of-magnitude, which in-turn, significantly reduce the size of reactors and hence reduce costs. This task is studying the catalytic decomposition of sulfuric acid and exploring catalyst activity, stability, and transport properties. The sulfuric acid decomposition catalyst is potentially problematic. The catalyst may not be stable and, thus, lose significant activity during the operating cycle. Although a platinum catalyst has been proposed, platinum catalysts sinter and lose significant activity at the high temperatures typical of the decomposition reaction. At present there is not a clear understanding of the rate-limiting variable in the decomposition.

The first part of this task was a literature review. Prior studies examined the reaction under idealized conditions using substantial volumes of inert gasses. A conceptual plan for a test system design was initially developed to study the reaction under industrially applicable conditions. Development of the final system design and operating conditions was greatly enhanced using information provided by researchers at the Japanese Atomic Energy Research Institute (JAERI).

A bench-top sulfuric acid catalytic decomposition reactor has been assembled. The reactor is composed of quartz and Teflon components and a ceramic piston pump. The system has been completely assembled and tested at temperatures up to 900°C. Catalysts have been identified and obtained. Several analytical titration techniques have been identified and tested for the anticipated reaction products ($SO_3$, $SO_2$, $H_2SO_4$).

*Materials*. The sulfuric acid decomposition loop was the focus of materials studies. Analysis of the GA process flow loop indicated that conditions ranged from 58 wt% sulfuric acid at 27 psi and 120°C up to 98 wt% sulfuric acid at 102 psi and 411°C. The conditions under the highest pressure correspond to 78 wt% sulfuric acid at 514 psi and 371°C. Corrosion resistant materials were selected

for testing under these conditions. Alloys were selected to have at least a modest amount of ductility for fabrication and safety purposes. Of seven alloys eventually selected, five (C-22, C-276, I-686, C-4 and HR-160) were nickel-based while the remaining two contained a significant amount of iron (I-800H and I-825). Corrosion studies were carried out initially at atmospheric pressure. Results have been obtained for two conditions: 98 wt% sulfuric acid at 200°C and 58 wt% sulfuric acid at 110°C. Experiments were performed in static sulfuric acid and the change in sample weight with corrosion time (up to 240 hours) was tracked. Alloy C-22 performed the best at 98 wt% sulfuric acid at 200°C and exhibited a decreasing corrosion rate as the experiment progressed. The average corrosion rate after 240 hours was ~10 mpy (mills per year). No corrosion products were deposited on the sample. Alloys C-4 and C-276 also exhibited low corrosion rates at ~20 mpy. These alloys were not as corrosion resistant at the lower sulfuric acid concentrations. Alloy I-825 exhibited the best corrosion resistance at 58 wt% sulfuric acid at 110°C with a corrosion rate of around 5 mpy. C-22, C-276 and C-4 exhibited corrosion rates of 118, 66 and 325 mpy, respectively.

The results indicate corrosion behavior is dependent on sulfuric acid concentration. Alloys I-825 and C-22 are promising for use in different areas of the sulfuric acid decomposition cycle but will require elevated pressure corrosion studies. Preparations also were made for corrosion testing at elevated pressures and temperatures. A pressure vessel capable of pressures in excess of 1000 psi at 600°C was obtained. Elevated pressure corrosion testing will commence early next fiscal year, studying the same alloys identified above as well as a few additional alloys recently identified.

*Separations*. Chemical separations in extremely acidic and thermally elevated conditions are one of the most significant barriers to implementation of thermochemical cycles. The goal of this task is to define and address the technological hurdles through literature and laboratory research of the most promising cycle, the SI cycle. Through an initial investigation of the problem, gas separations for the purification of hydrogen and liquid-liquid separations in acidic environments were identified as the major barriers. In fact, it was suggested that membrane technology could be utilized to accomplish the required separations. However, a GA report published in 1981 indicated that the state of the art in membrane technology was inadequate. Liquid-liquid separations work during FY03 concentrated on removing the water from a mix of $I_2$, HI, and water. During cycle operation, this separation must be accomplished at temperatures ranging from 120°-350°C. Materials investigated during this fiscal year include polydimethylsiloxane (PDMS), polyphosphazene (PPOP), and a polyvinyl alcohol/polysulfone composite (GFT). All three membranes passed initial stability testing.

Membrane testing was then performed using a technique called pervaporation. In pervaporation, the feed is kept at negligible pressure as it is flowed across the membrane surface. On the permeate side of the membrane, reduced pressure is used to facilitate transport. Pervaporation is effective for separations where the desired permeate is somewhat volatile. Water meets this requirement. The GFT membrane gave positive results with a good flux of water (~ 0.1 $Kg/m^2h$) that contained very low concentrations of both HI and $I_2$. An instrument to measure gas permeation was constructed for the investigation of gas transport through membranes at high temperature, up to 850°C. For the temperature required, it is envisioned that ceramic membranes with controlled pore sizes will be the best candidates. Future work will address specific membrane formulations.

*Electrolysis step of the Westinghouse process*. The objective of this task is to reexamine the electrolysis step of the Westinghouse Sulfur Cycle process in light of new electrochemical technology developed in the 25 years since the first publication of the process. The express purpose of the Westinghouse Sulfur Cycle is to reduce the electricity consumed in water electrolysis by oxidizing $SO_2$ at the anode rather than producing $O_2$. In this process, sulfuric acid is first converted to sulfur dioxide and water *via* a thermally driven chemical reaction. The sulfur dioxide and water are then sent to an electrolyzer where hydrogen is produced at

the cathode and the sulfur dioxide is electrolytically converted back to sulfuric acid at the anode. The electrolysis of water to $H_2$ and $O_2$ requires an overall cell voltage of 2.35V while the generation of $H_2$ coupled with the oxidation of $SO_2$ under the same conditions requires only 0.91V. This reduction in the required cell voltage results in an energy savings of 38 kWh/kg of $H_2$ produced at 10 mA/$cm^2$. In addition to verifying the advantages of $SO_2$ depolarization of the anode, potential electrode materials were investigated using standard electrochemical techniques including cyclic voltammetry, Tafel analysis, and electrochemical impedance spectroscopy. Potential cathode materials tested this year included platinum, nickel, and several high-nickel-content alloys. Anode materials investigated included platinum, graphite, lead, and Ebonex® (a substoichiometric oxide of Ti).

The growth of the "hydrogen economy" and the required R&D to support the transition to hydrogen as an energy carrier are significant growth opportunities for the INEEL. A specific strategic goal of this LDRD is to gain recognition for INEEL as a major player in the development of hydrogen production using high temperature nuclear reactors. This goal is being realized. Significant investment is expected from DOE-NE to include the building of a VHTR reactor in Idaho in the 2015 timeframe for the express purpose of hydrogen production. For the nearer term, a preliminary meeting with General Atomics was held to discuss cooperation in the development of thermochemical cycles and additional meetings with Sandia National Lab and others are planned for October 2004.

# Hydrogen Technologies R&D

*Raymond P. Anderson, Paul A. Lessing, Kendall B. Johnson*

## *Storing hydrogen in carbon*

NE125

A major problem with hydrogen as a transportation fuel is that insufficient hydrogen can be stored in existing, high-pressure, compressed-gas cylinders to meet DOE storage goals. This is a critical barrier that needs to be eliminated before Photon Exchange Membrane (PEM) fuel cell "engines" can achieve an acceptable driving range using pure hydrogen.

The objective of this LDRD is to create new hydrogen absorbing materials to be placed within the fuel tanks. Various forms of graphite fibers were investigated and experiments were performed to "prop open" the graphite's "c" planes, using metal atoms to create atom-sized internal pores that should absorb hydrogen molecules. Measurements were conducted to determine if a sufficient amount of hydrogen would be absorbed to meet the DOE storage goals. A second task was to develop a method for the economical production of carbon nanotubes, another potential hydrogen absorbent.

Technical objectives for fiscal year 2003:

- Complete experiments that intercalate Group 1A and VIIIA atomic elements between fibrous graphite's c-planes.
- Conduct x-ray diffraction experiments to characterize the structural changes within various graphite fiber materials after intercalation.
- Ship samples of intercalated graphite fibers to an independent laboratory for hydrogen absorption/desorption measurements.
- Complete a cooperative research and development agreement (CRADA) with a leading manufacturer of high-pressure, composite, hydrogen gas storage tanks.
- Investigate the plasma arc synthesis of carbon nanotubes, which, if successful, could open the potential for inexpensive high-volume production.

*Intercalated Graphite* — Experiments were conducted to "prop open" graphite's "c" planes by inserting metal atoms in between the planes via a chemical intercalation process. The experiments were designed using a partial factorial (Taguchi) array of various sources of graphite (Torayca, 3-types, ThermalGraph, 2-types, and EnerGraph) with Group 1A (Li, K, Cs) and Group VIIIA (Fe, Ni) intercalant atoms. Group VIIIA atoms were investigated for the possibility that they would perform a catalytic function.

To successfully perform the intercalation experiments, technical problems were overcome with the glove box's inert-gas atmosphere and Vycor reaction cell (design obtained from journal literature). A new, improved reaction cell was designed and fabricated from stainless steel.

Well-intercalated samples were produced using potassium (K) and cesium (Cs), but lithium (Li) intercalated samples could not be produced. There were two difficulties with lithium: its low vapor pressure and reaction with the Vycor cell. The cell redesign solved the unwanted reaction problem, but the low vapor pressure remained a problem due to temperature limitations of current equipment. The new stainless steel cell was demonstrated to perform better than the old Vycor cell and the stainless cell is re-usable for reduced experimental costs. About twelve well-intercalated samples were produced using the new cell design.

The samples were characterized using x-ray diffraction (XRD) to determine how intercalation affected the original graphite's internal crystal structure. XRD experiments were conducted using an "Anton Paar TTK-450" inert gas cell. However, the results were less than optimal. The TTK-450 cell's 25-micron thick "Capton" windows resulted in low x-ray signal amplitudes and the seals allowed hydrolysis reactions. Further experiments with thin-walled (10 micron) glass capillary tubes did not produce acceptable signal intensities. Finally a sealing technique was devised for special thin-walled polymeric bag material with low water permeability. These bags were combined with a special adjustable-height sample holder and Gobels mirror to optimize XRD peak intensity.

Examples of XRD spectra measured using the special techniques are shown in Figures 1 and 2. After successful intercalation, each sample's graphite sheet separation 002 reflection ("c" peak at theoretical value of 3.35 Å) was completely eliminated. In some K intercalated samples, new peaks (8.8 Å and 2.9 Å ) developed that were indexed as $KC_{24}$ (with an additional new reflection at 1.74 Å). In some Cs intercalated samples, new peaks concurrently developed at 3.95 Å (expanded planes) and 3.05 Å (compressed planes). Other K intercalated graphite samples exhibited new plane reflections at 4.25 Å (expanded) and 3.10 Å (compressed). Three representative samples (K, Cs, and Cs/Fe) were sent to an independent laboratory

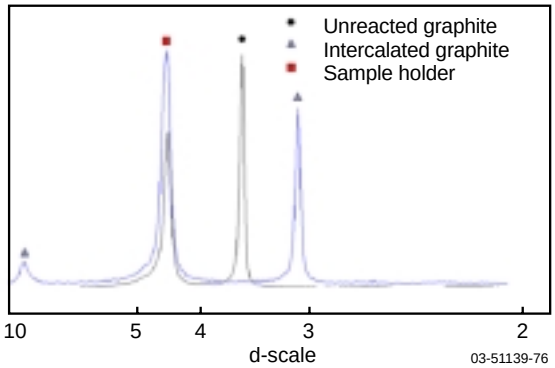


*FIGURE 1. XRD Intensity vs d-spacing (Å) for a K-intercalated graphite.*

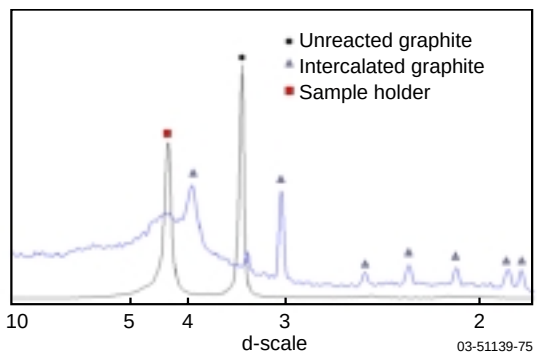


*FIGURE 2. XRD Intensity vs d-spacing (Å) for a Cs-intercalated graphite.*

for hydrogen absorption/desorption measurements. These results were not available at the time of writing.

*Carbon Nanotubes* — Emphasis during FY03 was placed on conducting as many experiments as possible with the plasma torch/reaction chamber developed during the previous year to find conditions that would produce carbon nanotubes. Variables investigated included using iron and tungsten powders and ferrocene as catalyst precursors. Methane and carbon monoxide were used as feedstocks. Other parameters included torch powers from 25 to 60 kW, chamber pressures from 65 to 450 torr and chamber temperatures from 300° to 900°C. The soot from each experiment was examined by TEM (transmission electron microscope) and SEM (scanning electron microscope). The soot from some experiments showed graphitic-like sheets and fiber-like materials. Catalyst particles on the nanometer scale were found in some of the experiments; this is important, as producing nano catalyst particles is a necessary condition for nanotube production. However, no tube-like structures were identified.

While no nanotubes were obtained in these experiments, the parameter space used was just the beginning of the parameter space that could be investigated; however, lack of additional funds and time prevented further investigation. Additional parameters of interest include higher temperatures, pressures, dwell times, and various metal-organic catalyst precursors as well as variations in the concentration of these parameters versus the feedstock and torch gasses.

This research has resulted in the signing of a CRADA between INEEL and Quantum Fuel Systems Technologies Worldwide, Inc. Quantum is the world's leading manufacturer of high-pressure, composite, gas storage tanks, and is an OEM supplier of hydrogen tanks for General Motors and fuel-cell vehicle manufacturers in Japan.

# Stable Enzymes for Hemicellulose Hydrolysis

*William Apel, Vicki Thompson*

***Using natural enzymes to convert biomass to industrial sugars***

CE111

Thermal/acid stable enzymes can potentially be used to hydrolyze hemicellulose found in agricultural biomass. If successful, the use of these enzymes on an industrial level could decrease acid hydrolysis pretreatment costs and convert hemicellulose to its monomeric sugars, which can then be used for production of fuels and chemicals.

The purpose of this LDRD is to investigate thermal/acid stable hemicellulases that can be used industrially. There are six categories of hemicellulases. In this project, thermal/acid stable hemicellulases will be isolated and characterized from two of these categories: endoxylanase (EC 3.2.1.8) and exoxylanase (EC 3.2.1.37). These two enzymes were selected because together they can hydrolyze the majority of hemicellulose found in agricultural biomass, the targeted feedstock of this research. Little research has been done on thermal/acid stable xylanases to date, and the xylanases that have been reported are insufficiently stable for industrial application. This LDRD will work with xylanases from extremophilic microbes (e.g., thermo-acidophiles) that will be obtained from both established culture collections and via enrichment/isolation from environmental samples.

Technical objectives for fiscal year 2003:

- Screen culture collections for thermo-acidophilic organisms with xylanase activity.
- Perform enrichments from environmental samples collected at Yellowstone National Park.
- Screen environmental enrichments for organisms with xylanase activity.

Culture collections, including American Type Culture Collection and German Collection of Microorganisms and Cell Cultures, were searched for thermo-acidophiles whose optimum growth conditions were at temperatures greater than 60°C and at pHs less than 4.0. The four cultures selected for further examination were *Picrophilus torridus*, *Thermoplasma volcanium*, *Thermoplasma acidophilus* and *Alicyclobacillus acidocaldarius*. The recommended medium for growth was prepared for each culture with the carbon source replaced by ground corncobs, a rich source of xylan. Only one of these cultures was able to grow on the xylan medium, *Alicyclobacillus acidocaldarius* (ATCC 43030), and was assumed to produce a xylanase enzyme. Environmental samples were obtained from two sampling trips to the Norris Geyser Basin of Yellowstone National Park (Fig. 1). This geyser basin has numerous high temperature and acidic thermal features.

The pools sampled were:

- Bathtub Spring was too deep to get accurate temperature and pH measurements (~ 96°C and ~ pH 4.0).
- Mud Springs (92.8°C and pH 4.4).
- Black Hermit Cauldron (85°C and pH 2.95),
- Branch Spring (81.3°C and pH 4.01).
- Son of Green Dragon (83°C and pH 3.3).
- Yellow Funnel (89°C and pH 3.4).

*FIGURE 1. Sampling at Branch Spring, Yellowstone National Park.*

Samples obtained from the hot springs were inoculated into a selective medium adjusted to pH 3.0 and supplemented with ground corncobs as the xylan carbon source. The cultures were incubated with shaking at 80°C and monitored periodically for growth. Growth was observed in cultures inoculated from Bathtub Spring, Mud Spring, and Black Hermit Cauldron samples. As in the case of

the culture collection organisms, it was assumed that xylanase activity was present if the organisms were able to grow on the xylan substrate.

A xylanase assay was developed to screen the cultures obtained definitively for xylanase activity. The assay used a commercially available insoluble birch azo-xylan that is dyed with Remazol Brilliant Blue R such that there is approximately one dye molecule per 30 sugar residues. When the xylan substrate is acted upon by a xylanase enzyme low molecular weight soluble dyed fragments are released. The sample is then centrifuged to remove the unreacted high molecular weight xylan and the absorption of the supernatant is measured. Figure 2 shows the absorbance versus enzyme concentration for a commercially obtained xylanase enzyme.

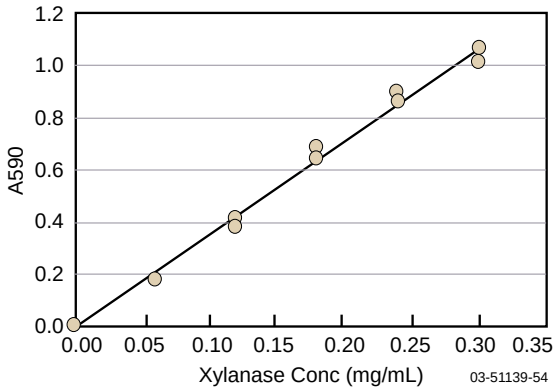


*FIGURE 2. Absorbance vs. enzyme concentration for a commercial xylanase.*

The assay will be used in FY04 to test the above cultures for xylanase activity and to quantify the amount of activity present. Once xylanase activity is definitively determined, the culture with the highest level of activity will be grown in liter quantities and the xylanase will be purified using standard protein purification techniques.

This is the first year of a three-year LDRD. This research will position INEEL to better respond to proposals for biomass conversion in support of the nation's alternative energy strategies. This topic also has been presented to the Consortium for Extremophile Research (CER) and received favorable feedback from that organization.

# $^{93m}$Nb, A Portable Excitation Source for Elemental Analysis

*John D. Baker, Robert J. Gehrke*

***Producing new x-ray sources for metals detection***

NE128

A cost-efficient method for producing pure, high-specific activity Nb-93m to be used as an x-ray fluorescence excitation source would be beneficial to efforts for locating hazardous metals. The isotope $^{93m}$Nb, daughter of $^{93}$Zr, emits niobium x-rays of which those at 16.6 and 18.6 KeV are extremely useful for the x-ray K shell fluorescence of elements between iron and rubidium and the L shell fluorescence of elements between lutetium and lead, which can then be detected using a thin-window photon detector.

This LDRD investigates radiochemical purification methods for a captured zirconium-containing stream at Oak Ridge National Laboratory (ORNL) that would produce $^{93m}$Nb. Efficient production of 16.1-year $^{93m}$Nb of high-purity and high-specific activity in millicurie quantities has been demonstrated including development of purification methods of the captured zirconium-containing stream. Significant progress also has been made toward the follow-on purification of gram quantities of its parent $^{93}$Zr.

While a number of $^{93m}$Nb production mechanisms where initially considered only one, production from fission, seemed to satisfy all of the criteria: millicurie quantities, high purity, and high-specific activity. The production scheme chosen involves the collection of the zirconium fission product fraction containing $1.5 \times 10^6$ -year $^{93}$Zr from very old fission products. The $^{93}$Zr radionuclide can be obtained in gram quantities after high burn-up of the fissile material. After suitable grow-in, the separation of the 16.1-year $^{93m}$Nb daughter is undertaken. Because only the $^{93m}$Nb that has grown in from the parent is collected, contamination by $^{94}$Nb is avoided.

Technical objectives for fiscal year 2003:

- Identify and develop chemical separation techniques to highly purify Nb-93m from sample effluent material furnished by ORNL.

A cost-efficient method for producing pure, high-specific activity Nb-93m has been identified and developed in collaboration with C.A. Alexander of ORNL. For this phase of the program, the investigators developed chemical separation techniques to highly purify Zr-93 from the ORNL-supplied sample effluent material. This material was collected from an effluent stream containing zirconium fission products. ORNL has been and will continue to further purify the totally collected zirconium-containing fraction from the irradiated assemblies over a period of years. This material will be further purified by ORNL using this LDRD's developed radiochemical separation scheme. The Zr-93 will then be let to decay to Nb-93m at which time the ORNL team will separate the $^{93m}$Nb from the Zr material. Either ORNL or this project's researchers will then electroplate the $^{93m}$Nb onto a backing for use as an x-ray fluorescence excitation source in this LDRD. Based on availability of funding, the x-ray fluorescence source will be tested as to its ability to detect part-per-million concentrations of the elements As, Hg and Pb.

The present approach to this year's objectives involved a minor modification to the chemical campaign at ORNL to recover $^{242}$Pu from irradiated Mark 42 assemblies for Los Alamos National Laboratory (LANL). These assemblies initially contained 3.3 kg of $^{239}$Pu and were irradiated at the Savannah River Site to 60 to 70% burn-up in the 1980s. When the investigators first learned of the campaigns being carried out at ORNL, only the actinide elements were being recovered with the fission products disposed to waste. Previous to this collaboration some interest was generated at ORNL to recover the precious metals of palladium, rhodium and ruthenium and some interest was shown in the recovery of the fission product $^{93}$Zr for cross-section measurements by ORNL.

Preliminary studies of the various effluent streams from the separation of Pu, Am and Cm from the high burn-up Mark 42 fuel assemblies were undertaken at the Radiochemical Engineering Development Center (REDC) at ORNL to determine which contained the Zr. The flow sheet for the purification of the plutonium isotopes, and later the transplutonium isotopes, are shown in Figure 1. The dissolution of the assembly was accomplished using a two-step process: caustic (NaOH) dissolution to remove the Al cladding and most of the Cs, Sr and Tc. The caustic solution is decanted and this is followed by a nitric acid addition to dissolve the actinides and the remainder of the fission products. The Pu is extracted in the Pubex process and the Am, Cm and Zr is extracted in the Cleanex process. After back-extracting the Am and Cm, the Zr remained in the extractant. To remove the zirconium fraction from the acid stripped HDEHP, this extractant was first diluted and then back extracted with oxalic acid.

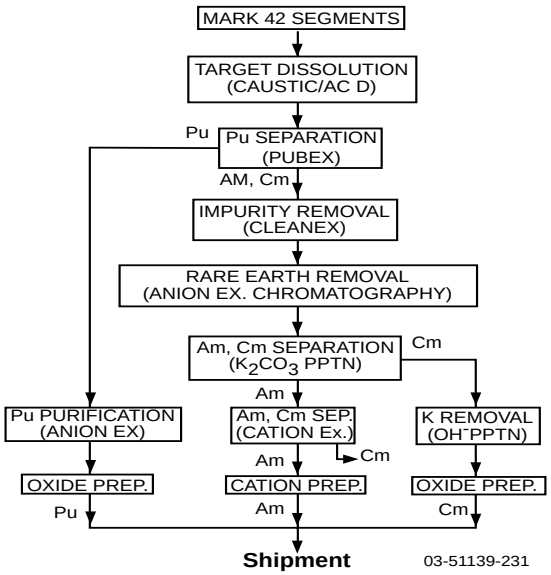


*FIGURE 1. ORNL Mark 42 element processing schematic.*

The oxalic acid solution was analyzed by ICPMS and mass 93 (Zr) was identified in amounts close to that of ORIGEN calculations (~39 g $^{93}$Zr per assembly). A small aliquot (sample) of this material was analyzed by gamma-ray and alpha spectrometry that showed the Zr was contaminated with $^{241,243}$Am, $^{242,244}$Cm, $^{238,239,240,241,242}$Pu, $^{239}$Np, $^{152,154}$Eu, $^{125}$Sb, $^{126}$Sn-$^{126}$Sb, $^{108,110m}$Ag, $^{106}$Ru-$^{106}$Rh, $^{137}$Cs and lesser amounts of other fission products.

ORNL sent a sample of the above solution to INEEL and chemical separations were performed to develop the following technique to produce radiochemically pure Zr. Since there were elements from most of the groups in the periodic table, it was obvious that one simple separation step would not suffice. Therefore, evaluating anion exchange became the first step.

Since the Zr was in oxalic acid, either this needed to be destroyed or the Zr removed from this matrix. The sample did not have macro amounts of Zr, so ~2 mg of natural Zr was added and the Zr was precipitated as $BaZrF_6$, by adding HF to the solution and then adding $Ba(NO_3)_2$. The Zr precipitate was washed with water and re-dissolved in $HNO_3/H_3BO_3$. The investigators added ~2 mg La to the solution and precipitated $LaF_3$ to carry most of the actinides and the lanthanide elements. The solution containing the Zr was made 10 M HCl, and NaHOCl was added to oxidize the Sb to the +5 oxidation state. This solution was passed through an anion exchange column to which the Zr and Sb sticks and the Zr eluted by reducing the acidity to 5 M HCl. There is still a trace amount of $^{106}$Ru-$^{106}$Rh in the Zr fraction, but this will be removed when the $^{93m}$Nb is separated from the Zr. This step has been performed many times on lesser amounts of $^{93}$Zr from samples separated from other fission product solutions. The Nb is separated from the Zr parent by dissolving the Zr in 6 M $H_2SO_4$/2 M HF and extracting the Nb into 20% Diisobutylcarbinol in Heptane. The Nb is back-extracted using $H_2O$.

The techniques to purify the Zr and separate the Nb from the Zr have been transmitted to ORNL so that larger amounts of Zr/Nb can be purified as they become available. Production of an electroplated $^{93m}$Nb x-ray fluorescence source could not be carried out due to the lack, at present, of sufficient activity of $^{93m}$Nb from grow-in from the parent $^{93}$Zr separated material.

This LDRD resulted in collaboration with ORNL. An Invention Disclosure Record also was submitted as a result of this research.

# Contaminants and Improved Energy Production: Laboratory Studies

*Richard D. Boardman, Robert A. Carrington*

***Using an abundant underdeveloped natural resource to address pollutants***

NE121

The development of cost-effective sorbents to remove sulfur and chlorine pollutants and toxic metals (especially mercury) from coal combustion, gasifier offgas, and other thermal conversion processes continues to lead DOE and EPA research and technology development objectives.

This LDRD is investigating a natural resource that has sorbent properties for multi-pollutant control. The thermal gravimetric tests and pollutant capture tests for the novel sorbent particles were completed in FY03. Material and energy balances were completed for one specific application of the sorbent in a coal-fired reactor. An Invention Disclosure Request will be submitted in FY04 and a patent application is currently being prepared. The technical and economical data obtained thus far are being used to support the patent application.

Due to the sensitivity of proprietary information, specific details regarding the technical accomplishments in FY03 are being withheld from this report. Interested parties may contact the project principals, Richard Boardman and Robert Carrington, for additional information. This LDRD is continuing next year. A detailed report of results will be provided in the FY04 annual report, pending completion of the patent application.

# Two-Phase Mass Flow Measurement for Geothermal Wells

*Robert P. Evans, Joe Keller*

***Measuring two-phase flow in a single instrument***

NE108

Accurate measurement of two-phase flow is not available either intrusively or non-intrusively in a single instrument. Yet, such an instrument would provide significant benefit to geothermal well sites, as well as to the oil and gas, thermal hydraulics, and nuclear industries.

The objective of this LDRD is to investigate the basis for a low-cost, non-intrusive, mass flow measurement system for single-phase and two-phase flow conditions. The technique explored is based on the relationship between flow noise, defined as the standard deviation of the time-series signal as measured by an accelerometer and mass flow rate. Using flow noise to measure mass flow employs an approach never before used in the measurement of mass flow.

Technical objectives for fiscal year 2003:

- Acquire experimental data for various piping materials, pipe sizes, and mass flow rates.
- Develop a relationship between the mass flow rate and the flow noise.
- Develop a theoretical basis for the relationship.
- Develop a numerical model validating the experimental data.
- Present results at internationally recognized forums.

A two-pronged approach was taken with this project, consisting of experimental testing backed by numerical model validation. In FY03, one focus was to determine a relationship between the signal noise, as measured by an accelerometer attached to the pipe, and the mass flow rate. Flow testing was performed at the Idaho State University flow laboratory using 0.5”, 1.5”, 3” and 4”diameter pipe test sections. Test section materials included 304/304L stainless steel, clear poly-vinyl chloride, and aluminum. The accelerometer data were acquired using a two-second time span at a sample rate of 2,048 samples per second. Anti-aliasing filters were used with a cut-off frequency of 800 Hz. The accelerometer time series data were transformed to the frequency domain using a Fast Fourier Transform.

Ten datasets were averaged in the frequency domain, filtered to remove pump vibrations, and transformed back to the time domain. The standard deviation of the filtered, time-series signal was plotted against the mass flow rate for the various pipe materials and pipe diameters. (Signal noise was computed as an average of the standard deviation of the accelerator signal.)

The test data indicate there is a strong relationship between the flow noise and the mass flow rate for single-phase flow. The effects of pipe material and pipe diameter were compensated for in the relationship. Test results indicate an exponential relationship between the mass flow rate and the standard deviation of the measurement signal, as shown in Figure 1. Based on this research, it can be concluded that a signal noise-based, flow measurement technique has potential. However, questions remain regarding calibration.

Using a statistical approach and the equations of motion (i.e., time-averaged quantities and a fluctuation term), an empirical relationship also was developed between the standard deviation of the time-series pipe vibrations and the fluid mean flow in a pipe.

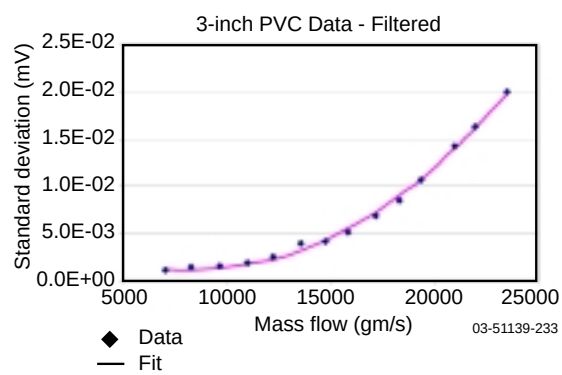


*FIGURE 1. Signal noise vs. mass flow for the 3” PVC test section.*

Another goal of this research was to develop a numerical-based approach to determine the impact of turbulent eddies on the vibration of a pipe with internal flow. A model of fully developed turbulent flow in a pipe was developed to investigate the contribution of turbulent flow to pipe vibration. It was determined that the turbulent flow contributes to pipe vibration to an extent that can be measured with an accelerometer.

The procedure for determining the relationship between flow rate and pipe vibration consisted of first solving the flow problem. So that others could

repeat this process, commercial software was used when possible. The Large Eddy Simulator (LES) model of the flow field was obtained through the commercial software package FLUENT. Once the solution to the flow field had been obtained, the pressure field on the pipe wall was exported to a commercially available structural finite element package known as ANSYS.

To determine the effects of turbulent flow on the vibration of the pipe, six discrete flow rates were investigated. At each time step in the flow solution, the pressure fluctuations were exported for use in the structural model. As the flow rate increases, the standard deviation of the pressure field also increases. The standard deviation of the pressure field for the six flow rates was computed and fit with a second order polynomial. The fit equation, which relates the standard deviation of the pressure field to the flow rate, has an $R^2$ fit of 0.998. Since pressure is the source of energy transfer between the fluid and the structure, it is assumed that a similar relationship between flow rate and pipe acceleration exists. In the flow model, fully developed flow conditions were initiated and periodic boundary conditions were used to reduce the length of the pipe and the number of elements. In the structural solution, however, the entire pipe was modeled such that the appropriate boundary conditions could be applied.

By comparison with other experimental results, the contribution of the turbulent flow to the pipe vibration at low flow rates is a rather small component of the overall pipe vibration. However, as the flow rate is increased, the turbulent flow-induced vibration becomes a more significant component of the total response. From this research it also was concluded that the pressure fluctuations on the pipe wall have a quadratic relationship with the flow rate. Furthermore, it was concluded that there is a definite relationship between the acceleration of the pipe (pipe vibration) and the flow rate. Figure 2 shows a relationship between the experimental and the simulated data. These last two concepts open possible avenues for the development of a non-intrusive mass flow sensor.

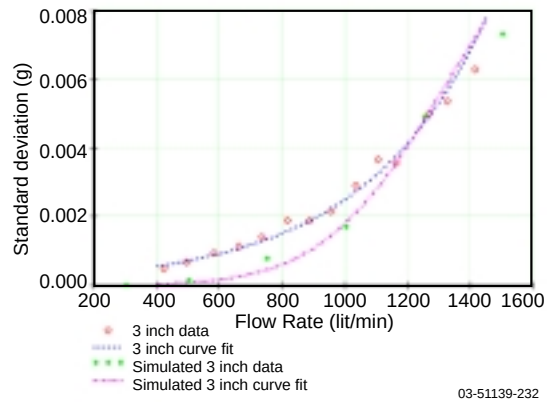


*FIGURE 2. Experimental vs. numerical data with curve fits.*

The results of the experimental testing and model development have been published or submitted for publication in four peer-reviewed publications and an invited paper, in addition to supporting a master's thesis, and a doctoral dissertation. This research has been performed in collaboration with investigators at the INEEL, Idaho State University, and Brigham Young University. A patent was awarded on the concept in July 2002. This LDRD supports DOE energy objectives and has generated interest among the oil and gas industries as well as the thermal hydraulics and nuclear industries.

# Advanced Test Reactor Three Dimensional Neutronics Modeling

*Hans D. Gougar, D. Scott Lucas, Paul Roth, Charles Wemple, Bruce Schnitzler*

***Enhancing accuracy and fidelity of reactor analysis***

NE119

The Advanced Test Reactor (ATR) is a premier materials test reactor with capabilities not found elsewhere. Its authorization basis, however, is based on safety analyses and methods that are decades old. Recent programmatic requirements and operational reviews have identified serious deficiencies in the ATR safety basis that threaten the long-term viability of the facility.

The purpose of this LDRD is to demonstrate the feasibility of using a 3-D deterministic transport code to perform global (core-wide) criticality and flux distribution calculations for the ATR. The effectiveness of the technique will be demonstrated through comparisons with experimental data and calculations that use alternative methods. Successful completion of this project will result in a more accurate and powerful tool that, compared to current methods, requires fewer modeling assumptions for determining safety-significant parameters.

Deterministic methods provide full core maps of core power and flux that are not possible with the Monte Carlo methods currently employed. These developments will allow the ATR to operate safely over a larger operating range while reducing reliance on expensive Advanced Test Reactor Critical (ATRC) facility measurements and conservative assumptions that contribute significantly to the cost of experiments. The resulting method also can be used for Generation IV reactor analysis to provide enhanced accuracy and fidelity.

Technical objectives for fiscal year 2003:

- Acquire and install the 3-D transport code, preprocessor software, manuals, and sample cases.
- Develop a 3-D (R-Z) model of the northeast quarter of the ATR including the reflector, control cylinders, fuel, and the Multiple Irradiation Capsule Experiment (MICE) mockup facility for the ATRC.
- Construct a full core 3-D model of ATR based on an existing MCNP (Monte Carlo) “clean core” deck. Verify geometric accuracy against drawings.
- Run decks to generate data on core eigenvalue, flux, and power distributions for fresh fuel elements.
- Compare results and execution times for the MCNP and Attila cases. Evaluate and compare the effort in writing input decks for each analysis tool.
- Generate a Statement of Work document specifying the tasks and objectives of the Atilla-ORIGEN Coupling utility and the performers.

The neutron transport code Attila was originally developed at Los Alamos National Laboratory (LANL) with ICEM-CFD (ANSYS) contracted to provide a mesh generator. The principals in that partnership formed Radion, Inc. to further develop and market the software. This LDRD has been conducted in close cooperation with Radion, Inc. The original Attila code licensed by Radion required two front-end codes to develop the appropriate finite element mesh. Solidworks computer-aided design (CAD) software was acquired and used to generate accurate 3-D geometric models of ATR components. The ICEM-CFD software converted the CAD models into a finite element mesh suitable for transport analysis. Licensing issues between the INEEL and ANSYS (the parent company of ICEM-CFD) prevented acquisition of the permanent ICEM license until six months into the fiscal year. However, progress was slowly made using temporary licenses on limited versions of the software. The latest version of Attila (in delivery) has its own mesh generation package and will eliminate the need for ICEM-CFD.

Attila has been installed on a number of high performance computing platforms maintained by the Numerical Simulation Laboratory including: a Sun V880 server, an SGI 64-processor SMP computer, an Opteron cluster, and a Cray Vector computer. A full-core model of the ATR was executed on the first three of these to compare run times with the following results:

- Sun V880 750MHz UltraSPARC III, 8GB RAM
  100 hours
- SGI Origin 3800 64 GB RAM
  100 hours
- Dual Opteron 246 1.8GHz with 8GB RAM
  12.5 hours

Geometrically accurate models of all ATR components and major experiment facilities were constructed using the Solidworks CAD software. A short training session on Solidworks was delivered by Radion staff to three of the project investigators. Most of the ATR models resulted from this activity.

A quarter-core model of the ATR East Flux Trap containing the Advanced Fuel Cycle (AFC) lead

experiment was developed. This facility was chosen rather than the northeast MICE experiment because of the unique challenges to core safety posed by the AFC cadmium baskets. Ease of model development and the speed of available computers (the Opteron in particular) allowed the progression to a full-core ATR model (Fig. 1) that included the AFC experiment along with the Irradiation Test Vehicle (ITV) in the center lobe, MICE, and other facilities in the current core.

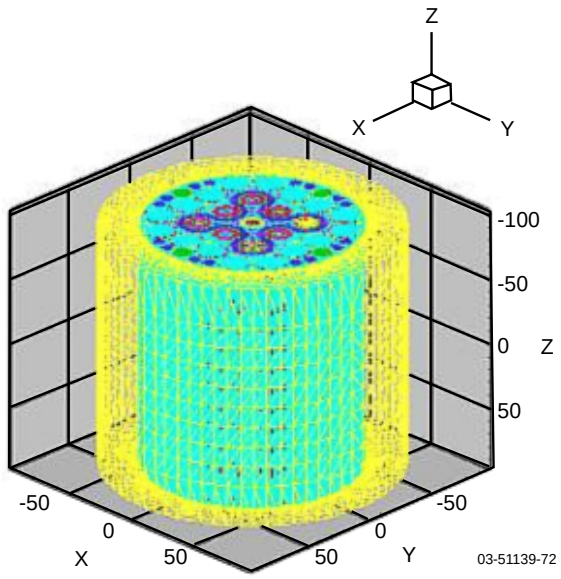


*FIGURE 1. 3-D Attila model of ATR core.*

The Attila software is still under development, and compatibility and licensing issues prevented extensive comparison with ATRC flux wire data and Monte Carlo calculations as of this date. The MCNP model of the ATR flux run from cycle 73-A has only recently been updated and cross-section sets between the two models are being synchronized. However, preliminary results of the Attila model of ATR with the AFC experiment were compared to the ATCR experiment that included this test. That experiment included the AFC test in the south flux trap. The shim positions, which gave a critical core multiplication factor ($k_{eff}$ = 1.000), were measured at 47.4°. The Attila model result gave a core $k_{eff}$ = 0.9900 with the shim positions at 50°. The legacy diffusion theory code PDQ, currently used for ATR safety analysis, also was used to model this ATRC experiment. It yielded a value of 0.9901 for a shim position of 51.2°. Even with this preliminary model, the Attila code yielded satisfactory reactivity agreement with measured data and PDQ. Axial profile and void reactivity results are pending the completion of the current analysis run.

Three-dimensional deterministic neutral particle transport calculations for core-wide applications have until recently been beyond the capacity of computational methods and machines. The methods developed for Attila combined with processors such as the Opteron now make feasible full-core, highly accurate reactor physics analyses and the generation of flux and power maps (Fig. 2).

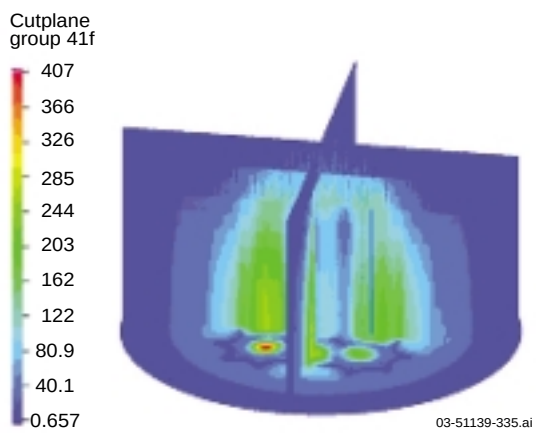


*FIGURE 2. Attila-computed thermal flux in ATR.*

Attila does not possess depletion capability, i.e., the ability to compute changes in core composition over time. This feature is essential for proper ATR cycle safety and experiment analysis. However, Attila can be coupled to the depletion code ORIGEN using code-coupling software. The creation of such software is the principal deliverable of the second phase of this LDRD. Such a coupling utility (MOCUP) was developed at the INEEL to link MCNP to ORIGEN. The MOCUP knowledge bases will be exploited for this project. A mutually beneficial agreement will be negotiated, possibly via a CRADA, which would license the coupling utility to Radion in return for a license to use Attila at the INEEL.

At mid-year (June 2003) a poster titled "Application of the 3D Finite Element Neutron Transport Code," describing work to date, was presented to the DOE EFCOG Safety Analysis Working Group

conference in Salt Lake City. A summary of the ATR modeling work also has been submitted to the American Nuclear Society PHYSOR topical meeting to be held in Chicago in April 2004.

Successful completion of this project will attract a renewed commitment to ATR by both Naval Reactors and DOE-NE. The tools and expertise in advanced reactor physics analysis being developed are not currently being investigated at any other site in the complex. This effort will help cement INEEL's position as reactor technology lead laboratory and place it in a position to lead Generation IV design and analysis work.

# Computational Fluid Dynamics Model Based Control of Two-Phase Flow

*Kurt D. Hamman, Christopher T. Wright*

***Controlling fluid dynamic processes for improved product designs***

CE109

Computational Fluid Dynamics (CFD) is a computer simulation tool originally developed for academic and aerospace research. It is now being used extensively in several industries. Since single-phase and multi-component fluid dynamic processes are fundamental to all aspects of industry, accurate measurement of system fluid properties and good control of these processes is essential to ensuring that industrial systems operate efficiently and in an environmentally sound manner.

However, most control technologies used in industrial systems have been based on indirect measures of fluid properties, such as pressure gages and thermocouples, instead of "primary" measures such as fluid density, momentum, vorticity and energy. A more accurate and less intrusive way to measure fluid properties for use in the control of industrial systems would be extremely beneficial.

This LDRD is demonstrating the feasibility of real-time CFD-based control. A simple experiment was constructed and coupled with commercial CFD software to simulate a 3-D piping system and demonstrate the use of open loop control of an industrial system. The overall intent was to keep the study simple, and then add complexities such as multi-component flow models after the first objective was completed successfully.

Technical objectives for fiscal year 2003:

- Use commercial CFD software to demonstrate open loop control in an industrial system designed to transport a single-phase working fluid (i.e., air).
- Use commercial CFD software to demonstrate open loop control in an industrial system designed to transport a multi-component working fluid (i.e., air and sand).

A control demonstration approach was pursued. The approach taken was to construct a simple piping and valve arrangement and to develop a CFD model of this arrangement (Figs. 1 and 2).

The first technical objective was completed successfully. The experiment demonstrated the application of open loop control of an industrial system using Fluent 6.1 commercial CFD software coupled with an experimental apparatus consisting of a plastic pipe and a valve that opens and shuts. Fluent 6.1 was chosen for this study based on minimizing project costs and the following:

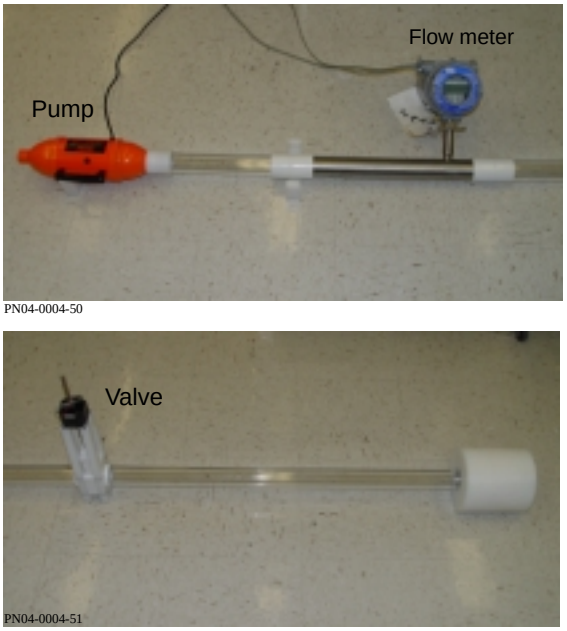


*FIGURE 1. Experimental apparatus.*

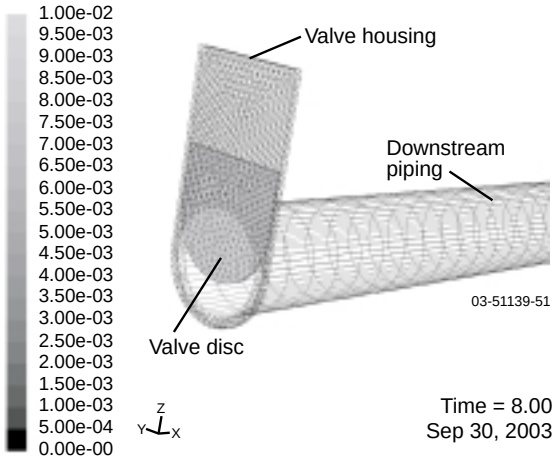


*FIGURE 2. CFD model geometry (upstream piping not shown).*

- INEEL currently maintains several Fluent licenses, so no additional cost was required to purchase software.
- Fluent has a parallel solver that executes on several of the INEEL's high performance computers, significantly reducing computational time.
- Fluent has moving-deformable mesh capabilities, making simulation of control surfaces, such as valves, relatively simple.
- Fluent has the capability to interface, using user-defined functions and data files, with experimental data via commercially available data acquisition systems such as those developed by National Instruments.

The experimental arrangement and the CFD model were coupled using LabVIEW, commercial data acquisition (DAQ) software, and DAQ hardware developed by National Instruments. The CFD software was executed on a 12-node Linux high-performance computer, and the DAQ software was executed on a single-processor Windows XP desktop computer. Samba and Exceed software allowed the Linux operating system to interoperate with the Microsoft Windows operating system.

The major components of the experimental apparatus included an electric air pump, a mass flow meter, a knife valve actuated with a small stepper motor, and approximately 13 feet of clear acrylic piping. The air pump was capable of forcing 25-cfm of air at 0.5 psi of pressure down the length of pipe. A mass flowmeter was placed inline between the pump and the knife valve to measure the actual mass flow of air being forced through the pipe during experimental operation.

The LabVIEW program was designed to perform two main functions. First, it would monitor the mass flow rate of the system and write the data to a file. This file would, in turn, be read by the CFD software and used as an inlet boundary condition for the flow simulation. Next, it would monitor an output file from the CFD software and compare the data to a preset condition that would represent an abnormal condition in an industrial system. If the preset condition were met, the program would shut or open the valve, depending on the desired conditions.

The second technical objective was not investigated during this fiscal year.

This LDRD enabled a team of scientists and engineers to gain valuable expertise in the integration of analytical software, high-performance computers and experimental apparatuses. Numerous industrial applications exist for this technology. Specific examples include control of reactor plant safety systems, inputs to virtual engineering platforms for visualization of experimental data, and inputs to artificial intelligence control systems. This effort set the tone for bridging the analytical and experimental "gap," enabling the INEEL to better position itself for research involving the integration of analytical and experimental tools.

# Active Neutron Spectrometry for Neutron Capture Beam Characterization

*Jack K. Hartwell, David W. Nigg*

***Improving cancer treatment planning***

NE 117

The INEEL has had a long-standing interest in the development of neutron-based radiotherapy. Boron neutron capture therapy (BNCT), which has been of particular interest at the INEEL, is a form of neutron-based therapy that uses blood-borne boron compounds and a carefully tailored neutron energy spectrum to enhance the therapeutic dose to cancer tumors.

Cancer treatment planning for BNCT requires detailed information regarding the neutron energy spectrum of the therapy beam. The INEEL's BNCT research group is internationally recognized for its expertise in the characterization of the energy spectrum of fast and epithermal neutron therapy beams. Neutron energy spectroscopy is a challenging measurement under the best of conditions, but is even more difficult in the high neutron and gamma ray fluence environment presented in actual neutron therapy beams.

The INEEL's measurement protocol relies on the activation of threshold foils, the induced activity of which can be analyzed to determine the neutron flux profile in various energy groups. These measurements lack detail in the critical neutron energy region from about 50 keV to 2 MeV.

In prior years, this LDRD demonstrated the efficacy of neutron measurements using superheated drop detectors (SDDs), implemented these measurements into the BNCT protocol, and demonstrated excellent results on measurements of the pre-clinical beam at Washington State University (WSU).

Technical objectives for fiscal year 2003:

- Investigate methods of extending active spectrometric techniques to high neutron energies.

The SDD neutron spectrometer that has produced much success in this LDRD is a product of Apfel Enterprises, Inc. (New Haven, CT). A number of successful measurements were made with the SDD spectrometer in FY02 (Fig. 1) and were reported in detail in the INEEL 2002 Advanced Radiotherapy Annual Report. Though Apfel Enterprises officially closed in December 2002, the SDD media tubes required periodically to support measurements are available on a full cost recovery basis through Dr. F. d'Errico (Yale University).

Also of note is a recent paper by Dr. F. d'Errico et. al. that reports response functions for the Apfel SDD spectrometric media tubes extending to

PN04-

*FIGURE 1. SDD spectrometer head positioned in the source plane for measurements at WSU.*

neutron energies of 134 MeV. Prior to this work, SDD response functions were available only to 20 MeV. The measurement and publication of these response functions facilitates the use of the SDD spectrometer in this LDRD. With the extended response functions and a supply of media tubes, the Apfel SDD spectrometer provides a method of performing coarse group neutron spectroscopy on therapy beams with energies up to 134 MeV. The spectrometer can be used and will provide an active neutron spectroscopy capability for this LDRD's beam characterization program; however, the tenuous nature of media supply and customer support is clearly a concern with this device.

Two alternative active spectroscopy candidates (that were to be the initial focus of this LDRD prior to the availability of the SDD spectrometer) are organic liquid scintillators and double scatter neutron spectroscopy. Some preliminary investigations on the liquid scintillation option were conducted in FY03.

Organic liquid scintillation detectors, such as NE213 and BC501A, have been successfully used to determine neutron energy spectra in the energy region from about 600 keV to more than 100 MeV. These scintillators have very short fluorescence lifetimes (3.2 ns), and thus, are capable of operation at very high input rates if such rates can be supported by the signal processing electronics. They have good detection efficiency even at very high neutron energies and are sufficiently rugged and compact to allow reasonable use as field spectrometers. However, since they are proton recoil detectors, spectral analysis is complicated. Also to avoid contamination of the neutron spectral data with gamma-ray events, electronic discrimination between neutron-generated proton recoil events and gamma ray-generated electron recoil events must be provided. Innovative techniques to provide this discrimination were investigated.

Success has been reported with the use of charge integration over a "short gate" (capturing the pulse rise time) and a "long gate" (capturing the pulse decay time) as a method of distinguishing between gamma ray-generated recoil electron events and neutron-generated proton recoil events. The total pulse duration of electron pulses is much shorter than that of proton recoil events, thus, the ratio of charge in the long gate to charge in the short gate can be used to differentiate between event types.

The investigators have available a couple of digital signal processors (DSPs) for radiation spectroscopy. DSPs in general, are highly input-rate-capable devices, a feature that matches well with the high-count rate capability of organic liquid scintillators. The specific units available are capable of capturing digitized input waveforms and storing them for later processing (much like digital oscilloscopes.) The software to recall and manipulate the waveforms is somewhat specialized, but can be developed.

Under this LDRD, a test was initiated to see if discrimination methods that had previously been implemented using analog signal processing could be performed using purely digital techniques. Sets of input waveforms for gamma-ray sources alone, and for a mixed $n$-$\gamma$ source ($^{252}$Cf) were carefully acquired. These data were taken in event-by-event mode using a 50 cm X 50 cm BC501A scintillation detector with a Phillips XP2020 photo multiplier input directly to a CAMAC-based XIA DGF-4E digital signal processor. A subset of these data was processed using a code that roughly implements previous techniques. The results on the test data set were quite good. Figure 2 (next page)presents the neutron/gamma discrimination results.

While the determination of an n-$\gamma$ discrimination technique is an important step forward in the integration of liquid scintillation counters and digital signal processors, a great deal of work remains to complete the implementation. This includes implementation of code to extract and histogram just the neutron section of the neutron/gamma-ray data, careful calibration of the energy response scale of the BC501A scintillators in electron equivalent energy, and the computation and implementation of detector-specific response functions. However, the work of Figure 2 is a proof of principle in this larger implementation task.

The INEEL is presently in its 15th year of a BNCT Research Program funded through the DOE's Office of Science. The INEEL's contributions to this program include its capability to characterize BNCT therapy beams for those parameters important to treatment planning and dosimetry.

INEEL researchers have assisted the international neutron capture therapy community by characterization of epithermal BNCT beams at the

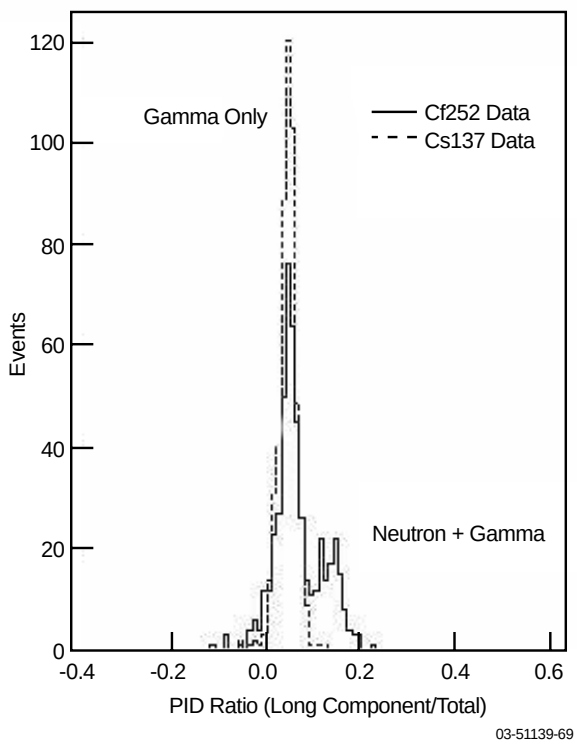


*FIGURE 2. Demonstrations of n-γ discrimination with a DSP. The dashed curve is γ-rays only, while the solid curve is both γ-rays and neutrons. The small peak above a PID of about 0.1 is the separated neutron data.*

Brookhaven Medical Research reactor (BMRR) at BNL, the Petten High Flux Reactor Facility (HFR) in the Netherlands, the Finnish Research Reactor Facility (FiR1) outside of Helsinki, and the Swedish Studsvik Nuclear Research Center (R2-0), near Nyköping, Sweden. BNCT clinical trials have been completed at these facilities, and the foreign beams are presently treating brain cancer patients. Additionally, the INEEL neutron spectroscopy team performed beam characterization measurements on the fast neutron therapy beam at the University of Washington both before and after installation of an INEEL-designed neutron filter. This filter was designed to provide a boron therapy "boost" to the fast neutron beam to enhance the control of certain lung cancer tumors. Measurements are being completed at an INEEL-designed beam facility installed on the Washington State University TRIGA reactor for large animal studies. In the U.S., plans for modification of reactors at Davis-McLlelan, New Hampshire, and Columbia (Missouri) have been proposed. Other proposed sites worldwide are in the Czech Republic, Italy, Portugal, Argentina, Brazil and Russia.

Implementation of a superheated drop detector-based spectrometer investigated in this research into beam characterization protocol has enhanced the INEEL's ability to detail the neutron spectrum in the energy region above 100 keV. Since these higher-energy neutrons contribute to an undesirable dose to healthy tissue, their quantification is important for treatment planning.

There is research interest in the use of neutron capture to augment currently implemented fast-neutron therapy techniques. The INEEL has collaborated in this research by the design of beam filters and characterization of beam neutronics. This year's LDRD research investigated and provided initial direction to the development of active spectrometric techniques to enhance the INEEL's foil activation protocol for these high-energy beam measurements.

# Development of Analytical Decision-Making Tools for Energy Efficient Agricultural Biomass Production

*Reed Hoskinson*

## *Creating a site-specific recipe for fertilizer application*

CE110

Presently, farmers fertilize and grow wheat with the objective of producing the economically optimum crop of wheat *grain*. With today's growing demand for energy, the wheat *stems* are becoming a valuable bioenergy source. The farmer's ideal would be to grow an economically optimum combination of both grain and straw stems.

This LDRD investigates methods for the optimum, simultaneous production of both grain and straw stems. To achieve this objective, the capability of the Decision Support System for Agriculture (DSS4Ag) has been extended to generate a spatially variable, site-specific recipe for application of fertilizers such that the economically optimum simultaneous production of both grain and biomass will be achieved.

Technical objectives for fiscal year 2003:

- Enhance the optimization function of DSS4Ag to take into consideration the costs/benefits for both grain and biomass.
- Generate a spatially variable site-specific recipe for fertilization of the farm field.
- Fertilize the field with the recipe in a treatment pattern suitable for statistical evaluation of results.
- Intensively monitor site-specific production of both grain and biomass at harvest.

A fertilizer recipe was field-tested during the FY02 growing season that was based on historic yield and biomass data collected in 1997 from a farm over 50 miles away from the test field. During FY03 the field tests were repeated on another field within three miles of the FY02 field, using the FY02 yield and biomass data as the historic data for the DSS4Ag. The historic data used to generate the 2003 fertilizer recipe included the 2002 grain and biomass yield (Fig. 1).

The current data comprised the existing test field soil chemistry determined from soil samples collected in April 2003, current fertilizer costs, and the farmer's forecast market price of $2.55/bushel for the grain at harvest. The control recipe of fertilizers was as specified by the farmer and his agronomic consultant. Two treatments were developed, one based on straw at a value of $10/ton to reflect current market conditions of minimal value of the straw, and the other at a value of $50/ton to reflect possible market conditions when a bioenergy market exists.

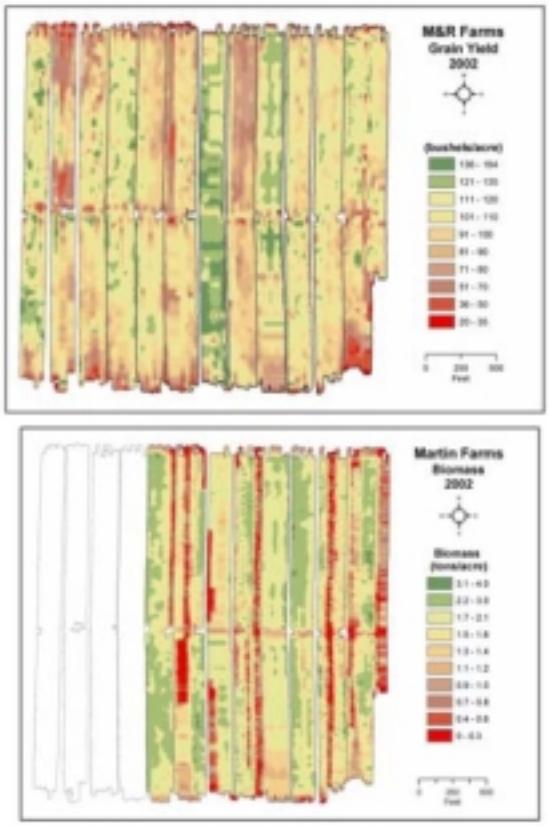


PN04-0004-55

*FIGURE 1. Historic 2002 grain and biomass yield data.*

Based on the current data and the knowledge from the historic data, the DSS4Ag generated spatially variable fertilizer recipes. Specifications for these

recipes were input to the Falcon controller system on a variable-rate fertilizer spreader and the fertilizers were spread as shown in Figure 2 on May 6, 2003.

The control fertilizer recipe cost $38.74/acre, the $10/ton treatment cost $19.08, and the $50/ton treatment cost $32.46/acre.

The field was harvested in September 2003 using a grain combine equipped with a GPS and yield monitor, as well as two biomass sensor systems being developed at INEEL. These harvest data will be analyzed with the economic data to determine the success of the field tests.

As the U.S. role in the national and international bioenergy markets grows, this DSS4Ag analytical tool for optimizing the production of the grain crop as well as the biomass feedstock will have significant potential. This expectation is strengthened by other INEEL research in collaboration with a major agricultural equipment manufacturer that suggests that there will be machinery available to harvest both the crop and the biomass feedstock.

The research supports the INEEL Bioenergy Initiative concept of "whole-crop utilization," and enhances the INEEL's expertise and contributions to the DOE Bioenergy Initiative.

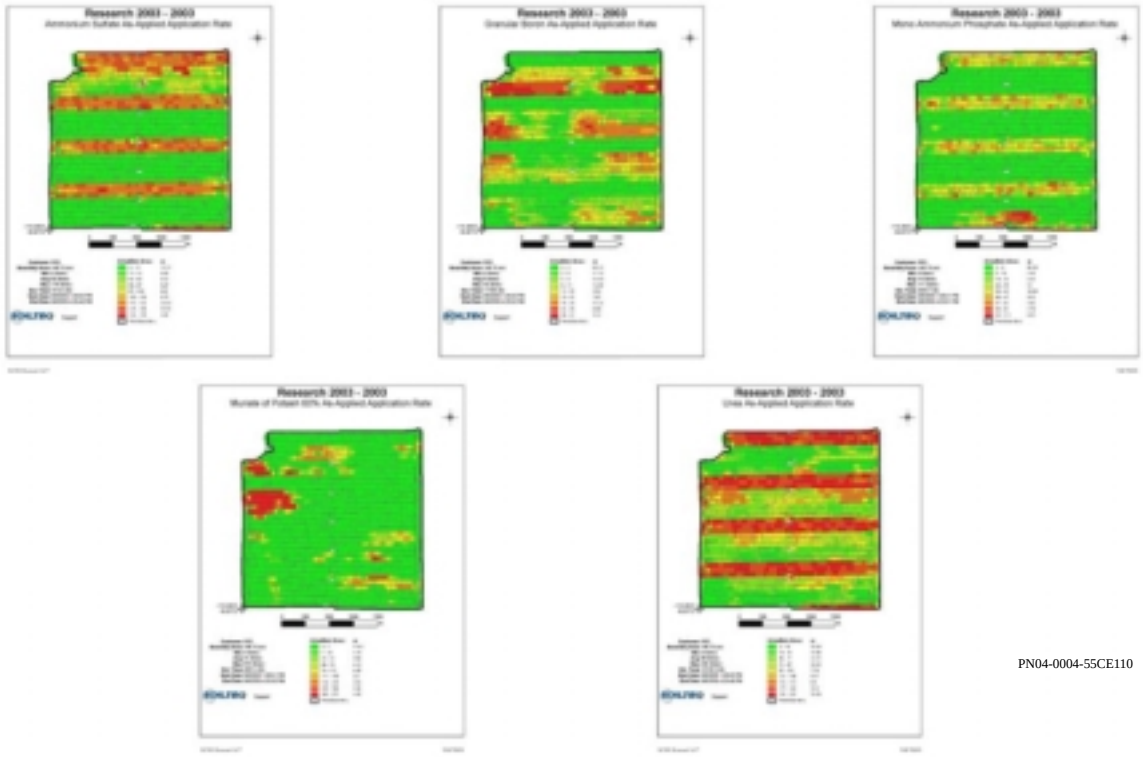


PN04-0004-55CE110

*FIGURE 2. Variable-rate fertilization as applied.*

# Flow Characterization of Complex Biomass Flows for Bioenergy Feedstock Development

*Kevin L. Kenney, Kurt D. Hamman, Christopher T. Wright*

***Separating biomass feedstock from crop residue***

CE113

Agricultural biomass is a significant source of alternative and renewable fuels. However, not all agricultural biomass components are suitable sources of bioenergy, which requires that the desired bioenergy feedstock be separated from the other crop residues before it can be effectively and broadly utilized. This requires the development of equipment and techniques to separate the feedstock material from the crop residues. As separation processes for biomass feedstock are very complex, they require innovative application of proven flow characterization techniques, used in fluid dynamics research, to evaluate them.

The objective of this LDRD is to develop a Particle Image Velocimetry (PIV) flow characterization technique to evaluate biomass flows within a separation chamber of a grain combine. PIV was developed and is generally used for examining controlled flows in a laboratory environment, so the inherent complexities of the biomass and the biomass flow field environment present significant challenges. Through the development of an imaging head that allows a PIV camera to be positioned directly in the flow field, and optimization of the image acquisition parameters, the investigators successfully applied PIV to quantitatively study biomass flows in the separation chamber of a grain combine. While this capability provides immediate benefits to INEEL's bioenergy feedstock development effort, it may eventually be used to engineer and design the next generation of harvesting and collection equipment needed to support the Bioenergy Industry.

Technical objectives for fiscal year 2003:

- Design PIV imaging hardware for positioning a video camera and lighting hardware directly in the flow while:
  - eliminating near-field biomass that obstructs the view of the image plane.
  - minimizing the intrusive effects on the flow field.
  - enabling the acquisition of PIV images at near full-load levels.
- Optimize image acquisition variables of camera focus and aperture, light sheet thickness and intensity, image magnification/resolution, and pulse separation.

In Figure 1, the improvements resulting from this LDRD are clearly illustrated. Figure 1a is a PIV map obtained prior to the developments of this project. Evaluation of this image shows that the biomass particles are not in clear focus, the image plane is somewhat obscured by the near-field particles (those between the camera and the image plane), and there are regions of the flow in which erroneous velocity vectors were predicted (large arrows).

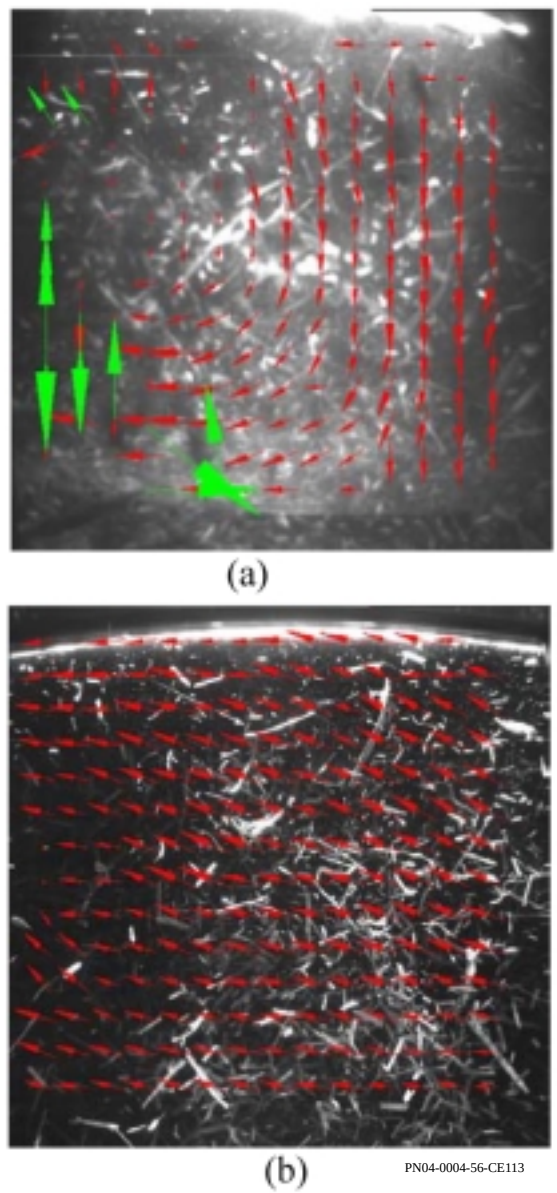


*FIGURE 1. PIV quality before (a) and after (b) the improvements accomplished under this LDRD.*

Figure 1b is a similar PIV map illustrating the improvements from this project. In this representative image, the biomass particles are in sharp focus, there is no near-field biomass to obstruct the view of the image plane, and there are no erroneous vectors. Additionally, the former PIV map was obtained at unusually low biomass loadings whereas the latter is representative of near-normal harvest conditions. These improvements were accomplished through the design of an imaging head that permitted the camera to be positioned directly in the flow while eliminating the near-field flow, and through optimization of the image acquisition parameters.

*Imaging System Design and Optimization* — Most PIV applications enable the camera to be positioned outside the flow where it can see through the near-field flow (region between the illumination plane and the camera) to the flow illuminated by the light sheet. Since the camera can see through the near-field flow, the entire depth of the flow field volume can be imaged with the camera isolated from the flow. Biomass flows, on the other hand, are much more complex, as the biomass particles are so large that the camera cannot see through the near-field particles. Consequently, to minimize the amount of near-field biomass obstructing the camera's view and to see beyond the outer perimeter of the flow field volume, the camera must be positioned directly in the flow and as near the illumination plane as possible (determined by the focal length of the camera lens).

Since the quality of the PIV images is directly related to the ability to see through the near-field biomass, a primary objective of this LDRD project was to develop techniques and hardware to minimize or entirely eliminate the near-field biomass. The proposed technique suggested partitioning the combine separation chamber using a transparent Lexan baffle, which enabled the camera to be positioned on one side of the baffle where its intrusive effects were isolated from the observed flow on the opposite side of the transparent baffle. However, since this solution involves a modification to the combine rather than a robust solution to the problem, a PIV imaging head was developed that accomplished the same objective without modifications to the combine itself.

A picture of the PIV imaging head designed, fabricated and tested for this LDRD project is shown installed in the separation chamber of a combine in Figure 2. The shroud was designed to enclose the camera and the near-field region to create a dead space between the camera and the focal plane. Its geometry is based on the angle-of-view and the field-of-view at the minimum working distance of the camera lens to minimize the size of the shroud. The geometry of the shroud as it extends from the camera head mimics the angle-of-view of the camera lens with the dimensions of the opening of the shroud determined by the field-of-view of the camera at the minimum object distance. A flow diversion plate extends 12" from the upstream edge of the shroud to divert the biomass flow in advance of the shroud to minimize the intrusive effects.

PN04-0004-056-CE113b

*FIGURE 2. PIV imaging head for acquiring images of biomass flows in a grain combine.*

The initial shroud design included a glass window that covered the opening of the shroud to shield the camera from dust and biomass particles in the flow. During field-testing however, the accumulation of dust on the glass, combined with illumination of the glass surface by the light positioned in the same plane as the glass, generated too much glare and resulted in poor image quality. Efforts to reduce the dust build-up included the use of anti-static coatings on the glass as well as replacing the glass with Plexiglas, but these provided no improvements. Finally, since efforts to prevent the accumulation of dust on the glass failed, the glass was removed, leaving the front of the shroud open. Subsequent tests showed dramatic improvement in image quality, but dust accumulation on the camera lens also proved problematic. Finally, an air knife

was installed to provide a continuous air curtain that shields the lens and prevents the accumulation of dust on the surface of the camera lens. The imaging head is cantilevered off a cross-rail (shown in Fig. 1) that permits easy positioning across the width of the combine separation chamber. A computational fluid dynamics (CFD) model was performed to determine the distance the imaging head must be positioned upstream of the cross-rail to not see the effects of the rail in the flow images.

*Image Acquisition Optimization* — Image acquisition is typically the most difficult aspect of PIV measurement and requires careful optimization of all the experimental parameters. Optimization of PIV image acquisition relies on the adjustment of a number of parameters, and was a major objective of this LDRD. Camera focus and aperture, light sheet thickness and intensity, and image magnification and pulse separation were all parameters that received careful consideration.

Optimum camera focus at a nominal object distance of 6” was obtained with the addition of a 0.25-mm spacer ring positioned between the camera and the lens. The optimum aperture setting was determined empirically to control image exposure, as the optimum setting changes with biomass loading. Typically the aperture also is used to control the depth of field, but since the exposure time is fixed, the aperture is used to control the exposure of the image, and the light sheet thickness controls the depth of field. The light sheet thickness controls the volume of biomass that is illuminated.

The light line is composed of optical fibers with an approximate angle of divergence of 60 degrees. Across the 10” field-of-view, the light sheet thickness increases by about 11”. This problem became apparent at the end of the project, and a rod lens has been purchased that will produce a collimated light sheet nominally 0.5” thick. Although the effect of the rod lens will not be evaluated with this LDRD, it will certainly offer improvements that will be realized with future applications. The light sheet intensity also was evaluated and adjustments were made to provide consistent lighting from the two xenon strobes.

Image magnification is determined by the focal length of the camera lens. The biomass particles are large enough to afford a large field-of-view, so a 6.5 mm wide-angle lens was selected in order to maximize the field-of-view. Perhaps the biggest improvement in image acquisition was the optimization of the pulse separation, i.e., the time delay between the two exposures for PIV analysis. The pulse separation is configurable and should be selected to provide 4 to 5 pixels of particle displacement between the two exposures. The appropriate pulse separation is empirically determined, based on the velocity of the imaged particles.

Biomass separation capabilities are critical to the selective harvest concept endorsed by the DOE Office of Biomass. As the lead research institute for bioenergy feedstock development, the INEEL must continue to develop these capabilities. The utilization of Particle Image Velocimetry for quantitative characterization of biomass separation processes enhances INEEL’s position in bioenergy feedstock development. Additionally, this project has improved the INEEL’s CFD modeling capabilities by providing an essential tool for developing and validating biomass separation models.

This project also has advanced the state-of-the-art of PIV technology. The flow of granular material is important to many industries such as pharmaceutical, food processing and construction. It is conceivable that the PIV capability developed through this LDRD could be useful for many other applications as well.

# Radiation Chemistry of Supercritical Water

*Bruce J. Mincher*

***Enabling direct measurement of corrosive species***

NE129

Pulse radiolysis is a technique used to measure yields and reaction rates of radicals and other products in irradiated systems. The short-lived, reactive species are measured spectroscopically, but many cannot be directly observed by conventional molecular spectroscopic techniques because they either weakly absorb UV-Vis light, or do not absorb any light at convenient wavelengths.

The coupling of state-of-the-art molecular spectroscopic techniques such as laser-induced fluorescence with pulse radiolysis will enable direct measurements of important products such as hydroxyl radical and peroxide that have only been measured previously by indirect means. The ability to directly measure these species has important applications in radiobiology for the investigation of hydroxyl radical and peroxide reactions with biological macromolecules; in atmospheric chemistry for the investigation of chlorocarbon removal from the atmosphere by photolytically produced hydroxyl radical; in basic radiation chemistry for the measurement of fundamental rate constants; and in reactor design to measure the rates at which the products of irradiated supercritical water and carbon dioxide are produced. The rates of production and reactivities of corrosive radical species are unknown in these proposed reactor coolant media.

This LDRD is establishing a pulse radiolysis capability at the INEEL with the ability to conduct novel spectroscopic measurements not performed at the handful of existing pulse radiolysis facilities. If successful, this project will result in a functional pulse radiolysis system and fundamental data regarding radiation chemistry in the form of peer-reviewed journal papers. The INEEL is well positioned to perform this work because of access to the 30 MeV LINAC at the Idaho Accelerator Center (IAC). This accelerator is one of the fastest in the country and, thus, is uniquely suited to provide the very fast radiation pulses necessary to study fast free-radical reactions.

Technical objectives for fiscal year 2003:

- Directly measure hydroxyl radical or peroxide using laser spectroscopy.
- Couple the spectroscopic technique with accelerator pulse radiolysis to make measurements of yields and reaction rates of transient radicals.
- Measure absolute rate constants for reaction of hydroxyl radical, peroxide and other transients with species of interest under varying pressure and temperature.

During FY03, a laser-spectroscopy system was constructed from existing equipment. In its current configuration, 1064 nm light is generated with a Class IV Nd:YAG laser, and the 2nd (532 nm) and 4th (266 nm) harmonics are split. The 266 nm light is transmitted down the table to the sample compartment to photolyze the sample to produce hydroxyl radical. The 532 nm light is used to pump a dye laser. The dye laser output is about 580 nm. The output of the dye laser (580 nm) is run through a UVT doubler, which produces tunable UV light. Thus, the 580 nm emission is doubled to 290 nm and can be tuned down to 280 nm or 281 nm where the hydroxyl radical absorbs. This is referred to as a “two-color experiment,” where one wavelength is used to produce the hydroxyl radical and the other to laser-excite the hydroxyl radical species. When the hydroxyl radical absorbs 280-281 nm, it fluoresces at ~306 nm to 308 nm. A chromagraph equipped with a TE-cooled CCD camera, capable of looking at all wavelengths from about 200 nm up to about 800 nm, is then used to measure the fluorescence, which is in direct correlation to the concentration of hydroxyl radical.

The Class IV laser spectroscopy system has been successfully constructed and the lasers operated; however, hydroxyl radical spectra have not yet been acquired. The UVT doubler uses a series of four doubling crystals specific for different input and output ranges and mixing crystals that can mix wavelengths. The UVT that was available from existing equipment came with a single mixing crystal (MCC-1), which is not able to supply 280-281 nm of excitation light to the sample compartment. At this time, hydroxyl radical can be generated but not fluoresced. Excitation of hydroxyl radical species requires the purchase of an appropriate doubling crystal. This aspect of the work is planned for early FY04.

In addition to acquiring suitable laser laboratory space, building the system, and operating the lasers, the necessary optics to build the system at IRC and an optical table were purchased. Another set of the lasers was transferred to the IAC that will be used

for coupling with pulse radiolysis in FY04. With continued funding in FY04, the investigators anticipate making measurements using the accelerator as a source of hydroxyl radical.

This LDRD addresses a Generation IV reactor research and development need, and expands the INEEL's radiation chemistry capability with development of possibly the fastest pulse radiolysis system in the U.S. Such a system is expected to become a national user facility. The 30 MeV LINAC at the IAC is uniquely suited to providing the very fast radiation pulses necessary to study fast reactions in supercritical water. Building upon previous INEEL radiation chemistry and laser spectroscopy experience, and IAC experience with accelerator applications and laser spectroscopy, this research will position the INEEL to become a premier radiation chemistry laboratory. These factors will significantly increase INEEL's ability to do new work for DOE-NE on the effects of radiation on materials and chemical compounds, on pollutant remediation by radiolysis, and in the areas of radiobiology and atmospheric chemistry.

# Estimation of Neutron Irradiation-Induced Displacements-Per-Atom

*Abderrafi M. Ougouag, Charles A. Wemple, Thomas J. Dolan, Clinton D. Van Siclen, David A. Petti, Hans D. Gougar*

***Determining potential materials damage from irradiation***

NE127

The Advanced Test Reactor (ATR) is a prime INEEL facility with national and international impact. Qualification of its irradiation facilities for the materials to be tested in the future is essential to maintaining its competitiveness. An irradiation facility in which an accurate estimate of the displacements-per-atom (dpa) in a given material is provided for specified neutron fluences is naturally preferable to a facility in which the estimate is less accurate for irradiation experiments involving that material.

This two-year LDRD investigates a state-of-the-art methodology and associated data for the computation of dpa for irradiation in various ATR irradiation facilities. The first year tasks focused on developing and enhancing the methods for calculation of the displacement kerma cross-sections and defining "best" values from the literature for the displacement threshold energy for the many materials of interest to the U.S. Navy, NASA, and Generation-IV reactor concepts. A method for automatically folding said data with spectra and fluences received in ATR facilities will be devised, and the capability will be generalized to other DOE complex facilities. The chosen approach is similar to that embodied in recent ASTM standards. The project requires modifying the NJOY code, then repeatedly using it on the various materials. Currently the folding is performed via spreadsheets. Later, a code will be devised.

Technical objectives for fiscal year 2003:

- Modify NJOY to use the NRT model, enable $E_d$ changes, and allow different primary-knock-on-atom (PKA) from background.
- Apply code to Mo and SiC, testing against Si and GaAs and Fe, for which published data are available, and finding correct or best values for $E_d$.
- Report and publish findings.

Atomic displacements are accepted as the principal underlying radiation damage mechanism for energetic neutron radiation in many materials. It is believed that accumulated (and remaining/permanent) displacements at the microscopic level (radiation damage) form the basis for the changes in material properties at the macroscopic level (radiation effects). Therefore, it is important to quantify the amount of displacements caused to such materials in the radiation field corresponding to their intended use. Such a characterization is seldom possible, and it is common practice to conduct accelerated irradiation tests in which a comparable, albeit preferably much stronger, irradiation field is used. Theory is then used to correlate the observable experimental effects to the expected behavior in the actual, intended operational field. If it were accepted that the total number of accumulated displacements determines the effect in the material, then dpa would provide a means for correlating damage in a given experimental testing field to damage in the operational field. It follows that a reliable method for ascertaining the number of displacements is highly desirable for all possible irradiation fields. In the foregoing statements, it is implicitly assumed that the same dpa number results in the same overall remaining damage configuration, regardless of field. (Departures from this assumption – because of rate effects, temperature effects, displacement damage cluster size effects, etc. – are valid concerns and are currently areas of further advanced research.)

The rational calculation of dpa requires the availability of displacement kerma cross-sections for the materials of interest. The displacement kerma cross-section has been a useful tool in calculating dpa because it enables the integration of the energy-dependent response of the material to the neutron radiation environment. The NJOY99 code is widely used for nuclear data processing. It operates on evaluated cross-section data and transforms them into pointwise or groupwise cross-sections suitable for use in other nuclear analysis codes. Functionality is available to reconstruct and Doppler-broaden resonances, construct kerma data, and produce a variety of output formats. The HEATR module within NJOY99 provides the facility for computing displacement kerma cross-sections. The displacement kerma cross-section is the product of the reaction cross-section and the damage energy resulting from said reaction summed over all reactions.

The damage energy is calculated by determining the emitted particles from the reaction, calculating the energy for each emitted particle, and then computing the fraction of this energy available to cause displacements in the lattice. This latter computation uses the Robinson version of the

Lindhard partition function for each emitted particle. The Lindhard partition function is essentially a damage efficiency, describing the fraction of the particle energy available to cause displacement damage in the lattice. It accounts for the effects of the differences in recoil particle and lattice atom electronic charges and masses on the damage energy. Conservation of energy for the reaction is maintained by forcing the emitted particles to carry off the energy remaining after subtracting off the recoil, or PKA, nucleus kinetic energy from the energy available for the reaction.

The modified Kinchin-Pease model of displacement damage, also referred to as the NRT model, is a widely accepted method for calculating damage in materials, especially metals. The model was originally formulated as a way to provide an expression for the number of displacements caused by a particle with damage energy E; however, it may be easily recast to provide an expression for the damage energy. When conforming to the NRT model, the equation for the damage energy is given by:

$$E = \begin{cases} 0, & E < E_d \\ 2.5E_d, & E_d < E < 2.5E_d \\ E, & E \geq 2.5E_d \end{cases}$$

where $E_d$ is the average threshold energy for displacement.

The HEATR module of the NJOY99 code was modified to include the NRT damage model. Additional modifications were made to account more accurately for the kinematics of multiple particle emission reactions. The partition of the reaction energy between the PKA and emitted particles is determined by the kinematics of the particle emission. For single particle emission, or charged particle emission following emission of one or more neutrons, the kinematics equations are easily solved. However, for multiple charged particle emissions, the equations are undetermined, and a closed form solution is not possible without additional information. To approximate this, a two-stage process was used. First, the PKA energy was calculated by solving the kinematics equations for the emission of a "lump" consisting of all the emitted charged particles. The remaining energy from the reaction was assigned to the "lump," which instantaneously decays into its constituents. The "lump" energy is divided amongst the emitted particles in inverse proportion to the particle masses, while maintaining the fundamental kinematic ratios (e.g., a particle of mass two will carry off twice as much energy as a particle of mass four). Numerical experiments have shown that this approximation will introduce errors of no more than 1-2% in the damage energy calculation.

This energy partition model is applied only to reactions that do not have a detailed energy-angle description of particle emission (File 6) in the ENDF neutron reaction data. All allowed reaction types emitting secondary charged particles were modeled by this method. An additional option flag was added to the HEATR user input to allow the user to either bypass or invoke the NRT model. Also, two other new input parameters enable the user to make the distinction between recoiling and lattice nuclei in the Lindhard partition function, thus more accurately modeling damage in non-monatomic solids.

The modified code was used to calculate displacement kerma cross-sections for Fe, Si, and GaAs, for which well-established standard data are available as verification cases. Additional calculations were performed for more recent Si cross-section data, SiC and graphite. These materials have well-established values for the $E_d$. Such values are not well known for Mo, ZrC, and other materials. To account for this, bounding values were chosen, and calculations were performed to provide interpolation tables for the displacement kerma cross-sections. These calculations will be refined as better $E_d$ values become available.

To determine the "best" values for $E_d$ for the materials of interest, a comprehensive literature search was launched to find published experimental or calculated values for Mo, ZrC, $UO_2$, $PuO_2$, $UC_2$, W, Ta, and Nb. This literature search will continue well into the second year of the project, as the literature in this field is vast. The results of this search will be collected, tabulated, and published as an INEEL external report. To supplement this, exploration of methods for calculating $E_d$ values from first principles has begun.

The results of this LDRD to date have been accepted for presentation at the GLOBAL 2003 embedded topical meeting at the ANS Winter Meeting in New Orleans (November 2003). A full-

length paper was included in the meeting proceedings. Submission of several journal articles is planned and work on these will continue in the second year of the project.

The tasks for the final year of the project will build upon these foundations. The literature search for suitable $E_d$ values will continue, with the goal of either finding well-established values for the materials of interest, or indicating a need for continued calculation of $E_d$ values from first principles. Calculation of $E_d$ from first principles will be performed as necessary. Refinement of the displacement kerma cross-section calculations for Mo, ZrC, $UO_2$, $PuO_2$, $UC_2$, W, Ta, and Nb will be carried out, as better $E_d$ values become available. A code will be written to fold multigroup neutron spectra with displacement kerma cross-sections to compute dpa. This code will include methods to correctly interpolate the neutron spectrum onto the same energy grid as the displacement kerma cross-sections. Additional conference presentations and journal articles will be published, as well as external reports on the literature search results.

# Energy Efficient Building Simulation and Technologies

*William D. Richins, Thomas K. Larson, Jeb E. Blakely*

***Integrating energy efficiency into the building envelope***

NE114

Conditioning air is the single largest energy cost in most buildings. This LDRD investigates whole-building integration of energy efficiency and air infiltration in residential housing. New technologies to detect air infiltration, products that reduce energy demands, and methods to evaluate energy usage were developed and/or tested using manufactured homes as proof-of-principle. Two homes were instrumented to measure continuous energy usage and air infiltration with respect to environmental conditions. Initial tests on these homes included tracer gas monitoring, blower door fans, duct blaster leakage tests, and infrared video scans. INEEL engineers also monitored the energy benefits of a prototype ground source cooling loop installed in trenches for an off-grid home. These data were used to evaluate energy use, calibrate a new air infiltration monitoring device, identify design and material improvements, and quantify the benefits of new transpired solar wall and ground source cooling systems for residential housing. The results of this project will support design and inspection guidelines and provide datasets useful for energy analysis and air infiltration computer code verification.

Technical objectives for fiscal year 2003:

- Investigate new air infiltration evaluation technologies.
- Develop expertise in monitoring building air infiltration.
- Develop, verify, and/or improve simulation software for energy efficiency evaluation.
- Apply and test the above technologies.
- Evaluate renewable technologies and new building products.

Whole building integration of energy efficiency and air infiltration in residential housing was investigated in this LDRD. New technologies to detect infiltration and calibrate simulation tools, and products that reduce energy demands were developed/investigated and tested. During 2001-2003, single- and double-section manufactured homes were instrumented to measure continuous energy usage and air infiltration with respect to the environmental conditions of a windy cold dry climate. The test site near Arlington, Wyoming, is ideal for testing the energy (and structural) performance of manufactured housing due to the naturally occurring high winds and temperature extremes (+35º to -35ºC).

Tests conducted by the investigators included tracer gas monitoring, pressurized leakage tests, and infrared video scans. Extensive arrays of instrumentation for calculating thermal efficiency of the homes were designed and installed. Thermocouple arrays were placed to measure vertical temperature profiles in various locations in the homes. At each location, the air temperature in the crawl space, belly pan, near-floor, room center, ceiling, and attic were monitored. Additional temperature measurements were located at the furnace thermostat and return air plenum, heater vents, combustion air inlet, and flue gas exit. Electrical power consumption and propane flow completed the measurements required for monitoring thermal efficiency.

INEEL and Solar Unlimited Inc. engineers (July 2003-Sept. 2003) monitored the energy benefits of a prototype ground source cooling loop installed in trenches for an off-grid home near Cedar City, Utah. Water was pumped through 12.7 mm (1/2”) diameter PEX-type tubing then passed through a heat exchanger installed in the furnace fan intake duct. Thermocouples were used to measure temperature of the ground at several locations, water circulating in the loop, air in the ducts, and the house interior. Other instrumentation monitored weather conditions, cooling loop pressure, and the electrical current required to operate the system. Controls for the cooling loop system were completely manual.

An automated air infiltration sensor based on $CO_2$ concentration decay rates was developed and shown to be an effective method to measure air infiltration in windy climates. Test results indicate that adequate mixing within the building is critical to achieve high quality and consistent results. Air infiltration tests using $CO_2$ decay rates show a near linear correlation between air changes per hour and wind speed.

The energy benefits of supplementing space heating with a transpired solar panel system were investigated. When the outside air temperature was above about -5ºC and the transpired solar collector was exposed to sunlight, the system provided a significant percentage of the energy required to heat the home — up to 40% when the outside air temperature was about +10ºC. An efficient

transpired solar panel installation in a new manufactured home might also duct warm air directly into the air plenum of the furnace for pre-heating and to meet ventilation requirements to take advantage of air that is warm but not warm enough to comfortably discharge into the living space. A control system would be required to more efficiently handle the airflow either directly into the home or to the furnace plenum.

An EnergyPlus model of a double-section manufactured home was developed. Calculated interior home temperatures compared well with measured values. While some modeling issues exist, the model can now be used to simulate the energy benefits of better insulation, a more efficient furnace system, improved windows, etc.

Analyses of the energy benefits available from the ground source cooling system are still underway. The system was installed during the hot summer months resulting in rather warm ground temperatures (68° to 70°F). The ground temperatures are expected to stabilize at a significantly lower temperature (~60°F) after the trench has been filled in for several months.

The following figures are representative of the project research results and test hardware.

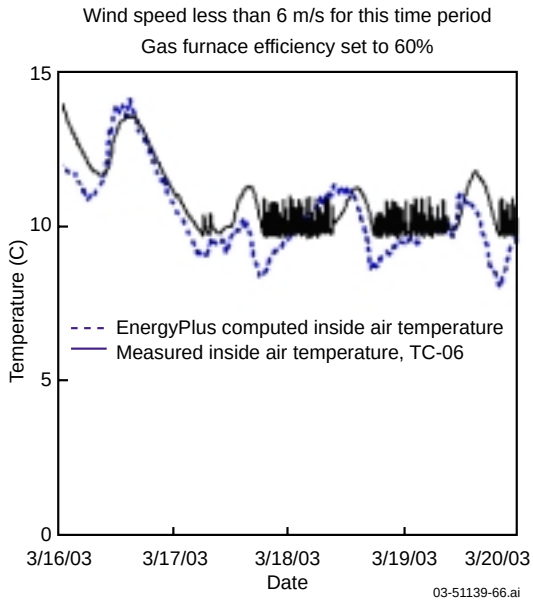


*FIGURE 1. EnergyPlus (DOE software) computed inside air temperature with furnace efficiency of 60% and measured inside air temperature as a function of time.*

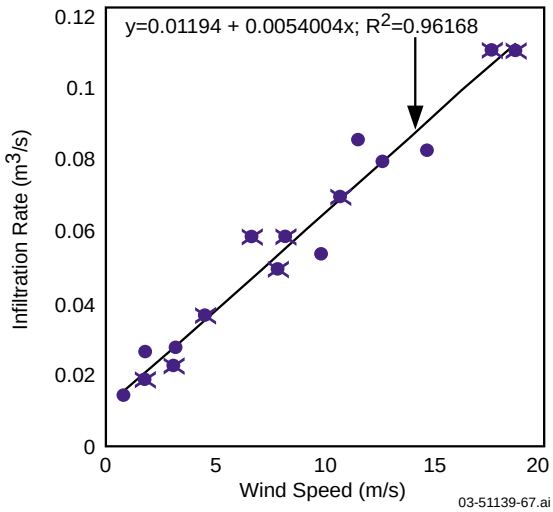


*FIGURE 2. Infiltration rate data and linear regression as a function of wind speed for double-section manufactured home.*

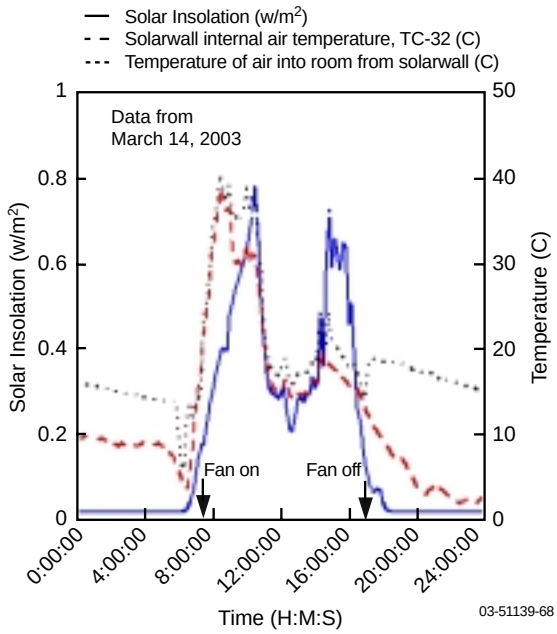


*FIGURE 3. Comparison of transpired solar panel internal air and exhaust temperatures and solar insulation.*

PN04-0004-61

*FIGURE 4. Ground source loop cooling system, including INEEL hardware, Cedar City, Ut.*

The expertise in EnergyPlus modeling gained through this project has attracted DOE and private interest to assist with energy modeling for Yellowstone National Park Service employee housing in Gardner, Montana. The Park Service approached INEEL for technical assistance on this project with the goal of becoming the first LEED™ certified residential housing in the National Park Service. In April 2003, the investigators also visited solar energy researchers at National Renewable Energy Laboratory (NREL), Golden, CO, to discuss joint proposal opportunities.

A proposal resulting from this LDRD has been submitted to the State Technologies Advancement Collaborative: "Controlled Low-Energy Heating and Cooling of Residential Housing." The project would integrate and prototype control systems for transpired solar roof/wall panels and ground source cooling/heating systems designed to provide low-energy heating and cooling for residential housing.

In addition, this LDRD benefits DOE and INEEL buildings programs and operations by providing better measurement and modeling of building airflow. An Intellectual Property review is under-way for Invention Disclosure Record "B-279 Automated tracer gas method to measure air infiltration" to investigate the potential of a device for monitoring air infiltration.

# Friction Stir Welding of Lightweight Materials

*Herschel B. Smartt, Denis E. Clark*

***Solid state welding of difficult metals and metal combinations***

NE111

Friction Stir Welding (FSW) is a relatively new welding process that joins metals by mechanically stirring them together at elevated temperatures, but without melting. This emerging solid-state process holds promise to dramatically increase the ability to weld difficult material combinations needed in "bi-material" structures for automotive and other applications.

The purpose of this LDRD is to research a computer-controlled friction-welding machine and develop advanced process control algorithms to support experimental studies of FSW process physics.

Technical objectives for fiscal year 2003:

- Complete development of an experimental FSW machine.
- Conduct experimental studies to develop a fundamental scientific understanding of heat and mass transfer in the FSW.
- Develop understanding of relationships between process control parameters and weld quality to support process optimization.
- Incorporate feedback control of FSW machine functions.
- Study fundamental issues involved in joining of dissimilar metals by FSW process.
- Establish collaborative working relationship with Vanderbilt University.

This research has been coordinated with ongoing Friction Stir Welding (FSW) work at Vanderbilt University under the direction of Professor George Cook. The investigators began working with Cook and his graduate students using tool designs and welding parameters initially developed at Vanderbilt. In addition, data acquisition and visualization software was developed at the INEEL that allowed the easy visualization of welding parameters immediately after a weld, and the comparison of two or more welds.

As part of this year's research, an experimental FSW machine was built (Fig. 1). The machine includes an infrared (IR) camera for measuring the temperature distributions in both the weldment and tool, and a multi-axis dynamometer for measuring principle forces and tool torque. Control of the machine is based on distributed control architecture with self-configuring, modular software. Experimental studies were conducted to identify principle forces and torque as a function of tool rotation speed and welding travel speed. This work also included experimental studies to identify causes of wormholes in weld roots. The effects of both process operating parameters and tool design on wormholes were studied, leading to the design of a threaded pin tool. Finally, test welds were made to study joining of steel to aluminum and to investigate the phenomena of chaotic mixing in the process.

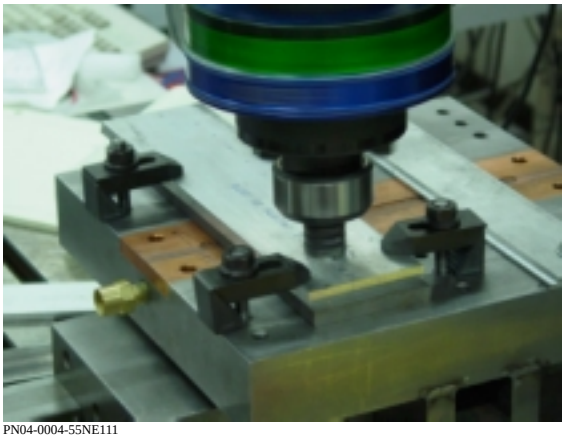

PN04-0004-55NE111

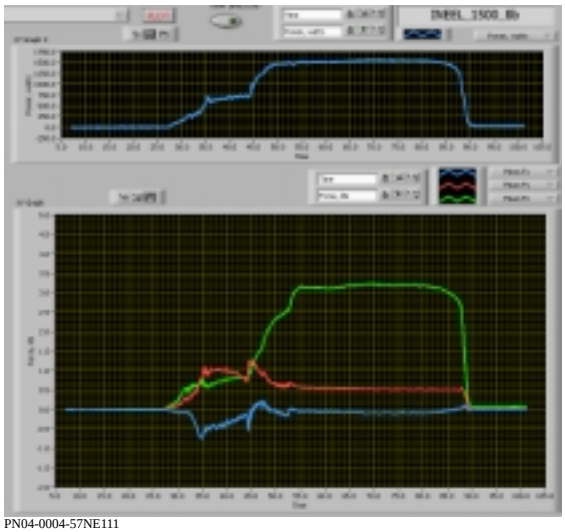

PN04-0004-57NE111

*FIGURE 1. Friction stir weld being made on the INEEL FSW machine (left). Associated forces and power measured by the dynamometer (right).*

Figure 2 shows the cross-section of a weld in a 6061-T651 aluminum plate, made with the "small Vanderbilt tool," with a smooth pin about 4 mm in diameter. This weld was made approximately in the middle of a matrix that included spindle speeds ranging from 1000 to 3000 RPM and travel speeds ranging from 4 inches to 32 inches per minute.

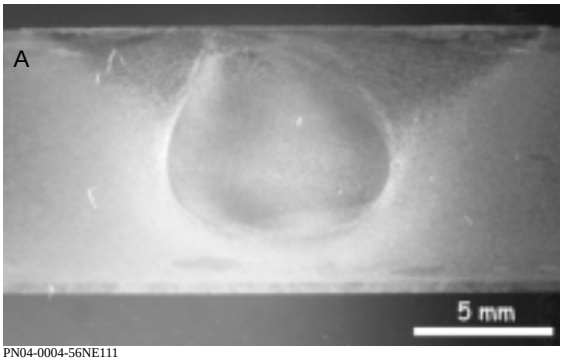


PN04-0004-56NE111

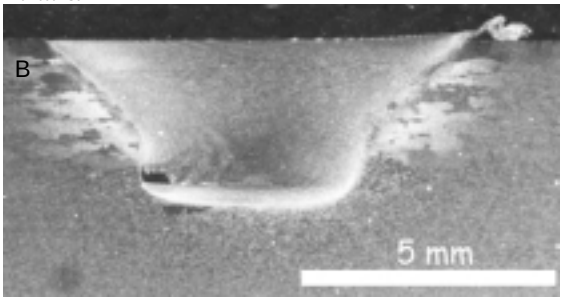


PN04-0004-59NE111

*FIGURE 2 A) Friction stir weld being made with smooth pin tool showing characteristic wormhole defect in root. B) Friction stir weld being made with threaded pin tool showing elimination of wormhole defect.*

The hole (lower left corner of the weld in Figure 2a) occurs on the side where the tangential rotational tool motion is in the same direction as the tool travel. The wormhole cavity extends the length of the weld, resulting from a net material movement from lower left to upper right in the photomicrograph, although the actual material flow path circulates a number of times in a widening upward helix and typically starts at the beginning of the weld as the pin enters the material. This hole was nearly, but not quite, eliminated with slower travel speeds and higher spindle speeds. It also shifted in shape and location under some parameters (lower spindle speeds, higher travel speeds), forming a vertical feature that, in extreme cases, splits the weld from top to bottom and, in other cases (higher spindle speeds, lower travel speeds), forms a horizontal feature near the bottom of the weld. Smooth tools of various sizes and shapes gave similar results.

A threaded tool, with a pin ~ 6 mm in diameter and extending ~ 6.4 mm into the material during welding, also was developed to influence the direction of material flow in the weld. A weld made with this tool at 1500 RPM and 8 inches per minute travel speed is shown in Figure 2b. The weld cross-section shows that this tool was successful in eliminating the wormhole defect experienced with smooth pin tools. The bulbous shape of the weld zone is due to material moving outward after being forced downward by the threads on the tool pin.

The control system for the FSW machine builds on earlier work performed on modular, distributed control software. In this LDRD, a capability for the machine to self-configure its operation without changing the source code was added. This capability has many applications, especially in flexible manufacturing and remote systems, and enables an operator to change the functional characteristics of a machine without reprogramming.

Portions of this work resulted in a joint publication with Vanderbilt ("Considerations for Robotic FSW," June 2003). A second joint work for publication has been submitted to the journal *Industrial Robot*.

This LDRD research is providing a basis for future development and improvement of a joining process for use in critical "bi-material" structures by U.S. industry and the DOE complex. The investigators have begun discussions with the Emerging Technologies Department at U. S. Army Tank Automotive Research Development and Engineering Center (TARDEC) on welding of armor components.

A DOE proposal also is in review on friction welding of waste package materials. This work would require addition of a new fixture to the FSW machine, but would rely on the dynamometer and IR camera to obtain experimental results. Work on the self-configuring, modular control systems is being extended in FY04 with application of this approach to software design for control of the Yucca Mountain Waste Package Closure System. A proposal to NASA on a radically new method for obtaining self-configuration in intelligent machines also has resulted from this research.

# Genetic Control of Straw Stem Ultrastructure that Affects the Biomechanics of Stem Separation

*Eric D. Steffler, J. Richard Hess and Thomas H. Ulrich*

***A genetic approach to bioproducts processing***

CE108

As part of the nation's energy strategy, cellulosic crops are expected to become the feedstock of choice for biomass-derived fuels and chemicals. A limiting factor for their use, however, has been the lack of equipment and methods to harvest, store, and fractionate biomass for subsequent conversion processes. Harvesting improvements can directly address economic and environmental issues for bioproducts processing of higher value cellulosic stem while leaving behind the remaining residue to supply soil organic matter and maintain soil nutrient levels.

This LDRD is researching practical testing tools and identifying ultrastructural phenotypic and molecular markers that will be useful for selecting genotypes with improved stem component separation. It is hypothesized that the biomechanical properties that differentiate the stem tissues of different genotypes result from functional gene expression that can be identified, characterized, and used to build selection tools for breeding new varieties with improved stem separation characteristics. These new cereal genotypes will be bred to withstand field stresses, but succumb to harvesting stresses.

Technical objectives for fiscal year 2003:

- Develop and apply standard mechanical testing procedures to several pre-selected varieties of wheat and barley stems.
- Compare and contrast the respective mechanical properties of each stem type.
- Detect mechanical differences between several types of wheat and barley, and numerically model these differences.

To develop proper testing procedures for bio-based materials such as wheat and barley it was necessary to treat the structures as complex composites and utilize fundamental evaluative techniques established for engineered composite systems. The suite of tests suitable for determining the biomechanical properties of wheat and barley are axial tension, axial compression, transverse tension, 3-point bend, 4-point bend, lateral shear, and axial torsion tests. These tests can identify failure modes and locations that will eventually point to plant tissues and their resulting composite structures that affect the stem's biomechanical properties. The biomechanical characteristics can then be related to the plant's tissue structure by comparing stem images and test data for several different varieties of wheat and barley.

To illustrate the relationship between stem mechanics and the stem structure, as well as show the success of this project, three sets of data collected from the axial compression, 3-point bend, and 4-point bend tests are presented. These data include two varieties of wheat, Amadon and West Bred 936, and two varieties of barley, Bowman and GSO Fragile Stem. The results from the axial compression tests are shown in Figure 1a. This figure shows that the stress vs. strain relationships for the four types of stems indicate measurable differences in their mechanical behavior. These differences can certainly be attributed to the individual structure of the stems as shown in the respective cross-sectional pictures of the four varieties. These structural differences can principally be attributed to the size of the cell structures and vascular bundles that are common to all stem varieties, also shown in Figure 1a.

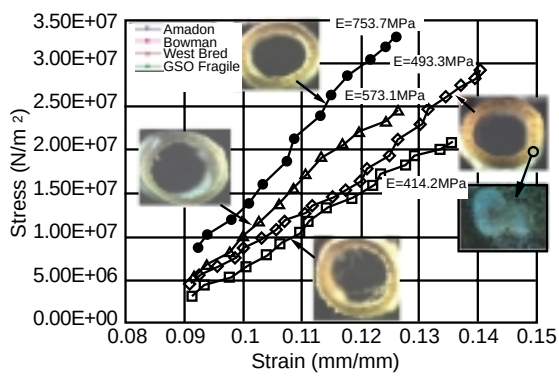


*FIGURE 1a. Stress vs. strain relationship for two varieties of wheat, Amadon and West Bred, and two varieties of barley, Bowman and GSO fragile stem.*

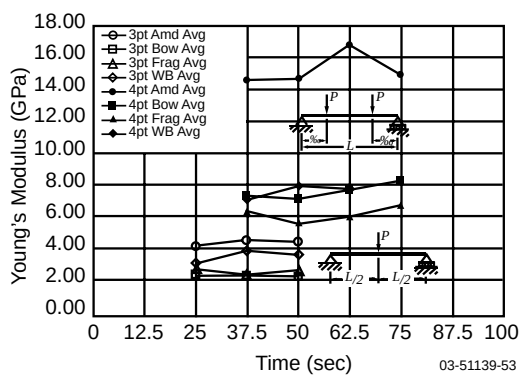


*FIGURE 1b. Change in the modulus of elasticity over time for both the 3-point and 4-point bend tests.*

Figure 1b combines the results from the 3- and 4-point bend tests. Once again, it is apparent that the modulus of elasticity is different for the separate varieties of stems tested. In addition, the modulus of elasticity is different in the bend test compared to those reported in the compression test. These results can be related to the placement of the loads and the different modes of failure inherent in the particular type of test. Both Figures 1a and 1b meet the research objective of distinguishing varying types of wheat and barley straw through comparing their mechanical properties. These results are now available for additional inclusion in numerical models and further parametric studies.

A preliminary structural analysis of an Amadon wheat stem, shown in cross-section in Figure 2a, was performed using a commercial finite element analysis (FEA) software, Abaqus 6.3. A representative geometry, which includes the main structural components of the stem, was extracted from Figure 2a and is shown in Figure 2b. Material property data was obtained both from INEEL measurements obtained as described above and published results from other researchers. The model is preliminary because a limited amount of property data was available. The linear mixture modeling approach used also assumes the wheat material is isotropic and elastic. The predicted axial stress for a stem

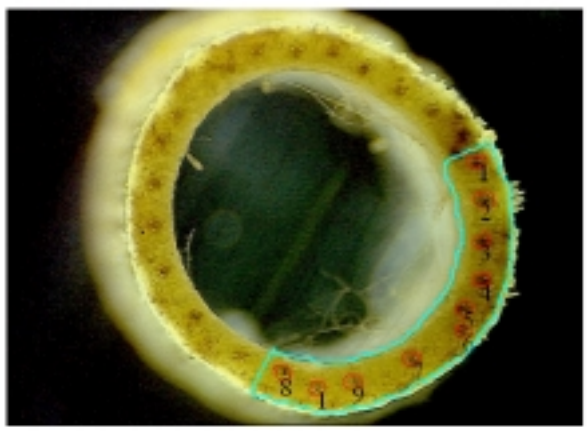

*FIGURE 2a. Wheat stem cross-section.*

03-GA51139-08

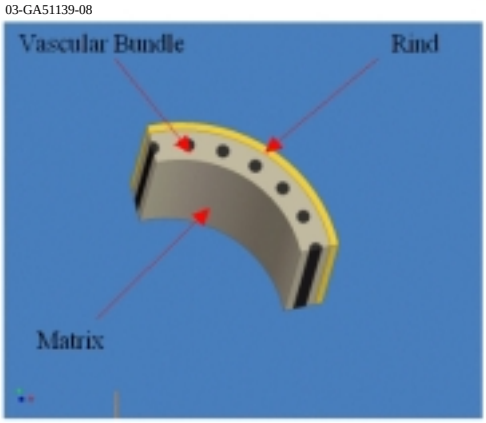


*FIGURE 2b. Wheat stem geometry.*

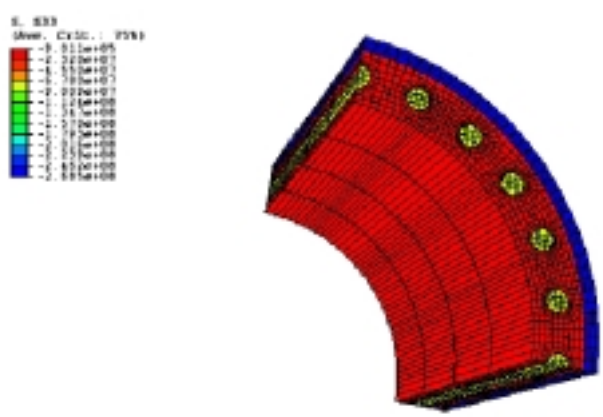

*FIGURE 2c. Wheat stem axial stress analysis [Pascal (N/m$^2$)]*

under compression, shown in Figure 2c, was compared with theoretical calculations. As expected, the rind, which has the largest modulus of elasticity, exhibits the largest compressive stress, whereas the matrix exhibits the smallest stress. Future work will use calculated results to compare with experimental measurements of mechanical behavior.

This LDRD has produced practical testing tools and identified ultrastructural features and behavior that will enable identification of the associated phenotypic and molecular markers that are required. This information, combined with validated numerical models, will be useful for selecting genotypes with optimal stem component separation attributes. This project addresses the biological issues associated with biomass harvesting and contributes to the nation's strategies for alternative energy resources.

# Laser Ultrasonic Corrosion Monitor

*Ken Telschow, Dave Hurley, Dave Cottle, Rob Schley, John Walter*

***Predicting corrosion in nuclear reactors***

NE118

The absence of real-time in-pile kinetic data continues to hinder the development of an accurate mechanistic model for predicting Zircaloy corrosion in nuclear reactors. High-resolution monitors have been developed that exploit the dependence of ultrasonic wave propagation properties to determine Zircaloy oxide film properties. However, a monitor of this type that can be employed in a high-radiation reactor environment is needed.

Laser ultrasonics is a totally noncontacting technology for performing ultrasonic measurements that can potentially operate in this hostile situation and resolve features such as film or coating thickness while requiring only optical access to the material surface. This LDRD project focuses on the implementation and measurement results of the laser ultrasonic approach for real-time material mechanical property/corrosion monitoring in high radiation environments.

Technical objectives for fiscal year 2003:

- Investigate detectability of different types of corrosion films (dry oxidation, wet high pressure oxidation, thickness dependence, film morphology, etc.).
- Investigate technological approaches most appropriate for Zircaloy films in situ in a hot water autoclave or other simulation environment (surface wave dispersion, single point pulse echo, picosecond acoustic).
- Install laser ultrasonic measurement equipment in the gamma tube facility at the Advanced Test Reactor (ATR) and initiate validation and test measurements.
- Determine requirements for an in situ ultrasonic corrosion monitor probe to be inserted into a hot cell or the ATR and initiate fabrication alterations necessary on existing gamma tube equipment and/or construct new equipment as needed.

This project has two major related goals: 1) determining the capability for laser ultrasonic measurements for characterizing corrosion films on Zircaloy, and 2) initiating remote measurements in a high radiation environment using techniques developed at the INEEL and elsewhere. Major advances have been made on both goals.

Several different laser acoustic methods have been explored for corrosion film measurements. One utilizes traveling surface waves and successfully measures the film thickness over an extended area. Another utilizes ultra high frequency acoustic microscopy to measure film properties at single points and over surfaces with high spatial resolution. Both of these results show that laser ultrasonics provide the capability for measuring corrosion film properties in situ using UHF laser acoustic methods, as only optical access is required.

A remote operation laser ultrasonic system for making measurements on sample materials in a high gamma radiation field at ATR was successfully developed, tested and installed. Measurements of several vibration modes have been made on a tubular sample before, during and after the movement of fuel to the vicinity of the gamma tube. The following results describe these measurements that are ongoing in the high gamma radiation field at the present time.

*Narrowband Surface Acoustic Waves (SAWs)* — Generation of narrowband SAWs was accomplished by modulating the absorbed optical energy at the sample surface using an optical interference grating. Propagation of the SAW was perpendicular to the grating axis along the sample surface with a frequency determined by the grating spacing and the SAW velocity. SAWs of different frequencies were produced through changing the separation between the interfering beams before they were combined through a cylindrical lens. The current setup is capable of producing grating spacing from ~20 μm to ~100 μm. The acoustic displacement was detected along the SAW propagation direction using a path-stabilized Michelson interferometer. Dispersion of the SAW for an oxide coating on Zircaloy results in the high frequency components of the wave arriving before the lower frequency components at the detection point. This dispersive effect increases with propagation distance. Measurements taken at different distances allow direct determination of the wave phase velocity with frequency that can be compared with predictions from elastic wave theory given the material properties and the film thickness.

The measured dispersion curve agreed with the prediction to within about 10% using the properties of Zirconium and Zirconium Oxide from the literature and the nominal film thickness as determined from weight change measurements. Although somewhat difficult to implement at more

than one surface point, this technique offers relatively high precision in determination of the average film thickness over the SAW propagation path.

*Transient Bulk Longitudinal Wave Measurement* — Capability has been established to perform laser ultrasonic measurements of longitudinal wave generation and reflection from thin corrosion films at single points. Implementation in a microscope has been accomplished providing spatial resolution of a few microns at a bandwidth greater than 1 GHz. This enables measurements with time resolution of a nanosecond or better for discriminating between echoes coming from thin film interfaces. The apparatus allows control over laser excitation and detection energy and spot size, and provides for scanning over the surface of a part to produce images of thin-film uniformity.

Initial measurements made of samples prepared with corrosion films with thickness from 0.8 µm to 36 µm show distinct effects that relate to the film's optical, thermal, dimensional, and elastic properties. Significant optical absorption of the excitation laser pulse occurred in the corrosion film, shielding the underlying metal. This was evident in the large increase in optical damage threshold observed for the samples with thicker films. Figure 1 shows the signals measured at the maximum source laser pulse intensity for films of varying thickness. The thinnest three films show sharp initial pulses that are a result of material ablation from the film. Also shown in Figure 1 is the intensity level (indicated by the amplitude of the optical pulse, Vdc) used to obtain this waveform. One can see from the figure that the thinner films ablate at significantly smaller intensity levels than the thicker films, showing that the ablation threshold is a strong function of film thickness.

Further measurements delineating the origin of this ablation effect and exploring its film thickness dependence are underway. Mechanisms for precisely controlling the excitation laser pulse energy and spot size are being installed on the microscope. In addition to acoustic parameters, optical/thermal effects of the film contribute to this film thickness dependence of the ablation threshold. These effects may significantly augment the arsenal of measurement parameters that laser ultrasonic methods provide for corrosion film property measurement.

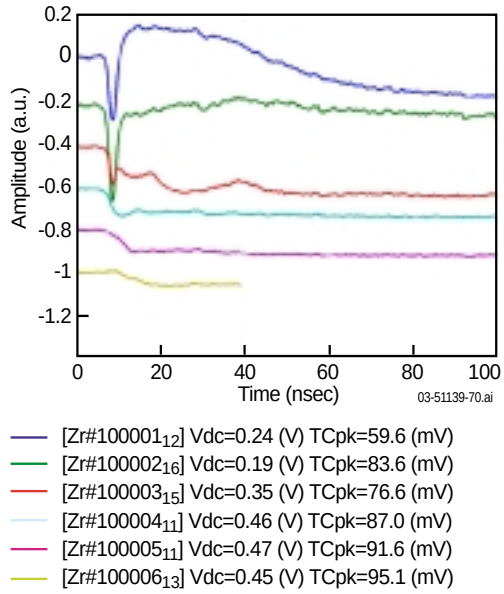


*FIGURE 1. Longitudinal wave measurements as a function of film thickness. The three thinnest films with a sharp initial leading pulse show the effects of ablation.*

*Laser Ultrasonic Measurements in the ATR Gamma Tube* — A mechanical light pipe tube was constructed with sample holder positioned in the high radiation area at the bottom of the gamma tube. Laser beams for both generation and detection of ultrasonic waves in the sample were directed into the light pipe tube from the top and traveled in a free-space manner to the bottom, approximately 30 feet from the laser equipment. A small curved mirror, near the bottom of the tube, focused the source laser beam onto the sample surface. A second parabolic mirror, also near the bottom of the tube, focused the detection laser beam onto the sample (located near the bottom of the tube) and collected the scattered light. Full positioning control of the sample and all mirror orientations were designed into the top of the light pipe tube. An interferometric detection scheme that could be used in an industrial setting was constructed using a high-speed photorefractive system to demodulate the reflected light, thereby measuring the ultrasonic displacement motion directly on the sample surface. This form of interferometer system automatically adjusts for environmental vibrations and can form interference with diffuse or multiple speckle

reflection from the rough sample surface and requires no stabilization feedback system. Provisions were made for both source and detection with contact piezoelectric transducers as well as the lasers for a redundancy on the measurement setup. Figure 2 shows measurement results of low frequency flexural modes recorded in situ before, during, and after fuel rods were placed in the vicinity around the tube.

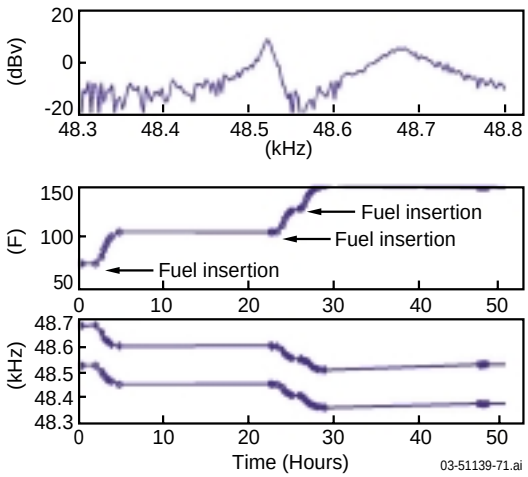


*FIGURE 2. Top: two resonant modes measured by the laser ultrasonic method in the gamma tube. Middle: temperature as a function of time showing the times fuel was inserted. Bottom: resonant mode frequencies as a function of time showing changes that follow the sample temperature.*

Resonances were recorded with signal-to-noise ratios of better than 10 using a source pulse energy of ~10 millijoules. The figure shows the resonant modes recorded and changes in their resonant frequencies as the fuel is inserted. The middle graph shows the change in temperature of the sample as a function of time. One can see that the sample temperature increases significantly each time the radiation level is increased. Correspondingly, the resonant mode frequencies decrease in a corresponding fashion. Changes in resonant mode frequency occur due to thermal expansion and material property temperature dependence. Modeling calculations of the resonant ultrasound process are underway to delineate the full impact of these observations. These results dramatically show that noncontacting optical ultrasonic measurements can be readily made in a high radiation environment.

This LDRD was performed to provide new diagnostic technology for inspection in high nuclear radiation environments. The results to date show that noncontact laser ultrasonic methods are promising for investigation of corrosion processes in situ. Further work shall delineate capability for in situ measurements and demonstrate real-time measurements during the corrosion process. Strong collaboration has been developed between researchers at the INEEL and customers of the ATR. Efforts are underway to obtain direct funding through DOE-NE and/or other agencies to fully implement this technology into the core area of ATR and at hot cells at other facilities.

# Hollow Waveguide Laser Ultrasonics

*Ken Telschow, Vance Deason, Dave Cottle, Rob Schley*

***Improving delivery and recovery systems in challenging environments***

NE126

Hollow waveguides greatly reduce the exposure of critical waveguide components to radiation effects and still provide flexible confinement of the electromagnetic energy for the noncontacting ultrasonic measurement process. The use of long electromagnetic wavelengths in the near infrared region and beyond offers reduced sensitivity to radiation effects of the materials used in waveguides as the longer wavelengths average over large regions containing many defects.

This LDRD investigates the use of hollow waveguides and long optical wavelengths to provide improved, mechanically flexible delivery and recovery systems for laser ultrasonic material diagnostics in high radiation environments. This three-year project is investigating the limitations of waveguide materials and manufactured hollow fibers, making laboratory measurements of the performance of suitable candidates for generating and detecting ultrasonic waves and implementing a hollow waveguide measurement in situ in a "hot-cell" or the gamma tube at the Advanced Test Reactor (ATR).

Technical objectives for fiscal year 2003:

- Survey approaches for using wavelengths in the visible, NIR, IR, THz and microwave with hollow waveguides for delivery and recovery of electromagnetic energy to a specimen for generation and detection of ultrasound.
- Investigate modeling approaches for suitable hollow waveguide modes in commercially available hollow waveguides to determine delivery and recovery properties for laser ultrasonic applications.
- Select one or two most feasible approaches for experimental and theoretical verification.
- Determine available waveguide manufacturing resources (commercial and/or specialty fabrication subcontract), and procure waveguides.
- Begin experimental determination of attenuation of delivery (laser generation) pulses to a specimen through the waveguide, investigating the effects of bore radius and bends.
- Begin experimental determination of the limitations of recovery (laser detection) beams to a specimen through the waveguide, investigating the affects of bore radius and bends.

A survey of the hollow waveguide literature has revealed only a relatively small number of researchers involved with this technology. Research has largely been limited to long wavelengths in the near infrared regions greater than 1µm. Commercial use has evolved for the 10.6 µm $CO_2$ laser systems as energy delivery units for drilling in the dental industry. Through assembly of this bibliography, the investigators now have detailed research results concerning the optical mode structure, propagation characteristics, and launch and retrieval requirements for successful use of hollow waveguides. This information is very helpful for modeling characterization of hollow waveguide properties for laser ultrasonic applications. In addition, information on gamma and neutron radiation effects on solid optical fibers has been assembled. Reports in the literature and from NASA tests of radiation damage to optical fibers indicate that substantial darkening occurs over time in conventional fibers, but the damage accumulation is highly dependent on the radiation type and dose. These data provide a useful background from which to judge the efficacy of hollow waveguides for radiation environments.

Two commercial companies (Polymicro Technologies, LLC of Phoenix, AZ, and Global Fiber-Optics Corp. of Mississauga, Ontario) have been found as sources for hollow silica fibers. Polymicro sent three samples (two hollow silica waveguides and one radiation-hardened fiber optic) for evaluation on this project. The hollow waveguides available commercially are only 3-10 meters long, due to limitations of their fiber draw tower, and relatively expensive. Transmission loss increases significantly at short wavelengths due to absorption, and hollow waveguides with different internal coatings are not currently available. Polymicro does not generally make custom hollow waveguides, but information was obtained on solid optical fibers that can be used in high gamma fields approximately 20 to 100 hours at the $5x10^6$ Rad/hr ATR Gamma tube dosage. Liquid-filled hollow waveguides also are being investigated and a company has been contacted that produces various index of refraction fluids (Cargille Laboratories, Inc).

Photonic Crystal Fibers (PCF) waveguides consist of arrays of air-filled holes/tubes in glass or silica matrices and offer some interesting properties. Several recent reports of their development have appeared in the literature. These may permit the

transmission of single transverse mode laser beams in an air core. Information on these new types of waveguides is being collected to see if this will offer any advantages in the high radiation environment. Contacts have been made with researchers fabricating their own hollow fibers and future collaboration is being setup for characterization of these samples at the INEEL for laser ultrasonic purposes. In particular, researchers at MIT are producing a multi-layer cladding hollow core fiber; however, nothing is known about its radiation resistance. The fiber is fabricated by rolling a stack of alternating index sheets into a tube, fusing them and then drawing them into a fiber form. The walls exhibit an index of refraction profile that resembles a quarter wave stack used for highly reflective surface coatings. MIT would be amenable to supplying samples for radiation testing. Currently these are rather short, due to the limitations of the MIT fiber draw tower where they are fabricated. Two other hollow waveguide manufacturers have been identified that produce PCF hollow waveguides commercially, BlazePhotonics Ltd., Bath, U.K., and Crystal Fibre, Denmark. Samples of these PCFs have been received and are under evaluation.

*Laser Ultrasonic Measurement in Hollow Waveguides* — Capabilities for performing optical measurement of the transmission at various wavelengths from 532 nm to 10.6 µm are being developed at the INEEL. Of particular concern is the region around 1µm, as that is the most efficient region for laser ultrasonic use with conventional laser systems. A complete laser ultrasonic system employing the hollow waveguides for laser light delivery has been constructed. Optical transmittance measurements have been performed on a 500 µm diameter core waveguide from Polymicro as a function of bending. Figure 1 shows the transmission loss as a function of bending angle for light traversing down and back through a 25 cm long specimen. Significant loss was found, although this is extreme bending and longer fibers with a larger bending radius and smaller bending angles will exhibit significantly reduced transmission loss for the whole fiber system. Very high intensity pulsed lasers are used for ultrasonic excitation that should be able to easily make up for this type of loss. Also, for laser ultrasonic detection, large power (~10 watt) single frequency lasers are available for delivery through the fiber. Therefore,

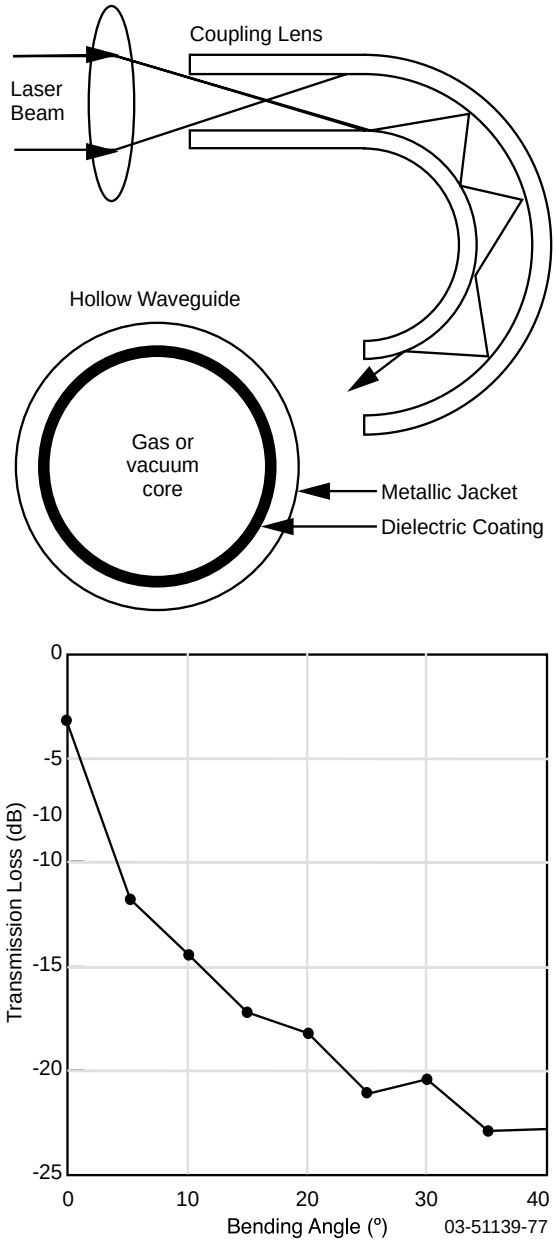


*FIGURE 1. Schematic of a hollow waveguide fiber showing multiple reflections of light traveling down a fiber. The insert shows the measured transmission loss for a 25 cm length (500 µm core) fiber as a function of bending angle.*

it is anticipated that there will be little difficulty in using fibers that exhibit transmission losses like those measured.

Transmission of light down the hollow waveguide for excitation is not very demanding. However, detection involves performing interfer-

ometry to demodulate the small optical phase shifts produced by the ultrasonic motion of the sample surface. While traversing the fiber, the light undergoes multiple reflections from curved surfaces that will significantly alter the optical wavefront of the light that comes back to the interferometer. This could pose a problem for some interferometer systems that use external reference beams for the interference. Interferometer systems based on using the photorefractive effect in nonlinear optical materials offer a very effective way to eliminate this wavefront distortion problem.

Figure 2 shows an interferometer system using 1064 nm light from a single frequency laser and GaAs as the photorefractive material. Interference within the GaAs produces a reference beam diffracted along the signal beam that has exactly the same wavefront as the signal beam. This is ideal for the final interference that occurs at the photodetector and produces a very robust interferometer that can easily demodulate complicated wavefronts from samples with rough surfaces and should take care of any additional distortion from multiple reflections within the hollow waveguide. Experimental measurements were performed to test this hypothesis. The insert of Figure 2 shows the results. Light along the signal leg of the interferometer was passed down and back through the hollow waveguide. Optical phase modulations were added to the light through electro-optic modulators in both the signal and reference legs of the interferometer. The insert shows that essentially the same signal was obtained for identical modulations along either the signal or reference legs. The sign reversal is because the phase difference between the two legs is what is measured in an interferometer. This test proves that laser ultrasonic measurements through a hollow waveguide pose no additional problems than measurements through free space if an adaptable photorefractive interferometer is used for demodulation.

Plans for next year include duplicating the Resonant Ultrasound Spectroscopy measurement system developed for the Gamma Tube at ATR using hollow waveguides. If these tests are successful, a new approach will be available for testing in the Gamma Tube that can be retrofitted to the existing Gamma

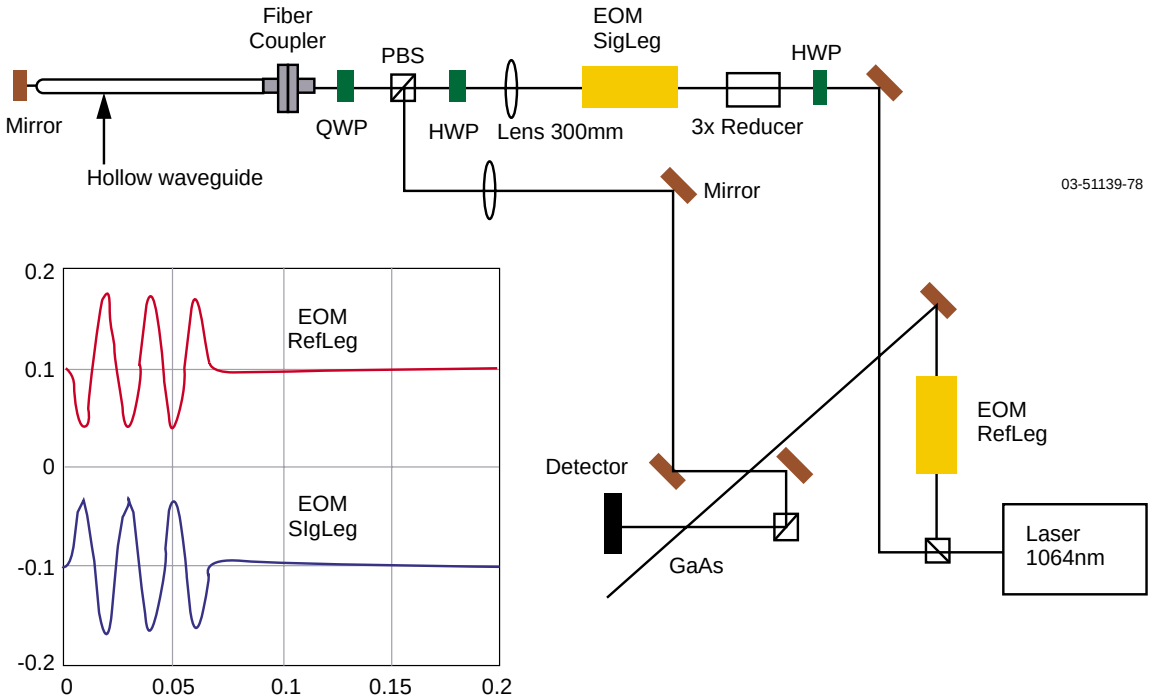


*FIGURE 2. Schematic layout for the laser ultrasonic detection measurements. The insert shows the simulated ultrasonic signals measured along either the signal or the reference legs of the interferometer, and illustrates the ability of this system to demodulate distorted wavefronts for the beam traversing down and back through the hollow waveguide.*

Tube probe. In this manner, actual measurements under high gamma radiation conditions shall be performed within a system that can be entirely enclosed (laser Class I) that will make future measurements simpler, more robust and safer.

This LDRD provides new diagnostic technology for inspection in high nuclear radiation environments. The results to date show that noncontact laser ultrasonic methods are promising for investigation of corrosion processes in situ. Further work shall delineate capability for in-situ measurements and demonstrate real-time measurements during the irradiation process. Strong collaboration has been developed between researchers at the INEEL and customers of the ATR. Efforts are underway to fully implement this technology into the core area of ATR and at hot cells at other facilities.

# Pretreatment Technologies for Cellulosic Biomass

*David N. Thompson*

***Improving use of wheat straw for industry***

CE112

Nearly one billion tons of usable lignocellulosic residues go to waste in the United States each year. This represents a significant and valuable renewable biomass resource. However, advancements must be made in feedstock harvest/preprocessing and enzymatic hydrolysis rates and yields before the complete biorefinery will be economically viable.

This LDRD addresses wheat straw composition and quality issues in wet storage systems, which can improve use of wheat straw as a source of fermentable sugars for industrial use.

Baling is typically used to collect and store agricultural residues. A biomass hydrolysis plant producing fermentable sugars from the biomass would be required to maintain a significant year-round feedstock inventory on site. However, substantial polysaccharide degradation occurs during bale storage due to aerobic microbial degradation even at low moisture contents. Anaerobic wet storage, or ensiling, has been used for many years in the non-wood pulping industry to stabilize lignocellulosic sugar cane residue (bagasse) during storage. An added benefit is that the wet bagasse compacts easily, reducing feedstock density. Ensiling techniques can potentially be adapted to stabilize these senescent feedstocks during storage. This research can potentially lead to the adaptation of ensiling to wheat straw and corn stover storage for the stabilization of polysaccharide compositions and sugar yields during long-term storage at or for hydrolysis plants.

Technical objectives for fiscal year 2003:

- Characterize the effects of wet storage of corn stover and straw on polysaccharide, lignin, and ash compositions.
- Determine whether corn stover and straw compositions can be stabilized during wet storage via ensiling.
- Determine the effect of wet storage and/or ensilage on the effectiveness of dilute acid pretreatment and enzymatic digestibility using cellulase enzymes.

Agricultural forage crops such as hay and residues such as cereal straws are typically baled and stored either at the side of the field (tarped or uncovered) or in covered storage (pole barns). Depending on the feedstock and location, typical collection, baling, storage, and transportation costs can range from $30 to $45/dry ton. Bulk storage methods (i.e., piles) that can stably store the biomass for a year or more would be helpful in maintaining a consistent feedstock supply for a biorefinery. For wet processes such as hydrolysis and fermentation, wet storage of biomass could be advantageous since it might eliminate the extra cost of drying and densification, and could result in a delivered cost of less than $30/dry ton.

Wet storage under anaerobic conditions has been successfully used to store sugar cane bagasse for non-wood pulping for over 50 years, and has been suggested as a storage method to stably maintain bagasse and other agricultural residues for hydrolysis plants. This storage method, which is essentially an ensiling or pickling system, preserves the lignocellulose by limiting oxygen supply to microorganisms in the biomass and lowering the pH of the water in the biomass to levels that are inhospitable to cellulose-degrading microorganisms. Given the difficulties in economically maintaining a consistent year-round source of corn stover and wheat straw for hydrolysis plants in non-arid regions, adapting ensiling to storage of these feedstocks seems necessary. However, there are many technical and logistical issues connected with wet feedstock that have yet to be considered or tested.

This project began testing in 2003 by conducting ensiling requirement tests for senescent wheat straw harvested in Idaho. Bench-scale ensiling assessments were conducted under controlled conditions with funding for the project commencing in February 2003. The purpose of these ensiling tests was to determine whether sugar, assimilable nitrogen, or inoculum additions would be necessary to successfully ensile wheat straw. The tests were designed to bracket the necessary starting conditions with respect to moisture content, nitrogen content, and carbon/nitrogen ratio (C/N) for wheat straw having an added inoculum of a fermentative bacterium (e.g., *Lactobacillus plantarum*).

An Independent Hazard Review was initiated in February and completed in May. A small-batch column ensiling system (60 columns) was constructed using 2” wide (ID) x 6” high glass columns. Wheat straw was obtained from Grant 4-D Farms (Rupert, Idaho) in the form of two large rectangular bales (~ 1/2 ton dry straw/bale) that had

been stored over the winter as center bales within a field-side stack. Before use, the straw bales were broken and ground in a commercial feed mill (tub grinder) to a particle size of 1/4” or less, sifted into a super-sack, and stored in covered storage at ambient temperature.

The ensiling tests were performed in the sealed glass columns, using about 20 g dry-weight of ground wheat straw in each column. The tests were performed in duplicate using a $3^3$ factorial design.

Initial moisture content was varied from 70-90% (unsaturated to over-saturated). The initial C/N ratio was varied by adding small amounts of yeast extract. An initial C/N of 30 is suggested for a robust compost heap; thus, a lower bound than C/N of 30 was used in the wet storage tests. The upper bound for C/N had no additions, i.e., about 80 for wheat straw. Molasses addition was varied from 0-39.4 mL/kg, based on requirements given in the literature for successfully ensiling sugar cane bagasse. Temperature within the pile during wet bagasse storage is optimal between 30°C and 40°C.

The tests were run at the midpoint temperature of 35°C for 82 days. Headspace oxygen was measured about every month, and biomass compositions in the top and bottom of the ensiling columns were measured initially and at the conclusion of the experiment using wet chemistry methods. The pH of the entrained liquid phase from the top and bottom of each column was measured in each column at the end of the experiment.

Liquid-phase pH results from the wheat straw ensiling tests are summarized in Figure 1. In general, ensiling occurred at many combinations of moisture, free sugars, and assimilable nitrogen, but the lowest pH values were attained in only limited cases at higher moisture content. Trends also were different at different moisture levels. At 70% moisture, if assimilable nitrogen was not added or if very high levels of assimilable nitrogen were added, ensiling (characterized by a drop in pH) did not occur. Similarly, if no free sugar was added or if very high levels of free sugar were added, ensiling did not occur. However, ensiling did occur if both nitrogen and free sugars were added at midpoint levels. At 80% moisture, ensiling did not occur when nitrogen or free sugars were not added, nor did ensiling occur when any level of nitrogen combined with high levels of free sugars was

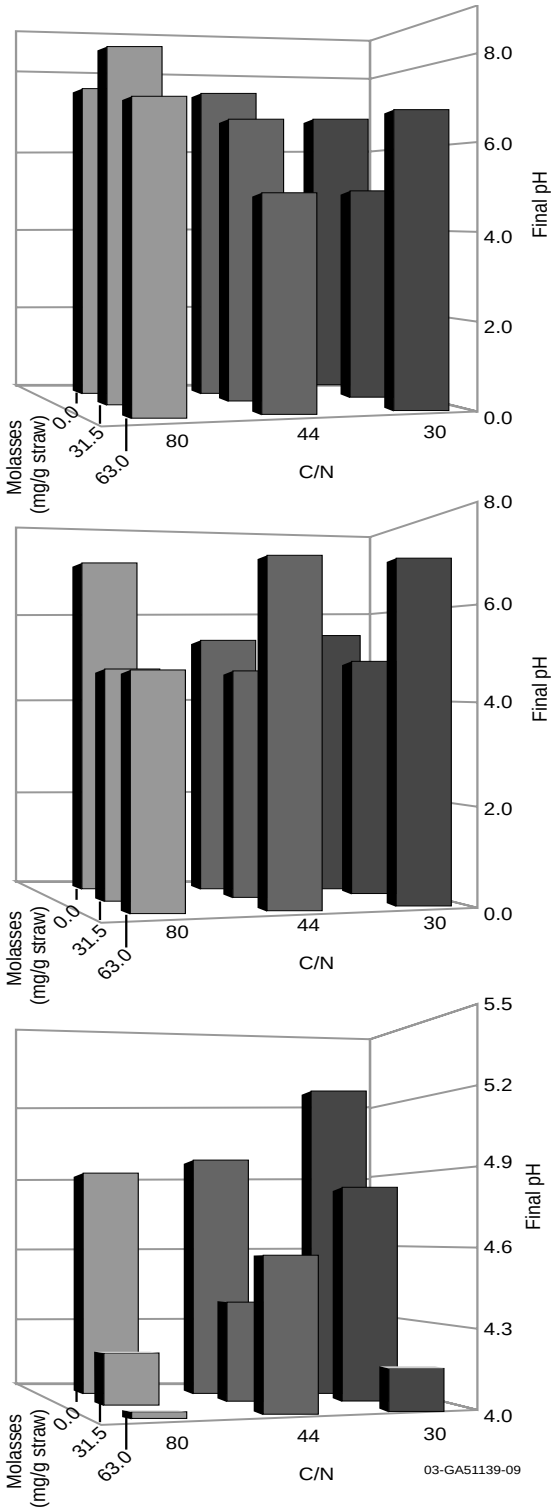


*FIGURE 1. The effect of adding free sugars (molasses) and assimilable nitrogen (yeast extract presented as C/N) on the final pH of the water in the ensiling columns. Tests were performed at 70%, 80% and 90% moisture (top to bottom).*

added. This result was consistent with production of cell mass rather than organic acids.

If only nitrogen or molasses was added at 80% moisture, ensiling occurred, but not as well with nitrogen as with molasses. When moderate levels of both nitrogen and free sugars were added together, ensiling also occurred. At 90% moisture, adding nitrogen generally worsened ensilability, while adding free sugars generally improved ensilability. The best ensiling occurred at the lowest nitrogen (highest C/N) but the highest free sugar.

The loss of dry matter and straw polysaccharides (cellulose and hemicellulose) in the ensiling columns is shown in Figure 2. The general trend showed that losses of each component increased as pH increased in the columns. That is, if ensiling did not occur, higher amounts of dry matter were lost, and yield losses were increased for both cellulose and hemicellulose. The lowest losses occurred below an average column pH (average of the pH values from top and bottom column fractions) of about 5.0. Therefore, it is necessary with this straw to attain an ensiled pH of no more than 5.0 to obtain the best stabilization of polysaccharide compositions and to minimize yield losses of these important fermentable sugar sources.

Many additional samples were taken for later analysis, including samples for microbial community analysis by traditional and molecular methods, samples for identification and quantification of organic acids produced, and statistical treatment of the factorial data set. This analysis will continue in the next fiscal year, as well as further work on the progression of the microbial community within the ensiling columns and its affect on the stability of the polysaccharide compositions and yields.

This work has demonstrated that ensiling the material and controlling moisture level through adaptation of wet storage/ensiling techniques can minimize variations in feedstock composition and yield. This LDRD aligns well with INEEL's recent designation by the Office of the Biomass Program (OBP) as the lead laboratory for Biorefinery Feedstock Development. In addition, successfully addressing these issues has helped to position the INEEL Bioenergy Initiative for direct funding from OBP, since their leadership favors the storage strategy advanced by this project. The Principal

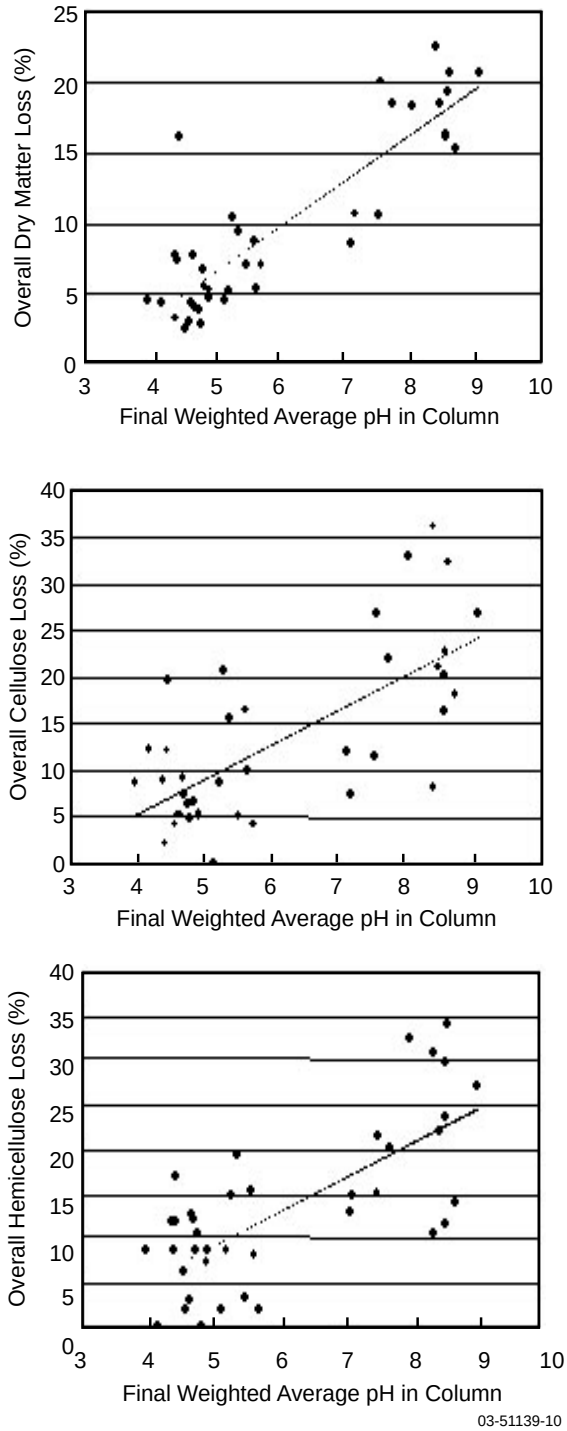


*FIGURE 2. Mass balances for (top to bottom) dry matter, cellulose, and hemicellulose in the ensiling columns. Losses are presented in each plot as percent of initial measurement. A maximum final pH of 5.0 is recommended for this straw for the best stabilization of fermentable carbohydrate compositions and yields.*

Investigator prepared significant work scope, developed in part from this LDRD, for inclusion in two proposals to the FY04 Biomass Research and Development Initiative (a joint call issued by DOE OBP and USDA). The PI has interest from BC International Corporation in partnering to test the effects of ensiling on pretreatment requirements, and Cargill Dow LLC also has expressed interest in a future collaboration to accomplish a similar scope for their pretreatment. DOE OBP will fund the ensiling testing portion of this LDRD for corn stover in coming years. Thus, work in FY04 on this project will focus on wheat straw alone.

INEEL

# Environmental

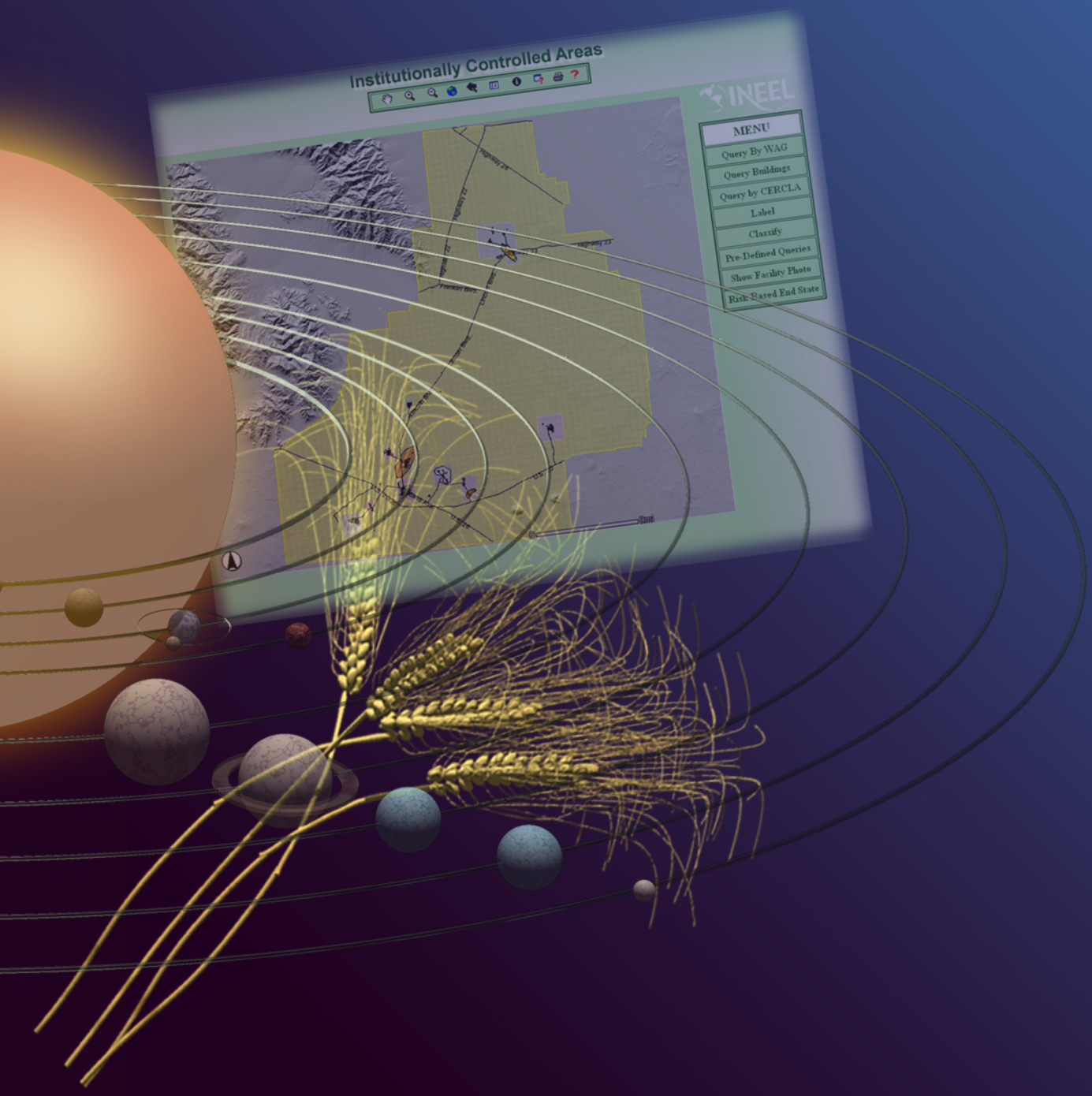

# Elemental Tracers and Multi-Variate Receptor Modeling Methods in Assessing Air Pollution

*Michael L. Abbott, Jeff Einerson*

***Predicting area contributions to regional pollution***

ET110

Regulatory permitting and stakeholder acceptance of important waste treatment projects at the INEEL (e.g., Advanced Mixed Waste Treatment Project incinerator, New Waste Calciner Facility) and other DOE and commercial sites have been impacted in the past by the inability to provide accurate predictions of long-range atmospheric transport of pollutants and by a general lack of scientific understanding of air pathway transport. Current methods of addressing this issue rely on either univariate measurements of a few ubiquitous pollutants (e.g., NOx, PM-10), which cannot discern a source's contribution in the mixture, or relatively simple air dispersion models that have large uncertainties beyond short-range distances (20-km) and lack site-specific validation.

This LDRD is investigating a measurement-based air pollution assessment method that provides information on the relative contributions of regional sources (e.g., cities, industrial areas, background input) to air pollutant fallout at downwind areas where pollutants from these sources mix. The research method uses a "receptor modeling" approach that consists of: 1) ultra-clean snow sampling techniques around known source areas and at downwind sites where pollutants mix with those from other sources, 2) analysis by inductively coupled plasma-mass spectrometry and ion chromatography (IC) to provide a broad suite of trace elements and common ions at very low levels, 3) principal component analysis to identify "source area profiles"—unique combinations of elements emitted from specific geographical source areas (e.g., INTEC, Idaho Falls, natural background), and 4) classical least-squares regression (CLS) and alternating least squares regression (ALS) to determine the fraction of the measured fallout mixture that originates from a specific source area.

Understanding who contributes what to air pollution at sensitive downwind locations will enhance permitting of new INEEL operations and stakeholder understanding of the impacts of INEEL sources relative to other regional sources, and help develop sound emission control strategies that avoid costly over-controls on industries that have little impact.

Technical objectives for fiscal year 2003:

- Collect and analyze over 450 snow samples to produce a large database of chemical constituents (trace elements and common ions) in air pollutant fallout on the INEEL and regionally across the Eastern Snake River Plain (ESRP).
- Develop sample design methods that permit use of CLS and ALS modeling techniques to source apportion fallout at distances more than 50 km from sources.
- Apply the CLS and ALS modeling techniques to two regional test cases: 1) ESRP sources and 2) a municipal waste incinerator in Thayne, Wyoming.
- Present results on the ESRP test case at industry conferences.
- Published results in the peer-reviewed journals.

More than 450 snow samples were collected over three winters using ultra-clean sampling methods. Samples were analyzed for a broad suite of trace elements using inductively coupled plasma mass spectrometry and common ions at the U.S. Geological Survey National Research Program laboratory in Boulder, CO. In 2002, a sampling design was developed for CLS source apportionment, consisting of upwind and downwind sampling around potential source areas and downwind sampling in mixing zones where plumes from numerous sources overlapped. In FY03, the sampling design was modified for ALS source apportionment (Fig. 1).

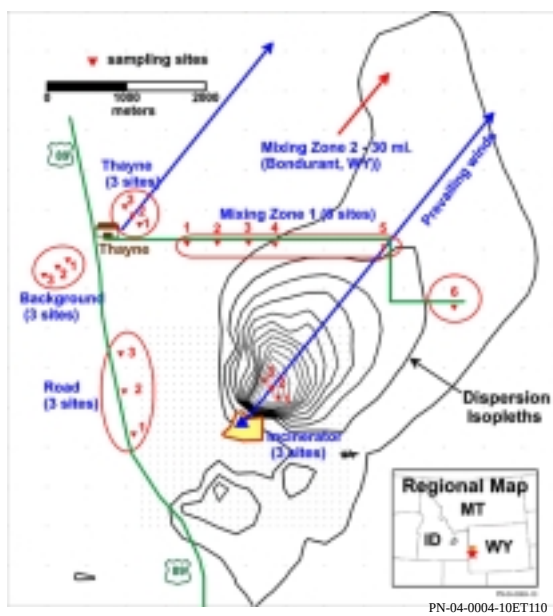


PN-04-0004-10ET110

*FIGURE 1. Sampling design test case for ALS source apportionment near a municipal waste incinerator in Thayne, WY, March 3-4, 2003.*

The elements and ions detected in most samples in 2002 and 2003 are shown in Table 1.

*TABLE 1. Analytes detected in most snow samples during 2002 and 2003.*

| | 2002 | 2003 |
|---|---|---|
| Elements | Al, AS, Ba, Cd, Ce, Co, Cs, Cu, Dy, Er, Eu, Gd, Ho, La, Li, Lu, Mn, Nd,Ni, Pb, Pr,Rb, Sb, Sm, Sr, Tb, Te, Tl, Tm, U, V, W, Y, Yb, Zn, Zr | Al, As, Ba, Cd, CE, Co, Cu, Dy, Gd, Ho, La, Li, Mn, Nd, Ni, Pr, Rb, Sm, Sr, Tb, U, V, W, Y, Zn, Zr |
| Ions | Ca, Cl, F, Mg, Na, $NO_3$, $SO_4$ | Cl, K, Na, $NH_4$, $SO_4$ |

03-51139-05a

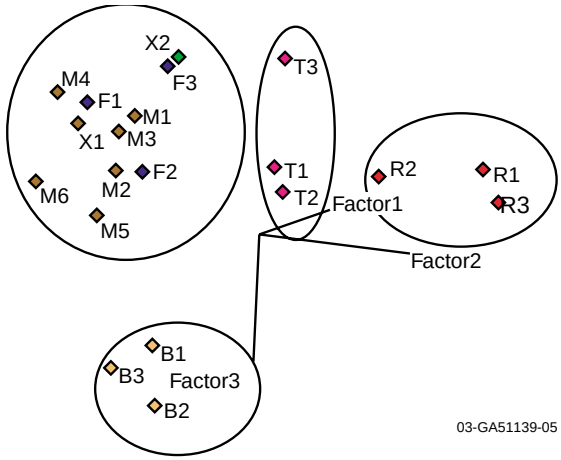


*FIGURE 2. PCA scores of sampling data around the incinerator at Thayne, WY.*

The 2001-2002 data showed the highest regional concentrations near the two largest cities in the area (Pocatello and Idaho Falls) and the lowest concentrations on the INEEL. Principal Component Analysis (PCA) of the 2001 data showed two distinct ESRP source categories: 1) fugitive emissions from the phosphorus industry in Pocatello and crustal (blowing dust) input, and 2) other emissions from phosphorus processing and oil combustion. Source apportionment of the 2002 ESRP data using ALS regression gave good results. Three major source areas were identified—Pocatello, Idaho Falls, and Rexburg—with reasonable fractional fallout contributions predicted at mixing zones east of Idaho Falls and Rexburg given the wind patterns that existed during the snowfall event.

The 2003 Thayne incinerator test case showed distinct PCA clusters for the background (B), road (R), Thayne (T) samples, indicating unique source emission profiles (chemical signatures) from these sources (Fig. 2). The clustering of the incinerator (F) and mixing site (M) samples with samples taken 50-km downwind (X) indicate a widespread incinerator emission profile that is distinct from background and other local source inputs.

The receptor modeling methods developed in this work provide a measurement-based assessment tool that can be used to augment traditional theoretical modeling approaches. This year's research resulted in presentation of test case results at the 2003 Gordon Research conference on Statistics in Chemistry and Chemical Engineering, July 27-August 1, Mount Holyoke College, MA, and publication in the peer-reviewed journal Fuel Processing Technology.

Permitting of important waste treatment projects at the INEEL and at other DOE and commercial sites has been impacted in the past by the inability to provide accurate predictions of long-range atmospheric transport of pollutants and by a general lack of scientific understanding of air pathway transport. Understanding who is responsible for what fraction of the pollution measured at sensitive downwind locations will enhance stakeholder understanding of the relative source impacts in the region, facilitate regulatory permitting of DOE facilities, and help develop sound and cost effective emission control strategies. The need for alternative, measurement-based pollution assessment tools also will likely become more important as a final waste treatment technology is selected for the remaining sodium bearing waste at the Idaho Nuclear Technology and Engineering Center.

# Improving Stakeholder Interactions: A Stakeholder-Based Research Methodology for Reaching Decisions on Polarized Issues

*R. Sam Alessi, Michael Mayhew, Jeffery Joe*

***A relationship-oriented approach to problem solving***

ET108

The political and emotional charge of DOE issues, historical distrust of the government, and expensive solutions that negate the interests of the community, have typically been barriers to achieving DOE's established policy of public participation.

This LDRD applies human systems science to show how stakeholders organize their thinking around complex problematic issues. The thesis is that it is necessary and prudent to understand the characteristics of stakeholder beliefs and rationalizations prior to invoking any decision-making method. An approach has been created that incorporates elements from anthropology, systems design, and systems therapy. The approach produces a deep, fundamental understanding of stakeholder concerns. The knowledge gained can be used to balance meaningful human needs with technological advancements that will benefit all parties. Additionally, traditional survey techniques have been used to study issues related to fatalistic beliefs observed across all stakeholder groups.

Technical objectives for fiscal year 2003:

- Gain a deeper understanding of the initial viewpoints of stakeholders involved in the long-term future of the INEEL, specifically,
  - A fatalistic belief that "messiness" in government prevents efficient decision-making, and
  - A fatalistic belief that "human nature" prevents citizen involvement unless specific personal items are threatened.
- Investigate how fatalistic beliefs and attitudes in youth and adults affect their ability to make good decisions and become effective future citizens.

This research seeks to analyze the interactions between DOE and stakeholders and to produce scientific data that will be used to strengthen sustainable relationships between these diverse groups. Failure to intervene and foster positive discussions can deadlock projects and create a deep regional impact because unpopular decisions are mandated without considering the values or interests of the local community. Approaches are needed that will fortify the community by building trust while striving to achieve common goals.

The proposed methodology integrates approaches from science and engineering disciplines including anthropology, therapy, and systems design to focus on the task of social and technical problem solving. First, anthropological methods are used to describe communication patterns and underlying assumptions among stakeholders. Next, therapeutic concepts are used to interrupt divisive communication patterns between participants and to assist the members in acknowledging and respecting the views of the others. Stakeholders participate in creating a new communication patterns, underlying assumptions, and physical solutions. The beliefs and perceptions of the stakeholders become intrinsically incorporated into the model and are a template of critical stakeholder requirements.

*Eastern Idaho Adult Stakeholders* - Adult stakeholders were selected for greatest diversity possible and then trimmed to 10 members through a ranking process that involved stakeholders both external and internal to the INEEL. Stakeholder affiliations included preservationist, professor, activist, DOE Citizen Advisory Member, local governance, media, Native American, environmentalist, and governmental regulator. Two separate two-hour sessions were convened and audio taped. The recording was transcribed literally and the only editing of the text was the removal of any identifiable information about the participants.

Initial findings are published in a report that was checked with stakeholders for accuracy and intent. Additionally, the results have been presented to the American Nuclear Society (Alessi et al., 2002). The emergent themes were identified from actual language of the stakeholders, thus any quotes are literal and left in the form in which they were spoken.

The focus group began with a very broad opening question:

"Since the end of the cold war, it's been hoped that sites could be cleaned up and returned to the public. For a variety of reasons, DOE feels that they cannot completely clean up sites, but need to leave some waste in place, but in a safe manner. My question to you is, in response, what would you like to input into that? What would you say in response to that? [Pause] So if you had decision-makers here and policyholders or someone like that here, and with that set before them, what would you like to say?"

The purpose of this question is to try and focus the discussion on the issue of long-term stewardship of INEEL waste. To do this the issue was

stated in its narrowest sense even though not all sites will leave waste in place or attempt to transfer land to the public.

The main topics and issues discussed included concerns about the process for making decisions, including the need for public involvement, full disclosure of information, respect for the public, the honest assessment of the situation, and inclusion of community values. Public involvement was discussed more fully including public attitudes on involvement and needs associated with public involvement. Additionally, science associated with waste management was discussed in terms of its complexity and whether that complexity is fundamentally social or technical. The narrative was also analyzed for the "impact on stakeholders" that affects the apparent lack of public involvement, unclear INEEL plans, and the overall influence of what was called messy government by stakeholders.

Overall, the results indicate a rather gloomy future. Uncertainty and confusion has led these stakeholders to fatalistic and cynical viewpoints that anything can be different. This negative view saps creativity about a positive future. Some stakeholders feel that decisions are made in a way that begs a fight (i.e., "Here's the decision, now come up and fight it if you want to fight it."). This research uncovered a number of paradoxes among the stakeholders that cripple the ability to create a beneficial future. Fatalistic beliefs and behavior are mirrored against a fundamental desire to help and not hurt. Beliefs that the future cannot be different are contrasted with some successes (e.g., KYNF stoppage of the INEEL incinerator), though the successes are negative. No "courageous" leadership could be identified by the group, yet stakeholders have a desire to be led and articulated a clear description of the needed leader. Overall, creative thinking is subsumed by dialogue that is saturated in the problem and any passion to create a better future is eclipsed by the overarching fatalism.

It was noted that some voices are marginalized from the discourse. Activist said, "And I find that that's really quite predominant in my experience as an activist over the years and not only with issues that I held, but other issues…and that so many cases you see the decision being made—'Here's the decision, now come up and fight it if you want to fight it.'" These voices are responded to by speaking in absolutes while maintaining an overall aura of cynicism. Initially, it was noted that the marginalized tend to be the weak and powerless. Ultimately, however, everyone feels marginalized. The strategy of the marginalized is to revert to attempts at destroying plans instead of participating in proactive effort.

The overall problem saturation, cynicism, and fatalism made it difficult for the group to think of how it might be different. Stakeholders did finally identify a solution that could lead to better regional relationships and a more creative future for Eastern Idaho. They expressed a desire for monthly dialogue and as stated by one stakeholder, *"…for discussions to exist, there has to be a forum. I don't think we'll necessarily resolve anything or there's going to be some panacea as a result of that. But right now it's discussions through third and fourth parties, and…we know that model doesn't work…."* This desire for a new way to interact promotes the possibility for cooperation, rather than condemning ourselves to more long years of contention and a near-gridlock for projects that appears threatening to some stakeholders. Forming a direct dialogue and redirecting the issues discussed can create a path to a more productive future in which stakeholders accept and even assist development, while using their influence and innovative ideas to provide new possibilities and directions. This idea was brought to INEEL leadership but proved too extreme and was not adopted.

*Eastern Idaho Teen Stakeholder* — An emergent finding from the 2001 INEEL qualitative study with regional youth (Hill-Molder et al., 2001) was the indication that teenagers in Eastern Idaho have a fatalistic outlook that influences their ability to plan for the future. Literature research indicates growing fatalism worldwide. The investigators hypothesized that fatalism will negatively impact levels of trust and interfere with sound, positive decision-making skills in both the personal and public domains.

Since findings from adults also indicated fatalistic beliefs, a survey instrument was constructed to determine the level of fatalism existing in Eastern Idaho. Causes of fatalism (locus of control, explanatory style, and religious dogmatism), and how fatalism affects the level of trust toward nuclear weapons, nuclear power and the storage of nuclear waste were included. Trust in self, the INEEL, and the federal government will also be studied and compared with demographic variables like age, sex, level of community involvement, and parents' occupations. Finally, decision-making skills and how they are affected by fatalistic attitudes were added items to the survey.

The survey instrument was pilot-tested with an opportunistic sample of 55 participants from Eastern Idaho. They represented teenagers age 13 through 19 from three separate counties in Eastern Idaho. The pilot test results showed that 18% to 32% of the test population was somewhat to very fatalistic. There was also a portion of that population that showed lower levels of trust and that did not believe their choices could make a difference.

In 2003, psychological measures of fatalism, namely locus of control (LOC) and mastery, were administered, along with measures of decision-making, interpersonal trust, delinquency, and nuclear energy attitudes. Peer pressure was also assessed in participants to account for its affects on maladaptive decision-making and delinquent behavior. Results showed that LOC, mastery, and peer pressure were significantly correlated to decision-making and delinquency. Religious orientation was also significantly correlated to decision-making, but not to delinquency. Results indicate that those who were more fatalistic in their beliefs, as indicated by an extrinsic LOC and lack of mastery, also tended to be more maladaptive in their decision-making. This relationship between fatalistic attitudes and maladaptive decision-making was significant across all dimensions of decision-making ability. That is, fatalism was correlated to lower self-confidence, less vigilance, more evasiveness, greater complacency, and greater panic in the process of making decisions. An extrinsic religious orientation also was related to four of the five dimensions of maladaptive decision-making (panic excluded). Based on these results, it is advised that some intervention be taken to reduce the negative implications of fatalistic beliefs in youth and adults.

Direct benefits from this research are that the INEEL, regional stakeholders and the DOE will gain a better understanding of different viewpoints that influence the progress of projects at the INEEL. Additionally, INEEL plans will benefit from clearer knowledge of stakeholder needs. Design engineers benefit by being able to create technology that will not raise stakeholder concerns. INEEL's capability to work with stakeholders to understand fundamental needs and to include this information in the construction of plans and in technology designs is a national asset. Since many investigations into failures of large-scale complex technologies are traceable to faulty requirements and misunderstood stakeholder need, this research will put the INEEL on the cutting edge of advanced planning and engineering design.

The DOE is committed to encouraging public participation and fostering a viable relationship with stakeholders. The approach described in this research facilitates the interaction between agencies, entities, and stakeholders to develop trust and enrich decisions that will impact future generations.

# Biologically Based Catalysts for Processing and Detection in Harsh Service Environments

*William A. Apel, Frank Roberto, Vicki Thompson*

***Detecting heavy metals with microbes***

ET105

Extremophilic microbes live at life's extremes; i.e., very high and very low pHs, high and low temperatures, high osmotic pressures, high barometric pressures, etc. Enzymes from extremophilic microbes often share the microbes' resistance to extremes, and can potentially be used to create biosensors and biocatalysts that have the high degree of specificity normally associated with enzymes while being stable under a variety of environmental extremes that would typically inactivate enzymes.

The goal of this LDRD is to develop enzymes from extremophilic microbes for use as biosensors to detect and monitor environmental contaminants such as toxic metals, and for use as bio-catalyses for industrial, energy, and national security applications. The initial thrust of this project entails two tasks: 1) characterization and evaluation of different classes of extremophilic enzymes for use in biosensors and/or industrial catalysts, and 2) development of genomic information to allow improved extremophilic enzyme stability through structural modification using molecular techniques.

Technical objectives for fiscal year 2003:

- Continue *Halomonas campisalis* genomic sequencing with focus on metal-binding homologs.
- Acquire extremophiles from high radiation and temperature environments for use in molecular evolution studies.
- Prepare report on draft genomic sequence of *Halomonas campisalis.*
- Complete comparison of thermostable catalase with commercially available enzymes.
- Develop and characterize immobilization methods for catalase enzyme.
- Publicize and present results of research.

The thermo-alkali-stable catalase previously isolated from *Thermus brockianus* was compared with catalases derived from beef liver and *Aspergillus niger* for the ability to degrade hydrogen peroxide in simulated industrial hydrogen peroxide waste streams. The optimum temperatures and pHs for activity of each enzyme were determined to be pH 7 and 40°C for the beef liver catalase, pH 7 and 50°C for the *A. niger* catalase, and pH 8 and 90°C for the *T. brockianus* catalase. The stability of each enzyme was examined at conditions of pH 10 and 11, and at temperatures of 25°C and 70°C with results shown in Table 1. The beef liver catalase showed the least stability with half lives at 25°C of two hours at pH 10 and 15 minutes at pH 11, and showed a complete loss of activity when incubated at 70°C and pH 10 and 11. The *A. niger* catalase was intermediate in stability with half lives at 25°C of 50 hours at pH 10 and 100 hours at pH 11, and half lives at 70°C of 15 seconds at pH 10 and 30 seconds at pH 11. The *T. brockianus* catalase was extremely stable under all conditions examined with the exception of pH 11 and 70°C. Measured half lives for this enzyme at 25°C were 44 days at pH 10 and 100 days at pH 11, and half lives at 70°C were 15 days at pH 10 and 15 seconds at pH 11.

*TABLE 1. Stability of catalases from various sources as a function of temperature and pH.*

| Catalase Source | Enzyme Half-Life | | | |
|---|---|---|---|---|
| | pH 10 | | pH 11 | |
| | 25°C | 70°C | 25°C | 70°C |
| *Aspergillus niger* | 50 hrs | 15 sec | 100 hrs | 30 sec |
| Beef liver | 2 hrs | Not stable | 15 min | not stable |
| *Thermus brockianus* | 44 days | 15 days | 100 days | 15 sec |

03-51139-07b

Several commercially available immobilization matrices were assessed for their ability to efficiently bind the catalase enzymes while retaining high levels of activity. Eupergit C beads yielded the best results and were used for subsequent characterization of immobilized enzyme properties. Beef liver, *A. niger*, and *T. brockianus* catalases were immobilized on Eupergit C beads and the Michaelis-Menton constant, $K_m$, determined. $K_m$ values of 22, 169, and 17 mM, respectively, were determined. These values were lower than the $K_m$ for each enzyme determined in solution, which is opposite the usual behavior for immobilized enzymes. Stability of the immobilized beef liver and *A. niger* catalases was determined at pH 10 and 70°C. The beef liver catalase stability increased from no stability at those conditions to having

activity for five minutes. The *A. niger* catalase stability increased 100 fold from a half-life of 15 seconds to a half-life of 26 minutes.

In FY03, the genomics task had a number of accomplishments. Sampling for radiotolerant bacteria and fungi was performed in cooperation with Idaho Nuclear Technology and Engineering Center (INTEC) operations staff during the decommissioning process for INTEC-603 fuel storage facility. Sludges were pumped to the surface and inoculated into a variety of bacterial and fungal medias. Enrichment cultures and individual isolates were removed to the IRC after elimination of residual radioactive materials during successive culture passages. Splits of the cultures were provided to Idaho State University where the bacterial isolates were characterized. No appreciable radiotolerance was found.

With the assistance of summer intern, an additional 1.39 Mb of *H. campisalis* sequence was obtained. This new sequence is currently being analyzed with the newly integrated bioinformatics tools in the Numerical Simulation Lab.

To support pursuit of a patent in the thermophilic enzyme task led by several INEEL investigators have cloned the catalase gene from *Thermus brockianus*. The sequence of this gene is currently being generated for comparison with other *Thermus* catalase sequences in GenBank. Partial amino acid sequence information provided by Dr. Thompson suggests a high degree of similarity with other *Thermus* catalases.

The capabilities developed under this LDRD effectively support environmental initiatives, as well as initiatives directed towards the development of clean energy and chemicals from renewables.

In FY03 a number of positive opportunities resulted from this project. An intellectual disclosure record was filed titled “High temperature and alkaline stable catalase.” A patent application based on this IDR is in preparation. An NSF Microbial Observatory project titled “Microbial Observatories: Viruses from Yellowstone Thermal Acidic Environments” was funded. A poster titled “Genomic sequencing of a halophilic, alkaliphilic bacterium, *Halomonas campisalis*, for potential use in bioremediation of mixed hazardous waste,” was presented as part of the INEEL summer intern program. The Consortium for Extremophile Research, formed between INEEL, Washington State University and Concurrent Technologies Corp., is pursuing further extremophile research at the member institutions. In addition, presentations on the catalase work have been made at two national technical conferences: the 2002 American Institute of Chemical Engineers annual meeting held in Indianapolis, IN, in November, and the 2003 American Society for Microbiology annual meeting held in Washington D.C. in May. A manuscript based on the *T. brockianus* catalase also was published in Biotechnology Progress, and two manuscripts based on the Microbial Observatory project are in review.

# Atmospheric Pressure Surface Analysis Mass Spectrometry

*Anthony D. Appelhans, Richard C. Martineau, David A. Dahl*

***Obtaining chemical information from samples in natural environments***

SC117

Research needs in chemistry, materials, environmental, and biological sciences are increasingly demanding that chemical information be obtained at conditions more representative of the samples' natural environment, often under harsh conditions (high temperature, aggressive gas composition). For example, in environmental science many of the chemical processes of interest are manifested in the presence of water vapor and other atmospheric gases (e.g., $CO_2$). Similarly, in materials science and catalysis research, the operational conditions include reactive species at atmospheric pressures, often at elevated temperature; conditions heretofore unsuitable for mass spectrometry analysis.

This LDRD investigates the technology needed for a new field of mass spectrometry, Atmospheric Pressure Surface Analysis Mass Spectrometry (APSAMS), that will enable the chemistry at the surface of a sample to be investigated while the sample is at atmospheric pressure conditions. To accomplish this, current state-of-the-art technologies in laser desorption coupled with corona discharge chemical ionization will be integrated. Advanced fluid dynamics and ion transport simulation models are being developed and applied to the design to maximize the efficiency of ionization and transport of the ions from atmospheric pressure the mass spectrometer vacuum conditions. This will enable ionization of neutral molecules desorbed from samples held at atmospheric pressure, and subsequent chemical analysis of the desorbed compounds via mass spectrometry.

Technical objectives for fiscal year 2003:

- Integrate current state-of-the-art technologies in laser desorption and corona discharge chemical ionization to enable ionization of desorbed neutral molecules from samples held at atmospheric pressure and transport of the ions into a mass spectrometer for analysis.
- Develop and apply state-of-the-art computational fluid dynamics modeling capability and apply it to optimize the geometry of the flow domain to maximize the transport of sample ions into the mass spectrometer.
- Develop state-of-the-art atmospheric pressure ion-neutral collisional modeling capability and integrate it into the SIMION ion optics program to enable design of ion optical components that operate at atmospheric pressure.
- Develop the capability to link the computational fluid dynamics predicted flow, pressure, and temperature parameters into the ion optics model so that the coupled mechanical and electrostatic forces are applied in calculating ion trajectories.

A functional representation of the APSAMS concept is shown in Figure 1.

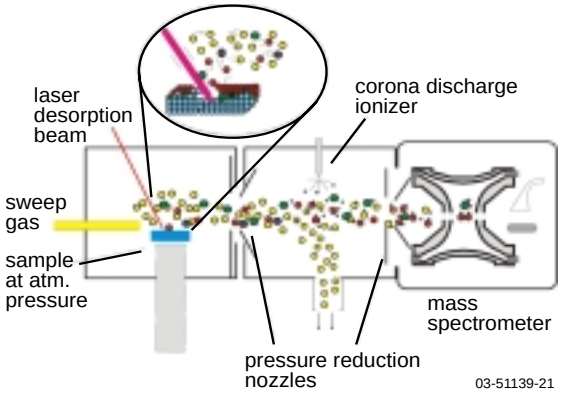


*Figure 1. Molecules desorbed from the sample at atmospheric pressure are chemically ionized and the ions are transported into an ion trap mass spectrometer for analysis.*

The focus for year one in this project was on detailed study, design, and testing of the sampling and ionization chambers and the pressure reduction nozzles. To accomplish this, the fluid dynamics and ion optical code capabilities have been developed and are being applied to identify the controlling mechanisms and develop design criteria to optimize performance. Collaboration with Dr. W. Harrison, University of Florida, has been established. Scoping studies of the ion signatures from INEEL model samples have been conducted using an instrument at the UF, and the ion transport and fluid dynamics of this instrument have been modeled and compared with experiment results.

*Computational Fluid Dynamics:* INEEL computational fluid dynamics computer codes have been modified to handle the extreme flow conditions present in the pressure reduction nozzles, and different nozzle designs have been explored. The APSAMS apparatus presents a particularly challenging flow field resolution problem and difficult numerical problems. The most obvious of these

flow features is the large pressure drop between the sample chamber and the ion collection chamber, on the order of 500 to 1. This pressure drop guarantees supersonic flow conditions in an unconfined flow domain. The main requirement of the sample chamber design is that the ablated sample be transported through the pressure reduction nozzle in as high of a concentration as possible. This requires a short travel time to avoid significant diffusion and flow streamlines that smoothly converge to the pressure reduction nozzle system. Several axisymmetric geometries were designed and simulated in an effort to meet these design requirements. The geometries ranged from a simple, small-diameter straight tube to the more complex pressure reduction nozzle–ion skimmer configuration shown in Figure 2. These geometries were simulated with a new 2-D CFD code employing the PCICE-FEM scheme (developed at the INEEL by Dr. Martineau). Currently, the PCICE-FEM code is capable of simulating either 2-D planar or axisymmetric single-phase, viscous compressible flows, and is fully capable of reaching a stable solution for the large pressure drop defined in the APSAMS flow domain. A paper detailing the advances in the model is in preparation.

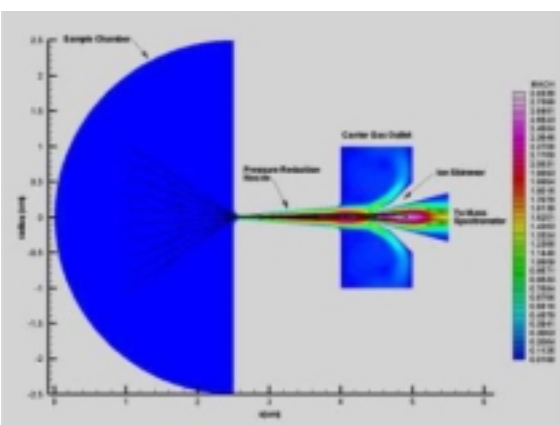

PN04-0004-84a

*FIGURE 2. Pressure reduction nozzle.*

*Atmospheric Pressure Ion-Neutral Collision Model*: An ion-neutral collisional model suitable for atmospheric pressure has been developed and integrated into the SIMION ion optics program. Standard mechanistic kinetic collision models are impractical for use at atmospheric pressure because the number of collisions is so high (2 million collisions per mm) that the time to calculate an ion trajectory with a mechanistic collision model becomes unreasonably long (hours per ion). Modeling this process, even by Monte Carlo methods, can be extremely time-consuming. To speed up the calculation time, a statistical model was developed that enables the ion trajectory to be calculated in seconds, making it practical for use. The statistical based model has been compared against the mechanistic kinetic model, and the agreement is quite good. (Note that generation of the data with the kinetic model required three computers operating for a month just to get 500 trajectories, while the same data set was generated with the statistical model in minutes.)

The statistical model has been used to analyze the ion source region of an atmospheric sampling instrument at the University of Florida. The predicted performance agreed well with the experiment results. After further experimental confirmation of the statistically based collision model, the model will be expanded to include the gas flow fields calculated with the fluid dynamics model. This will provide the ability to identify the controlling mechanisms at each stage in the ion transport and develop an optimum design for the sampling and ion transfer sections of the instrument.

The tools (computer simulation codes) developed in this LDRD will put the INEEL in a unique position to develop new instruments that address research needs in environmental science (chemistry at surfaces of soils and minerals), materials science (corrosion and chemical changes at surfaces of metals and oxides, such as advanced nuclear fuels and reactor components), and new instruments for detection of hazardous materials such as chemical and biological weapons. It is anticipated that these tools will be instrumental in the INEEL's ability to demonstrate a unique capability when responding to calls for proposals in these areas, and improve the laboratory's ability to attract new research and development programs. In particular, INEEL expertise in this area was instrumental in the laboratory's participation in the recent Joint Laboratory proposal to the Office of Homeland Defense.

# Long-Term Record Storage for Long-Term Stewardship

*Sharon Berrett*

***Tracking site-specific records with barcodes***

ST108

Long-term record storage and retrieval will become increasingly more important to DOE as their role in Long-Term Stewardship (LTS) continues. The ability to track and recover pertinent data is measured by decades rather than years. Regulatory and stakeholder acceptance of long-term stewardship activities relies upon their confidence in the sufficiency and credibility of the historical information supporting the remedy decisions and in the subsequent monitoring data validating the protectiveness of the remedies. The complexities involved in managing this information for many years into the future is arguably one of the most pressing tasks currently facing the INEEL LTS Program.

This LDRD investigates two new automatic identification technologies – touch memory buttons and 2-D barcodes — coupled with new hand-held, portable computing devices to develop a prototype demonstrating how these issues might be resolved. Effectively, these devices allow storage of container or facility-specific database records directly on the container or facility itself, thus saving both time and money as well as relieving the dependence on remote computer systems. Both storage devices have the potential to maintain information in excess of 100 years. The application can be a stand-alone function that is self-contained, eliminating the need for connection to a remote system or dependence on electrical power.

Technical objectives for fiscal year 2003:

- Identify a subset of LTS data for storage on button memory and 2-D barcode.
- Modify a hand-held computer (modification by vendor).
- Develop data conversion method.
- Develop a process to transfer data to buttons and 2-D barcodes.
- Develop application to run on hand-held computer.

This LDRD project uses standard desktop and hand-held hardware platforms, operating systems and software with some modifications. In general, a desktop software module retrieves sample LTS records from an existing database and converts the records to a standard flat file format. The workstation module then downloads the records to the hand-held computer using standard hand-held communications software. In turn, the hand-held downloads the data to the button memory device already attached to the selected object. Information retrieval from the memory button operates in reverse order. Both the desktop and hand-held applications display the data on the device screens. The hand-held application has the additional capability of interfacing with barcode printers for conversion of the data to printed barcode labels. The hand-held application is generic and portable to any site with standard hand-held hardware and accessories.

A typical scenario might be as follows: Selected data is retrieved from a database, formatted and downloaded to a hand-held computer. The hand-held is carried to the monument, facility or container location and the data downloaded to the memory button attached to the object. The button is then locked using an encryption key. Another organization, at another site if the object has been shipped, with a hand-held computer and the encryption key retrieves the application and the data. The data and/or application can be used locally on the hand-held or uploaded to another workstation for use by any other system as flat files.

The system employs both memory buttons and 2-D barcodes as storage devices. Each has unique characteristics that complement each other. Both have long-term storage capabilities and can be used separately or in combination as redundant backups. For example, the read/write capabilities of the buttons make them an ideal choice for applications that require periodic modifications; whereas the labels, encoded on specialized materials, may provide the best long-lasting storage.

This LDRD project has demonstrated the ability to store critical information at the LTS site itself for long periods of time. This ability allows information to be accessed in real time during emergency or power outage situations.

The applications developed in this project have proven to be of interest to EPA for Institutional Controls tracking and DOD for equipment and supplies tracking during deployment activities. The INEEL is now in a position to team with DOD, specifically the Army, to support the Army Research Laboratory. There are also opportunities to assist EPA to develop Institutional Controls system.

# Development of the Scientific Basis for Landscape Management of Federal Lands

*Robert P. Breckenridge, Jerry L. Harbour, Randy D. Lee*

***Using advanced concepts to Identify and map landscape characteristics***

ET122

Many federal lands are subject to creeping environmental problems that often go unnoticed on a site-specific basis, but when reviewed from a landscape level can have dramatic impacts on natural resource management (e.g., threatened and endangered species, invasive weeds, fire).

This LDRD is researching the use of advanced concepts in landscape ecology and remote sensing to develop a unified theory for management of Federal lands. Development of a unified theory that takes advantage of advanced technologies for identification and mapping of landscape features will enhance resource management to meet appropriate regulations, facilitate future facility siting, and enhance the scientific basis for evaluating options for future management of these lands.

Technical objectives for fiscal year 2003:

- Develop a theoretical model for land cover and land use on and around the INEEL.
- Develop ecological health indicators needed to support end state planning and risk assessment.
- Develop computational technologies to evaluate landscape characteristics for improving data for future use analysis.
- Define the long-term research niche for INEEL in understanding sagebrush steppe ecosystems.

This LDRD started late (August) in FY03, thus results to date are limited. However, the following progress has been made.

*Development of theoretical model.* DOE Headquarters developed a new policy in August of 2003 to use risk-based end state for planning future use of DOE properties that are appropriately protective of human health and the environment. The theoretical model being developed in this LDRD is evaluating the framework for addressing end state planning and will help DOE achieve two aspects of its mission associated with the INEEL. These aspects are to understand the future use for sagebrush ecosystems as well as to take actions to ensure future NE and EM missions are achieved as efficiently as possible.

*Evaluation of ecological health indicators*. The research team has been invited by the Sustainable Rangeland Executive Committee to join their group in identifying criteria and indicators for sustainable rangeland management. Current activities have focused on identifying critical linkages between ecological parameters and how these will support long-term risk management for rangeland systems. Currently 64 criteria and indicators have been identified. Over the next year, these criteria will be evaluated in conjunction with the Sustainable Rangeland organization to identify those most appropriate for INEEL.

*Evaluate landscape characteristics*. Analysis of landscape level changes requires the analysis of data at multiple temporal and spatial scales. Evaluations are being conducted to determine appropriate remotely sensed data that may be applicable, and existing geo-spatial data, when available, are being compiled. A combination of on-the-ground data collection, unmanned areal vehicles using camera and sensor technologies, and remote sensing techniques are being evaluated as a multi-scale approach for evaluating creeping environmental problems on and around the INEEL.

*Long-term niche for INEEL in this research area*. A series of meetings and conference calls have been held with senior representatives from the Department of Interior, United States Geological Survey (USGS), Fish and Wildlife Service, and Nature Conservancy to evaluate long-term uses for INEEL as a sagebrush steppe research facility. The National Academy of Science also has recently endorsed the creation of an ambitious network of ecological research stations that the National Science Foundation (NSF) has been advocating for the past six years. INEEL, along with university collaborators, will pursue involvement in the National Ecological Observatory Network (NEON). A presentation is being developed and will be provided to NSF in FY04 identifying INEEL's role in supporting the NEON concept.

# Advanced Multi-Operation Control Architectures for Human-Robot Synergy in Complex Domains

*David Bruemmer*

***Robot "autonomy" offers peer-peer interaction***

ET116

Intelligent robots provide the potential of reducing operator workload and error while promoting safety and efficiency for remote tasks in a variety of environmental, military, and industrial applications.

This LDRD is investigating innovative tools for interaction between human operators and intelligent robots. The goal is not super-intelligent robots that never need human assistance, but rather a highly flexible control architecture that assumes limitations on both sides and provides means for mutual support. The control system being developed provides an effective means to merge human cognition with the efficiency of reactive robot control, sensor fusion, and automated decision-making. By allowing the human and robot to do what each can do best, this work increases mission capabilities in terms of speed, quality of data collected, human trust in the system, and overall reliability of the system.

A human-centered, multi-modal interface has been developed that can support meaningful cognitive interaction, allowing humans and robots to share knowledge, goals, and intentions "on the fly." The flexibility and power of this interface is supported by a platform-general robot behavior architecture that provides intrinsic intelligence necessary in the face of unforeseen events and changing levels of human input. This work will enable robots to be used across a much wider range of remote search and detection tasks by providing an intelligent robotic system that can adapt its level of autonomy to handle changes in task goals, operational constraints, data-link connectivity and workload.

Technical objectives for fiscal year 2003:

- Reduce operator workload and error while promoting operation safety and efficiency.
- Develop innovative perceptual capabilities that permit robots to form abstract representations of the environment.
- Create new interfaces that promote true teamwork between humans and robots.
- Develop comms payload and protocol to permit robust communication.
- Provide a complete robotic system, including software control architecture, interfaces, robotic hardware and sensor suite for accomplishing challenging remote tasks.
- Allow remote sensor deployment to be accomplished in days rather than months.

One of the most significant accomplishments in FY03 has been porting the architecture to four different robotic systems varying in size from 35 to 300 pounds. To support this effort, the control software was revamped into a new object-oriented "universal" robot program that can be applied to a wide variety of mobile robot platforms. The software now adapts to the robot's sensors and geometry partly through a process of self-discovery and partly by reading from a parameter file. In fact, this new code is more portable, more stable, more readable and more configurable.

To support human-robot teams, an innovative tool was developed with which to maintain awareness of the environment and task and cooperatively pursue mission objectives using a common substrate – a collaborative cognitive workspace. The workspace is a real-time semantic map, constructed collaboratively by human and machines, that serves as the basis for a spectrum of mutual human-robot interactions including tasking, situation awareness, human-assisted perception, and collaborative environmental "understanding."

A foremost goal of this LDRD has been to improve task efficiency due to the multiple modes of autonomy. Consequently, the investigators designed and executed a human subject experiment to evaluate the change in task efficiency due to the adjustable autonomy architecture developed. In particular, the experiment measured performance for each level of autonomy when used exclusively, as well as when operators are permitted to shift at will between levels of autonomy. Through this human-subject testing, it was found that mixed teams of humans and robots may exceed the limitations of either fully autonomous or teleoperated systems. However, the benefits of mixed teams can easily be overshadowed by control challenges inherent to developing and deploying mixed teams. It was found that some operators utilized multiple modalities presented within the interface such as mapping, vision, and abstracted range sensing, while others seemed unable to cognitively process this much information and often focused entirely on the video display. Some

users seemed quite willing to utilize the autonomous capabilities of the robot while others fought with the robot for control, losing efficiency to "mode switching."

Although the interface already offers an effective means to mediate between human and robot team members, the usability study indicated opportunities for improvement. A new interface design has been implemented with several new capabilities. The interface shown in Figure 1 provides the human user with graphical and textual representations of the environment and task that are appropriate for the current mode. New additions to the interface include the ability to monitor communications status (shown at the bottom of the robot status window). Also, the Sensor Status window (upper right) is a new powerful addition that allows the user to monitor the status of each sensor and select which sensors will be used. New interactive map capabilities provide a means to collaboratively build a shared understanding of the environment and then communicate based on the emerging representation.

Using this architecture and interface, the INEEL human-robot team won the 2003 AAAI Robot Rescue Competition held in Acapulco, Mexico, finding 18 victims within a collapsed building structure over the course of five allotted runs. Not only did the INEEL robot win first place in the competition, it was able to enter areas inaccessible

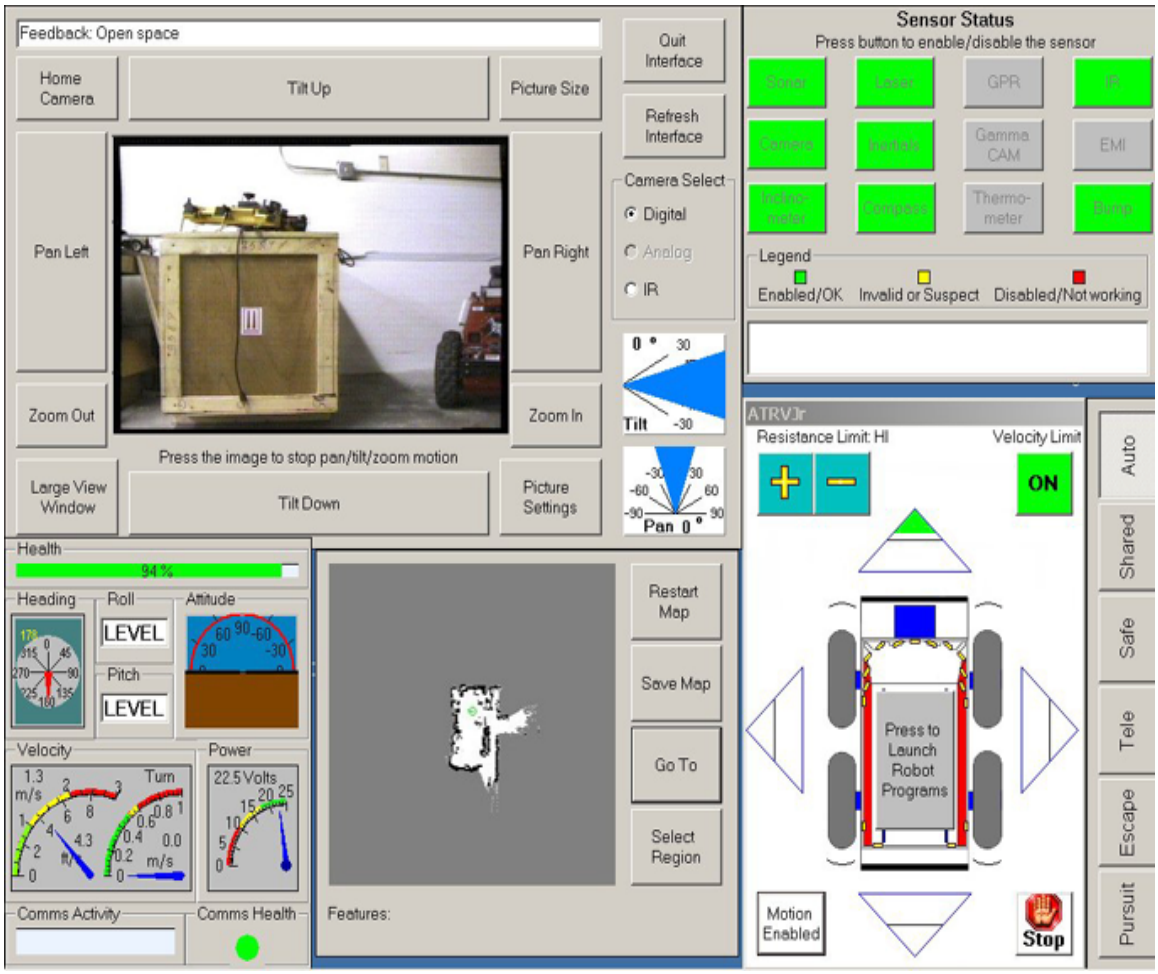


03-51139-236

*FIGURE 1. Interface for control of multi-level autonomy system.*

to other competitors and was able to reliably identify the victims ID tags, their location within the building, and whether or not they were still alive. INEEL's best run was more than double that of the next highest competitor's, showing that INEEL has achieved a leadership status in the area of intelligent mobile robots. The competition, sponsored by the Defense Advanced Research Projects Agency, the National Institute for Standards and Technology, and the National Science Foundation, was held in conjunction with the International Joint Conference on Artificial Intelligence and represents a recognized benchmark for the field of robotics and artificial intelligence community.

The success of this LDRD is evidenced by a number of new contracts and agreements that marry the INEEL's work in this area with other top institutions including the Naval Research Laboratory, the U.S. Army Maneuver Support Center at Ft. Leonard Wood, Missouri, the U.S. Navy Space and Naval Warfare Command in San Diego, California, and university collaborations with Georgia Institute of Technology and Washington University at St. Louis.

# Intelligent Control of Multi-Nodal Systems

*Cal Christensen*

***Decision-making sensors***

ET118

In today's environment, the need for intelligent systems is increasing exponentially. Sensors and processors are being placed on everything from toasters to the family car. These sensors are being used to obtain data that can then be used to make operating decisions that increase system performance. As the number of sensors and the amount of information gathered increases, intelligent systems are needed to interpret complex sensor data, evaluate sensor data from multiple sensor systems, discern good and bad data and prioritize data for decision-making processes. Additionally, as the complexity of systems increases, the requirements for "intelligent" decision-making capabilities is being moved farther down the control architecture to the individual sensor systems.

The objective of this LDRD is to investigate control architectures that will utilize multiple sensor systems, interpret complex sensor data, evaluate and prioritize sensor data, and then make decisions at the sensor level.

Technical objectives for fiscal year 2003:

- Create working computer model.
- Demonstrate remote vehicle operation using computer model.
- Develop intelligent video interpolation algorithm for vehicle guidance.
- Begin research on sensors.

In collaboration with the University of Idaho, a working computer model was created to demonstrate the operation of a remote vehicle in a wooded environment. Three identical sensors working in concert were simulated. The objective of the model was to show the operation of a vehicle under conventional collision avoidance approaches and then compare against an intelligent control system that used a fuzzy logic control algorithm and a training/optimization algorithm to enhance the performance of the vehicle in a wooded environment.

In collaboration with the University of Idaho, an intelligent video interpolation algorithm was developed. The objective of this algorithm was to use video images in the decision-making for vehicle guidance as shown in Figure 1.

A series of acoustic sensors have been procured and are being assembled into a sensor suite. Infrared sensors, a laser system, and infrared cameras and interface boards have been procured. Due to delays in receiving these systems, not all were made operational in FY03.

Literature searches and data gathering have begun on sensors that will support the basic multi-sensor suite. To date, research has begun on acoustic sensors, vision systems, and radar systems. Additional sensor systems will be added as applicable.

In FY04, all of the sensors presently obtained will be made operational. Data sets using the sensors will be obtained, and control algorithms using the data sets will be developed. The objective will be to establish parameters for the data, its "quality," and those attributes that make the data distinct from other sensors. A paper on multi-sensor system control also is planned.

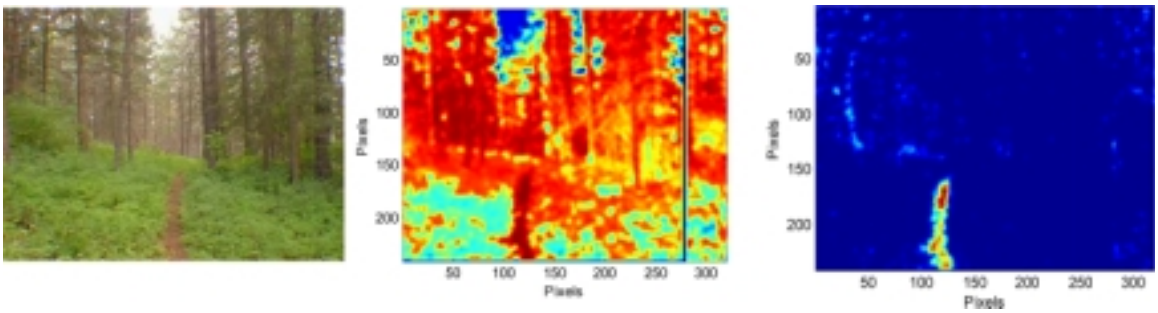


*FIGURE 1. Intelligent video interpolation algorithm uses video images to assist decision-making.*

PN-04-0004-13aET118

# Characterization of Legacy Risk

*Steven A. Eide*

***Improving long-term risk information and performance indicators***

PH102

A key issue related to the INEEL's strategic thrust in environmental management (EM) is the evaluation of risk from environmental waste in its present state or in its end state for long-term stewardship.

This LDRD comprehensively characterizes what is termed the legacy risk or long-term risk burden from environmental waste. This work includes the development of a strong risk foundation for the concept of legacy risk. Appropriate characterizations of legacy risk allow a variety of risk comparisons to be performed: prioritization of site and DOE complex environmental wastes based on risk, evaluation of the risk effectiveness of waste management programs, site and DOE complex risk reduction (by year) as waste management programs progress, and the evaluation of risks of various proposed end states. Such risk information is an essential input to complex environmental decision-making and helps explain DOE EM programs to stakeholders. Finally, such risk information provides risk-based performance indicators to help DOE, Congress, and other stakeholders measure DOE progress in the cleanup area.

Technical objectives for fiscal year 2003:

- Develop human safety and health risk models and a software code to support the following types of evaluations:
  - Risk evaluation of an entire waste management (WM) or environmental restoration (ER) program.
  - Risk comparisons of alternative programs or activities.
  - Comparisons of risk benefit vs. risk cost for activities or entire programs.
  - Ranking of programs or activities by risk.
  - Ranking of wastes/materials by risk.
  - Evaluation of site risk changes with time as WM/ER activities progress.
  - Integrated performance measurement using indicators such as injury/death and radiological exposure rates.

During the 2-1/2 years of this LDRD, the concept of legacy risk (long-term, no-action risk from wastes/materials) was refined and presented to peers at two Waste Management Conferences (2000

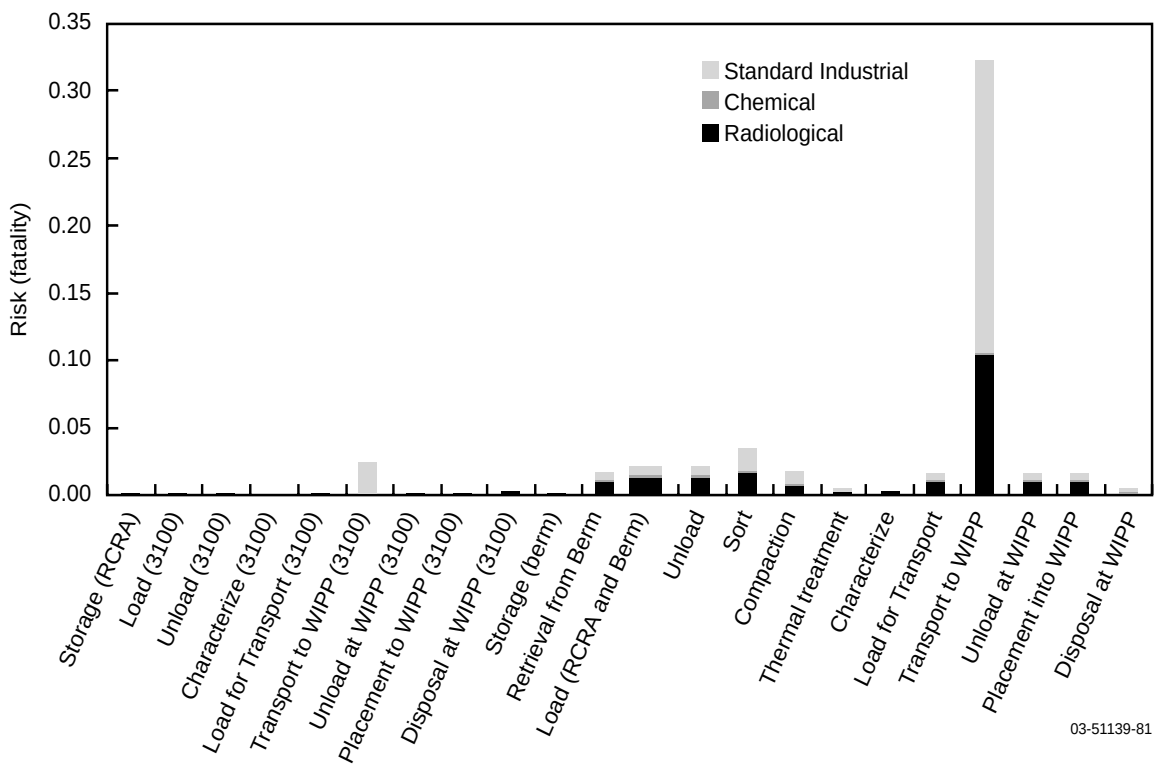


*FIGURE 1. INEEL aboveground CH-TRUW program risk by activity.*

and 2002). Comprehensive and consistent risk models capable of predicting human health and safety risk from a wide range of WM/ER activities were developed. The investigators developed the Environment, Safety, and Health Risk Assessment Program (ESHRAP) software code to implement the risk models and legacy risk concept. And the philosophy and supporting risk models were documented with an INEEL report.

An example of the risk evaluation of an entire WM program, performed using ESHRAP, is presented in Figure 1. The WM program covers the aboveground contact-handled transuranic waste (CH-TRUW) at the INEEL. Human safety and health risks were evaluated for activities covering present storage conditions, ongoing and future waste preparation and treatment, transport to the Waste Isolation Pilot Plant (WIPP), and final disposal. As indicated in the figure, the dominant risks for the entire CH-TRUW program lie in the transportation to WIPP (i.e., mostly non-radiological, standard industrial risks from transport vehicles colliding with other vehicles). Also, long-term risk from disposal is negligible compared with other activities.

The risk benefit vs. risk cost for this program is illustrated in Figure 2. Risk benefit is defined as the human safety and health legacy risk of the CH-TRUW in its present environmental setting minus the legacy risk when disposed at WIPP. Risk cost is defined as the total human safety and health risk from program activities. As indicated in the figure, even though there are significant transportation risks associated with the aboveground CH-TRUW program, the risk benefit is much larger than the risk cost. Therefore, moving the aboveground CH-TRUW from its present location at the INEEL to final disposal at WIPP makes sense from a human safety and health risk basis.

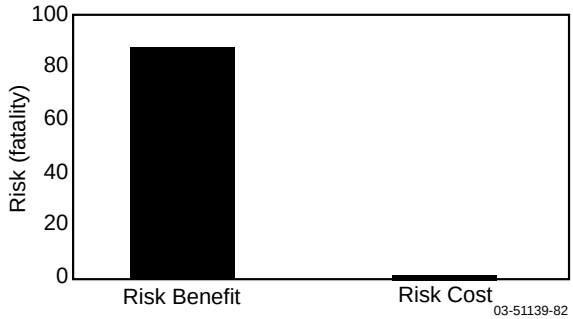


*FIGURE 2. INEEL aboveground CH-TRUW program risk benefit vs. risk cost comparison.*

Characterization of legacy risk included several technical tasks:

- Characterize a risk methodology capable of performing a wide range of risk-related applications.
- Develop risk models sufficient to support such applications.
- Assemble the risk models in a software code package for efficient risk analyses.
- Perform quality assurance on the risk models as implemented in the software code package.
- Document the risk models and software.
- Perform trial applications on INEEL WM and ER programs.

The risk methodology is capable of performing a wide variety of risk analyses for WM and ER activities and programs. Activities covered include storage, handling, treatment, transportation, and disposal of wastes and materials. Construction, operation, and D&D phases also are covered. Risk models developed to support these risk analyses include radiological atmospheric releases from natural phenomena and operational accidents, direct radiation exposure, normal air exposure from off gas or air entrainment releases, vadose zone and groundwater pathway releases, and standard industrial accidents. Human safety and health effects are evaluated for workers, other site personnel, and the public within 50 miles. Site characteristics (populations, air dispersion characteristics, vadose zone and groundwater parameters, etc.) were tabulated for many DOE sites, as were characteristics of various types of wastes and materials. Also, for disposal and legacy risk calculations, intrusion scenarios include scavengers, drilling crews, and residential families. All of these risk models include a moderate level of detail and are internally consistent (a requirement to perform the types of risk analyses listed).

The ESHRAP software code was developed to implement the risk models. This code was developed using Microsoft Access 2000™. ESHRAP allows for efficient risk evaluations using a wide range of user options to support sensitivity studies. Quality assurance of ESHRAP included comparing

code predictions with hand-calculated results using the same risk models and limited comparisons of code predictions with actual experience (e.g., worker exposures, transportation accidents, and other information).

Work performed as part of this LDRD has been documented in the INEEL report *Environment, Safety, and Health Risk Assessment Program (ESHRAP)*. Included in the report is a description of the overall risk model philosophy, technical specifications against which to judge the risk models and software code, risk models, site characteristics, waste and material characteristics, legacy risk models, and example risk analyses. Also, interim results were presented for peer review at various conferences.

Finally, as part of the demonstration phase for the ESHRAP code, analyses were performed for the INEEL aboveground and belowground CH-TRUW WM/ER programs. Example results are presented in Figures 1 and 2.

The legacy risk concept and ESHRAP code developed with this LDRD provide the INEEL with a risk capability not available at any other DOE site. With these capabilities, the entire WM and ER program at the INEEL can be modeled. Important information available from such a model includes the following: ranking of wastes and materials by long-term legacy risk, ranking of WM and ER activities and/or entire programs by risk, and evaluation of site risk reduction as WM and ER activities continue and are completed. Also, yearly site performance data such as accident rates and radiation exposure levels can be inserted into the model to evaluate the integrated impacts on risk.

Legacy risk and ESHRAP applications at the INEEL during the LDRD have included ranking of site wastes by legacy risk, evaluation of program alternatives related to the underground CH-TRUW, and ranking of D&D facilities by risk. The next step is to implement the overall risk model framework using the final ESHRAP risk models and software for the entire INEEL. Results could be used in the yearly Performance and Accountability Report to measure actual risk reduction from WM and ER activities completed during the year. If this is successful, then the same methodology could be extended to the entire DOE complex. At this time, funding is not in place for these follow-on activities. Finally, ESHRAP could easily be expanded to support risk studies for Generation IV reactor concepts and the Advanced Fuel Cycle Initiative.

# Use of Engineered Nano-Particles for Nutrient Delivery and Bioremediation in Subsurface Environments

*Yoshiko Fujita, Glenn Moore, George Redden*

***Delivering food to microbes for bioremediation***

ET114

Effective subsurface bioremediation requires the simultaneous co-localization of contaminants, capable microorganisms, and nutrients for microbial stimulation. The goal of this LDRD is to demonstrate that synthetic nano-particles, or colloids, can be used to deliver nutrients for in situ bioremediation in porous media.

This project addresses the problems of biofouling and subsequent aquifer clogging caused by nutrient utilization at the injection point, and the need for more effective nutrient delivery to contaminated zones. The focus is on development of nano-particles that transport and release nutrients in a gradual release fashion, enabling 1) the prevention of microbial overgrowth around the injection well caused by a sudden drastic increase in substrate concentrations, 2) the delivery of intact substrate farther away from the point of introduction, and 3) a long-term source of nutrition, reducing the frequency of required nutrient applications.

One of the major challenges in this project was the development of methods to synthesize appropriate particles. Over the course of this 2-1/2 year LDRD the investigators tested approaches where the substrate was incorporated into the structural matrix during synthesis, infused into the colloid following particle synthesis, and where the nutrient itself (or a derivative of it) comprised the colloid matrix. Phenol and lactate were the two substrates selected for the experiments. In the end, it was determined that colloids made of polylactide were most promising. It was demonstrated that polylactide colloids of appropriate size (< 500 nm) can be synthesized and can transport through porous media to support microbial growth.

Technical objectives for fiscal year 2003:

- Develop methods to synthesize nano-particles carrying nutrients suitable for subsurface bioremediation.
- Test whether substrate carried in nano-particles is available for microbial utilization.
- Conduct column experiments to demonstrate that nano-particles can transport through porous media.
- Preliminary modeling of nano-particle transport in porous media and release of substrate.
- Prepare at least one paper for a peer-reviewed journal describing work performed for this project.

For this LDRD two substrates, phenol and lactate, were considered for delivery by colloidal suspension. Both compounds have been demonstrated to support the growth of microorganisms that can degrade trichloroethylene (TCE), a common groundwater pollutant at many sites including DOE facilities. Several different synthesis strategies and materials were evaluated for the colloids. With respect to bioavailability and biodegradation of substrates, the investigators developed protocols to assess the bioavailability of phenol, and conducted experiments to evaluate the biodegradability of polylactide particles. In addition, column transport studies were conducted with colloidal suspensions. These activities are summarized briefly below.

*Evaluation of colloid synthesis techniques*. Colloid synthesis was the most challenging aspect of this project. Efforts initially focused on processing of mesoporous silica colloids using the sol-gel process. In this process, a silicon ethoxide is hydrolyzed and then condensed in the presence of either an ionic or nonionic surfactant. A variety of formulations were prepared. Several problems, however, were encountered with this process: namely, narrow size distributions were not obtained in the submicron regime, and the pyrolysis step used to remove the templating agent created significant agglomeration of the colloidal particles. It was also established that both phenol and lactate were too quickly released from the 20-30 nm pores of the silica colloids. Thus, the desired time-release characteristics were not realized.

Next, polymeric colloidal synthesis approaches were evaluated. The first polymer evaluated was poly(propylene carbonate) QPAC40 (Empower Materials, Newark DE), a water insoluble polymer that could be dissolved in acetone and subsequently mixed with water to form 200-600 nm colloids. The acetone was removed by evaporation and dialysis. The resulting aqueous colloidal suspensions were stable for several months. Electrophoretic measurements determined that the QPAC colloids had a zeta potential in simulated groundwater of -17 to -20 mV, similar to that of natural colloids found in INEEL Spreading Area B soil

samples (-15 mV). Unfortunately, with these colloids the investigators were unable to load a significant amount of nutrient into the particles. Subsequently, polyphosphazene polymers were investigated with primary focus on poly (bis phenoxy) phosphazene (PPOP). With an emulsion technique, PPOP particle size distributions with mean diameters of 175 - 240 nm could be generated. Phenol could be incorporated into the PPOP, but thin film experiments indicated that, although phenol release could be detected over 1 week, approximately 90% of the phenol was released within the first five hours. This release rate was likely to be even faster with nano-particles because of their high surface area, and this was deemed too fast for use as a gradual release system.

Because of the difficulties with phenol, the investigators decided to concentrate on the preparation of particles from polylactic acid (PLA). It was hypothesized that hydrolysis of the polylactide, either abiotically or biotically, could be a mechanism for generating bioavailable lactate, as lactate is a commonly used carbon source for microorganisms. Two approaches were tried for synthesis of PLA nano-particles, a supercritical anti-solvent (SAS) process and an ultrasonic mixing and precipitation technique. The SAS process did not attain the desired particle size (<500 nm diameter), but the ultrasonic mixing technique did, generating a median particle size of approximately 390 nm.

*Bioavailability of phenol*. Simultaneous to the work on the synthesis of phenol-laden particles, the investigators focused on developing a rapid method for determining whether phenol was effectively delivered to cells for metabolism. The bacterium *Burkholderia cepacia* G4, a common rhizosphere organism that can cometabolically degrade TCE using the enzyme toluene-2-monooxygenase was used in the laboratory experiments. This enzyme can be induced by phenol, and its activity in the cell can be observed by the production of a fluorescent product from the enzymatic substrate 3-hydroxyphenylacetylene (3-HPA). Conditions for maximal 3-HPA oxidation (formation of fluorescent product) were determined and optimized by members of the research team, and this resulted in both a presentation at a national meeting, and the preparation and publication of a peer-reviewed paper on this technique. The investigators also verified that the candidate carrier materials themselves were not inhibitory to G4's growth.

*Biodegradation of polylactide particles*. The ability of the PLA particles to support microbial growth was tested in two experiments: one anaerobic, one aerobic. In the anaerobic experiment, PLA particles were provided to inocula derived from mixed cultures from INEEL Test Area North aquifer samples that had been maintained on sodium lactate. Microbial activity was monitored for eight months. Triplicate vials were compared with triplicate samples from three other treatments: culture with lactate provided at the same mass concentration as the PLA, culture without PLA or lactate, and a killed ($ZnCl_2$) control with the colloids. The parameters measured included volatile fatty acids (VFA), acridine orange (AO) total cell counts, and lactate. At the end of the experiment, the investigators also measured headspace $CO_2$ and methane, and estimated ATP content of the cells using a fluorescent assay (G.E. Betz BIOSCAN 2). Unfortunately, the VFA analyses showed no significant differences between the live culture treatments during the course of the experiments, and lactate measurements were not possible because of apparent interferences from the particles. Total cell counts also were problematic because the colloids (of similar size to the cells) were stained by AO. $CO_2$ and methane measurements were similarly inconclusive; only the ATP measurements appeared to indicate a significant difference ($P < 0.05$; Student's t-test) between the PLA treatments and the other three treatments. The ATP concentrations were highest in the PLA-amended cultures, suggesting that the PLA colloids were more effective at supporting microbial activity over an extended time period than the lactate solution.

Aerobic biodegradation experiments were conducting using the bacterial culture *B. cepacia* G4, which, in addition to phenol, is known to grow on lactate. In these experiments, growth of G4 on PLA (triplicate vials) was compared to growth on an equivalent mass of lactate. The experiments were conducted in a minimal salts medium, and the following controls also were set up: 1) G4 added to the medium alone, and 2) PLA in the medium

without G4. The treatments were monitored for cell growth by AO. After two weeks, results indicated that although G4 did not appear to grow on the PLA, an apparent bacterial contaminant derived from the colloid suspension itself was growing on the PLA. The PLA had not been autoclaved prior to the experiment because of concerns that autoclaving would alter the colloidal properties of the PLA. Over the course of two weeks the cell numbers in the PLA treatment without G4 increased by 3 orders of magnitude. The morphology was different from the G4 cells, indicating that this was a different species (or multiple species). However, additional experiments will be required to confirm that PLA can support growth.

*Column transport experiments*. Bench-scale columns (4.1 cm i.d., 5 cm length) containing crushed INEEL basalt (300-600 nm size; pore volume 17 ml) were constructed for transport studies with the synthetic colloids. Effluent was collected in a fraction collector and analyzed with a Coulter N4 submicron particle size analyzer. PLA colloids were suspended in DI water and also in aqueous solutions of varying ionic strength (adjusted with NaCl), and breakthrough of pulses of the colloid suspensions was monitored. Results indicated that PLA colloid transport did not follow the expected behavior for colloid transport with respect to the measured zeta potential. Even at zeta potentials where the colloid would be expected to be stable in suspension, minimal breakthrough was observed. Flocculation and/or sorption were apparently occurring. Resources were not available to pursue this surprising result further.

*Modeling of colloid transport and release of substrate*. Modeling for this application must include both transport of the colloid in porous media, and release of the carried substrate from the particle. It was determined that currently available models, based on filtration theory in a continuum, would be appropriate for predicting and simulating colloid transport behavior. However, these models lack a kinetic term that will permit modeling slow diffusion of solutes from a mobile source (colloid). The investigators planned to modify the models to incorporate solute diffusion from a spherical particle based on Fick's law, which is already well established in the literature. However, because of the aforementioned difficulties with respect to particle synthesis and demonstrating effective transport of the particles, and the consequent diversion of project resources, development and parameterization of a model to describe colloid transport in conjunction with slow diffusion of a solute from the colloid was not further pursued.

Despite the challenges that arose during this LDRD, research efforts resulted in increased experience on the part of INEEL personnel with respect to nano-particle synthesis and characterization, and the development of a method for the reproducible generation of polylactide colloids that may be able to serve as microbial nutrients. These capabilities should benefit future research requiring the synthesis, characterization, and testing of nano-particles for environmental applications.

Recent progress with respect to the synthesis of PLA particles, and hints at their ability to support microbial growth over long time periods, suggest that this line of research may be worth pursuing. The investigators have discussed this project work with researchers at other universities, and collaborations are being pursued. In the long term, if this research line proves fruitful, it could ultimately lead to significant cost savings to DOE by providing a more efficient means of delivering nutrients to a subsurface contaminated zone undergoing bioremediation.

# Supercritical Fluid Catalyst Regeneration Chemistry

*Daniel M. Ginosar*

***Increasing catalyst longevity and industrial safety***

SC116

Recently, the INEEL has developed a novel, non-oxidative regeneration technology for solid acid catalysts. The regeneration process, termed reactive supercritical fluid regeneration (RSFR), exploits the extractive properties of supercritical fluids (SCFs) to dissolve and remove hydrocarbonaceous compounds from catalyst surfaces to restore catalyst activity. The RSFR technique could have a huge technical and economic impact on industrial heterogeneous catalytic reactions by reversing catalyst fouling, increasing catalyst longevity and energy efficiency, and enhancing industrial safety. To appreciate the advantages and limitations of the RSFR method, it is necessary to develop knowledge of the compounds that deposit and buildup on the catalyst surface, to understand which compounds are either reacted/solubilized by the SCF or trapped by the catalyst itself. Although several studies have explored the coking of isobutane/butene alkylation catalysts, these studies showed that deactivation is highly dependent on the specific catalyst and reaction conditions.

This LDRD is focused on understanding the chemical nature of the coke deposited on a USY zeolite used for isobutane/butene alkylation reaction at 60°C (333 K) and 1,600 psi (11032 kPa). Catalysts were deactivated to different levels by running the reaction for different times on stream (TOS) ranging from 0 to 380 min, removed from the reactor, and interrogated by various off-line spectroscopic and instrumental techniques to determine the chemical species formed on the catalyst surface. These data were needed to establish a base case for comparison with future catalyst regeneration data.

Technical objectives for fiscal year 2003:

- Determine the nature of chemical and physical phenomena occurring on the heterogeneous catalyst surface
- Develop an understanding of how coke compounds and catalyst fouling change as a function of reaction time on stream (TOS).
- Determine what compounds the reactive supercritical fluid regeneration (RSFR) process can remove from the deactivated catalyst.
- Determine how the catalyst pore structure affects the RSFR process.

The research work performed so far has focused on understanding the chemical nature of the coke deposited on a USY zeolite utilized for isobutane/butene alkylation reaction at 60°C and 1600 psig. The catalysts were deactivated to different levels by running the reaction for different times on stream (TOSs) ranging from 0 to 380 min. The used catalysts were removed from the reactor and submitted to TPO, DRIFTS and UV-Vis spectroscopy measurements to determine the chemical nature of the species being formed on the catalyst surface before regeneration. Surface area and pore volume of fresh and used catalysts were determined by traditional $N_2$ physisorption techniques. Ammonia chemisorption was utilized to determine catalyst acidity. Elemental analysis was performed to account for the carbon content of the catalyst samples.

The mass of hydrocarbon species retained on the catalyst surface increased with TOS. At the onset of the deactivation stage, the amount of weakly adsorbed hydrocarbon species reached a maximum and an increase of heavier species was found afterwards. Hydrocarbon adsorption and aging produced a marked decrease in micropore volume and internal surface area indicating that most of the coke was deposited inside the zeolite micropores. A very small amount of hydrocarbons was adsorbed while pressurizing the system with isobutane before starting the alkylation reaction. After contact with the feed containing butene, mainly paraffinic and small amounts of alkenyl-like species were found adsorbed in the zeolite micropores. Both the chain length of those species and their degree of unsaturation/conjugation increased with TOS.

This LDRD project resulted in a presentation at a national societal meeting. Three additional presentations have been submitted and are currently under review.

Knowledge gained from this investigation will have significant impact on the use of heterogeneous catalysis and will lead to new research into SCF regeneration techniques. A better understanding of the regeneration chemistry will also lead to a broad array of heterogeneous catalyst applications. Successful work in this area will build the strengths of the chemistry department and position the

INEEL research team to develop successful proposals for external, follow-on projects specifically targeted to DOE-OS, DOE-EE, and DOE-FE customers. DOE-OS is currently working to develop a large multi-year program in catalyst science. Additional research opportunities include the DOE-EE Industry of the Future program, and DOE-FE gas-to-liquids and environmental programs. Having a strong technical foundation for this technology is imperative to obtaining government and industry support.

# Human Factors for Management of High Consequence Events

*Bruce Hallbert*

***Reducing risk to first responders***

ET121

First responders, the front-line groups that deal with the immediate effects of high-consequence events, are at the highest risk for their personal safety. A single catastrophic incident can account for the majority of first and other responder work-related fatalities in a single year. Depending on the nature of the event, first responders may include groups and organizations that are unaccustomed to working together. Such organizations may have very different accident management methods and techniques that could impede the effectiveness of co-intervention.

Effective command, control, and coordination among and between different accident responders are vital to minimize loss of life and property, contain and control the effects of the event, and to recover vital systems and operations. Information management and organizational performance is key to achieving effective command and control. Information is needed at all levels of the command hierarchy and throughout the distributed emergency response organization so that situational awareness is developed and maintained. In a diversely structured command and control organization such as those envisioned for high-consequence and mass casualty events, practices for the use and management of information are needed to ensure coordination among organizations and to provide protection – especially of first responders.

The objectives of this LDRD are two-fold: to investigate models of information management for high-consequence events that include models of the organizations involved to identify critical knowledge for response management, and to contribute to the development of the technical basis for effective emergency management.

Technical objectives for fiscal year 2003:

- Identify and select an aspect of the emergency management organization for study in this research.
- Develop necessary protocols for interacting with the selected organization.

This LDRD project was a late start in FY03. An objective of this first year's research was to characterize factors that affect the activation of functions involved in the response to mass casualty events. Vanderbilt University was recently awarded a national grant by the U.S. government to operate the National Center for Emergency Preparedness. Located in the medical school at Vanderbilt University, the Center will focus on research and training to prepare first responders from the medical and health care disciplines. The Center has indicated a willingness to collaborate with INEEL on research to better understand the human factors aspect of medical first response to mass casualty events. As a result of work conducted in FY03, the emergency medical healthcare delivery functions of emergency management operations have been selected for study in this project.

# Model-Based Decision Making

*Jerry L. Harbour*

***Turning decision models into valuable decision-support tools***

ET117

There is a need to better understand how decision models can be effectively translated into decision tools. This LDRD investigates this issue, and has led to the development of a computer-based decision tool termed *RapidOps*. *RapidOps* is a time- and probability-based modeling tool especially well suited for time-critical or time-sensitive operations. The system links time and probability modeling in a graphical, intuitive, easy-to-use, and field-deployable computer-assisted work environment. Specifically, it can assist decision makers in modeling and assessing time-critical operations, including evaluating emergency response capabilities, modeling physical security vulnerabilities and counter response capabilities, and supporting time-critical hazardous and other time-sensitive operations. Of particular note is the ability to quantitatively assess the contribution of new rapid response-type technologies and associated system configurations.

Technical objectives for fiscal year 2003:

- Pursue copyright approval for *RapidOps* software.
- Evaluate *RapidOps* applicability in limited operational settings.
- Make enhancements to version 1.0, including:
  - Add various graphics capabilities.
  - Modify associated database to allow user input.
  - Create embedded user guide.
  - Develop completely new Activity Time module with real-time support and statistical modeling capabilities.
    - Present papers at industry conferences and publish a peer-reviewed article.

FY03 efforts primarily involved enhancing *RapidOps* version 1.0, as well as creating new features. *RapidOps* is a time and probability-modeling tool especially well suited for assessing and evaluating time-critical or time-sensitive operations. The developed system links time and probability modeling in a graphical, intuitive, easy-to-use, and field-deployable computer-assisted work environment. Specifically, it can assist decision makers in modeling and assessing:

- Emergency response capabilities,
- Physical security vulnerabilities and counter-response capabilities, and
- Any time-critical or sensitive operation.

One such feature is *ActivityTimer* (Fig. 1). *ActivityTimer* allows real-time tracking of any activity and provides feed-forward information, permitting supported real-time decision-making. *ActivityTimer* also permits cumulative statistical analyses (Fig. 2). *ActivityTimer* has particular application in supporting work activities in contaminated operational settings (e.g., radioactive) where time-related monitoring and real-time tactical decision making is of utmost importance.

03-51139-250

*FIGURE 1. Screen capture illustrating the real-time tracking capability of* ActivityTimer.

03-51139-249

*FIGURE 2. Screen capture illustrating the statistical trending capability of* ActivityTimer.

Beta testing in FY03 indicated broad applicability and user-friendly applications. One initial insight gained in the beta testing is the importance of a user-modifiable database and robust, field-verified

time data. Consequently, the potential value of *ActivityTimer* in collecting field data is especially significant.

Copyright approval was received in FY03 on the *RapidOps* software. A paper was presented at MTS/IEEE Oceans 2002 Conference: "Assessing offshore vulnerabilities and counter-response capabilities using RapidOps," and an oral presentation was made at the 2002 Waste Management Conference. In addition, the investigator co-authored a paper, "Two Views of Public Participation," published in *Radwaste Solutions'* March/April 2003 issue.

*RapidOps* has potentially broad application including security, emergency response support or time-critical operational planning, assessment, and execution support. Of particular importance is its demonstrated ability to assist in quantitatively assessing response capabilities for a wide range of differing events, especially in terms of evaluating the contribution of various technologies and system configurations. The work completed under this LDRD has generated considerable interest by various government agencies, including the DOE, Army Corps of Engineers, and the Nuclear Regulatory Agency.

# Designing Advanced Emergency Response Planning Support Systems

*Jerry L. Harbour*

***A better model for understanding events as they occur***

ET120

The ability to rapidly and accurately plan an emergency response is of vital importance. In such situations, three key questions are frequently asked of response planners: 1) What is happening – requiring some type of descriptive model, 2) What could happen – requiring some type of predictive model, 3) What actions should be taken – requiring some type of action model.

This LDRD looks at how one might improve the use of spatial imagery (e.g., maps, aerial photos, satellite photos, etc.) in time-critical, emergency response "descriptive" modeling. Specifically, two questions were explored in this research.

- How rapidly and accurately do people detect changes (either during slow or rapid-onset disasters) using spatial imagery (e.g., such as when comparing two similar photos taken at differing times)?
- How can the detection of such changes be improved via advanced computer support presentation methods?

To answer these two important questions, an experiment was conducted involving a series of satellite imagery change detection tasks using three different presentation conditions. Results of the experiment indicated that one method was statistically significant in terms of both speed and accuracy.

Technical objectives for fiscal year 2003:

- Design an experiment to assess the ability of subjects to identify subtle changes in satellite imagery using three different, computer-based experimental conditions.
- Collect and prepare all satellite photos for subject viewing.
- Develop and test all experiment protocols.
- Obtain Internal Review Board (IRB) approval.
- Develop in-house, real-time tracking software required to conduct experiment.
- Conduct experiment using 45 subjects.
- Analyze data.
- Prepare in-house report.

In many emergency response planning situations, a "what is happening" descriptive model is required. Frequently, temporally sequenced spatial imagery is used to assist in answering this "what is happening" question. For example, spatial imagery may be used to plot the evolution of an emergency event through space and time, as illustrated by a spreading wildfire. A common use of spatial imagery, and in particular aerial-collected imagery, involves a comparison between two geographically referenced images with the intent to detect and assess any temporal changes.

Such a comparative analysis is termed *change detection* and refers to the technique of comparing a pair of images that have been collected from approximately the same geo-referenced areas but at different times (e.g., before, during, and/or after an event).

An experiment involving a series of satellite imagery change detection tasks and using 45 subjects, sought to explore how differing computer presentation modes can affect both change detection speed and accuracy. The three experimental conditions included:

- A side-by-side comparison method that presented the to-be compared images on two separate monitors.
- A flip-flop or "back and forth" method using one monitor.
- An altered flip-flop method (termed the flicker condition) using one monitor with a gray screen between the two displayed images that appeared for 150 ms. The purpose of this condition was to purposely dampen after-image and iconic sensory memory by creating a momentary "flicker" with the embedded gray screen.

The experiment was divided into two phases. In the first phase, subjects viewed satellite images that had been purposely altered. The reason underlying this manipulation was to allow the experimenters the ability to explicitly control changes in the images. Such manipulation ensured that participants would not learn to look in certain areas of the image for changes and that they also did not learn or try to predict what type of image change would occur next. In the second phase of the experiment, natural images of a similar geographic area taken at different times were used.

In all, twenty satellite images were used in the experiment. Both medium-resolution/wide area coverage LANDSAT images and high-resolution/

small area coverage IKONOS (from Space Imaging) images were used. Additionally, both black and white and color image sets were displayed.

Statistically significant differences among all three conditions for the amount of time required to detect changes (p = .0001) were observed. Mean times (per image) were 24.91 seconds for the flip-flop condition, 96.22 seconds for the flicker condition, and 156.65 seconds for the side-by-side condition. Post-hoc tests showed that participants in the flip-flop condition were significantly faster than participants in the side-by-side condition (p = .0001) and the flicker condition (p = .006). Participants in the flicker condition also were significantly faster than participants in the side-by-side condition (p = .021).

Statistically significant differences among all three conditions on accuracy (p = .0001) also were observed. Mean accuracy for the six, purposely changed images was 98.05% for the flip-flop condition, 61.34% for the flicker condition, and 78.48% for the side-by-side condition. Post-hoc tests showed that participants in the flip-flop condition were significantly more accurate than participants in the side-by-side condition (p = .0001) and the flicker condition (p = .0001). Participants in the side-by-side condition also were significantly more accurate than participants in the flicker condition (p = .008).

As experimentally demonstrated, presentation mode of spatial imagery (e.g., aerial imagery) can have a profound effect on both speed and accuracy. In these cases, the flip-flop condition was both faster and more accurate than the side-by-side condition and/or the flicker condition (Fig. 1). The side-by-side condition, although accurate, was slow. Conversely, the flicker condition was relatively fast, but not very accurate.

The experimental findings in this LDRD have practical application for any organization involved in varied imagery detection tasks. Particular opportunities include environmental monitoring and military applications, and support INEEL EM and security missions.

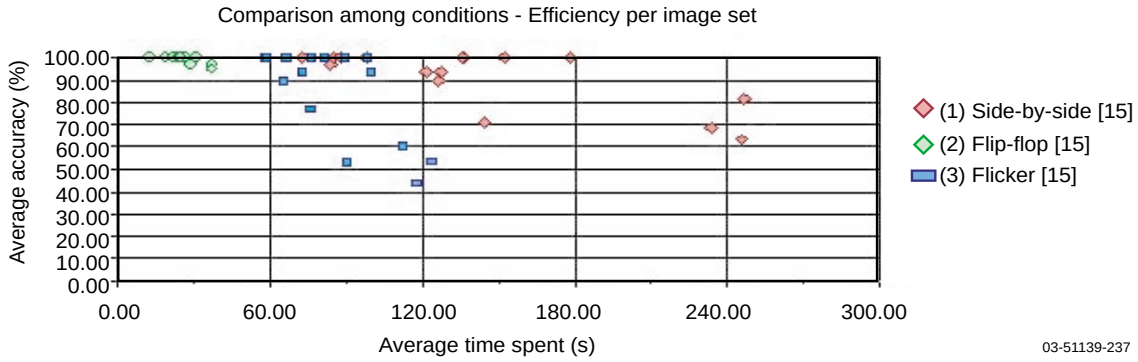


*FIGURE 1. A graphical plot comparing mean time vs. mean accuracy for each of the three experimental conditions.*

# Nanostructure Characterization for Sensing

*David Hurley*

## *Controlling material properties with acoustic waves*

NC101

Acoustically induced confinement is very appealing for use in structures with nanometer-size dimensions because the parameters that dictate the material properties of a confined system (i.e., confinement boundary conditions) can be easily controlled in situ by changing the parameters of the acoustic wave, such as wavelength and wave amplitude.

This LDRD focuses on methods to create quantum-confined devices using picosecond surface acoustic waves (SAWs). Supporting work conducted at the Applied Solid State Physics Laboratory, a division of the Physical Science and Engineering Graduate School at Hokkaido University, involved investigating the interaction of quasi-static electric fields with photoexcited carriers in piezoelectric semiconductors. This research will serve as a baseline to gauge the magnitude of the lateral confining potential provided by surface acoustic waves in GaAs quantum wells.

Technical objectives for fiscal year 2003:

- Modify an existing picosecond acoustic facility to measure photoluminescence of SAW-induced quantum structures at cryogenic temperatures.
- Devise and carry out experiments to study the interaction of photoexcited carriers with near-surface piezoelectric fields in AsGaAs.
- Devise and carry out experiments to generate and detect near THz shear waves using an off-axis detection scheme.

An experiment has been designed and implemented that measures the photoluminescence of samples placed in a cryostat. Optical access to the cryostat provides a means to generate and detect picosecond surface acoustic waves, as well as measure changes in the photoluminescence spectrum resulting from acoustic confinement. The photoluminescence setup uses a three grating spectrometer, a thermoelectrically cooled CCD

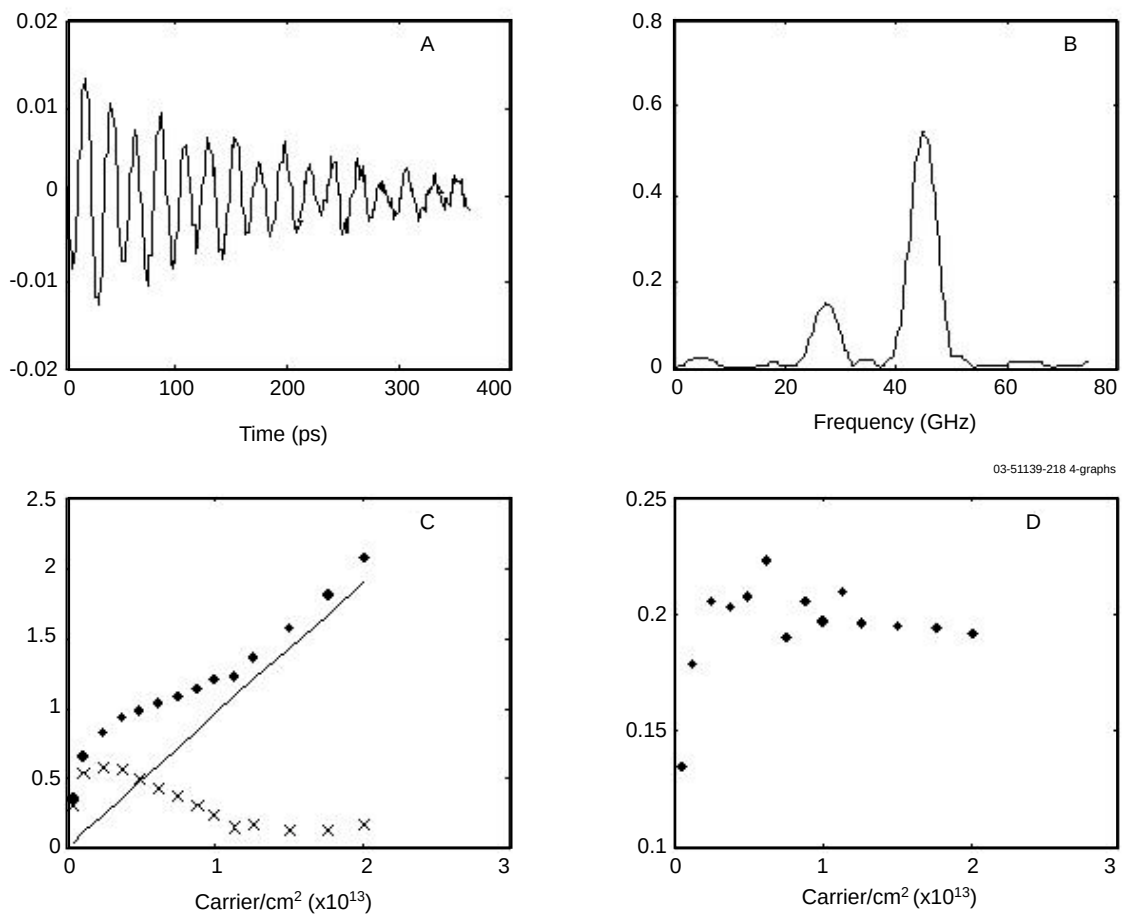


*FIGURE 1. a) Oscillatory portion of signal with background subtracted, b) Fourier transform of data, c) (dots) Fourier amplitude of longitudinal wave, (solid line) linear fit to last five data points, (x) solid line subtracted from dots, d) Fourier amplitude of shear wave.*

detector, and polarizing optics to maximize the throughput of the system. A specially designed AsGaAs quantum well sample with a 50 nm absorption grating for proof of principle studies has been constructed by OSEMI, Inc.

Picosecond acoustic waves were generated and detected in [114] GaAs using a pump/probe technique. Acoustic generation involved pumping the sample at normal incidence with the frequency-doubled output of a femtosecond Ti:sapphire laser (400 nm pump beam, spot size ~ 500 $\mu m^2$) and subsequent conversion of the absorbed energy into acoustic phonons. Laser detection of the acoustic pulses propagating into the sample was accomplished by monitoring strain-induced changes in the sample reflectivity using a delayed probe beam (800 nm, spot size ~ 50 $\mu m^2$, collinear with the pump beam). A typical plot of the reflectivity change as a function of delay time is shown in Figure 1a. The origin of the oscillatory portion of the reflectivity signal is as follows. A portion of the probe beam is reflected from the sample surface. Another portion of the probe beam is transmitted into the sample and is reflected from strain-induced changes in the refractive index associated with propagating bulk acoustic modes. These two beams constructively and destructively interfere as the acoustic pulse propagates away from the sample surface. These oscillations have two frequency components that are governed by $n=2vn/\lambda$, where v is either the shear or longitudinal velocity. Two frequency components are clearly discernable from this graph.

The Fourier amplitude spectrum of this data is plotted in Fig. 1b. The peak at 27.4 GHz is associated with the quasi-shear mode propagating at 3.02 μm/ns, and the peak at 45.0 GHz is associated with the quasi-longitudinal mode propagating at 4.97 μm/ns. These experimental frequencies correspond well with the predicted frequencies of 44.8 GHz and 27.3 GHz for the quasi-longitudinal and quasi-shear wave respectively ($n=2vn/\lambda$, n(810 nm)=3.66)). As predicted, the pure shear mode with a velocity of 3.24 μm/ns and a predicted frequency of 29.3 GHz is not excited. The role of anisotropy in the generation of acoustic waves due to thermoelastic, concentration deformation, and inverse piezoelectric mechanisms is currently being considered. Developing a clear understanding of these sources of shear acoustic waves will help determine the magnitude of the static electric field associated with surface acoustic waves in piezoelectric semiconductors.

This work was performed to better understand the interaction of acoustic waves with carriers in piezoelectric semiconductors and to understand the influence of quantum confinement on the nonlinear optical response of structures with nanometer size dimensions. This approach is of fundamental importance to the field of semiconductor physics as it holds the potential to develop new devices at the nanometer scale. To further bolster this research effort, collaborations have been established with the physics department at the University of Utah and researchers at the Naval Research Laboratory at Schott Glass. Efforts are underway to obtain direct funding through DOE-BES and/or other agencies to further the research pursued thus far.

# Surface-Sensitive Laser Acoustic Studies of Heterogeneous Catalysis

*David Hurley, Harry Rollins, Dan Ginosar, John Walter, Ken Telschow*

***Controlling the parameters of the catalytic process***

SC118

Research involving the fundamental microscopic details of catalytic processes is an emergent field that has been recently bolstered by new surface-sensitive analytical techniques. Realization of artificial control of the parameters that define the catalytic process will rely heavily on further development of surface-sensitive techniques.

This LDRD seeks to investigate and control heterogeneous catalysis using a novel surface-sensitive sonochemical technique that utilizes coupling between laser-generated surface acoustic waves (SAWs) in the catalyst material (laser ultrasonics) and surface reactivity. This work is a cross-disciplinary effort carried out in coordination with the Laser Ultrasonics Group and the Supercritical Fluids Group at the INEEL.

Technical objectives for fiscal year 2003:

- Design reaction cells amenable to contact acoustic experiments.
- Design and implement experiment that utilizes various acoustic transduction methods generating SAWs inside the reaction cell. This design should be capable of generating both standing and traveling SAWs.
- Develop spectroscopic techniques that give enhanced spatial resolution.

A reaction cell for investigation of the effects of surface acoustic waves on catalytic reactions has been designed and constructed (Fig. 1). The reaction cell will be connected to a gas phase circulation apparatus and the reactant and product concentrations will be determined by gas chromatography. The system temperature is maintained with a temperature controller and cartridge heaters. The reaction cell has a high temperature feed-through to allow the use of comb-type transducers for the generation of surface acoustic waves. The 2” square quartz window allows the catalyst surface to be imaged, both for characterization of the surface acoustic field, as well as for in situ spectroscopic determination of reactant and product distributions.

In a typical experiment, the system will be evacuated and the preheating zone and reactor brought to desired temperature and allowed to equilibrate. The valve to the vacuum pump will be closed, and the bellows pump will be turned on to circulate gas through the reactor. The desired quantity of ethanol will be drawn in by vacuum or introduced through a septa or sample injection valve. Then oxygen will be introduced using a regulator and needle valve. The pressure and temperature of the system are continuously monitored. Typically, reactions will be carried out at 60 torr (vacuum) and ~100ºC, although temperatures up to 400ºC may be used. The surface acoustic wave field will be characterized using interferometry. Determination of the reactant and product concentrations is discussed in the spectroscopic technique section of this report.

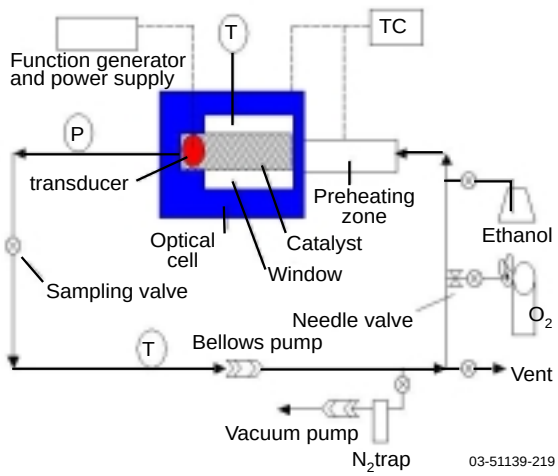


*FIGURE 1. Experimental configuration for examining the effects of surface acoustic waves on gas phase catalytic reactions.*

A comb transducer for generating narrowband SAWs has been fabricated and tested. Like its name suggests, acoustic transduction is accomplished by spatially modulating the contact surface between the transducer and the sample. The comb itself is made out of a high-temperature buffer rod to thermally isolate the hot sample surface from the longitudinal transducer. The center frequency of the comb is approximately 1 MHz and has a bandwidth of 0.3 MHz. The maximum out-of-

plane displacement of approximately 10 nm was measured using an electro-optic modulator placed in the reference arm of the interferometer. For a center frequency of 1 MHz, a 10 nm displacement corresponds to a strain on the order of $10^{-5}$. Two important experimental variables that dictate the effect of SAWs on surface catalysis, frequency, and strain amplitude are easily controlled with this setup.

In addition to mechanical transduction, current efforts are underway to generate narrowband SAWs using pulsed laser techniques. Figure 2 shows a typical interferometric trace for the out-of-plane displacement produced using a thermal grating set-up by crossing two laser beams at the sample surface. To avoid the unwanted effects due to laser heating of the gas phase reactants, future plans call for the introduction of the grating at the interface between the thin film catalysis and the transparent substrate.

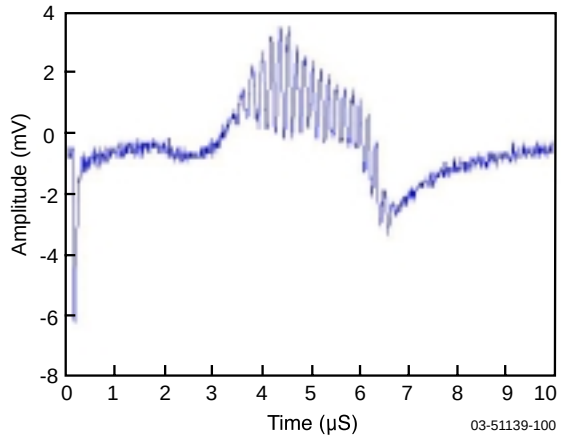


*FIGURE 2. Out-of-plane displacement of laser-generated narrowband surface acoustic wave.*

A Raman chemical species detection system that utilizes a three-grating spectrometer and a thermoelectrically cooled CCD detector is currently being developed. This system has been designed to be used concurrently with the interferometric acoustic detection system and uses the same laser (5 Watt diode-pump ND:YAG). Since the Raman signal is inherently weak, every effort has been made to boost the system sensitivity. In addition, preliminary experiments will involve catalytic systems that exhibit surface-enhanced effects such as silver substrates that have been chemically roughened.

This LDRD involves the development of a novel surface-sensitive sonochemical technique to study and control heterogeneous catalysis. Results from this research may serve as the framework for future work from various DOE Program Offices such as the Office of Science. Furthermore, since external control of the catalytic process is relevant to many energy-relevant chemical processes, this work also serves the missions of the DOE Office of Energy Efficiency and Renewable Energy and the Office of Fossil Energy.

# DOE Complex-Wide Long-term Stewardship Options Analysis System

*Jacob J. Jacobson, Sharon Berrett*

***Visualizing end-state site scenarios at INEEL***

ST107

The INEEL does not have a common repository or quick-retrieval method for documents for the multitude of operable units pertaining to waste site management. Currently, if documents need to be reviewed for a particular site, personnel have to search through archives trying to locate site identification numbers and site documents.

This LDRD is investigating a web-based application that can provide map-based, near-real-time information on current INEEL waste sites. The application gives users access to contact information for facilities, Waste Area Groups, related documents, activity status, contamination constituents, as well as proposed cleanup activities. In addition, this application examines, from a more holistic perspective, the cleanup activities at multiple sites to determine if the cleanup work at the individual sites is compatible with the entire area and with INEEL end-state planning.

Technical objectives for fiscal year 2003:

- Complete centralized web-based access to information about a site or facility.
- Enable web-based options analysis of cleanup strategies and effects on end-state planning.
- Develop expertise in System Dynamic modeling.
- Develop expertise in Bayesian Decision Network analysis.
- Develop expertise in Graphic Information Systems (GIS) and Geomatics (Graphical Analysis Systems).

The research performed under this LDRD is innovative in several ways. First, it combines several new technologies into a comprehensive tool. These technologies include computer simulation, GIS, and the Internet. The outcome will be a powerful simulation tool that is visually appealing, intrinsically easy to use, and operates over an Internet browser. Browser access bridges the computer operating system limitations and allows access to anyone with a network or modem connection to run the application regardless of the operating system and computer type.

Secondly, this research broadens the use of System Dynamics and computer simulations into the environmental management areas. This research also takes advantage of the ability of GIS to allow data management and access through a graphical display (Figs. 1 and 2).

FY03STI07_fullpage

*FIGURE 1. GIS interface allows the user to select different features for viewing and information retrieval.*

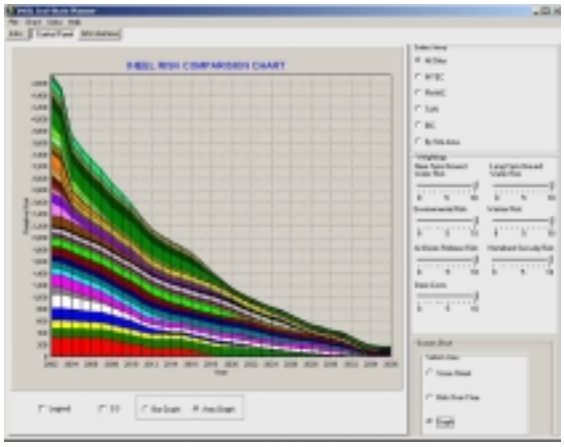

FY03STI07_RiskChart

*FIGURE 2. Screen view shows the cockpit for adjusting the risk weightings on seven different criteria and the resultant output of the profile of risk reduction throughout the cleanup operations at the INEEL. By adjusting the weightings between the various risk components, cleanup projects change in priority, and the user can determine whether certain projects should be started sooner or delayed.*

The end product of this effort is applicable to a wide range of areas. The rapidly developing field of decision-making models will benefit from the research conducted under this LDRD. It also is expected that the final products of this LDRD will improve the interface between science and public policy. The program is already being used in planning sessions for Test Area North and Power Burst Facility, and continued use is expected next year.

By centralizing vital information in a web-based, easily accessible form, this type of tool will be valuable at the INEEL, other DOE facilities, DOD, and Federal waste sites. Future development and implementation of this program is currently being planned for the Idaho Closure Project End State Planning, Long Term Stewardship (LTS) areas, and has been included in their work plan for FY04. In addition to being leveraged with other research in the Long-Term Stewardship Initiative, this tool is being looked at for use in specific management areas such as flood and fire control.

Discussions have been initiated with EPA and the Department of Interior over potential uses of this tool with each of their respected LTS Programs. Follow-up discussions with EPA are already scheduled. Contact with DOI will follow from this work with EPA. Additional proposals have resulted from this research including one with the U.S. Army Research Laboratory and a proposal to the U.S. Bureau of Reclamation. This work has been presented at several professional meetings, and a paper has been submitted to the American Nuclear Society for publications.

# Developing a Predictive Decision Network for Long-Term Stewardship

*Kevin M. Kostelnik, Jerry L. Harbour*

***Developing a predictive decision network for long-term stewardship***

PH103

Numerous activities generate hazardous byproducts. In many instances, such hazards cannot be completely removed and must reside in the environment for extended periods of time. The environmental management of such hazards is termed "residual hazards management." Residual hazards management may be defined as the identification/delineation, assessment, selective removal, control, and/or monitoring and maintenance of an enduring source of danger.

The goal of this LDRD is to define an improved sustainable environmental protection system for the management of residual hazards. A sustainable system would require the integration of both engineered and institutional controls to isolate residual contaminants, and thus minimize the associated hazards. *Engineered controls* are physical modifications to the natural setting and ecosystem including the site, facility, and/or the residual materials themselves to reduce or eliminate the potential for exposure to contaminants of concern. *Institutional controls* are processes, instruments, and mechanisms designed to influence human behavior and activity. These mechanisms generally take the form of legal or administrative restrictions, but also may include containment system monitoring and maintenance.

System failure can involve hazardous material escaping from the confinement because of system degradation (i.e., chronic or acute degradation) or by external intrusion of the biosphere into the contaminated material because of the loss of institutional control.

Technical objectives for fiscal year 2003:

- Make presentations of research results at Vanderbilt University and at the Annual Society of Risk Analysis Conference.
- Complete a case study paper and a paper on the practice of institutional controls.
- Conduct site visits and prepare follow-on reports of each.

The ongoing research conducted under this LDRD suggests that the significance of the loss of institutional control pathway is a critical pathway because decisions made during the operations/remedial action phase, as well as decisions made throughout the residual hazards management period, are key to the long-term success of the prescribed system. In fact, given that society has become more reliant on and confident of engineered controls, there appears to be a growing tendency to be even less concerned with institutional controls. As such, obtaining a better understanding of the factors that influence the failure of institutional controls becomes even more important and represents the key focus of this LDRD.

This research is assembling a series of historic and contemporary case studies to provide insight into how various residual hazard systems have performed historically and why some systems have failed or succeeded. The following objectives were accomplished this fiscal year.

Presentations made:

- "Residual Hazards Management," Vanderbilt University (November 5, 2002) and at the Annual Society of Risk Analysis Conference (December 5, 2002).
- "Institutional Controls of Residual Hazards," Vanderbilt University (March 12, 2003).
- "Improving Institutional Controls for Residual Hazards Management," U.S. Army Corps of Engineers (February 14, 2003).

Papers completed:

- "Case Study Protocol for Residual Hazards Management" (December 10, 2002)
- "State of the Practice of Institutional Controls" (March 10, 2003)
- "Residual Hazards Management Framework" (April 18, 2003)

In addition to the above accomplishments, site visits were conducted at Maxey Flats Disposal Facility, Love Canal Waste Disposal Site, Burrell UMTRA Disposal Cell, Canonsburg UMTRA Disposal Cell, and Rocky Mountain Arsenal. Case study reports were completed on Maxey Flats, Love Canal and Canonsburg.

An abstract titled "A Sustainable Environmental Protection System for the Management of Residual Hazards" also was accepted for the Society of Risk Analysis Annual Meeting 2003 Conference (December 8-10, 2003).

The work completed under this LDRD has application across the nation, both within and outside of the DOE complex. Indeed, any agency responsible for the management of residual hazards can directly benefit from this study.

# Enhanced Transport in Nano-Crystalline Ceramic Films

*Paul A. Lessing, Gary Huestis*

***Improving ionic conductivity***

NC 103

Some ceramic oxides have the potential for enhanced ionic transport due to nano-crystalline grain boundaries. This enhancement could bring orders of magnitude improvements to a number of applications, including extremely useful applications related to many hydrogen transport devices.

The goal of this LDRD is to investigate, using organo-metallic precursors, the synthesis and fabrication of nano-crystalline ceramic thin films that would exhibit greatly enhanced transport (e.g., 1000X faster) of ions (e.g., protons) through their grain boundaries. Dense, nano-crystalline films were successfully fabricated on silicon substrates using two separate synthesis routes for two different NASICON-type compositions. Deposition of multiple layers, deposition on micro-porous alumina substrates, and depositions on Pd/Ag electrodes were demonstrated.

Technical objectives for fiscal year 2003:

- Develop organic, non-hydrolytic, precursor route for Na-NASICON thin films.
- Develop techniques for multiple coatings using a chelated-polymer precursor route for Sn-NASION thin films.
- Develop coating techniques for deposition on substrates and electrodes having extremely fine pores.
- Submit paper to Journal of Membrane Science.

Two different NASICON compositions were fabricated: 1) $NaZr_2 Si_x P_{3-x} O_{12}$, and 2) $Na_{1+x} Sn_{2-x} In_x P_3 O_{12}$. The zirconium (Zr) compositions had previously proven to be difficult to work with due to complexities in the Zr chemistry that led to extremely fine precipitates (e.g., zirconium phosphate) when using the polymeric precursor (modified "Pechini") route. Therefore, a new route to produce Zr-NASICON thin films (using combination of organic compounds containing zirconium, sodium and phosphorus) was developed. Sols of $PCl_5/Zr(Obu)_4$/EtOH and $ZrCl_4$/TEOS/EtOH were combined, NaOEt added, followed by centrifugation and filtration to remove precipitated NaCl. Additional NaOEt was then added to adjust the stoichiometry, and the precursor solution was then used for spin casting of thin films.

Previous work with polymeric precursors on this project allowed the casting of Sn-NASICON thin films about 0.1 microns thick without cracking during firing. In FY03, the investigators successfully developed thicker fired-films by using multiple coatings (Fig. 1). TEM analyses showed nano-crystalline grain sizes and EDX qualitatively confirmed the proper elemental make-up of Sn-NASICON. An original research paper covering the Sn-NASICON films, titled "Nano-crystalline NASICON-type Thin Film Ceramics," was completed and submitted to the Journal of Membrane Science for publication.

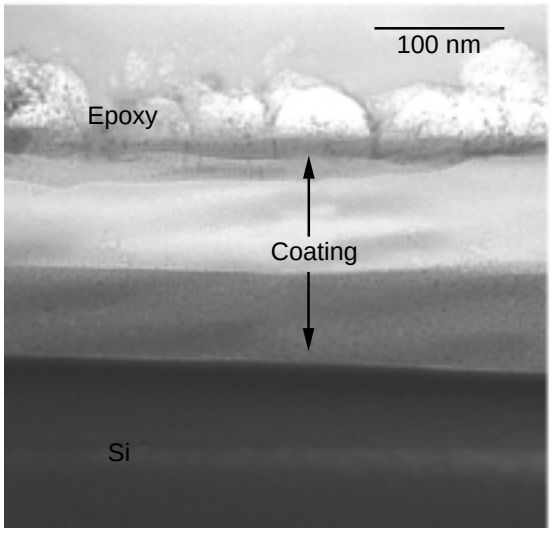


03-51139-62

*FIGURE 1. A bright-field TEM micrograph of the multiple coating of Sn-NASICON on silicon substrate.*

Practical devices (fuel cells, sensors, batteries, hydrogen-separation membranes) will need thin films applied to porous substrates, with electrodes to drive hydrogen transport with a voltage (electric field). The NASICON will then have to be ion-exchanged with protons from a mineral acid. Therefore, palladium-silver (Pd/Ag) was deposited upon different types of substrates using paint and fire, sputter coating, or physical vapor deposition

(PVD) coating. Of these three techniques, the PVD technique showed the most promise. Pd/Ag (Fig. 2) was deposited onto a porous alumina substrate (Fig. 3), followed by spin coating of the Sn-NASICON precursor and firing in ozone. The thickness of the coating is estimated to be about 250 nanometers based upon a 45-degree angle of view. The flaw in the center of the coating shown in Figure 2 allows clear observation of the underlying top surface of the Pd/Ag electrode.

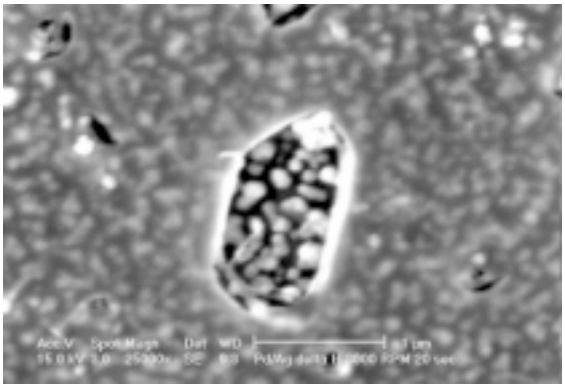

PN04-0004-131-NC103a

*FIGURE 2. Defect in Sn-NASICON precursor coating revealing underlying Pd/Ag coating. Heat-treated to 320°C in oxidizing (ozone) atmosphere.*

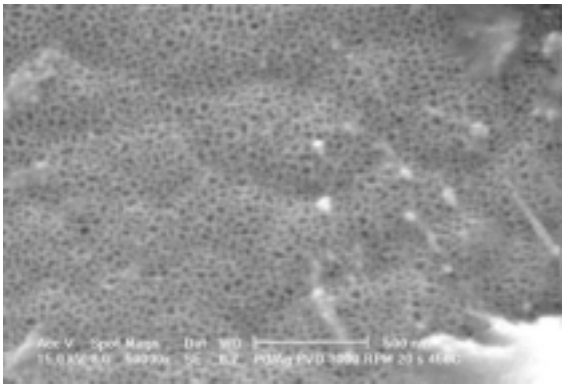

PN04-0004-131-NC103b

*FIGURE 3. Porous alumina substrate showing extremely small pores.*

Thin membranes showing fast proton transport are important to DOE because of their many uses in hydrogen-related applications, including: fuel cell electrolytes (hydrogen fueled), hydrogen sensors, batteries, hydrogen separation from reformed hydrocarbon fuels, and sealed removal of hydrogen from corroding spent nuclear fuel canisters. In the blossoming fuel cell industry, there is a need for proton-conducting membranes with higher operating temperatures (e.g., 150-300°C) such that waste heat can be rejected as steam rather than hot water. Steam is very useful and can be used in "bottoming cycles" to greatly increase the overall system efficiency. DARPA and NRL are interested in both nano-scale electrochemical materials and improved electrolytes for fuel cells and sensors. Therefore, proposals for continued development are a good possibility.

Collaboration has been ongoing with University of Idaho (Prof. Y-K Hong) for sputtered electrodes and Argonne National Laboratory (Dr. Jue) for TEM analysis. Joint proposals in the many areas of hydrogen (listed above) may be pursued.

There is a need for thin films of fast sodium or potassium ion conductors. The Bettis Atomic Power Laboratory is researching these devices to convert nuclear reactor heat into electricity. An example is the Alkali Metal Thermal to Electric Converter (AMTEC). This need was expressed in a letter of support for this LDRD from Dr. Wayne L. Ohlinger (Advisory Engineer, Advanced Materials Technology & Applications, Bechtel Bettis, Inc.).

# Development of Microelectrode Arrays for In Situ Detection of Localized Corrosion

*Tedd Lister*

***Understanding the effects of local chemistry on surroundings***

SC119

Scanning electrochemical microscopy (SECM) is a technique used to examine chemical species at surfaces in a spatially specific manner. To effectively use this technology to measure dynamic events, such as corrosion, it would be useful to acquire multiple data points on a surface simultaneously. This LDRD seeks to combine SECM with array technology to create a tool for researchers interested in mapping chemical species.

Technical objectives for fiscal year 2003:

- Design a multielectrode array microscope (MEAM) for mapping corrosion processes in spatial and temporal domains.
- Purchase materials and build the MEAM instrument.
- Conduct performance testing of MEAM instrument using a single point source electrode.
- Examine a previously examined model system by SECM to confirm detection of corrosion processes.
- Write draft of preliminary data for publication.
- Present preliminary results at industry conference and submit peer-reviewed papers.
- Begin examination of passive surfaces of Alloy 22.
- Examine a Ni-Cr-Mo-Gd alloy developed for use in Yucca Mountain Project as a neutron-absorbing construction material.

During the first year of this LDRD, work has focused on the building of the MEAM instrument and optimization of the microelectrode array and performing experimental work in corrosion.

The MEAM instrument (Fig. 1) combines the technique of scanning electrochemical microscopy with array technology. SECM is a technique used to examine chemical species at surfaces in a spatially specific manner. The use of an array allows the simultaneous acquisition of data at multiple points on a surface. This is useful in the measurement of dynamic events, such as corrosion. The construction of the instrument involved integrating the multi-channel microelectrode analyzer and software (Scribner and Associates) with arrays designed for implantation in living tissue (Bionic Technology). The array chosen had 100 elements in a square arrangement with a 400-micrometer spacing between electrodes. Two computers control the instrument, one operating the MEAM and a second to electrochemically control the sample for corrosion studies.

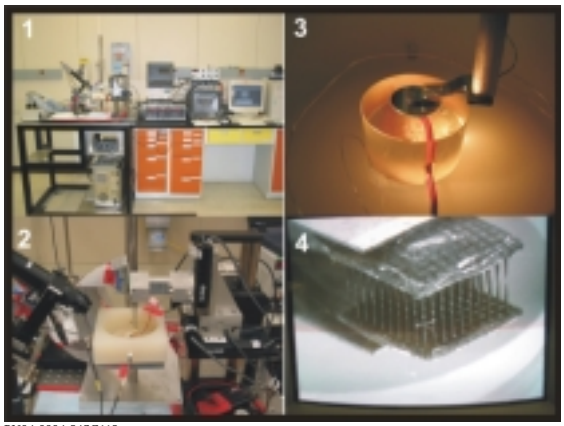


PN04-0004-84SC119

*FIGURE 1. 1) Image of instruments, 2) close-up of cell and array, 3) close-up of array positioned over a sample, and 4) video microscope image of array positioned above sample surface.*

The MMA is an instrument that allows the analysis of up to 100 microelectrodes simultaneously. For the purposes of the MEAM, the electrodes are held at a fixed potential and the current measured as a function of time (chronoamperometry). The potential is chosen such that the desired chemical specie is oxidized/reduced, with the current proportional to the concentration of that chemical specie.

The array used in this work is a unique design used to insert into living tissue. The elements of doped silicon spears protrude from the base and come to point coated with Pt. The entire device is insulated from solution contact except for the Pt tips, which are the sensing part of the element. The array tips are placed in close proximity to the electrode surface during measurements. Other parts of the instrument are part of the SECM instrument already in service, including the micro-positioning system, video microscope, and electrochemical cell.

Testing of the MEAM was performed to confirm the wiring of the array and measure the electrochemical characteristics of the array elements. This testing involved submerging the array in a solution of a redox compound and analyzing the response. An issue that was anticipated was bad connections to the arrays or poor electrochemical response. The performance of the arrays turned out to be better

than expected. No more that two elements were defective per array of the four used. The shape and size of the active areas of the arrays is still of concern. Ideally, the tip should have a disk shape parallel to the sample surface. It is envisioned that micro-machining technology will be used to create ideal array geometry. The elements were tested using a point source electrode to confirm the array was wired in a spatially correct manner.

Detection of corrosion events using SECM has been studied in this laboratory and has been documented in several papers. It was realized early in these experiments that the use of a single scanned probe resulted in an incomplete survey of the dynamic behavior of the surface. The obvious answer to this issue was to develop a parallel detection scheme. To test the MEAM, the same conditions used in those SECM studies were employed. These tests were performed on 304 SS containing a high sulfur composition (0.03%) in 10 mM KI with NaCl added in some cases. The $I^-$ ion acts as both corrosive agent and redox detection specie. Points of oxide breakdown become sites of electrochemical activity and oxidation of the $I^-$ occurs. The array microelectrodes, tuned to reduce iodine ($I_2$ or $I_3^-$), detect the formation of iodine. In these experiments, the arrays capture data at a relatively high frequency (up to 10 measurements per second). The data obtained from these experiments can be best presented as a video. However, data extracted from important points in a 24-hour experiment are shown in Figure 2. Figure 2A shows the current responses vs. time for all 100 elements of the array during a 304 SS corrosion experiment. Also shown (Fig. 2B) are maps taken at active points in Figure 2A.

This LDRD originally covered a three-year period, but has been condensed to two years. In FY04, additional mapping data will be acquired using the new instrument. However, the focus will be on understanding the effects of local chemistry on surroundings. This project supports the environmental missions of INEEL and DOE.

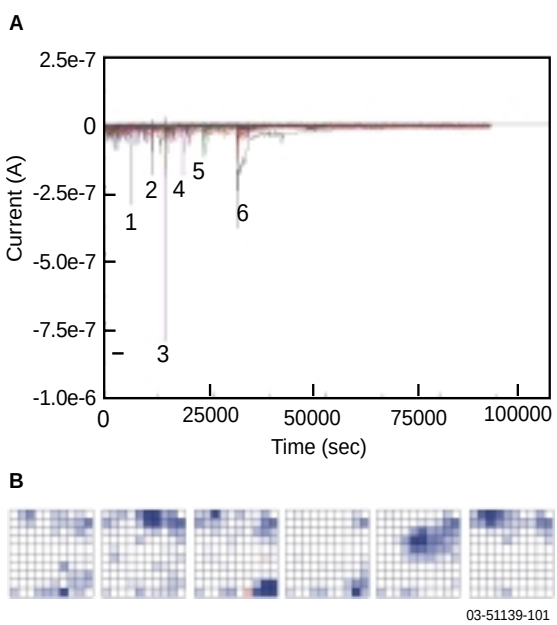


*FIGURE 2. MEAM experiment: A) current vs. time curves for all 100 elements during a 304 SS corrosion experiment, and B) array data extracted from points shown on (A).*

# Understanding Societal Issues Associated with Acceptance of Bioremediation Strategies

*Julie L. Marble*

***A model for stakeholder perception of risk***

ET119

Factors such as physical distance and exposure to scientific and risk information affect peoples' perception of risk in the context of bioremediation and biotechnologies.

This LDRD assesses how perceptions of risk associated with bioremediation efforts vary as a function of physical distance from them. Differences in how process trust evolves over time as decision makers are presented with more information also was investigated. Results from this project generally demonstrate that participants believe scientists are the most credible, trustworthy, and cautious in the cases where the bioremediation site was closer than when it was farther away. Results also showed that participants' risk perceptions are reduced as they learn more about that risk (especially if it is one they knew nothing about before). Distance between the remediation site and the decision maker was shown to significantly affect participants' subjective assessment of risk. This latter finding is critical for DOE remediation projects as it underscores the importance of identifying stakeholders close to the affected area. The perception of similarity between areas could be a critical factor that allows public decision makers who are removed from a site to identify more strongly with it. If so, it indicates that either emphasizing or de-emphasizing the similarities of the test location to the current location of the decision makers can sway decision-making. Future research should address these possibilities. Age, gender, and self-described political orientation all appeared to be good indicators of environmental attitudes. Based on these findings, a normative model of risk perception was created.

Technical objectives for fiscal year 2003:

- Develop a test method to allow assessment of risk perception at three disparate geographic locations nationally.
- Create opportunities for cross national research collaborations with Idaho State University (ISU) and Lake Forest College (LFC).
- Identify and assess risk perception in a representative cultural sample of participants from three national locations.
- Create a generic test scenario based on an actual remediation case that could be altered to assess the effect of potential factors affecting risk perception.
- Assess the affects on public perception of risk based on:
  - Physical proximity to the source of risk
  - Geographical location
  - Learning
  - Gender
  - Environmental attitudes
  - Self-described political orientation
  - Prior knowledge.
- Assess how trust in decision-making evolves in stakeholders based on the above factors.
- Develop a normative model of factors affecting risk perception relevant to DOE projects.

As expected, there were significant differences in the perception of risk based on the location at which the participants were tested associated with differing levels of awareness of bioremediation and the pros and cons of bioremediation before the start of the test. Prior awareness of bioremediation was associated with greater acceptance of bioremediation decisions and lessened perception of risk across all test locations. Further, the least knowledgeable group was more likely to indicate that their opinions regarding the risk of bioremediation would change if the location of the remediation were different. The probability that the decision makers would change their opinions was higher for those LFC participants who were assigned to the most distant remediation condition. In contrast, the two groups with some awareness of bioremediation (INEEL and ISU) indicated that changes in the location of remediation would have little effect on their opinions of the risk. It seems therefore, that prior awareness or education has a leveling affect on perception of risk with respect to physical distance.

Results also demonstrated that participants believed bioremediation would successfully solve environmental problems after reading through the entire set of information provided them, although

not at all assessment points. Participants' trust in the science behind bioremediation steadily improved as they received more information. These affects of physical distance and information gathering are important to DOE because of the historic lessons learned from the ability of affected groups to prevent or delay the implementation of remediation solutions.

Physical distance from the risk source to the decision maker significantly affected assessment of risk. Participants who were more distant to the proposed remediation site perceived less risk when presented with the same information as those who were closer. This finding is essential for DOE remediation projects as it underscores the importance of identifying stakeholders close to the affected area. However, this effect was not consistent for the intermediate distance condition (Lincoln, NE). One explanation, based on physical proximity, predicts that bias in location increases with the distance from a participant's home city or region. The perception of similarity between areas could be a critical factor that allows public decision makers who are removed from a site to identify more strongly with it. If so, it indicates either emphasizing or de-emphasizing the similarities of the test location to the current location of the decision makers can sway decision-making. Future research should address these possibilities.

There were fewer effects on perception of risk due to the amount of information obtained than expected. The lack of effects was surprising because of results from a recent study by Marble et al. (2002) that identified differences in decision style and decision certainty reflected in people's willingness and desire to seek more information during an environmental decision-making task. The results of this study imply that although participants' certainty of and desire for information may vary, their perception of associated risk does not differ. This is critical to DOE implementation of remediation solutions because it implies that desire for increased information does not concur with increased perception of risk. More importantly, age, gender, and self-described political orientation also appeared to correlate with various aspects of risk perception. Inclusive with the above factors, these have been incorporated into a normative model of risk perception (Fig. 1) that can be used as the basis for prediction of stakeholder acceptance of remediation solutions.

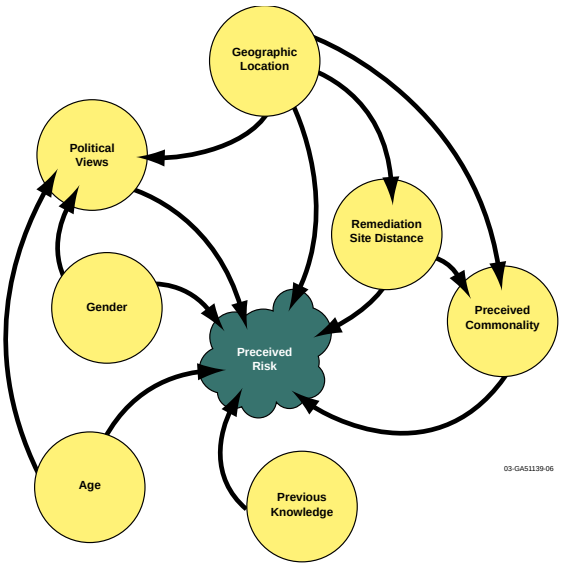


*FIGURE 1. Model of the factors contributing to perceived risk.*

This research identified factors that influence stakeholder perception of risk and modeled the potential impact and interactions of these factors to support DOE implementation of bioremediation solutions. The area of bioremediation holds tremendous promise for expanded use at the INEEL and throughout the world, but difficulties relating to stakeholder risk perception, communication of scientific data, and technology selection have limited the implementation of optimal bioremediation strategies. The greatest cost to a company lies not in investment in faulty technology, but in faulty implementation strategies that overlook stakeholder acceptance — a significant yet frequently neglected dimension of the likelihood of implementation. These are lessons that have been learned at the INEEL, as in the prevention of the implementation of an incineration plant. The DOE had given careful consideration to a

number of possible solutions, and determined that of the possible options, the use of an incinerator plant was the safest solution and posed little or no risk to the surrounding community and the environment. In this case, although stakeholder groups in Idaho next to the proposed site of the incinerator plant had been consulted and their acceptance of the proposed solution was gained, opposition arose from stakeholder groups located around Jackson Hole, WY, who were concerned that pollutants in the smoke from the incinerator plant would contaminate nearby Yellowstone National Park. Ultimately, this group effectively prevented implementation of the solution at a cost of several million dollars to the DOE. Early identification of stakeholders affected by a given bioremediation strategy who are likely to be interested and involved in the decision-making process is critical to successful implementation of a new technology. Although a given remediation strategy may have low risk from an industry standpoint, stakeholder perception of that risk (i.e., its perceived threat) is the overriding factor in the implementation of a technology and subsequent regulation of that technology.

This research was supported through collaborations with Idaho State University and Lake Forest College. The research represents the first opportunity for collaborative research between INEEL and Lake Forest College. Collaboration with LFC was highly successful. Dr. Matthew Kelley was a significant and important contributor to this work. Furthermore, a collaborative journal article and conference presentation between LFC, ISU, and INEEL are pending as an outcome of this research. It is expected that this collaboration will yield further opportunities for joint work between these three institutions.

This research has served as the basis for two proposals submitted to the DOE NABIR Program. The first proposal was to assess public perception of risk with reference to genetic testing, and was not selected. A second proposal, still under review, focused on public perception of risk due to perceived similarity between bioremediation, biotechnologies, and bioterrorism.

# The Controlled Synthesis, Structural, Electrical, and Optical Properties of One-Dimensional Metals

*Eric S. Peterson*

***Forming novel materials for next-generation wires***

SC115

Certain metal complexes can be polymerized in linear chains. These chains display metallic properties along the long axis but are non-metals along the other two. These novel materials offer an insight into the development of new strategies for forming wires at the molecular/nano level. Understanding how these materials behave at birth – nucleation and early growth phase – is critical to directing the system to form wires and devices (e.g., switches, resistors). The wires formed at the molecular/nano level offer the next generation of possible materials with specific, and to date unknown, properties. Since very few wires and devices have been formed at the molecular level, no one actually knows if these wires are quantum conductors, what their physical properties are going to be, if Peirl's distortions and charge density shifts will destroy conductivity, or if they can be used to provide novel properties. All of these types of questions are open for discovery and understanding.

The objective of this LDRD is to develop fundamental understanding of the processes that lead to the polymerization of the platinum chains. This is a critical first step to developing a characterization of the materials to the point that one can understand their flexibility for various applications.

Technical objectives for fiscal year 2003:

- Conduct rigorous literature review of work done on 1-D platinum-based wires.
- Investigate control of the fiber structure.
- Synthesize several complexes.
- Examine systematic effects upon the polymer bundle.
- Investigate encapsulation of 1-D polymers within polymer matrixes.

Certain heavy metal compounds can be caused to polymerize into linear chains. These chains display metallic properties along one cartesian/crystallographic axis but are non-metals along the other two. In collaboration with Montana State University (MSU), this LDRD is researching the synthesis and characterization of polymeric materials that display 1-D metallic properties. The investigators will develop systematic syntheses for the compounds (including nanoscale assembly of individual molecular/nano-wires), followed by probing the optical electrical, electo-optical, and chemo-optical properties of the polymers. Analogs of nano-diodes and other electronic components may result.

The optical electrical and electo-optical properties of the polymers are unique and of considerable practical value. Additionally, strategies are being developed to accomplish nanoscale assembly of individual molecular wires, and the synthesis of structures that should function as diodes and other electronic components. Finally, by combination of two known chemistries on closely related compounds, the investigators are working on a synthetic pathway to photo-switchable, 1-D conductors, a completely new set of materials. If successful, the resulting material would likely have photoconductivity far exceeding current polymers and also would display photoreflection and true photorefractive effects, novel materials that have not been observed previously. Applications for these materials include holography, optical routing and switching, phase conjugate amplification, and a variety of other nonlinear optical phenomena. Ultimately, these materials could be utilized in devices such as re-configurable antennas for satellite based Internet services, optical limiters, switches in fiber-optic networks, and aberration correction devices for remote sensing.

This project is the next logical step building on an existing collaboration between synthetic inorganic chemists, physicists, spectroscopists, and engineers at Montana State University and the INEEL. An important aspect is that the project is focused on the development of junior scientists. It is being carried out by a postdoctoral fellow, an undergraduate student, and a graduate student. These scientists are spending a fraction of their time at INEEL.

Year-to-date accomplishments include conducting a rigorous review of the literature, which has enabled the team to discover important precedents about the partially oxidized platinum complexes. This has enabled the investigators to more specifically direct their work.

In accordance with the working plan, control of the fiber structure by variation of the counter cation has been investigated. Several complexes were synthesized, and some of the systematic effects upon the polymer bundle have been examined. The results indicate that partial oxidation can occur with

larger cations than previously reported in the literature.

Encapsulation of the 1-D polymers within polymer matrixes also has been investigated. This offers numerous advantages including increased environmental stability (reduction in solvent losses), ease of handling and orientation, and the ability to incorporate optically active species into the polymer film (e.g., NLO active species). Nonconductive polyvinyl chloride and conductive polyaniline are the two polymeric species that have been concentrated on. Spin coating techniques coupled with molecular wire incorporation within spun filaments were examined. These experiments did not yield any significant results.

The collaboration with MSU has allowed training of personnel in the basic techniques for synthesis and handling of the materials. Additionally training in electron microscopy techniques (e.g., SEM, STM, AFM) has been ongoing both at MSU and at INEEL.

As an aside to the main work, the $Pt(DISN)_2$ complex was investigated (Fig. 1). This neutral square planar complex may be analogous to the other platinum complexes with platinum atom stacking. In solution, this complex produces a thin layer of material on the surface with a metallic sheen, suggesting a degree of platinum bond overlap. Further investigations are continuing.

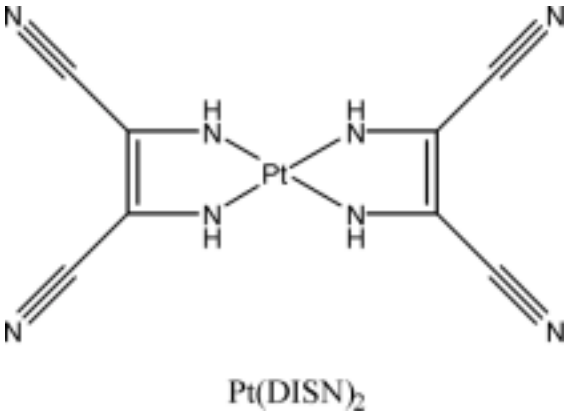


03-51139-131aSc115

*FIGURE 1. $Pt(DISN)_2$ complex.*

A key innovation of this project that is still under investigation is generation of possible nonlinear electronic effects resulting from the rope-like structure of the crystalline materials. The investigators have mapped out the degree of separation by counter ion that the system can tolerate, and are gaining significant understanding of how the systems work and what the functionality tolerances of the materials are. Additionally an entirely new ligand for these materials has been discovered.

The work performed under this LDRD offers a critical first step to characterizing these novel materials so that their flexibility for various applications can be understood. The materials researched have the potential for providing a chemical-specific or electro-optical sensor that could be applied in a number of situations in both the government and industry. Additionally, the potential for energy-saving devices exists with these materials, if they can be implemented as wires.

This LDRD is developing fundamental understandings that will provide the basis for future research in molecular/nano-materials development, and put INEEL and MSU at the forefront of this type of research for the next several years. Other benefits to INEEL include providing a set of significant technical advances within the INEEL's Office of Science mission driven by the desire for new technical understanding that creates a reputation for excellence and makes INEEL a preferred nanoscience provider, and forms the basis for new nanoscience missions.

# Making Sustainable Decisions Using the *K*ON*VER*GENCE Framework

*Steven J. Piet*

***A new framework for better science-based decisions***

ET106

Decisions on complex issues are often controversial, can be blocked, and are sometimes redone — some before implementation, some decades later. This is particularly true for decisions involving cleanup (decommissioning, environmental restoration, and waste management) of nuclear facilities and contaminated sites.

The goal of this LDRD is to explore approaches on how to make decisions easier, more robust, transparent, consistent, and sustainable through a holistic framework that emphasizes relevant time scales. Although this work was stimulated by the challenge of decision-making for cleanup of nuclear facilities and contaminated sites, it is applicable to other complex decisions with relatively long time horizons.

In this research, experiences and analyses were melded with ideas from decision science, action science, sociology, psychology, political science, ethics, history, "hard" sciences, risk assessment, and many engineering disciplines. The resulting *K*ON*VER*GENCE framework combines new ideas, modifications of others' ideas, and existing ideas. The framework includes the *K*ON*VER*GENCE mental model describing the underlying decision dynamics that require cleanup alternatives to be *konver*gent with knowledge of the problem and alternatives, values of those impacted by the decision, and resources needed to implement alternatives so that the decision works over time. Another key framework element is proper framing of the decision, including the need to consider the adaptability of alternatives to reduce the resistance to making decisions and increase the sustainability of decisions once made. The framework is also built on general values and principles to guide both process and result.

Technical objectives for fiscal year 2003:

- Complete the model, framework, guidebook, and publications.
- Test the model and framework.

The comprehensive *K*ON*VER*GENCE framework is a mental model that describes some of the underlying decision dynamics that require cleanup alternatives to be *konver*gent with knowledge, values, and resources so that the decision works over time. It includes:

- Strategic improvements to reframe the problem and expand the spectrum of alternatives to include adaptable alternatives and decision networks.
- Tactical improvements such as processes and analytical tools derived from experience, values/principles, and relevant literature.
- Initial extensions of existing risk and cost estimation tools to provide earlier and more comprehensive inputs to decision-making.
- Some implications for R&D into possible solutions that may increase adaptability while still reducing risk of residual hazards.

The framework developed by this research, models regulations as an imperfect overlay or "snapshot" of values. The fact that regulations can never totally substitute for values is one of the underlying challenges. Also, the number of participants in a decision is always less than the full set of stakeholders. The framework suggests a more effective, appropriate, and timely involvement and analysis to improve the validity of the values considered. An improved values component should make the decision more robust against "late entry" players.

The framework includes a generic set of values and 21 principles that are a starting point for establishing common ground on both the process and objectives. These principles advocate caution in differing ways. The first principle cautions against taking actions prematurely if the actions pose threat of irreversible harm. The second principle cautions against not taking action to protect against the threat of irreversible harm.

In FY03, the investigators conducted several tests, most notably groups of students worked through an INEEL cleanup problem and a focus group of INEEL employees worked through a question of siting a new nuclear facility at the INEEL.

*INEEL Cleanup test case:* The same information package was provided to three groups of students taking a University of Idaho environmental science class. Two groups used the *K*ON*VER*GENCE process; one used the normal NEPA process. Various questions were asked before and after the test to measure how much participants thought they had learned and whether some of their attitudes had changed.

The two groups using the *K*ON*V*E*R*GENCE process (Fig. 1) indeed converged on an alternative that they generated during the refinement step rather than a pre-selected alternative. This is consistent with other researchers' observations that people like alternatives more if they have been involved in their development. The investigators believe it also shows that participants were able to use the *K*ON*V*E*R*GENCE concepts and apply them to improve one or more of the original alternatives to address concerns that were raised during evaluations. Their alternatives were modifications of performance-based closure. The modifications allowed the groups to address their concerns using the concepts of adaptability and staging of decisions.

The group using the NEPA process was less supportive of performance-based closure, exhibited less satisfaction with the decision process, and indicated that they believed they had learned less about the problem and the INEEL than the two *konver*gence groups.

*Nuclear facility test case:* The *K*ON*V*E*R*GENCE decision-making process applied to a nuclear facility siting case yielded the following insights into the issues and challenges the INEEL will likely face when it moves forward with siting a new nuclear reactor facility.

Despite being a diverse group of INEEL employees, most with college degrees, many showed little understanding of relevant technical concepts and terminology. They supported siting a new facility *only* if various concerns and values were addressed. They also tended to articulate alternatives and desired additional information in terms of *why* would something new be built, and *how* have their values and concerns been addressed; i.e., "I don't care what it is you build as long as you address *my* concerns' and 'Show me that technical designers have a 'questioning attitude' and have not pre-selected alternatives."

In contrast, some technical members of the group tended to deny that many values were important; i.e., "Feelings don't matter." The investigators observed this in the test and believe that this attitude would not encourage collaboration with local stakeholders. All previously hypothesized issues arose, including waste generation, water contamination, water usage, public safety, and impact on local jobs and economy. Issues of local control, local benefit, and chemical hazards were stronger than hypothesized; i.e., "This new nuclear facility needs to be for us, by us."

From these focus groups, the investigators believe that:

- Nuclear and cleanup tests, and working with the INEEL Citizen's Advisory Board show the process very helpful for diagnosing a decision situation.
- These tests strongly suggest the process can help in increasing consensus, although real applications with public interest and focus groups are needed.

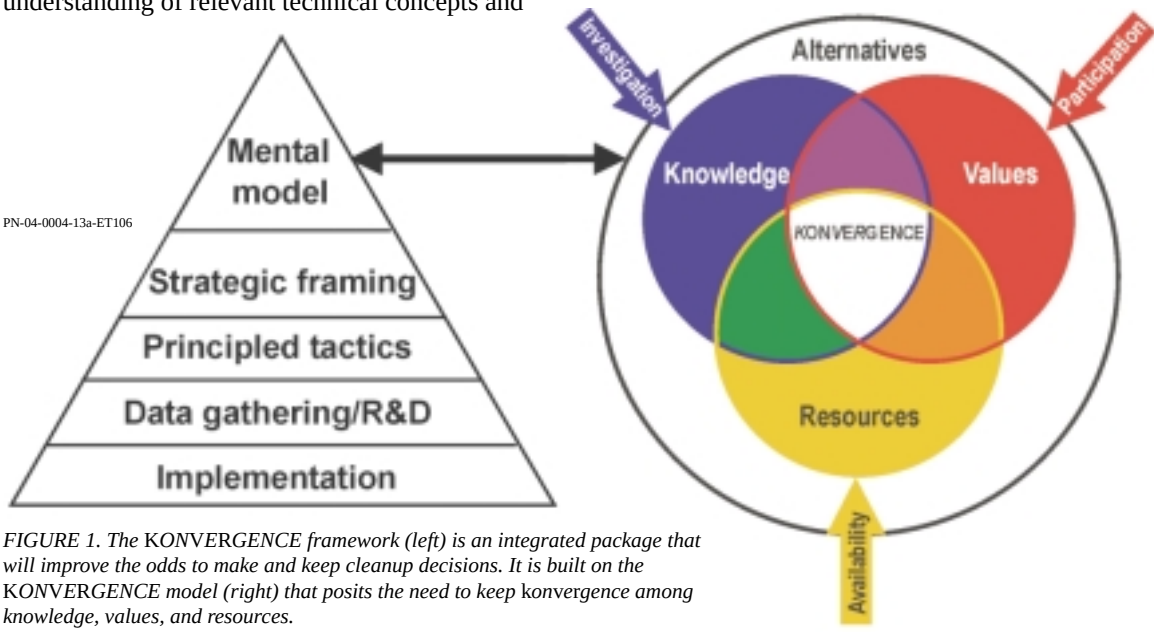


*FIGURE 1. The* KONVERGENCE *framework (left) is an integrated package that will improve the odds to make and keep cleanup decisions. It is built on the* KONVERGENCE *model (right) that posits the need to keep konvergence among knowledge, values, and resources.*

- Theories provide some basis for believing that the process leads to more sustainable decisions. (Of course, short-term tests cannot provide data on long-term sustainability.)

As alternatives are developed, diagnosis of opposition needs to be probed more deeply to provide a better basis for refinements, prior to spending millions of dollars on detailed engineering, while recognizing the limited potential to solve values problems with increased knowledge, etc. Finally, decision makers must recognize that knowledge, values and resources interact dynamically and change over time.

In FY03, the guidebook was completed, a paper was presented at the Waste Management 2003 conference, a paper and practice exercise were given at the International Association for Public Participation meeting in Ottawa, Canada, and two manuscripts were submitted to the Journal of Risk Analysis.

This LDRD is pursuing a science-based decision framework for decommissioning, stewardship, and waste decisions. This effort support EM Operations and better decision-making operations in general at the INEEL, within the DOE Complex, and elsewhere.

# Dependence of Coal Bed Permeability on Pore Pressure and Adsorbed Gas Composition

*Eric Robertson, Russel Hertzog*

***Modeling in situ stress in coal beds***

PH107

Permeability in coal, being dependent on cleat density and width, is not only a function of the effective stress and elastic moduli of the coal matrix, but also a function of the adsorbed gas content and composition. Current state-of-the-art coal bed permeability models that are based on elastic moduli and Langmuir strain curve parameters for coal saturated with pure methane are unable to achieve a satisfactory match of field data without significantly modifying the strain data obtained in the laboratory. Because the gas adsorbed in coal beds *is not* pure methane, permeability models might be significantly improved by incorporating parameters of an extended Langmuir strain curve for gas mixtures in coal.

The objective of this LDRD is to improve the ability to model changes in coal permeability as a function of in situ stress and adsorbed gas composition. Gas mixture strain parameters will be calculated based on the extended isotherm equation using the measured pure-gas isotherm curves. The gas-mixture-parameters more accurately portray field conditions and will be used to improve the permeability model. The model will be tested and refined by comparing changes in coal permeability measured in the laboratory with calculated permeability using the improved model. The refined permeability model could be incorporated into reservoir simulators to better predict permeability decline and rebound during traditional coal bed methane production operations, but may be even more applicable during simulation of $N_2$- or $CO_2$-enhanced methane recovery from coal beds and for $CO_2$-sequestration in coal beds.

Technical objectives for fiscal year 2003:

- Purchase equipment and set up at Colorado School of Mines (CSM).
- Make preliminary permeability measurements on sandstone to test equipment.
- Transfer laboratory equipment from CSM to INEEL.
- Purchase equipment necessary for measuring porosity.
- Measure permeability changes in coal.
- Measure coal strain as a function of pore pressure and gas composition.

Improving the ability to model changes in coal permeability, as a function of in situ stress and gas composition will be accomplished by incorporating parameters of extended Langmuir strain curves for gas mixtures in coal into a coal permeability model. Improving the ability to model coal permeability would greatly improve reservoir simulators' ability to predict permeability decline and rebound during traditional coal bed gas (CBG) production operations. However, results of this research may be

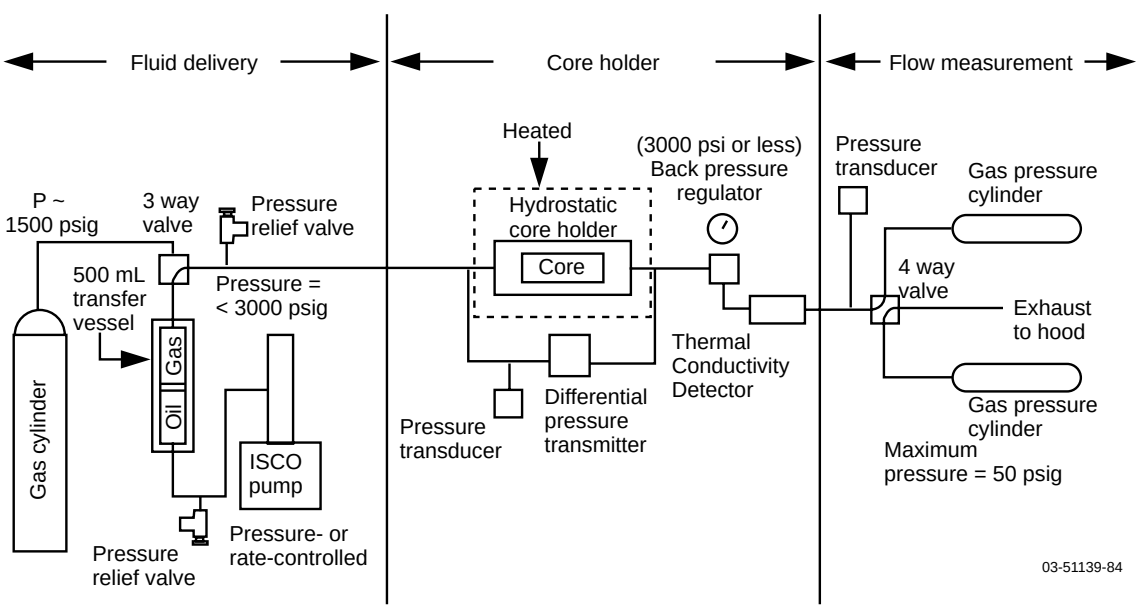


*FIGURE 1. Schematic of equipment used to measure coal permeability and porosity.*

even more applicable during simulation of $N_2$- or $CO_2$-enhanced methane recovery from coal beds, as well as for $CO_2$-sequestration in coal beds.

INEEL staff engineer Eric Robertson was transferred to the CSM campus in Golden, Colorado, on an out-plant assignment from August 2002 through May 2003 to work with qualified personnel there on the progress of the project. Under the direction of Dr. Richard Christiansen (associate professor, petroleum engineering, CSM, and collaborator on this project), laboratory space at CSM was obtained where the equipment was set up and tested. LabView™ software was selected to log data and control the equipment. The permeability experimental set-up can be seen in Figure 1.

After initial set-up and verification that the equipment was in working condition, the equipment was dismantled and transferred to an INEEL laboratory at the IRC building in May 2003. Samples of coal were obtained for initial study from local suppliers. Weathering and oxidation of the coal can cause damage to the coal and affect the gas adsorption process. Therefore, because the coal samples obtained from local suppliers had presumably been exposed to oxygen and were weathered for an unknown amount of time, they were only used to obtain some initial data collection and for proof-of-concept experiments. Collection of virgin coal samples from an underground mine face is planned in the future.

A number of permeability readings have been taken on a cylindrical coal sample 2 inches in diameter by 4 inches in length that was cut from a larger coal sample. These tests were designed to determine the effect of overburden pressure on cleat permeability. In these tests, the upstream pore pressure (supplied by a nitrogen gas cylinder) and the backpressure were left constant at 130 psig and 50 psig respectively, allowing the flow rate to vary. The overburden pressure was systematically increased from 500 psi to 1800 psi in regular steps and then decreased back down to 500 psi in the same manner. As expected, there was a strong correlation between overburden pressure and permeability: the higher the overburden pressure the lower the resulting permeability. The effect was found to be reversible with very little hysteresis, as the ending permeability was roughly equal to the initial value.

The equipment necessary to measure porosity in coal was purchased. An in-line thermal conductivity detector (TCD) will be used to calculate changes in coal porosity, with helium being used as a tracer because it does not interact with the coal. The TCD can be used to monitor helium transport through the coat in real time to calculate coal pore volume and porosity.

A novel method of measuring strain in coal as a function of pore pressure has been developed in which strain is measured optically. Previous researchers have used strain gauges that were glued onto the surfaces of a coal sample placed in a pressure vessel. Problems associated with the strain gauges include difficulty in adherence of the gauges for long periods of time; hysteresis of the gauges, which complicates interpretation; and possible chemical interaction between the epoxy and the adsorbance of the gas by the coal surfaces. An advantage of an optical measurement is that it is noninvasive, does not rely on problematic strain gauges, and multiple samples can be tested at the same time in one cell. This method uses high quality optics to note changes in coal lengths down to 0.5 microns. To date, only a proof-of-concept apparatus has been built and demonstrated that verifies that coal does indeed swell in the presence of $CO_2$ at 800 psig and that strain can be measured optically. In addition, the swelling/shrinkage process was shown to be reversible in the samples used in these experiments.

Figure 2 (next page) is a photograph of the current system used to detect coal strain as a function of pore pressure and gas composition. In the photo, a coal sample 1 inch in length with cross-section of 1/8 inch by 1/8 inch was placed in the Jerguson cell. The Cohu video camera with the large lens attached is connected to the video display. The end of the coal sample can be seen on the video screen.

Future work in this area will focus on quantitative measurements of coal strain as a function of pore pressure and gas composition using optical methods.

PN04-0004-65

*FIGURE 2. Photo of the equipment used to measure strain in coal as a function of pore pressure and adsorbed gas composition. Note the end of the coal sample seen on the video screen.*

Several abstracts have been submitted and accepted to professional symposia wherein this work will be presented in front of international audiences. Research to understand how different gases flow through coal is vital to accurately model $CO_2$-sequestration in coal, as well as enhanced gas production from coal by injecting other gases. Follow-on work after the project is finished will include, among other things, the applicability of sequestering flue gases from power plants into nearby coal seams.

# Nucleation and Growth of Nanoparticle Materials in Supercritical Fluid Processes

*Harry Rollins*

***New, versatile methods to control particle properties***

NC104

The novel optical, electronic and/or magnetic properparticle shape to be easily controlled and would be applicable to a wide variety of material systems. Numerous preparation methods have been reported, each with its inherent advantages and disadvantages. However, an ideal method has yet to emerge.

This LDRD is investigating new methods for the preparation of metal and semiconductor nanoparticle materials using supercritical fluids. A variety of nanoscale materials have been prepared and the effects of the preparation conditions on particle properties have been examined.

Technical objectives for fiscal year 2003:

- Evaluate effects of processing conditions on particle properties.
- Prepare and characterize metal nanoparticles (silver).
- Prepare and characterize semiconductor nanoparticles (silver sulfide).

Silver and silver sulfide nanoparticles with average diameters ~10 nm with narrow size distributions have been prepared using a reactive supercritical fluid processing method. In this method, a neutral metal salt is dissolved in $CO_2$ using tributyl phosphate. The supercritical solution of the metal salt is rapidly expanded into a liquid solution containing a second reactant, resulting in the formation of metal or metal sulfide nanoparticles. The nanoparticles have been characterized by powder x-ray diffraction, transmission electron microscopy, and absorption spectroscopy. Figure 1 shows a typical powder x-ray diffraction pattern of metallic silver nanoparticles. The average particle diameter was calculated using the Debye-Scherrer equation: $D = K\lambda/(\beta \cos(\theta))$, where K is a constant (equal to 1) related to the particle shape, $\lambda$ is the x-ray wavelength, $\beta$ is the peak width, and $\theta$ is the diffraction angle.

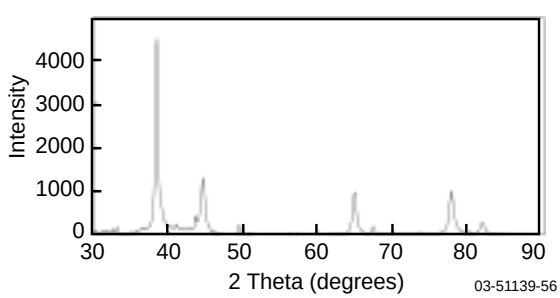


*FIGURE 1. Powder x-ray diffraction pattern of a typical silver nanoparticle sample.*

The effects of silver triflate and tributyl phosphate concentrations on particle properties were evaluated. Figure 2 shows the average particle diameter for a series of silver samples prepared using different silver triflate and tributyl phosphate concentrations. The concentration of silver in the final sample was determined by Inductively Coupled Plasma-Atomic Emission Spectroscopy (ICP-AES). Increasing the concentration of TBP or silver triflate resulted in the production of larger quantities of nanoparticles. The average particle diameter showed a weak dependence on silver triflate concentration, with larger particles being produced at higher concentrations of silver triflate.

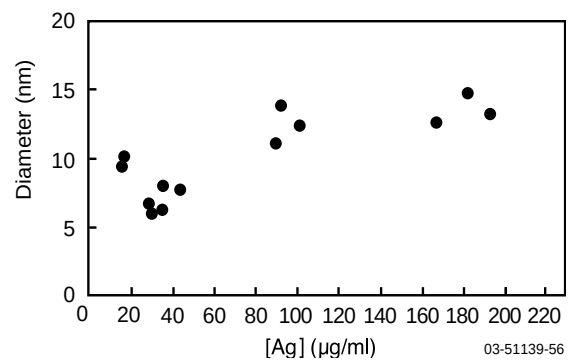


*FIGURE 2. Average particle diameter for silver nanoparticles as a function of silver triflate concentration.*

This LDRD project supports DOE EM missions and has resulted in additional funding from the Science Office for continued research that includes collaborators at Carnegie Mellon University. The purpose of this future project is to design, prepare, and characterize novel surfactant coated composite Iron/Palladium nanoparticle catalysts for the in situ degradation of chlorinated organic contaminates.

An article titled “Preparation of Metal and Metal-Sulfide Nanoparticles from Carbon Dioxide Solutions” was accepted for publication in the 1st edition of the Encyclopedia of Nanoscience and Nanotechnology, published by Marcel Dekker.

This LDRD also supported a summer undergraduate student through the INEEL Undergraduate Fellowship Program, and collaboration with Sara Majetich at Carnegie Mellon on the effects of supercritical fluid annealing of amorphous FePt nanoparticles.

The proposals, publications, and presentations resulting from this LDRD greatly enhance the capabilities of the INEEL in the preparation and characterization of nanomaterials and demonstrate the INEEL’s active involvement in basic and applied research and development.

# Development of an Integrated Watershed Information Management Tool for Long-Term Facilities Stewardship

*Ron Rope, Jerry Sehlke*

***Making better water resource decisions***

ST105

Significant watershed management issues occur throughout the world, many crossing national boundaries. Given the current stresses on natural systems, resulting from both anthropogenic and natural events, watershed issues are being discussed internationally. A system that could help manage these issues would be extremely timely.

The goal of this LDRD is to provide DOE with Integrated Watershed Information Management Tools (IWIMT) that integrate and leverage water and environmental management information leading to improved long-term stewardship decision-making on the INEEL and within the associated watersheds. The tools and methods being developed are transferable to other DOE and federal facilities and to address national/global watershed management issues. Key components of the system include data management, access and analysis tools, a Bayesian Decision Network (BDN), system dynamics model, and options analysis/decision support capabilities.

The approach is structured around a BDN description of the Big Lost River (BLR) watershed. The BDN will be developed for integrated water and environmental management, and to identify and account for uncertainties associated with the physical systems, water quantity and quality, and alternative long-term management options.

Work has involved data collection and database development for disparate data sources in the watershed and development of disciplinary data analysis and mathematical modeling tools to the BLR and INEEL. These tools will be integrated into a coherent IWIMT. Facility and water resource managers, along with stakeholders can use these tools to help evaluate information and management alternatives and communicate decisions to other interested parties.

Technical objectives for fiscal year 2003:

- Collect and disseminate data for the BLR and INEEL.
- Develop model and software.
- Perform BLR and INEEL site-specific modeling and data analysis.

The following data for the BLR and INEEL have been compiled and integrated into the BLR-Data Viewer (DV):

- Ground water: elevation and quality
- SNOTEL, Snow Course and other Meteorological data
- Wildlife Corridors for sensitive and focus species
- Surface water flow
- Surface water quality
- Soil erosion susceptibility
- Precipitation run-off forecasting model.

The data inventory table for the BLR-DV has been organized and updated. This data inventory table provides an example for what data are needed to support the tools and how to document and organize the data.

The MapWindow software used as the primary visualization tool and GIS engine for the BLR-DV has been re-engineered to be more efficient and stable. Plug-ins also have been revised.

The IWIMT component, including these revisions re-engineering, include:

- MapWindow 3.0 Programmable GIS with MapWindow Applications: Attribute Table Editor Plug-in, Grid Wizard Plug-in, Shape file Editor Plug-in, Feature Identifier Plug-in.
- MapWindow Watershed Information System Plug-ins: Water Quality Analyst, Streamflow Analyst, Photo Viewer.
- Additional IWIMT related plug-ins and tools: Model Manager, Bayesian Network Analyst, Hot-Linked Document Viewer, BLR Sediment Model, TAUDEM, TIN Builder/Viewer, MapWindow Application Builder. The Model Manager Plug-in can serve as a central hub linking separate models and providing for simple construction of scenarios in a common graphical user interface (GUI).
- Documentation: MapWinGIS ActiveX control developer documentation, MapWindow Application Plug-in developer documentation, Watershed Information System developer documentation, IWIMT Tools end-user documentation including questions and answers.
- BLR and INEEL Data sets: GIS data (streams, watersheds, land use, terrain, political boundaries), surface water quality, groundwater quality and streamflow data, BLR photo database, input data sets for the BLR sediment model, table of data sources and datasets.

A soil erosion risk model was developed for the BLR watershed. This model identifies key areas within the basin where soils are most susceptible to erosion and cause sediment problems in the streams. This is a key component to addressing sediment Total Daily Maximum Load (TMDL) issues in the BLR and will help land managers determine high priority areas for implementing best management practices.

A model identifying key wildlife corridors for sensitive and important vertebrate species has been developed for the BLR watershed. This component of the tool set is attempting to address terrestrial ecological sustainability, at least for the identified key species or species of concern. This model, along with the soil erosion model, can help identify high priority areas that if protected, could reduce sedimentation problems while also providing wildlife habitat.

The structure of the BLR Bayesian Decision Network has been completed (Fig. 1). The decision nodes are defined and the Conditional Probabilities Tables have been populated. Some modifications to the INEEL portion of the BDN are taking place to capture additional questions and decision associated with operation of the BLR diversion on the INEEL and Spreading Area management options.

The system dynamics (SD) model for surface water flow in the BLR is completed, but not calibrated. This model is used to predict stream flows based on different dam operation scenarios and its output will populate the conditional probability tables (CPTs) in the BDN. Filters to integrate the System Dynamics model with the BDN were explored and the mechanism to build them is

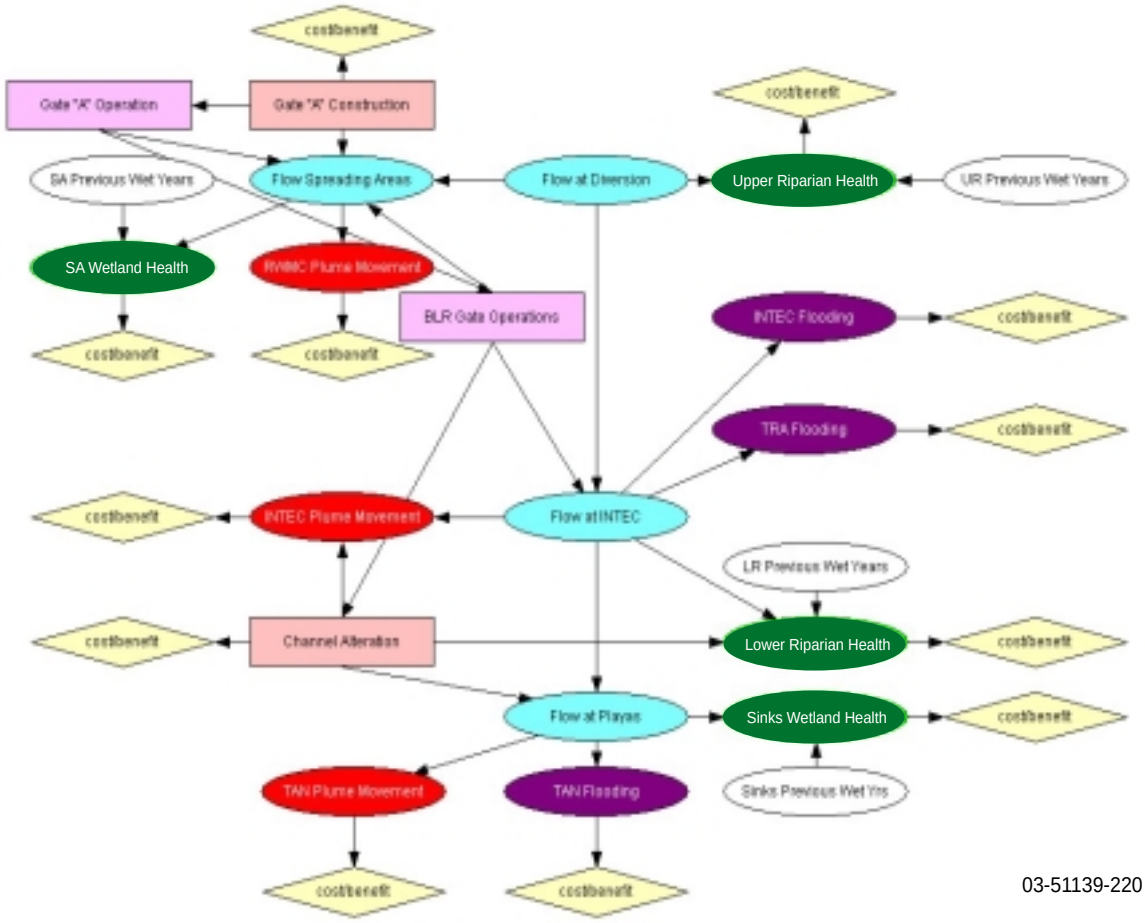


*FIGURE 1. BLR-INEEL network.*

now understood. The purpose of these filters are to allow the SD model to operate dynamically with the BDN allowing the BDN conditional probability tables to be automatically updated after the SD model is run using a different scenario. These filters were not developed fully due to lack of funding and because the system dynamics model and BDN were not finalized.

A precipitation runoff forecasting BDN was completed for the upper BLR basin above Howe Ranch gauge. This model utilizes historic snow-pack/snow water equivalent data, flow data, and northern sea surface water temperatures to provide probabilities of upcoming run-off conditions for the basin. Run-off is predicted in acre-feet based on five types of precipitation years: very low, low, normal, high, and very high. This model can provide information to water users regarding the amount of water they might expect in the coming year with and an uncertainty component to it.

A snow-cover run-off model has been completed for the Copper Basin portion of the BLR. It provides an estimate of total water run-off based on snow cover in early spring. This will provide an additional prediction tool for supporting management options for the Mackay Dam. It increases the accuracy and reduces the uncertainty associated with using SNOTEL data alone. This can increase the options dam operators will have for the amount and timing of water releases.

A license agreement between INEEL and Utah State University (USU) is under negotiation for using and distributing the software developed through this project. Documentation has been completed for the software developed and includes identification of issues and questions that can be supported by the developed tools. A workshop was conducted with INEEL and ID DEQ personnel to present and discuss uses of these tools. Other applications for the software have been developed and are being pursued. These include an interactive application to view INEEL facilities and infrastructure as a marketing tool for new work for the INEEL. An interactive application used for the INEEL Source Water Assessment to show wells and potential contaminant sources and protective buffer zones. An interactive application to compile and view data for the Coeur d'Alene Basin and associated contaminant issues.

# Elucidating the Photo-Physics of Complex Metal Ions Trapped in a Fourier Transform Mass Spectrometer

*Jill R. Scott, Paul L. Tremblay*

***Leading to new energy technologies***

SC111

A better understanding of electron and energy-transfer modalities could lead to the development of new energy technologies such as improved energy collection, conversion, and storage devices.

This LDRD is investigating sensitive techniques for the measurement of ground and excited-state energies from a number of complexes that have properties suitable for the conversion of light energy to chemical or electrical energy. The technical capabilities that will be developed at the INEEL are the integration of a sensitive optical detection system with a Fourier transform mass spectrometer (FTMS) for the study of chemical complexes with narrow absorption and emission bands in a solvent-free environment. The investigators have chosen fluorescence as their first emphasis because the sensitivity of fluorescence > absorption > infrared ˜ Raman.

While gas-phase data for atomic ions and a few small molecular ions exists, virtually no information exists about spectroscopic characteristics for large, non-volatile gas-phase ions. For example, extinction coefficients and quantum efficiencies are not available in the literature. Another complication is that the ions produced in the gas phase may not resemble those in solution or their behavior may be significantly different without the presence of solvent. The investigators have observed gas-phase fluorescence behavior of $Ru(bpy)_3^{+1}$ that has not been reported for this complex in solution. Additionally, the mechanism of ion production plays an important role in the structure of metal-bipyridine complex that would be difficult to see without the high resolution and mass accuracy of the FTMS.

Technical objectives for fiscal year 2003:

- Optimize integration of fluorescence spectra apparatus.
- Investigate ion production and stability for compounds of interest.
- Explore magnetic field effects on fluorescence lifetimes and spectra.
- Publish and present research results.

Metal polypyridines are excellent candidates for gas-phase optical experiments where their intrinsic properties can be studied without complications due to the presence of solvent. The fluorescence lifetimes of $[Ru(bpy)_3]^{1+}$ trapped in an optical detection cell within a Fourier transform mass spectrometer were obtained using matrix-assisted laser desorption/ionization to generate the ions with either 2,5-dihydroxybenzoic acid (DHB) or sinapinic acid (SA) as matrix. In light of the investigators' recent work that indicated the stability of $[Ru(bpy)_3]^{1+}$ generated by matrix-assisted laser desorption/ionization (MALDI) varies according to the matrix used, the results from experiments using DHB or SA as matrix were compared.

The emission transients recorded for $[Ru(bpy)_3]^{1+}$ generated with matrices DHB and SA vary significantly in intensity and rate of decay as illustrated in Figure 1, graphs B and C respectively. Both transients can be best described as approximately exponential. The rate constant obtained with $[Ru(bpy)_3]^{1+}$ generated using DHB (Fig. 1B) is = 4. x $10^7$ $s^{-1}$. The same experiment performed with SA as a matrix yields a rate constant of approximately 1 x $10^7$ $s^{-1}$. Thus, the measured rate constants are slower for the SA generated $[Ru(bpy)_3]^{1+}$ than for $[Ru(bpy)_3]^{1+}$ generated with DHB. In addition, the S/N is better with SA than with DHB. The number of photons contributing to the emission signal in Figure 1C is ~5400 compared to only ~1100 in Figure 1B.

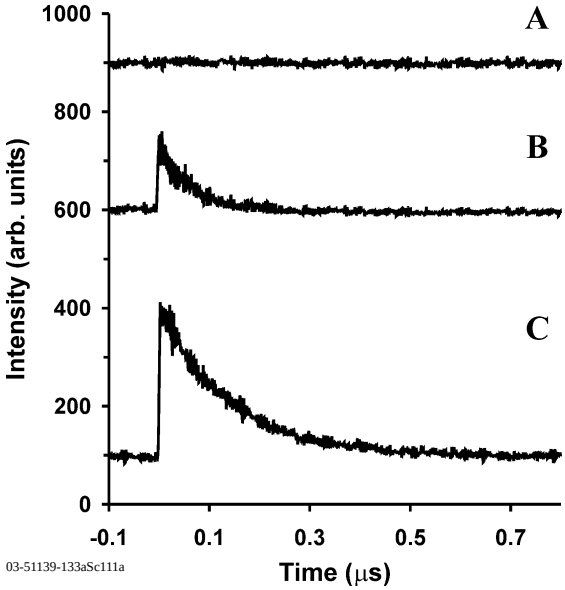


*FIGURE 1. Fluorescence lifetime transients: A) background prior to transfer of ions to optical detection cell, B) from ions generated using DHB as matrix, and C) from ions generated using SA as matrix.*

Based on solution experiments, emission from $[Ru(bpy)_3]^{1+}$ may seem unexpected; however, weak emission from ruthenium (I) polypyridines have been observed in frozen matrices where the solvent effects are minimized. In the gas phase, there is no solvent to couple to the vibrational and rotational modes of $[Ru(bpy)_3]^{1+}$ and quench fluorescence.

Based on previous work, it is possible that two ruthenium species are generated by MALDI that differ by one hydrogen atom as illustrated in reaction Scheme 1 (Fig. 2). A metal-nitrogen bond in structure A, $[Ru(bpy)_3]^{1+}$, is broken to produce structure B. Rotation of a pyridine ring and reformation of an ortho-metallated complex by a metal-C bond then produces structure C with concomitant loss of a hydrogen atom. Loss of one H to produce structure C is consistent with stabilization of the ruthenium complex by following the $18e^-$ rule. The most likely candidates for fluorophores are excited states of structures A and C. Even in the higher resolution FTMS spectra, the isotopic patterns for structures A and C would overlap and be difficult to distinguish. Additionally, there may be other conformations present that also fluoresce because very little is known about the behavior of large molecular ions, especially inorganic species, in the gas phase.

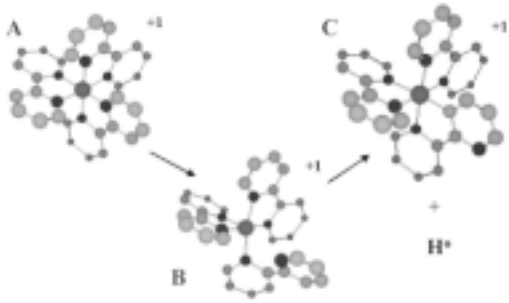


03-51139-133aSc111b

*FIGURE 2. Reaction scheme.*

Because more stable ions are generated by MALDI using SA compared to DHB, it is reasonable that distributions in energy levels are produced and account for some of the variability in the observed fluorescence signals. In solution, the energy levels of $[Ru(bpy)_3]^{2+}$drop to the singlet state in picoseconds before fluorescing because of solvent interaction with vibrational and rotational states of the metal complex. In the gas phase there are no solvent relaxation modes. While there may be some relaxation due to collisions, at a pressure of $10^{-8}$ Torr the calculated collision rate for $[Ru(bpy)_3]^{1+}$, assuming a molecular radius of 6.1 Å, is approximately 0.2 $s^{-1}$. However, the actual efficiency of collisional relaxation would depend on the size of the neutral involved in the collision. Therefore, molecular ions may be produced and trapped at multiple energy levels.

The results presented illustrate the powerful potential of combining mass spectrometry with gas-phase optical detection. While the mass spectra may indicate that only one species is present, the multi-exponential nature of the emission lifetimes suggests the presence of at least two optically active species. Using MALDI to generate the ions complicates interpretation because multiple structural conformations with a broad energy distribution can be created. Future experiments should utilize electrospray ionization (ESI) to generate ions to hopefully produce a single conformation with a narrower energy distribution. Additionally, ESI would allow production of the multiply-charged species $[Ru(bpy)_3]^{2+}$, which could be compared directly to solution experiments. Besides the ability to generate a well-defined population of large molecular ions, other technological challenges exist for the gas-phase spectroscopic study of molecular ions. For example, solution spectroscopy takes advantage of Beer's law. In the gas phase, Beer's law is difficult or impossible to apply because it is a non-trivial task to define the volume or determine the exact number of optically active ions; hence, extinction coefficients remain unknown. In essence, the study of the optical properties of molecular ions in the gas phase is at an embryonic stage similar to condensed-phase spectroscopic studies in the early 1900s.

This LDRD addresses the science need of DOE for basic fundamental knowledge that is not currently available. Specifically, this project addresses the need for information regarding intrinsic characteristics and reactivity of molecular ions in the absence of solvent. A primary DOE mission is also the development of new energy

technologies. This project will facilitate understanding of electron-and energy-transfer modalities, which may lead to development of improved energy collection, conversion, and storage devices. In addition, because many surface analysis techniques rely on mass spectrometers, including those at the INEEL, it is necessary to understand how the gas-phase ions generated during such analyses relate to the surfaces from which they are derived. Mass spectrometers cannot provide direct information about structural characteristics; therefore, it is necessary to incorporate the technology to directly measure the electronic and vibrational characteristics of gas-phase ions. Ultimately, it is expected that publications generated by this project will enhance INEEL opportunities to contribute to DOE programs, such as EM and SC, and encourage interest by outside sources.

# Recombinant Adhesive Protein Production and Investigation into Alternate Natural Adhesive Systems in Marine Mussels

*Heather Silverman, Frank Roberto*

***Super adhesives from marine mussels***

ET107

Exploitation of the natural adhesive systems in marine mussels can provide biomimetic glue products that are water impervious, inexpensive alternatives to conventional adhesives available today. The common blue mussel, *Mytilus edulis*, and a deep-sea methanotrophic mussel, *Bathymodiolus childressi*, are two organisms that produce strong, proteinaceous structures that are incredibly durable in an aqueous environment. Current purification methods for individual adhesive proteins from *Mytilus edulis* byssal structures yield only small quantities of proteins for further analysis. However, the adhesives industry requires large quantities of protein to perform adequate testing and analyses for future adhesive technologies.

This LDRD seeks to implement techniques for the identification of adhesive-related genes in two marine mussels, and to develop recombinant approaches for large-scale protein production of individual adhesive proteins. In addition, an investigation into the methanotrophic bacterial endosymbiont from *Bathymodiolus childressi* is proposed. Solutions to combat biofouling as well as identification of enzymes for industrial uses also may result from this research.

Marine mussels, like the edible blue mussel, *Mytilus edulis*, attach to a variety of surfaces in an aqueous environment using a natural adhesive. There are no conventional glues that can be applied in an aqueous environment that also are impervious to water and turbulent forces. Prior research has shown that one of the proteins in the adhesive, *Mytilus edulis* foot protein 1 (Mefp-1), bonds to glass, plastic, wood, concrete and Teflon. Eight other adhesive-related proteins from *Mytilus edulis* have been identified to date. Commercial recombinant products consisting of either the partial amino acid sequence of Mefp-1 or repeats of the unique decapeptide motif have been marketed. However, no commercial product incorporates any of the other proteins known to be involved in underwater adhesion by the *Mytilus edulis* mussel. Initial strategies for identifying the adhesive proteins of the byssus of *Mytilus edulis* involved purification of the proteins directly from the byssi of thousands of animals. About 10,000 mussels are needed to produce 1 gram of adhesive. Thus, subsequent purification and microscopic analysis require the sacrifice of many mussels, which is neither environmentally friendly nor economically practical.

This LDRD research is using reverse-genetics approaches to obtain complete adhesive-related gene sequences of transcripts actively expressed and transcribed by the *Mytilus edulis* mussel. With the complete gene sequences, an alternate host system can be employed to produce recombinant adhesive proteins for future analyses from protein chemistry, novel microscopy, and adhesive science disciplines. In addition, the investigation of an extreme, deep sea methanotrophic mussel, *Bathymodiolus childressi*, is proposed. The adhesive proteins of the deep-sea mussel also have not been examined to date. Symbiotic, methanotrophic bacteria are found to live within the gill tissues of this mussel, and may be a potential source of new enzymes for industrial applications.

Technical objectives for fiscal year 2003:

- Identify and confirm at least six adhesive-related genes for *Mytilus edulis* using reverse-genetic approaches: foot protein-1, -2 (three variants), -3, non-gradient byssal precursor, precollagen-D, precollagen-P.
- Obtain DNA information for an aromatic dioxygenase in *Mytilus edulis.*
- Perform small-and large-scale recombinant protein production studies for beta-galactosidase (control protein) and *Mytilus edulis* foot protein 1 (Mefp-1).
- Optimize purification strategies for acid-soluble adhesive proteins from *Mytilus edulis.*
- Isolate RNA from the foot organ of *Bathymodiolus childressi* mussels.
- Perform growth studies of a methanotrophic bacterial endosymbiont from the gill tissue of *Bathymodiolus childressi* mussels. Perform genomic screening of a methanotrophic bacterial endosymbiont from *Bathymodiolus childressi.*

The general scheme for identifying and expressing adhesive proteins from *Mytilus edulis*, as well as investigating the deep sea mussel, *Bathymodiolus childressi*, involves 1) reverse-genetic approaches for the identification and confirmation of adhesive-related gene sequences from *Mytilus edulis*, 2) large-scale recombinant protein production of adhesive-related proteins,

3) comparative analysis of adhesive-related proteins from *Mytilus edulis* with *Bathymodiolus childressi*, and 4) genomic screening of a methanotrophic bacterial endosymbiont from *Bathymodiolus childressi*. INEEL-Biotechnology capabilities in the areas of protein structure/function relationships, large-scale production of recombinant protein, and genomics of extreme environments (deep marine) can be gained from this research.

In FY01, the complementary DNAs (cDNAs) for six adhesive-related genes from *Mytilus edulis* were identified. This involved obtaining organisms, isolating messenger RNA (mRNA) from the foot organ, and converting mRNA to cDNAs using the enzyme reverse transcriptase and the polymerase chain reaction (RT-PCR). Screening of possible cDNAs was accomplished through high-throughput DNA sequencing. Full-length clones as well as other genes of interest (e.g., mussel genes encoding antibiotic proteins) were identified. The target adhesive protein genes for Mefp-1, -2, -3, nongradient byssal precursor, precollagen-D and precollagen-P were subcloned into a yeast expression vector (pYES2 or pYES2.1 TOPO-V5His; Invitrogen; Carlsbad, CA) and transformed into the yeast laboratory strain, INVSc1 (Invitrogen, Carlsbad, CA). Small-scale recombinant protein expression studies (e.g., milliliter volumes) using a control expression vector (for beta-galactosidase) and Mefp-1 and Mefp-2 yeast clones were initiated.

In FY02, small-scale heterologous expression of recombinant proteins was continued for beta-galactosidase and Mefp-1 (up to 2.0 liters maximum volumes). Results from 26-hour and 96-hour fed-batch experiments (e.g. galactose induction) revealed recombinant beta-galactosidase protein production at 8.4% and 12% of total protein production, respectively, by enzymatic assay procedures. Production of the adhesive protein Mefp-1 was not identified with the volumes used. Continued technical efforts focused primarily on methodologies for recombinant Mefp-1 due to potential business opportunities. Alternate strategies for induction of protein production (duration, cell densities, timing of galactose addition, concentration of galactose), yeast cell lysis (solutions, mechanical mechanisms), Mefp-1 protein solubilization (acid extraction techniques), and protein concentration (chemical and filter techniques) were tested. Screening of a cDNA library revealed DNA information for an aromatic dioxygenase gene that could be useful in identifying the catechol oxidase enzyme implicated in the adhesive structure of mussels. *Bathymodiolus childressi* mussels were obtained from an outside researcher and total RNA was isolated from excised foot organs. The RNA appeared intact and suitable for RT-PCR procedures based upon maintenance of ribosomal integrity (viewed by agarose gel electrophoresis). Homogenized gill tissue from the *Bathymodiolus childressi* mussels was processed for culturing of a methanotrophic bacterial endosymbiont. Cultures were maintained between 4-12°C in a methanotroph-specific media supplemented with a synthetic seawater formulation. Cultures were sparged with different methane gas mixtures to simulate the deep-sea environment. Results from microscopic images revealed a microorganism similar to that previously described in the literature.

In FY03, considerable time and effort was spent finalizing the cDNA gene sequence for the Mefp-1 clone. The difficulty in elucidating the complete DNA sequence was compounded by the fact that Mefp-1 protein isolated from byssal structures contains at least 80 decapeptide repeats with little substitution in the amino acid motif. Numerous internal sequencing primers were designed and tested to elucidate where the forward (5 prime) and reverse (3 prime) ends of the gene sequence overlap. A deletion cloning technique was also used to obtain additional sequence information. The cDNA clone was confirmed as a 1,698 base pair/565 amino acid sequence containing 39 decapeptide and 8 hexapeptide repeats, as well as a translational start and stop codon (estimated molecular weight of 62.6 kD).

It was determined that the clone was truncated from the original RT-PCR product obtained prior to cloning. This phenomenon of truncation has been reported before in the literature for repetitive-type gene sequences. Thus, the choice of expression organism appears to play a role in the maintenance of the original RT-PCR cDNA sequence with Mefp-1. Because other researchers have demonstrated adhesive properties in recombinant proteins using only partial Mefp-1 sequences, efforts to express recombinant protein from the Mefp-1 clone were continued. H. Silverman attended a short course in protein purification at Utah State University to gain experience in the theory and application

of various protein purification techniques and tools. Large-scale induction experiments (10.0 liters) were performed with both beta-galactosidase and Mefp-1 yeast clones in a 30 liter BioFlo 4500 fermentor (New Brunswick Scientific Co., Inc; Edison, NJ). Variables such as temperature, pH, optical density, agitation, dissolved oxygen, and gas flow rate were monitored for approximately 24 hours. The growth/induction profiles for the large-scale experiments paralleled those of the smaller scaled experiments, indicating that the modification of parameters for scale-up were appropriate. Purification for the acid-soluble Mefp-1 protein was performed with techniques that had been optimized in the pooling of samples from smaller scale experiments (zirconia beads plus mechanical shearing, formic acid extraction, dialysis for buffer exchange, and filter concentration). Following protein concentration measurements, ion exchange chromatography was performed with a linear salt gradient. Protein fraction profiles from the UV monitor showed the acid soluble recombinant protein eluting along the salt gradient, with another large elution occurring during the final regeneration step of the procedure. This profile is characteristic of Mefp-1 elution behavior (from earlier proprietary research performed by F. Roberto.) Mefp-1 protein fractions are currently stored for continued analysis and characterization. Three different cDNA clones for Mefp-2 also were confirmed through DNA sequencing. Their estimated sizes are 55.9 kD, 51.7 kD, and 47.6 kD. No published DNA sequence data is available for a foot protein -2 from *Mytilus edulis*, nor is there evidence for variations in "foot protein-2". The cDNA sequence data for Mefp-1 and Mefp-2 will be submitted to the National Center for Biotechnology Information (NCBI) database.

Bacterial genomic DNA was isolated from the methanotrophic cultures that were initiated in FY02. The polymerase chain reaction (PCR) was performed with primer pairs specific for the 16S rRNA gene (general bacterial, Type I methanotroph, and Type II methanotroph gene targets). A strong product was identified with the general primer set and non-specific products were present with the Type I and Type II primer sets. PCR also was performed with primers specific to two different forms of methane monooxygenase, an enzyme with industrial significance. No specific products were identified. Modifications in PCR reaction conditions will help in product specificity, and also may help to elucidate the presence of novel methanotrophic enzymes in the genome of the bacterial endosymbiont.

The range of applications for this research includes the biomedical, electronics, aviation, automotive, plastics, forest, pulp and paper, cosmetics, and veterinarian industries, among others.

An invention disclosure record was filed to protect intellectual property stemming from this research (IDR B-129; "Cloning and Expression of Recombinant Adhesive Proteins of the Blue Mussel, *Mytilus edulis*") in December 2000.

# Novel Materials for Evaluation of Generation IV Materials

*Terry C. Totemeier*

## *Characterizing steels in off-normal heat treatment conditions*

SC120

Ferritic-martensitic steels have been identified as the primary structural material for five of the seven Generation IV reactor concepts (and a secondary material for another). While there has been a good deal of effort to characterize these steels in normalized or peak strength conditions, less is known about their properties in off-normal heat treatment conditions that could occur in thick sections and welded structures.

To address these concerns, this LDRD is investigating the effect of off-normal heat treatment conditions on the microstructure and properties of two prototypical steels: T91(9Cr-1MoVNb) and Type 422 stainless (12Cr-MoVW). Two off-normal heat treatment conditions were studied: one that simulates improper austenization (annealing prior to quenching) and a second that simulates improper welding practices. The first off-normal condition is expected to result in a significant decrease in creep strength, while the second results in poor ductility and fracture resistance.

In this first year, tensile, creep, and impact test specimens were machined from both steels after standard and off-normal heat treatment. Room and elevated temperature tensile tests showed the first off-normal treatment to have slightly reduced strength at high temperatures, while the second heat treatment gave specimens that were hard and brittle. Creep testing was initiated and is in progress. In addition to the testing tasks described above, the creep testing capability at the IRC was upgraded to allow computer data acquisition, and a long-unused impact test machine was reinstalled and qualified for use.

Technical objectives for fiscal year 2003:

- Select off-normal heat treatment conditions for prototypic ferritic-martensitic steels to be used in Generation IV nuclear reactors.
- Study the effect of off-normal heat treatment on the microstructure and mechanical properties of these steels, including tensile, creep, and impact strength.
- Upgrade the creep testing capability at the IRC by installing a computerized data acquisition system.
- Install and qualify impact-testing capability at the IRC.

Funding for this program was approved in late January 2003. A review of the literature on the effects of heat treatment and welding on the microstructure and properties of the ferritic-martensitic steels was initially performed. Based on information gained in the literature review, two ferritic-martensitic steels and two off-normal heat treatment conditions were selected for study. The two steels, T91 (9Cr-1MoVNb) and AISI 422 (12Cr-1MoV) are prototypic of the 9Cr and 12Cr classes and were readily available commercially. The first off-normal heat treatment involves austenization at a temperature of 925°C instead of the normal 1050°C, followed by a standard 760°C tempering treatment. This heat treatment is intended to simulate potential inadequate austenization that might occur during treatment of large structures in the field. It also serves to simulate the "Type IV" region of weld heat-affected zones (HAZ). Such inadequate austenization has been shown in a previous study to dramatically reduce the creep strength.

The second off-normal heat treatment is intended to simulate the effects of improper welding. Welding of these steels requires closely following a complex weld procedure with specified pre-heat, interpass, intercooling, and post-weld heat treatment (PWHT) temperatures. Welds in T91 and 422 appear to be most sensitive to the intercooling temperature (cooling of the work piece after welding and prior to PWHT). Lack of sufficient intercooling results in untempered martensite formation during cool-down from the PWHT. Lack of proper intercooling was simulated for both steels by austenizing at the standard temperature of 1050°C, air cooling to only 300°C instead of room temperature, and immediately tempering at 760°C. Mechanical test specimens (tensile, creep, and impact) were machined at the North Holmes facility from each alloy heat treated in the three conditions (standard and two off-normal).

In parallel with the heat treatment and specimen production, the creep and impact test capability was upgraded. A new LabView-based data acquisition system for creep testing was developed and installed. This allows direct computer acquisition of creep data, rather than manual entry of printed data. The capability for in situ test monitoring and data plotting also was added. A non-functional, out-of-date fatigue test system was removed, and a Charpy impact tester, formerly in storage, was installed in its place. A heat-cool environmental

chamber was purchased and set up to enable Charpy impact testing at temperatures from -150 to 450°C. Use of the impact tester is pending review of qualification tests by NIST.

The microstructure of the two steels in the different heat treatment conditions was characterized using metallography and hardness measurements. Table 1 shows the results of micro-hardness measurements. For the T91 steel, the off-normal heat treatments did not significantly affect the microstructure observable at 1000X or the micro-hardness. In contrast, the 422 steel showed observable carbide coarsening following improper austenization, and a microstructure of untempered martensite following improper intercooling. Corresponding decreases and increases in micro-hardness are observed.

*TABLE 1. Micro-hardness data for T91 and AISI 422 in different heat treatment conditions.*

| Alloy | Heat Treatment | Micro-hardness (DPH) |
|---|---|---|
| T91 | Standard | 235 |
| T91 | Improper austenization | 237 |
| T91 | Improper weld intercooling | 230 |
| 422 | Standard | 307 |
| 422 | Improper austenization | 257 |
| 422 | Improper weld intercooling | 607 |

03-51139-130a

Room temperature tensile testing was performed for both alloys after standard and off-normal heat treatments. Tensile tests at elevated temperatures of 450, 550, and 650°C were performed for both alloys following standard and improper austenization heat treatments. The tensile strengths of the two alloys after heat treatment are shown in Figure 1. For both alloys a small decrease in tensile strength is observed for the off-normal heat treatment. This difference is less at 650°C than at lower temperatures. No significant change in ductility is observed. The second off-normal heat treatment (improper intercooling) appears to result in a slight reduction in room temperature tensile strength for T91, while for 422 this heat treatment results in very high strength (~1200 MPa yield) and poor ductility (~2%), commensurate with the untempered martensite structure.

Creep testing of T91 in the standard heat treatment has been completed and is pending analysis. An initial creep test on T91 after the first off-normal heat treatment has been started. Creep testing will be the focus of the second year of the program.

One of the objectives of this LDRD research was to revitalize the high-temperature test capability at the INEEL and allow INEEL researchers to come up to speed on materials issues in Generation IV reactor concepts. The knowledge gained to date has been very helpful in this regard, leading to creep testing work as part of a INERI program on the supercritical water reactor. The expanded knowledge base and test capability has allowed INEEL personnel to intelligently participate in NGNP materials research planning activities and assist INEEL-based Generation IV program managers with materials issues.

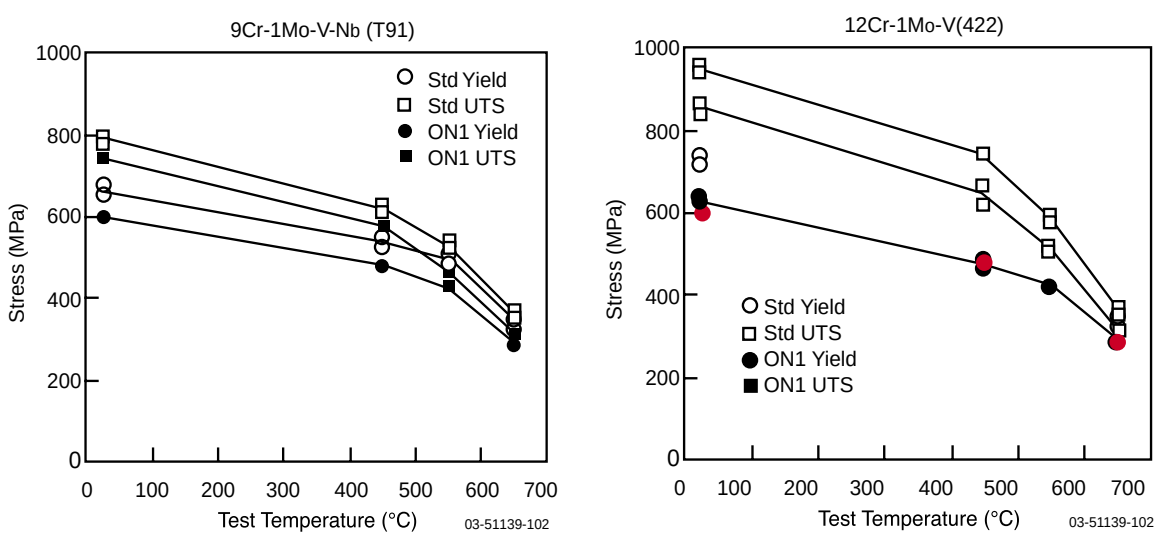


*FIGURE 1. Tensile strength of T91 and 422 in standard and off-normal heat treatment conditions.*

# Mechanical and Flow Properties of Dry Granular Media

*Clinton Van Siclen*

## *The role of granular disorder*

SC112

The storage, handling, and transport of granular materials are primary activities of many U.S. industries (e.g., pharmaceutical, food processing, construction). Despite this, the properties of granular media remain very poorly understood: grain silos still collapse, chutes and funnels directing granular flow become clogged, etc. The unusual static and dynamic properties, which may resemble those of a liquid or a solid depending on the circumstances, are produced by the collective behavior of the grains.

This LDRD considers the effects of disorder on the force structure of granular piles. In particular, a non-lattice model of a disordered pile was created that produces a probability distribution of normal forces on the substrate consistent with that found experimentally. Further, the model reveals the origin of this force distribution, and connects it with the probability distribution of intergranular forces in the pile interior. This is a significant accomplishment. This normal force distribution is evidently generic to disordered granular piles, in fact, it is the primary experimental result for granular piles since the interior forces are so difficult to measure, but it has not heretofore been satisfactorily explained.

Technical objectives for fiscal year 2003:

- Write computer code to create 2-D, frictionless piles of disks (representing grains).
- Write computer code to calculate the intergranular (contact) forces in the piles.
- Obtain force distributions from sets of piles characterized by their degree of structural disorder.
- Derive an analytic expression for the weight distribution on the substrate using the internal force distributions obtained from the frictionless piles.
- Prepare and submit report for publication.

Granular materials are of scientific interest due to their unusual static and dynamic properties, and of technological interest due to their ubiquity in industry. The unusual properties in the case of dry, non-cohesive granular material derive from the lack of an attractive intergranular force. Granular piles, which are considered here, are (meta-) stable only due to the opposing forces of intergranular friction and gravity. An important question is then the influence of friction on the static properties of a pile. Clearly friction, by acting against an applied force, directly affects the mechanical properties. But friction additionally permits structural disorder, which will influence properties as well.

A consequence of structural disorder is the existence of "force chains" (linear clusters of contacting grains at which compressive stress is concentrated) visible in experiments with photoelastic disks. These presumably are related to the exponential distribution of large normal forces on the substrate found both experimentally and in computer dynamics simulations. The latter additionally find the distribution not to be very sensitive to the choice of friction coefficient $\mu$.

Various lattice-based models have been developed in attempts to understand the production of normal forces much larger than the average force in nominally homogeneous granular piles. Disorder is introduced through the "coupling" between grains on a regular lattice; that is, by the allocation of the weight or forces on a grain to its supporting grains. Not surprisingly, such a procedure produces some normal forces at the substrate that are significantly larger than the average force, in a probability distribution that is exponential-like.

Thus, it is important to consider non-lattice granular piles where the structural disorder is built in as grains are added to stable positions at the top of the pile. This disorder is correlated to the extent that new grains are placed so as to accommodate the existing pile structure. Of interest are the probability distribution $P(w_s)$ of normal forces exerted on the substrate by the bottom layer of grains, and the probability distribution $p(w_{is})$ of contributions, made by the layer of grains above, to those normal forces. Knowledge of $p(w_{is})$ allows the construction of a simple theory that connects these distributions and produces an equation for $P(w_s)$ that holds for force fluctuations on the order of the average force as well as much smaller and larger forces. These distributions are of course affected by the degree of disorder in the pile, which is set by the template of grains placed on the substrate.

The 2-D piles of grains (identical disks) considered here were created by repeatedly placing a new grain atop a randomly chosen grain at the free surface of the pile and allowing it to fall to a stable position on the side at which it would lie lowest. However, some local configurations produced were

disallowed to ensure that each grain in the pile would be supported by exactly two grains, both of which lay at a lower elevation. This is a criterion for 2-D frictionless piles, so called because torques (due to friction) are not needed to achieve force balance at every grain. As evident in Figures 1 and 2, such disordered frictionless piles contain void defects common to frictional piles.

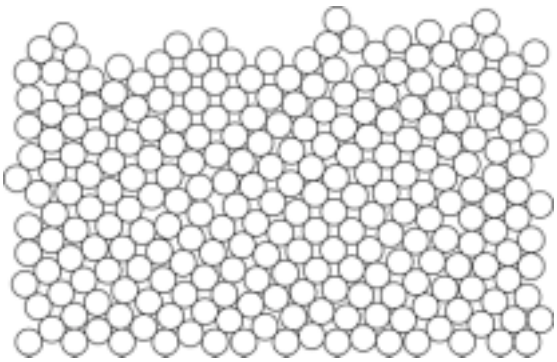

PN04-0004-135a-SC112

*FIGURE 1. Two-dimensional frictionless pile periodic in the horizontal direction. This pile, which is maximally disordered due to the initial random placement of grains on the substrate, shows the variety of possible defects.*

PN04-0004-135b-SC112

*FIGURE 2. Force network corresponding to the pile in Figure 1. The width of a bond connecting two nodes indicates the magnitude of the contact force between the two corresponding grains (the scale is not quite linear, since there is a minimum width). The black or red color indicates whether that force is compressive or zero, respectively. The heavy black lines then identify "force chains."*

The intergranular forces may then be calculated grain-by-grain in a top-down manner (i.e., in the reverse order that grains were placed on the pile). When a tensile force is thereby obtained, only the vertical force balance is required to be satisfied at that contact. This preserves the total weight of a pile and produces a small set of "zero force" contacts within the pile. A heuristic argument relates this procedure to the force structure in frictional piles.

The force distributions $P(w_s)$ and $p(w_{is})$ were obtained for piles characterized by degree of disorder. In the case of maximally disordered piles, $p(w_{is})$ was found to be an exponential function, which permitted a derivation of $P(w_s)$. The resulting expression is

$$P(w_s) = \left( \frac{N}{\langle w_s \rangle} \right)^N \frac{w_s^{\,N-1}}{(N-1)!} \exp(-N w_s / \langle w_s \rangle),$$

where $N$ is the number of grains supported by a substrate grain (so $N$=2 for these 2-D frictionless piles). This distribution fits experimental data obtained from real, frictional piles as well as the simulated, frictionless piles considered here.

The research presented here will be published in the journal *Physica A*, and is preliminary to a study of the force structure of conical sand piles where it is well known that the spatial distribution of normal forces on the substrate is strongly dependent on the method of pile construction. This dependence is not understood at present, and remains a research problem of considerable experimental and theoretical interest in the granular media community.

This LDRD was initiated in response to interest from DOE-BES. Contacts with other researchers, made at a DOE-sponsored workshop on granular media in January, and visibility via publication of the LDRD research may lead to future opportunities. In addition, familiarity with the research field was gained that may benefit various activities at the INEEL (e.g., biomass flow and separation, design of "pebble bed" nuclear reactors).

# Developing Collaborative Approaches to Long-Term Environmental Stewardship

*Greg J. White, William Keener*

***Understanding natural systems in the intermountain west***

ST106

Stewardship of biological resources at the INEEL is critical. Yet a lack of understanding of fundamental ecological patterns and processes is a significant barrier to the development of sustainable management practices. This LDRD establishes a collaborative research program between Idaho State University (ISU) and the INEEL for addressing local and regional environmental issues relating to long-term environmental stewardship. Both ISU and the INEEL have significant scientific expertise and distinct complementary capabilities to meet these varied environmental challenges.

Research efforts focused on two areas: 1) development of enzyme-specific probes for screening and characterizing environmental samples, and 2) assessment of the effects of climate change on the stability of protective caps for isolating buried hazardous wastes. These efforts are representative of the approaches necessary to meet environmental challenges and support the DOE goal of long-term stewardship at the INEEL.

Technical objectives for fiscal year 2003:

- Develop enzyme-specific probes.
  - Perform genetic and probe analysis of bacterial isolates from INEEL Test Area North site.
  - Perform additional experiments verifying probe response from groundwater isolates.
  - Present results of above experiments at a technical conference and prepare manuscripts for submission to scientific journals.
- Analyze effects of climate change on protective caps.
  - Perform soil profiling and heterogeneity analysis at the Protective Cap Biobarrier Experiment (PC/BE) plots.
  - Prepare report on the relationships between Walkley-Black organic carbon analysis and alternative methods for soils of the Snake River Plain.
  - Prepare and submit manuscripts on the development of resource islands under sagebrush plants.

*Development of enzyme-specific probes*. During FY03, significant progress was made in applying the enzyme activity-dependent probes and assays to field situations. These tools have been developed for the evaluation of microbial processes related to bioremediation in subsurface environments. Novel approaches have been incorporated into this work, including molecular probe and coupled fluorescence microscopy techniques. Two field studies in collaboration with Northwind, Inc., were completed that investigated the potential for microbial oxygenase activity in TCE contaminated groundwater at the INEEL Test Area North site. Using a variety of probes, related assays, and control experiments, significant levels of oxygenase activity within this system have been demonstrated. Specifically, activity of soluble methane monooxygenase and several toluene oxygenases has been demonstrated. These results are compelling since each of these enzyme systems co-metabolizes TCE.

Significant progress has also been made in developing molecular techniques based on gene sequences for these enzymes. Molecular probes have been applied to groundwater from this field site and have verified the enzyme activity probe results and further demonstrated oxygenase activity within aerobic regions of the TCE plume. These results have garnered considerable interest in private and governmental sectors due to the potential for demonstrating natural attenuation.

Specific research accomplishments this year include the successful demonstration of DNA and RNA probes for toluene and methane oxygenases. Amplification of soluble methane monooxygenase sequences from groundwater samples was also successful with two complete field tests being conducted. Experimental microcosm systems were developed for manipulative studies. TCE degradation directly linked to probe response was demonstrated. Successful amplification was demonstrated of toluene oxygenase sequences from environmental isolates using primers developed in the laboratory.

*Effects on protective caps of climate change*. Soil profile and heterogeneity analyses have been completed. Soils were sampled eight years after the PC/BE plots were created with a uniform soil. The results indicate that vertical and horizontal heterogeneity in soils has developed very rapidly on the PC/BE plots. This suggests that processes characteristic of undisturbed sagebrush steppe communities that are linked to soil heterogeneity may be manifested on constructed protective caps more quickly than anticipated, which has important potential ramifications in the performance of a

vegetative cap. Monitoring of soil moisture on experimental plots continued through FY03. Results of soil profile and heterogeneity development on the PC/BE plots at the INEEL were presented at the Soil Science Society of America annual meeting in November 2003.

Research conducted under these two tasks benefits not only the INEEL, but DOE and the Nation, by providing a better understanding of how the natural systems in the intermountain west can be managed to help protect human health and natural systems from hazardous and radioactive wastes. The research provides an increased bank of useful subsurface techniques, including subsurface microbiology methodologies, a field that is still in its infancy and expected to grow substantially over the next few decades. The research also resulted in increased visibility for both the INEEL and for ISU, and the completion of several more advanced degrees by INEEL employees.

This year's research resulted in the publication of two manuscripts and several research presentations, including two invited. Another manuscript has been submitted and three more have been prepared and are ready for submission.

The research conducted under this LDRD is focused on two independent, but related research areas. Both tasks address uncertainties regarding the effectiveness of natural systems in degrading and/or isolating anthropogenic contaminants in belowground systems. These tasks are critical to the mission of the INEEL.

This LDRD may lead to potential applications for enzyme probe development work involving different types of organisms and/or enzymes to address the problems of organic contaminants other than the chlorinated solvents that are currently being studied. Furthermore, enzyme probes may potentially be developed and applied in deeper subsurface strata to help clean up contaminated groundwater. As for the Restoration Ecology portion of the LDRD, the work conducted has already led to the development of several proposals for related research. These include proposals to INRA and the DOE. Additional proposals to DOE, National Science Foundation, and U.S. Department of Agriculture for ecological research are being discussed.

The basis for this LDRD project was to develop collaborations between researchers at the INEEL and Idaho State University that relate to DOE long-term environmental stewardship. As such, this project was essentially shared between personnel from the INEEL and ISU. ISU involvement includes both faculty and several students.

INEEL

# National Defense

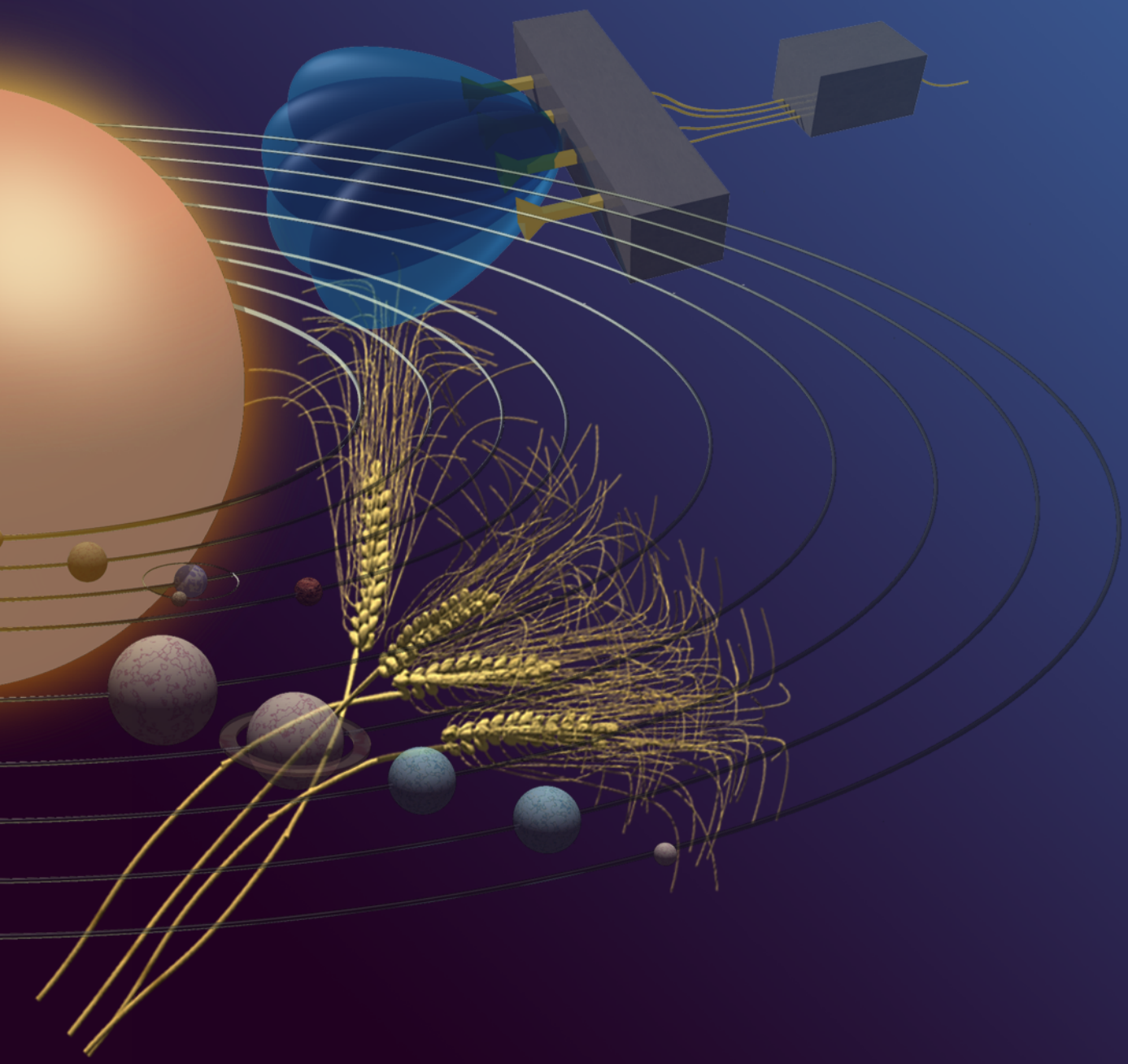

# Enhanced Isotope Ratio Measurement Sensitivity

*Anthony D. Appelhans, James E. Delmore*

***Improving detection capability even with smaller samples***

NS 134

Isotope ratio mass spectrometry is used in a wide variety of applications ranging from geochronology, to tracking manufacture of materials used in weapons of mass destruction. Current needs require analysis of ever-smaller samples and increased sensitivity. The sensitivity of isotope ratio measurements (chlorine, iodine, strontium, uranium, plutonium and others) is dependent upon the efficiency of the ion source and the associated optics of the ion lens that accelerates and focuses the ions into the mass spectrometer. Increasing the throughput efficiency of the ion lens will improve the absolute limit of detection (lower limit of the mass of an isotope that can be detected) and reduce the size of the sample required to make a measurement. The existing ion sources and lenses used in commercial and special-purpose isotope ratio mass spectrometers are based on a design that is over 35 years old and was developed prior to the availability of 3-D ion optics modeling programs. Preliminary analyses indicate that the performance of these ion sources and lenses is marginal. Indeed, the ion lens acts primarily as a collimator rather than a focusing device.

In this LDRD, modern 3-D ion optics modeling programs are being used to design a more efficient ion source and lens. The new ion source and lens will be fabricated and then tested on a triple sector isotope ratio mass spectrometer. The goal is to achieve at least an order of magnitude increase in sensitivity and reduce the amount of sample needed to make a measurement.

Technical objectives for fiscal year 2003:

- Generate a full 3-D ion optics model of a complete triple sector (two magnetic sectors and an electrostatic energy analyzer) isotope ratio mass spectrometer.
- Predict key performance indicators with the model and compare with measured values.
- Use the verified model to define the optimum input envelope of ion angular and positional dispersion required as performance criteria for the yet-to-be-designed ion-accelerating lens.
- Model and verify by experiment the existing ion accelerating lens.
- Design an advanced ion source and conduct preliminary testing in an ion optics test bench.

A 3-D ion optics model has been generated of a complete triple sector isotope ratio mass spectrometer. Key performance indicators (magnet focal points, z focusing of asymmetric magnet poles, mass resolution, and beam shape) were predicted with the model and compared with measured values (Fig. 1). Ion beam cross-section profiles were measured at the focal plane of the first magnetic sector of the triple sector mass spectrometer and as predicted by the SIMION ion optics model of the instrument. The measured beam profiles were projected onto a phosphor screen and photographed. The predicted beam profiles were generated using the experiment settings for the ion source voltages and magnetic field. The agreement demonstrates that the Z focusing of the off-normal magnet inlet and outlet pole faces is being properly modeled, and that the predicted mass resolution (dispersion of the two beams) agrees with the measurment. This close agreement between the model and experiment allows the model to be used to determine the optimum input characteristics for the magnetic sector, parameters required for design of a more efficient ion source and accelerating lens.

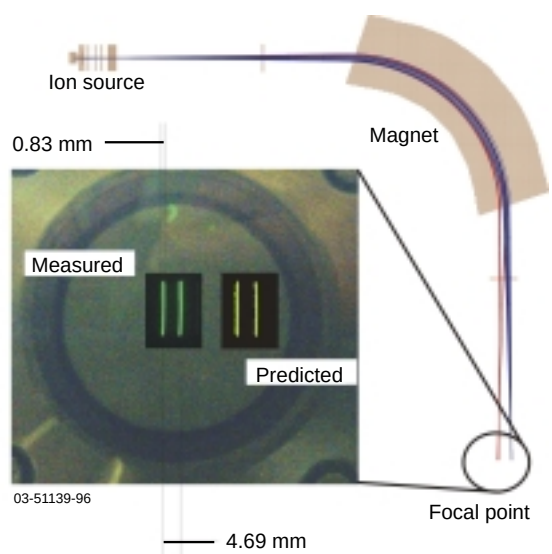


*FIGURE 1. Ion beam cross-section profiles measured at the focal plane of the first magnetic sector of the triple sector mass spectrometer and as predicted by the ion optics model of the instrument.*

The model was then used to define performance criteria for a new ion-accelerating lens. The existing ion-accelerating lens was modeled. Verification experiments clearly demonstrated its shortcomings, pointing out the opportunity for increased performance. In the course of analysis, a new design for an isotope ratio mass spectrometer with wide dispersion was discovered. Modeling indicates the design would provide significant advantages for actinide isotope ratio analysis. The design allows full-sized, low-noise, high-efficiency electron multipliers to be used for simultaneous measurement of multiple isotopes (7 or more) of an element. A patent idea record has been submitted and a proposal for development of an advanced isotope ratio mass spectrometer has been prepared and submitted.

Demonstration of INEEL's modeling capability has resulted in numerous requests from another national laboratory for assistance in modeling and analyzing several different mass spectrometers. This has resulted in a collaborative program for the measurement of Tc isotopes with DOE's Pacific Northwest National Laboratory, and request from a customer for submission of a proposal for design and construction of a wide dispersion isotope ratio mass spectrometer. Advanced isotope ratio mass spectrometry capabilities support both the national security programs of the INEEL, and the new mission relative to nuclear energy production.

# Security of Cyber Systems

*Wayne Austad, Steve Novack*

NS137

The final report for this LDRD project has a restricted distribution to only those approved personnel with a need to know access, and is not for public distribution. Requests for further information need to come through official channels.

# Wireless Security Research

*Wayne Austad, Scott Bauer*

***Increasing security in wireless communications***

NS140

The use of wireless systems is rapidly expanding in our nation's public and national security infrastructures. Many new protocols are being developed to carry both wireless voice and data, including Internet Protocol (IP)-based cellular and Land Mobile Radio (LMR) systems. The deployment of new secure protocols is often hindered by the need for compatibility with legacy systems. Architecture based on Intrusion Detection Systems (IDS) and hostile "packet scrubbing" provides independence from specific protocols, and makes possible a "black-box" security deployment on either legacy or new systems.

The objective of this LDRD is two-fold: to investigate the network aspects of security, and to investigate a novel approach to the physical aspects of wireless infrastructure security. In many situations the ability to "dynamically" enhance a specific cellular coverage area offers a significant advantage to homeland security, local law enforcement, federal agencies, search and rescue, unmanned missions, or intelligence personnel. This effort will use Autonomous Unmanned Aerial Vehicles (AUAVs) to carry "nano" versions of cellular controllers to extend coverage in a rapid, *ad hoc* fashion.

Technical objectives for fiscal year 2003:

- Install protocol sensor nodes on the Bechtel/INEEL Wireless Test Bed (WTB) for security R&D.
- Develop a trial IDS/packet-scrubbing system to test its viability on new cellular protocols.
- Investigate the applicability to new IP-based systems used by emergency responders and DOD.
- Install a nano-cell base station as small AUAV payload to aerially extend coverage.
- Test bi-directional control of AUAV using cellular data protocols on the WTB.
- Evaluate the security implications of such aerial-mounted devices.

This is a multiyear LDRD started late in FY03. During this first year, the investigators completed a background study of 2nd Generation (Global System for Mobile, GSM) and 3rd Generation (Universal Mobile Telecommunication System, UMTS) cell systems and analysis of architecture and interfaces for optimal locations for IDS nodes. Portable Linux-based PC systems were procured to support data traffic collection and IDS development, and two locations were investigated to probe and analyze traffic on WTB: 1) Abis link between radio Base Transceiver Station (BTS) and Base Station Controller (BSC), and 2) A-line link between BSC and Mobile Switching Center (MSC).

Detailed training WTB equipment also was completed this year as well as communication-link troubleshooting. Investigators also reviewed Session Initiation Protocol (SIP) control protocol for Voice-over-IP (VoIP) and procured two SIP Internet phones for probing and testing in the Cyber Security Lab and the WTB.

*Detailed Description of Traffic Probing:* The WTB structure (Figure 1), consists of three cell tower sites that provide a coverage area for mobile stations (MS). Each site is equipped with RF interfaces for processing radio to digital information. The Base Transceiver Station (BTS) is the GSM device used to accomplish transmitting radio frequencies over the air interface. In the WTB, the three cell tower sites are each equipped with a BTS. These sites, Gate-1, EBR-1, and CFA-609, are connected to the core system located at CFA-609. The CFA BTS is connected directly to the Base Station Controller (BSC) that is responsible for controlling traffic on the Abis link between it and the BTS. The BSC is functionally responsible for radio resource allocation to the MS, frequency administration, and handover between the BTS's controlled by the BSC. Additionally, the BSC is connected to the Mobile Switching Center (MSC). The MSC is a telecommunications switch or exchange within a cellular network and interfaces with location databases, such as the Home Location

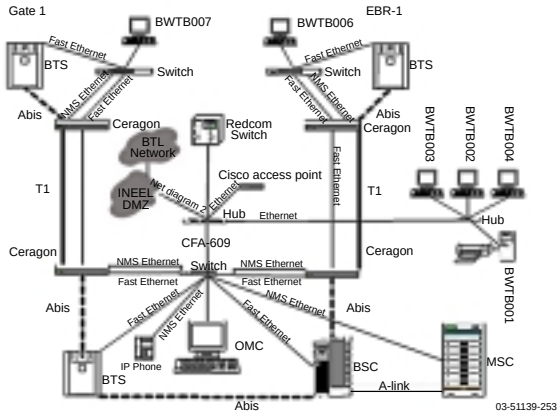


*FIGURE 1. Wireless Test Bed (WTB) structure for cellular testing.*

Register (HLR) and Visitor Location Register (VLR). The MSC is connected to the Operation and Maintenance Console (OMC) that performs operation and maintenance on the WTB networked system. The OMC functions include configuring, testing, event and error reporting, etc.

Because of the late start of this LDRD and difficulties in "tearing apart" the different layers within these links in such a short time, a functional IDS system will not be deployed until FY04. But many technical probes were tried and much was learned about the control signals within the cellular grid. The Abis link permits investigation of traffic from wired network as close as possible to the RF interface. Strategically this would impede the propagation of any malicious activity initiated from a hostile MS before it got into core network. The Abis link traffic flow uses protocol tunneling (protocols within protocols) and is described in the following manner: T1 to PPP, PPP to LAPD, and LAPD to DATA (InterWAVE message structure). Hardware analyzers also were used to trap such communications to decode the structure further, but the objective of this work ultimately requires access to the packets at a software level to implement INEEL's IDS and packet scrubber modules.

A conceptual design was completed on how to implement INEEL's packet scrubber code into such a structure, with additional T1 communications cards and new software drivers for INEEL's code. However, when authentication and encryption are deployed, this will make it difficult to analyze traffic using any security sensor. Another good location for monitoring traffic is at the BSC. Because the BSC employs Ethernet, this location is more compatible with present monitoring equipment and IDS software. It is also at the heart of most control signals initiated from either a MS or from the core network side, making it a nice single point for monitoring both sources of potential hostile activity. Implementation of this approach was started at the end of FY03. Additionally, work began on a test plan for probing SIP phones that transport voice calls over standard Internet lines in the Cyber Lab.

Physical security applications, the second aspect of this LDRD, included completion of the following efforts. FAA Certification of Authorization (COA) was established for operation of Remotely Operated Aircraft (ROA) at the INEEL as part of the National Air Space (NAS) System. The investigators purchased and modified a "surrogate" unmanned aircraft capable of simulating and demonstrating wireless CDMA 1x or GSM cellular communications. An "objective" unmanned aircraft was also purchased that is capable of carrying payloads up to 25 lbs for up to 4 to 6 hours. The investigators purchased and installed a highly autonomous autopilot system capable of 100% autonomy with or without pilot intervention on both "surrogate" and "objective" aircraft. The autopilot system and ground station were tested for tolerance of communication interruptions and safety. Additional efforts included:

- Purchased, configured, and tested CDMA 1x cellular interfaces, computer bridge / access points, and small board computers capable of payload integration in the "objective" unmanned aircraft. Tested configuration using the "surrogate" AUAV.
- Purchased, modified, and tested lightweight/ energy-dense Li-Polymer battery systems for the power of on-board AUAV communications payload.
- Investigated potential pico-cell relay systems to augment terrestrial cell base stations.
- Investigated RF propagation gains attributed to managing and flying an AUAV based Cellular Airborne Communication Node (Cell-ACN).

*Detailed description of AUAV mobile ad hoc cellular communications*: Research efforts have begun for investigation of using CDMA 1x cellular modem technology for the command and control of small AUAV platforms. This effort has included two different methods: A) the ability for a remote operator in the existing AUAV ground station control link to conduct a full command and control mission, and B) assembly of embedded system hardware designed to be carried on-board the AUAV that will provide a secondary command and control link completely independent of the existing AUAV ground station control.

*"Surrogate" Method*. Two cellular modems were purchased with one modem being used as a server for an encrypted Virtual Private Network (VPN), and the second modem being used as a client into that network (Fig. 2 next page). The VPN server was networked with the existing AUAV ground station providing a bridge between the cellular and

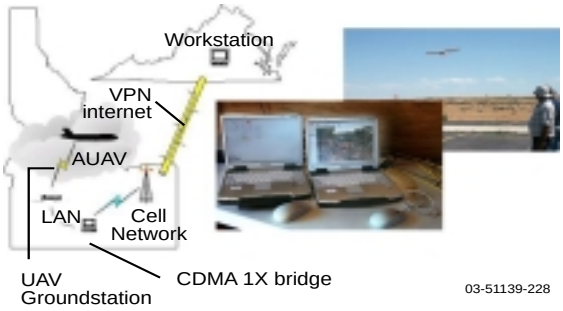


*FIGURE 2. AUAV "surrogate" method of cellular communications: conceptual and actual.*

RF ground control. The second cellular modem was placed in a laptop running a full operator interface to the AUAV. This system was then used to demonstrate the ability for a remote operator to log into the VPN server to monitor and control the AUAV as if they were sitting at the UAV ground station, but with the added ability to locate anywhere cellular connectivity can be established. Connectivity also was exercised from a remote Internet location to the wireless connection. Results to date have been outstanding.

*"Objective" Method*. Hardware suitable for integration onto the AUAV has been identified and purchased. This hardware includes a PC104 embedded processor, compact flash hard drive, PCMCIA adapter, and one of the cellular modems from method 1. This system has just been received and development activities are underway to integrate UAV command and control software with the cellular modem. All application development done for the surrogate method will be directly transferable.

INEEL cyber staff are co-authors of the most widely used open source IDS and packet scrubbing solutions (Snort and Hogwash) for standard computer networks. In addition, INEEL has developed custom IDS solutions, for use in defending its own networks, that are not published back to the open source community but have been used to trap and actively respond to "zero-day" exploits previously unseen. INEEL has extensive deployment experience and maintains dozens of these types of network abuse sensors as part of the INEEL Cyber Test Bed and for outside DOD customers.

Applying this expertise to INEEL WTB to advance the state of wireless control channel security is a natural and strategic extension. The WTB is isolated from the Public Switched Telephone Network (PSTN) so tests can be performed without impacting our own telecommunications infrastructure. Bechtel Telecoms is establishing itself as serious players in the higher-valued engineering services in the cellular industry (RF planning, etc.), but does not have the breadth or depth of INEEL's experience in writing new IDS security solutions. All of Bechtel Telecoms' clients have expressed that security is a "big concern," but few can articulate a definitive technological path forward. The vender of the present WTB equipment, InterWAVE, is very interested in the security of their telecommunications gear and has expressed an interest in collaborating on research. If a viable or inspiring security technology can be demonstrated as part of the WTB customer visits, it could greatly enhance WTB and Cyber Test Bed work opportunities for the INEEL Critical Infrastructure Test Range, a strategic initiative for the National Security Division.

A significant issue with all unmanned systems is the ability to communicate non-line-of-site for mission plan changes, monitoring health status, and data collection. Additionally, in many situations the ability to dynamically enhance a specific coverage area could offer a significant advantage as well as provide other *ad hoc* potentials. The ability to relay several channels of cell communications from a hot spot or diminished area could provide a significant advantage to personnel involved in homeland security, local law enforcement, federal agencies, search and rescue, recovery applications, unmanned required missions, or intelligence related CONUS (Continental US) or non-CONUS needs.

This LDRD effort has targeted a novel approach of using secure encrypted bi-directional cellular based communications for UAV mission control, and the installation of a nano-cell relay to dynamically extend cellular coverage. Potential clients for both efforts include various entities within the Department of Homeland Security, Department of Defense, Law Enforcement, DOE Physical Security, and the Intelligence Community. All are important customers to the National Security Division. Presentations on preliminary results during visits to the INEEL have generated positive feedback and opportunities for programmatic funding, if results of FY04 work are successful.

# Novel Threat-Risk Index Using Probabilistic Risk Assessment and Human Reliability Analysis

*George Beitel*

***Identifying and quantifying risk to U.S. infrastructure***

NS139

Over the past 25 years, the value of the basic event tree/fault tree approach to risk analysis models has been demonstrated by the INEEL with nuclear power plants. The same basic tool used to model terrorist attacks could be of general applicability to power plants, transmission systems, pipelines, transportation, and other infrastructure systems.

The objective of this LDRD is to demonstrate the applicability of SAPHIRE, an event tree/fault tree package, to provide an integrated assessment of infrastructure/industrial systems. Specifically this research will lead to development of a model sensitive to human factor parameters, physical system parameters, economic engineering principles, and failure mode calculations. The model could be used to calculate a threat-risk index on a quantitative variant or basis for updating the current qualitative National Color-coded Threat Alert.

The long-term objective is to develop a technology that government agencies or industries can use across domains (dams, navigation systems, ports, rail, energy systems, chemical plants, and harbors) to assess, track, and support the planning process for reducing terrorist threat risk. For this investigation, the investigators chose to develop an application using a system of dams and hydroelectric facilities in the State of Idaho.

Technical objectives for fiscal year 2003:

- Determine a set of models to be integrated into a single comprehensive model that results in a quantitative risk assessment.
- Analyze terrorist attack probability for varied targets and compare with existing modeling approaches.
- Present and discuss results with USACE and USBOR.

A set of models has been successfully integrated into a single comprehensive model that results in a quantitative risk assessment. The resulting Quantitative Threat-Risk Index Model (QTRIM) is being compared with other contemporary approaches that use qualitative information to populate generalized risk matrices and uniformly apply the same threat index number to terrorist attack probability for varied targets. The results from the QTRIM were presented to and discussed with the U.S Army Corps of Engineers (USACE) and with the U.S. Bureau of Reclamation (USBOR). Both USACE and USBOR have expressed continued interest in this work.

QTRIM consists of:

1. The targeting model that estimates the probability of terrorist attack.
2. The human reliability model, consisting of a series of human response logic models.
3. The physical impacts model that, as applied to the hydroelectric system, includes dam failure models, flood inundation model, and loss of service model.
4. The probabilistic risk analysis model, SAPHIRE, an INEEL event tree/fault tree software program.
5. The consequence/loss model, providing a socioeconomic account of the attractiveness of potential targets, or, alternatively, the potential economic damage from an attack.

Based on a Sandia-developed model, RAM-D, and as accepted by the Interagency Forum on Infrastructure Protection (IFIP) — a consortium of hydropower generators, government dam owners, transmission system operators, and anti-terrorism experts — security risk assessments have been performed on most high-risk dams during the past five years.

The RAM-D process involves a thorough dam-by-dam inspection and calculates the risk (Probability x Consequence) of each respective asset using the equation:

$$R = P_A*(1-P_{eff})*C,$$

Where the probability of attack, $P_A$, is set equal to MEDIUM for all high-risk dams and consequence, C, is equal to HIGH for all dams considered. Since two of the three variables are constant, the risk assessment defaults to assessment of $P_{eff}$ — the effectiveness of the facility to detect, delay, and respond, thereby, preventing success of a terrorist attack. The INEEL model calculates risk using the same general approach, but actually calculates $P_A$, estimates dollar values for C for all levels of damage, and considers a system of dams with automatic prioritization.

The above summary of RAM-D was excerpted from: "*Risk Assessment Methodology for Dams (RAM-D)*," by R. V. Matalucci, proceedings of the

6th International Conference on Probabilistic Safety Assessment and Management (PSAM6), San Juan, Puerto Rico, USA, June 2002.

Approaches such as those used in RAM-D provide no mechanism to prioritize or compare one dam against another, nor do they evaluate the impact of a failure of one or more facility in a system on the other(s). The RAM-D model is based on the nuclear materials protection approach, an evaluation technique where risk is generally mitigated by adding guards and guns. However, dams are public assets and, as often as not, viewed as visitor attractions and recreational facilities.

The major advances associated with the QTRIM are a better approximation of the threat and priority of a specific dam as a target, integration of human factors and reliability information, and consideration of multiple dams including downstream effects that may greatly enhance the overall effectiveness and consequence of a terrorist attack. It demonstrates that the probability of attack and failure from terrorist attacks is so low for most dams, and that the risk from attacks by groups such as ecoterrorists who seek less damage may, in fact, be the greater risk. The model is still not validated; even so, it provides estimates of probability of attack that correspond with published terrorist activity.

QTRIM represents a highly successful and well-received study and proof of principle using proven software modeling (SAPHIRE) in conjunction with an integrated systems approach to identify and quantify risk. The utility of a quantitative approach in replacing or supplementing the current qualitative approach is readily apparent. Both the USACE and USBOR are faced with prioritizing available funding to address security improvements. Huge cost savings can be realized by identifying (region-by-region and then state-by-state) which targets are at risk, what is their priority, and where resources should be directed. State and National Legislatures and security agencies can potentially save millions in taxpayer dollars by limiting spending to the higher priority threats identified by this risk analysis approach. QTRIM can be used to support actions to preserve valuable natural resources that then can be used to direct other activities useful in reducing the national threat to terrorist entities. The QTRIM model approach should be of general applicability to power plants, transmission systems, pipelines, transportation, and other infrastructure systems.

# Smart Antenna Systems in a Wireless Local Area Network

*Lynda L. Brighton*

***Enhancing quality of service, spectral reuse and improved security***

NS135

A typical antenna for a wireless local area network (WLAN) system transmits RF energy equally in all horizontal directions (i.e., equal coverage over 360° in azimuth) and only has one RF output. As clients make a connection, the effective data rate decreases proportionally to the number of clients. "Smart Antennas" can be defined as a Switched Multibeam Antenna or Adaptive Arrays. The benefits of Smart Antennas in Wireless Systems include: 1) a significant increase in range for clients from feet to miles, 2) an independent/directive channel (array beam) for each client that improves performance by increasing the available data rate and minimizing the number of packets lost and bit error rate (BER), and 3) optimized coverage for each client while minimizing coverage in all other directions, thereby, significantly decreasing opportunities for those other than the intended client to receive the signal and increasing security at the RF level.

This LDRD effort evaluates antenna systems to support multiple simultaneous clients without degradation and with improved security.

Technical objectives for fiscal year 2003:

- Develop or procure Wireless Local Area Network (WLAN) Smart Antenna Systems
- Evaluate/procure WLAN performance monitoring tools.
- Characterize WLAN performance for Smart Antennas vs. typical (omni-directional) Access Point Antennas.
- Research Algorithms for a Space Time Adaptive Processor (STAP) WLAN System.
- Research Digital Signal Processing (DSP) Boards, Real-Time Operating Systems (RTOS) and Network Interface Controller (NIC) cards.

Smart Antennas can significantly improve the performance of wireless systems by providing higher antenna/diversity gain to extend the range; multi-path mitigation interference suppression to improve quality, capacity and security; suppression of delayed signals resulting in quality improvement and higher data rates; and multiple signals (clients) in the same or different bandwidth resulting in higher data rates and increased capacity.

Several Smart Antenna Systems were evaluated under this effort. The choices were narrowed down to two antenna systems. The first is a Simultaneous Switched Multibeam antenna, designed and constructed under this effort. The second smart antenna system was procured from Vivato Inc. and is a Simultaneous Multibeam Antenna/WIFI Switch. To determine the benefits of using a smart antenna system in a WLAN, performance tests were conducted on both of these antenna systems as well as a typical WLAN Access Point (AP) Omni Antenna.

The Omni-Directional Cisco Aironet 350 system consisted of an omni-directional antenna connected to each client of an *ad hoc* system consisting of Cisco Aironet 350 PCMCIA and PCI network interface cards. The Vivato Smart Antenna/Switch WLAN system consisted of a planar phased array antenna access point system with all necessary RF components, processing capability, and LAN switching functionality. This system has thirteen high-gain fixed receive beams that are serviced by three high-gain electronically phased steered transmit beams. The array azimuth 3 dB beam width is between 6° and 7° and the elevation beam width is approximately 12°. This system supports the simultaneous use of three channels of different frequencies, one each on each of the three transmit beams.

For the Switched Multibeam, a pseudo wireless LAN access point was constructed by positioning a series of seven high-gain panel antennas in a semi-circular array pattern. Each element had an approximate 3dB horizontal beam width of 14°and an elevation beam width of 90°. Each of the antennas in the array was connected to one of eight rows of an 8-row by 4-column RF matrix switch. Three of the four columns were used to channel the bi-directional RF signals from three network interface cards (NIC) to three antenna elements of the array. This system supported three transmit/receive beams.

Chariot, a network performance-testing software package, was used to measure throughput and other performance parameters. Four different data transmission protocols were monitored with the Chariot software in all tests, e.g., TCP, UDP, RTP, and VoIP. Each test was run for two minutes with the sampled performance data averaged.

The following sections are a brief summary of the measurement results.

*Range vs. Antenna Type*. Tests were completed outdoors at Iona Hill north of Idaho Falls. The omni-directional and the switched-beam systems were configured using a Cisco access point. The range between the antenna under test (AUT) and a single client was systematically increased until the throughput dropped below 1 Mbps or the signal was lost. Network performance data was collected with Chariot at three different elevations (average above the data points for range distance evaluated) for the AUTs: WP 18 ≅ 140 ft, WP 22 ≅ 60 ft, WP 24 ≅ 40 ft. Typical data results are shown in Figures 1a and 1b.

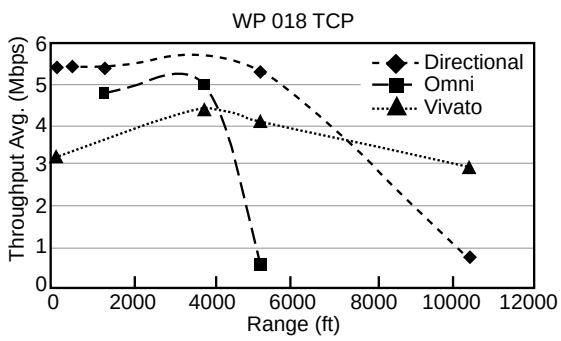


*FIGURE 1a. WP 018 TCP results.*

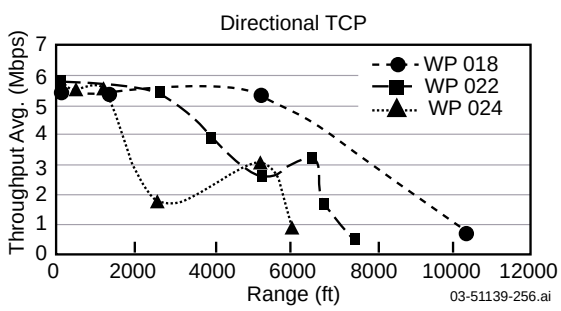


*FIGURE 1b. Directional TCP results.*

The range data collected showed that: 1) the Vivato and the Directional Antenna (Switched Multibeam) could typically operate over a much longer range than the omni antenna, with the Vivato typically slightly surpassing the Directional Antenna system; and 2) the higher the antenna system is placed (relative to the client location/ elevation), the longer the range over which the system will operate. (This is true for all three antenna systems evaluated).

*Client Load vs. Antenna Type*. Tests were completed outdoors next to the INEEL Heyrend Facility in Idaho Falls. The omni-directional and the switched-beam systems were configured in an *ad hoc* mode with no access point. The clients were placed 100 feet from each other or from the Vivato panel. The number of clients was systematically increased to measure the effect on network performance parameters for each of the antenna types.

Tests showed that the Vivato system scanned for the directions of highest signal level. It was therefore difficult to control the pointing direction through which the system communicated. In other words, as a client was placed in one of the receive beams and throughput was being measured, the system did not remain focused and locked to that receive beam. It was observed that when more than one client used the same Wi-Fi frequency channel, the data throughput was shared among the clients and thus was divided by the number of clients. When the clients were operating on different channels, the throughput remained high for each of the clients up to three clients. Beyond three clients, the throughput decreased in a similar fashion to a typical AP. The system was able to service multiple clients located in multiple directions or a three-fold increase in capacity over a typical AP.

Within the 100-foot operating range, and for one client and one channel, the omni-directional antenna system generally performed with slightly higher throughput than the Vivato system. However, only one channel was allowed. As the number of clients increased above one, the throughput was divided by the number of clients connected to the WLAN. As expected, the signal level as measured at the clients was always lower than that of either the Vivato or the switched beam systems.

As in the Vivato system, the Switched Multibeam System allowed multiple clients and three different channel frequencies to be used simultaneously. This system operated somewhat differently than the Vivato system, however, when more than one client was used with the same channel frequency. In this case, the data throughput was unexpectedly shared disproportionately among the clients. Some additional testing was performed and preliminary results showed that co-channel interference between beams was the direct cause of throughput sharing. However throughput was higher when the

clients were located in separate beams. When the clients were operating on different channels the throughput remained high for each of the clients up to three clients. Beyond three clients the throughput decreased in a similar fashion to a typical AP. The system was able to service multiple clients located in multiple directions, or a three-fold increase in capacity over a typical AP.

*Algorithms reviewed*. The development of the DSP algorithm has been performed in two stages: researching algorithms and algorithm development. A number of methods exist that can be used for smart and beam-forming antennas. An extensive amount of effort went into researching tried-and-true methods and studying the algorithms. Several algorithms were reviewed to identify an appropriate algorithm for the STAP system. There are two basic types of algorithms: those that require or assume *apriori* knowledge of the direction of an arriving signal and adaptive beam forming, and those that do not require direction of arrival knowledge.

Once a greater understanding of the beam-forming process was gained, an existing implementation was selected as a base line to develop the STAP algorithm for the project. An outline for the process was developed and represented in an N-Squared chart as well as in a System Design Document. The space-time adaptive beam-forming algorithm proposed uses a combination of time delay and direction approximation based on Choleski solving methods. This algorithm applies a predetermined time delay to the signal sample to create three apertures: early, on time, and late. The early and late signals are used to form a covariance matrix. The Choleski method is then applied, and the beam-forming weights are determined. Follow-on effort will include refinement of the algorithm and system design.

*Hardware review*. Several DSP boards, real time operating systems and WLAN interface cards (NIC) were investigated for potential use for the ultimate WLAN STAP system. From what was investigated from the DSP and RTOS products available, it seems that the algorithm will be the determining factor for selection. Most of the DSP cards had on-board memory and/or FPGA support. Many products are on the market, use the same few chipsets in slightly different configurations, and utilize all the common bus footprints (e.g., VME, PCI, PMC). After the algorithm, issues of throughput and ease of coming up to speed will make the biggest difference in selection.

The antenna systems evaluated in this LDRD that support multiple simultaneous beams proved out the concept that multiple clients can be supported without degradation in throughput if the beams are configured to different RF channels. A three-fold improvement was measured over a typical omni AP point antenna in network performance, i.e., the amount of bandwidth available to a client is equal to the maximum available bandwidth until the fourth client makes a connection to the WLAN. The antenna systems that support directive array beams proved out the concept that range can be significantly increased over an Omni AP Antenna; i.e., a two-to-6-times improvement in range was measured for the directive antenna systems over the Omni AP Antenna.

A STAP algorithm has been proposed for implementation in the follow-on LDRD effort after extensive research was conducted to select the best algorithm for an Adaptive WLAN System. Once the algorithm has been fully defined, then the DSP and RTOS can be identified and implemented, based on the research completed.

# Automated Control and Electronic Signal Acquisition/Processing Systems for Sprayed Distributed Sensors

*Robert Carrington, John Richardson, Karen Moore*

***Spray-on sensors for damage detection***

NS132

Assuring the reliability and security of the nation's infrastructure – from pipelines to bridges – requires the ability to monitor operations and structures in near real time. This LDRD characterizes and demonstrates the acquisition and transmission of encrypted digital information, utilizing a data communications network communicating via thermally sprayed conductive traces. The system is applicable to a variety of infrastructure security applications where the sensor and communications network can be imbedded in physical systems such as pipelines, bridges, building structures, etc. Additionally, project activity developed a Process Flow Diagram for an industrial data trace application system. The prototypic application used for both the communications and application system evaluation was for a natural gas pipeline. The Process Flow Diagram was developed with input from Delphi Research Co., gas pipeline fabrication/coating industry, and natural gas pipeline operators.

Technical objectives for fiscal year 2003:

- Perform system design of data network.
- Specify and design trace electrical interface.
- Design and fabricate pipeline electrical simulator.
- Test network hardware and electrical interface.
- Design and fabricate data acquisition system.
- Develop a Process Flow Diagram for an operational data trace system within a pipe mill for a prototypic gas pipeline application.

The overall objective of the data communications portion of this project was to show that data could be acquired, and encrypted information transmitted between pumping stations along a gas pipeline utilizing conductive thermally sprayed traces placed on a pipe wall. The data network topology was first defined and a balanced IEEE-485 selected as the interface.

The investigators developed a model to simulate the overall goal of transmitting data over 20 miles (32 km). The model was produced using a Spice-based program named MultiSim and configured as a modified classical lossy transmission line. As part of pipe damage detection research being done for the National Energy Technology Laboratory (NETL), a nine-foot pipe had multiple thermally sprayed traces applied to it. This physical system served as a basis for the construction of the theoretical computer model. The pipe study included the measurement and collection of raw data for analysis and calculation of the basic model parameters such as resistance, inductance, and capacitance of different areas of the sprayed pipe. A theoretical electrical model was developed and simplified that closely matched the physical characteristics of the pipeline system. Once a good model was developed, it was simplified and tested in the frequency and time domains to determine the effective properties of actually sending data down the length of the pipeline. Then a series of 20 one-mile, lumped, parameter simulators were built to simulate the goal transmission length of twenty miles (Fig. 1).

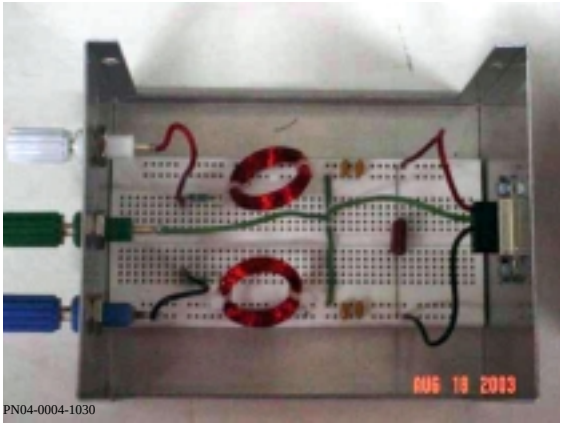


PN04-0004-1030

*FIGURE 1. One-mile pipeline electrical simulator.*

The resulting simulator was tested to see how fast data could be transmitted down the pipeline (bandwidth). Finally the basic system was reinvestigated to see how the bandwidth could be improved by changing the physical dimensions of the physical plasma-sprayed system.

The investigators also prepared data communications hardware and data acquisition hardware. A software package was generated to transfer information and provide command sequences to the remote data acquistion electronics. These were interfaced to the same scaled, prototype pipeline section used to quantify physical electrical characteristics earlier. Both remote data acquisition and encrypted data communications were successfully demonstrated during laboratory testing (Fig. 2).

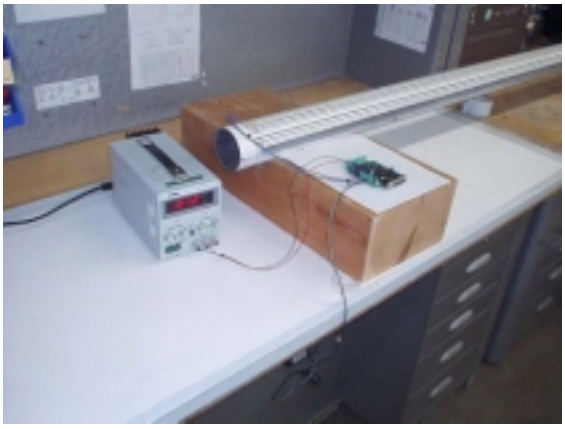

PN04-0004-103b

*FIGURE 2. Encrypted data communications test.*

Another task in this LDRD was to explore the automation of the spray control systems to enable application of sprayed traces within the specified tolerances required for deployment of the technology. The knowledge gained in fabricating pipe for the NETL-funded work suggests that a level of process control required for either sensor or communications applications is significantly higher than that used in typical thermal spray coating applications. The spray system must have a very consistent process that integrates gas flow, traverse speed, mechanical position, and electrical power using feedback controls that monitor temperature, acceleration, force, and angles. In addition, the system must rapidly measure resistance values per length on completed traces for verification.

The investigators worked with Delphi Research Co., a supplier of industrial spray systems, and Flame Spray Inc., a specialty spray shop, to identify technical issues for an industrial spray system capable of meeting the more stringent requirements for sensor or communications applications including cost targets. Process improvement issues that were addressed included elimination of manually applied masking prior to trace application and alternatives to the alumina-insulating coat. Elimination of the masking may be accomplished utilizing Delphi Research Co. proprietary spray gun design that controls the trace edge properties using a distributed particle velocity spray pattern. Because of the low-temperature application proposed for early demonstration on gas pipelines, plastic coatings have been proposed as an alternative to the alumina insulation coat. While this will provide adequate isolation for communications applications, there is still an open question regarding use of the trace as a strain sensor. The ability of the plastic to properly transfer strain between the pipe and the trace must still be verified. A detailed process flow diagram has been created to document and relate requirements for separate components, and define process and subsystem interactions and enclosure constraints.

The sensor technology investigated under this LDRD has potential application to a number of security, reliability and transportation uses where it can be used to remotely detect damage, monitor operations and be used to improve decision-making processes.

# Thermomechanical Processing of Titanium 10V-2A1-3Fe

*Henry Chu, Thomas Lillo, Kevin McHugh*

***Building ever-stronger armor for combat missions***

NS141

The armor community is in need of improved structural armor material that can be used to build the combat systems of the future. Titanium alloys have been identified as the materials that possess the best balance of mechanical and physical properties. A current structural armor candidate is standard Grade-A Titanium 6Al-4V. However, other titanium alloys may hold even greater promise for satisfying the strength and hardness needs of armor, if process issues can be resolved.

This LDRD investigates developing a suitable titanium-based structural armor material using Titanium 10V-2A1-Fe, an alloy that may offer higher performance than titanium 6A1-4V. Titanium 10V-2A1-Fe is expensive and currently only used in specialized applications. As a result of this limited use, little knowledge exists of the alloy's process parameters. To develop the thermomechanical (TMP) process parameters to transform ingots into plates suitable for structural armor application, a small as-cast Titanium 10V-2A1-3Fe ingot was purchased. Rolling slabs were sliced from the ingot and hot-rolled uni-directionally and cross-directionally into plates approximately 0.7" thick. The rolled plates were subsequently solution heat-treated according to one of the schedules reported by a previous Army Research Lab (ARL) study. The heat-treated plates were ballistic tested against 30-cal armor-piercing (AP) projectiles at muzzle velocity together with a commercial Grade A Ti 6Al-4V plate and a factory-forged Ti 10V-2A1-3Fe plate for comparison purpose.

As a subtask in this LDRD, improved manufacturing methods for transparent aluminum oxynitride (ALON) also were investigated. The concept of using a gelcast process for fabrication potentially offers a more cost-effective manufacturing method to produce windshield-sized, conformal, transparent armor for vehicles. Attempts were made to fabricate transparent ALON from elemental powders by gelcasting followed by pressureless sintering. Eleven different formulations, containing boron metal powder, boron oxide, or lithium aluminate as sintering aids, were explored. It was demonstrated that gelcasting could be used to make samples exceeding 0.5" thickness. However, sintering of the gelcasting failed to yield fully transparent material.

Technical objectives for fiscal year 2003:

Main Task:

- Develop the thermomechanical (TMP) process parameters to transform ingots into plates suitable for structural armor application.
- Develop joining/welding process for the Ti 10V-2A1-3Fe alloy.
- Evaluate for ballistic properties.

Subtask:

- Explore gelcasting of elemental powders to produce ALON.
- Explore sintering aids and develop samples for ballistics testing.

The investigators originally planned to procure inexpensive, electron beam re-melted, high-purity Ti 10V-2A1-3Fe (Ti-10-2-3) ingots from the TITAN Production-Research center of the Paton Research Institute at Ukraine for this study. The quoted price for a typical (5.6" x 18" x 60") ingot was $10 per pound, which was subsequently lowered to under $8 per pound due to favorable currency exchange rates and the quantity of ingots requested. Unfortunately, during the month of August, the Ukraine production facility was in summer recess and could not respond to the purchase order in time for this fiscal year's work. To initiate the TMP development phase and get a feel for the material, a special small ingot (about 38 lb) was purchased from TIMET, the only U.S. source of Ti-10-2-3 materials, at a cost of $56 per pound.

Two rolling slabs were machined from a half-cylindrical ingot. The initial process of ingot was double re-melt and cast in vacuum with no further heat-treatment or forging. Initial slab dimensions were 9.75" x 5.5" x 1.43" and 5"x 5" x 1.43". Slab #1 was rolled in a predominately longitudinal direction (UR) and the rolling direction was reversed by 180 degrees after each pass. Slab #2 was cross-rolled (CR) with a 90-degree turn after each pass. All slabs were pre-heated in nitrogen atmosphere at the transus temperature of 780 - 800°C for 25 minutes before each pass. Seven passes were required to reduce the 1-1/2"-thick slabs to approximately ∫"-thick plates. An additional skim pass was required to flatten the uni-directionally rolled (UR) plate.

Based on one of the heat-treatment schedules (SCH F) previously reported by the U.S. Army Research Lab at the Aberdeen Proving Ground (APG), the two rolled plates were simultaneously solution-heat-treated at 730°C for 1 hour, followed by an air cool outside the furnace to room temperature of about 25°C. The temperature ram rate was set at 600°C/hr. The two plates were finally aged at 600°C for 8 hours (temperature ram rate was 600°C/hr), followed by an air cool outside the furnace to room temperature. After final cool down, the plates were trimmed into several 4” x 6” targets for ballistic tests.

A standard Grade-A titanium 6Al-4V was also prepared as a baseline target. Additionally, a commercially forged (standard commercial practice) Ti 10-2-3 plate was purchased and prepared as a comparison target. The ballistic test was performed at the INEEL live-fire range using 30-cal, armor-piercing projectiles launched at muzzle velocity of 2800 ± 25 ft/sec. The target was clamped on to a steel picture frame placed at a standoff distance of 20 feet from the muzzle of the rifle per Mil-Std-662. A bundle of 24 pieces of 10” x 12” x 5/16”-thick dry wall panels were placed 6” behind the target to capture the residual projectile and to gage the approximate residual energy in the event the projectile perforated the target completely. The results of the test are summarized in Table 1.

Note that in the previous ARL study the test rounds were 22-cal fragment simulated projectiles (FSP), and the 30-cal AP rounds used in the present study represent orders of magnitude higher threats. It is anticipated that the threshold threat level for the titanium alloy would be a 50-cal AP round.

It is shown that the Ti 6-4 alloy performs better than the rolled/HT and the forged Ti 10-2-3, and the cross-rolled (CR) Ti 10-2-3 performs slightly better than the uni-directional-rolled (UR) one. The preliminary results seem to indicate that the differences in the hardness may have some influence on the ballistic performance. However, the current three-month study period is too limited to allow more in-depth investigation and achieve better ballistic performance. Further parametric studies of the thermomechanical process on the final properties of Ti 10-2-3 will be continued in FY04. (Effort to procure a ˚-tone ingot from the Ukraine to produce full-sized armor plates also will continue in FY04.).

A high-capacity drive motor was procured to upgrade the present INEEL friction stir weld (FSW) setup in anticipation of demonstrating the feasibility of this advanced technique in joining Ti 10-2-3 plate stocks. Development of an FSW process on this titanium alloy will continue.

*Investigation of gelcasting method for manufacturing ALON:* Eleven different recipes containing various sintering aids (boron, boron oxide or lithium aluminate) were mixed with elemental powders (alumina and aluminum nitride) in the proper ratio to produce ALON consisting 20 to 30 mol% AlN. The sintering aid additions ranged from 1 to 7.5 wt% of the elemental powders. Samples were gelcast as either 1”-diameter disks approximately 1” thick or as a single bar 0.88” x 0.88” x 4”. Both sample forms exhibited shallow cracks on the top surface of the gelcasting but otherwise were largely free of cracks, demonstrating the potential of gelcasting to produce large

*Table 1. Ballistic test comparison of titanium alloys*

| | Thickness | Hardness | Velocity | Result |
|---|---|---|---|---|
| UR Ti 10-2-3 | 0.757 in | 32.8 Rc | 2799 ft/sec | Perforated + 16 pcs of dry wall |
| CR Ti 10-2-3 | 0.774 in | 32.6 Rc | 2811 ft/sec | Perforated + 4 pcs of dry wall |
| Forged Ti 10-2-3 | 0.762 in | TBD | 2802 ft/sec | Perforated + 13 pcs of dry wall |
| Grade A Ti 6-4 | 0.772 in | 33.4 Rc | 2793 ft/sec | Projectile stopped |

03-51139-99a

(>3” diameter x 0.5” thick) samples. After drying, the gelcasting exhibited a density of ~30-45% of theoretical density.

Sintering of the gelcast samples produced final samples that were translucent to various degrees. However, none of the samples exhibited full transparency, even after polishing. None of the samples exceeded 98% of theoretical density, which is probably the reason for the lack of transparency (residual porosity causing light scattering). The samples with $LiAlO_2$ were the most translucent. Sintering times were only on the order of six hours and most likely longer times would produce more transparent samples. The severely limited project duration of three working weeks did not permit the sintered material to be evaluated for ballistic properties. Higher concentrations of $LiAlO_2$ and longer sintering times should be used in the future to obtain transparent material.

The investigators believe that a gelcast process could be successfully developed via the adjustment of the pressureless sintering process and/or incorporation of a final hot-isostatic-press phase. However, the results of the current gelcast development effort may be too ambiguous to attract further funding.

This LDRD was initiated based on interest by the U.S. Army and U.S. Treasury for improved armor materials. The U.S. Army Research Lab has been briefed on this continuous effort and agreed to support future testing of the processed titanium 10-2-3 plates. It is expected that successful completion of the main task will bring follow-on support from the U.S. Army to advance the technology to Technology Readiness level (TRL) of six (scale-up production demonstration) and higher (production ready).

# Client/Server Architecture for High-Performance Computing

*Greg Corbett, Kurt Welker, Andrew Shewmaker*

***Easing implementation of high-performance applications***

NS136

While the hardware costs associated with high-performance computing (HPC) have decreased dramatically, the costs of creating applications to take advantage of HPC have remained prohibitive. The reasons for this include the high cost of labor, the complexity of managing distributed resources, and the increasingly heterogeneous environments in which these applications must run. Java, and recent Java-related technologies promise to reduce the difficulty of implementing parallel applications that can operate in heterogeneous distributed computing environments.

This LDRD is investigating a parallel high-performance computing architecture based on Java, the Java Management Extensions (JMX), and the Jini distributed services protocol. This architecture follows the client/server model in that client applications are able to directly control their distributed processes. It is simpler, has good cross-platform capabilities, and provides more extensive management capabilities than other distributed computing architectures. Two versions of this architecture were developed. The Parallel Computing Architecture for Java (Pca4j) is based on Java and Jini and provides a low overhead method for distributing tasks in a distributed computing environment. The Parallel Computing Architecture for JMX (Pca4jmx) is based on Java and JMX and gives the user much more control over its distributed processes.

This research also addresses a deficiency in the INEEL's high-performance computing capabilities, namely classified cluster computing. This capability now enables scientists to use high-performance compute clusters to create more realistic models than are on existing classified workstations. This project addresses the classified cluster's hardware, software, and security needs; implements a security plan to address these needs; and examines the cluster environment's usability for two projects.

Technical objectives for fiscal year 2003:

- Design and implement a parallel computing architecture based on Java, the Java Management Extensions, and the Jini distributed services protocol that is easy to use, supports many platforms, and gives the client a rich management interface to its running processes.
- Develop a pilot application that demonstrates the capabilities of this architecture.
- Demonstrate the architecture using a real-world application – the USAF Model for Electronic Support and Attack (MESA), a Java-based mission-planning tool.
- Demonstrate the feasibility of using the classified computing cluster at the INEEL for multiple projects.

Pca4jmx uses the JMX to provide a rich interface through which a client application can manage its tasks while they are running on remote servers. Pca4jmx encapsulates some of the key components of the JMX architecture to provide a simpler interface to the user. The primary components of the Pca4jmx architecture are identified in **Error! Reference source not found.** These components consist of:

- Client Application – An application that has created a number of task objects that it wishes to run in parallel.
- Tasks – Java objects that contain the data and code necessary to perform a certain job.
- Pca4jmxAgent – A process that manages a pool of Pca4jmxServers.
- Pca4jmxServer – A process that is capable of running a task object. Pca4jmxServers reside on distributed nodes throughout a computing system.

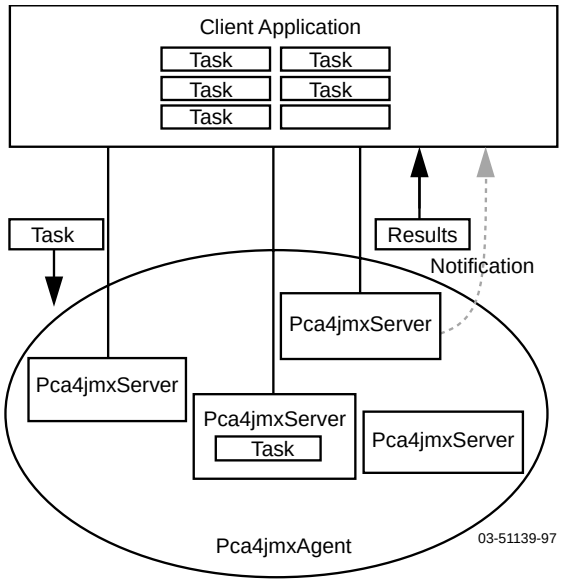


*FIGURE 1. Overview of the Pca4jmx architecture.*

There are several steps for running a parallel job using this architecture. First, the Client Application breaks up its overall job into smaller tasks that can be run in parallel. It also connects to the Pca4jmxAgent and requests a number of available Pca4jmxServers. The Client Application then assigns a task to each Pca4jmxServer. When a task completes, a notification is sent to the Client Application. The Client Application can then retrieve the results of the task. While a task is executing, a Client Application can get and set attributes, and invoke methods on the task through the JMX interface. The Client Application also can perform complex JMX queries on its tasks.

Pca4j is similar in architecture to Pca4jmx, but is based on the Jini distributed service protocol. This results in a faster, lighter-weight architecture, but also removes many of the management capabilities of Pca4jmx.

A parallel version of MESA was implemented using Pca4j. In one benchmark test the parallel version of MESA used 60 processors to complete a job in 4:49 that took 3:54:26 in serial — a 49-times speedup. The SAPHIRE application also was parallelized with Pca4j and experienced similar speedup. For both applications the implementation using Pca4j was simple and straightforward.

A classified compute cluster was set up at the INEEL. A security plan for the cluster was implemented and approved. The CTH hydrodynamics software was installed and tested on the cluster. This cluster uses diskless nodes, and supports multiple classified projects through use of a removable disk on the head node. To change the current project using the cluster, the removable disk containing that project's workspace must be locked in a safe and replaced with the new project's disk. This method also requires the locks on the door to the room to be changed between each project which may cause some inconveniences. However, the cost for a project to run on the classified cluster is reasonable, approximately 40 hours for security (lock changes, classification guide, etc.) and 10 hours for system administration (initial system configuration, user training, etc.).

This classified cluster is just a temporary solution to the needs of scientists and engineers at the INEEL. A compartmentalized facility, and an operating system with certified and proven isolation of different users, such as Trusted Solaris, would be needed to allow multiple projects with different "need to know" status to use a cluster simultaneously.

Although Pca4j will be used by the MESA and SAPHIRE applications, and possibly other potential USAF customers, there are still several issues to address. These include: improved security policies, a configurable priority policy, and an improved fault tolerance and fault recovery.

An Invention Disclosure Record for Pca4j and Pca4jmx is currently being processed. A paper describing the results of this research is being prepared for submission to a peer-reviewed journal or conference.

Through this LDRD the INEEL has now demonstrated a classified computing capability, positioning the INEEL to participate in such research as simulating critical infrastructure protection, and modeling and simulation of ballistics and armor.

# Development of Enzyme-Activity-Based Assays for Potential Bioterrorist Agents Designed for Use With Current Detection Platforms

*William Keener, Thomas Ward, Joni Barnes*

***Detecting likely bioterrorist toxins***

NS138

N-glycoslases and proteases are some of the most serious biothreat agents in the world. N-glycoslase agents include ricin, one gram of which could theoretically kill between 350 and 1,000 people. One gram of botulinum (BoNT) could kill 1.5 million people if perfectly distributed. BoNTs, tetanus (TeNT), and ricin are threat agents of immediate concern due to their potencies, their availability, and their usefulness in native, unaltered forms. Ricin is a significant component of a byproduct of castor oil production. Production facilities around the world could theoretically yield about 20,000 tons of purified ricin each year for possible use by terrorists.

This LDRD evaluates enzyme-activity-based assays for detecting toxins that are likely bioterrorist agents. Research plans utilized polymerase chain reaction (PCR) techniques and concentrated on detecting activities of two different enzyme classes: N-glycosylases and proteases. N-Glycosylases include the biothreat agents ricin, abrin, and shiga toxin. Protease toxins regarded as biothreat agents include botulinum neurotoxins and tetanus neurotoxin. Based on the specific toxin-catalyzed, enzymatic cleavage reactions that cause the toxic effects *in vivo*, alternative substrates in the proposed assays were designed to be specifically cleaved to yield products detectable upon their formation (i.e., real time) or after product-dependent, PCR-based signal amplification.

For this research, safe unregulated toxin surrogates were used. Complementary assay strategies for both N-glycosylase and protease activity detection could allow quantitative, real-time detection, or highly sensitive detection based on PCR. Selectivity and speed are made possible by specific cleavage reactions involving stable substrate reagents and minimal steps to produce signals from the cleaved products, respectively. Specific toxin capture and activation processes also should enhance selectivity. Activity-based detection will provide a response that is commensurate with the actual threat, and will be less fallible to engineered toxin threat agents than immunoassays or DNA tests for toxin genes. LDRD-funded development of new activity assays will be followed by integration with known toxin capture and activation methods. These combined methods will be incorporated into existing PCR-based detection platforms through phased efforts emphasizing early incorporation with subsequent improvements.

Technical objectives for fiscal year 2003:

- Examine potential activity assays for ricin-like, N-glycosylase toxins using surrogates.

The initial funding period for this LDRD was June-September 2003. The main objective of the research was to demonstrate proof-of-concept for key elements of new approaches to detecting protein toxins on the basis of their enzymatic activities. Ricin-like toxins were the treat agents initially considered in this project.

Several technical considerations have influenced the project scope. For example, to minimize dependence on infrastructure in putting the detection methods into practice, the diversity of reagents and the necessary instrumentation must be minimized. In practice, this will best be accomplished with detection strategies applicable to toxin classes, not just individual toxins, using reagents suited to detection platforms that currently exist. Platforms that include the polymerase chain reaction (PCR) for detection of DNA are widely used and effective. This project's assays incorporated such a platform as a means of amplifying the activity-dependent signal to improve sensitivity and minimize false negative results. Like PCR, the detection chemistries will require different probes (e.g., oligonucleotides) to permit the identification of each specific agent, but the detection mechanisms and many of the reagents need not vary. Toxin-contaminated samples will include complex background components that, if not removed, can cause false positive or negative signals. The use of known toxin capture strategies will enable the timely co-integration of the novel activity assays, along with methods for rapidly concentrating and purifying the toxins, into existing PCR platforms.

During the initial four-month period of experimentation, research demonstrated a highly sensitive assay using three N-glycosylase surrogates for ricin toxin. This three-step assay involves a glycosylase-catalyzed conversion of an artificial substrate, followed by PCR-style thermocylcing to amplify the signal, and measurement of the signal by gel-based analysis (Fig. 1 next page). The investigators

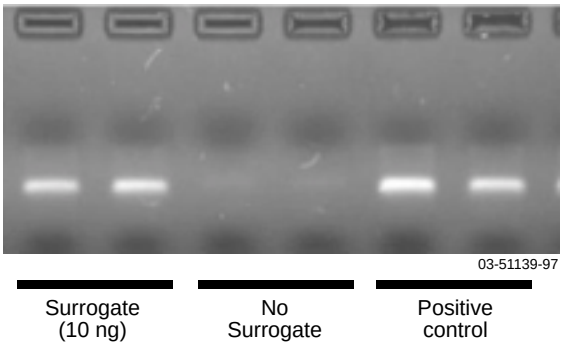


*FIGURE 1. Gel-based analysis of the reaction products amplified from surrogate-catalyzed reactions (30 min, 30°C).*

succeeded in detecting 1/4 of one nanogram of a ricin surrogate (1 billion nanograms = 1 gram), with just 10-minute reactions for the toxin activity (first) part of the assay. This current detection limit is theoretically equivalent to 1/4,000,000th of a lethal dose of ricin. Furthermore, the assay signal is proportional to the amount of toxin activity in the sample (i.e., the more toxin, the greater the signal). In future work, time required for the second part of the assay (thermocycling will be reduced, and the need for the last part (gel analysis) will be eliminated by using fluorescence-based signal analysis during termocycling. It is anticipated that the total assay time can be reduced below one hour.

The mission of the National Security Division at the INEEL is to support the non-proliferation of weapons of mass destruction, including bioweapons. This brief, fast-paced LDRD effort represents an opportunity for the INEEL to enter into a new niche of biodefense research, leading the way in activity-based detection of threat agents. Indeed, opportunities to effectively enter and compete in the field of biodetection are very limited, especially opportunities requiring a small investment. Early in FY04, the intellectual property demonstrated to date would be protected by the standard process. CRADA opportunities are now being explored. In addition, collaborative interactions are being pursued to enable testing with authentic toxins. Work on developing a more fieldable protocol will be given a high priority.

# Cermet Filters for Hazardous Material, Chemical and Biological Weapon Agent Destruction

*Peter C. Kong, Larry D. Zuck, Gary M. Huestis, Robert Pink, Brent Detering, Arnold W. Erickson*

***Extending high-temperature cermet filter applications***

ES101

In the aftermath of 9/11 and the subsequent anthrax attack on America in 2001, the nation is propelled to develop new technologies for critical infrastructure protection, environmental security, and national security. The U.S. military, fighting against unconventional enemies, needs the utmost protection against weapons of mass destruction.

Functional, high-temperature cermet filters have potential application in hazardous chemical and biological agent destruction. This technology is adaptable for command structures and combat equipment protection on battlefields, making the research and development of cermet filter technology a high priority.

This LDRD investigates cermet filters for hazardous chemical and biological weapon agent destruction. A single-step combustion synthesis process manufactures the cermet filters. Metal powder, ceramic oxide powder, sacrificial fillers, and doping material are mixed and compacted to form green filter discs and thin cylindrical filter shells. The compact is fired at high temperatures to initiate the combustion synthesis process to form a net shape structure. The cermet filter can be brazed to metal during synthesis. Material properties include inexpensive starting materials, high melting temperatures, high-heat capacity, good thermal-shock resistance, low thermal-expansion coefficient, electrically resistive self-heating, lightweight strength, ability to produce ammonia and hydrocarbon gases with water, and high particulate removal efficiency. Bench-scale destruction tests of tributyl phosphate (TBP), a simulant of chemical weapon agent VX, have been completely successful. A larger-scale destruction reactor was designed and constructed for contaminated infrastructure cleanup simulation tests.

Technical objectives for fiscal year 2003:

- Continue research and development of cermet filter systems.
- Continue small bench-scale cermet filter destruction of chemical weapon agent simulants.
- Design and construct a large-scale reactor for chemical weapon agent simulants destruction.
- Conduct large-scale chemical weapon agent simulant destruction tests.
- Simulate contaminated infrastructure cleanup.

The final phase of this LDRD focuses on the manufacturing of thin cylindrical filter shells, small bench-scale destruction of chemical weapon agent simulant, and the design and construction of a large-scale cermet filter reactor for contaminated infrastructure cleanup simulation tests.

As reported at the end of FY02, the initial development of thin cylindrical filter shells was unsuccessful. The thin cylinder shells had no structural strength even though no filler materials were used to increase the porosity of the filter. The filters partially crumbled after the combustion synthesis step. The difficulty came from developing a method to compact a thin wall (0.125”) hollow cylinder with significant diameter and length. High porosity requirements to maintain low-pressure drop for the cylinder filter shells further compounded the technical challenge. After months of research and development work, the technical obstacles were finally conquered. A double reversed compaction method was developed to form the green body compact in the mold. A new cermet composition was developed to carry out a thermite combustion synthesis reaction in the mold to form the final cylinder thin shells. The thermite combustion synthesis released much higher reaction heat than ordinary combustion synthesis reactions. The higher combustion heat produced significantly stronger filter shells that allowed machining operations if modifications were needed on the filters. Equations (1) and (2) below represent the *ordinary combustion synthesis* and the *thermite combustion synthesis* throughout this research.

$$2Al + 2Fe + Al_2O_3 \rightarrow 2FeAl + Al_2O_3 \qquad (1)$$

$$4Al + Fe_2O_3 \rightarrow 2FeAl + Al_2O_3 \qquad (2)$$

In reaction (1) the alumina does not participate in any reaction and the heat of reaction only comes from FeAl formation. However, in reaction (2) half of the aluminum involves in the reduction of the iron oxide and the formation of alumina while the remaining half of the aluminum involves in the formation of FeAl. Therefore, the heat of reaction for reaction (2) comes from both the formation of FeAl and alumina.

It is obvious that the thermite combustion synthesis reaction will produce much stronger final structures. The investigators were able to produce

very porous and strong thin filter shells with a 1:1 volume ratio between the cermet powder and the filler material. It was also found that coffee grounds were very effective filler materials. The cermet filter material composition was further refined to increase the electrical resistivity for self-heating. As synthesized, the thin filter shells showed a very low electrical resistance (<1Ω). This low electrical resistance will not permit the filter to produce high self-heating temperatures. However, doping with other metals can increase the bulk resistivity of the cermet filter, thus raising the self-heating temperature.

Research determined that adding 1 wt% of a high resistance metal to the cermet material composition would increase the bulk resistance of the filter shell to about 4Ω. Experiments had shown that adding 1-3 wt% of high resistance metals to the cermet material composition produced filter shells with bulk electrical resistance ranging between 3-9Ω. Figure 1 shows the self-heating test for a short cylinder. The temperature of the bright glow part of the filter shell reached well over 700°C; however, the heating was not uniform over the entire cylinder. Achieving complete uniform self-heating remains a technical challenge.

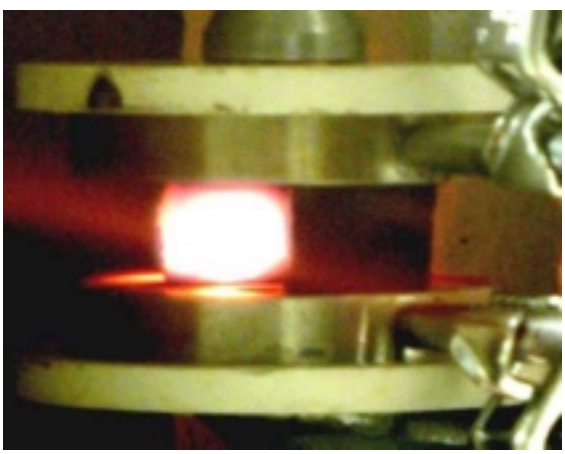

PN04-0004-100a

*FIGURE 1. Self-heating test.*

Several agents and their simulants were identified for the cermet filter destruction tests. These agents included mustard gas, sarin, and VX. Among these agents, VX has a nontoxic simulant, Tributyl phosphate (TBP) that closely resembles that of the real agent. TBP has a molecular weight and structure extremely close to VX. If the cermet filter can destroy the TBP, very likely it can destroy VX, which is highly toxic, and other highly toxic agents. The molecular composition of VX is $[(CH_3)_2CH_2]_3(CH)_2NSPO_2$ with a molecular weight of 267. The nontoxic simulant TBP has a molecular composition of $[CH_3(CH_2)_3]_3(CH)_2PO_4$ and a molecular weight of 266. TBP is a sticky oily substance and has a fairly high boiling temperature.

During the tests, TBP was injected at a rate of 0.01 cc/min into the heated cermet filter reactor. The filters were 1” x 0.25” discs. Air was the oxidant, and the flow rate was set at 500 cc/min. The destruction product was captured in cold traps using liquid-nitrogen-cooled ethylene glycol as coolant and large Teflon trap bags for product analysis. Besides air, steam also was used as an oxidant for TBP destruction. The destruction product was analyzed by gas chromatograph (GC) for residue TBP. A coated polymer fiber extraction probe was used to extract the destruction products from the traps. Using the coated polymer fiber extraction probe, the GC detection limit was 1 ppb. One ppb is below the lethal limit for VX, and a destruction process must achieve this value. At 1 ppb GC detection limit all results showed that TBP was not present in the trapped gas.

A larger scale cermet filter reactor was designed and constructed to simulate the continuous cleanup of a contaminated area or prevention of toxins from breaching a confined structure. The reactor system consisted of a ceramic reactor housing made of lava stone. The thin wall hollow filter cylinder was mounted inside a heater that was enclosed in the reactor housing. Because of electrical penetration for the heater, ceramic was chosen as the housing material. The ceramic reactor housing is attached to an aluminum box, which houses a heat exchanger for cooling the heated processed air to ambient temperature before it enters the confined structure. The Plexiglas box represents the confined structure where occupants are protected from external toxins. A blower fan connecting the Plexiglas box and the destruction reactor represents the make-up air system that recirculates the air in the confined structure through the destruction reactor for processing. An injection port located just in front of the reactor simulates the air intake vent where airborne toxins (TBP vapor) enter the confined structure. Extraction ports were installed

in the heat exchanger housing and the Plexiglas chamber for processed air sampling to detect the level of toxins remaining in the structure.

The complex ceramic reactor housing was machined from green lava stone stock. Green lava stone is very fragile, and machining was a painfully slow and careful process. The machined parts were fired in a furnace at 1250 °C at a ramping rate of 50°C/hr and then soaked for five days before being cooled down to room temperature at the same ramping rate. The fully cured lava stone parts would turn from dark gray to pinkish tan color. If the lava stone parts were fired too hastily, they would thermal-shock to pieces or crack and warp. During assembly of the first reactor, mechanical stress broke the metal pipe and ceramic junction coupling. The coupling method was redesigned and a second reactor was built. However, during pre-heating of the reactor (at a very slow heating rate) in preparation for TBP injection, thermal stress caused the reactor housing to crack. The insert in Figure 2 shows the crack developed on the reactor housing during the pre-heating process. Because of the crack on the housing, TBP injection was not carried out. The inability to complete this last task in FY03 reveals that the reactor housing needs to be constructed of metal, and the heater must be mounted externally.

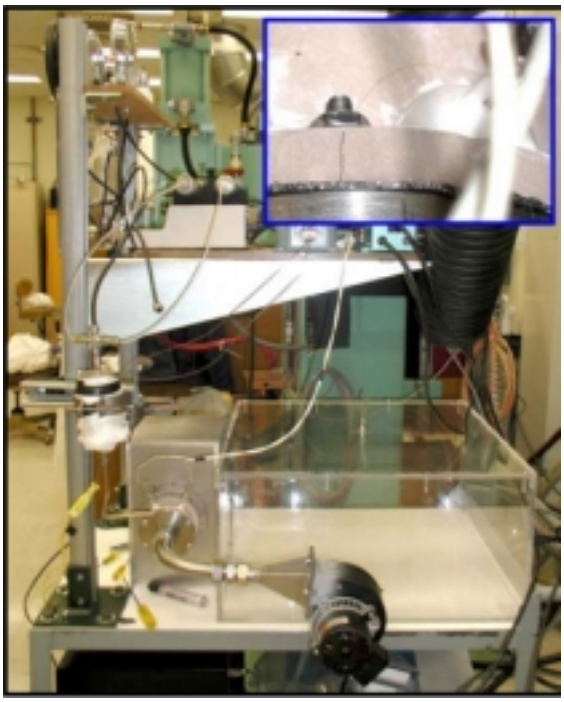

PN04-00040-100b

*FIGURE 2. Cermet filter for contaminated infrastructure cleanup simulation.*

Research into new cermet material compositions to enhance the strength of the thin cylindrical filter shells has led to a new class of cermet material formulation. The new cermet material composition shows an extreme energetic reaction during the combustion synthesis process. These new, energetic cermet materials have strong application for the military, law enforcement agencies, and other entities. For example, the cermet filter technology has been extended to address the emission problems ($NO_x$, $SO_x$, carbon particulate, and hydrocarbons) associated with diesel exhaust. A diesel engine exhaust treatment company in Canada has expressed interest in this technology for this application. A new cermet formulation used in the thermite combustion synthesis (reaction 2) of cermet filters has shown to release very high amounts of combustion energy. This new cermet formulation is being tested for use in energetic projectiles. Successful demonstration of the energetic projectile concept using this cermet material would support U.S. military and law enforcement agency objectives. In addition, a white paper resulting from this research was submitted in FY03 to the Air Force Research Lab in response to a Broad Area Announcement solicitation on chemical reactors for hazardous waste treatment or energy conversion.

# Microantenna Infrared Tags

*Dale Kotter*

***Identifying "assets" with unique infrared patterns***

NS124

In national security and military operations there is a need to tag, track, and locate "assets" from standoff and remote distances. One such means is through the measurement of the unique thermal infrared emissions from the asset. It is recognized that the thermal signatures of assets can be masked or distorted by environmental noise and high background interference, resulting in false detection. Current technologies have unacceptable infrared signature discrimination at standoff distances to resolve a single asset from a common group. In life, critical friend-or-foe monitoring application tag errors are not acceptable.

This LDRD is investigating a tagging technology to enhance the infrared signatures of controlled assets. Surface treatments have been developed that provide a tailored infrared signature. The treatment can be applied to the exterior surface of a controlled item to enhance the object's emission in the portion of the infrared (IR) band that thermal imagers are typically configured to detect. Preliminary results have demonstrated that the technology results in unique tag signatures that are immune to deception and which greatly reduce tag errors. The tags are completely passive and covert until interrogated.

Technical objectives for fiscal year 2003:

- Form research collaboration with University of Central Florida for fabrication of microstructure surface treatments.
- Design and fabricate a "dielectric-on-metal barcode" prototype.
- Design and fabricate a "diffraction-based Tag" prototype.
- Perform optical characterization tests.
- Demonstrate that the tags can be remotely monitored using standard thermal imagery and can discriminate friend from foe.

The INEEL, in collaboration with the University of Central Florida, has been at the forefront in the research of micro-antenna structures. They have demonstrated that antenna structures, in tandem with dielectric-on-metal surface treatments, can alter the infrared emissions of the item they are embedded on. This ongoing research has served as the basis for the development of surface treatments that emit unique infrared signatures. Research has centered on two tagging methods: 1) Infrared barcode, and 2) Infrared diffraction tags.

*Infrared Barcode*. Modeling efforts have demonstrated that the appropriate combination of composition/thickness of metal films and dielectric overcoats allows thermal emissivity to be selectively enhanced or reduced in desired regions. From this basis, a barcode was designed and fabricated using a bilayer of titanium and amorphous silicon on a flexible Kapton substrate. Portions of the barcode were designed to be anti-reflective (AR) in the infrared band, while portions were designed to be highly reflective (HR).

The tags were manufactured with various combinations of the AR and HR materials, resulting in unique binary and/or visual patterns. When the tags were passively activated by natural solar radiation an excellent contrast was achieved between the AR and HR states. The performance was characterized with an infrared imaging system in the 8 to 12µm spectral region. The AR layer had a maximum absorption of >95%. The HR layer had a minimum absorption of <19%. In the visible spectrum (400 to 700nm) the barcode appears as an untreated, uniform metal sheet. The visible signature remains uniform while concealing the barcode information.

*Barcode Demonstration*. A practical application of the barcode was demonstrated. The tag was applied to the surface of an automobile (Fig. 1). The flexible substrate allowed the tag to contour to the car's natural structure. The tag was remotely interrogated using a thermal camera in the 8-12 µm region. It was demonstrated that the high-contrast barcode information is only evident in the infrared bands, leaving the visible signature unaffected by ambient conditions.

*FIGURE 1. Conformal application of the thin-film barcode, imaged at 8-12 micron wavelengths using an infrared thermal camera.*

*Diffraction Tag*. It was experimentally demonstrated that when a slotted microantenna array is illuminated by infrared energy, the array's surface reflects a unique diffraction pattern. This is the phenomenon exhibited by an infrared wavefront that, when passing by the antenna array, is modulated, thereby causing a redistribution of energy within the wavefront. This redistribution of energy results in a unique infrared optical spectrum – like a fingerprint (Fig. 2). The spectrum provides the basis for fabricating a tag to generate specific coded diffraction patterns that can serve as a fingerprint for positive identification of the tagged item. Studies have demonstrated that the retro-reflective response is a direct function of the physical antenna array geometry. The array geometry can be configured to generate infinite diffraction tag patterns.

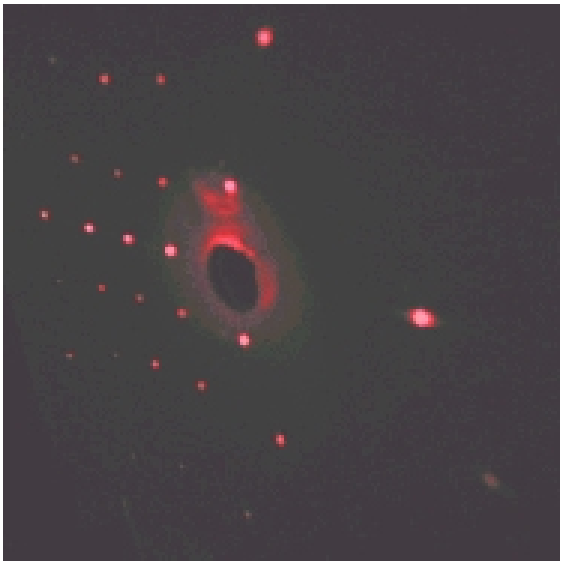

PN04-0004-70N

*FIGURE 2. Diffracted response of IR microantenna tag.*

The microantenna array tag requires no power or external electronics and acts as a receptor of IR energy. The antenna structure is "tuned" to resonate at a specific infrared frequency. The antenna structure acts as a diachronic filter of infrared emissions, independent of whether it is excited by broadband sunlight or an external laser source. The antenna has an inherent gain and generates current waves at the excitation frequency resulting results in a distinct and enhanced IR signature.

*Diffraction Tag Demonstration*. A diffractive tag image-recognition system was designed consisting of the diffraction tag, CCD camera/frame grabber, and image processing software. When the tag is illuminated with a He-Ne laser ($\lambda$ = 632.8 nm), a unique diffraction pattern is generated and recorded with a CCD camera. Redundant information about the tag is encoded at each diffracted order, however it is only necessary to acquire a single order, thus greatly relaxing the alignment tolerances for standoff detection. An image-processing algorithm compares each scanned image from the "tagged" target to the template library, and decodes the tag information. Real-time diffraction images are recognized and processed by an autocorrelation template-matching approach.

Bench-scale tests have demonstrated that unique diffraction patterns can be generated and provide the means for positive identification of the tagged item. When fully reduced to practice, a tag can be remotely monitored using standard FTIR or thermal imaging technology and tailored to enhance long-distance standoff monitoring.

Research-to-date has focused on the development of static tags with embedded permanent codes and information. Future research will develop electronic tunable antenna structures that will provide the basis of dynamic tags capable of being reprogrammed. This will provide additional security measures and the ability for closed-loop optical data communication.

This LDRD addresses critical technology gaps in the remote tagging and tracking of sensitive assets. Primary end users are in defense and security applications such as Homeland Security and DoD. This project fostered collaboration with the Center for Research and Education in Lasers and Optics (CREOL) at the University of Central Florida. This collaboration has led to related research in frequency selective surfaces under the sponsorship of the DOE Advanced Technology Program.

# Novel Fabrication of Blast and Penetration Resistant Materials

*Thomas M. Lillo, Henry S. Chu, Kevin McHugh*

***Defeating high-level threats with new armor materials***

NS133

There is an increasing need to develop blast- and penetration-resistant materials and systems for the protection of various vulnerable areas on vehicles, personnel and buildings. The INEEL has developed expertise in the areas of ceramics fabrication, materials characterization, and design of armor systems to develop advanced lightweight armor systems for national security applications. In previous work (LDRD CS116), pressureless sintered silicon carbide (SiC) armor tiles were developed by the INEEL and Superior Graphite Co. (SGC). However, the tiles were found to contain two types of impurity phases and a sintered grain size exceeding commercial, hot-pressed SiC material. Ballistic tests of pressureless sintered material showed that the hot-pressed SiC performed better.

This LDRD is investigating ways to improve the ballistic properties of the pressureless sintered material. During this first year, the two impurity phases were successfully removed while attempts at pinning the grain size were ambiguous. Improvement in ballistic properties of the modified pressureless sintered SiC tiles ranged from 5 to 16%.

Multi-hit capability was pursued by gelcasting SiC slurries with additions of carbon fibers followed by pressureless sintering. Carbon fiber levels were low and the gelcast matrix did not sinter properly, resulting in low-fired densities. The INEEL's proprietary metal spray forming process was used to pursue a more promising method of obtaining multi-hit capability. Lightweight aluminum alloys were sprayed onto pressureless sintered SiC and subjected to ballistic testing. The spray-formed aluminum encapsulated SiC system defeated the first shot by a 30-cal armor-piercing (AP) round but did not stop the second shot.

Technical objectives for fiscal year 2003:

- Characterize the mechanical and ballistic properties of pressureless sintered SiC produced under a previous LDRD.
- Reduce/eliminate impurity phases found in the pressureless sintered silicon carbide.
- Reduce grain size to improve the ballistic performance of pressureless sintered SiC.
- Apply pressureless sintered SiC technology to boron carbide-based ceramic armor.
- Develop methodologies to impart multi-hit capability to pressureless sintered SiC armor.
- Present and publish results at various national and international conferences.

*Characterization of Pressureless Sintered SiC* - Bend bars and targets for Modulus of Rupture (MOR) and ballistic evaluations respectively, were prepared from pressureless sintered SiC and tested. The following table summarizes the mechanical properties and compares them to two commercially hot-pressed SiC.

*Table 1. Comparision of mechanical properties: hot presses SiC and INEEL pressureless sintered Sic.*

| Typical Properties | Cercom (hot pressed) | Cercom (hot pressed) | Superior Graphite Co (SGC)/INEEL | Superior Graphite Co (SGC)/INEEL | Superior Graphite Co (SGC)/INEEL |
|---|---|---|---|---|---|
| Grade of SiC (Tile Thickness) | SiC-B (N/A) | SiC-N (N/A) | HSC490 (12.7 mm) | HSC490 (19.1 mm) | HSC490 (27.9 mm) |
| Bulk Density $g/cm^3$ | 3.20 | 3.20 | 3.17 | 3.18 | 3.17 |
| Average Grain Size µm | 3-5 | 3-5 | 5-10 | 5-12 | 5-15 |
| Average Flexural Strength, MPa (4-Pt MOR) | 560 | 580 | 286 | 382 | 421 |
| Characteristic Strength, MPa | 595 | 600 | 307 | 404 | 455 |
| Weibull Modulus (m) | 11 | 17 | 6.5 | 8.5 | 5.9 |

03-51139-100a

The density is slightly lower while the grain size is slightly larger than commercial material. Most notable is the low flexural strength and the Weibull Modulus, which describes the variability of strength from sample to sample. Variability in density and flexural strength through the tile thickness was revealed and suggested the need for adjustments to the sintering schedule for thicker SiC tiles. Even with these significant differences in properties these tiles performed comparably with the commercially hot-pressed material during ballistic testing performed at the INEEL and confirmed by the Armor Mechanics Branch of the Army Research Laboratory (ARL), Aberdeen Proving Ground, MD. The $V_{50}$ Protective Ballistic Limit (PBL) was 750 and 728 m/s for the Cercom SiC-B and the INEEL-SGC materials, respectively.

Differences in properties between the INEEL-SGC and the Cercom materials were thought to arise from the slightly lower sintered density, larger grain size, and the presence of impurities in the INEEL-SGC material. Steps were taken during this LDRD to correct these differences and hopefully achieve mechanical and ballistic properties closer to the Cercom material.

*Reduce/Eliminate Impurity Phases* - The SiC tiles are made with a SiC powder specially mixed by SGC to contain the necessary ingredients to pressureless sinter to > 98% of theoretical density. Two types of impurity particles: Mo- and C-rich particles were found in the sintered SiC. The source of the Mo-rich particles, approximately 0.5 µm in diameter, originated from the milling media (through wear of the media) used to produce the powder. SGC eliminated this contamination by switching to autogenous milling in which the milling media is also SiC. The carbon particle originated from a phenolic resin binder used as a binder and as a source of carbon needed for proper densification during sintering. Excess resin was present in the milled powder from SGC and resulted in residual carbon particles, approximately 2 µm, in the sintered microstructure. Elimination of these carbon particles, and the associated crack nucleation sites was achieved by simply adding a small amount (≤1 wt%) of SiC powder that did not contain binder. The sintered density was not adversely affected and still consistently exceeded 98% of theoretical density.

*Reduction of Grain Size* – Small inert particles were used to pin grain boundaries against movement during sintering, effectively stopping grain growth. Two pinning particle types were tried, $TiB_2$ and TiC. Samples containing 2, 5 or 7% by volume were prepared and fired. Additions of TiC resulted in poor densification. Sintered density was no more than 80%, making TiC an unsuitable pinning particle. Samples containing $TiB_2$ sintered to high density (~98% of theoretical) in laboratory sintering runs. Optical metallography of the sintered samples revealed ambiguous grain size pinning behavior. However, large control samples (~3" diameter) containing 0, 7 and 10 V% of $TiB_2$, were prepared at the INEEL and sintered at SGC (INEEL can only fire parts that are <2" in diameter) for ballistic tests. Samples were fired according to two different sintering schedules, the proprietary

*TABLE 2. Depth of Penetration test results.*

| Sample | Density g/cc | Thickness (cm) | Velocity (ft/s) | Penetration (cm) | Mass Efficiency |
|---|---|---|---|---|---|
| SiC + 0% $TiB_2$ | 3.09 | 0.572 | 2828 | 0.62 | 3.61 |
| SiC + 7% $TiB_2$ [1] | 3.15 | 0.572 | 2787 | 0.04 | 6.21 |
| SiC + 7% $TiB_2$ | 3.23 | 0.572 | 2786 | 0.11 | 5.58 |
| SiC + 10% $TiB_2$ | 3.25 | 0.566 | 2790 | 0.07 | 5.62 |
| SiC [2] | 3.17 | 0.447 | 2825 | 0.34 | 5.35 |
| Cercom SiC-B [3] | 3.22 | 0.445 | 2780 | 0.15 | 6.51 |

03-51139-100b

[1] Sintered at temperature of > 2375 degree C

[2] Previous result from LDRD CS1160

[3] Commercially hot pressed SiC supplied by Cercom Inc.

schedule used by SGC and a schedule developed at the INEEL that included a high temperature hold (~1750°C for 3 hrs) to allow the sample to outgas before increasing the temperature to the final sintering temperature (2200°C for 1 hr). The sintering results from SGC were somewhat disappointing in that neither sintering schedule produced densities greater than 98% of theoretical, as in previous work. Also a furnace malfunction during one run resulted in an over-temperature condition with the part reaching >2375°C.

Time and funding dictated that only four of the 18 tiles could be subjected to ballistic testing at the INEEL firing range. The tiles consisted of one tile of each variety (0,7 and 10 V% $TiB_2$), fired according to the INEEL schedule as well as one of the tiles that experienced the over-temperature condition. Testing was in the form of a Depth of Penetration (DOP) test and the results are presented in Table 2 (previous page).

*Boron Carbide-based Ceramics* – SGC is in the process of developing a grade of boron carbide powder that would allow pressureless sintering. However it was not developed in time for this year's research.

*Multi-Hit Capability* – Two methods to obtain multi-hit capability for SiC were pursued. The first attempted to incorporate long or continuous carbon fibers into the SiC matrix that would carry the load and hold the SiC fragments together for additional ballistic impacts. Previous attempts utilizing simple uni-axial pressing of SiC powder around carbon fibers followed by pressureless sintering, revealed the carbon fibers acted as crack nucleation sites following uni-axial pressing prior to sintering. Gelcasting was chosen to cast the SiC powder around the carbon fibers. A summer intern student, Joseph Murphy, was assigned the task to develop the gelcasting system and procedures to produce high-density SiC. He encountered difficulty in obtaining slurries with a high loading of SiC powder that was necessary for subsequent sintering to high density. The best gelcast samples (without carbon fibers) attained a density far short (~80%) of the desired 98%. Further work will be required to develop the gelcasting method to the point where the addition of carbon fibers can be explored.

The second method for developing multi-hit capability used the INEEL proprietary spray forming technology to encapsulate SiC tile within a metal alloy coating. The relatively ductile metal coating provides toughness and constraint to the ceramic tile during a ballistic impact, keeping the fragments of the tile together for subsequent impacts.

Two aluminum alloys, 5083 and 2195, were sprayed onto various pressureless sintered SiC tiles. The first tiles encapsulated used inferior beta-phase SiC tiles and explored spraying parameters. These tiles failed during first hits. However, the spray-deposited metal coating stayed intact without the de-lamination typically seen in encapsulation methods that use conventional casting. The second spraying iteration used high-quality, pressureless-sintered, alpha-phase SiC. Ballistic results are presented in Table 3.

Results indicated that only target 1 has a sufficiently robust configuration to stop a 30-cal AP projectile fired at muzzle velocity. However, it failed to stop a second hit at a location of 1.5" away

*TABLE 3. Ballistic results.*

| Target Configuration (cm) | | | Velocity (ft/s) | Results |
|---|---|---|---|---|
| 1 | 5083-Al | Front = 0.457, SiC core = 0.914, back = 1.372, side = 0.914 | 2793 | Shot #1 stopped<br>Shot #2 perforated target |
| 2 | 5083-Al | Front = 0.318, SiC core = 0.660, back = 0.947, side = 0.660 | 2805 | Shot #1 perforated target |
| 3 | 2195-Al | Front = 0.406, SiC core = 0.899, back = 1.461, side = 0.899 | 2787 | Shot #1 perforated target |

03-51139-100c

from the last hit. It was determined that the 10 x 10 cm surface area of the SiC core did not provide enough hard material to erode the second projectile. Fabrication of a larger target for re-testing will be explored in the future.

This research has led to the development of SiC ceramics for armor applications by a relatively inexpensive and high-throughput manufacturing process compared to current commercial methods. At this time, it is estimated that at production quantities, the cost of pressureless sintered SiC would be no more than 60% of the current commercial armor-grade SiC. Inexpensive SiC ceramic armor will enable various law enforcement agencies and defense departments to equip their personnel with effective body armor capable of defeating very high levels of threat such as the AP rifle projectiles. Diplomatic and military armored personnel vehicles equipped with the SiC based lightweight armor system would have a balance performance in terms of protection, speed, mobility, and cost.

This LDRD resulted in presentations at two conferences: The 27th Annual Cocoa Beach Conference and Exposition on Advanced Ceramics & Composites, and the 105th Annual Meeting & Exposition of the American Ceramics Society. Each conference required a paper to be published in a peer-reviewed journal.

In addition, this LDRD resulted in collaboration with Superior Graphite Company in the form of a CRADA, that has greatly aided in research at the INEEL to further improve this product to match the ballistic properties of commercial SiC materials produced by more expensive, low-productivity methods. In this collaboration, the INEEL has been the characterization and R&D institution while SGC has been the raw material supplier and the commercialization arm of the collaboration.

Contacts with individuals at the Army Research Laboratory have been established through this research resulting in testing of prototype materials and guidance. The high productivity rate and relatively inexpensive finished cost are attractive to various projects including the Future Combat Systems program. This research and other armor programs at the INEEL have enhanced the reputation of the INEEL within the armor community.

# Novel Selective Matrix for Collection and Identification of Priority Pathogens

*Frank Roberto, Vance Deason, Heather Silverman, Amber Miller, Joni Barnes, Cindy Breckenridge, Scott Watson*

***A novel strategy for detecting bioterrorism agents***

NS118

New, reliable and sensitive methods of detecting pathogens, especially those that might be used by bioterrorists, are sorely needed, as was demonstrated as our nation attempted to deal with anthrax spores dispersed through the U.S. Postal Service, federal and private mail facilities. The focus of this LDRD research is to develop a nano-pattern recognition strategy (nanosensor) based on the derivatization of selective matrixes for the detection of pathogenic microorganisms or toxins.

Organically modified sol-gels, commonly referred to as ormogels, are polymers containing both organic and inorganic moieties. These sol-gels can be polymerized using laser holography to produce 3-D structures with both geometric and chemical matches or affinities; e.g., for particular bacterial cells or proteins. The silica backbone of ormogels provides mechanical strength, while the organic components consist of organic monomers that can be polymerized to provide reactive groups to which antibodies and fluorescent or other sensing and reporting mechanisms can be attached covalently. Polymerized composite ormogel material has a high degree of optical transparency that enables the use of conventional light-based detection strategies.

Holographic structures, complementary to a microorganism or protein of interest, can be written into ormogels using a UV laser. The resulting size of the pathogen-specific pattern within the ormogel is very small — approximately 200 nanometers. The fabrication of an inorganic/organic hybrid composite material (hybrid glass) with antibodies or other ligands to produce a stable polymeric matrix, or "nanotrap", provides a means of both identifying and capturing relatively small numbers of pathogenic toxins and microorganisms. In addition to serving as a novel strategy for detecting bioterrorism agents, other uses for the holographic imprinting technique could include the detection or remediation of environmental contaminants.

Technical objectives for fiscal year 2003:

- Select and fabricate a composite surface using ormogel chemistries.
- Demonstrate specificity of antibodies to a pathogenic microorganism.
- Cross-link proteins to the fabricated surface for enhanced orientation of antibodies.
- Bind or capture the pathogen(s) of interest.
- Detect and enumerate the bound pathogen(s).

Binding of a pathogenic organism to specific antibodies was evaluated in solution, solid-matrix, and sol-gel slide formats using both enzyme-based and fluorescence-based assay techniques. Visualization and quantification strategies included colorimetric, fluorescence, direct cell counts, and imaging methods. The use of fluorescent probes for monitoring individual cross-linking and binding steps in the design of the biosensor was determined to be the most sensitive and quantitative.

In FY01, prepolymer formulations of ormogels were received from Dr. Anna Wojcik (Hybrid Glass Technologies, Inc.; Rutgers University Department of Ceramic and Materials Engineering), and evaluated for use in creating regular nanometer-scale patterns with a Coherent Argon-Ion laser operating at 365 nm wavelength of about 80mW power. An M3 matrix was chosen for the fabrication of a prototype model that has been used for presentations in describing the project. Glass slides with sol-gel films derivatized with organic reactive groups (urethane and primary-amine groups, primary-amine groups only, and primary- and secondary-amine groups; "F2, F3, and F4") also were received from Dr. Wojcik for investigating selective binding of proteins and whole microbial cells to the reactive surfaces.

In FY02, the binding properties of a specific pathogenic strain of *Escherichia coli* containing cell-surface O-antigens (O18, O44, O112 and O125) was evaluated and optimized against $IgG_2$ antibodies using colorimetric enzyme linked immunosorbent assay (ELISA) techniques. A solution-based assay was optimized in microfuge-tube format followed by testing on standard polystyrene microplates (used in medical-based ELISA research). Because the standard microplate experiments yielded elevated levels of background color, microbe-antibody binding also was tested with specialized microplates grafted with amine functional groups (CovaLink NH - Nalge Nunc International, Naperville, IL). These solid supports were intended to mimic the specialized slide surfaces obtained through the sol-gel process. CovaLink studies involving the passive binding of Protein A or Protein G, as well as the cross-linking of Protein A or Protein G (with the

homobifunctional chemical dissuccinimidyl suberate (DSS), revealed an increased binding potential with Protein A and an increased binding potential with the use of DSS. DSS cross-linking experiments with the prepolymer film formulations F2, F3, and F4 on slide surfaces indicated successful colorimetric detection of microbe-antibody interactions as well (Table 1). Atomic force microscopy (AFM) revealed the presence of cells on the prepolymer film surfaces. However, whether the cells were trapped due to AFM preparatory steps or actually bound via cross-linking and specific binding could not be determined. In addition, the prepolymer surfaces appeared to be negatively affected by the chemical conditions used for the ELISA procedures.

In FY03, the microbe-antibody and surface-antibody-microbe binding steps were specifically monitored with the use of fluorescent probes. Additional prepolymer formulations also were tested in the slide format. First, the $IgG2_b$ antibody was labeled with the red Alexa Fluor 568 dye (Molecular Probes, Eugene, OR). The new probe was tested at varying concentrations with different concentrations of *E. coli* #12793 and a non-pathogenic organism (*Shewanella putrefaciens*). Cell suspensions were visualized using epifluorescence microscopy. Cells of *E. coli* #12793 appeared more fluorescent than the control cells, indicating antibody specificity to the pathogenic microbe. To obtain a more sensitive and quantitative measurement, the cell suspensions were evaluated using fluorometry. Cells of *E. coli* #12793 were more fluorescent at all concentrations of labeled antibody than cells of the non-pathogenic organism, *S. putrefaciens*. A probe concentration of 1.5 µg/mL appeared to be optimal for distinguishing E. *coli* #12793 from *S. putrefaciens* (Table 2).

Next, the labeled antibody was cross-linked to the amine groups on slide coatings using the homobifunctional cross-linker, glutaraldehyde. Additional prepolymer coatings containing the M3 matrix (that was optimal for laser patterning) were obtained from Dr. Wojcik (designations 42-F3 and 42-F4). Two different reaction times were examined, 4 hours and overnight, for the addition of the crosslinker to F3, 42-F3, F4 and 42-F4 prepolymer slide coatings. Prolonged incubations appeared to alter the F3 and F4 slide surfaces. The activated coatings were incubated with labeled antibody, followed by incubation with cells of *E. coli* #12793 or *S. putrefaciens*. The slides were examined for bound cells using microscopy and fluorometry. The fluorometer revealed that the labeled antibody was not effectively cross-linked to the slide coating. Consistent with this result, microscopy showed that

*TABLE 1. Colorimetric detection of prepolymer film formulations and Covalink NH microplate modules. Readings were obtained on a BioRad 450 Microplate Reader at $OD_{495}$. For prepolymer film formulations, YES indicates colorimetric detection. For CovaLink NH microplate modules, mean optical density is indicated.*

| **Prepolymer Film Formulations** | | **CovaLink NH Microplate Module** | | | |
|---|---|---|---|---|---|
| Designation/Reactive Group | Result | Protein A | Protein A/DSS | Protein G | Protein G/DSS |
| F2/urethane and amine | YES | 0.883 | 0.995 | 0.580 | 0.869 |
| F3/amine | YES | | | | |
| F4/amine | YES | | | | |

03-51139-101a

*TABLE 2. Fluoresence quantitation of Alexa Fluor 568-labeled Antibody $IgG2_b$ with Pathogenic* E. coli *#12793 and Control Microorganism* S. putrefaciens*. At all concentrations tested,* E. coli *presented a greater fluorescent response than* S. putrefaciens*. A probe concentration of 1.5 µg/mL gave the greatest difference in fluorescence readings.*

| Alexa Flour 568-$IgG2_b$ | Fluoresence Quantitation: Instrument Response (mV) | |
|---|---|---|
| Concentration (µg/mL) | *E. coli* #12793 | S. *putrefaciens* |
| 1.5 | $1.8 \times 10^4$ | $9.0 \times 10^3$ |
| 10 | $1.5 \times 10^4$ | $1.4 \times 10^4$ |
| 50 | $8.1 \times 10^5$ | $2.5 \times 10^5$ |

03-51139-101b

no cells were bound to the slide surface. Therefore, the methodology used to cross-link labeled probe via glutaraldehyde was not successful.

During the final period of this project, the fabrication effort focused on materials and techniques to improve the quality and ease of fabrication of the micro-patterns. Dr. Wojcik assisted a major effort involving the search for suitable visible photo cross-linking or activating agents. Near the end of the fiscal year, a set of three mixtures was received based on the successful M3 mix perfected earlier for ultraviolet printing. As has been seen in the past, these mixes are fairly unstable and tend to polymerize spontaneously during storage. Shipping time compounded by slow delivery once the package is at the INEEL has been problematic. In the last series of mixes, mix 2 was gelled on arrival, and tests were run on mixes 1 and 3. While both samples produced patterning with visible (532 nm laser light produced by a Coherent 5 Watt diode pumped frequency doubled solid state Verdi (TM) Laser), mix 3 was found to produce better (brighter) diffraction effects, and to do so more consistently than mix 1. A series of experiments to determine ideal exposure and processing was performed and a set of good patterns produced.

Other improvements involved better preparation of the base coating using a carefully honed "blade" made of a hand-beveled microscope slide to spread the mix in an even coat over the sample substrate. This improvement eliminated much of the streaking seen earlier, presumably caused by small chips or irregularities in the edge of the blade. Also, a slight (<5%) addition of acetone to the final (of 3) rinse baths seemed to better clean off the residual unreacted material prior to final baking.

Future work on this research may include:

- Modified chemistries for cross-linking with glutaraldehye, DSS, or other options to take into account variables such as salt concentration, pH, incubation time and temperature.
- Cross-linking to prepolymer surfaces with Alexa Fluor-labeled Protein A and/or Protein G followed by binding of $IgG2_b$ to evaluate increased sensitivity with the addition of available antibody binding sites.
- Antibodies raised specifically to the model pathogenic microorganism to improve sensitivity.

This LDRD seeks to develop materials that can selectively capture and detect pathogenic microorganisms. These materials could serve as "monitoring sentinels" detecting pathogens that might be used in bioterrorism, supporting National Defense missions. Progress on biosensor development was briefed to a variety of potential and existing national defense customers in FY03.

# Imaging of Heavy Metals and Nuclear Materials

*Tim Roney, Tim White*

***Supporting non-intrusive, nondestructive inspection***

NS121

X-ray fluorescence (XRF) is an established technique for elemental identification and characterization of materials. This LDRD focuses on expanding the traditional application areas of XRF to induced-emission imaging of materials in containers of various sizes. Application areas include determination of heavy metals and RCRA materials in environmental and nuclear waste containers, and detection of nuclear weapons materials or shielding materials in transport containers (luggage, baggage, pallets, cargo containers).

Prior efforts in XRF imaging have occurred mostly at locations where there is a high-intensity monochromatic x-ray source, such as a synchrotron facility. These facilities provide an x-ray beam that works well on very small, low-density objects. The interest in this LDRD research is to combine XRF with 2-D and 3-D x-ray tomography methods using more portable, higher-energy, broadband x-ray sources. This would avoid the requirement for a synchrotron x-ray source and allow access to larger packages. Concepts for XRF imaging investigated in this project include the use of Bremstrahlung (broadband) x-ray sources including both linear accelerators and x-ray generators, XRF tomographic imaging of high density materials, and combined conventional transmission x-ray imaging with region-of-interest XRF. Bremstrahlung sources (linear accelerators and generators) produce very-high-energy x-ray beams (6MeV and 300kVp, respectively for this work) allowing for deep penetration of the excitation radiation in dense or thick objects. Applying tomographic principles in XRF imaging allows for material identification, spatial location, and shape of materials embedded in packages. Region-of-interest (ROI) XRF based on high-speed x-ray transmission allows for very rapid inspection of containers.

Technical objectives for fiscal year 2003:

- Investigate tomographic imaging potential of accelerator-based XRF (AXRF).
- Develop a tomographic imaging protocol for XRF imaging.
- Construct laboratory prototype x-ray imaging system for imaging of small objects.
- Acquire image data on test object.

X-ray fluorescence occurs when an incoming x-ray photon causes the ejection of a bound electron from an element. Subsequently a free electron (or an electron in an outer shell), drops into the vacancy established by the interaction, and an x-ray photon that is characteristic of the transition (and hence the element) is emitted. This phenomenon occurs in all elements. The energy of the characteristic photon increases with the Z-number of the element. For this investigation, elements of interest are those that are higher Z and hence produce higher energy photons. This group includes mercury, lead, uranium, and plutonium — elements that are of interest for environmental concerns and for national defense (homeland security). This project seeks to develop screening and quantitative methods for determining heavy elements and nuclear materials in containers.

In fiscal year FY02, the investigators and collaborators at Idaho State University (ISU) became interested in the use of broadband x-ray sources for x-ray fluorescence emission imaging. The Compton Backscatter project was redirected to focus on the XRF imaging application in FY03. Two laboratory studies were initiated. The first experiment set used a high-energy (6MeV) linear accelerator and a 300kVp x-ray generator located in the physics building at ISU. The second experiment used a lower-energy (300kVp) x-ray generator located in the INEEL's Digital Radiography and Computed Tomography (DRCT) laboratory at ISU for both XRF imaging and combined transmission x-ray region of interest XRF.

*High-Energy XRF Imaging:* This experiment used a highly collimated 6 MeV pulsed linear accelerator to induce XRF in samples of uranium and mercury (in 25 mm diameter cylinders) in a 16-cm diameter sand-filled can (Fig. 1A). The can was translated through the beam in a direction normal to the beam direction. At each step, spectra were collected (Fig. 1B) with a high-purity germanium (HPGe) detector. Due to collimation in this geometry, the detectors are not sensitive to the direct excitation Bremsstrahlung beam. However, the detectors are sensitive to photons that have Compton-scattered from the object or fluorescence photons generated by x-ray interactions in the high-density materials. Figure 1C shows a clear spatial response for both $K\alpha$ and $K\beta$ lines of mercury and uranium. These

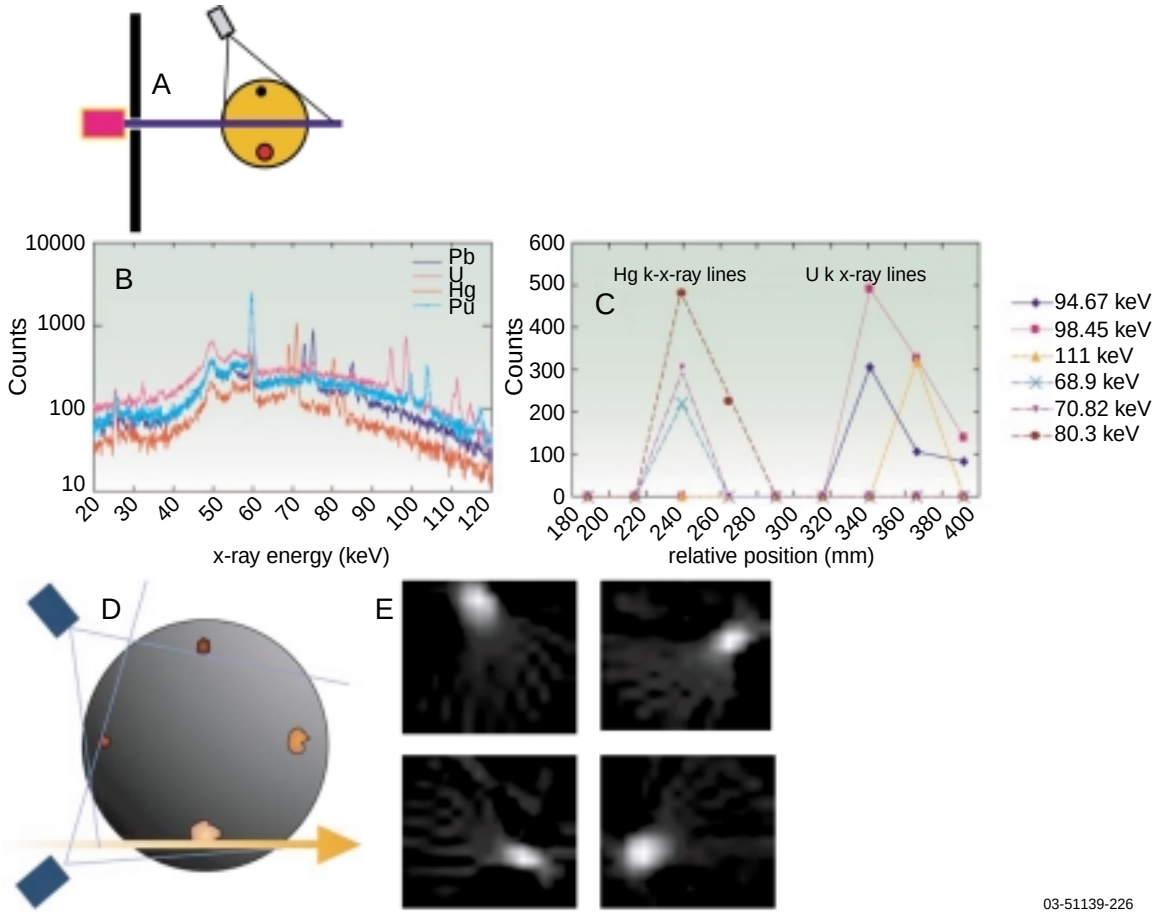


*FIGURE 1. Initial XRF imaging tests: A) A high-energy x-ray source is placed behind a thick wall to support collimation of the x-ray beam and reduction of undesirable scattered radiation. B) Typical x-ray fluorescence spectra from several elements. C) Results of a linear translation scan of the x-ray beam across the object. The mercury and uranium lines separate spatially indicating their placement in the can. D) Setup for first tomographic scan. E) Four tomographic reconstructions, one for each element placed in the can of sand.*

results demonstrate the potential of linear accelerators in induced-emission imaging.

*XRF Imaging with a 300kVp X-ray generator*. The second set of tests studied the feasibility of high-energy XRF imaging with a continuous 300 kVp x-ray generator. A 16-cm diameter, sand-filled can containing four vials of high-density material was used as a test object. The density of the sand was about 1.5gm/cm$^3$. The diameter of the vials ranged from 2.5 cm to 3.75 cm. Each contained only one material: lead, uranium oxide, mercuric chloride, or plutonium. The first three items were in powder form. The plutonium was in the form of two flat disks. Each Pu disk was 1g and embedded in a low-density resin. The x-ray generator was collimated to a ~2.5-cm pencil beam for irradiation of the sample. The four elements were spatially separated so that in certain orientations the excitation beam would only probe one element. The experimental setup is shown in Figure 1D for beam collimation, but data acquisition includes both translation and rotation of the object in a typical tomographic scan. In Figure 1D the large circular shell represents the can and defines the edge of the object space. The four smaller objects represent the high-density materials within the can. The horizontal line represents the pencil beam of x-rays. Two

thin germanium detectors with beryllium entrance windows were used as x-ray detectors. Figure 1E shows the tomographic reconstruction of the four individual elements.

A configuration with higher spatial resolution was set up for a third test. In this system (Fig. 2B), the source is collimated to a pencil beam of about 3.5mm diameter. An object consisting of a small cup with holes bored in the bottom to accommodate small vials of high-density materials was constructed (Fig. 2A). This object was loaded with several materials (tantalum, mercuric chloride, lead, and uranium oxide) in separate vials and then filled with water to serve as an attenuating matrix. A complete 2-D tomographic scan was acquired by translating the object in 28 steps of 3mm each and rotating 60 times at 6 degrees per rotation (Fig. 2B). Spectrum acquisition time for each data point was 15 seconds. With motion overhead, the data collection required 11 hours. This time was governed by the source characteristics and the use of only one low-efficiency detector. Using an x-ray generator tailored to this application (lower voltage, much higher current), and a more efficient multiple-detector system, a much higher throughput rate is possible. The resulting 2-D tomographic slice image of the four materials in the cup is shown in Figure 2C.

*Combined Transmission X-ray Imaging and XRF Region of Interest Inspection*. A likely scenario for the deployment of XRF inspection for either environmental applications or weapons of mass destruction is to combine conventional x-ray transmission imaging with XRF. In many situations, transmission x-ray imaging is already an accepted method of inspection. Adding in XRF to verify presence of specific materials when suspicious images are encountered may greatly improve the

03-51139-217

*FIGURE 2. High-energy x-ray fluorescence tomography with a generator x-ray source. Four materials placed in cup at left are scanned on the XRF tomography system (center). The resulting tomographic slice reconstruction is shown at right.*

statistics for true positives and reduce false alarm rates. With this in mind, the investigators set up an experiment to demonstrate transmission x-ray region-of-interest XRF inspection. The samples used in the XRF tomography experiment were dispersed throughout a bucket of sand, and high-resolution transmission x-ray imaging (radiography and tomography) was performed on the bucket. A high-contrast x-ray image readily provides the means to determine where suspicious high-density material may reside in a lower-density matrix. In this case, the x-ray CT images allowed the investigators to locate each vial of material. The bucket of sand was then strategically placed on the XRF imaging equipment so that a single pencil-beam of radiation from the x-ray generator collides with the material of interest. Then an XRF spectrum is acquired that provides immediate information on the region of interest. Results indicate that ROI XRF may be performed on 55-gallon drums of waste and on transportation packages including luggage, pallets, and cargo containers.

This research has application in the identification, location, and quantification of RCRA materials and heavy elements in containerized waste. Areas for environmental application continue to be pursued through DOE. Another application is in the detection and location of nuclear materials or the materials that shield radiation from nuclear materials. This is a homeland security application that may be deployed at border inspection stations, ports of entry for cargo, and airports. This application will be pursued with white paper submissions throughout the year.

INEEL

# Advanced Computing Initiative

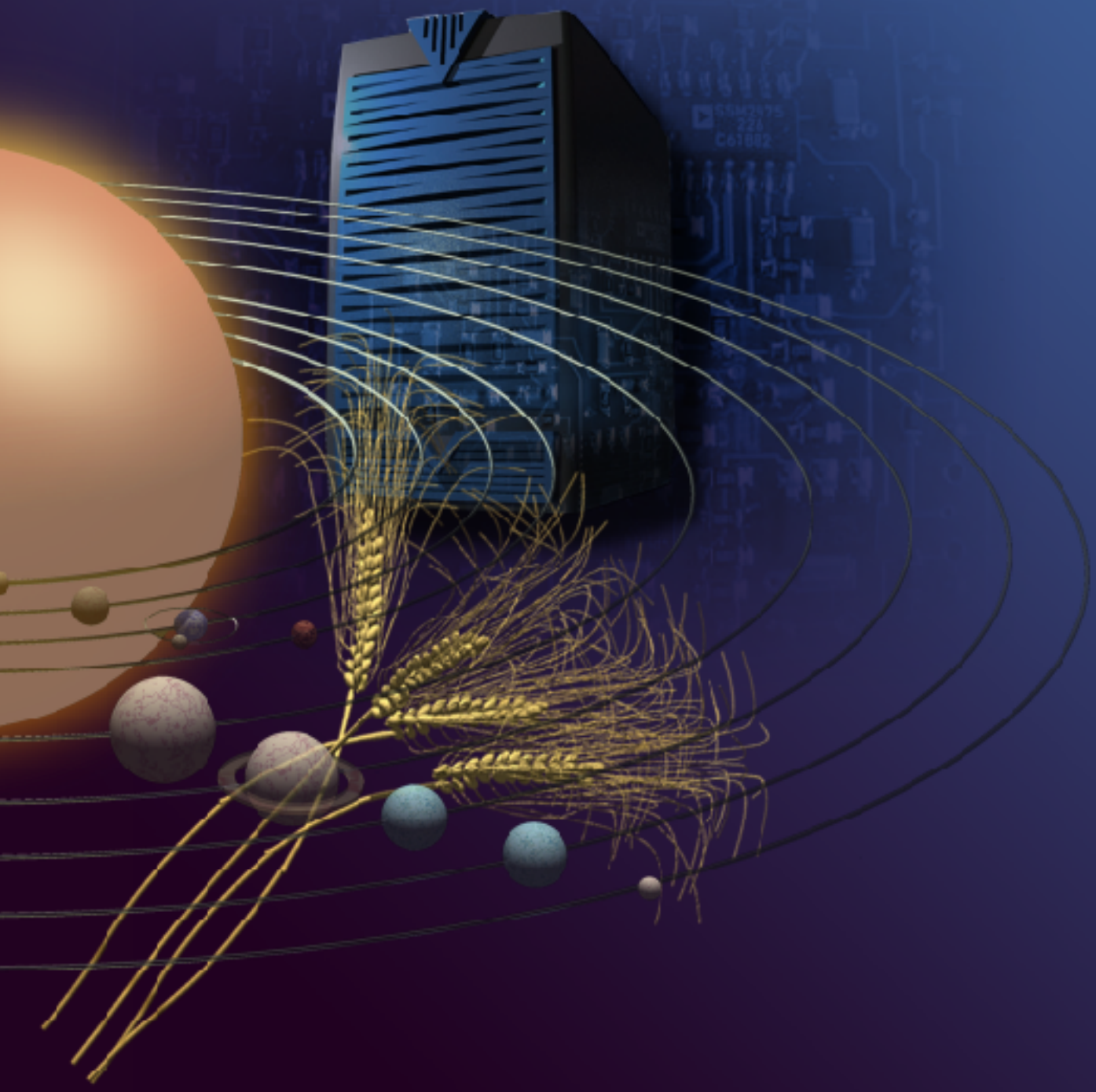

# Development and Validation of Advanced Simulation and Collaboration Capability

*L. Eric Greenwade*

***Advancing computational and collaborative work at INEEL***

AC 104

A more robust, advanced computer simulation and collaboration environment is needed at the INEEL to promote additional scientific and engineering work. This LDRD extends and validates three of the five fundamental components of an advanced computing and collaboration capability at the INEEL. The five components are terascale data management, data abstraction models, performance optimization, parallelization, and visualization. Specific aspects of three of these areas (performance optimization, parallelization, visualization) will be developed and validated as well as an overall integration among the components. The near-term focus of these efforts will be in the area of subsurface science while incorporating the flexibility and extensibility for application to other INEEL mission areas, such as critical infrastructure protection and nuclear energy.

Technical objectives for fiscal year 2003:

- Implement the AccessGrid node (Agnode).
- Create functioning powerwall within INEEL Visualization Laboratory.
- Acquire new visualization applications and apply to INEEL Numerical Simulation Laboratory (NSL) environments.
- Port applications to improve NSL's high-performance computing capabilities.

The AccessGrid node (AGnode) was successfully implemented and has been used for a number of collaborative activities. There were several substantial hurdles to overcome that were not foreseen at the beginning of this activity. These hurdles were due to the particular security requirements at the INEEL. Thus, the processes developed at other DOE facilities, which guided the work package specifics, were not employable at the INEEL. Eventually, all but one of the issues was resolved and the AGnode has been utilized in a number of expected and unexpected ways. The outstanding issue is related to a repetitive dropping of packets by the INEEL network. The cause has not been determined, and appears to be related to the complex networking infrastructure. Presently, it is annoying but tolerable.

The AGnode has been used to provide a number of collaboration opportunities. The first of these was the presentation of an Intermediate MPI (Message Passing Interface) class. Approximately a dozen INEEL staff were able to participate in this class, presented by the Ohio State and Boston universities. Several sessions of a virtual reality tutorial presented by the University of Manchester in the U.K. also were presented on the INEEL's AGnode. An INEEL staff member working on a Ph.D. at the University of Idaho used the AGnode for his dissertation proposal defense, avoiding the need for the staff member and his Idaho Falls-based committee members to travel to Moscow.

Three additional classes are scheduled for FY04. The first is an Introduction to MPI that will be presented by the National Computational Science Alliance's Partners for Advanced Computational Services, primarily the Ohio Supercomputer Center. The second is a graduate level computer science class, CS580 Parallel Processing, being offered by the University of Montana. This course is focused specifically at the INEEL and is expected to be well received. The third class is an MPICH-G2 Workshop, again sponsored by the National Computational Science Alliance's Partners for Advanced Computational Services. This workshop will focus on the integration of MPI, the most commonly used parallel programming methodology, with the second generation of the Globus toolkit, the most widely used grid-computing framework. Finally, an INRA subsurface science course is in development that could take place on the AccessGrid.

The powerwall is now up and functional within the INEEL's Visualization Lab (VizLab). The powerwall is a very large display device (basically a computer monitor) that is 6-feet high and 12-feet long. Six high-resolution projectors, each connected to a very high-end, hardware-accelerated computer drive it. Therefore, the display is capable of providing a hardware-accelerated display of almost 8 million pixels in an application-independent fashion. The display has been shown to work with both openGL and X-windows, the two primary drawing interfaces for science and engineering applications. The powerwall has been used for display applications that need either a large number of pixels and/or display area, and for group interactions that are impossible on a standard computer monitor. The powerwall has been successfully operated with the major visualization packages at INEEL.

Two new visualization applications have been acquired and ported to the INEEL Numerical

Simulation Laboratory (NSL) environments. The *visit* code is from Lawrence Livermore National Laboratory (LLNL) and the *paraview* code for Los Alamos National Laboratory (LANL). These were both developed within DOE's ASCI program. Although the *paraview* code has many interesting design attributes, the *visit* code is a fully functional visualization tool ready to be placed in the hands of users. For this reason it is *visit* that has received the majority of the attention in this activity. Both visualization tools are design to read for a common data storage mechanism, reducing the need to create custom tools for each application. Two INEEL applications, one each from the NE and EM program areas, were ported to these standardized data storage mechanisms and integrated with the *visit* visualization application. As *visit* is based on the openGL drawing interface, both the NE and EM visualization are presentable for a number of display devices, ranging for laptops and desktops, to the powerwall. Therefore, both the NE and EM communities at the INEEL can leverage the significant work performed by the DOE ASCI program, and utilize state-of-the-art visualization and display technologies.

The latest version of *visit* has been obtained from LLNL. It has been successfully compiled and install on all three primary Unix advanced computing environments at the lab, Linux, Solaris and Irix. *Visit* continues to be applied to an ever-increasing number of laboratory applications and the frequent feature updates provided by LLNL continue to increase its applicability. It has become the primary visualization tool of the DOE ASCI program, ensuring a robust future for the application.

As part of the ongoing efforts to characterize the NSL high-performance computing (HPC) capabilities, several applications were successfully ported to the Cray, as this machine represents the most recent addition to the NSL's capabilities. These codes were selected by their importance to the INEEL Nuclear Engineering (NE) and Environmental Management (EM) communities. The codes were: TETRAD, GAMESS, PEBBED, Attila, and RELAP5.

- TETRAD (groundwater modeling code) — Some source code modification was required to run TETRAD on the Cray. It was found to be a highly scalar code that does not vectorize well. A large effort would be required to rewrite the source code enough to gain significant speedup on the Cray.
- GAMESS (General Atomic and Molecular Electronic Structure System) — This was found to be a scalar code that does not vectorize well. An alternative code exists that would perform better on the Cray. No significant vectorization effort was spent on this code.
- PEBBED (code for analysis of pebble bed nuclear reactors) — The most significant amount of application optimization time was spent on this code, which was developed at the INEEL. Source code modifications were initially performed to correct errors that the Cray compiler caught. Once PEBBED was running, it was profiled using two inputs, a 2-D and 3-D model. Profiling indicated that two different subroutines accounted for the majority of the run time, one for the 2-D case and the other for the 3-D case. Numerous modifications have been made to the algorithms used to enable the compiler to vectorize the source code. This has resulted in significant speedup for both models as compared to the initial run times. For the 2-D case, the total run time (measured in CPU seconds) was decreased 47%, floating point operations per second (FLOPS) for the entire code were increased 189%, and FLOPS in the most significant subroutine were increased 374%. For the 3-D case, total run time was decreased 86%, and FLOPS for the entire code were increased 541%. Code optimization efforts are ongoing, as PEBBED is under active development.
- Attila (NE radiation transport code) — This code is used to perform analyses of the ATR. Porting it to the Cray uncovered a compiler bug that had to be resolved before Attila could be run. Some slight source code modification was required due to the Attila's default use of double-precision variables. Converting the code to use single precision on the Cray (equivalent to double precision on other platforms) increased its speed 11 times as compared to the initial installation. Profiling of Attila has been performed, indicating a single subroutine that accounts for 84% of the total run time. Vectorization efforts to improve the performance

of that subroutine are ongoing as well as some very large memory runs that surpass, or very closely approach, the current memory limits of the INEEL hardware.

- RELAP5 (nuclear plant simulation code) — This application (developed at the INEEL) was run on a Cray 10 years ago, but subsequent code development was performed when no Cray was available for testing. This alteration has inhibited vectorization in previously vectorizable routines. The RELAP5 code developers have expressed an interest in porting it to a Cray again. Code profiling has been performed on several input models to determine where to focus optimization efforts. Some testing of the OpenMP directives that have been added to RELAP5 is anticipated to gauge its performance on multiple processors, and 256 Mflops have been achieved on a single processor.

This LDRD was successful in meeting all planned objectives for the year. There were several planned changes to the INEEL network environment that will impact the use of the AGnode. These network changes were to have been completed prior to the end of FY03; however, they have now been postponed. It is anticipated that FY04 activities on this LDRD will in part, respond to these network changes to retain the current capabilities of the AGnode. Version 2.1 of the AG software needs to be brought up for the INEEL to participate in future Supercomputing Global activity. The new software and the firewall changes should enable the AG node to be moved to within the INEEL firewall, greatly reducing the special security requirements now in place.

The work performed under this LDRD will drive additional development of advanced simulation and collaboration activities, continuing to enhance the state of scientific research and engineering at the INEEL.

# Parallel Computing with Cluster Technology

*Thomas K. Larson, Charles R. Tolle*

***Advancing high-performance computing***

AC101

Revitalization and advancement of high-performance computing (HPC) is a critical component of the INEEL Institutional Plan that supports all laboratory research and development activities. This LDRD is conducting a group of tasks to facilitate development and use of a more robust HPC capability. This work supports a cross-section of initiatives and users. Tasks represent a multi-pronged capability evaluation and development effort to address some of the major stated computing needs, including parallel computing tools and distributed architectures, computational methods, data visualization and repository, and code optimization/parallelization. The primary effort centers on improving understanding and use of distributed computing or cluster technology where appropriate and possible. An over-arching driver in this work is low-cost, high-performance computing – in other words, to minimize hardware cost and maximize computer performance for the specific problems of interest. This work is being conducted in collaboration with universities and other institutions to leverage relevant ongoing research.

Technical objectives for fiscal year 2003:

- Investigate methods to achieve performance and scalability using inexpensive components and a systematic methodology to optimize cluster topology and connectivity for specific computational problems.
- Investigate tools to help the average scientist focus more on the task of algorithm development than on parallel implementation.
- Evaluate cluster file- and load-balancing systems and scheduling algorithm development.
- Initiate building additional INEEL computational fluid dynamics (CFD) modeling and simulation capability using an existing particle method and high-performance computing.
- Review integrated scientific data management and expanded visualization capability at the INEEL.
- Optimize TETRAD and parallel evaluation.

*Cluster Networking Optimization* – INEEL instigated collaboration with the University of California, Santa Barbara (UCSB), and MetaHeuristics LLC (Santa Barbara, CA) to study performance and scalability of computer cluster topology and connectivity for specific computational problems. The motivations for such work are cost advantages and the availability (ownership) of distributed memory environments relative to large shared-memory machines. The scope of this work was completed in February 2003 and findings documented. The work conducted included efficiency/optimization investigation of a hybrid network connection topology known as a flat network neighborhood (FNN) where each node in the cluster has multiple network interface cards (NICs) and each processor is connected to another through only one switch as shown in Figure 1. With a selected optimized network back-plane topology, investigation of cluster performance was done using three different 3-D computer codes for different grid domain sizes and orientations, and number of CPUs on the USB 16 node (32 CPU) cluster. Three-dimensional codes used for performance evaluation included both explicit finite difference and spectral heat conduction solutions and a parallel FFT from the FFTW library. Each cluster node has three network communication cards for versatility in back-plane communications routing.

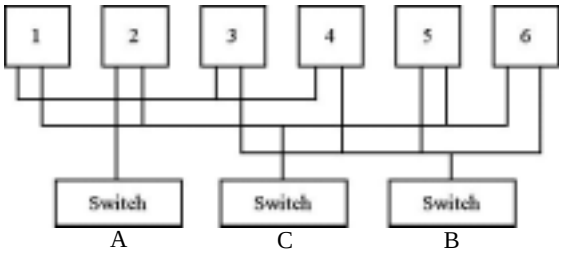


PN04-0004-140-AC101a

*FIGURE 1. Sketch of FNN topology. Numbered boxes represent compute nodes.*

In the investigation of how to design the optimal FFN topology, no analytical way of generating all the possible wiring patterns could be found. However, an iterative "rule based" procedure was found that works well and is able to find a selection of connection patterns in a reasonable amount of computer time. Changing the configuration of the cluster was found to have significant performance influence (up to 10% on speed of computation). The best arrangements appear to be ones in which the distribution is such that pairs of CPUs that need to communicate are in the same node to the extent

possible although more experimentation needs to be done. Figure 2 shows results for one of the spectral heat conduction cases evaluated where speedup is plotted as a function of the number of machines (i.e., from 2-32 CPUs) used and the grid size of the problem.

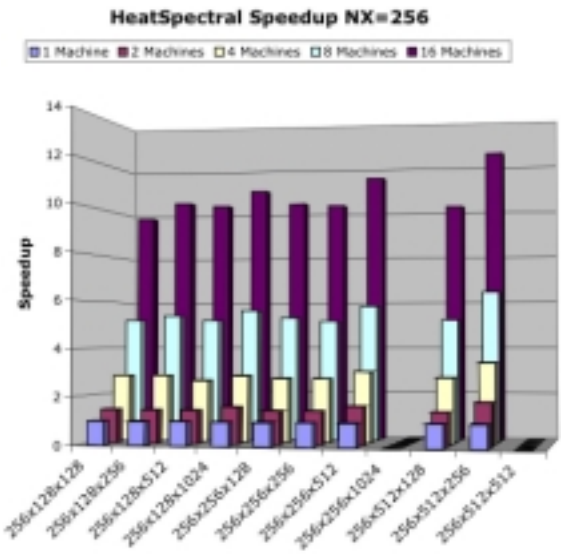


PN04-0004-140-AC101

*FIGURE 2. Spectral heat conduction code speedup with respect to number of nodes used and domain grid size.*

It was found that the larger domain size problems performed well with the computational speed rising almost linearly with the number of processors in some cases. Smaller problems do not show such significant speed-ups; this was expected, since the ratio of communication to computation decreases with domain size. Poorer performance on small problems is not an issue when one considers that clusters would normally be used for very large problems requiring significant memory.

*Cluster Parallel Tool* - In investigating the development of Filk, it was learned that Fortran's syntax has significant issues with Lex and YACC parsing. Fortran does not follow the standard syntax used in the development of a modern compiler. This complicates the development of a Fortran-based implementation of Cilk, since the lexer and parser routines must be developed from scratch instead of using existing Lex and YACC tools, a significant increase in effort. Also, an investigation began into the baseline tools needed to expand Cilk and Filk to a distributed architecture system (Beowulf cluster), it became clear that Message Passing Interface (MPI) does not have the required ability to spawn new processor subtasks "on the fly" while the program is under execution. This ability is available within Parallel Virtual Machine (PVM) and is the most likely the reason why past distributed Cilk implementations have been developed using PVM.

The investigators continued researching the best implementation methods for creating Filk and distributed Filk/Cilk during the remainder of the year. They supported Dr. Ken Bosworth (Idaho State University) in his initial efforts in obtaining EPSCORE funding to jointly work with the INEEL team on the distributed Cilk/Filk project next year and into the future. A conceptual framework for a new genetically inspired computing (GIC) parallel computing concept was developed that is distinctly different from genetic-based computing currently in the literature. The GIC concept employs a computing engine and source code basically identical to DNA and has the flexibility or plasticity to literally morph into vast numbers of end-use configurations in response to temporal, near neighbor, external environmental, and other factors. The concept presents robustness and adaptability far beyond that exhibited by man-made control systems, intelligent or otherwise.

*Cluster File System/Load Balancing Evaluation and Scheduling Algorithm Development* – The INEEL investigators initiated review, selection, and evaluation of several different cluster Distributed Resource Managers (DRM) and Distributed File Systems (DFS) to gain insight on implementation and performance issues and learn how to take full advantage of the products. A portion of an existing INEEL cluster (20 nodes of the "dawulf" Athlon cluster) was used for product evaluations. Based on the results, Sun Grid Engine (SGE) was selected for permanent installation. Experience to date indicates that Sun Grid Engine is stable and performs well. The project installation does not use the SGE failover support for the qmaster server, but SGE is robust enough that the jobs it controls on other machines will continue to run to completion even if the server is down. Implementing a failover qmaster is still desirable in case the main server experiences catastrophic failure and also so that job

submission is more robust (jobs cannot be submitted while the qmaster is down). Check-pointing functionality, while desirable, does not seem to be necessary. Lessons learned indicate that additional SGE administrators are needed so that expert administration support is not a single point of failure. Focus on SGE user training also is desirable. Primary users of SGE, mostly TETRAD and Monte Carlo N-Particle (MCNP) transport code users, are pleased with the resource manager.

New scheduling algorithms were developed to improve the efficiency of distributed computing environments. The algorithms were implemented with C++ and installed on a cluster of LINUX machines at the University of Idaho. The proposed algorithms include 1) a model for task-to-task communications, 2) an efficient method for mapping task order to a locally optimum schedule, 3) a random search mechanism that approximates a globally optimum schedule, and 4) static and dynamic scheduling methods. The proposed algorithms were evaluated by comparison to existing baseline algorithms and by simulating various computational load scenarios and distributed computing environments. The simulated computational load characteristics, including task heterogeneity, cost-matrix consistency, and level of inter-task communications, were varied over a broad range. The simulated computing environment characteristics, including machine heterogeneity and number of machines, also were varied. The results of these simulated experiments shows that the proposed algorithms performed better than the baseline algorithms for most of the cases studied. Proposed algorithm performance was within 10% of the best baseline algorithm in all cases, and has the advantages of fewer tuning parameters and lower memory requirements.

*Computational Fluid Dynamics Method Development* – In FY03, work continued on the particle model CFD code and its validation. A momentum interpolation scheme developed by Mizanur Rahman of the Helsinki University of Technology was implemented in the particle code. Momentum interpolation is necessary to prevent pressure checker boarding when using a collocated solution scheme. A collocated scheme is being pursued to eliminate the need for ghost cells when decomposing the solution domain for implementation on parallel processors. The test solution appears very stable, but converges to an incorrect solution. Dr. Rahman was contacted and provided a piece of the computer code that implements his momentum interpolation scheme. His coding is being dissected to determine the cause of the incorrect convergence. In February, many team members attended the Alliance Partners for Advanced Computational Services Intermediate MPI Programming class via the INEEL Access Grid Node. While the class was informative, the learning curve for MPI is steep. Acquisition of a CFD code that already incorporates the logic necessary to implement MPI calls, such as LANL Telluride code, was pursued to assist in the incorporation of MPI calls into the particle code.

*Scientific Data Repository and Visualization* – Earlier in this LDRD, an effort was initiated to address integrated scientific data management and expanded visualization capability needs at the INEEL. Pilot studies were conducted to evaluate the Landmark Graphics Corporation (LGC) product suite applicability to some or all of the INEEL needs. The goal of the pilot study was to provide an opportunity for participants from various disciplines (nuclear engineering, GIS visualization, hydrology, fossil energy technologies, geosciences research, and database administration) to evaluate LGC products and provide recommendations for requirements development. As expected, none of the participants concluded that the LGC suite was a solution to all of the INEEL data management and visualization needs, but many suggested that it was a powerful tool that would meet many of their individual visualization and analysis needs. Results of the pilot study have been compiled and captured in a draft report.

*TETRAD Optimization/Parallelization Evaluation*-TETRAD is a large legacy single-processor code widely used at the INEEL for subsurface fate and transport. This task evaluated the performance and parallelization potential of TETRAD. Several versions of TETRAD exist each having specific modifications related to speed-up attempts and addition of capabilities to meet particular needs. In early FY03, various versions of TETRAD were evaluated in order to select an INEEL standard. The version selected, 12.7MS, was examined for

code efficiency and performance. Results of this performance testing were used along with input from subsurface scientist users to identify bottlenecks/inefficiencies and remove TETRAD features not used for INEEL purposes. During the program final version selection, TETRAD was evaluated for parallelization and use in a cluster environment using the utility flow and by tracing the subroutine calls. Based on this evaluation, the following possibilities for further enhancement of TETRAD include:

- *Develop New Parallel Program* – The physical problem that TETRAD solves is inherently parallel and a new parallel program providing a highly scalable solution is feasible. Such an effort would be extensive (multi-year) requiring a team of developers that not only have parallel computing and programming skills, but also a geoscientist with in-depth knowledge of the problem statement and governing equations.
- *Parallelize Portions of TETRAD Version* – While the physical problem that TETRAD solves is highly parallel, the current implementation of TETRAD is not. Four subroutines in the program account for approximately 60% of the run time. While parallel versions of these subroutines could be created (a year effort for a team possessing extensive knowledge of the program, the analysis needs, and parallel programming skills), ideal results suggest that elimination of 60% of the run time would produce a 2.5 time speedup at best.
- *Non-Parallel Solutions* – Non-parallel options for enhancing the performance of TETRAD exist including software, hardware, and problem statement clarification efforts. Such effort would require programming performance skills as well as expertise from a geoscientist.

This LDRD has resulted in the submission of a proposal ("Genetic Inspired Computing") to the NASA Intelligent Systems Research Announcement to develop a GIC simulation system in which GIC computing paradigm (design/development of algorithms, operating kernel, etc.) can be developed and tested. The preliminary proposal received favorable reviews and a more detailed proposal has been requested and delivered. The GIC concept and several other advanced computing program ideas stemming from this research were submitted to Dr. Chuck Romine (Mathematical, Information, and Computational Science program manager), DOE-Office of Science, in the summer of 2003. In response to the project team's expression of interest, Dr. Romine requested that Thomas K. Larson become the Science Office point of contact at the INEEL for applied mathematics and that INEEL personnel be involved in planning and organizing computing research needs workshops for DOE to be conducted in the near future. Work conducted during this project also led to the submission of a proposal to the DOE Advanced Technology Program.

# Aerospace Situation Awareness and Risk Monitor Tool

*Steven D. Novack*

***Developing a functional model to support operational personnel***

AC103

Government and industry are recognizing the importance of using risk assessment tools to support complicated operations and management decisions. Risk analyses, including probabilistic risk assessment (PRA), help to formulate and present a wide variety of essential information for optimizing operation, maintenance, and training tasks for operators of complex systems. However, logic models which are often the underlying basis for PRA, and their powerful insights, are difficult to communicate to operators.

The nuclear power community has pioneered advances in risk assessment for the last 20 years. The aerospace industry, and in particular NASA, has recently focused on implementing nuclear power advances into their analyses. This is evidenced by some of the work the INEEL Nuclear Risk, Reliability, and Regulatory organization is participating in for the space shuttle and the upcoming international space station. As technology advances and the complexity of systems increases, the ability to understand the interdependencies, various weaknesses, and vulnerabilities of these dynamic systems becomes much more difficult. There is a need for model-based situation awareness and risk-monitoring technology to support ground control and crew decision-making. This ability could make the difference between success and failure for critical national missions in space.

This LDRD is developing situation awareness and risk monitoring software to support aeronautics and space missions. The software and decision tool will be applied to the SAPHIRE models for the space shuttle, and in the near future, international space station models that are being developed by NASA. The effort builds on a previous LDRD (ES106 — "Risk Monitor for SAPHIRE") that enhances and supports decision-making associated with nuclear power plant risks. The project also takes advantage of experience gained in the development of Virtual Reality Reliability, Availability, and Maintainability (VRAM) applications. The software will help to enhance aerospace activities with a focus on mission success.

The software focuses on the three major stages of aerospace missions: take-off and ascent, orbiting, and descent. A helpful visual interface is under development to assist with task management and risk awareness. The software also incorporates the INEEL's recent advances in common cause failure (CCF) methodology to increase the accuracy of the resultant calculations and investigate Binary Decision Diagrams (BDDs) to greatly enhance computational speed of solving PRA models. Speed enhancement from the BDD concept to SAPHIRE would be substantial such that SAPHIRE could be used as a real-time risk-monitoring tool. This could greatly extend the use of SAPHIRE and the risk monitor into industries and government agencies that require real-time situation awareness tools such as aerospace and DoD applications.

The objective of this software application is to communicate to control room operators, astronauts, and NASA management, the current levels of risk (average and instantaneous) of a Loss of Crew and Equipment accident for a multi-phased operation based on the up-to-date SAPHIRE risk models. These models consider such factors as the operational mode, out of service (failed) components, and components undergoing maintenance. As the operational mode changes or components are restored or removed from service, the risk model is recalculated and the results are displayed.

Technical objectives for fiscal year 2003:

- Design an operational graphical user interface.
- Update the advanced features of the INEEL Risk Monitor.
- Propose and modify the environment to NASA.
- Identify modifications and enhancements required for SAPHIRE.

The standalone graphical user interface (GUI) encompasses an easy-to-use interface for navigation, the ability to initiate mission status information, and a reporting feature tailored to control room operators. The interface is developed as an MS Windows program supported by a multi-user distributed database such as SQL 7.0. This program is an application that interconnects with the SAPHIRE database and uses API calls to interact with the logic model stored in SAPHIRE.

There are three aspects to the GUI: a baseline mission status, a reporting feature, and a SAPHIRE

interface module. The baseline mission status consists of a space shuttle and/or a space station status database, the graphical interface to identify information to the control room personnel, and a mapping function that interprets the graphical interface to the SAPHIRE database.

Baseline mission status information requires the software to set and store the status of events and maintenance considerations for use by the control room personnel. It is anticipated that this portion of the software will project information that provides a time-based mode (e.g., pre-launch, take-off and ascent, orbiting, and decent) graphical interface that integrates into NASA's current control room system status information.

The mapping interface, which is separated into functions, systems, subsystems (e.g., train) and components, provides a method of directing the operator to choose information that can quickly be mapped to the SAPHIRE database. This interface uses graphical methods such as 2-D (P&ID) or 3-D (3-D models) drawings and a hierarchical tree to present information to the control room operator and crew members. The mapping function will then take this information and accumulate a list of components and their associated failure modes that are considered to be unavailable for the period of time presented. This information is then passed to the SAPHIRE interface module.

The SAPHIRE interface module receives the information from the baseline mission status module and performs the recalculation or update of the Loss of Crew and Equipment from the baseline space shuttle or international space station model. CCF information will be modified in this module based on the work and algorithms developed at the INEEL. This result is then sent to the database to be used in the reporting module of the risk monitor software.

The reporting module takes the information from the SAPHIRE interface module, interprets the quantitative results, and presents the information to control operators as a colored risk meter. This risk meter can report risk based on various periods of time from hours to months. These reports will be in a time-based mode format and will directly correspond to the events identified in the baseline mission status module. The flow chart in Figure 1 depicts the interconnections of the modules and the associated databases.

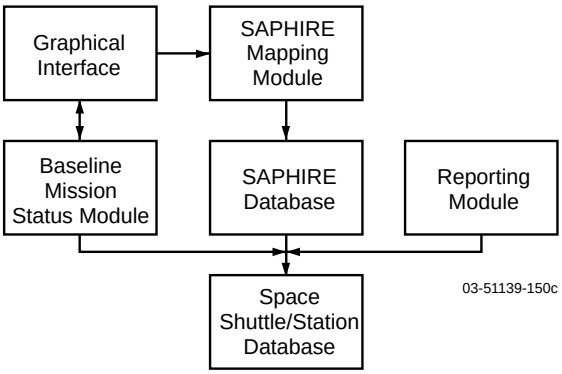


*FIGURE 1. Module and database flow chart.*

Development and incorporation of BDD methods and algorithms for SAPHIRE play an essential role in preparing INEEL's SAPHIRE for a future role in risk assessment and risk monitoring for national and international levels. The work scope involves converting documented steps for the development of Shannon Trees into source code, optimization/reduction of Shannon Trees to an efficient BDD, applying the BDD to SAPHIRE quantification to replace current min/max solutions, and testing and validating SAPHIRE modifications.

The reworking of the 3-D interface in Direct X Version 9 is 75% complete. Component hierarchy has been researched and a plan is available to add this to the risk monitor. A high-level functional model has been developed for the ISS and sent to Johnson Space Center for comments. The response was very positive from Jerry Holsenbach, director of safety and mission assurance at JSC.

- The addition of functional models has been included for an operational focus.

The risk monitor has been modularized into three areas. The first module corresponds the mapping components represented in the SAPHIRE model to plant components as viewed by the operators (Fig. 2 next page).

The second module allows supervisors to plan periodic maintenance activities based on knowledge

of the system status at the current state of time. This allows the effects of safety systems or components that are unavailable due to testing and maintenance or random failures to be included in the estimation of risk of core damage. The core of this interface is based on scheduling and hierarchy concepts (Fig. 3).

Lastly, the ability to manage risk levels for the current state of the plant and anticipated future concerns relies on the ability to communicate risk in an easily understood manner. The risk management module provides a calendar view that immediately explains the day and projected future risk levels (Fig. 4).

This work has enabled the INEEL to use the extensive static risk models developed in SAPHIRE to monitor risk on a changing plant or system. This LDRD project also has opened doors for international collaborative work with prestigious research facilities such as the RRC Kurchatov Institute. The addition of a risk monitor for SAPHIRE will greatly benefit the INEEL in its goal of establishing expertise and tools to perform risk assessment.

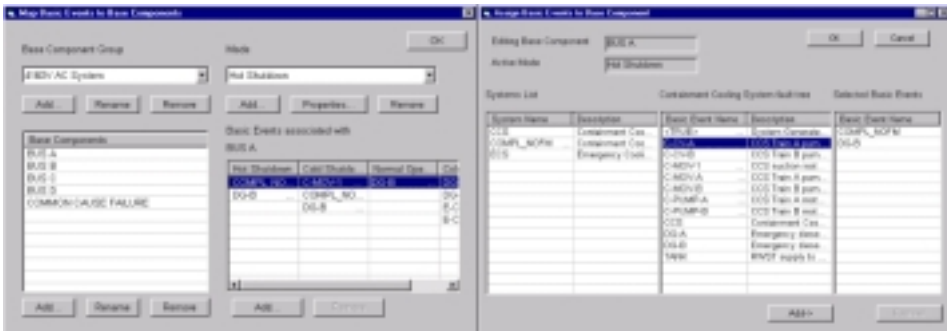

PN04-0004-151-AC103a

*FIGURE 2. Mapping interface between SAPHIRE and the risk monitor.*

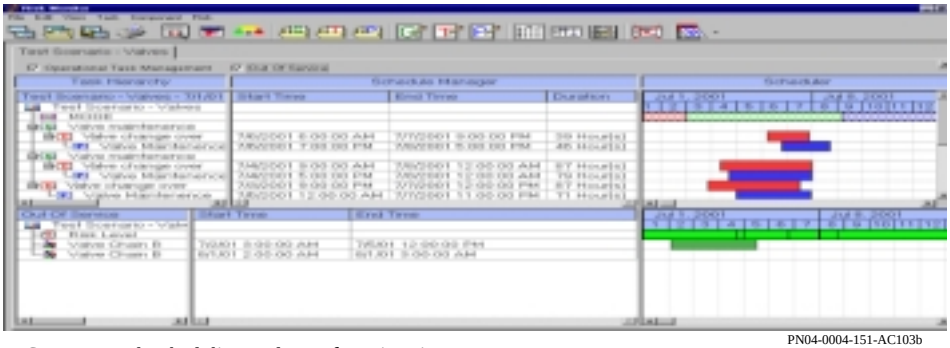

PN04-0004-151-AC103b

*FIGURE 3. Task scheduling and out-of-service view.*

PN04-0004-151-AC103c

*FIGURE 4. Calendar and daily risk view.*

# Improving Numerical Model Efficiency of an Existing, In-House Simulation Model

*G. Michael Shook, J. Hope Forsmann, M. Elena Velasquez, Swen O. Magnuson*

***TETRAD updated to meet INEEL research needs***

AC102

The numerical model TETRAD is used in a variety of studies at the INEEL, including Environmental Restoration (ER), Geothermal Engineering, and Oil and Gas studies. Due to design considerations that were valid a decade ago (but are no longer), TETRAD runs relatively slowly on "typical" ER model studies.

The objective of this LDRD is to improve the efficiency of TETRAD. Several code modifications were identified, as were a suite of test problems representative of ER model studies. Performance tools were used to identify inefficient routines in TETRAD, and code modifications were performed. Finally, recognizing the potential for inefficiencies due to input structure, input typical of ER simulations was analyzed and modified as needed. The suite of approaches taken resulted in up to 5-fold improvements in speed, depending on the test problem.

Technical objectives for fiscal year 2003:

- Reduce TETRAD execution times for "typical" ER problems by 1 order of magnitude.
- Make numerical solution modifications, identify bottlenecks in the program via performance measure software, and revise input structures to enhance stability.
- Test improvements against a suite of example problems provided by WAG 7.

As with any fluid flow model, TETRAD is based on the conservation of mass, energy and momentum. To describe the current limitations in TETRAD efficiency, it is important to discuss conservation of mass and what changes were investigated. The conservation of component i (for i=1, total number of components, or $N_c$) can be written as:

$$E_i = \frac{\partial}{\partial t}\left(\sum_{j=1}^{Np} \varphi\rho_j S_j \omega_{ij} + (1-\varphi)\rho_s \omega_{is}\right) + \frac{\rho}{\nabla}\left(\sum_{j=1}^{Np} \rho_j \overset{\rho}{u}\omega_{ij} - \overset{\rho}{K}_{ij} \cdot \frac{\rho}{\nabla}(\rho_j \omega_{ij})\right) + q_i = R_i = 0 \quad (1)$$

The first term in equation 1 above is the accumulation of component i, the second is the net flux (which includes advection and dispersion), $q_i$ is the source/sink of component i, and $R_i$ is formation/destruction of i from reaction or decay. The solution of these $N_c$ coupled equations is accomplished through a Newton-Raphson procedure as shown below.

$$\tilde{E}(t+\Delta t, \tilde{x}) = \tilde{E}(t, \tilde{x}) + \frac{\partial \tilde{E}}{\partial \tilde{x}} \cdot \delta\tilde{x} = \tilde{E}(t, \tilde{x}) + J(\tilde{x}) \cdot \delta\tilde{x} = 0 \quad (2)$$

For a variety of reasons, instead of solving equation 2 to identically zero, the equations were solved to some predetermined convergence tolerance, $\tilde{E}_i < \varepsilon$. In the standard version of TETRAD, $\varepsilon$ is a scalar. From material balance considerations, it must be substantially less than the smallest concentration being solved; however, there is no reason that mass balance convergence cannot be specie-dependant. Therefore, the first code modification investigated was to implement convergence criteria on a per-specie basis. This modified convergence criteria will be referred to as $\varepsilon(i)$ for each of $i=1,N_c$ components.

Also investigated in the previous year was a means to implement a sequential implicit scheme for solving the mass balance equations. Noting that water and air alone dictate the pressure, saturation, and flow field (i.e., trace contaminants do not affect phase behavior), the investigators considered solving only these two mass balance equations implicitly, determining the flow field, and solving the balance of the equations explicitly. Implicit formulations have the advantage of being unconditionally stable; however, solving all conservation equations implicitly requires simultaneous solution of $N_c$ equations (the sequential implicit scheme requires 2 equations solved simultaneously and $N_c$-2 solved sequentially). Thus, while there are potential time step-size limitations, sequential implicit formulations were also investigated. Another activity in this project was to evaluate the program's performance using the SpeedShop performance tools. This analysis typically consists of examining how the program makes use of the machine resources, breaking down the program into subtasks, identifying the bottleneck within each subtask, and correcting the cause of the bottleneck. Finally, a variety of input structures for ER simula-

tion were evaluated. There are various means of describing steady initial conditions in TETRAD. Input options were investigated that provided the most stable and rapid initialization for the problems of interest.

Following are the results of these investigations.

Species-dependant convergence criteria were implemented in a test version of TETRAD. Code modifications included introducing a scale factor, SCALE(I), for each of the $N_c$ conservation equations. Mass balance convergence criteria for each component is the product of ε*SCALE(I), as shown in Table 1.

Note that, while convergence criteria for water and air have increased, their *relative* accuracy (i.e., their mass balance accuracy) is the same as the other components.

A stability analysis was conducted to evaluate sequential implicit schemes for the example problems. The analysis indicated that numerical instabilities existed for typical flow rates (Courant numbers in excess of 0.5). As the instabilities were difficult to treat efficiently, sequential implicit schemes were abandoned.

Performance analysis of the program execution identified the subroutines DISPER and AREAIB as inefficient and potential areas for improvement. Forty-five percent of the total run time is spent on these two subroutines. The subroutines were modified to eliminate unnecessary branch statements without apparent improvement. A set of example problems was devised that illustrated the problem succinctly. These examples were subsequently forwarded to the code author, who is making a separate analysis. It is expected that this problem will be addressed outside of the scope of this project. However, it should be noted that whatever improvements are made are directly due to this LDRD. In addition, subroutines not used in INEEL WAG simulations were removed from TETRAD. This did not reduce execution time, but did reduce the footprint of the code.

Finally, review of typical input and initialization for WAG7 problems indicated that numerical solutions for the problems were consistently too loose. Improvements in the time-step selector and implicit iteration scheme led to more efficient problem initializations for the test cases.

A suite of test problems were identified by WAG 7 personnel for benchmarking modified versions of TETRAD. The problems involve varying degrees of geologic complexity, problem dimensionality, number of components, initialization and simulated time, etc. A program was written to compare output from the various versions of TETRAD; results were in excellent agreement for each problem statement. A simple problem description is given in Table 2, which also shows CPU timings for the original and revised codes, and relative speedup. The improvement in execution is obviously problem-dependant, but ranges up to about a factor of 5. The investigators did not achieve their target of 10-fold reduction in CPU time; however, it is noted that hardware upgrades could increase this factor to more than 10-fold.

The goal of this work was to reduce run times of TETRAD by 1 order of magnitude in FY02-03. This goal was not met. Speedups in execution range

*Table 1. Comparison in convergence criteria for original vs. modified TETRAD*

| Component | Order of magnitude mol fraction | Original Version | Revised Version | | |
|---|---|---|---|---|---|
| | | $\varepsilon_2$ | $\varepsilon_2$ | Scale (I) | $\varepsilon_2(i)$ |
| Water | 0.1-1. | $10^{-7}$ | $10^{-2}$ | 1. | $10^{-2}$ |
| Air | 0.1-1. | $10^{-7}$ | $10^{-2}$ | 1. | $10^{-2}$ |
| Aq. Contam. #1 | $10^{-4}$-$10^{-6}$ | $10^{-7}$ | $10^{-2}$ | $10^{-5}$ | $10^{-7}$ |
| Aq. Contam. #2 | $10^{-4}$-$10^{-6}$ | $10^{-7}$ | $10^{-2}$ | $10^{-5}$ | $10^{-7}$ |

03-51139-150a

*Table 2. Summary of timings for test problems*

| Problem | Description | Baseline CPU (Orig. TETRAD) | Revised CPU (Revised TETRAD) | Relative Speed |
|---|---|---|---|---|
| Base Case | Simple geometry, Vadose zone + aquifer, uniform BCs | 00:6:16 | 00:1:14 | 4.88 |
| Ex3dt | Subset of Vadose Zone simulations, simple geometry, 4 components | 00:6:08 | 00:1:53 | 3.26 |
| Combgrp9 | Full SDA simulation to t=270 yrs, complex geometry and BCs | 56:50:00 | 25:29:00 | 2.25 |

03-51139-150b

up to about 5-fold. The project team evaluated the utility in rewriting more portions of TETRAD for efficiency improvements, but concluded the cost in manpower would outweigh improvements. It appears that the most efficient way to improve execution of the code is to purchase newer hardware. For example, current processor speeds are approximately three times faster than the cluster in current use. This upgrade would reduce CPU times 3-fold.

There are additional enhancements being made to TETRAD that make the code particularly attractive for continued use. For example, an automatic history match (aka parameter estimation) version of TETRAD, known as $Tet^{-1}$, is being developed in the Renewable Energy program. TETRAD also is being coupled with a suite of geophysics models. This program and the next generation of $Tet^{-1}$ that uses both the fluid flow and geophysics models in history match algorithms ($TetGeo^{-1}$) will be useful for designing and interpreting experiments at all scales. These improved, efficient numerical models are expected to be useful to experimentalists involved in INEEL's Subsurface Science Initiative.

INEEL

# Advanced Waste Management Solutions Initiative

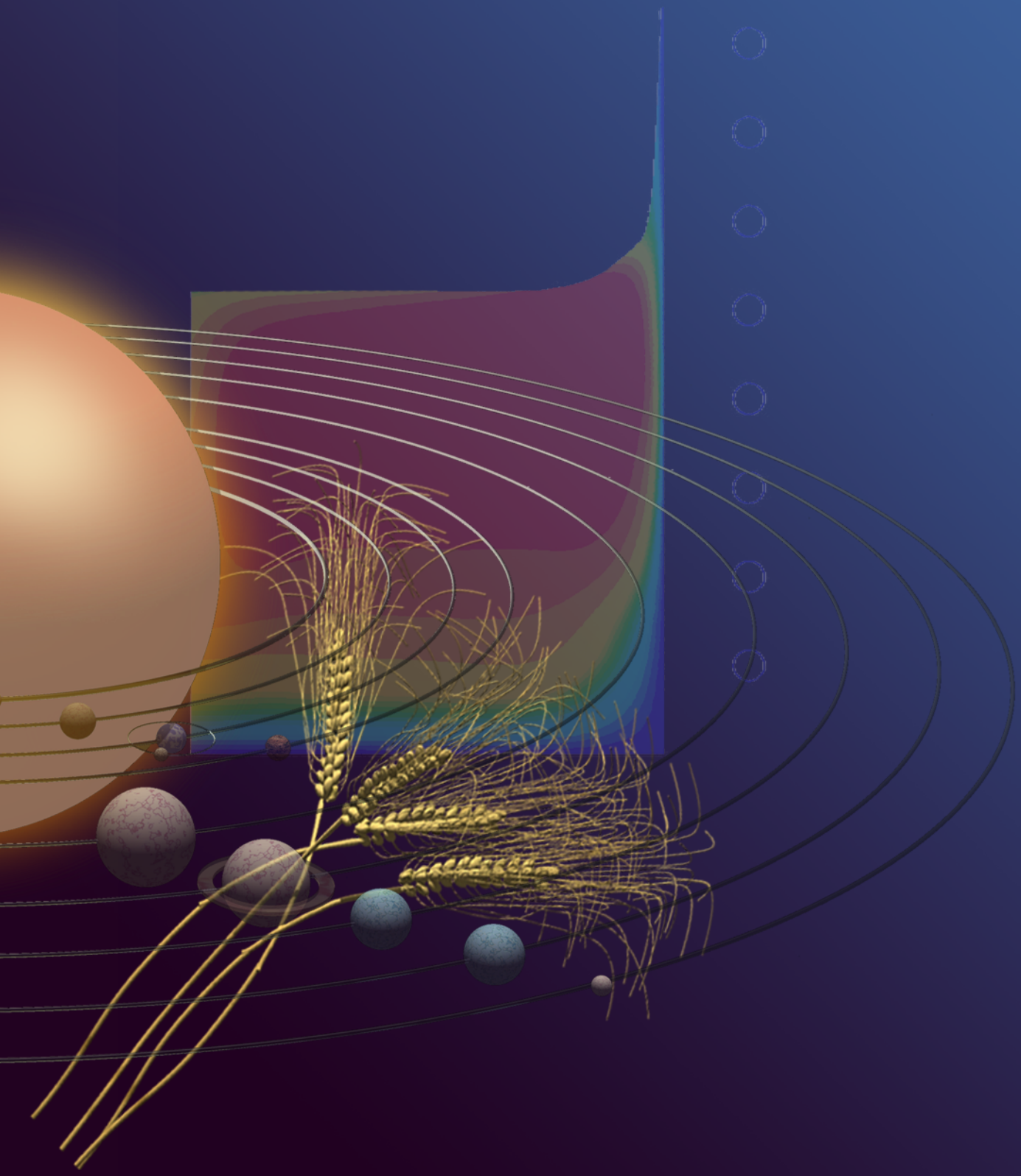

# Thermally Hot Offgas Cleanup Sorbent Technology Development

*Richard D. Boardman*

***Removing pollutants during power generation***

WT115

Offgas treatment generally requires offgas cooling to remove gaseous sulfur pollutants and volatile mercury by wet scrubbing or adsorption systems. In some cases, such as coal gasification, it is desirable to maintain the thermal heat of syngas prior to combustion in a gas turbine for power generation. It is also necessary to remove sulfur pollutants and halide-containing pollutants prior to combustion to avoid corrosion in the turbine. Thermally hot, and pressurized offgas treatment is, therefore, needed to improve process conversion efficiency.

This LDRD is evaluating the design, fabrication, set-up, and demonstration of a heated tubular or fluidized-bed reactor that will enable thermally hot offgas cleanup sorbent technology development and testing.

Technical objectives for fiscal year 2003:

- Design a high-temperature, high-pressure reactor that can operate as a fixed-bed or fluid-bed reactor to perform thermally hot, pressurized offgas sorbent development and testing.
- Model reactor operating conditions, flow sheet conditions, and material balance calculations using HYSYS.
- Identify, screen, and select candidate high-temperature sorbents for $SO_2$, $H_2S$, HCl, and Hg capture for future testing.
- Complete and/or initiate an Air Permit Applicability Determination and Independent Hazards Review.
- Demonstrate high-temperature sorbent testing and screening in a tubular reactor.

During FY03, a thermally heated, high-pressure reactor was designed and fabricated to perform novel sorbent development and testing. Design objectives for the reactor included the ability to test at high temperature (up to 900°C) and high pressure (up to 10 atm). The reactor design requirements included dynamic sorbent loading and bed sampling capability, internal temperature and pressure monitoring instrumentation, and gas mixing and flow control capability to simulate various process gases including coal gasification syngas, mixed-waste process offgas, etc. Efficient fluidization and mixing of the sorbent bed at minimal gas flow rates also was required of the reactor to minimize the volume or supply gas and emissions associated with each test. Other design criteria included article filtration to maintain the particles in the bed, and internal heating to minimize heat loss and interference with feed lines and instruments. The new reactor will be used for future research activities related to mixed-waste thermal process cleaning and fossil fuel process offgas cleaning.

The fluidized bed is illustrated in Figure 1. The reactor is constructed from 3-inch schedule 40, 304 stainless steel (ss) pipe with a length of approximately 6.2 inches. This bed has a total volume of about 1.0 L. A sintered metal (316 ss) fluidizing media with a 2-micron porosity is used for the gas distribution/fluidizing plate. The top of the bed is covered and sealed with a standard blind flange. Thermocouple and pressure tubes penetrate the flange. A 1/2 inch cartridge heater and gas takeoff port also are tapped into the top flange. A sintered metal filter is threaded to the bottom of the gas outlet. A series of valve alignments allows for a nitrogen or carbon dioxide gas blowback of the filter to prevent blockage by small particles. Six

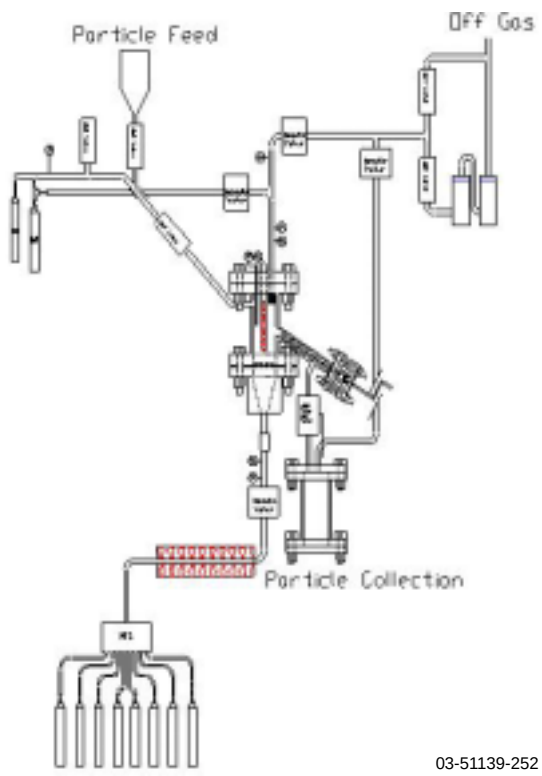


*FIGURE 1. High-temperature, high-pressure sorbent reactor.*

compressed gas cylinders are used to obtain variable synthetic offgas mixtures. Sorbent feed particles are pressure fed into the reactor through 1/2 inch stainless steel tubing located near the top of the vessel. Solids feed is regulated by a ball valve before reaching a "tee" joint. One stream off the tee joint extends to a pressure relief valve and ultimately to a nitrogen or carbon dioxide compressed gas cylinder. This enables sorbent particles to be pressurized and charged into the reactor during operation of a test. An auger is used to collect the product (Fig. 2). The auger is welded at a 30-degree angle to assist in the removal of the bed particles. Sorbent particles are conveyed from the reaction bed and eventually fall into a collection chamber.

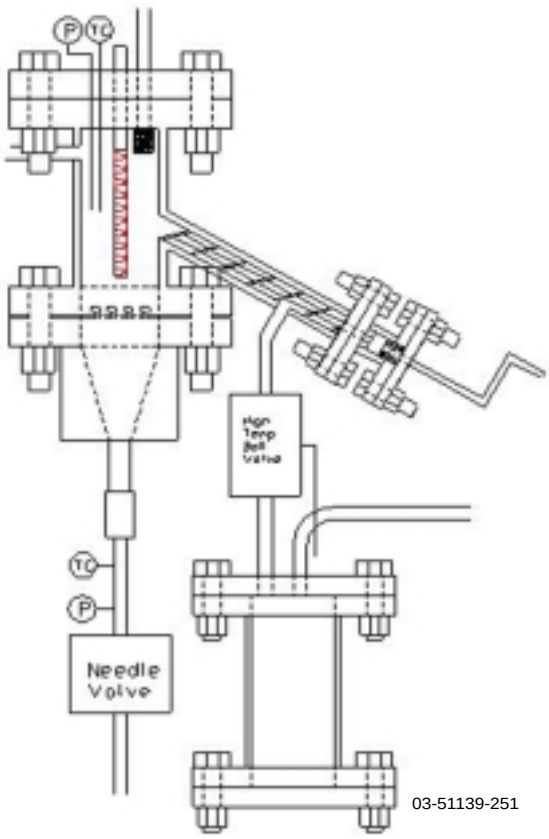


*FIGURE 2. Sorbent reactor dynamic sample collection design.*

The reactor is suitable for a variety of sorbent development tests, including:

- Pollutant sorption/de-sorption thermal cycling investigations.
- Kinetic rate of adsorption/de-sorption determination.
- Particle attrition testing as a function of thermal cycling and fluidization intensity, etc.

A literature review of ongoing research by the Gasification Technology Council and DOE-NETL research program on air pollutant control was completed during FY03 to identify sorbents that are suitable for acid gas capture (i.e., $SO_2$, HCl, HF), and for mercury sorption at elevated temperature. The literature review identified myriad sorbents that have been tested for pollutant adsorption, but only a few that are viable for high-temperature conditions. Table 1 summarizes the most promising sorbents that were selected for possible testing under this LDRD. Screening criteria included: 1) suitable isotherms for target pollutant adsorption and desorption — i.e., regeneration of sorbent, 2) sorbent particles that do not easily attrite when subjected to periodic thermal cycling, 3) favorable production or availability costs, and 4) toxicity of waste product.

*TABLE 1. High-temperature pollutant sorbent candidates.*

| Target Pollutants | Potential High-Temperature Sorbents |
|---|---|
| HCl | alumina, calcium oxide, zinc oxides |
| $SO_2$, $H_2S$ | calcium oxide, zinc oxide, zinc titinates |
| Hg | amended silicates, I-impregnated activated carbon, sulfide-ore minerals, selenium-loaded solids |

03-51139-34a

Limited high-temperature testing was completed for $SO_2$ and $H_2S$ adsorption in a tubular reactor; however, no testing was completed in the new fluidized reactor mainly due to schedule limitations. The principal investigator attended two conferences during the fiscal year. Professional contacts were made, and opportunities to support DOE, EPA, and industry with high-temperature sorbent development were identified and are now being pursued.

# Direct Dissolution of Plutonium and Neptunium Species Using Chelated Agents in Supercritical Fluid Carbon Dioxide

*Robert Vincent Fox*

***Improving metals extraction from soils and solid surfaces***

WT 107

Metal complexation followed by supercritical fluid extraction (SFE) is a new extraction technique that involves solubility and chemical reaction phenomena in the supercritical fluid phase. In metal complexation/SFE, metals are rendered into extractable forms by in situ derivatization with soluble complexing agents. Extraction of metals from solid surfaces and soil has been demonstrated using complexing agents in supercritical carbon dioxide ($scCO_2$). Extraction efficiencies are generally high, however variable results have been reported, and quantitative extraction of strongly bound and recalcitrant metals from soil has not been achieved. The causes for incomplete extraction of metal from soil are directly related to the complexation reaction. Whereas knowledge of solubility in supercritical fluids (SCFs) is sufficiently advanced, current knowledge of metal-complexation reactions in SCF solvents is shallow.

This LDRD investigates metal-complexation reactions in supercritical fluid carbon dioxide using lanthanides and organophosphorus complexing agents. Complexation reactions also were investigated for lanthanides and beta-diketones, and for dual ligand synergistic systems comprised of organophosphorus reagents and beta-diketones together. Metal-complexation reactions were studied in this unique solvent system to determine the influence of solvent conditions and reaction components on metal-complexation chemistry, metal complex limiting stoichiometry, and the conditional extraction coefficient of the various complexes. By investigating known metal-complexation reactions, solvent conditions and reaction components can be explored that lead to enhanced extraction of recalcitrant radionuclides from environmental media.

Technical objectives for fiscal year 2003:

- Determine the influence of water, ligand type, and metal type on limiting complex stoichiometry and conditional extraction coefficient.

This project focused on metal-complexation reactions between lanthanides, organophosphorus reagents, and beta-diketones in $scCO_2$. Titration reactions were performed and product stoichiometry determined. Reactions using both single-ligand systems and dual-ligand synergistic systems were studied. The products dissolved in the supercritical fluid phase were quantitatively measured using spectroscopic techniques. Spectra were examined using both univariate and multivariate analyses. Conditional extraction coefficients and conditional formation constants were calculated from the spectral data using least-squares regression and hard-equilibria models.

Reactions between neodymium, praseodymium, and tributyl phosphate in $scCO_2$ at 35°C (308 K) and pressures greater than 4,000 psi (27.5 MPa) gave rise to complexes having metal-to-ligand stoichiometric ratios of 1:4. Holmium-produced complexes had stoichiometric ratios of 1:2 and 1:4 depending on the amount of ligand added. Complexation of neodymium with tributyl phosphine oxide produced 1:5 complexes, whereas complexation with tributyl phosphite produced 1:8 complexes. Extraction coefficients computed for the different lanthanide-organophosphorus reactions in $scCO_2$ were found to be 4 to 6 orders of magnitude higher than in hexane.

Synergistic complexation of lanthanides with tributyl phosphate and several beta-diketones was shown to result in increased extraction coefficients and additional displacement of coordinated water. The more acidic beta-diketone hexafluoroacetylacetone resulted in production of stable, soluble complexes having a higher extraction coefficient than the thenoyltrifluoroacetone-tributyl phosphate complexes.

Addition of water to the complexation reaction between tributyl phosphate and the different lanthanides reduced the stoichiometry from 1:4 to 1:3, which is similar to what is found in conventional solvent extraction processes. Additionally, as the extraction temperature increased from 35°C to 65°C, the complexes fell apart producing 1:3 metal-ligand complexes. The addition of water to beta-diketone reactions increased the conditional extraction coefficient. Whereas water competes with tributyl phosphate, water aids in dissociation of beta-diketones to form the reactive enolate ion, leading to a more complete reaction of the beta-diketone with the metal.

This LDRD project resulted in two peer-reviewed journal articles and three presentations at national societal meetings. Four additional peer-review manuscripts have been prepared, two of which have been submitted and are currently under review. The other two manuscripts will be submitted later this

calendar year. Finally, this LDRD project supported, in part, the completion of the investigator's Ph.D. in chemistry through the University of Idaho.

Gaining expertise in the area of supercritical fluid metal-complexation reactions supports INEEL environmental initiatives and has already led to a Work For Others agreement with Molycorp (Mountain Pass, CA). Molycorp is the only producer of lanthanide-rich bastnasite ore in the U.S. The ore contains small amounts of natural thorium that is causing concern to customers. The understandings gained through this LDRD research will help support development of a process for selective removal of thorium from the lanthanide rich ore.

# Cold Crucible Design Parameters for Next Generation High Level Waste Melters

*Dirk Gombert*

***Solving challenging melting concerns***

WT101

The Cold Crucible Induction Melter (CCIM) represents a potential next-generation melter technology for high-level waste and high-purity or high-melting-point commercial materials. The internal surfaces of the new melter are water cooled, establishing a cold skull of the melt material that isolates the crucible from corrosion while allowing melt temperatures that are much greater than metallic surfaces could normally withstand. This LDRD project represents a complimentary theoretical aspect to engineering development of CCIM technology, specifically pilot plant design. The model is a unique capability to the INEEL.

Activities undertaken this fiscal year successfully quantified the internal state and processes in the melt including temperature profile, heat deposition distribution, convection, and subsidence. Also described is a bulk-properties model that provides the basis for a melter control system by calculating a net-melt resistance and relating that to melt power.

Technical objectives for fiscal year 2003:

- Quantify the relationship between thermal profile, convective mixing, deposition energy level, frequency, and melter topology in CCIMs.
- Devise a feedback control scheme to maintain melt state by developing a way to represent the melt as a single, controllable parameter.

INEEL has developed two complementary models. The first, a finite element model, simulates the internal state and processes in the melt, including temperature profiles, thermal deposition, subsidence, convective mixing and inactive regions. This model has been reviewed and revised on a continuing basis with the help of the Electrotechnical University in St. Petersburg, Russia. The second model is a bulk electrical properties model that represents the melt as a single load conductance across the induction coil, and is the basis for the assessment of a control algorithm. The INEEL and Montana Technical University (MTU) are developing this model jointly. Figure 1 shows the INEEL melter in operation pouring molten glass.

PN04-0004-170d

*FIGURE 1. CCIM pouring molten glass at INEEL.*

Heat transfer engineers at the INEEL have taken a commercial finite element heat transfer and computational fluid dynamics code and used it to solve magnetic field equations that couple as a heat source for the energy equation. The commercial finite element heat transfer code FIDAP (Fluent Inc.) was used to compute the electromagnetic field and heat transfer. This model calculates the magnetic vector potential that has a real and an imaginary component. The purpose of this model is to deterministically assess the transient startup of a melt configuration. The induction coil is taken as a nine-turn copper tube coil. The material in the crucible is PSCM-20 glass and has been used in other melters. A strategically placed graphite ring generates heat and causes the surrounding glass to melt. After a sufficient amount of glass has melted, the electrical conductivity of the melt is sufficient to produce heat and permit the melt to grow.

This model includes natural convection of the glass due to density differences. The model also incorporates subsidence of the melt when the

density of the glass changes from a powdered frit to the molten glass. Figure 2 shows the finite element mesh deformed due to subsidence. Also included in this model is a power controller that adjusts the current in the induction coil to generate 60 kW of heat in the glass melt and crucible. The power controller limits the current in the coil to 70 Amps. Figure 3 shows the power and current histories with the implemented controller. Figure 4 shows the temperature distribution at 3600 seconds. Dynamically, the model shows the molten region growing and melting more of the glass with time.

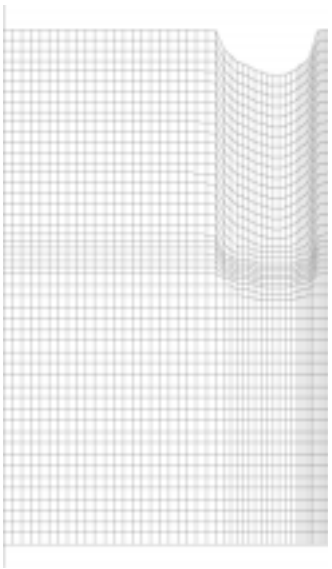

PN04-0004170e

*FIGURE 2. Deformed finite element mesh.*

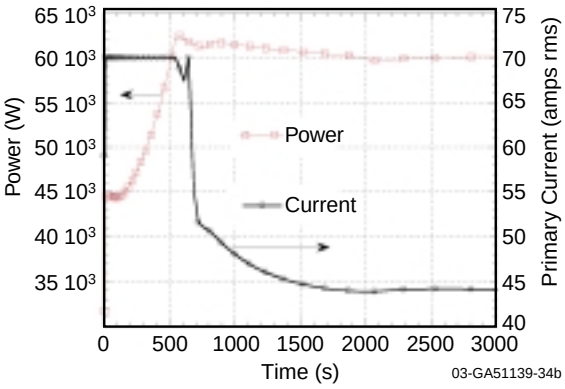


*FIGURE 3. Power and current history with controller.*

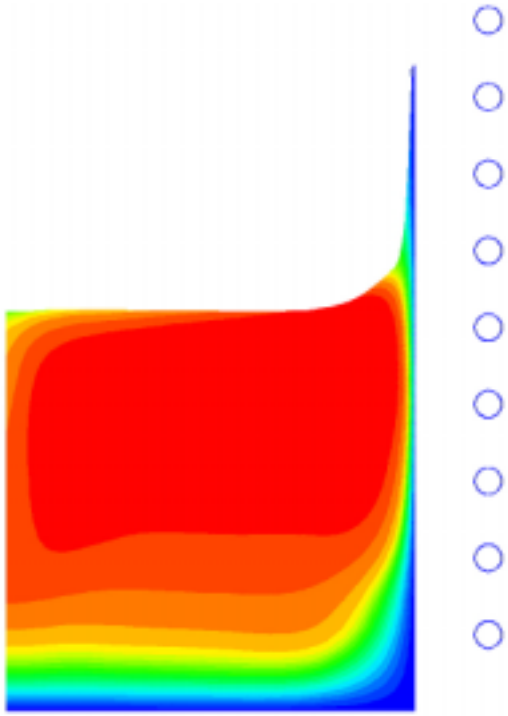

PN04-0004-170a

*FIGURE 4. Temperature contours at 3600 seconds with deformed mesh.*

FIDAP solved the magnetic equations as a set of highly coupled steady-state equations and used this information as a heat source for the transient heat transfer model. Preliminary results indicate that the modeling effort agrees with experimental efforts with the recently completed melter. Collaboration with professors from the Electrotechnical University in St. Petersburg Russia has been completed during FY03 as part of this LDRD. The Russian professors visited the INEEL, September 15-18, 2003.

*Bulk Electrical Properties Model* — As a complement to the Electromagnetic, Heat Transfer and Thermodynamics Model, the measurement basis for a melter control algorithm was completed based on a bulk-electrical properties model. During FY03 the model was expanded to account for skin effect

losses, a sophisticated circuit equivalent model was developed of the primary inductor and power supply system, and a technique was derived to estimate all parameters.

As frequency increases, the depth of penetration of current into a conductor falls off as an exponential. This is known as the skin effect. The decay of current into the conductor was modeled with conductivity being a function of depth into the conductor, and the expression for the skin depth resistance of the copper tubing that the CCIM coil is fabricated from was determined as

$$R = \frac{l}{2\pi\sigma_o}\left\{\frac{1}{\gamma}\left(R_O - R_i e^{-\gamma(R_O - R_i)}\right) + \frac{1}{\gamma^2}\left(e^{-\gamma(R_O - R_i)} - 1\right)\right\}^{-1}$$

The CCIM Equivalent Circuit Model was expanded so that with measurements of $\vec{V}_{in}$, $\vec{I}_{in}$ are measured then melt power, $P_{melt}$ can be determined. An in situ parameter estimation technique was developed to obtain model parameters for the refined electrical equivalent circuit model of the CCIM. Figure 5 illustrates the schematic of the refined model and the parameters that can be measured directly or estimated.

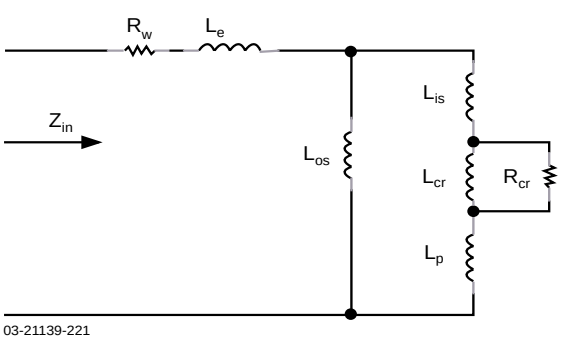


*FIGURE 5. Refined CCIM electrical model.*

The inclusion of $L_{IS}$ is considered important because during summer testing at INEEL, the spacing between the induction coil and the crucible was increased to eliminate electrical arcing. The expressions for the model parameters in terms of in situ measurements were derived and it was shown that all could be determined by laboratory measurements.

These three tasks completed the work necessary for a control scheme based on model estimates of melt power $P_{melt}$ to be tested.

The CCIM technology offers distinct and recognized advantages over conventional vitrification technologies (e.g., refractory-lined and electrode-type melters). Several studies have been conducted within DOE that identify CCIMs as the best potential alternative to the baseline technology, and recommend that additional research and technology testing be conducted. The work completed for this LDRD has significantly advanced the understanding of CCIM operations and parameters, while strengthening the INEEL capabilities through university partnerships with St. Petersburg Electrotechnical University and Montana Technical University. This LDRD project has enabled INEEL engineers to design and fabricate an innovative CCIM test system that is unparalleled in North America. Additionally, significant intellectual property has resulted from these efforts.

# Novel Abrasion Resistant Enhanced Flux UF Membranes

*R. Scott Herbst, Nick R. Mann*

***Developing a key to the success of alternative energy sources***

WT117

Past experimental studies regarding abrasion mechanisms of ultrafiltration membranes resulted in the concept of an "embedded membrane" for use in ultrafiltration applications. There has been little research on membrane abrasion in the past; however, commercial membrane companies and many end users know that this is a critical issue in the commercialization of membranes for numerous high-volume applications. Both the DOE and INEEL have a keen interest in developing renewable and sustainable energy sources relating to bioenergy, nuclear energy, and hydrogen production. The development of advanced filtration technologies is key to the success of these renewable and sustainable alternative energy sources.

This LDRD, a collaboration with Amalgamated Research Inc. (ARi), investigates a concept for fabricating novel embedded membranes that could potentially revolutionize ultrafiltration membrane technology by providing substaintially higher permeate fluxes and reduced membrane abrasion characteristics. The objective of this project is to explore the development of embedded membranes by parametrically designing, fabricating, and testing a number of composite embedded membrane filter elements. The embedded membrane concept relies on incorporating smaller particles of one material (e.g., $TiO_2$) in the interstices of a macro-porous support (e.g., sintered stainless steel) in the absence of a surface coating of the finer "active" material. The resulting composite membrane is resilient to abrasive processes since only the substrate material is subjected to the harsh hydrodynamic properties of the flowing bulk process fluid, protecting the layer of finer particles that provides the necessary filtration efficiency. Furthermore, the embedded layer of particles results in less resistance to permeate flow (compared to coating the porous substrate surface with a thin layer of finer particles), resulting in enhanced permeate fluxes without loss of filter efficiency or permeate clarity.

Technical objectives for fiscal year 2003:

- Complete subcontract with Amalgamated Research Inc.
- Determine and procure candidate substrate materials (tubular 5 ìm nominal cutoff sintered stainless steel manufactured by both Pall Corp. and Mott Metallurgical) and appropriate samples of $TiO_2$ to be embedded in the substrates.
- Develop membrane preparation techniques and test protocol.
- Present research results at a technical conference.
- Prepare initial samples of embedded membranes.

Initial fabrication attempts included a simple slip-cast technique with 40 wt.% $TiO_2$ slurry in water. The fabrication technique was designed for complete recycle and reuse of the unused $TiO_2$ slurry. To slip cast the membranes, one end of a 3-inch long, 0.5-inch ID (interior diameter) tubular sintered stainless steel membrane (samples from both Pall Corp. and Mott Metallurgical were used) was plugged and filled with 40 wt% $TiO_2$ slurry. The slurry was allowed to stand in the tube for two hours, after which the slurry was poured away and the tube allowed to air dry. After drying, the tube was cut lengthwise and then broken to examine the fracture edge. It was determined that a coating approximately 100 microns thick was embedded into the membrane with this technique. However, instead of filling the interstices of the sintered metal at the interior wall, the $TiO_2$ migrated to the exterior of the tube. This phenomenon was observed with both the Mott and Pall sintered metal tubes. A SEM micrograph indicating the 100-ìm thick layer of embedded $TiO_2$ prepared by the slip casting method is shown in Figure 1.

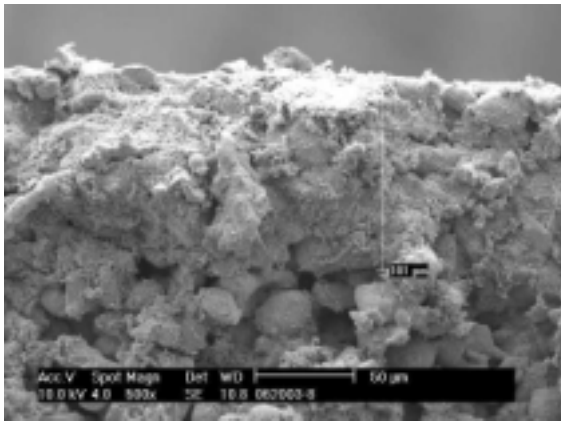

PN04-0004-170a

*FIGURE 1. SEM micrograph of an ~100 µm thick $TiO_2$ layer embedded in the sintered stainless steel substrate.*

In an attempt to understand the migration of $TiO_2$ particles to the exterior of the membrane, residence time experiments were performed where the length of soak time for the $TiO_2$ slurry was varied. It was determined that the longer the slurry was allowed to

reside in the tube, the further from the inside edge the embedded $TiO_2$ migrated. It was determined that at a residence time of five minutes, the embedded $TiO_2$ layer remained predominately at the interior wall of the tubular sintered stainless steel. However, the problem with this fabrication technique was that it resulted in residual coating on the inner surface of the tube.

An additional matrix of experiments was performed using slight vacuum starting at 500 torr with incremental decreases in pressure by 50 torr to facilitate transfer of the embedded layer into the substrate. From these experiments it became obvious that the hydrostatic pressure felt by a 3-inch length of tube is minimal since samples at the lowest pressures did not exhibit a coating within the cross-section at all. The $TiO_2$ cake formed on the exterior of these tubes was of the same consistency found in the earlier experiments using the slip cast method. Figure 2 shows an embedded membrane sample fabricated under vacuum.

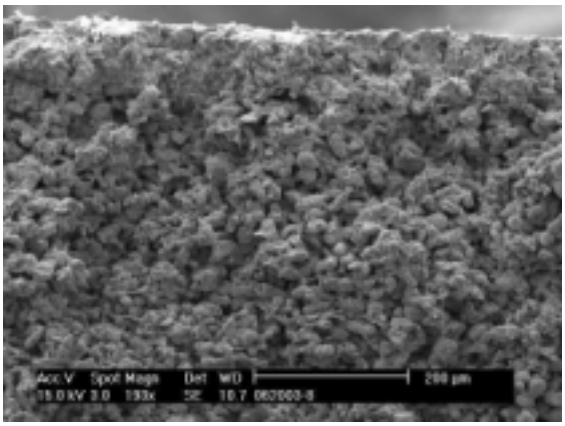

PN04-0004-170g

*FIGURE 2. SEM micrograph of embedded membrane fabricated under vacuum. The $TiO_2$ coating (top) is embedded ~ 100 µm deep in the sintered metal substrate.*

Finally, experiments are currently in progress where the vacuum used on the sample is minimal. Samples prepared in this manner indicate the most promise with regard to controlling the thickness and location of the embedded $TiO_2$ layer. Another option of slurry fabrication was explored in the event that a surface coating could not be avoided. This technique used added acrylic binders in a combination similar to that of tape casting so that after drying, the surface coating would be peeled leaving a virtually particle-free or uncoated surface.

This LDRD has resulted in the filing of two Invention Disclosure Records (IDRs) in collaboration with ARi, and future collaboration with another industry partner, Ceramem Corp., to evaluate embedded membranes (prepared by Ceramem) based on incorporating metal oxides into a ceramic substrate. Future activities include the continued evaluation of embedding techniques and methods. Embedded membrane samples will be prepared and evaluated to determine flux through the samples with water and solids-containing slurries using the existing Cells Unit Filter apparatus under cross-flow process conditions.

The research produced under this LDRD supports INEEL and DOE bioenergy and nuclear energy missions.

# Development of Advanced Aqueous Processing to Support the Nuclear Fuel Cycle

*Jack D. Law, D. R. Peterman*

***Minimizing nuclear waste and proliferation risk***

WT116

A major goal of the Office of Nuclear Energy is to expand nuclear energy as a reliable, affordable, and clean energy source for the nation. A major obstacle to expanded use of nuclear energy is the generation and disposal of the large quantities of spent fuel that result from a once-through process. Advanced reprocessing technologies are needed that allow for complete actinide recycle and minimization of nuclear waste.

This LDRD investigates the potential of advanced aqueous reprocessing of spent fuel to provide a versatile method for reducing waste generation and eliminating proliferation potential in the nuclear fuel cycle. Research was performed to support an advanced aqueous reprocessing flowsheet allowing complete actinide recycle. Work in FY03 focused on the separation of Am/Cm from lanthanides. Computer modeling was performed for the processes that likely would precede this extraction process to determine the feed composition. Purification and testing of a solvent extraction process using CYANEX-301 was initiated. Additionally, a proprietary dithiophosphinic acid derivative was identified that should have a significantly lower $pK_a$ than the alkyl dithiophosphinic acid extractant (CYANEX-301), enabling extraction in more acidic solutions (pH < 1). Development of a synthetic pathway for this ligand is underway.

Technical objectives for fiscal year 2003:

- Complete literature search/review of the use of CYANEX-301 for the separation of actinides from lanthanides.
- Perform modeling of the UREX + flow sheet for the treatment of spent LWR fuel to determine a feed composition for the CYANEX process.
- Procure CYANEX-301 extractant, evaluate purification methods for the CYANEX-301, and purify the extractant for use in batch contact experiments.
- Initiate batch contact experiments to evaluate performance of the process as a function of pH.
- Begin evaluation of potential use of the ammonium salt of CYANEX-301 as opposed to the use of the acid form.
- Identify, through the use of modeling, a proprietary dithiophosphinic acid derivative that should have a significantly lower $pK_a$ than the alkyl dithiophosphinic acid extractant (CYANEX-301), enabling extraction in more acidic solutions (pH < 1).
- Develop a potential synthetic scheme for this novel extractant.

A literature review of existing technologies for the separation of actinides from the lanthanides has been performed. Two approaches are being taken in developing an actinide/lanthanide separations process. One is application of a commercially available alkyl dithiophosphinic acid extractant-based (CYANEX-301) solvent extraction process in an advanced aqueous reprocessing flowsheet for the treatment of light water reactor (LWR) fuel. The CYANEX process is being considered by the AFCI Program for the actinide/lanthanide separation. However, this process operates most effectively at a solution pH > 4.0, requiring some feed adjustments. The second approach being taken is the development of a novel dithiophosphinic acid extractant that is effective with higher acidity feed solutions.

Computer modeling has been completed for an advanced aqueous reprocessing flowsheet that consists of the UREX process for the separation of U and Tc, a CDC/PEG process for the extraction of Cs and Sr, the TRUEX process for the extraction of Np/Pu and Am/Cm/lanthanides, and a CYANEX process for the separation of Am/Cm from the lanthanides. Feed simulant for the development of the Am/Ln separations process will be based on the results of this modeling.

The CYANEX-301 extractant (Cytex, Canada) has been obtained for use in developing a CYANEX flowsheet. As received, CYANEX-301 is a mixture of approximately 70% of the active extractant, bis(2,4,4-trimethylpentyl)dithiophosphinic acid, with the balance being synthetic byproducts. The CYANEX-301 has been purified by recrystallization of the ammonium salt from toluene. The purity of the final product increased to >99.9% (determined by $^{31}P$ NMR), as the bis(2,4,4-trimethylpentyl)dithiophosphinic acid, with a yield

of approximately 75%. The purified CYANEX-301 has been used to perform batch contact tests of the process.

Initial batch contact tests were performed using 0.5 M CYANEX and 0.55 M tributyl phosphate (TBP) in n-dodecane. Leached spent LWR fuel simulant spiked with Am-241 and Eu-154 was used. Extraction distribution coefficients were measured as a function of pH using a buffered solution of ammonium acetate and acetic acid. Distribution coefficients for Am were > 1,000 while the Eu distribution coefficients were typically < 40, with the lowest value being 8.5. With these distribution coefficients, both Am and Eu will extract; however, using a lower CYANEX concentration in the solvent, along with an appropriate scrub solution should yield good separation between the Am and Eu. Testing is planned under these conditions.

The purified CYANEX-301 decomposed from 99.9% purity to 97% purity over a four-week period (stored at room temperature under a nitrogen atmosphere). The purification process for the CYANEX-301 includes crystallizing the CYANEX as an ammonium salt then re-dissolving the salt and converting it to the acid form. The second part of the procedure is difficult and results in a solvent that decomposes as described above. Crystallizing the CYANEX as an ammonium salt is not difficult and results in a more stable product. With an ammonium acetate/acetic acid based feed to the CYANEX process (ammonium acetate/acetic acid can be used to strip the actinides and lanthanides from the TRUEX solvent in the previous process), potentially a CYANEX flowsheet can be designed that will allow for the use of the ammonium salt in TBP and n-dodecane. This would substantially decrease the complexity of the purification process and increase the stability of the solvent. Batch contact tests have been initiated using the ammonium salt dissolved directly in a TBP/n-dodecane solution. The initial results of a long-term stability study indicate the ammonium salt of CYANEX-301 is significantly more stable than the acidic form.

Computer modeling has been performed on several dialkyl dithiophosphinic acid derivatives to identify favorable candidates for synthesis. The primary criterion for evaluation of possible extractant structures was the $pK_a$ of the acidic thiol hydrogen. In the case of the bis(2,4,4-trimethylpentyl)dithiophosphinic acid, the $pK_a$ value of approximately 3 limits the usefulness of this extractant to mildly acidic (pH ~ 3) solutions. The results of the computer modeling identified a proprietary dithiophosphinic acid derivative that should have a significantly lower $pK_a$, enabling extraction in more acidic solutions (pH < 1). This new compound is not commercially available. A synthetic scheme has been developed and is currently being pursued for this ligand.

The mission of the INEEL has recently been realigned to the Office of Nuclear Energy, establishing the INEEL as the nation's leading center of nuclear energy research and development. The major goal of the Office of Nuclear Energy is to expand nuclear energy as a reliable, affordable, and clean energy source for the nation. A major obstacle to the expanded use of nuclear energy is disposal of spent fuel. An integral part of the nuclear fuel cycle is development of advanced reprocessing technologies that allow for complete actinide recycle and minimization of nuclear waste. This LDRD supports development of advanced aqueous reprocessing. The work will enhance the INEEL's capabilities and expertise in the area of nuclear fuel reprocessing. Currently, separations research and development direct funding at the INEEL from the Advanced Fuel Cycle Initiative is limited to the separation of Cs and Sr from dissolved LWR fuel. This direct funding resulted from previously demonstrated expertise in Cs and Sr separations for the treatment of waste solutions at the INEEL. Developing expertise in other areas of the AFCI separations program should lead to additional opportunities from the AFCI program in future years.

# Investigation and Modeling of Dynamic Strain Rate Effects on Structural Material Response

*Dana K. Morton*

***Leading to design affordability and longer life cycles of construction materials***

WT114

Most structural design acceptance criteria are stress-based. These stress-based criteria are prudent for normal operating conditions where static loading due to pressure, weight, and thermal loads dominate. Years of experience have repeatedly demonstrated that these criteria (e.g., ASME B31.1 Power Piping Code) have achieved successful designs. However, many component designs become excessively conservative trying to satisfy these stress-based criteria for the high stresses typically resulting from low-probability, off-normal dynamic events such as an accidental drop. This conservatism frequently manifests itself as thicker material. The downside of thicker material is that it can significantly elevate life-cycle costs and potentially degrade structural performance over the design life of the component.

The goal of this LDRD is to develop a test capability at the INEEL that can accurately determine stress-strain response models of commonly used construction materials, addressing both strain rate and temperature effects. As a first step, an apparatus was constructed that would permit such material testing. This apparatus, using a dropped weight, is called the Impact Testing Machine (ITM). By extending the knowledge of material responses beyond the standard "quasi-static" uniaxial tensile test process, the accuracy of stresses/strains predicted by finite element plastic analysis computer codes for low-probability (but design-governing) dynamic events, such as accidental drops, can be improved. Accurate knowledge of the actual responses of components or structures to dynamic loads means improved designs, safer designs, more cost-effective designs, and better overall engineered solutions to the many problems at hand.

The first year's goal was to build the impact test apparatus. Future funding will be used to perform material testing that will determine the dynamic stress-strain material responses and demonstrate the capabilities of the ITM. Besides carbon, stainless, and alloy steels, concrete can be tested to determine penetration, perforation, spalling, and scabbing insights. In addition, test documentation and ITM capabilities information will be developed.

Technical objectives for fiscal year 2003:

- Finalize the ITM design.
- Fabricate major components for the ITM.
- Assemble the major components and prepare the ITM for use.

During FY03, the ITM was taken from the conceptual design stage to a completed test apparatus (Fig. 1). Major components of the tower, the drop weight, and the test specimen fixture that holds the test specimens were fabricated. The major components of the drop tower were then assembled (Fig. 2). An enclosure was installed to eliminate potential fragments and reduce noise concerns for the test personnel.

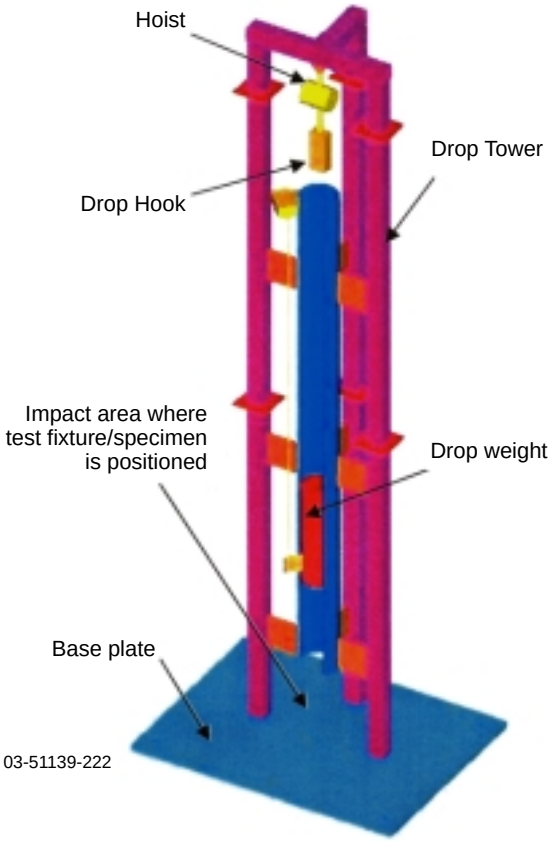


*FIGURE 1. Impact Testing Machine (ITM).*

PN04-0004-170f

*FIGURE 2. Assembled drop tower.*

Although the ITM has not yet been used, this year's effort resulted in a new INEEL test capability that is expected to generate data to support improved structural evaluations of cans, canisters, and transportation packaging used to carry spent nuclear fuel and radioactive wastes. This information also can be used to assess vulnerabilities to terrorist attacks or be used to improve or evaluate countermeasures against terrorist attacks. Industries that could benefit from improved structural evaluations are nuclear power plants, fossil power plants, refineries, chemical plants, data centers, water plants, financial institutions, and other infrastructure sites deemed potential terrorist targets. Other areas in which this research task may have application include vehicle crash studies, roadside barrier design improvements, shipping containers for hazardous chemical and biological materials, codes and standards organizations, government agencies and private industries interested in databases for computer software validation, and more.

Virtually any structure, system, or component design can benefit from this research task if imposed dynamic loads induce plastic strains at the achievable strain rates (expected to be from 50 $sec^{-1}$ to 200 $sec^{-1}$). This is an area of research that has been largely overlooked and where the INEEL can now play a significant role in offering this test capability.

Having more accurate material response data directly supports the DOE-EM mission of reducing cost, risk, and schedule while safely disposing of the nation's radioactive wastes. Two programs funded through DOE-EM have already established FY04 work plans to use the ITM to test materials associated with canister performance during drop tests. DOE's Office of Civilian Radioactive Waste Management also can benefit from accurate material response data in terms of improved repository surface facility and container designs so that spent nuclear fuel and radioactive wastes can be safely handled and disposed. Generating more accurate stress-strain material response data with the ITM can be extended to support other government agencies such as the Department of Transportation, the Office of Homeland Security, and the Nuclear Regulatory Commission. In addition, this new test capability will enable the INEEL to pursue university collaborations in this area.

The new test capability positions the INEEL to attract other significant efforts such as helping to establish the basis for changing stress-based structural design criteria (e.g., the ASME Boiler and Pressure Vessel Code) to strain-based criteria for low probability dynamic events. This could have a major impact on the nuclear industry, including Generation IV reactor development applications, and enhance the INEEL's newly assigned role as DOE's preeminent facility for advanced nuclear and engineering research.

# Thermodynamic Modeling of High-Ionic Non-Ideal Solutions

*Todd T. Nichols, Dean D. Taylor*

***Bringing new capabilities to INEEL process modeling***

WT111

Association-based parameters for the Pitzer model would enable practitioners to perform process design involving liquid speciation, vapor-liquid equilibria and solid-liquid equilibria of high ionic-strength, complex, electrolyte mixtures at 0-100°C within process simulators where Pitzer's model has been implemented. Association-based parameterizations would enhance the INEEL's process simulation capability in particular because of their compatibility with ASPEN Plus, the simulator selected for INEEL process modeling. The purpose of this LDRD is to obtain association-based Pitzer parameters for use with ASPEN Plus.

Technical objectives for fiscal year 2003:

- Obtain association-based parameterizations of the Pitzer model for key volatile solutes.
- Extend the applicability of the Pitzer model from 6 up to 16-20 molal.

Compatibility with ASPEN Plus requires that the Pitzer model used be limited to the third virial coefficient and have the values of $b$ and $\alpha_1$ as originally proposed by Pitzer. Two aqueous models for 0-110°C at atmospheric pressure were parameterized in FY03. The model for the aqueous $H^+$-$K^+$-$Na^+$-$Cl^-$ system is applicable for 0-16 molal, and the $HNO_3$-H2O for 0-20 molal. An association-based Pitzer activity coefficient model is combined with Henry's law to predict activity/osmotic coefficients and VLE. The chloride model also predicts KCl and NaCl solubility, while the nitric acid model has the unique capability of predicting extent of dissociation with an average absolute deviation of 1.43%. Both models are readily usable in ASPEN Plus. Results are summarized in Table 1.

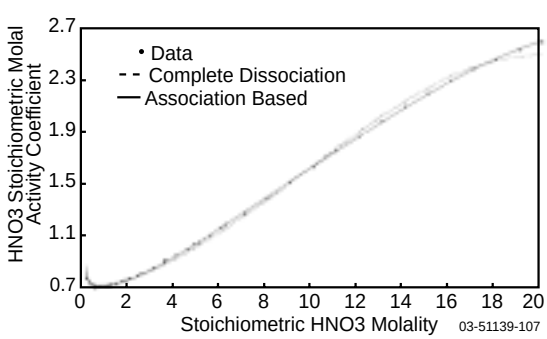


*FIGURE 1. Comparison of association-based and complete-dissociation Pizter models: HN03 at 25°C*

The association-based approach extends the utility of the molality-based Pitzer model up to 16-20 molal to predict activity/osmotic coefficients. The average absolute deviation of the association-based approach for HCl up to 16 molal, for example, is almost as small as that of the complete-dissociation approach when limited to only 6 molal. In the case of $HNO_3$, a solute undergoing significant association, the association-based approach can reproduce activity and osmotic coefficient data reasonably well (average absolute deviation $\approx$ 0.4%) up to 20 molal, as well as accurately predict extent of dissociation. The complete-dissociation approach of the molality-based Pitzer model, on the other hand, produces a significant under-predict/over-predict cycle in the predicted activity/osmotic coefficients of HCl and $HNO_3$ when the regressed data extends much past 6 molal. This is visible for the $HNO_3$ stoichiometric molal activity coefficient in Figure 1. The approach based on association has the additional benefit of enabling the Pitzer model to be fully utilized in simulators (such as ASPEN Plus) that implement Henry's law in terms of molecular species.

The parameterization of the model for the $H^+$-$K^+$-$Na^+$-$Cl^-$ system was achieved by: (a) performing isothermal regressions of HCl-$H_2O$ activity/osmotic coefficient data to establish temperature-dependent correlations for the HCl association-based binary Pitzer parameters, (b) regressing HCl partial pressure data to establish a temperature-dependent correlation for the Henry's law constant, (c) regressing solubility and activity coefficient data from HCl-KCl and HCl-NaCl ternary subsystems to determine the corresponding Pitzer mixing parameters, and (d) utilizing mixing parameters for KCl-NaCl from the literature. A reasonable dissociation constant for HCl from the literature was used, but extent of dissociation data is not available. Temperature-dependent correlations for the solubility product of KCl and NaCl were obtained from solubility and saturation activity coefficient data reported in the literature.

The parameterization of the model for nitric acid was developed by estimating stoichiometric activity coefficient values at temperatures other than 25°C with the correlation of Clegg & Brimblecombe (1990) as referenced to the values of Hamer & Wu (1972) and Redlich et al. (1968) at 25°C. Isothermal regressions of activity coefficient and extent of

dissociation data were then performed at 0, 25, and 70°C. The van't Hoff expression was used to describe the temperature dependence of the dissociation constant from these three isothermal regressions. Holding the expression for the dissociation constant fixed, isothermal regressions were performed at other temperatures, from which temperature-dependent correlations were fitted for the Pitzer parameters. A multi-temperature Henry's law correlation was subsequently regressed from $HNO_3$ partial pressures.

This LDRD advances the Nuclear and Environmental operations at the INEEL in support of DOE initiatives.

*TABLE 1. Summary of Association-Based Parameterization Results: Average Absolute Deviation Between Predicted and Experimental Values.**

| Aqueous System | $\gamma_{\pm,st}$ | $\phi_{st}$ | Vapor-Liquid Equilibrium | Solid-Liquid Equilibrium | Extent of Dissociation |
|---|---|---|---|---|---|
| HCI | (0-50°C, 0 < m ≤ 16; 60-110°C, 0 < m ≤ 7) 0.6% (5-55°C, 0 < m ≤ 4) **0.24%** (70-80°C, 7 < m ≤ 11) **4.5%** | 0.3% (25, 60-110°C) | ($p_{HCI}$: 0-50°C) 2.05% ($p_{HCI}$: 60-110°C) 4.41% ($p_{HCI}$: 0-110°C) 2.70% ** ($p_{Total}$: 50-121°C, 1 < m ≤ 13.5) **1.36%** | N/A | N/A |
| HCI-NaCI | (0-50°C, 0 < 1 ≤ 3 m $\gamma_{\pm,st(HCI)}$) 0.42% *** (25°C, 0 < 1 ≤ 7 m $\gamma_{\pm,st(HCI)}$) 1.44% | N/A | N/A | (0-30°C, 6 ≤ I ≤ 17.5 m) 4.92% *** (25°C, 6 ≤ I ≤ 19 m) 4.21% | |
| HCI-KCI | (0-50°C, 0 < 1 ≤ 3.5 m $\gamma_{\pm,st(HCI)}$) 1.06% (25°C, 0 < 1 ≤ 5 m $\gamma_{\pm,st(HCI)}$) 1.28% (5-45°C, 0 < 1 ≤ 1.5 m $\gamma_{\pm,st(HCI)}$) **0.60%** **** | N/A | N/A | (0°C, 3.8 ≤ I ≤ 17.4 m) 6.42% (0°C, 19 ≤ I ≤ 20.8 m) **4.21%** (25°C, 5 ≤ I ≤ 16 m) 2.02% (25°C, I = 17.6 m) **0.64%** | |
| HCI-KCI-NaCI @25°C | 4 ≤ 1 ≤ 6 m) 3.12% | N/A | ($p_{HCI}$: I = 5 m) **5.64%** | (7 ≤ I ≤ 14 m) 6.08% | |
| $HNO_3$ | (25°C) 0.51% (Clegg & Brimblecombe "input" 0-110°C) 0.14% *** | 0.32% (25°C) | ($p_{HCI}$: 5-120°C, 4-24 m) 14.0% ($p_{HCI}$: 106-117°C, 6-20 m) **14.8%** | N/A | 1.43% (0, 25, & 70°C) **3.45%** 00 & 50°C) |

* Unless stated otherwise, the ionic strength and temperature ranges are 0-16 m: 0-110˚C (chloride systems) and 0-20 molal: 0-120˚C ($HNO_3$). Bolded averages indicate that the corresponding data was not used to regress model parameters. Absolute deviation = |data-predicted|/data. Average absolute deviation = $\frac{\sum_{i}^{n} \frac{|data_i - predicted_i|}{data_i}}{n}$ where the summation is over all data points i, and n is the number of data points. Deviations given in terms of percentages are merely multiplied by one hundred. For solubility data, $data_i$ and $predicted_i$ refer to the thermodynamic solubility product and the predicted ionic product at saturation, respectively. Details of the association-based parameterization process, data reconciliation, results, and predictive accuracy can be found in Nichols & Taylor (2003). Details of the regression algorithm used are given in Taylor & Nichols (2003).

** Total average for two previous cell entries at 0-50˚ and 60-110˚C.

*** Excludes data at 25˚C.

**** Data is distinct from that of other entries in the cell.

# Electrochemical Recovery of Mercury from Nuclear Industry Process Solutions

*Darryl D. Siemer*

***Removing mercury from radioactive waste***

WT112

Strongly acidic radioactive waste solutions generally consist of either raffinates generated when PUREX and/or REDOX actinide separation processes are applied to solutions generated by either: 1) mercury-catalyzed nitric acid dissolution of aluminum-clad fuel rods, or 2) offgas scrub solutions produced when such wastes are subjected to any treatment that volatilizes mercury (e.g., calcination). The extremely high salt content, acidity, and oxidizing nature of these solutions render conventional mercury recovery technologies, such as cementation (displacement from solution by a more readily oxidized metal) absorption onto thio-based ion exchangers or absorption onto activated charcoal, ineffective.

This LDRD is determining how to design a practical system to electrowin (recover) mercury from these strongly acidic radioactive waste solutions. A simple, vertically oriented, concentric-cylinder reactor that serves double-duty as a solution-circulation pump proved to be the most promising approach. Straightforward methods were developed to enhance the degree to which the mercury (volatilized from a calciner, etc.) could be scrubbed into a solution amenable to electrowinning, as well as ways to determine the acidity of such solutions.

Technical objectives for fiscal year 2003:

- Determine why a previous attempt to electrowin mercury from INEEL reprocessing waste simulants failed.
- Design a workable system based on the above findings and characterize it.
- Develop ancillary devices necessary for the successful implementation of mercury electrowinning in a real-world situation.

Some of the processes routinely implemented in nuclear fuel reprocessing facilities generate solutions that contain a large amount of mercury. An immediately relevant example is the offgas-scrub solution generated when INEEL's New Waste Calcination Facility treats sodium-bearing waste. Because that scrub solution is periodically recycled back to the calciner's feed tank, mercury tends to accumulate in the calciner-scrubber-scrub tank system throughout the entire calcination campaign. Consequently, it would be very desirable to remove mercury from that scrub solution. Unfortunately, those scrub solutions are all too corrosive, salty, acidic, oxidizing, and contain too much undissolved particulate matter to be successfully treated by conventional mercury removal technologies.

The first portion of this year's study determined that a previous attempt to develop a system to electrowin mercury from the solution failed for two reasons: 1) the mercury pool-based system was inappropriate for such corrosive solutions; and 2) the system was operated in a way that exacerbated that problem.

The second part of the current study determined that a successful system would require:

- Temperature control: with the temperature of the solution not to exceed ~40ºC.
- Acid control: the solution should contain no more than 4 M free acid.
- Voltage control: the cathode's potential should be controlled with a potentiostat.
- Better cell configuration: implement the "mercury electrode electrowinning" concept in a fashion that discourages redissolution of the working electrode.

Achieving adequate temperature control proved simple, and was resolved by putting a water jacket around the system's inlet pipe. On the other hand, real-time control of the scrub solution's acidity would require that some sort of "acid meter" be installed. A few days of experimentation revealed that one way to accomplish this control would be to add a conductivity meter to the calciner's existing suite of solution-monitoring equipment. Because "acid" and "salt" influence the conductivity and specific gravity (SpG) of nitrate solutions differently, it is possible to estimate both influences to the required degree of accuracy if a scrub's temperature, SpG, and conductivity are known. Algorithms to do that calculation were developed.

The commercial high-power potentiostat purchased for the previous study proved unreliable, so a simple, homemade, "unipolar" power supply was built to replace it. Five new electrowinners were built and tested. The last and best example is shown in Figure 1.

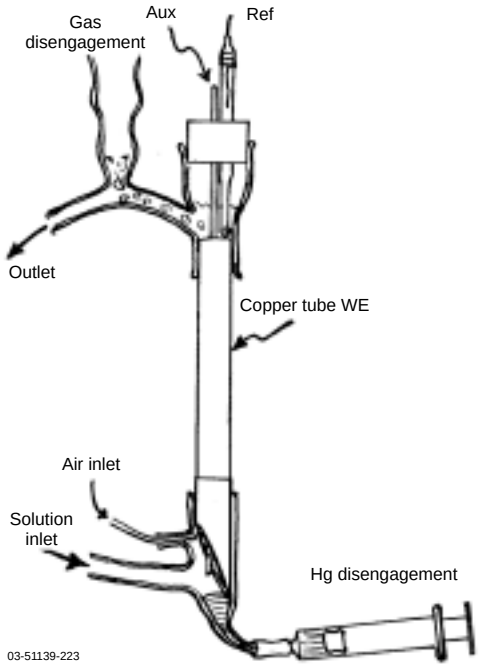


*FIGURE 1. Airlift electrowinner.*

The airlift electrowinner has a cathode comprised of a vertically oriented metal pipe. A thin film of mercury plated-out onto its inner surface comprises the "working electrode" (WE). The metal pipe has a solution outlet at its top and an inlet at the bottom. The anode ("auxiliary electrode") is a platinum rod running through the center of the pipe. There is an $Ag/AgCl/Cl^-$ reference electrode situated next to the surface of the top of the cathode. A stream of gas bubbles (usually air) is introduced into the electrolyte solution at the bottom of the pipe. The rising bubbles enhance mass transfer at the electrode surfaces and obviate the need for a mechanical liquid pump. The bottom end of the pipe (cathode) is cut off diagonally so that its tip can contact a pool of liquid mercury. This pool serves to disengage and collect plated-out mercury. The combination of solution and gas bubbles exiting the top end of the pipe is directed to an inverted Y-shaped "gas disengager," which separates the two.

Figure 2 depicts results of a typical batch electrodeposition with the following conditions: WE area = 17 $cm^2$; $E_{WE\ vs\ SHE}$ = - 0.3 V; solution volume = 32 $cm^3$; air flow =115 $cm^3$/min; initial $HgCl_n^{2-n}$ = 0.144 M; initial free acid =1.35 M (+/- 0.03); nitrate = 1.79 M; chloride = 0.63 M, no sulfamate.

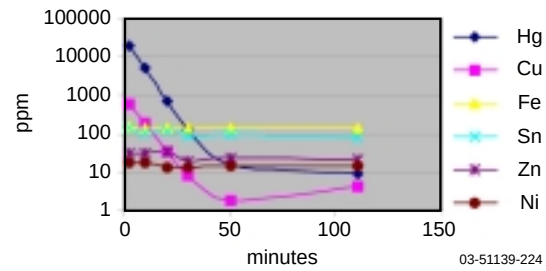


*FIGURE 2. Typical batch plate-out behavior.*

Plate-out of the chloride-complexed mercury was rapid (effective Nernst diffusion layer thickness =0.0021 cm) and it obediently joined that in the disengagement pool. The concentrations of concomitant metals (iron, nickel, tin, zinc, and copper) present in both the simulant and many real radioactive waste solutions are plotted on the same graph. The only metal co-plating with mercury was copper (there is generally much more mercury than copper in real radioactive waste solutions) and the solution's free acid concentration remained virtually unchanged.

The system's advantages include: 1) no mechanical pump, 2) "pump gas" that also serves to enhance mass transfer at electrode surfaces, 3) gravity-driven mercury collection, and 4) a vertical orientation that discourages the accumulation of particulate crud on electrode surfaces. A straightforward calculation suggests that if a similar device possessing a working electrode area equivalent to that of the inside surface of a single ten-foot length of half-inch copper pipe were to be close-coupled to INEEL's calciner and applied to INEEL's ~1 million gallons of sodium-bearing waste, it would recover ~98% of the mercury within one year. It would be equally simple (and

economical) to apply a similar system to any thermal waste treatment device (e.g., glass melter) that generates similar scrub solutions.

Finally, a good deal of thought and some experimentation were devoted to improving the mercury collection efficiency of the nuclear industry's gas scrubbers. The conclusion was that implementation of the following ideas would probably enhance their performance:

- Enhance the offgas ability to oxidize elemental mercury by adding ozone if it contains NO and chlorine (or bromine) if it doesn't. (The Hg electrowinner's offgas often contains chlorine.)
- Follow the primary offgas scrubber with one dedicated to recovering mercuric chloride vapor. It should possess two or three "plate equivalents" and cross-system scrub/gas flows should be countercurrent. (Flows can be co-current across individual plates.)

This LDRD directly contributes to advanced waste management objectives at the INEEL that will benefit other sites containing sodium-bearing waste. In addition, the research performed as a result of this project appears to have broader application to thermal waste treatment devices producing similar scrub solutions such as glass melters.

# Highly Selective Sorbents for the Removal of Arsenic from Drinking Water

*Terry Todd, Troy Tranter, Scott Herbst*

***Meeting a worldwide need for cost-effective water treatment***

WT113

Arsenic (As) occurs naturally in rocks and soils around the world. It enters into water supplies when the minerals in these formations dissolve, or when released by mining or industry.

This LDRD is researching the potential of a novel ion exchange/adsorption resin to remove arsenic contamination, in the oxy-anion/neutral form, from water. The resin material developed through this project has exhibited substantially higher capacity for arsenic than existing exchange materials. It also has maintained selectivity for arsenic in the presence of other potentially competing anions such as phosphate and nitrate. The material is especially applicable to the removal of indigenous arsenic contamination from drinking water, but also would have application for treating/remediating contaminated waters resulting from industrial activities.

Technical objectives for fiscal year 2003:

- Develop techniques for synthesizing composite materials with high selectivity and capacity for arsenic removal.
- Perform batch contacts with the newly developed composite material to obtain equilibrium data.
- Initiate process for securing intellectual property rights for the newly developed materials.
- Present initial results at an international conference.

The first arsenic standard in the U.S. for drinking water was set in 1942 at 50 ug/L (or parts per billion, ppb). A National Academy of Science study in September 2001 concluded that even trace amounts of arsenic can cause bladder and lung cancer. This led to the Environmental Protection Agency (EPA) reducing the maximum concentration limit (MCL) for arsenic to 10 ppb. This new MCL for As will be enforced in 2006, which allows only a few years for adequate technologies to be developed and tested. The new MCL for arsenic in drinking water affects over 4000 municipal water supplies and potentially tens of thousands of private drinking water supplies, primarily in the western U.S.

Large cities that have centralized water treatment facilities will probably be able to achieve compliance using existing technology such as precipitation or coagulation treatment. However, small and mid-sized municipalities do not have centralized treatment facilities, but typically use point-of-origin treatment schemes such as chlorination at the wellhead prior to distribution. Due to a smaller customer base, it is not economically feasible for these suppliers to build a treatment facility at each point of origin or a centralized treatment facility, which would be required for current arsenic removal technologies. Thus, a new sorbent material with high arsenic removal capacity would provide an economical treatment alternative for the small to mid-sized suppliers. For example, a material of this type would be used in a packed bed (similar to a water softener) at the wellhead or point of origin to remove arsenic from potable water prior to distribution. This approach would provide arsenic removal to meet the new MCL with much lower capital and operating cost than that required for a large treatment facility.

Numerous papers are reported in the literature describing arsenic separation via ion exchange (IX) or adsorption. It has been shown that conventional IX resins do not have the specificity for economically removing arsenic from feed streams of low concentration, such as contaminated drinking water. Work with various metal oxides or hydroxides in granular form indicates these compounds to be much more selective for arsenic, but they exhibit low capacity and poor kinetic properties due to low porosity.

The goal of this research is to synthesize or distribute metal hydroxides/oxide compounds within a highly porous polyacrylonitrile (PAN) matrix to form beads amenable to operation in a packed bed. This approach seeks to combine the high arsenic adsorption attributes of the metal compounds with the porous, high-surface-area characteristics of a polymer to form a bead with good mechanical and kinetic properties. As a result of the first year's effort, a proprietary technique has been developed to produce composite materials of metal hydroxides/oxides (typically those of Fe, Zr, La, Ce, or a combination of these) and PAN. As an

example, a SEM micrograph of the surface of a $Fe(OH)_3$-PAN composite bead is shown in Figure 1, which depicts the high surface area of the material.

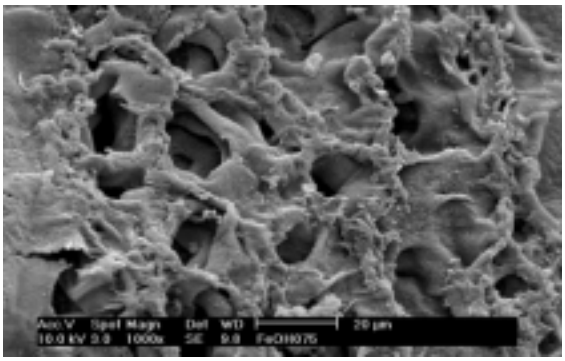

PN04-0004-170

*FIGURE 1: SEM micrograph of the surface of $Fe(OH)_3$-PAN composite bead.*

Numerous batches of these materials have been prepared and tested to determine equilibrium arsenic capacity at various feed concentrations. In these tests, a known weight of the sorbent material is contacted with a ground water solution spiked to yield a specific concentration of $HAsO_4^{2-}$. These contacts are done repeatedly with different sorbent weights to obtain a plot of equilibrium arsenic concentration in the solid phase vs. equilibrium arsenic concentration in the liquid phase. Plots of these data for the $Fe(OH)_3$-PAN composite sorbent are shown in Figure 2. The curves in Figure 2, known as equilibrium isotherms, are shown for three different Fe:PAN ratios. Note that these isotherms are not complete, but only provide data at very low liquid arsenic concentrations. Thus, they are termed region of interest (ROI) isotherms, since they provide data at or near the low arsenic concentrations existing in potable water in the U.S. Inspection of Figure 2 indicates that the sorbent material gives arsenic loading of about 3 mg/g at equilibrium with 20 ppb arsenic in the feed. Since the liquid phase arsenic concentration is very low (20 ppb) there is a correspondingly low concentration gradient or driving force for mass diffusion into the solid phase. Thus, 3 mg/g arsenic in the solid phase is quite high.

Results from the initial testing of this new technology are very promising and show substantial improvement over existing ion exchange technologies. Further testing to maximize available surface area is in progress, as well as experiments to test the efficacy of other metal hydroxide/oxide-PAN composites. It also is anticipated that these materials will have an affinity for oxy-compounds of antimony and selenium. Therefore, experiments with these contaminants also are planned in FY04. A paper describing initial results of this work was presented at the 10th International Conference on Separation of Ionic Solutes, Podbanske, Slovakia, in September 2003. An application for U.S. patent on the newly developed technology was also filed in September 2003.

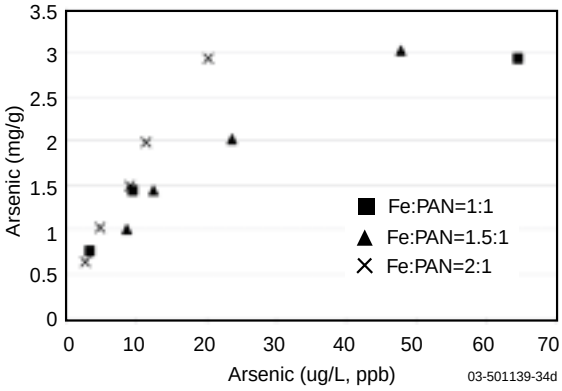


*FIGURE 2: ROI Isotherms for $Fe(OH)_3$-PAN at various Fe:PAN ratios.*

This LDRD is leading to a demonstrated, cost-effective arsenic removal technology that can significantly benefit U.S. and international water treatment needs. The present need in the U.S. is tremendous and it is likely the growing international market will be several orders of magnitude larger than the U.S. market during the next decade. This is especially true in developing countries that cannot afford to use the currently available technologies. The arsenic removal technology developed under this LDRD project would also be applicable to the clean-up/remediation of contaminated surface waters or effluents resulting from industrial activities such as mining. Efforts are in progress to partner with Amalgamated Research Inc. in order to perform testing of the new material at pilot scale with actual groundwater.

INEEL

# Critical Infrastructure Protection Initiative

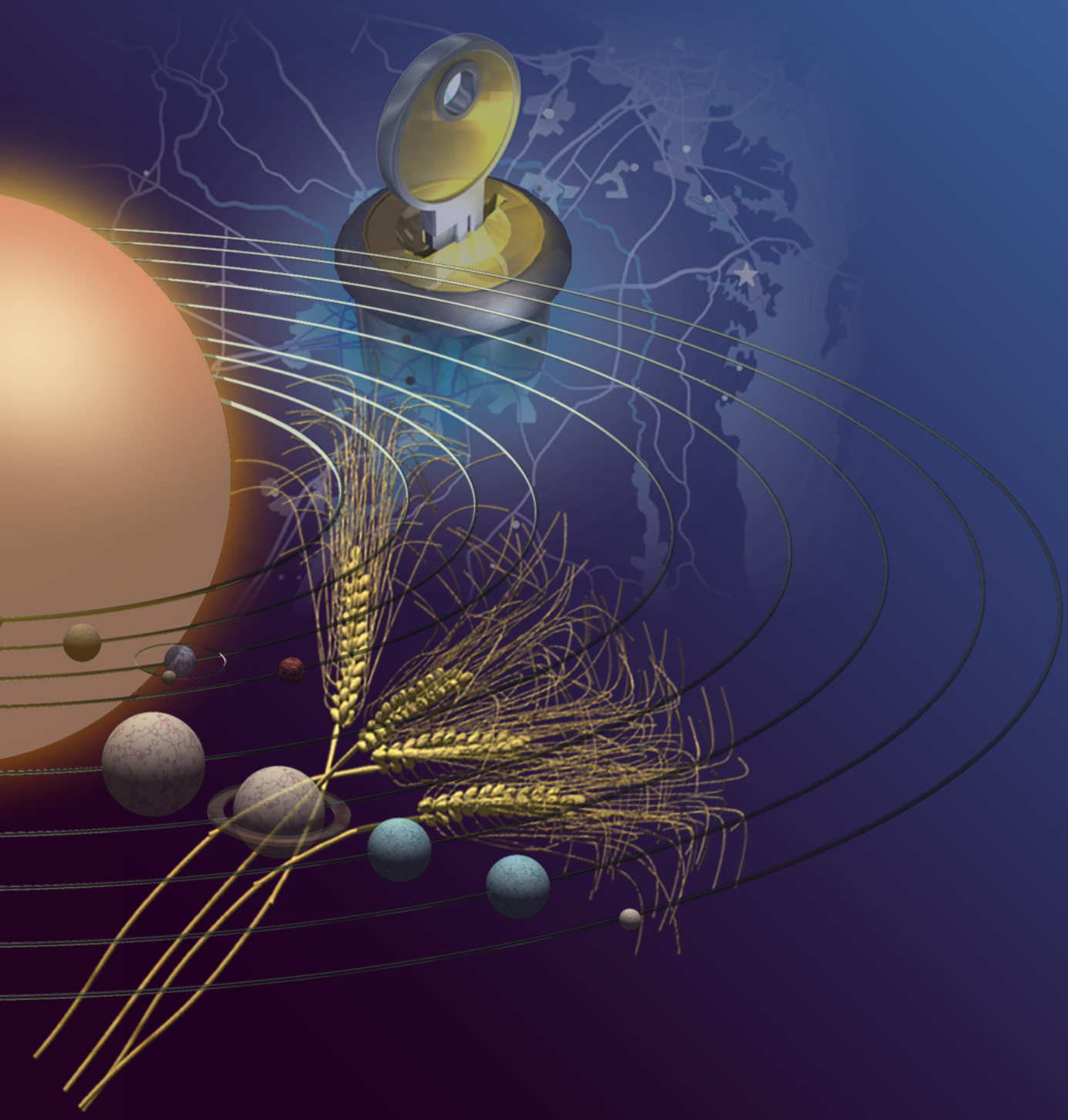

# Critical Infrastructure Critical Sub-network

*Don Dudenhoeffer*

***Reducing the vulnerability of critical national assets***

CS114

Critical infrastructures are those physical and cyber-based systems essential to the minimum operations of the economy and government. They include telecommunications, energy, banking and finance, transportation, water systems, and emergency services.

Due to advances in information technology (IT) and the necessity of improved efficiency, infrastructures have become increasingly automated and interlinked. Most modern commercial infrastructures are composed of a collection of interconnected networks that serve different purposes and have different owners. Even parts of the information residing on a single sub-network may have different purposes and different owners. Critical information is passed between these component elements to coordinate necessary functions. The complexity and interdependency of this critical information flow introduces vulnerabilities into the entire critical infrastructure. Deliberate attacks or accidental system failures may result in serious consequences to the nation.

This LDRD is researching the interdependencies that exist between multiple infrastructure networks. Through modeling, simulation, and algorithmic development, an understanding of these intricacies will be gained. It is only through this insight that the true vulnerabilities can be understood and, thus, prevented or mitigated.

Technical objectives for fiscal year 2003:

- Develop methods to identify the "Irreducible Critical Sub-network." The Irreducible Critical Sub-network is the smallest part of an infrastructure(s) that can still execute its critical function to support a defined mission. Within this scope, the assets that are both critical and vulnerable will be identified.
- Identify emergent behaviors that result from interdependencies between infrastructures. Infrastructures under consideration include: Energy, Information and Communication, Emergency Services, Water Systems, Transportation, and SCADA systems. Dependencies may be the result of a direct link like electrical power to a computer LAN system or the dependencies may exist due to physical proximity of infrastructure items.
- Develop approaches and methodologies to assist in vulnerability assessment, resource allocation, and remediation against knowledgeable and capable attacks.
- Develop visualization methods to assist decision-makers in conducting system assessment during both normal and abnormal situations.

This research has evolved from the National Security Division's division-wide initiative addressing the broad needs of Critical Infrastructure Protection established by Presidential Decision Direction 63 (May 1998) and Presidential Executive Order 13231: Critical Infrastructure Protection in the Information Age (October 16, 2001). The issue of Critical Infrastructure Protection is a vital research area to support critical national assets. The approach to this project includes the development of decision support tools that will aid decision makers in identifying and evaluating infrastructure interrelationships and potential vulnerabilities that result from these relationships.

The interweaving of infrastructure elements creates a complex system. A complex system is defined as "one whose component parts interact with sufficient intricacy that they cannot be predicted by standard linear equations; so many variables are at work in the system that its overall behavior can only be understood as an emergent consequence of the holistic sum of all the myriad behaviors embedded within." (Levy 1992)

These interactions result in emergent behaviors. The objective is to understand these behaviors and, specifically, the vulnerability that they create. The decision support tools being developed to gain this understanding and quantify vulnerabilities will consist of a modeling and simulation framework coupled with analytical methods. The need for such understanding was never so evident as with the blackout that occurred in the Northeast on August 14, 2003. A series of events led to a cascading loss of electrical power as illustrated by the dark area over the Northeast in Figure 1 (next page).

This research is using the Idaho Nuclear Technology and Engineering Center (INTEC) as a resource for analytical tool development and evaluation. Using this framework, decision tools will be used in wargame-like scenarios in which attack vectors

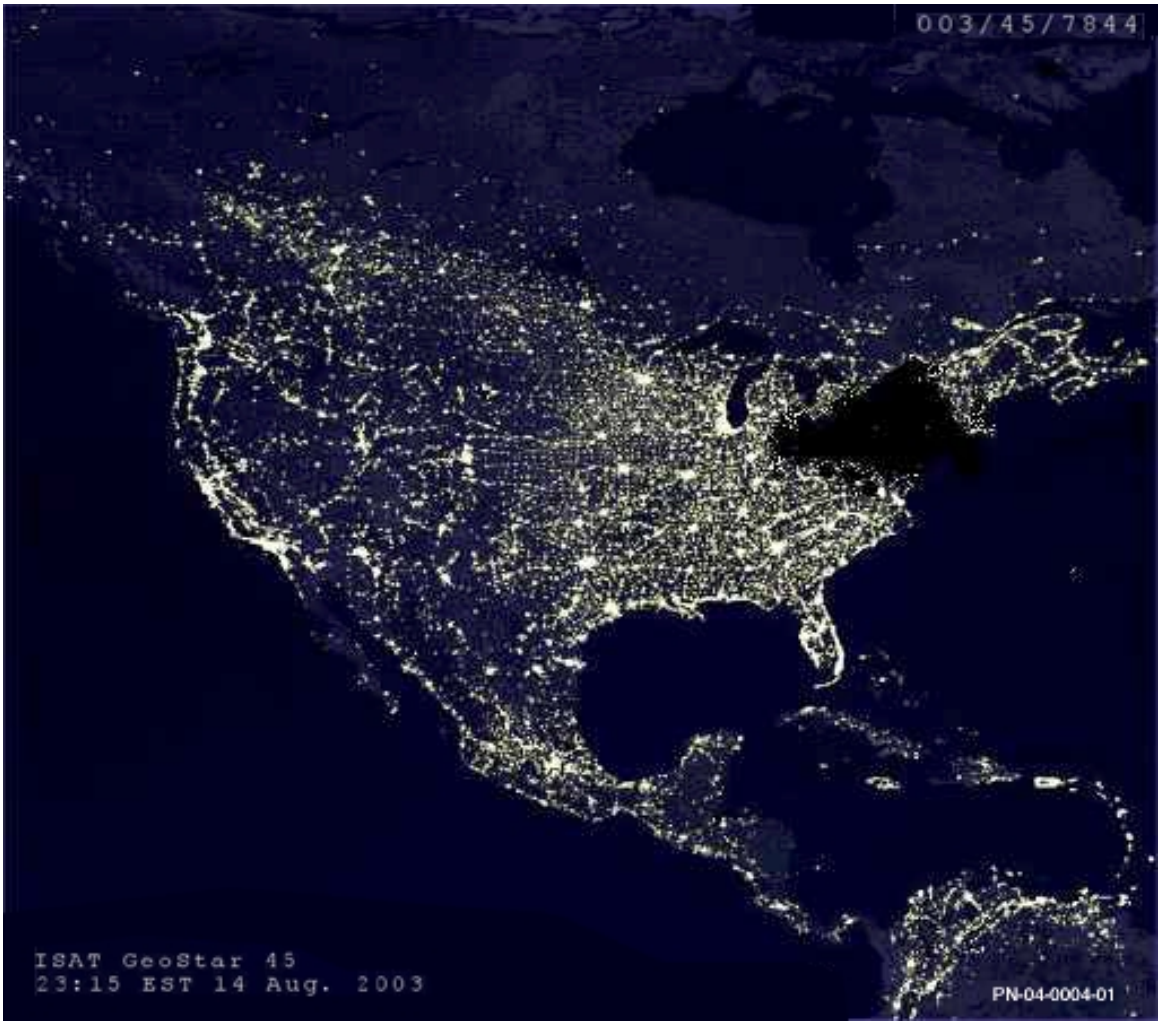


PN04-0004-01

*FIGURE 1. A series of events led to the cascading loss of electrical power in the Northeast U.S. on August 14, 2003.*

target selected infrastructure elements within defined critical missions. The simulation will be interactive to allow scripted events and/or user-inserted events.

During FY03, a beta version of a parallel simulation environment was developed. Initial testing shows the ability to model over 200,000 nodes. In addition, a beta Windows PC version was developed to support portability and infield analysis. Advanced visualization techniques were developed, including the ability to build 3-D Studio MAX images to represent infrastructure elements. These elements have the ability to move and interact with each other. A demonstration model showing simple SCADA interactions at INTEC was completed in FY03, and demonstrations and briefings were conducted for Steve Rinaldi, NISAC Director, Carl Bauer, NETL-DOE, and Ken Friedmen, OEA-DOE.

Much development is still required to increase capability and reliability of the system. Many challenges exist in this project including the development of parallel algorithms, data management in terms of shear mass and quality, visualization and information presentation, and simulation model development.

Figure 2 represents the visualization being developed to support user interaction. Pictured are infrastructure elements at INTEC. The cubes

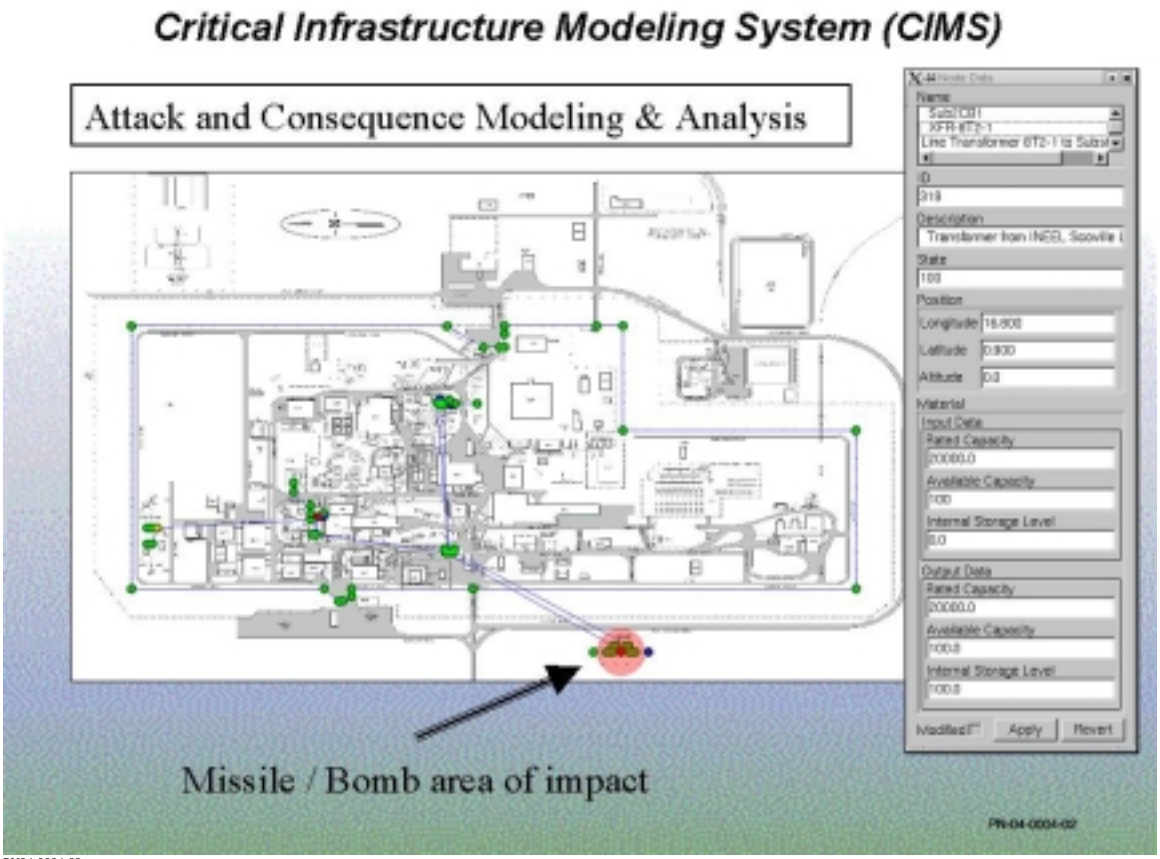


PN04-0004-02

*FIGURE 2. Critical Infrastructure Modeling System (CIMS).*

represent infrastructure assets. Vertical separation between nodes illustrates the various infrastructures being modeled. The edges between nodes represent flow paths (e.g., roads, pipes, wires). The visualization is presented in a 3-D environment. Users can select edges or nodes to examine the state, and have the capability to change various parameters. During the simulation, the nodes and edges change color to represent a change of state. This presents a visual representation of the emergent behavior.

This LDRD directly supports the Critical Infrastructure Initiative at the INEEL, and has resulted in the call for additional proposals. The project was leveraged in a joint INEEL-LANL-General Electric proposal for the DOE National Energy Technology Laboratory call for Deploying Technologies and Methodologies for Assurance of the U.S. Energy Infrastructure. This was the only winning proposal at the INEEL for this DOE call. As part of the project, a demonstration for Secretary Abraham is planned for August. The project is currently being evaluated as a visualization tool for the national power grid to assist DOE in emergency monitoring and management. The Commanding Officer of Naval Magazine Indian Island Washington is interested in using this tool as a means for modeling base vulnerabilities and operations. This modeling is scheduled to be conducted as a proof of concept demonstration for the LDRD in FY04. A successful demonstration could lead to further case studies at DOD bases. CIMS is also being evaluated as a tool for use on the SCADA testbed at the INEEL.

# Development of a Compact Laser-Compton X-ray Source

*James L. Jones, Greg D. Lancaster*

***Expanding regional capabilities***

CS117

There is great industrial and scientific interest in bright, monochromatic and tunable x-ray sources. These sources are being widely used in various scientific research fields as well as in medical, technology and industrial fields. For example, this technology can directly support: 1) investigations of sub-micron and sub-nanometer structures on silicon (wafer) surfaces; 2) imaging for material probing, chemical identification, spatial element mapping in materials or stressed materials; and 3) medical radiation therapy using very focused, tunable photon energies resulting in desired monitoring reactions or in the most favorable dose distributions to the patient.

Previously in this LDRD, the production of unique, tunable, mono-energetic x-rays was successfully demonstrated using the Laser-Compton Scattering (LCS) effect, whereby optical laser photons are collided with a 20-MeV, relativistic electron beam. This demonstration used a large linear accelerator (LINAC) approximately 10 meters long and a laser/detection system separated from the LINAC by a 2-meter thick cement wall.

This year's effort was to develop a similar system in a compact package having a smaller LINAC and a laser/detection system co-located with the LINAC. Where the shielding between the LINAC and the laser was previously a 2-meter thick cement wall, FY03's effort incorporated only blocks of polyethylene and lead shielding. The developed compact configuration design imposed significant challenges in the collection of the x-ray data. While no LCS x-rays were observed with the selected configuration using only available hardware and a 13-MeV electron beam operation, the investigation provided considerable insight into the development of a successful and versatile compact system.

Technical objectives for fiscal year 2003:

- Relocate and set up INEEL/ISU (Idaho State University) laser system and begin operational assessments.
- Design laser/electron beam interaction requirements.
- Select, assemble, and operationally test a compact ISU electron beam LINAC system.
- Integrate and test laser system with the LINAC operation.
- Complete initial characterization of a compact LCS source.

The initial experimental LCS setup is shown in Figure 1. The electron beam from the 13 MeV LINAC is deflected by a 45-degree bending magnet. A pair of horizontal and vertical steering magnets enabled the operator to steer the electron beam toward the beam transport line axis. The electron beam was then focused to the center of the interaction region ("flag") for optimum collision with the laser beam. The transmitted electron beam is then deflected with another 45-degree bending magnet toward the beam dump. The beam dump consisted of a 2.54-cm thick aluminum block surrounded by blocks of polyethylene and lead. The aluminum enabled measurement of electron beam current and pulse width. Lead was used to shield photon emissions from the beam dump. Using an in/out fluorescent screen at the flag allowed monitoring of the electron beam spot size and position. The maximum electron beam current recorded was 100 mA (peak current) and the electron beam pulse width was 12-15 ns.

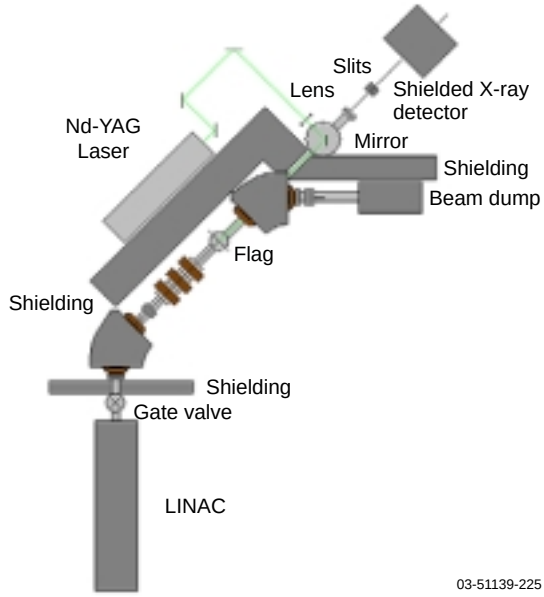


*FIGURE 1. Experimental setup.*

The optical/laser setup consisted of an Nd:YaG laser and several mirrors for focusing and steering. The laser spot size at the interaction cross was about 3 mm to match the transverse size of the electron beam. The laser alignment with the transport beam centerline was performed using a HeNe laser. An AMPTEK pin detector was used that had a near unity efficiency for an x-ray energy ranging from 5 to 10 keV. The detector was enclosed in a lead shielding configured so as to provide a 6-mm diameter lead collimation toward the interaction region. In addition, a pair of lead slits (1mm) were placed between the detector and exit window. The energy and wavelength of the Nd:Yag laser was 220 mJ and 532 nm, respectively. The LINAC and laser repetition rate was 7 Hz. The electron beam made an angle of about 3.6-mrad with respect to the laser beam. Observing an interaction signal from the electron beam dump enabled the monitoring of the time delay between the electron beam and the laser pulse. This time delay was varied from –50 to 50 ns. Using 13-MeV electrons, the expected LCS x-rays would be about 6.5 keV. At this x-ray energy, the kapton window (in vacuum system) and the air between the window and the detector, will result in only 15.4% transmission efficiency.

Three primary reasons are given for not having observed LCS x-rays with this compact configuration: 1) the kapton window attenuated the LCS x-rays more than expected; 2) the selected LINAC limited effective electron beam energy operations to 13 MeV, induced temporal jitters between an accelerator pulse and a laser pulse, and required the utilization of lower-than-expected electron beam currents; and 3) the high radio frequency and bremsstrahlung “noise” backgrounds related to signal detection using the selected compact configuration (i.e., polyethylene blocks instead of cement walls).

This LDRD has resulted in collaboration with Idaho State University and the presentation of scientific papers for conference presentation and publication. The research performed under this project is enhancing the reputation of the INEEL in this advanced research area.

# Advanced Automated Ion Mobility Spectrometer for Explosives Detection

*Carla J. Miller, Jill R. Scott, Paul L. Tremblay, Timothy R. McJunkin*

***Improving detection of contraband and chemical warfare agents***

CS118

Ion mobility spectrometry (IMS) is a very sensitive, selective, low cost, low maintenance, field-portable instrument providing near real-time detection. It is currently the state-of-the-art for explosives, narcotics, and chemical warfare detection. In IMS, the chemical substances are characterized by using gas-phase ion mobility determined by the velocity of an ion along a drift tube at atmospheric pressure. Even with all the advantages of this system, there is a need to improve signal-to-noise and the spectral interpretation, increasing the chances of a positive detection of contraband and chemical warfare agents and decreasing the relatively high false alarm rate. Additionally, most IMS systems are designed to look at either the positive ions (drugs, some explosives, nerve agents) or negative ions (most explosives and blister agents). Current "dual-mode" IMS systems are designed to alternately detect positive and negative ions. Ideally, a system will be designed where both positive and negative ions will be generated and detected simultaneously.

The focus of this LDRD is to determine the feasibility of a simultaneous dual-mode IMS with a unique automated spectral interpretation system. Alternative ionization schemes and other techniques to selectively enhance ion harvesting also will be studied. Ultimately, this instrument will increase detection limits and resolution while enabling the detection of a greater number of compounds simultaneously.

Technical objectives for fiscal year 2003:

- Provide an automated spectral interpretation system for improved data interpretation and reliability from IMS-based instruments, removing human error.
- Provide novel advances to IMS instrumentation by building a unique dual-mode detection system (positive and negative ions will be detected simultaneously).
- Present and publish spectral interpretation results.
- Submit an invention disclosure for "Advanced Dual Mode Ion Mobility Spectrometer."

This is the first of a three-year LDRD aimed at developing a smarter, more selective, ion mobility spectrometer. The first step was to develop software that would improve the spectral interpretation of the IMS system. To accomplish this, standards of trinitrotoluene (TNT), pentaerythritol tetranitrate (PETN) and cyclo-1,3,5-trimethylene-2,4,6-trinitramine (RDX) were introduced into two commercial ion mobility spectrometers to obtain "clean" spectra of common military explosives. These spectra were used to assist in locating the peaks within an IMS spectrum. Mixed standards (standards containing all three components) also were used to assist in locating the peaks that may result from a shift due to competing ions. The spectra obtained from the commercial instruments were then used to create software that could readily identify peak positions and automatically adjust for changes in temperature and pressure, creating a "smart" ion mobility spectrometer.

For the smart, automated, inference engine, the process of detecting substances begins with calculating an expected time for a calibrant peak based on the measured temperature, pressure, and electric field strength in the drift tube. The plasmagram is searched for the peak nearest the expected time for the calibrant. Assuming that the calibrant peak is found within some error bound, a conversion factor is calculated to translate time-of-flight to reduced mobility. This conversion factor accounts for other non-explicit factors in the instrument operation. If the calibrant peak is not found with the calculated boundaries, then the instrument is not operating within specifications or there is an error in sample preparation and/or injection. All peaks and peak widths are then identified. The peak width is found using the steepest slope on both sides of the peak, using the side that has the greatest distance fromthe peak center to define the half width. All peak width end points are converted to reduced mobilities by the conversion factor and displayed as trapezoids with a base of twice the width as can be seen in Figure 1. From a database of substances, sets of indicator peaks with defined full confidence thresholds are compared to the mobility peak trapezoids. A membership value for each indicator peak is found based on the ratio of the intersection with the trapezoids and the full confidence threshold. The individual memberships are then combined using fuzzy logic operations. Finally, a threshold based on required sensitivity is applied to determine if a substance is detected.

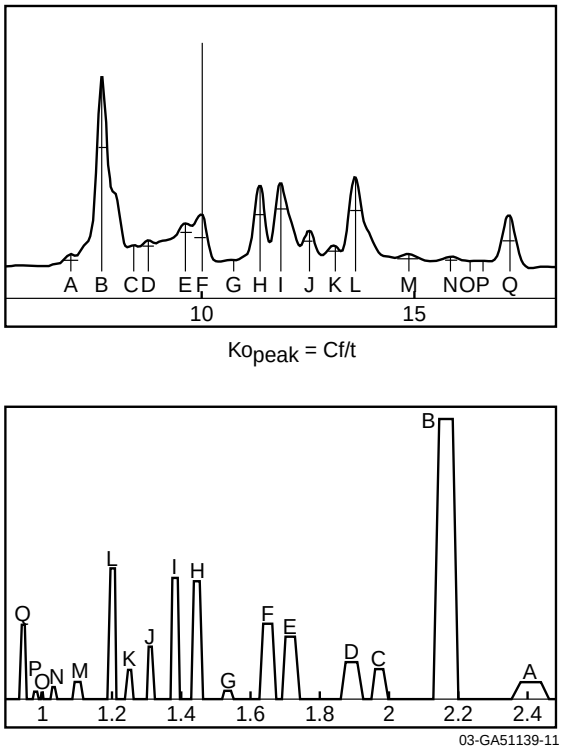


*FIGURE 1. Conversion from drift time ($t_{peak}$) to reduced mobilities ($ko_{peak}$) using correction factor (Cf).*

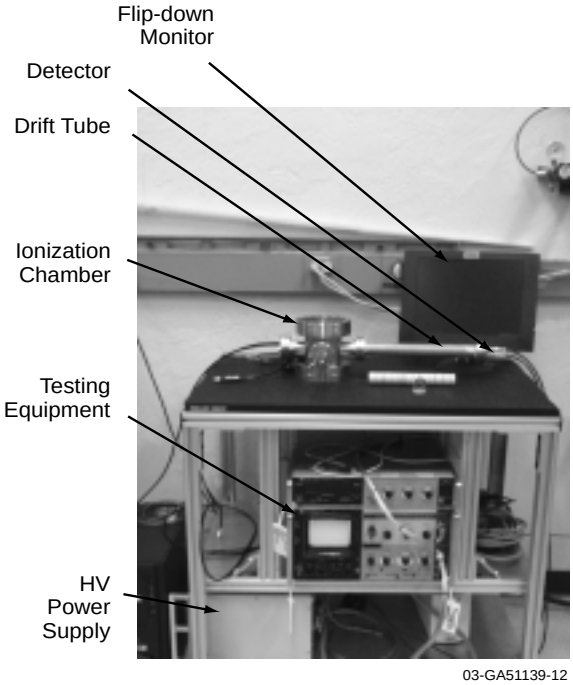


*FIGURE 2. Benchtop experimental ion mobility spectrometer test unit.*

This technique has been tested on unknown samples taken from an explosives testing facility. The unknown samples not only had the potential to be contaminated with mixed explosives, but also contained contaminants from dirt, hair, and the surrounding environment. These samples were used to ensure the reliability of the detection algorithm for real detection scenarios.

The second objective for the fiscal year was to provide novel advances to IMS instrumentation by building a dual-mode ion mobility spectrometer. To accomplish this, a benchtop experimental test unit was designed and built to determine if any variations in design and materials different from commercial ion mobility spectrometers would create unforeseen problems when utilized with a high voltage system at atmospheric pressure. Some of the things that were tested were the electrostatic charge build-up along the drift tube and the differences in charge gradients over different materials. The current experimental test unit design is shown in Figure 2, as well as a spectrum generated on this system using laser ionization. Only one polarization was used to determine the feasibility of using this setup for the prototype.

The next step was to model ion trajectories through a drift tube at atmospheric pressure using SIMION with a special user program. This task was performed under a subcontract with David A. Dahl. The ion trajectories were modeled taking into account diffusion, external pressure changes, charge gradients, and temperature through a tube operated at atmospheric pressure. This information was used to design an efficient drift tube for the dual-mode system. Several instrument designs have been incorporated into an invention disclosure for “Advanced Dual Mode Ion Mobility Spectrometer”—Tracking #139. Modeling of the flows through the various designs will help to determine the most efficient information prior to manufacturing the ion mobility spectrometer.

The third task was to begin the requisition process for parts to be used on the prototype. This part of the project is ahead of schedule since the majority of the parts were going to be purchased in the second year of the LDRD. However, all the preliminary tests provided enough confidence in the

data to purchase the majority of the prototype parts this year.

This LDRD has opened several doors of opportunity. A presentation was given at the 12th International Conference on Ion Mobility Spectrometry and results of the spectral interpretation work were published in the International Journal for Ion Mobility Spectrometry. A great amount of interest has been shown in the concept of a "smart" ion mobility spectrometer. A nondisclosure agreement has been put in place with Draper Laboratories to use this programming technique for joint proposals to obtain future funding. In addition, interest has been shown by Sionex for the spectral interpretation algorithms. A nondisclosure agreement and possibly a software copyright will be put in place prior to information exchanges with this company. Once the project is completed, it will provide the INEEL with a highly sensitive dual-mode ion mobility spectrometer that will place the laboratory in the forefront of the IMS community.

INEEL

# Generation IV Nuclear Reactor Initiative

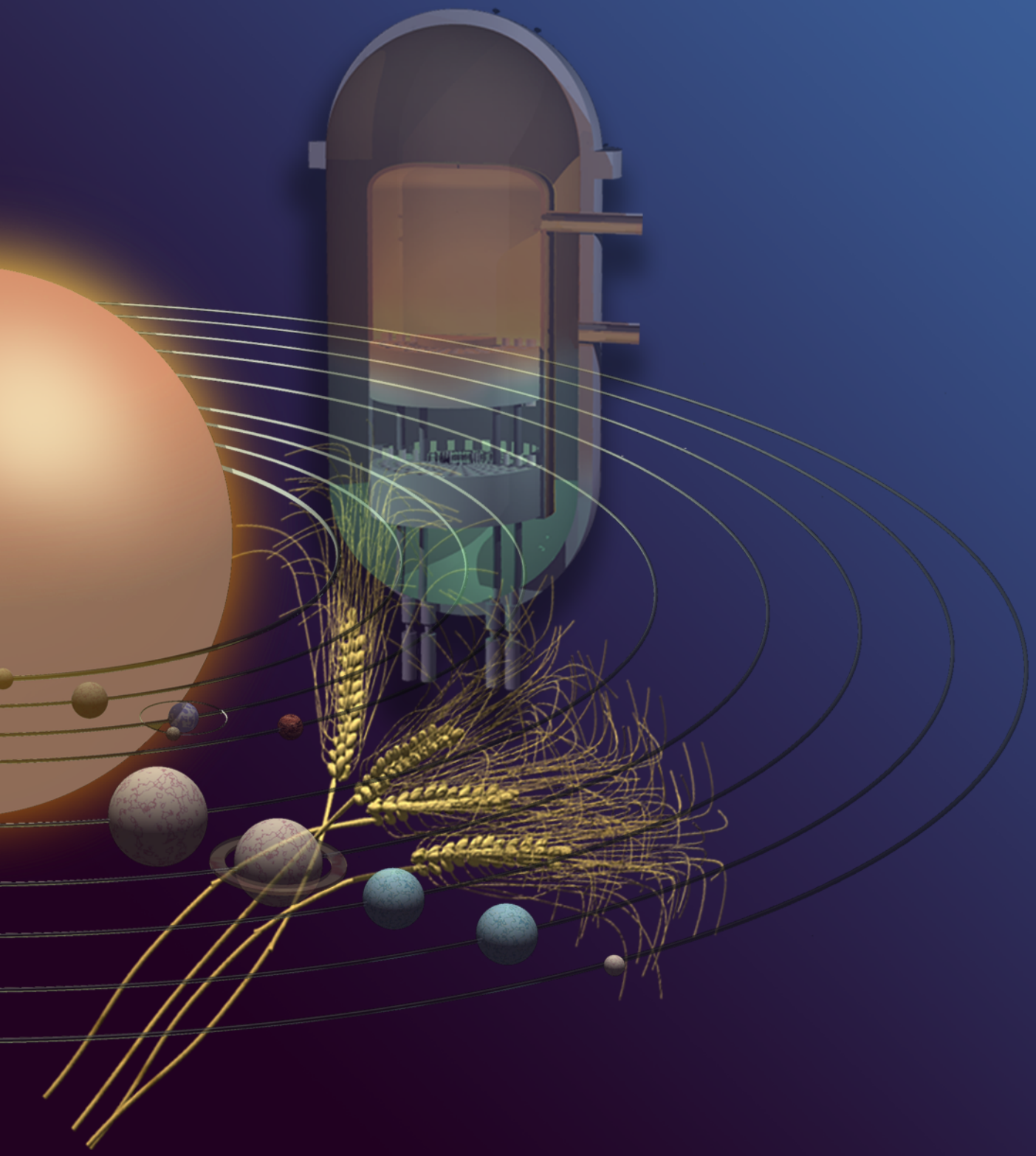

# Advanced Fission Product Detection Systems for Generation IV Fuel Testing

*Jack K. Hartwell, E. Wayne Killian, Rahmat Aryaeinejad, Dawn M. Scates*

***Improving fuels for Gen IV reactors***

GE108

The Fuel Cycle Crosscut Group Summary report developed in support of the Generation IV Roadmap concluded that improvement of fuels and advanced fuels is important to the next development effort "no matter what fuel cycle is chosen." The report further concludes that these fuel development efforts will require "both in pile and out of pile testing (including safety tests) before the fuel is ready for deployment."

This LDRD is conducting initial work into the development of the advanced fission product detection systems that will be required to support the testing of next-generation fuels regardless of the fuel concept chosen. The INEEL, and specifically the investigators on this project, have extensive experience in the design and operation of online fission product monitoring systems. This project exploits that experience, along with recent advances in digital signal processing techniques, new detector materials, and active guard systems used in high-energy physics research, to develop and evaluate state-of-the-art fission product detection systems for fuel testing. An additional activity is the evaluation of candidate sample transport systems.

During the first year of this research, the investigators specified and conducted preliminary tests on promising alternative detector materials, enhanced the capabilities of the INEEL's PCGAP© gamma-ray spectral analysis and control code, evaluated certain capabilities of commercial digital signal processors, and initiated evaluation of an active Compton suppression system. The investigators also are collaborating in the design of a fission product monitoring system for the Advanced Gas Reactor (AGR) fuel tests scheduled for installation in the ATR.

Technical objectives for fiscal year 2003:

- Specify and purchase a special active Compton guard mated to a commercial Cadmium Zinc Telluride (CZT) detector, and document the performance of this unit.
- Test the performance of commercial digital signal processors (DSPs) with high-purity germanium (HPGe) detectors.
- Implement the tailing function required to properly fit spectral peaks in spectra acquired with a CZT detector in the PCGAP analysis code.
- Test and document the combined performance of the DSP-supported active Compton-guarded CZT spectrometer.

For research into the efficacy of active anti-Compton guard detectors to improve the peak-to-Compton performance of small room temperature semiconductor detectors, a specially designed NaI(Tl) scintillation detector (the guard) and two specially designed Cadmium Zinc Telluride (CZT) gamma-ray detectors were ordered from a commercial detector company. The NaI(Tl) detector was a 7.62 cm diameter by 7.62 cm long right circular cylindrical detector manufactured with two connecting 2.0 cm diameter "ports". One of these ports, centered on the long axis of the cylinder, provides a path for gamma rays from a sample to reach the primary CZT detector that is inserted through the second port that penetrates the NaI(Tl) detector radius and intersects the first port at the guard detector center. To mate with this unit, two CZT detectors were specified, both mounted with an external preamplifier and on a "finger" that extends into the guard detector port.

The vendor of choice quoted delivery on May 30, 2003; however, fabrication problems plagued these units. The NaI(Tl) guard detector and one of the two CZT detectors were not received until September 4, 2003. The investigators have determined that the physical dimensions of these units are correct, and that they operate properly individually. Integral testing will be completed next year.

Gamma-ray photopeaks acquired with certain room temperature semiconductor detectors (like CZT) have a pronounced low energy tail. As part of this fiscal year's work, the PCGAPÓ gamma-ray spectral analysis code was modified to incorporate a low-energy tailing function. Preliminary testing on this modified code is promising.

Prior experience with online fission product monitoring systems highlighted the necessity of real-time performance monitoring as provided by pulse injection with subsequent removal. Under this research a protocol was devised that should enable implementation of this pulse injection technique on any digital signal processor that has the requisite auxiliary inputs and microcode. A DSP manufacturer was located that was willing to provide the modifications to one of their DSPs at a modest price. The DSP (a POLARIS from XIA

Corp.) was received in June, and the hardware/firmware update to implement pulse injection with subsequent removal arrived in August. The upgrade has not yet been installed, pending completion of the testing described further on in this report.

From this and other projects, the investigators have the newest generation DSPs from three different manufacturers. These include the POLARIS (from XIA Corporation), the DIGIDART (from ORTEC Instruments), and the INSPECTOR 2000 (from Canberra Industries). These are small, highly capable digital spectrometry systems, and the latter two are capable of running on battery power. Since spectrometer performance at high input rates can be a key requirement for fission product monitoring systems, the performance characteristics of these three units have been tested. The test procedures were similar to those used earlier to test larger "desktop" DSP spectrometers. The units were similarly configured and tested with the same HPGe detector and a set of proportional $^{152}$Eu. Spectra were acquired in triplicate at precisely known input rates from 417 c/s to greater than 235,000 c/s. The spectra are being analyzed to compare the throughput, gain stability, accuracy, and peak shape performance of each spectrometer. Figure 1 compares the preliminary measured throughput (in stored counts per real-time second) versus input rate for the three units. When all of the test results are finalized a journal article reporting these results will be prepared.

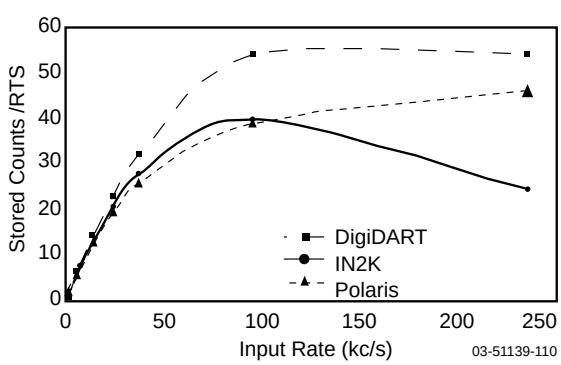


*FIGURE 1. Preliminary comparison of the throughput performance of the DigiDart, the Inspector 2K, and the Polaris DSPs using $^{152}$Eu.*

Recent developments in the area of gamma-ray scintillation detectors resulted in the acquisition and testing of an entirely new type of room temperature detector. Classically, gamma-ray scintillation detectors, of which thallium-activated sodium iodide [NaI(Tl)] detectors are the best known example, while they operate at room temperature, are limited in their resolution (ability to separate close-lying peaks.) This limits their utility in a fission product monitor for anything other than gross count rate applications.

Resolution is generally specified as the full width of a spectral peak (like the 662 keV $^{137}$Cs gamma-ray peak) at half the maximum peak height. This is abbreviated as FWHM, and may be specified either in keV or as a percentage of the peak energy. Typical values at 662 keV are 1.5 keV (0.23%) for high purity germanium detectors, 13 keV (2.0%) for CZT detectors, and 49 keV (7.5%) for NaI(Tl) scintillation detectors. Recent work at Delft University of Technology reported exciting results on a family of cerium-activated lanthanum halide scintillators. These are room temperature scintillation detectors with an energy resolution at 662 keV of about 20 keV (3%). Since scintillation detectors can generally be manufactured in large sizes (liters in volume) this factor-of-two resolution breakthrough makes these units attractive.

Under this project one of the first commercially available cerium-activated lanthanum halide scintillators was purchased. The unit is a 1.0 cm-diameter-by-1.5 cm-deep $LaCl_3$(10% Ce) crystal packaged by the vendor, Saint-Gobain. This unit was coupled to a well-matched Hamamatsu 4177 PMT using GE Viscosil 600M. High voltage (negative) was supplied through and the signal extracted using a tube base purchased specifically for this tube. The fast anode output was input to an Ortec 572 linear amplifier, given 0.5 microsecond semiGaussian shaping, and then input to an Amptek

8000A MCA. Although the resolution performance was near that reported (Figure 2) each acquired spectrum contained artifact peaks at 1950, 2080, and 2211 keV. While these spurious peaks are probably due to either optical or electronic mismatches, it is interesting that they have been noted by at least one other researcher.

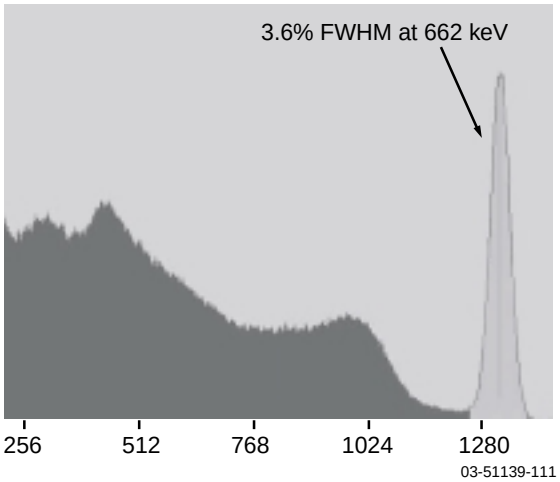


*FIGURE 2. Spectrum acquired with 1.0 cm x 1.5 cm $LaCl_3$(10% Ce) scintillator.*

This LDRD research exploits the extensive experience and institutional knowledge derived from numerous fuel behavior experiments to investigate advanced systems for the fission product monitoring systems that will be required for advanced Generation IV fuel testing both in and out of pile. Publications and presentations developed as a result of this research will augment the INEEL's reputation as a premier reactor testing facility, strengthen its position in competing for test programs, and enhance the information derived from fuel test programs conducted at the INEEL.

The investigators are involved in the planning and design of the Advanced Gas Reactor (AGR) fuel tests to be conducted in the Advanced Test Reactor (ATR) beginning in CY2004. Research conducted under this LDRD has already been useful to the AGR fuel test program, and the investigators expect a continuing contribution to this and other next-generation fuel test programs.

# Advanced Transient Analysis Capabilities for Generation IV Reactors

*Edwin A. Harvego*

***Supporting advanced nuclear reactor concepts***

GE102

The importance of nuclear energy as a vital and strategic resource in the U.S. energy supply mix has led to the need to develop and demonstrate new and improved reactor technologies. Generation IV reactor concepts are expected to substantially improve the economics, safety, proliferation resistance, and waste characteristics of current generation reactors. Although a number of light water reactors (LWRs) have been proposed as Generation IV candidates, the majority of these concepts have fundamentally different characteristics than current operating LWRs.

The intent of this three-year LDRD project is to develop and/or extend current INEEL transient analysis capabilities to support future reactor design, development, and assessment needs. In FY01, more than 100 proposed reactor concepts were reviewed and a report prepared describing the characteristics of four general nuclear reactor categories (gas-cooled, liquid metal-cooled, molten salt, and light water), along with their transient analysis needs. Based on this report, additions/improvements to existing INEEL analysis capabilities for two particular reactor concepts, gas-cooled and supercritical-water reactors, were identified as high priority needs. In FY02, a conceptual model design report was completed and initial improvements/additions for the modeling of gas-cooled reactors were incorporated into the SCDAP/RELAP5-3D/ATHENA code. In this fiscal year, a second conceptual model design report was prepared for supercritical-water reactors, and modeling improvements from this report were incorporated into SCDAP/RELAP5-3D/ATHENA. Initial assessments of the new modeling capabilities for both the gas-cooled and supercritical-water reactors also were completed in FY03.

Technical objectives for fiscal year 2003:

- Revise and update detailed conceptual designs of modeling extensions for transient analysis of gas-cooled reactors.
- Complete detailed conceptual designs of modeling extensions for transient analyses of supercritical-water reactors.
- Submit and present a peer-reviewed technical paper for the ICONE-11 conference on transient analysis of Generation IV reactors.
- Submit an abstract of a technical paper for presentation at the ICONE-12 conference to be held in April 2004.
- Complete revisions and updates to models for transient analyses of gas-cooled reactor concepts.
- Complete code updates and modeling extensions for transient analyses of supercritical-water reactors.
- Perform selected assessments of new modeling capabilities implemented into the SCDAP/RELAP5-3D/ATHENA code.

A review of these proposed Generation IV reactor concepts, performed in the first year of this LDRD, led to the identification of both near-term and long-term transient analysis needs. The near-term development needs were those required to establish a basic capability to support anticipated DOE needs during the initial Generation IV evaluation process. The long-term development needs were those that would allow more refined analyses of the complex phenomena that will become more important as the reactor system designs evolve.

Based on the results of the first-year study, high priority model development tasks were defined for two reactor concepts (i.e., gas-cooled and supercritical-water reactors) that appeared to offer the most promise for future development within the U.S. During the second year, the focus was on completing modeling improvement for the gas-cooled reactors. Although the initial intent was to focus on the pebble-bed modular reactor (PBMR) design, it was subsequently decided to develop a more general analysis capability that would allow transient modeling of both pebble-bed and graphite-block reactor core designs. The gas-cooled reactor modeling activities were largely completed in FY02, and the modeling improvements associated with the transient analyses of supercritical-water reactors were completed this fiscal year. The specific code improvement activities associated with the gas-cooled and supercritical-water reactor concepts are briefly summarized as follows.

For gas-cooled reactor concepts, models were developed to enable the SCDAP/RELAP5-3D/ATHENA code to predict important phenomena occurring in either pebble-bed or block-type (prismatic) reactor core designs. These models were (1) graphite oxidation in air and water, (2) heat transfer and flow losses through a pebble-bed reactor core design, and (3) 2-D conduction and radiation heat

removal from a pebble-bed or graphite-block reactor core following a complete loss-of-coolant accident. The complete loss-of-coolant (or conduction cool-down) accident represents one of the more challenging events for the passive safety features of a gas-cooled reactor, and also one of the more difficult transients to accurately model. Modeling improvements made to the code have simplified the detailed modeling of decay heat removal paths from the center of the reactor core to the ultimate earth or atmospheric heat sink, while preserving the high fidelity modeling capabilities of the code. An example calculation for a conduction cool-down event in a passively cooled block-type gas reactor is depicted in Figure 1. In this analysis, air was calculated to flow at a rate of about 1.5 m/s up through the risers surrounding the reactor vessel. After about 50 hours, the rate of heat transfer to the atmosphere was about equal to the rate of decay heat production in the reactor core, and thus no subsequent heat up of the reactor core was calculated to occur.

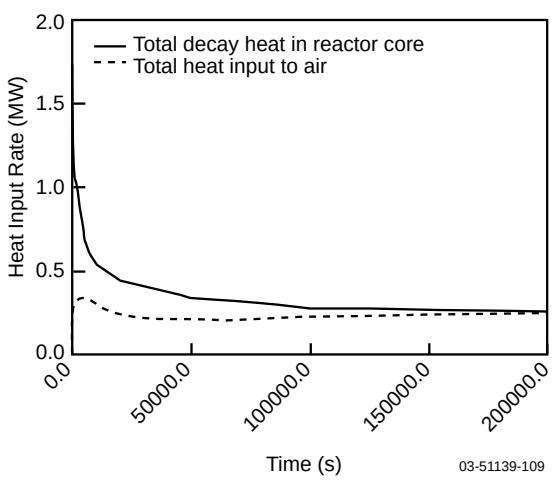


*FIGURE 1. Comparison of rate of heat production in reactor core to rate of heat removal from block-type core.*

For supercritical reactor concepts, modeling primarily focused on improvements in material and fluid properties applicable to these reactor concepts, and on modeling heat transfer processes between the fuel, cladding, and fluid. Modeling improvements included (1) thermal and structural properties of fuel-rod cladding suitable for the high core exit temperatures of supercritical-water reactors, (2) models for calculating the conductance at fuel-cladding interfaces where pellet-cladding mechanical interaction occurs, (3) models for calculating convective heat transfer in supercritical water, and (4) refinement of the water properties tables to more accurately calculate the thermodynamic state of supercritical water. The fuel-rod cladding properties incorporated into the code were for Inconel 718 and Alloy MA956 in the temperature range of 300ºK to 1300ºK, and included correlations for thermal conductivity, heat capacity, thermal expansion, modulus of elasticity, yield strength, ultimate strength, and total elongation.

The modeling of conductance at fuel-cladding interfaces where pellet-cladding interactions occur accounts for fuel-cladding interface pressure, the roughness of the surfaces of the fuel and cladding, and the composition and temperature of the gas at the fuel-cladding interface. Three different correlations were implemented for calculating convective heat transfer in supercritical water. However, these correlations are provided as user options, as they calculated significantly different rates of heat transfer for coolant temperatures near the pseudo-critical temperature, and insufficient experimental data is available for assessment of the results. Finally, an increase in the number of temperature and pressure entries in the water property table has resulted in decreased ranges of property interpolations and, thus, a more accurate calculation of water properties and less chance for code execution failures due to non-convergence on water properties.

As the lead laboratory for nuclear energy, INEEL is in a position to provide strong technical leadership in support of DOE's Generation IV reactor initiative. Although INEEL is the internationally recognized leader in light water reactor safety analyses, the laboratory's capability to perform transient analyses of other reactor concepts has been limited. Therefore, the advanced transient analysis capabilities developed through this LDRD will position the INEEL for major roles in support of DOE's Generation IV reactor initiative and related missions. The development of these essential capabilities has coincided with the evolving development of Generation IV reactor concepts, so that the INEEL capabilities have been available when needed by DOE and its Generation IV partners.

In addition to potential follow-on work associated with DOE's Generation IV reactor initiative, the development of advanced reactor transient analysis capabilities may lead to externally funded collaborative research and development in other areas.

# Advanced Nuclear Fuels for Enhanced Proliferation Resistance

*J. Stephen Herring, Kevan Weaver, Philip MacDonald*

***Investigating Thorium-based fuels for Light Water Reactors***

GE104

Advanced fuels for thermal reactors will be needed in the future to reduce the production of plutonium for proliferation resistance and to create robust fuel/waste forms. The fuel/waste form matrix holds the fission products and actinides in a permanent repository or in temporary storage awaiting reprocessing. Thoria ($ThO_2$) fuels appear promising as a matrix for plutonium and the minor actinides during mono-recycling in Light Water Reactors (LWRs). Thorium-based fuels reduce the total amount of plutonium created and produce a mixture of plutonium isotopes high in Pu-238. Because of the high decay heat and spontaneous neutron generation of Pu-238, this isotope provides intrinsic proliferation resistance. Thoria also is difficult to dissolve, making the diversion of spent fuel for weapons production more difficult.

This LDRD is determining if thorium-based fuels can be used to further increase the proliferation resistance of LWR fuels. For this research, a LWR fuel cycle was developed where the reactor core primarily consists of standard uranium-dioxide ($UO_2$) fuel rods with typical U-235 enrichment, along with a small fraction of thoria-urania ($ThO_2$-$UO_2$) or yttria-stabilized zirconia fertile-free fuel rods containing the plutonium and minor actinides produced in earlier cores. The goals of this mono-recycling strategy or "twice-through fuel cycle" are to transmute the great majority of the long-lived actinides in existing LWRs and to discharge a very robust waste form whose isotopic content is very proliferation resistant.

The incorporation of plutonium into a $ThO_2$ or yttria-stabilized zirconia fertile-free matrix results in the consumption of already separated plutonium without breeding significant additional Pu-239. The minor actinides (e.g., neptunium, americium, curium, berkelium, californium) also are included in the $ThO_2$ or fertile-free transmuter fuel rods to further reduce the overall long-term radiotoxicity of the fuel cycle. The investigators' analyses have shown that thorium-based or fertile-free fuels can reduce the amount of Pu-239 needing further transmutation or going to a repository by about 90%. Also, thorium-based fuels produce a mixture of plutonium isotopes high in Pu-238. Because of the high decay heat and spontaneous neutron generation of Pu-238, this isotope provides intrinsic proliferation resistance.

Technical objectives for fiscal year 2003:

- Analyze isotopic generation and depletion for 22 different thoria and fertile-free fuel types.
- Balance fission heat production in transmuter fuel and surrounding $UO_2$ fuel.
- Develop parameters for use of fertile-free fuel in LWRs.
- Determine void coefficients for thoria and fertile-free fuel assemblies.
- Compare thoria and fertile-free fuels for effective destruction of plutonium and minor actinides.

To determine the effectiveness of the various transmutation schemes, the amounts of the various actinides produced in the $UO_2$ fuels and the transmuter pins was calculated and compared with the actinide production in a standard $UO_2$ once-through fuel cycle. The $UO_2$ baseline case consists of a once-through irradiation of the $UO_2$ fuel to 61.5 MW-d/kg, followed by disposal of all the pins in a repository.

The comparison has been carried out for two scenarios. In the first scenario, it is assumed that the plutonium and minor actinides from previous cycles are placed in the transmuter pin and that all the pins in the assembly, both the surrounding $UO_2$ pins and the transmuter pins, are sent to a repository at the end of one 61-MW-d/kg irradiation. The net production of selected actinides is compared with the $UO_2$ baseline on a percentage basis. The net production of Pu-238 in the overall assembly has increased by 150% to 250% while the net production of the other plutonium isotopes has decreased by 30% to nearly 100%. The net Pu-241 production is slightly higher than the once-through $UO_2$ baseline because of the higher inventory of Pu-240 in the transmuter pins compared with the baseline. The net production of Np-237 and its precursors is reduced by about 25% to 75% from the $UO_2$ baseline. The 13-pin case with the large annular transmuter pin clearly provides the best results.

The second scenario assumes that only the transmuter pins are sent to further transmutation or to a repository. The plutonium and minor actinides and about 1% of the uranium in the surrounding $UO_2$ pins are chemically separated after a 30-year decay time and fabricated into future transmuter pins. Because the thorium-based or inert matrix transmuter pins would be more difficult to process chemically, those pins are assumed to be sent directly to a geological repository or processed using more advanced separation technologies.
The masses of each of the actinides sent to further transmutation or to a repository are shown in Figure 1.

Note that the Pu-239 leaving the LWR system has been reduced by as much as an order of magnitude, but that Pu-238 has increased by as much as a factor of 2. Though small, the Am-242 going to further transmutation or to a repository is slightly higher than in the

$UO_2$ baseline case. The Am-242 will decay into Pu-238 and then U-234. On the other hand, the rest of the plutonium isotopes have been reduced. The percentage changes in the amounts of actinides going to further transmutation or a geological repository, compared with the once-through fuel cycle, are shown in Figure 2. As was the case with the net production comparisons, the amounts of Pu-238 leaving the LWR system are increased by 25% to 160%. The Pu-239 is reduced by 85% to 100% and the rest of the plutonium isotopes by lesser amounts. The Np-237 and its precursors are reduced by as much as 75%.

The development of these fertile-free fuels has contributed to the Advanced Fuel Cycle Initiative (AFCI), which has the goal of greatly reducing the repository capacity needed for continuing, a sustainable nuclear fuel cycle. This LDRD has led to the award of a NERI grant for the investigation of mixed thoria-uranium fuels in LWRs and to work at the INEEL on the AFCI.

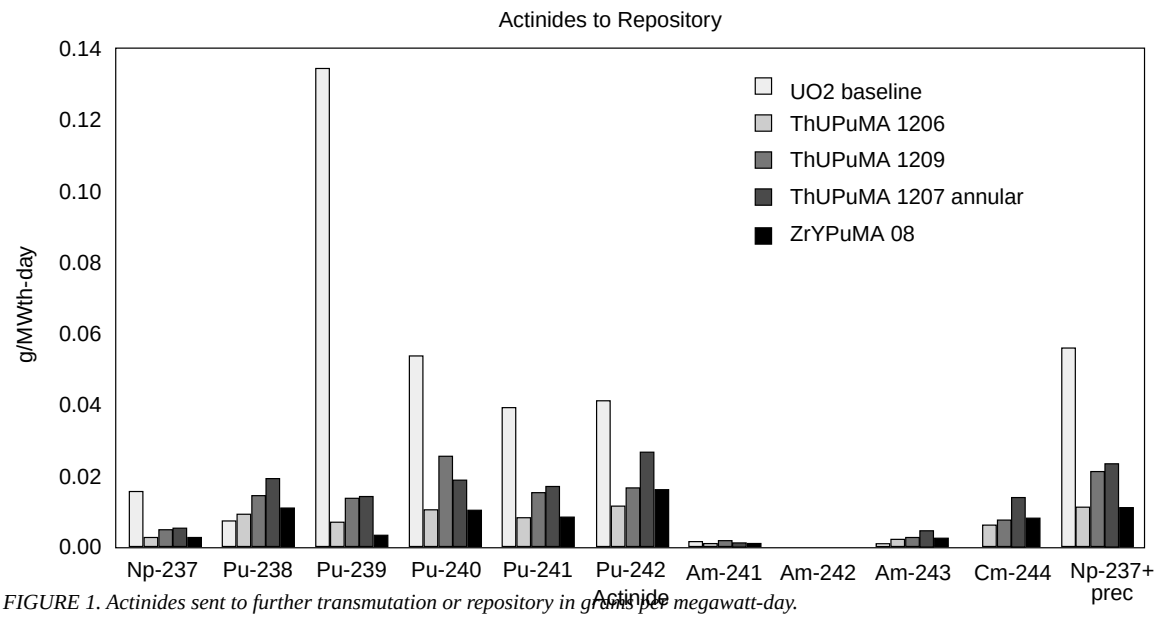


*FIGURE 1. Actinides sent to further transmutation or repository in grams per megawatt-day.*

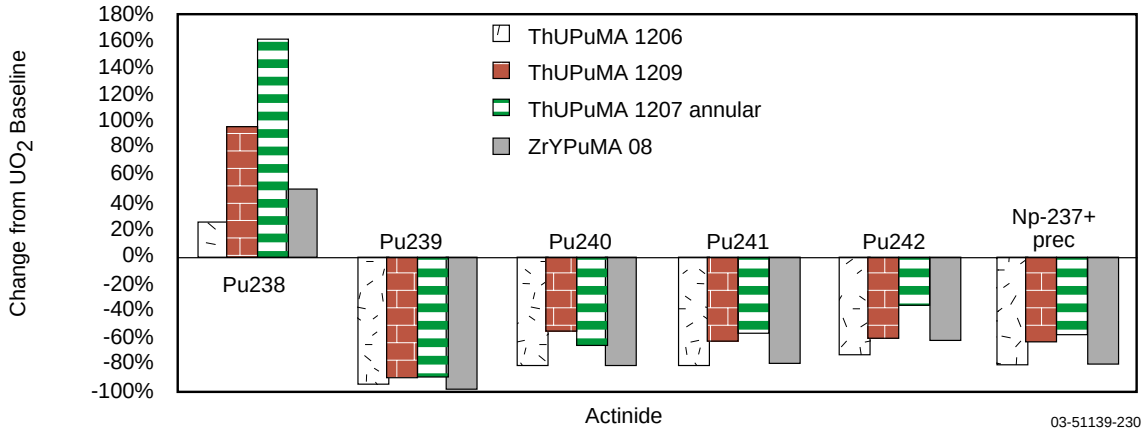


*FIGURE 2. Change in actinides going to further transmutation of a geological repository.*

# Design of an Actinide Burning, Lead or Lead-Bismuth Reactor That Produces Low Cost Electricity

*Eric Loewen, Jacopo Buongiorno, Cliff Davis, Kevan Weaver*

***Safely meeting the world's expanding energy needs***

GE105

As the earth's population grows, so will the demand for energy. Simply expanding energy use based on today's mix of production options will continue to have adverse environmental impacts and potential long-term consequences from global warming. Currently nuclear power plants produce 16% of the world's electricity. However, new and better reactor designs are needed to compete economically with coal and natural gas-fired power plants while maintaining safety, increasing proliferation resistance, and minimizing waste.

The objective of this LDRD is to identify and analyze the key technical issues in core neutronics, materials, thermal-hydraulics, fuels, and the economics associated with development of a Pb or Pb-Bi cooled fast reactor. The project evaluated the abilities of a Pb or Pb-Bi cooled fast reactor to detoxify current high-level waste (actinide burning), as well as produce low-cost electricity. The project explored Pb and Pb-Bi coolants for realistic and futuristic versions of fast fission reactor concepts.

The research from this project indicates that a Pb/Pb-Bi reactor would minimize and manage its nuclear waste to reduce long-term stewardship concerns, excel in safety and reliability with a very low likelihood and degree of reactor core damage in the event of an accident, and deliver sustainable energy that meets clean air objectives. This LDRD was performed in collaboration with investigators at Massachusetts Institute of Technology (MIT).

Technical objectives for fiscal year 2003:

- Examine different core design concepts to maximize actinide consumption and minimize electricity production cost.
- Assess transient plant performance and steady-state plant performance to determine maximum allowable power and associated capital cost for a plant system with the primary coolant under natural vs. forced circulation, and a steam He or supercritical $CO_2$ secondary coolant system.
- Conduct circulation corrosion studies focused on commercially available materials.
- Characterize Po removal from a Pb-Bi primary coolant in response to the formation of $H_2Po$ and rare-earth elements, and develop an alkaline extraction technology for removal of Po from a Pb-Bi primary coolant.

For the past three years, this LDRD has investigated safety and operation-related issues for molten Pb-alloy coolant reactor as shown in Figure 1. The project evaluated Pb/Pb-Bi coolants to ensure that a different scientific concept was explored for realistic and futuristic versions of fast fission reactor concepts. Four reactor design concepts were studied over the course of this research; three for waste management and one for producing electricity. The important features of these four designs (all configured like the general system shown in Figure 1) are summarized as follows:

*Fertile-Free Actinide Burner (ABR)* – The ABR achieves a maximum actinide-burning rate comparable to that of accelerator-driven systems while not separating the Pu during the cycle. The fuel, fertile-free TRUs and Zr, is burned and recycled repeatedly. A particular advantage of the ABR is the preferential Pu isotopes discharged from the burner, since they are poorer than the original spent LWR fuel.

*Fertile-Free Minor Actinide Burner (MABR)* – The MABR attains a maximum minor actinide destruction rate. Unlike the previous design, the MABR approach assumes that the Pu from spent LWR fuel is incinerated in fertile-free fuel LWR assemblies while the minor actinides are combined with a small amount of Pu and burned in the MABR core. In general, the number of reactors and therefore the capital costs for this approach will be less than for the ABR, but the reprocessing costs will be high. The MABR fuel will have a very small delayed neutron fraction, a zero or positive fuel temperature coefficient, and a very large coolant void worth that makes the design of a safety system extremely difficult, although the proposed design successfully meets this challenge.

*Actinide-Burning Reactor with Thorium (ABRT)* – The ABRT produces economical electricity while reducing TRUs from spent LWR fuel. The main difference between this and the ABR and MABR concepts is the addition of Th and U to the TRUs in the fuel matrix. The addition of a fertile material can reduce reactivity swings during burn up, thus reducing the number of control rods but conversely reducing the TRU destruction rate.

*Once-Through Electricity Producing Concept (OTC)* – The OTC produces low cost electricity by eliminating costs associated with fuel reprocessing. This design has low moderation, reduced leakage,

modest burn up, and a harder neutron spectrum. If the in-core breeding ratio is approximately 1, blankets are not needed, the void reactivity is improved, and excellent safety characteristics can be obtained. The main drawbacks, as with any fast reactor once-through cycle, are the issues of waste, waste disposal, and proliferation.

Of the concepts analyzed, the ABR and MABR offer the best potential to meet the actinide-burning mission and objectives of the Generation IV initiative. A 700 MWth modular reactor with forced-convection Pb-alloy cooling, passive decay heat removal, and a supercritical CO2 power cycle is the recommended approach to best exploit the Pb-alloy-cooled reactor concept for actinide burning.

The Generation IV roadmap identifies six concepts with potential to meet the Nation's energy needs in a sustainable, economic and safe manner. The concepts of the Pb-cooled Fast Reactor System developed by this LDRD put the INEEL in an excellent position to support the development of this reactor concept for the DOE. The expertise gained from the work on this LDRD also led to a design concept for a heavy water cooled and Pb-Bi scattered fast test reactor that captured the attention of DOE/NE-1 who requested a personal presentation.

Two internal Invention Disclosures were submitted based on this LDRD research: 1) A Corrosion Control Process for a Liquid (Molten) Metal Alloy System Using Oxide Film Management, and 2) Molten Len Alloy Online Impurity Removal System. In addition, this LDRD resulted in the completion of studies and submittal of nine integrated papers for a special issue of the American Nuclear Society journal *Nuclear Technology*, reporting on this project. The report from the LDRD team members will provide future researchers and evaluators with an inclusive review of this project. MIT and INEEL also published or presented three papers at ICONE-11.

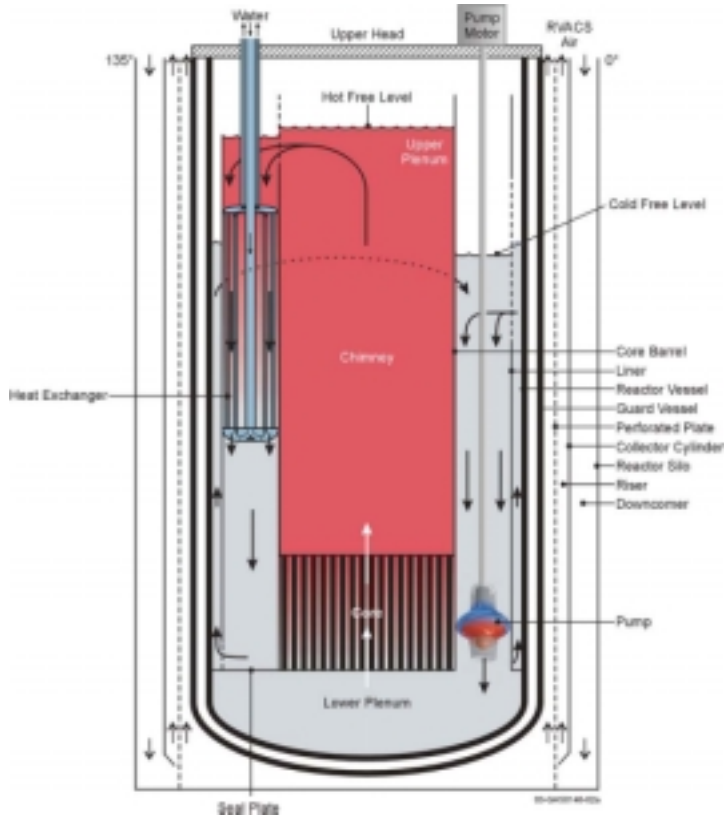


*FIGURE 1. Pb / Pb-Bi cooled fast reactor concept.*

# Modular Pebble Bed Reactor

*David Petti*

***Benchmarking core design tools***

GE101

The Modular Pebble-Bed Gas-Cooled Reactor (MPBR) is a leading Generation IV reactor concept for an electric generation station whose viability has been proven by the operation of experimental MPBR reactors. However, many technical issues must be addressed before construction of MPBR reactors becomes commercially practical.

This LDRD explores some of these issues, building on the strong capabilities at INEEL for reactor core neutronics, thermal hydraulic design, and nuclear safety analysis. INEEL is involved in the development of fuel performance, neutronics, thermal hydraulics, and safety analysis computational models necessary to design the MPBR. This work is focused on developing and benchmarking these core design tools so that INEEL can assess the key technical issues associated with the technology.

Technical objectives for fiscal year 2003:

- Complete quality assurance testing of the pebble-bed reactor physics code PEBBED.
- Develop an optimized pebble fuel form.
- Perform analysis of the degree of oxidation that occurs in the core and lower reflector of a pebble-bed design.

PEBBED is a new reactor physics code developed as part of this LDRD project. PEBBED has the unique ability to perform reactor physics analysis and fuel cycle optimization on reactors in which the reactor core consists of flowing pebbles. As national and international interest in the MPBR grows, the need for accurate analysis tools will become pressing.

In FY02, the 3-D version of PEBBED (PEBBED3) was begun. PEBBED3 provides two options for solving the neutron diffusion equation in general 3-D cylindrical geometry. The first option is a standard finite-difference solution that is now fully operational. The second option is a nodal solution; that is still being implemented. Research in FY03 focused on validating the finite-difference solution method currently employed in PEBBED. An effort was launched to validate PEBBED results against simple cases in which analytical solutions exist. A series of test cases was constructed and some of the results are shown in Table 1.

In a related effort, a new method for analyzing isotope depletion in pebble-bed fuel was investigated. The Kernel-by-Kernel Fuel (KbKF) model, developed by G. S. Chang of the INEEL, has been proposed for gas reactor fuel burnup analysis. A Monte Carlo neutral particle transport code (MCNP), is coupled to an isotope depletion code ORIGEN-2 via a UNIX-script (MCWO). With MCWO, the KbKF model can be used to deplete the fuel kernels individually. Infinite core multipli-

*Table 1: Results of PEBBED Analytical Benchmark Calculations*

| Case Geometry | Number of Energy Groups | Analytical Eigenvalue | PEBBED Eigenvalue |
|---|---|---|---|
| Bare Critical One-Dimensional Cylinder | 1 | 1 | 1.00002 |
| Bare Critical One-Dimensional Slab | 1 | 1 | 1.00002 |
| Bare Critical Two-Dimensional Slab | 1 | 1 | |
| Bare Critical Two-Dimensional Cylinder | 1 | 1 | 1.00001 |
| Bare Critical Three-Dimensional Cylinder | 1 | 1 | 1.00001 |
| Infinite Two-Dimensional Slab | 1 | 2.6069 | 2.6069 |
| Reflected Critical One-Dimensional Cylinder | 1 | 1 | 1.00002 |
| Reflected Critical One-Dimensional Slab | 1 | 1 | 1.00018 |
| Bare Critical Two-Dimensional Cylinder | 2 | 1 | 1.00019 |
| Bare Critical Two-Dimensional Slab | 2 | 1 | 0.99980 |

03-51139-111a

cation factors, time-dependent actinide concentrations, and detailed radial fuel kernel fission power profiles are obtained using this method. While validation and verification of the MCWO is not likely to happen soon, a joint study comparing the MCWO with other pebble-bed analysis methods falls within the MPBR methods development scope. Such a joint study has been initiated with Mitsubishi Heavy Industries, LTD (MHI), in which their proposed technique, MVP-BURN, is being compared to the MCWO-KbKF approach.

One of the criteria in the standard definition of spent fuel, as defined by the National Academy of Sciences, is that the isotopic compositions of the discharged fuel should be about the same as the light water reactor $UO_2$ spent fuel. In particular, the $^{240}$Pu/Pu ratio should be greater than 24%. The $^{240}$Pu/Pu ratio calculated using the KbKF model indicates that the average $^{240}$Pu/Pu ratio of the benchmark LEUPRO-1 fuel kernel with burnup at the end of 925 effective full power (750 W per pebble) days reached 22.88%, which is very close to the spent fuel standard value. Further results, along with those from the ongoing MVP-BURN analysis, will be published in the technical literature.

An application of the PEBBED code illustrates the potential for optimization of the pebble-bed reactor. The standard pebble design used in most reactors under consideration is not a result of an extensive optimization process. A number of parameters can be varied in a full-scale optimization effort, but this is outside the scope of this project. However, one such parameter was varied (radius of fueled region within pebble) to examine the potential for pebble fuel optimization. Figure 1 shows the insertion of reactivity (increase in $k_{eff}$) that results when steam inadvertently enters a Very High Temperature pebble-bed reactor core. For both the 600MWt and 300MWt designs shown, an optimized pebble design yields a significantly reduced reactivity insertion. This translates into a power plant that is much more immune to this accident scenario. The data also indicate clearly superior fuel economy as discussed in the mid-year report. The results of this optimization study were presented in a report on the conceptual design of a Next Generation Nuclear Plant that is planned for construction at the INEEL.

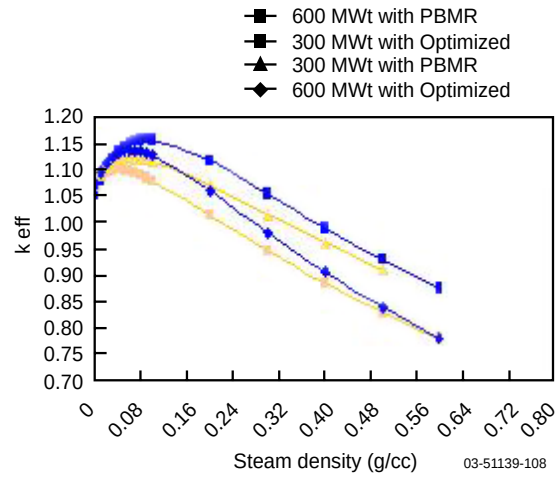


*FIGURE 1. Core multiplication factor for PBRs with different pebble designs.*

The subcontract work with the Georgia Institute of Technology continued this fiscal year. The codes, COMBINE and TORT, originally planned for use in cross-section processing, had been shown in FY01 to be unsuitable. In FY03 the codes WIMS and EVENT were selected, tested, and shown to be appropriate.

Since PEBBED is being developed as a practical tool to answer questions about the performance of real pebble-bed reactors (PBRs), it is appropriate to test its capabilities at each stage in its development by applying it to address practical issues. During FY03, PEBBED was used to develop a conceptual design of a Very High Temperature Reactor (VHTR), a Generation IV Advanced Reactor concept slated for construction at the INEEL. PEBBED now possesses a genetic algorithm advanced optimization feature making it the only reactor analysis code capable of rapid design and analysis of recirculating pebble-bed reactors. Five papers describing the application of PEBBED to proliferation studies, optimal pebble design, VHTR design, and optimal core design were presented or submitted to ANS and other conferences for publication during FY03.

Graphite oxidation can occur if a pebble-bed reactor is subjected to a beyond-design-basis air ingress accident, causing significant fuel failure and radionuclide release. As indicated in the Gen IV

roadmap, this is a significant issue for all pebble-bed reactors and is also a concern in other gas reactor concepts that use graphite in the core as a moderator and reflector material. Although analyses of air ingress accidents have been done in Germany, Japan, and China that show this event to be of limited consequence, the INEEL effort funded by this LDRD is the first in the U.S. to use an existing (validated for Light Water Reactors) thermal-hydraulic code (MELCOR) to address this scenario. The Nuclear Regulatory Commission (NRC) has referred to results from this work during the development of Pebble-Bed Reactors Phenomenon Identification and Ranking Table (PIRT) and has since contacted the INEEL with more interest in the project. The work resulting from this project also has been very beneficial in the development of a Pebble-Bed Reactor point design for the VHTR that is being considered for development at the INEEL. Specifically:

- German graphite oxidation rates were obtained and compared to the oxidation rates used in MELCOR code to generate the results presented in the FY01 and FY02 annual reports. The German oxidation rates fall between the previously used rates in the temperature range of 800°K to 1250°K. Below 800°K the German oxidation rate is higher, which could have an impact on the long-term release of radionuclides in the core. The discrepancies in oxidation rates suggest that more controlled experiments are needed to generate better oxidation rate data.
- A new effective pebble-bed thermal conductivity as described in IAEA-TECDOC-1163 was incorporated into the MELCOR code. Using the new effective conductivity has reduced the maximum predicted core temperature approximately 100°C to a value less than 1600°C, which is presently the upper limit for assured resistance of the fuel to thermal failure.
- A new heat transfer correlation, which better represents flow through a pebble bed, has been added to the MELCOR code.
- Heating values obtained from the INEEL PEBBED code are now being used in the MELCOR code.

Since the mid-year LDRD progress report, the pebble-bed model developed through this project has been used to study the sensitivity of fuel oxidation in the core of a PBR to various reactor parameters such as the effective core thermal conductivity, leakage from the top head of the reactor, no oxidation in the lower reflector, and reduced flow resistance in the core. The results from this study will be used by the NRC to help in the development of a PIRT document, which will be used, in the assessment of important phenomena to be considered in the licensing of PBRs. An NRC NUREG report is to be published in the near future containing the results from this study. The pebble-bed model also has been used in the VHTR point design effort at the INEEL. A journal article describing the model and important air ingress results obtained from the model is being prepared.

This LDRD has greatly enhanced the stature of the INEEL in the international PBR research community. The project team met or surpassed all major goals. Eight papers were published in archival journals and refereed conference proceedings, one of which was invited, and the investigator has participated in a panel discussion as an invited panelist. At least three more papers have been submitted based on recent design work. Copyrights have been asserted on the PEBBED code and the recirculation formulation used within. The cumulative results of this LDRD over the past three years have led directly to the awarding of three NERI projects being led or supported by the INEEL.

# Generation IV Gas-Cooled Reactor System Analysis Tools

*Richard R. Schultz, Walter L. Weaver III*

***Coupling two software codes to create one powerful tool***

GE103

To study advanced nuclear plant behavior, as well as thermal-hydraulic behavior of advanced systems in other industries, new analysis tools are needed. Currently, the Fluent Computational Fluid Dynamics (CFD) code is designed to perform detailed analyses of system components, predicting and analyzing the 3-D behavior of the working fluid. However, the code has no accommodations to handle rapidly changing boundary conditions at the component inlet and exit to analyze the component during a rapid transient as part of a system.

This LDRD has developed a new analysis tool by coupling the CFD code to the RELAP5-3D/ATHENA advanced thermal-hydraulic (TH) analysis code. This tool enables researchers to perform detailed, 3-D analyses using CFD capability while the boundary conditions required by the Fluent calculation are provided by the balance-of-system model created using RELAP5-3D / ATHENA. Both steady state and transient calculations can be performed using many working fluids and also point-to-3-D neutronics. Prior to this research, there was no means to analyze the quick-transient TH behavior of a reactor system component using a CFD code.

The Fluent/RELAP5-3D coupled code is a state-of-the-art tool to study the behavior of systems with single-phase working fluids, such as advanced gas-cooled reactors, metal-cooled reactors, and portions of water-cooled reactor systems. The coupled code can be used with Fluent 5 on Digital Equipment Corporation (DEC) workstations or Fluent 6 on Sun workstations (both UNIX operating systems).

To demonstrate the applicability of the tool to an existing gas-cooled reactor system, a collaborative agreement between General Atomics (GA), Fluent, and INEEL was formed. A demonstration of Fluent's capability to model a GA prismatic reactor component was completed by modeling the reactor's lower plenum and by performing a preliminary study of the exit temperature profile. A demonstration of Fluent and RELAP5-3D being used in the coupled mode was accomplished by linking a Fluent model of a test section to a RELAP5 model of the balance-of-system with helium as the working fluid.

Technical objectives for fiscal year 2003

- Couple the Fluent CFD code and the RELAP5-3D systems analysis code to enable them to work together by passing boundary conditions between them so transient analyses of systems can be performed.
- Demonstrate that the coupled codes are properly coupled and function as expected.
- Create a validation & verification (V&V) matrix that can ultimately be used to demonstrate Fluent's capability to analyze gas-cooled reactor systems.
- Develop a collaborative technical relationship between a commercial CFD provider and at least one gas-cooled reactor designer and demonstrate the feasibility of using the coupled tool.

Fluent and RELAP5-3D©/ATHENA are linked using an Executive Program that (a) monitors the calculational progression in each code, (b) determines when each code has converged, (c) governs the information interchanges between the codes, and (d) issues permission to allow each code to progress to the next time step. The linkage is operational with Fluent 5 on DEC workstations and with Fluent 6 on Sun workstations.

The Fluent/RELAP5-3D coupling was first completed using Fluent 5 on a DEC workstation. The coupling between the codes was demonstrated and validated by modeling a pipe test section using Fluent and by modeling the balance-of-system using RELAP5-3D. This work was documented in a paper presented at the 11th International Conference on Nuclear Engineering, Tokyo, Japan.

A preliminary V&V matrix was created to use as the basis for studying the applicability of the Fluent CFD code and the RELAP5-3D code for analyzing gas-cooled systems. V&V, performed using the first case in the matrix, indicated Fluent has the desired capabilities. The V&V matrix, later supplemented by studies performed by the Generation IV system product managers, was presented at the 10th International Conference on Nuclear Engineering, Arlington, VA.

A collaborative relationship was formed between INEEL, the Fluent Corporation, and GA to demonstrate the feasibility of using the new tool for analyzing gas-cooled reactor systems. To accomplish this task the lower plenum of a GA prismatic gas-cooled reactor was modeled using the Fluent CFD code, and a gas system using helium as working fluid, was modeled using the coupled code. This work, documented in a Web Seminar in

April, shows a preliminary analysis of the temperature distribution in the lower plenum (Fig. 1) of the GA GT-MHR gas-cooled reactor. The coupled case was performed using Fluent 6 on a Sun workstation (Fig. 2).

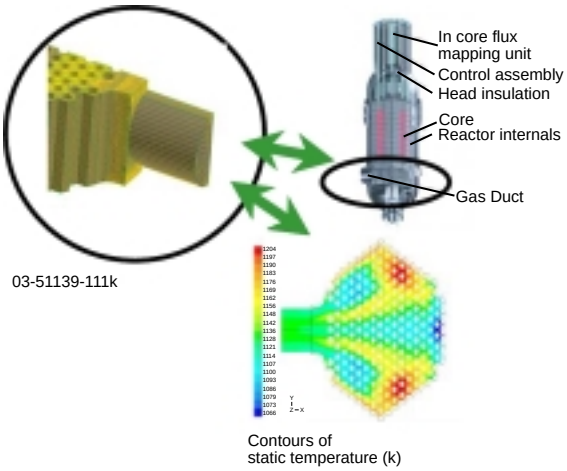


*FIGURE 1. Fluent model: GT-MHR lower plenum.*

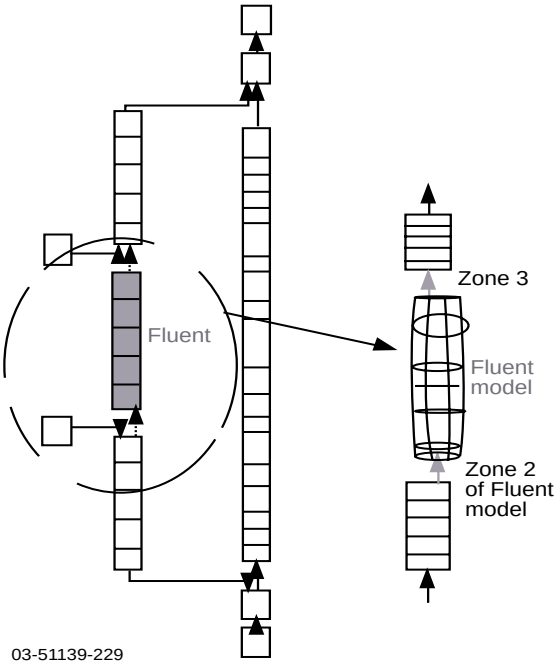


*FIGURE 2. Model using coupled code.*

Because it is sometimes difficult to judge whether to use a CFD code such as Fluent or a systems analysis code such as RELAP5-3D for analysis of a system, a user guideline was written as part of this LDRD. In addition, a more informal user guideline was created to guide an analyst in using the Fluent/RELAP5-3D coupled code.

In summary, the Fluent CFD code and RELAP5-3D advanced thermal-hydraulic systems code have been coupled, and the coupled tool was demonstrated to work using a model with helium as the working fluid. Also, Fluent has been shown to be an excellent candidate to perform CFD analyses of the behavior of gas-cooled reactors systems. The coupled tool is available for use. The Fluent/RELAP5-3D tool adds an analysis capability that was previously unavailable; this capability has recently been shown to be essential for analysis of advanced reactor systems. Prior to the development of this tool there was no means to analyze the transient TH behavior of a reactor system using a CFD code since there was no means to update the boundary conditions during a rapid transient or to take into the consideration the interactions between the CFD model and the remainder of the system.

Since this LDRD began in 2000, the importance of combining CFD software with systems analysis codes has come to the forefront of R&D efforts in many nuclear industry-focused organizations throughout the world. The French have more than two efforts ongoing in this area; the European community has work in progress; and the U.S. Nuclear Regulatory Commission has discussed linking its systems analysis code, TRACE, to a CFD code, to name the most prominent efforts. In addition, the IAEA sponsored the first conference (November 2002) to focus specifically on the subject of software linkages and, in particular, on the coupling of CFD and systems analysis codes. INEEL participated in the IAEA conference.

Concurrent with the interest in linking CFD codes and system analysis codes other than the Fluent/RELAP5-3D combination, there has been substantial interest in the linked product of this LDRD. Interested parties include Westinghouse, Framatome, General Atomic, and Oak Ridge National Laboratory. A number of other commercial organizations and universities also have indicated their interest in this product.

# An Innovative Gas-Cooled Fast Reactor

*Kevan D. Weaver, James Sterbentz, James Fisher, Rick Gregg, Eric Loewen, Cliff Davis*

***Safe, economical electricity production***

GE107

The fourth generation of nuclear power reactors will have to compete economically with coal- and natural gas-fired power plants, while maintaining safety, increasing proliferation resistance, and minimizing waste. The goal is to identify, analyze, and resolve the key technical issues associated with the development of the Generation IV reactor concept to meet these criteria. The major issues involved are loss-of-coolant/loss-of-flow accidents, long-life core/fuel designs, and materials compatibility at high temperatures and pressures.

This LDRD is investigating various fuel, core, coolant, plant, and material designs of gas-cooled fast reactors that would meet these criteria by producing low-cost electricity while consuming actinides to reduce waste, increase proliferation resistance, and retain high safety margins. The specific tasks undertaken to accomplish these goals are: 1) reactor physics and core design where long-life cores (including fuels) are studied to optimize the transuranic destruction rate, minimize waste production, and maintain a low lifetime reactivity swing; 2) plant engineering design where supercritical pressure and temperature $CO_2$ as a coolant is being studied; and 3) high temperature material studies, including $CO_2$ steady-state and air ingress experiments of candidate cladding and structural materials.

Technical objectives for fiscal year 2003:

- Analyze and resolve the key technical issues associated with:
  - Reactor physics and core design
  - Plant engineering design
  - Material studies.

*Reactor physics and core design* — Work was accomplished on both the pebble/particle and block matrix cores, with emphasis in the following areas: suitable materials for the diluent/clad and reflector, and initiation of reactivity coefficient calculations. Specific results based on parametric studies are as follows:

- GFR reflector albedo is only ~ 80% even for the better materials: 10% less than the best thermal reactor reflectors.
- Low $\sigma_a$ is only a rough guide to suitability. This is consistent with superiority of Ca, Ba, Sr, Pb and their sulfides. But some with higher $\sigma_a$ (e.g., most transition metals/rare earths) are good performers despite their unsuitability as in-core diluents. This increases the enrichment requirements, but produces a negative void worth.
- For U-235, Ni confers a negative coolant void $\Delta k$ and many others keep $\Delta k_{void} < \beta$, but for fissile Pu, all give approximately the same $\Delta k_{void}$ and $> \beta$.
- No single material is best overall. BaS, which melts at 2220°C, appears to be an interesting compromise.
- The best reflectors provide reactivity-limited burnup slightly better than a conventional uranium blanket.
- Internal fertile blankets of natural uranium or thorium extending the length of the core axially were found to decrease coolant void $\Delta k$.
- A totally internal fertile blanket region (an axial "parfait" blanket) decreases coolant void $\Delta k$ significantly. A core 2.4 m tall with a natural uranium parfait blanket region 1.2 m tall gave a coolant void $\Delta k$ of $1.17 with supercritical $CO_2$ at 20 MPa. A similar core with only external blankets had a coolant void $\Delta k$ of greater than $2.
- Reducing pressure of either $CO_2$ or He from 20MPa to 10MPa reduces void $\Delta k$ by about a factor of two in most cases.

Additional work includes the development of methods to reduce the positive reactivity effect of coolant voiding. Approaches studied were configuration modification, materials selection, and conceptualization of special reactivity feedback devices. The most promising finding was that the use of titanium as reflector and/or core fuel matrix material reduced $CO_2$ void reactivity to << ß (or even rendered it negative). This is documented in a paper prepared for the GLOBAL 2003 meeting in November. At the parallel ANS Conference, the investigators also are presenting papers on three innovative passive reactivity devices developed under this LDRD project.

*Plant Engineering Design* — Work was completed to define a reference supercritical $CO_2$ Brayton Cycle. A generic indirect-cycle power plant of this type would be suitable for use with all GEN IV advanced reactors having core outlet temperatures $\geq$ 500°C. Currently in progress are PRA-guided system studies aimed at accommodating loss-of-coolant (LOCA) events, the oft-cited

Achilles heel of the GFR. Promising results are indicated if one employs dual purpose shutdown/emergency cooling loops with gas accumulators that passively come online to power gas turbine drives as another diverse energy source should station electric power be lost. It is expected that further analysis of this approach will indicate core damage frequencies significantly less than the generic GEN-IV goal of $<10^{-5}$ per reactor year. In addition, past designs and proposed design concepts were reviewed to determine which systems and/or components (e.g., blowers, compressors, compressed-gas storage) are potentially significant contributors to risk and/or reliability. In support of this effort, a literature search was performed on "HEATRIC Heat Exchangers" to assess their reliability versus conventional heat exchangers.

The RELAP5-3D (INEEL 2002) computer code is being used in the analysis of gas-cooled fast reactors. Improvements were made to the code to support the analysis of these reactors during the first half of the fiscal year. Specifically, the Gnielinski (1979) heat transfer correlation was added to the code to facilitate analytical comparisons with Massachusetts Institute of Technology (MIT), a collaborator on this project, and the turbine model was improved. The Gnielinski (1979) correlation represents forced convection heat transfer for turbulent flow in pipes and channels. The Gnielinski correlation simulates additional phenomena, including entrance effects, heated wall effects, and the transition between turbulent and laminar flow, compared to the correlations previously used in the code. The RELAP5-3D turbine model was evaluated for the $CO_2$ turbine described by Dostal et al. (2002). The model in the original code was deficient because the power added to the shaft was not always consistent with the power removed from the fluid, as shown in Figure 1. This deficiency was resolved by adding a dissipation term to the turbine energy equation. The shaft and hydraulic powers are now consistent for a wide range of flow rates. (The results shown in Figure 1 were obtained for exit Mach numbers between 0.25 and 0.70.) The flexibility of the turbine model was increased by allowing the user to account for variable frictional torque and variable moment of inertia, and by adding a new type of turbine in which the user can specify the efficiency as a function of normalized speed and load.

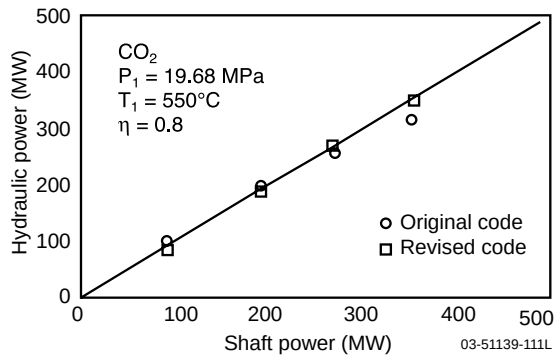


*FIGURE 1. A comparison of hydraulic and shaft powers for a $CO_2$ turbine.*

Additional RELAP5-3D work includes the capability to model a compressor. The characteristics of this component are similar to those of a pump. Provisions were made for input of data for the new component. Included are the capability to use a speed table, which optionally can be controlled with a trip, and the capability to use a torque-inertia equation, with or without a motor torque table. Unlike the pump component that has two associated junctions, the compressor includes a required junction at the inlet and an optional junction at the outlet that provides the capability of connecting the outlet of the compressor to the inlet of another compressor or to a non-compressor component. The model is functional, and results of test cases show reasonable agreement between theoretical and actual performance. The difference occurs because an approximation of fluid density is used, which avoids an entropy-based fluid property table lookup (a capability that is not available within RELAP5). The error introduced by the density approximation can be made arbitrarily small, however, by using compressor components with low-pressure ratios and cascading them in series to obtain the desired overall pressure ratio. Preliminary investigations have been done for data input options, but additional work is necessary to finalize the method for input of data to the code. One possibility is to input the data into homologous form, as is done with the pump. An advantage is that the derivative of head with speed should be continuous. This is important because these discontinuities introduce "steps" in the performance and introduce time-step limitations. A disadvantage is that distortions and inaccuracies are introduced because homologous theory is based on the

Buckingham Pi groups that assume an incompressible fluid. Density-based corrections were shown to improve the accuracy somewhat, however the form of the density correction varies from fluid to fluid and is apparently dependent on fluid compressibility.

Linear interpolation also was investigated. It was found necessary to interpolate along lines of constant efficiency. This is problematic because of the non-orthogonality of a speed-versus-efficiency coordinate system, and because the derivative of head with speed has a discontinuity at each input speed value. Bicubic interpolation also was briefly investigated, but restricted in scope because of funding limitations. Bicubic splines guarantee a continuous derivative of head with speed, but may not be applicable in non-orthogonal coordinate systems, particularly in regions of the map where efficiency values cannot be matched.

*Material Studies* — A supercritical $CO_2$ corrosion apparatus, shown in Figure 2, was deployed at the May Street North Facility. When corrosion experiments start next fiscal year, this apparatus will enable the characterization of corrosion rates with different materials at variable temperature, pressure and flow rates. The test loop constructed for the investigation of $CO_2$ corrosion consists of a high-purity $CO_2$ cylinder, high-pressure $CO_2$ pumps, filters, a flow meter, a pre-heated test section, and high-pressure fittings and valves. This once-through apparatus is used to simulate a fast-neutron reactor operated with a temperature range of 100° to 600°C, and a pressure range of 15 to 30 MPa. $CO_2$ with a purity of 99.9999% will feed into the test loop from the compressed $CO_2$ cylinder, and will be pumped to the experimental operating pressure by an ISCO D-series syringe pump Model 500D. The pump takes an input pressure of 5.7 MPa, and discharges up to 30 MPa with a maximum volumetric flow rate of 170 ml/min. The heated corrosion samples can be made from 0.3175 cm, 0.635 cm or 1.27 cm OD tubes at a length of 124.5 cm. This length provides sufficient flow development lengths from the entrance. The apparatus is designed to operate at varying and precisely adjustable pressure, temperature, and $CO_2$ flow rates within the design limits.

This project supports the Generation IV initiative in advanced reactor design, which has become a prominent focus of the INEEL. It is evaluating an optional gas-cooled fast reactor (GFR) design not being studied or funded under DOE's Generation IV initiative, but that shows high potential for safe, economical electricity production at modest temperatures while meeting Generation IV goals. Previous and continued work on this project has positioned the INEEL as a leader in this area.

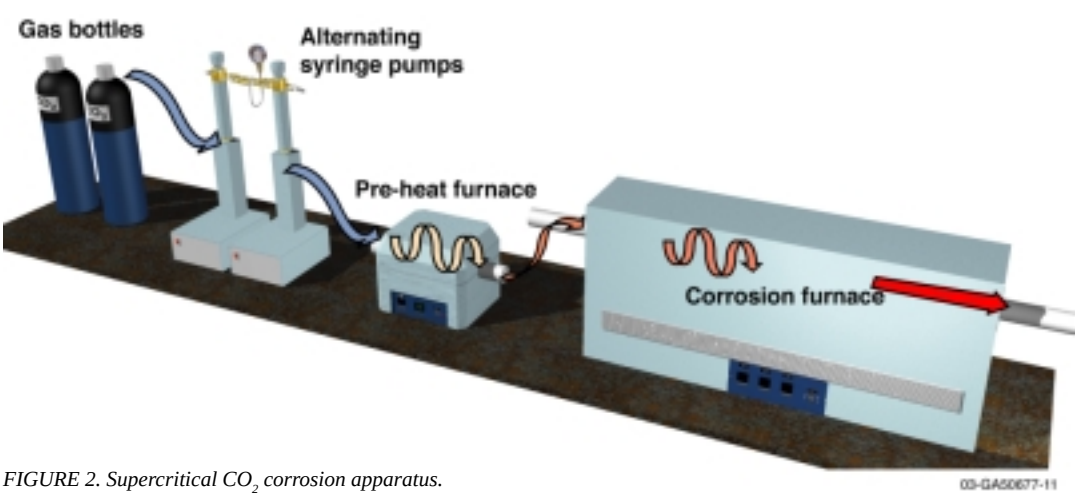


*FIGURE 2. Supercritical $CO_2$ corrosion apparatus.*

INEEL

# Subsurface Science Initiative

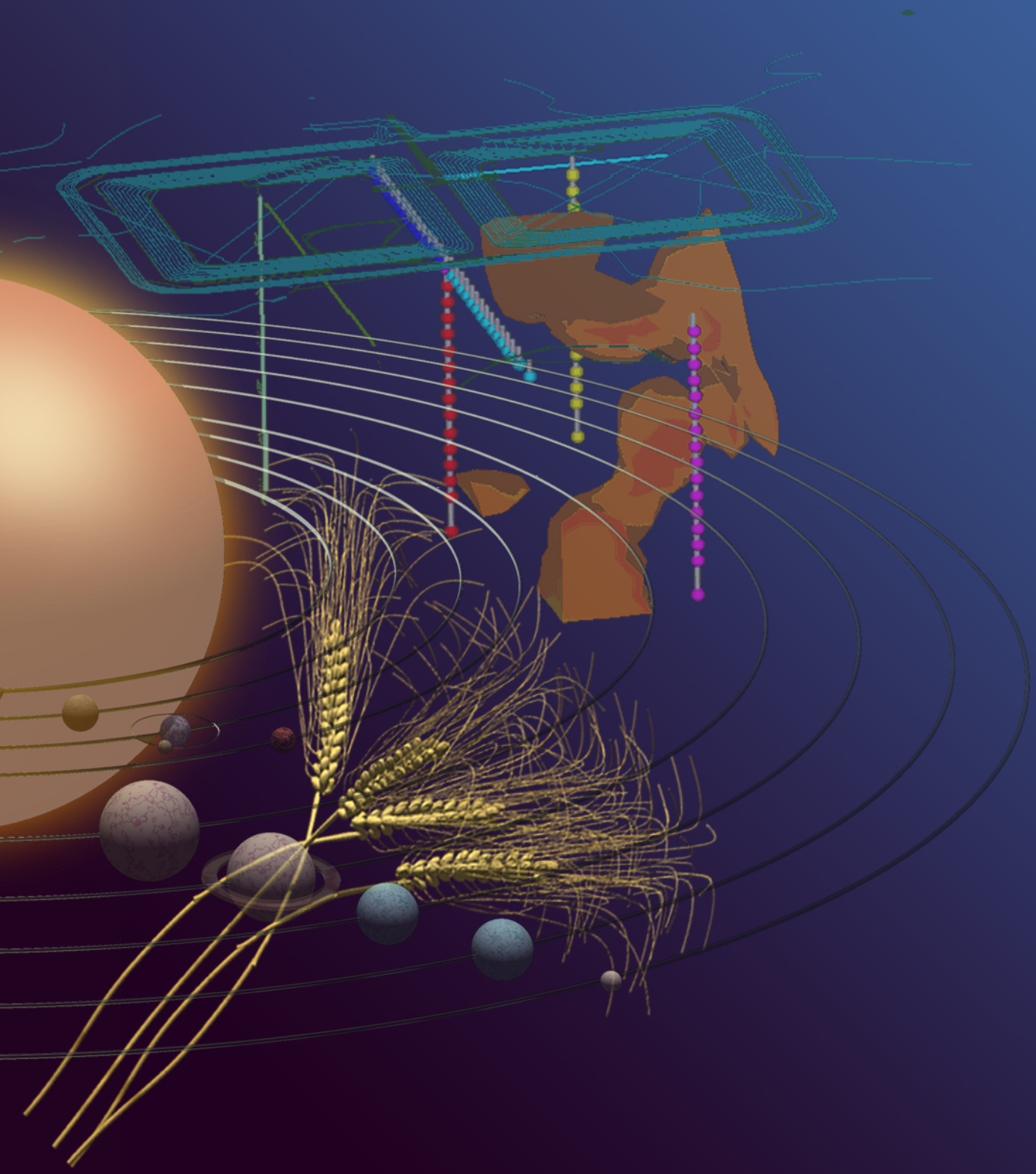

# Use of Molecular Markers for Detection and Tracking of Environmental Bacteria

*Joni M. Barnes, Bill Bauer, Frank Roberto, Debby Bruhn*

***Tracking microbe interaction with mineral surfaces***

GC124

At almost all DOE sites, groundwater contamination with radionuclides, heavy metals, or chlorinated solvents is a problem. Subsurface microbes use minerals and mineral surfaces to facilitate metabolic processes. These in turn influence redox chemistry and pH of groundwaters and can affect the fate of contaminants such as chlorinated hydrocarbons, chromium, uranium, and plutonium. Therefore, information relative to the transport and fate of microorganisms in natural environments is important in the development of bioremediation strategies as well as predicting and monitoring natural attenuation.

Studies designed to assess the interaction of microbes with soil and mineral surfaces frequently use light, electron, or confocal scanning laser microscopy to visualize the cells. However, sample preparation techniques can physically alter the sample, change bacterial surface properties, and kill the cells. To eliminate these artifact problems, simple, non-invasive bacterial tagging agents are needed.

This LDRD investigates using molecular markers as a means to detect and track environmental bacteria. Over the course of the project, work has focused on the use of green fluorescent protein (GFP) as a non-invasive cell marker. Cells that have been genetically altered with the GFP gene produce a stable internal chromophore, which fluoresces in the absence of other substrates or cofactors. Cells expressing GFP emit a bright green fluorescence that can be visualized using epifluorescent or confocal microscopy. In addition, blue and yellow color variants of GFP and a red fluorescent protein are commercially available, providing a method to simultaneously monitor mixed cell populations.

Technical objectives for fiscal year 2003:

- Develop molecular techniques for inserting GFP genes onto the chromosome of environmental bacteria.
- Continue laboratory studies using GFP tagged bacteria.
- Evaluate maturation and emission properties of red fluorescent protein markers.

This is the final year of a three-year project. In the first year, a plasmid vector (pRK415npt$_2$gfp) was constructed that provides an appropriate antibiotic resistance gene and an optimum promoter for environmental bacteria. The plasmid, which carries genes for tetracycline resistance, expresses GFP from the constitutive neomycin-phosphotransferase (npt$_2$) promoter and contains restriction sites that allow easy insertion of commercially available GFP color variants (CLONTECH Laboratories, Inc., Palo Alto, CA). Electroporation and conjugation techniques also were developed for introducing the plasmid into host cells. Using these tools, the investigators successfully tagged a variety of environmental bacteria, including iron-, sulfate-, and nitrate-reducing bacteria, with fluorescent markers. Tagged cells emitted bright fluorescence that was easily detected by direct epifluorescent microscopy.

In FY02, studies were done to determine the affect of the GFP plasmid on host cell metabolism. For this work, *Shewanella putrefaciens*, a facultative iron-reducing microbe was used as a model bacterium. *S. putrefaciens* is widespread in the environment and under anaerobic conditions can use an array of electron acceptors including insoluble manganese (IV) and iron (III) oxides. *S. putrefaciens* cells were tagged with GFP using pRK415npt$_2$gfp as described above. Similar growth and iron reduction rates were measured in studies using cultures with and without the plasmid. Also, when cells carrying the plasmid were grown in the absence of tetracycline, no plasmid loss was observed after 24 hours, and 83% of the cells still retained the plasmid after 72 hours (36 generations). These findings indicate that pRK415npt$_2$gfp places minimal stress on *S. putrefaciens*, and that cells tagged with GFP can be used in the absence of selective pressure for short-term studies. Similar results were observed when these experiments were conducted using *Pseudomonas putida*.

Over the course of the project, effective epifluorescent microscopy techniques and fluorometric methods were developed that enable detection of labeled cells. Also, a flow cell system was constructed for real-time detection and tracking of GFP-tagged bacteria. In the flow cell studies, bacteria were grown in simulated groundwater and pumped through a laminar flow cell that contained a hematite pellet. Throughout the experiment, cells that attached and adhered to the hematite surface were observed by placing the flow chamber directly on the stage of a Nikon Eclipse E600 microscope

(Fig. 1). The E600 is equipped with a water immersion objective lens (60x, NA=1.20), a 100-watt mercury arc lamp and various filter sets for viewing different fluorescent colors. Cells were imaged using a Peltier-cooled CCD camera. Using these techniques, the investigators were able to demonstrate that GFP provides an effective non-invasive means to monitor cell activity over time and, by using different color variants, up to three cell populations can be monitored concomitantly.

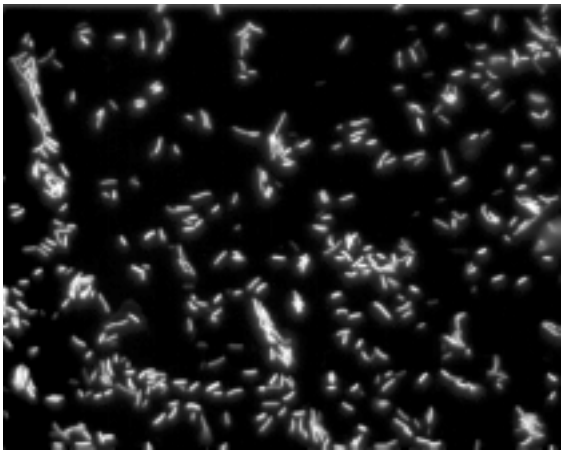

PN04-004-155

*FIGURE 1. Epifluorescence photomicrograph of* Shewanella putrefaciens *attached to a hematite surface. The cells, which are tagged with GFP, were grown for 44 hours in a laminar flow cell operated under aerobic conditions.*

In FY03, work focused on the development of molecular techniques for inserting GFP directly onto the chromosome of environmental bacteria. Marking the chromosome maximizes genetic stability and reduces the risk of transferring the genetic marker to other microorganisms — characteristics that are needed for long-term bench-scale or field studies. In this work, the investigators successfully used a miniTn5 delivery system (pUTmini-Tn5gfp) and conjugal transfer techniques to randomly insert GFP genes onto the chromosome of *Pseudomonas putida* F-1 and *Comamonas DA001*. Although chromosomally tagged cells with a single integrated copy of GFP emitted lower fluorescence than cells carrying multiple copy plasmids, they were clearly visible and could be detected and monitored using epifluorescent microscopy, fluorometry, and flow cytometry.

The investigators also evaluated using DsRed-Express (CLONTECH Laboratories, Inc., Palo Alto, CA), a new fluorescent protein derived from the coral *Discosoma.* In the first year of the project, cells were tagged with the original variant of the red fluorescent protein (DsRed), but the results were disappointing. DsRed-labeled cells required 72 hours to achieve maximum fluorescence; whereas, GFP-tagged cells or cells expressing blue and yellow variants reached maximum fluorescence in less than 24 hours. Due to the slow maturation of DsRed, it couldn't be used in combination with the other molecular markers. However, this problem was resolved when DsRed-Express, a variant of the *Discosoma* red fluorescent protein, became available. The investigators evaluated DsRd-Express in *E. coli*, and found that the new protein attained fluorescence as fast as those tagged with GFP and emitted similar intensity.

As a result of this LDRD project, a valuable research tool has been developed for evaluating the interaction of microbes with a variety of surfaces at the INEEL and other DOE sites. The work directly supports Subsurface Science Initiative projects that need to evaluate the role of bacteria in complex environmental samples and can be used to study biocorrosion and biofouling related to nuclear and conventional power systems.

# A New Hydrogeophysical Method for Characterizing and Monitoring Preferential Flow Paths in Complex Layered and Fractured Basalt

*Carolyn W. Bishop, Russell C. Hertzog, Mike D. Knoll*

***Improving non-invasive techniques for subsurface characterization***

PH106

Across the DOE complex, monitoring of contaminant transport in the subsurface has greatly exceeded predicted transport suggesting that current predictions contain serious errors. Prediction inaccuracy is related to computer model uncertainty. Model uncertainty is directly related to the ability to accurately describe the system being modeled. Specifically, the predictive failure can be attributed to scaling issues involved with hydraulic property estimation, limited ability to use proxy information, failure to understand vadose zone processes, and inability to monitor flow in preferential flow pathways.

The purpose of this LDRD is to evaluate and test an integrated hydrogeophysical methodology for identifying, characterizing, and monitoring preferential flow paths in complex, layered, and fractured basalt sequences. In particular, this research is vital to developing better techniques to characterize subsurface heterogeneity, estimate hydraulic properties, and characterize and monitor fluid flow and contaminant transport through extremely complex fractured rock systems.

Technical objectives for fiscal year 2003:

- Conduct crosshole seismic tomography in TAN-34 and TAN-35.
- Assemble well logs for TAN-34 and TAN-35.
- Conduct seismic Level-Run Analysis.
- Integrate crosshole seismic and radar data.
- Develop advanced data processing and inversion methods.
- Prepare and present research.

Seismic data collected in TAN-34 and TAN-35 in FY02 were analyzed and the data representing about the bottom quarter of both holes were found to be noisy and unpickable. Therefore, Boise State and INEEL researchers re-collected the data in FY03. This time, data quality was excellent as data points were stacked as many as 32 times.

In FY03, investigators focused on data analysis and integration. Seismic and radar data were successfully integrated with the goal of imaging the seismic and radar velocity structure of the fractured basalt aquifer between the TAN wells. Seismic and radar velocity values still need to be compared to geophysical well logs to investigate the relationship between seismic and radar velocity, neutron counts, bulk and fluid electrical conductivity, and porosity for water-saturated basalt.

The optical televiewer (OTV) logs, collected in FY02, provided oriented visual images of the rock around open holes, or “virtual core,” with millimeter-scale resolution. These images were used in conjunction with the caliper logs to identify and locate rubble zones and zones of dense basalt at well locations. The OTV images also provided information about the location, orientation, and aperture of fractures that intersect boreholes. Around some fractures, rock discoloration or staining is observed. This observation is used as a direct indicator of groundwater flow through the fracture. The OTV images also help to constrain geologic and hydrologic interpretations of other geophysical data. The neutron logs provide quantitative information about porosity variations near the borehole. Reflections in the single-hole radar data indicate the presence of near-vertical fractures, which in some cases intersect boreholes but in other cases do not.

The crosswell radar and seismic data show significant variations in the travel times and amplitudes of direct arrivals. The radar data were inverted to construct velocity and attenuation tomograms of the interwell region. The radar velocity tomogram also was used with a calibrated petrophysical model between radar velocity and water-saturated porosity to estimate porosity values between the wells. Zones in the radar tomograms that exhibit both low velocity and high attenuation are well correlated with the presence of either rubbly material (interbed zone) or abundant sub-horizontal fractures as observed in the OTV data. These zones also tended to exhibit low seismic compressional-wave velocities, high seismic attenuations, and high hydraulic conductivity values as inferred from borehole electromagnetic flowmeter measurements.

Spatial correlations between geophysical and hydrologic attributes were used to identify six zones of porous and permeable basalt. The zone that appears to have the greatest affect on flow and transport occurs at depths between 94 and 98 m and corresponds to a thick, weathered, rubble zone between two distinct basalt flows, as interpreted from the OTV and other hydrogeophysical data. The tomograms and well log data suggest that there is a dense basalt unit at depths between 98 and 110 m that extends between the wells and may be a barrier to the downward movement of contaminants and water.

The functional hydraulic components of the fractured basalt at this site include both conduits and barriers to flow. The dominant conduits are interflow rubble zones and zones of abundant, open, shallow-dipping fractures. Steeply dipping fractures, as interpreted from the single-hole reflection data, also may be important conduits for flow if they are laterally continuous. The dominant barriers are thick, laterally extensive, basalt flows with dense interiors.

By using geophysics to improve the density and resolution of subsurface sampling, targeting hydraulic measurements at specific zones, and taking into account the scale-dependent petrophysical relationships between geophysical and hydraulic parameters, the investigators demonstrated a methodology for identifying and mapping the key hydraulic components of a fractured basalt system (Fig. 1). Development of this method is a corroborative effort between researchers at the INEEL and Boise State University. Follow up research is planned.

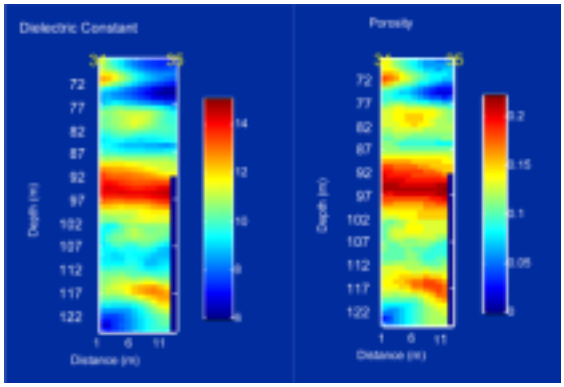


PN04-0004-151

*FIGURE 1. Dielectric constant and porosity tomograms for the region between wells TAN-34 and TAN-35.*

This LDRD research meets the science needs expressed by the National Research Council (NRC 2000) for improved understanding of subsurface processes, scale issues, and characterization and monitoring methods for DOE and other stakeholders.

# Characterizing Microbial Population Shifts in Response to Alternative Electron Donors and Their Effect on TCE-Dechlorination Efficiency

*David E. Cummings, Kent Sorenson*

***Creating dynamic bioremediation strategies***

GC131

Contamination of the subsurface environment with industrial chlorinated solvents such as trichloroethylene (TCE) threatens our nation's limited drinking water supplies. Some experts estimate that TCE is the most widespread subsurface contaminant in the U.S. and possibly the world. Active remediation of a TCE plume at the INEEL Test Area North (TAN) provides a unique opportunity for focused research on the mechanisms underlying the success of the biological treatment.

This LDRD aspires to understand the microbially catalyzed dechlorination of TCE to ethene at TAN, and examine the dechlorination efficiency of the TAN community when presented with alternative electron donors. The TAN community is dominated by the lactate-fermenting homoacetogen *Acetobacterium* and several other fermentative bacteria in the order *Clostridiales*. Also present are the dechlorinators *Dehalococcoides*, *Sulfurospirillum*, and *Trichlorobacter*. A TCE-dechlorinating laboratory consortium established with TAN groundwater was challenged with alternative electron donors and examined for dechlorination efficiency, community diversity, and active populations within the community. All electron donors tested (lactate, acetate, propionate, and butyrate) dechlorinated with equal efficiency in the short term (160 days). *Dehalococcoides* dominated nearly all treatments with the exception of propionate, which was dominated by *Sulfurospirillum*. Combined, these two populations comprised between 12-30% of the total populations present, and between 37-70% of the total active fraction of the amended microcosm communities. *Acetobacterium* spp. were only present in the lactate-amended consortium, and were only active while lactate was still available, suggesting that $H_2$/$CO_2$-fixing acetogenesis was not present to compete for $H_2$ with the dechlorinating populations. Methane remained below 120 µM in all microcosms.

In conclusion, lactate injections at TAN have selected for a community that ferments the lactate to acetate and $H_2$, followed by dechlorination of TCE to ethene coupled to acetate and hydrogen oxidation. This same community can catalyze TCE dechlorination with alternative electron donors that may be more efficient for long-term treatments.

Technical objectives for fiscal year 2003:

- Develop and apply methods to distinguish metabolically active populations from dormant populations in complex dechlorinating communities.
- Utilize the TCE-dechlorinating consortium, methods, and bioreactors developed in FY01-FY03 to determine the chemical and microbiological responses of the TAN consortium to alternative electron donors.

For three years, the goal of this research has been to define the TCE-dechlorinating, complex microbial community that has developed at TAN in response to regular lactate additions, and determine the response of this community to stimulation with electron donors other than lactate. Accomplishment of this objective has required the design of a new bioreactor that met specific criteria (FY01), establishment of a dechlorinating consortium in the bioreactor from TAN groundwater (FY01), and implementation of molecular biology techniques that allow the investigators to readily query the consortium for composition and activities (FY01-FY03). Furthermore, interpretation of the laboratory results has required thorough characterization of the community extant in the TAN subsurface (FY02).

Work in years one and two has indicated that the dechlorinating community in the field is predominated by acetogenic and fermentative Gram-positive *Bacteria* (*Acetobacterium* and *Clostridium* spp.) that produce acetate, propionate, butyrate, and molecular hydrogen from lactate. In addition, three populations of dechlorinating *Bacteria* (*Sulfurospirillum*, *Trichlorobacter*, and *Dehalococcoides* spp.) have been identified. *Dehalococcoides* is the only single organism known to completely dechlorinate PCE and TCE to ethene, and some have speculated that it is essential to achieve complete dechlorination in the field. The *Archaeal* portion of the community consists exclusively of methanogens (methane-producing organisms), and is dominated by acetoclastic (acetate-utilizing) species. Carbon and electron flow from lactate, then, appears to proceed first through acetogens and other fermenters that generate acetate, propionate, butyrate, and hydrogen. Propionate and butyrate are slowly fermented to $CO_2$ and hydrogen. The resulting pool of acetate and hydrogen supplies electrons for the dechlorinating populations as well as methanogens. Methane is probably a dead-end in terms of electron flow to

chloroethenes, and management of the site should include a plan to minimize methanogenesis and maximize dechlorinating populations.

The laboratory consortium is very similar to the natural community at TAN, with a predominance of acetogenic, fermentative *Bacteria*, and acetoclastic methanogens. The two systems shared in common several members of the *Clostridiales*, including a phylotype affiliated with *Acetobacterium carbinolicum* and four others that were not identifiable. Additionally, two *Sphingobacteriales* phylotypes that were present in the field were also present in the laboratory consortium, as was one of the two *Spirochaetales*. PCR amplification with *Dehalococcoides*-specific primers confirmed their presence in the laboratory consortium. Absent from the laboratory consortium, however, were the dechlorinating *Trichlorobacter* and *Sulfurospirillum* populations present in the field.

During the course of this work it became apparent that a method to distinguish metabolically active populations from dead or dormant ones would be of immense value. To accomplish this, the investigators examined not only DNA from the dechlorinating consortia, but also RNA. Specifically, the investigators amplified the 16S ribosomal RNA (rRNA) for which the 16S rRNA gene (rDNA) encodes. This molecule is only produced by metabolically active cells. Thus, it was possible to identify which populations in a complex community were active under a given set of conditions, and relate the active populations to chemical transformations catalyzed under those conditions.

For the pivotal experiment of this study – determining the influence of alternative electron donors on dechlorination efficiency and microbial community structure – cellular RNA and DNA were interrogated. The dechlorinating laboratory consortium originating from TAN groundwater was stimulated with lactate, acetate, propionate, or butyrate, and analyzed for dechlorination efficiency, DNA-based community structure (rDNA), and RNA-based ***active*** community structure (rRNA). All four electron donors supported TCE dechlorination with equal rates of ethene production (Fig. 1). In terms of electron transfer efficiency (unit electron donor used per unit TCE dechlorinated), however, propionate proved the most efficient followed by butyrate, acetate, and lactate.

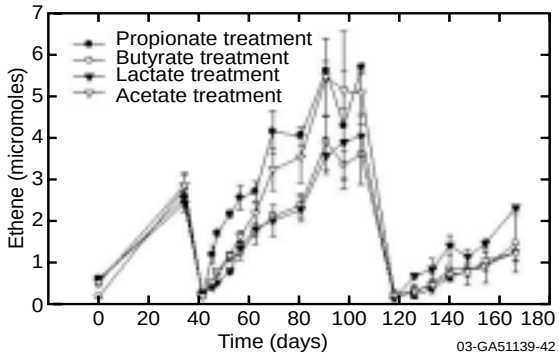


*FIGURE 1. Production of ethene by the TAN consortium with various electron donors.*

Hydrogen production from electron donor fermentation is thought to play a critical role in sustained dechlorination. Maximal $H_2$ concentrations for butyrate and propionate fermentation were near 150 nM, while as much as 240 nM $H_2$ was generated from lactate fermentation and 275 nM $H_2$ was generated from acetate. Conversely, methane is considered a dead-end for electron flow, and is thus avoided. The least methane produced (maximal concentration during the fermentation) was 75 μM from propionate followed by 100 mM from lactate, 110 μM from butyrate, and 120 μM from acetate. It appears that, while acetate generated the highest $H_2$ concentrations (desirable), it also generated the highest methane concentrations (undesirable). Lactate, on the other hand, produced intermediate concentrations of both.

Microbial diversity and activity in the different microcosms were analyzed with T-RFLP profiles generated from rDNA as well as from reverse transcription of the rRNA itself, which is only produced by metabolically active cells. An example of a combined T-RFLP stemming from both rDNA and rRNA present in the microcosms is provided in Figure 2. In all cases, the diversity of rDNAs was greater than the diversity of rRNAs. The lactate-stimulated microcosms supported the most diverse microbial community with 47 distinct rDNAs and 24 rRNAs, indicating that approximately half of the populations present were metabolically active at the time of sampling. The acetate-stimulated microcosms showed similar diversity, containing rDNA from 42 populations and rRNA from 19 populations. Diversity of the propionate- and butyrate-stimulated microcosms was approximately half that of the lactate and acetate microcosms.

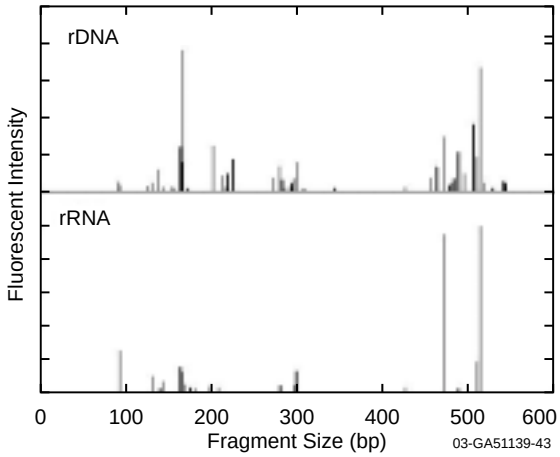


*FIGURE 2. Terminal restriction fragment length polymorphism (T-RFLP) analysis of the TCE-dechlorinating microbial community stimulated by acetate. rDNA represents populations present in the community. rRNA represents metabolically active populations.*

The dechlorinating taxa *Dehalococcoides* and *Sulfurospirillum* spp. were abundant in all treatments. *Dehalococcoides* was most abundant, surprisingly, in the acetate-amended microcosms in which it comprised 13% of the rDNA and 32% of the rRNA. In other words, 13% of the total community present in the acetate-amended culture was *Dehalococcoides*, and fully 32% of the active cells were *Dehalococcoides*. The composition in the other three treatments was very similar to that of the acetate culture. *Sulfurospirillum* also was present in all four treatments, but was clearly most active in the propionate-amended culture, comprising 40% of the active cells. It was least important in the lactate-amended consortium, making up only 5.5% of the active community. The TCA degrader *Trichlorobacter thiogenes* was relatively unimportant in all treatments, with the possible exception of the acetate microcosms in which it comprised 5.5% of the active community.

The homoacetogen *Acetobacterium* is numerically the most important population in the field at TAN where lactate is provided as the electron donor to support dechlorination. The lactate microcosms contained 24% *Acetobacterium* rDNA, but only 2% *Acetobacterium* rRNA at the time of sampling. This finding suggests that *Acetobacterium* is only important for the transformation of lactate to acetate after which it becomes metabolically dormant. It is further supported by the lack of this population in any of the other microcosms. This finding has important implications for electron competition, suggesting that the acetogens present at TAN do not compete with dechlorinating populations for available hydrogen.

In the late 1990s, an alternative strategy to affect TCE dechlorination at Test Area North was proposed in which lactate, a rich source of carbon and electrons for microbial activity, would be added directly to the subsurface to stimulate in situ anaerobic reductive dechlorination by native microorganisms. A pilot test was successful, and the Record of Decision for TAN was amended to implement this method as the selected remedy. Already, millions of dollars in operation and maintenance costs have likely been saved, and the remedial action should be completed with further cost savings and in a shorter timeframe. This LDRD-funded research was initiated to elucidate the mechanisms whereby dechlorination is occurring and to examine the potential use of alternative electron donors with the goal of improving both understanding and efficiency of the treatment. Both of these objectives have been met and even surpassed. The results from the last three years of research have already begun to influence the way the INEEL and the nation think about and manage TCE-contaminated sites.

Much of the new knowledge is being applied by North Wind Environmental, Inc., a local Idaho Falls company that has contracts with the DOE, DoD, and EPA to clean up TCE/PCE-contaminated sites across the nation. At the same time, the INEEL has been in the spotlight of dechlorination technology, and core competencies at the laboratory have been advanced. The INEEL collaboration with North Wind should continue for many years in other areas. Four manuscripts describing the research performed under this LDRD will be published in international, high-visibility journals (*Applied and Environmental Microbiology* and *Environmental Science and Technology*).

# Uptake and Translocation Patterns of Strontium by Sagebrush Steppe Ecosystem Plants

*Melinda A. Hamilton*

***Using plants as bio-indicators***

GC149

Radionuclides and heavy metals are primary contaminants of concern at the INEEL and many DOE sites. Soil and groundwater contaminated with Strontium-90 pose a significant challenge in environmental restoration and long-term stewardship at each of these sites. Two essential components to long-term management of legacy waste sites are the 1) monitoring of sites in which residual hazards remain after cleanup is completed, and 2) reducing the technical uncertainty associated with predictions of contaminant fate.

Plants may play a critical role both as a tool for monitoring contaminants and as an agent for affecting their potential migration. Although phytoextraction (plant uptake of metals/radionuclides) is widely known to occur, only gross uptake data has been published, and many assumptions are used when trying to use plants as bio-indicators.

This LDRD is developing a scientific basis for using plants as accurate and reliable indicators of surface and near-surface contaminant concentrations, and changes in contaminant mobility over time. The first objective is to develop a fundamental understanding of the impacts of environmental factors and plant physiology on Sr-90 uptake and translocation. The establishment of this new information will aid in the development of accurate and reliable predictive models that could elucidate changes in contaminant risk based on combinations of environmental and seasonal factors. The second objective is to develop a non-destructive, aboveground imaging system that will provide information about changes in plant development and biomass concentrations of $^{90}Sr$.

Technical objective for fiscal year 2003:

- Examine the uptake and partitioning of Sr in crested wheatgrass grown in soil columns, and compare the results to those obtained from hydroponic studies.
- Determine the partitioning of Sr in crested wheatgrass between bound and unbound fractions by measuring total and soluble Sr in plant tissues.
- Determine if there are correlations between spectral transmission and Sr concentrations in crested wheatgrass leaves.

To understand and ultimately predict Sr-90 uptake and translocation in crested wheatgrass, actual Sr uptake rates and extents, Sr translocation patterns, and Sr effects on crested wheatgrass must first be understood. Studies to elucidate these phenomena, as well as parallel studies designed to define the ability to identify Sr presence in leaves with spectral imaging techniques, were undertaken.

Working collaboratively with Dr. Bruce Bugbee of Utah State University (USU), two hydroponic greenhouse trials were completed with crested wheatgrass. In trial 1, three available Sr concentrations were compared, 0, 100, and 1000 micromolar, four with 4 replicates of each treatment in a randomized block design. In trial 2, four Sr concentrations were included, 0, 3, 10, and 100 micromolar, with three replicates of each treatment in a randomized block design.

Crested wheatgrass seedlings were planted in quarter-strength Hoaglands nutrient solution and grown under constant greenhouse conditions. Strontium was added to the desired solution concentration as Sr-Cl salt. Calcium concentration was maintained at 1 mmol available solution Ca in all treatments. Nitric acid (HNO3) was added to maintain pH. Temperature, humidity, and solution pH were monitored continuously.

Throughout these studies, weekly samples of leaves, stems, and roots were collected and analyzed for Sr and Ca concentrations, other trace metal and nutrient concentrations, and biomass (dry wt.). Plant growth was measured by several methods including biomass, radiation capture, transpiration, and NO3 addition requirements. The heads of the plants also were analyzed once they appeared at about seven weeks.

Crested wheatgrass also was grown in soil columns to determine the effect on Sr uptake and partitioning, as well as to identify any impacts ammonium may have on that translocation. Two sandy loam soils with similar native Sr content (~20 mg/kg) were used. One of the soils had a total Ca + Mg concentration that was ~50% higher than the other. Four treatments were applied per each soil type, for a total of eight treatments. Each treatment was replicated three times, for a total of 24 columns. The four treatments were: 1) planted and watered with ammonium and nitrate, 2) planted and watered with nitrate only, 3) unplanted and watered with ammonium and nitrate, and 4) unplanted and watered with nitrate only. Each of the two soils was mixed with sand (50/50, v/v) to improve drainage. To minimize the natural bacterial

transformation of ammonium to nitrate by nitrification, nitrapyrin was applied to the columns receiving ammonium every eight weeks.

Hydroponics Sr uptake studies ran until the crested wheatgrass plants were approximately nine weeks old. Results indicate that the concentrations of Sr tested, had little to no effect on measured parameters of plant growth, with the possible exception of the highest concentration (1 mmol). Sr uptake was similar to Ca uptake on a molar basis as well as on a translocation basis. Both Sr and Ca were found to concentrate primarily into the crested wheatgrass leaves (50% w/w) with stems, roots, and heads containing lower concentrations respectively. Sr uptake was fairly constant with biomass increase (Fig. 1).

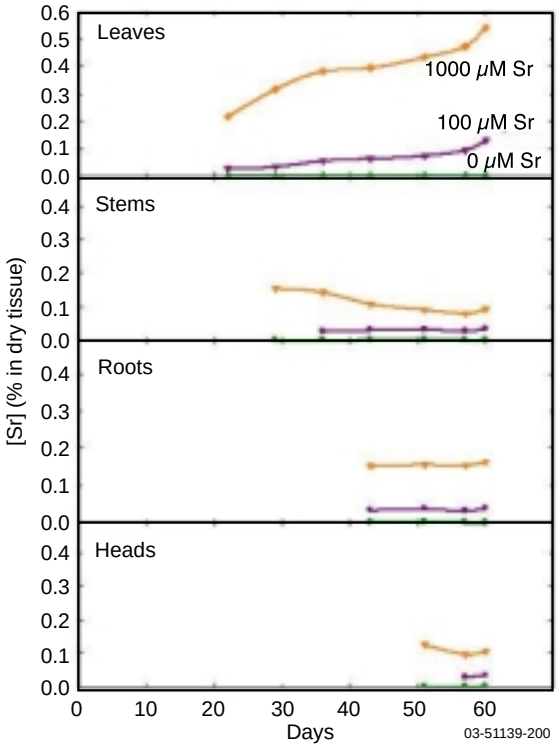


*FIGURE 1. Sr partitioning in crested wheatgrass plant structures over time of growth.*

The presence of ammonium in the soil columns was consistently detected only in the "unplanted with ammonium added" columns, indicating that the ammonium in the planted columns was assimilated by the plants. Sr, Ca, and Mg were found at higher concentrations in the leachates of "planted with ammonium added" columns. This is likely due to the fact that as plants take up ammonium, they acidify the rhizosphere, which could result in higher cation solubility. Sr, Ca, and Mg concentrations were not influenced by soil type, elevated ammonium, or sampling method (Fig. 2).

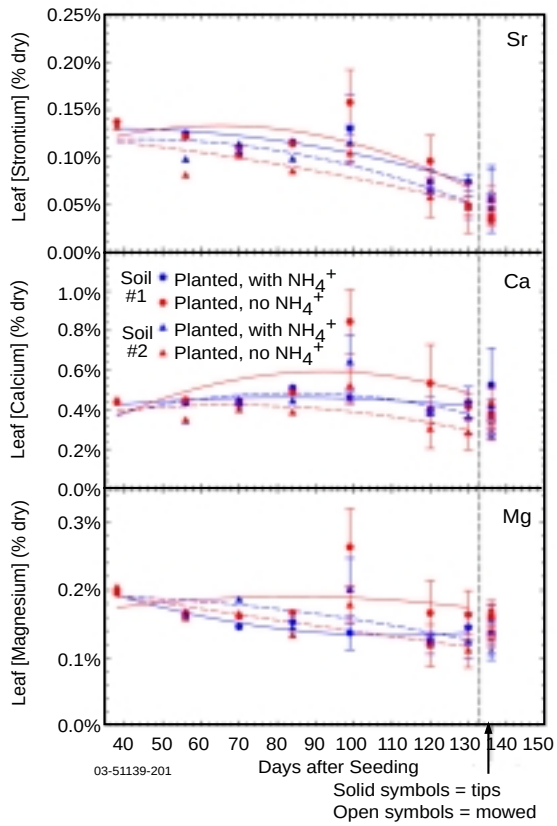


*FIGURE 2. Sr, Ca, and Mg content of crested wheatgrass leaves over time. The final data point is from samples that were obtained by mowing rather than leaf tip clipping.*

Spectral imaging, to determine if the presence of Sr in the plant leaves could be detected by light transmittance/reflectance measurements, was also conducted at USU's Crop Physiology Lab. This was done by performing spectral reflectance measurements on crested wheatgrass leaves that contained high Sr concentrations due to plant uptake, and comparing the results to control plant leaves that were grown in the absence of Sr. Wavelengths of 450 through 850 (nm) were used for these measurements and compared by standardizing to 820nm.

The development of a capability to detect high concentrations of Sr in crested wheatgrass leaves was not completed during the first year of work. While spectral reflectance varied with Sr concentrations, the differences were not statistically significant at the low Sr concentrations used. It is expected that by using a broader range of wavelengths (up to 2350 nm), spectral signals at these low Sr concentrations will be more pronounced and significant differences will be detected. Development of this method will continue in next year's work (Fig 3).

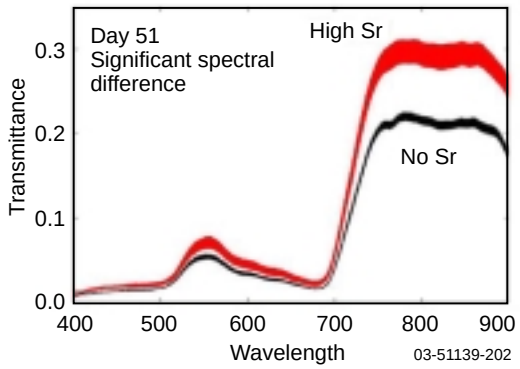


*FIGURE 3. Comparison of transmittance measurements for crested wheatgrass leaves with and without Sr incorporated.*

Results of this research indicate that Sr is readily taken up by crested wheatgrass (just as Ca is); however, it does not result in easily detectable physiological or morphological changes in the plant. This suggests that crested wheatgrass growing in Sr-90 contaminated areas is likely to take up Sr-90, but until nondestructive measurement techniques are developed, would require harvesting, digesting, and analyzing the samples to verify uptake rates and extents. Therefore, research to date still indicates a need for a "screening method" and some predictive tools for determining the rate of Sr-90 uptake and entry into the food chain. This research is still on track to provide these tools.

Long-Term Stewardship of DOE sites in the West will need to rely on low-cost methodologies to constantly evaluate risks associated with leaving low-levels of contaminants in place. This LDRD is designed to provide a basis for doing just that for Sr-contaminated surface soils initially, and then, potentially, for other contaminants of concern. The first step toward this goal was to establish baseline data for Sr uptake by crested wheatgrass. This goal was accomplished.

Three areas for follow on work are being considered and will be evaluated as the research progresses. The three topics are: follow-on fieldwork at a Sr-contaminated site at INEEL to validate the model, greenhouse studies with other sagebrush steppe ecosystem plants and other contaminants and expansion of the model to include these plants and contaminants, and development of remote sensing for bioindicator applications. The DOE's Environmental Management (EM) Office is a potential sponsor for field validation of the model. In addition to continuing the established collaboration with Utah State University, this project intends to collaborate with remote sensing projects at the INEEL to explore approaches for remotely obtaining spectral data that can be used to estimate plant concentrations of contaminants.

# Hybrid Nanocomposite Materials as Subsurface Permeable Reactive Barriers

*Mason K. Harrup, Michael Jones, Linda Polson, Byron White*

***Designing novel methods of contaminant containment***

GC111

The development of effective subsurface barriers could be a tremendous aid for the containment of contaminants in the vadose zone, directly solving one of DOE's toughest problems at the INEEL Site.

This LDRD is investigating the effectiveness of recently developed, novel nanocomposite materials for subsurface permeable reactive barrier (PRB) applications. These new materials are Type I nanocomposite. That is, they are preformed organic polymers embedded in an inorganic matrix without significant covalent bonding between the components. The required properties for these materials to function efficiently are: 1) a tunable water passing rate to approximate the hydraulic conductivity of the subsurface environment where the PRB will be placed, 2) sufficient mechanical strength (both wet and dry) to maintain barrier integrity, 3) the ability to incorporate selective metal sequestration agents so that they remain active – yet do not leach from the barrier, and 4) to be deployable through direct injection methods such that trenching is not needed. Additionally, there is a need to keep the technology as low cost as possible, while remaining reliable. Results obtained from the third year of this multi-year project show that this technology has considerable promise for in situ subsurface remediation of metals.

Technical objectives for fiscal year 2003:

- Set up a subcontract and continue collaboration with Dr. Robert Paine at the University of New Mexico (UNM) to provide new sequestration agents for incorporation into nanocomposites.
- Incorporate the new sequestration agents into nanocomposite systems and evaluate.
- Examine at least five new hydrophillic polymer families, formulate into nanocomposites and compare to the existing systems.
- Examine water flow behavior through leading nanocomposites. Reevaluate contaminant sequestration (particularly cesium) in a flowing system.
- Characterize representative barrier materials.

*New Nanocomposite Formulations*. The theoretical work performed during last year's effort revealed that the specific chemical affinity of any molecule can be described as a summation of the individual "parts," as described by group contributions. Using this group contribution model, it was determined that the most relevant chemical affinities of a molecule may be described in terms of Hansen solubility parameters where the polar ($\delta_p$), dispersion ($\delta_d$) and hydrogen bonding ($\delta_h$) aspects of chemical affinity are represented. Since Type I nanocomposites were desired, and since one of the largest contributors to $\delta_h$ is the hydroxyl functionality, this parameter could reasonably be ignored for these initial studies. Fourteen polymers were characterized for $\delta_p$ and $\delta_d$ using published procedures, and the results of this study were used to select five new polymer families to investigate for suitability in new nanocomposite formulations. New polymer systems that were explored were: cellulose acetate, (CA) polyepichlorohydrin, (PEC) polyepichlorohydrin-co-ethylene oxide, (PEC-PEO) polyacrylamide, (PA) and polyacrylamide-co-acrylic acid (PA-AA). Each of these new formulations was ultimately found to be inferior to the original polyvinyl alcohol (PVA) and polyvinyl acetate (PVAc) systems for various reasons. The CA was found to be too hydrophobic to dissolve in water or water/ethanol mixtures in sufficient levels to form a suitable nanocomposite. Both PEC and PEC-PEO also suffered from solvent compatibility problems and no suitable nanocomposites were formed. Both the PA and the PA-AA were solvent compatible and nanocomposites were formed out of each of these systems. The nanocomposites formed from the PA-AA were found to be exceptionally brittle. This likely was due to direct covalent binding between the ceramic and the polymer phases, joined through the acrylic acid functionality of the polymer component. Due to this poor mechanical performance, this system was not investigated further. Finally, nanocomposites of the PA were formed. These were of acceptable mechanical integrity when dry, but upon immersion in water the extreme hydrophilicity of the PA caused the nanocomposite to swell greatly and shatter. This was caused by the internal hydrostatic pressure created during water uptake overcoming the mechanical strength of the ceramic network in the nanocomposite. Based upon these results, the

balance of the research effort was concentrated on the PVA and PVAc systems.

*New Sequestration Agents*. A suite of new sequestration agents, applicable for the removal of actinides (such as Am and Pu), was obtained and evaluated. The first of these suites were the thiophosphinic derivatives. Two of these agents were chosen, as they are known to be active in the selective extraction of actinides in two-phase liquid-liquid extraction processes associated with nuclear fuel processing (Figure 1).

PN04-0004-155g

*FIGURE 1. Nanocomposites formulated with the new sequestration agents. In the left nanocomposite, the sequestration agent (a thiophosphinic acid derivative) has phased out of the material during synthesis. In the right nanocomposite is incorporated one of the tripodal sequestration agents exhibiting a homogeneous distribution throughout the matrix.*

Nanocomposites based on both PVA and PVAc systems were synthesized with these sequestration agents. Although the nanocomposites were successfully formed, the low polarity of the sequestration agents caused the agents to phase out of the system during the final drying process, forming crystals on the surface of the nanocomposite. This was found to be ineffective for metal ion capture (in model studies with Eu) as the agents were not entombed within the nanocomposite and simply washed off the surface.

The second suite of two agents evaluated was tripodal ligands, also well studied in liquid-liquid extraction processes and known to be highly effective in binding the actinides. Again, nanocomposites based on both PVA and PVAc systems were synthesized with these sequestration agents. In each of these composites, there was no observed phase-out behavior and the composites were then subjected to metal uptake trials. In these trials, Eu was used as a non-radioactive model for Am. Poor ion uptake was noted for each of these systems, generally between 8-15% of the theoretical uptake values calculated from the binding stoichiometry. After discussions with Dr. Paine, it was concluded that this poor efficiency was likely due to pH effects. These tripodal ligands are known to function more effectively at low pH, yet these studies had to be conducted at neutral pH, the pH of common groundwater. Because of this practical limitation low pH studies were not conducted.

*Flowing Barrier System Studies*. Work with both the PVA and PVAc systems was expanded to introduce a flow component to assess the breadth of water flow rates achievable. Laboratory scale barriers were formed in sea sand to ensure that the barrier material zone was the zone limiting total hydraulic conductivity. The setup is shown in Figure 2.

PN04-0004-155f

*FIGURE 2. Left, close-up of a single barrier column, sand above and below, with a PVAc/AMP barrier (slurry emplaced) in the middle. Right, entire setup including water introduction apparatus.*

The barrier columns were formed in a variety of methods, but the one technique that functioned the best involved grinding the nanocomposite materials

into small fragments and then slurring them with water. This nanocomposite/water slurry was then injected into the column to form the distinct barrier zone. (Fig. 2, left) Water was then flowed through the column and the rates measured. It was found that the rate could be varied greatly, from nearly zero measurable flow (70 µl/minute) up to a flow that matched blanks run with pure sea sand (29ml/min). *This range represents a variance in flow rates of over 400x*. This wide range of tunable hydraulic conductivity is one of the critical properties needed for practical deployment of this technology. Further flow studies were conducted with these two systems employing the cesium sequestration agent ammonium molybdophosphate (AMP). At the time of this writing, the raw cesium sequestration data has been collected on six systems, with varying AMP concentration, cesium concentration, and flow rates. These data will be analyzed and presented in peer-reviewed literature in the near future.

The new type of subsurface barrier resulting from this LDRD research could be of tremendous aid for contaminants in the vadose zone – directly solving one of the DOE's toughest problems at the INEEL Site. The work has already attracted the interest of environmental firms in Oregon and Hong Kong. This project also represents collaboration with the University of New Mexico, strengthening the INEEL's technology. This LDRD has produced one patent application and another is in the IDR stage, capturing the key intellectual property developed in this project.

# Advanced Technology for Mapping Subsurface Water Conductivity

*Gail Heath, John Svoboda*

***Combining two techniques for better subsurface characterization***

GC108

Traditional subsurface resistivity or conductivity distribution mapping is a well-established subsurface characterization method. This method's potential resolution is not exploited to the fullest extent because the method is based only on bulk DC resistance measurements between multiple pairs of two points with subsequent data processing to estimate the subsurface resistivity distribution.

This LDRD is developing a unique variation of the existing technology that combines the traditional DC resistivity measurements with surface magnetic field measurements where the magnetic field is generated by subsurface current flow. Resistivity measurements are accomplished by passing current through a system of permanently installed subsurface electrodes at varying depths in the volume of interest. Surface magnetic field measurements are made with a 3-axis flux-gate magnetometer's output that is synchronously detected with the transmitted subsurface current. Magnetic field measurements are made at each map point for each frequency and electrode pair combination. Inversion algorithms will generate conductivity maps by utilizing the spatial magnetic data as well as the resistivity data. This data would then be used to determine the depth to groundwater, identification of contaminant plumes, and contaminant migration through comparison with background and historical conductivity values.

Technical objectives for fiscal year 2003:

- Design and test a magnetic field measurement system.
- Develop a magnetic field data post-processing package.
- Simulate electric and magnetic field data sets.
- Perform tests on actual field-collected data sets.
- Develop a 3-D inverse routine that combines magnetic and electric field measurements.

Electrical Resistance Tomography (ERT) is a technique for reconstruction of subsurface electrical resistivity distributions. The electrical resistivity distribution can lend information on the moisture content and distribution, movement of plumes, the geology, temperature, and most manmade materials present between the boreholes. As a result, ERT data provides good information on targets of interest between boreholes. The surface magnetic field measurements provide an orthogonal magnetic field surface view of the plumes and other conductive bodies between and outside the boreholes providing more information with less cost over existing systems. The data sets are collected by transmitting electrical current into a pair of electrodes while the electrical potentials are measured at other electrode pair combinations and the magnetic field is measured at the surface or within bore holes. ERT and surface magnetic field data sets have been collected at the new meso-scale test bed located at the Jefferson Canal Site. Baseline data collection was performed to test the INEEL B-field system and its incorporation into the Zonge ERT system. Software, primary field correction, and data interpretation have been tested using the data sets collected at the meso-scale site at Jefferson Canal Site.

During FY03, a synchronously detected, spatially resolved, 3-axis vector B-field measurement system was designed and incorporated into the operation of a Zonge GDP-32 resistivity measurement system for simultaneous surface magnetic field and subsurface electric field measurements.

The magnetic field measurement system consists of a 3-axis flux gate magnetometer, three lock-in amplifiers, and a Zonge GDP-32 ERT receiver. Alternating current (8 Hz) is passed through the subsurface volume of interest via electrode pairs located at several depths in each borehole pair. The subsurface excitation current is controlled and transmitted via the transmitter portion of the Zonge receiver. The Zonge receiver simultaneously measures the voltage across all non-transmitting electrode pairs. This constitutes the potential field data used by the inversion code. The 3-axis magnetometer output is fed to the lock-in amplifiers as unknown input, which allows for synchronous detection of any AC magnetic fields that are synchronous with the subsurface current excitation. The lock-ins direct current output is fed to spare Zonge receiver inputs where the magnetic field data is measured and recorded with the potential data. This constitutes the magnetic field data used by the inversion code.

Synchronous detection allows for the extraction of extremely small signal levels buried in noise. The lock-in amplifiers derive their reference from the transmitted subsurface current signal. All other fields not synchronized with the reference are averaged to zero. This technique provides detection of vector magnetic field components due to milliamps of current flow through subsurface volumes.

A post-processing package that corrects the magnetic field vector data for sensor orientation, calculates the inphase and quadrature components, and corrects for the B-field associated with the surface conductors that deliver the subsurface current was developed.

A full physics 3-D forward model capable of modeling subsurface electric fields and surface magnetic fields due to subsurface current flow was developed by Dr. David Alumbaugh of the University of Wisconsin and Dr. Greg Newman of Sandia National Labs. The model is capable of calculating electric and magnetic fields in mediums characterized by conductivity, permeability, and permitivity. The Newman-Alumbaugh model, as well as field data taken at the Jefferson Canal Site, is being used as a source for generating data sets capable of testing inversion code robustness.

Field data sets were collected at the meso-scale test site located at the Jefferson Canal Test Facility. Software, primary field correction, and data interpretation have been tested using the data sets collected at Jefferson Canal Site. The data sets include background with ERT and MMR for background, steel and copper targets. Figure 1 presents the results for ERT over the steel target that the ERT data has a difficult time distinguishing. The ERT method failed to see the target due to the location and orientation of the steel plate. Figure 2 shows the results of the same target and location as Figure 1 with the addition of the MMR data. The combined data sets, (ERT, MMR) show the steel target at the correct location as seen by the response in Figure 2. Resolution is increased with the MMR data incorporated.

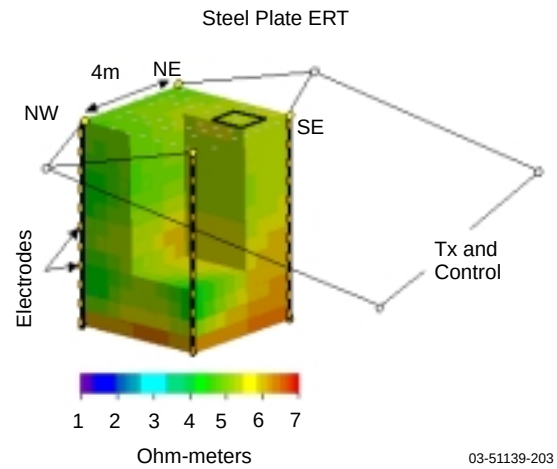


*FIGURE 1. Inversion results from ERT data alone.*

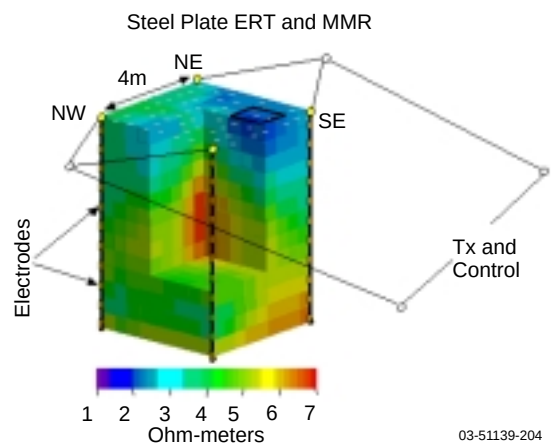


*FIGURE 2. Inversion results from MMR and ERT data.*

Closely related to ERT is the MagnetoMetric-Resistivity method (MMR) in which measurements are made on the magnetic fields generated by a more-or-less steady state electric subsurface current. The MMR method has seen occasional use in mineral exploration but has seen little, if any, application in engineering or environmental applications. One problem is that the equipment is more expensive than standard resistivity equipment

and is not readily available. As a stand-alone method, MMR has some significant limitations. Even for simple bodies the MMR responses are fairly complicated and thus interpretation is more difficult. A fully 3-D inversion routine is necessary to interpret the ERT/MMR data in terms of subsurface conductivity. In addition, the interpretation of ERT/MMR results is non-unique. The problems in uniqueness can be overcome by combining the magnetic and electric measurements in the same inversion code. Key to this research is that ERT is very good at delineating large structures such as layered earths; whereas MMR is more sensitive to small, 3-D structures. Therefore, combining the two methods will improve the overall resolution of the ERT method alone.

The project supported development of a fully 3-D inverse routine that combines magnetic and electric field measurements. The algorithm is designed and coded by Multi-Phase Technologies of Reno, NV, and is based on a 3-D finite difference forward algorithm. The magnetic fields are modeled by applying the reciprocity theorem to model the electric fields induced by a coil of unit moment at a frequency of one radian per second. Using this method allows for an adjoint formulation for calculating sensitivities of both magnetic and electric fields with respect to changes in the conductivities of individual cells within the finite-difference mesh.

This LDRD supports Environmental Quality and Energy Security by allowing for the mapping of subsurface contamination plumes and water, steam, and /or CO2 floods. Current collaboration includes the University of Wisconsin and Multiphase Technologies of Reno, NV. Both are involved with inversion code development.

# Electrical Resistivity Imaging to Define Preferred Flow Paths in a Heterogeneous, Layered Vadose Zone

*Gail Heath, Russ Hertzog*

***Understanding flow and transport in the vadose zone***

GC133

An important component of the hydrogeologic system at the INEEL is a thick (250 to 1,000-ft) unsaturated zone between the ground surface and the Snake River Plain Aquifer. This unsaturated zone (or vadose zone) presents a significant hurdle to assessing the impact of operational activities, waste disposal, and past contaminant releases on the aquifer. The DOE's Vadose Zone Science Program is being developed to coordinate interdisciplinary research for the purposes of improving understanding of processes occurring between land surface and underlying aquifers, and to develop the tools for using this knowledge to accurately predict and monitor the movement and transformation of contaminants in this region. The keys to successful environmental management lie in enhancing scientific understanding of the processes important for predicting and controlling vadose zone transport and remediation.

A search of the DOE EM-50 Science and Technology Coordination Group (STCG) "Technology Needs" database identified 17 technology needs associated with flow and transport in the vadose zone at Los Alamos, Sandia, Hanford, Nevada, and the INEEL. There are needs for a better understanding of vadose zone processes with specific areas identified in: conceptual modeling of complex environments, predicting behavior of contaminants in dynamic transport processes and complex geology, innovative characterization techniques, and basic data or methods to support long-term decisions.

This LDRD is developing conceptual models that will provide a significant advancement towards meeting many of these vadose zone science needs.

Technical objectives for fiscal year 2003:

- Select and install arrays for characterization of subsurface hydrologic processes.
- Collect data from the arrays using the prototype system.
- Design and implement new operating system for autonomous operation of the system.

Electrical resistance tomography (ERT) is a technique for reconstruction of subsurface electrical resistivity distributions. The electrical resistivity distribution can lend information on moisture content and distribution, movement of plumes, the geology, temperature, and most manmade materials present between the boreholes. The surface magnetic field measurements provide an orthogonal magnetic field surface view of the plumes and other conductive bodies between and outside the boreholes providing more information with less cost over existing systems. Transmitting electrical current into a pair of electrodes while the electrical potentials are measured at other electrode pair combinations results in the data sets.

The purpose of the project is to monitor infiltration on a pair of 61 m by 61 m ponds on the INEEL Site west of Idaho Falls, Idaho. The two ponds are separated by approximately 15 m and one pond is directly north of the other. The ponds lie on top of about 17 m (56 ft) of alluvial sand and gravel underlain interbedded basaltic lava flows and sediments. There are significant sediment beds at around 40 m and 60 m (Street et al. 2002) within the basalt flows.

Prior to flooding the site, five electrode arrays were installed: three vertical electrode arrays (VEAs) and two surface electrode arrays. One of the VEAs was centered between the ponds. The two surface arrays extend outward from this VEA along east-west lines between the ponds. Each surface array includes thirty electrodes at 6 m intervals. The other VEAs were located approximately 150 m apart in an east-west direction and 30 m south of the east-west line formed by the surface arrays. This positioned the VEAs one on each side of the south percolation pond, approximately 30 m distant from the pond, and at approximately 1/3 of the south extent of the pond. The depth of all three VEAs was 70 m and electrodes were placed at 2.5 m intervals.

Various electrical data were available for collection. The significant data collected during each time period include Schlumberger sounding/profiling along the surface arrays, common-well and cross-well dipole-dipole data, and cross-well horizontal transmitters with vertical dipole receivers. Pole-dipole-like data also was collected that used a vertical dipole in one VEA, a single electrode in a second well, and the reference electrode as the bottommost electrode in the third VEA.

The data collection schedules included a pre-flood background data set collected the morning of June 18. Subsequently data collection intervals were approximately every 5 hours. Continuous

cycling over each 24-hour period resulted in 5-6 collection intervals per day. Each collection interval started and ended autonomously.

Conductivity changes in the subsurface show the speed of fluid movements as well as the location of ponding. Figure 1 shows a wetting front moving through the system. The solid is wrapped around the conductivity values that are a 20% change over the background data. The ERT data will be compared to the hydrologic information to provide more insight into the geophysics. Quantification information could be extracted from the 3-D geophysics data and integrated into the hydrology point source data to give better wide-scale pictures of the subsurface processes.

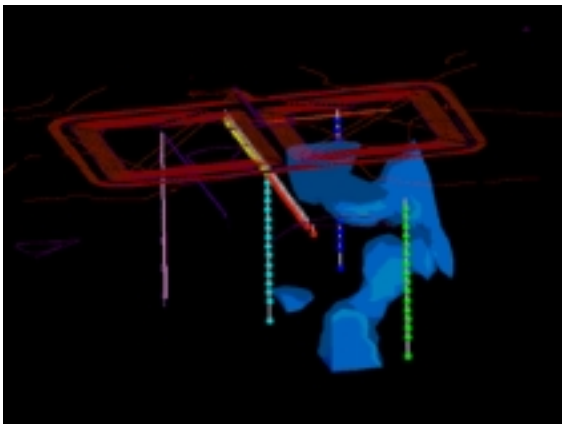

PN04-0004-155j

*FIGURE 1. A wetting front is shown moving through the subsurface.*

There are substantial advantages to applying a fully 3-D, autonomous system to long-term monitoring. Although all of the techniques possible with such a system have not been fully implemented, a prototype system successfully collected data using a variety of different arrays.

Data were collected over a two-week period essentially without an operator on the site. The data were used successfully to monitor the infiltration of the water in the interbedded sediment and basalts at the INEEL.

During the operation it was found that there was a need to develop a more sophisticated operating system dedicated to autonomous operation. This was addressed and a new operating system was written. The experience from using this method suggests that, in autonomous systems, the system needs to be able to continue operation, rather than halt, for any situation that does not threaten to damage the system, even in cases where only part of the data may be collected. Ideally, such a system should be able to adapt to problems and, if necessary, contact the operators remotely when problems occur.

ERT has been used widely in subsurface hydrology; however, some major limitations still exist to its optimum application. Specifically, data acquisition needs to be improved, and the combined effects of multiple components that contribute to the bulk electrical conductivity (e.g., water content, solute concentration, and medium properties) must be identified to allow for more quantitative analysis of heat or mass transport. This can be achieved through improved survey design that combines hydrologic understanding in the identification of suitable ERT targets and optimization of data acquisition for hydrologic interpretation. This LDRD demonstrates that wise selection of the arrays composing a survey can improve the ability to characterize subsurface hydrologic processes. The selection is based on comparisons of the sampling volumes of surface-based ERT arrays with those that make use of both surface and borehole electrodes. The method is applied to a specific example of vadose zone monitoring at the INEEL.

This LDRD supports Environmental Quality and Energy Security by allowing for the mapping of subsurface contamination plumes and water, steam, and /or CO2 floods.

Research completed on this project is now being applied to an EPA monitoring project on an acid mine waste site in South Dakota.

# Application of New Borehole Geophysical Methods for Stratigraphic Correlation and Identification of Non-Aqueous-Phase Contaminants

*Russel C. Hertzog, Catherine M. Helm-Clark*

***Defining new logging techniques for better subsurface characterization***

GC138

To improve environmental quality, definitive methods are needed to correlate lava flow units in the subsurface through quantitative rock property information for in situ conditions and for identification of non-aqueous contaminants in groundwater.

This LDRD is investigating new methods that will give the INEEL a unique capability to analyze results of state-of-the-art borehole logging measurements, and to provide drill-rig support for the deployment of the new logging tools in INEEL wells. As part of this research, state-of-the-art geochemical logging tools were deployed to develop new interpretation methodologies that could address the difficult problems of stratigraphic correlation of subsurface lava flows at the INEEL. The results of this research also will support other geophysics work in subsurface science, including ongoing work at the Vadose Zone Research Park and proposed electrical soundings for determination of aquifer and sediment interbed geometries.

Specific objectives of this project include the deployment of state-of-the-art geochemical logging tools, development of a calibration and oxide-closure model for these tools in unsaturated basalts, and producing a proof-of-principle study to show these tools are sufficient by themselves to geochemically fingerprint basalt flows and interbeds, thus enabling correlations of unsaturated basalts over large distances with great confidence. All project objectives were met with the exception of finishing a new oxide-closure model and calibration appropriate in unsaturated basalt – a task that requires input from a non-INEEL collaborator and is still in progress. Preliminary elemental analyses, though qualitative and based on a sedimentary rock calibration, demonstrate that unsaturated basalts have sufficiently unique multi-element geochemical signatures that can be used to correlate strata with great confidence of large distances.

Technical objectives for fiscal year 2003:

- *Task 1.* Finalize choice of wells for logging and provide support for removal and replacement of pumps and other well fixtures.
- *Task 2:* Develop new acquisition and processing protocol for geochemical logging in fresh water and unsaturated basalts.
- *Task 3:* Investigate augmenting geochemical logging with NMR and magnetic susceptibility tools for remnant magnetic correlation of lava flows.
- *Task 4:* Deploy geochemical logging tools at INEEL wells suitable for elemental-based stratigraphic correlation.

This LDRD started in January 2002. Tasks completed by the end of the FY02 included the identification of wells suitable for state-of-the-art geophysical logging methods, and an investigation to determine which geophysical tools would be deployed. Activities carried out during fiscal year 2003 are detailed in the following.

The first task for this project consisted of searching the inventory of wells at INEEL and surrounding region to identify wells of sufficient diameter, casing type, footage, and appropriate status for logging. The work plan was modified to include logging an additional well with the geochemical logging suite. As a result, this eliminated several wells from the short list developed during FY02. Additional work performed during FY03 included physical inspection of short-listed wells. Each short-listed well pair included a “control” well and a test well. Each control well was associated with a geochemical data set for cores collected at the well itself or at a well in the immediate vicinity. The geochemical data set would be used to establish and correlate the geochemical logging tools. The test well would be used to test the calibration of the new correlation model based on the geochemical data for the control well, since each control well/test well pair penetrated at least three shared basalt flows.

Other Task 1 work included the inspection of the control well/test well pair selected for geophysical logging. The final wells selected were RWMC-MON-A-065 as a control well and USGS-009 as the test well. The geochemical data set would be for USGS-118. USGS-118 is near RWMC-MON-A-065 and there is extremely good correlation of basalt flows between these two wells. USGS-009 is approximately three miles south of RWMC-MON-A-065, and penetrates some but not all of the flows present in RWMC-MON-A-065. Therefore, establishing correlations between this well with the control well would be a good demonstration of the correlation capability of the geochemical logging technology.

The pump and water-level access tube in USGS-009 were removed by INEEL well maintenance in late May 2003. No disassembly or reassembly was required at RWMC-MON-A-065 since this well has no pump or water-level tube. A caliper log and a video log were collected from the casings and screens in both wells to verify clearance for the Schlumberger specialty tools chosen for evaluation. This task also included the reassembly of the well-top assemblies. USGS-009 will be reassembled eventually. When the well box, water-access tube and pump were removed, it was obvious that the pump and its piping must be replaced because of extreme corrosion. Replacement of failed well equipment falls under the functions of INEEL well maintenance and therefore is no longer a task required of this LDRD project.

The second task of this project required the development of new acquisition and processing protocols for the geochemical logging tool to account for its use in unsaturated conditions. Schlumberger has developed geochemical-logging interpretations for saturated sedimentary environments such as those encountered by the oil and gas industry. Elsewhere, interpretations for igneous and metamorphic terrains for the Ocean Drill Program (ODP) and the International Continental Drilling Program (ICDP) have been developed at the Lamont-Doherty Geological Observatory, Columbia University. However, for INEEL unsaturated environments, a new interpretation model will be required. The INEEL vadose zone is comprised of unsaturated basalt formations and continental sediment interbeds, unlike those in the ODP or ICDP igneous models or the marine clastic-sediment models developed for the oil field applications. Geochemical interpretation models combine measurements from various conventional logging tools with thermal-neutron-capture gamma-ray measurements from nuclear spectroscopy tools, nuclear physics, and geochemical information to determine elemental concentrations.

Interpretation using the results of geochemical logging tools requires that a new "Oxides-Renormalization Model" (oxide-closure model) be defined for unsaturated basalt formations. This model is a critical component in converting nuclear spectroscopic measurements to elemental concentrations. In support of this task, a database of elemental concentrations has been compiled using basalt data from geochemical data libraries such as GEOROC and analytical results for subsurface INEEL basalts measured by colleagues at the Idaho State University geology department. These data include elemental concentrations from basalts throughout the western United States, sufficient for the comparison of INEEL basalts, East Snake River Plain basalts, and other Cordilleran basalts. The geochemical database is needed to develop an oxide-closure model and processing routine that will be applicable in all unsaturated basalts, not just those at the INEEL.

Analysis of the INEEL subsurface geochemical data shows that basalt flow groups each have a potentially unique geochemical signature or "fingerprint" of several elements combined, typically including Al, Fe, K, La, S, Si, Ti and Th. Successful deployment of geochemical logging tools could therefore provide unambiguous correlations of flow groups between wells, a capability never possible before the development of these tools.

Data collected by the Schlumberger logging crew in August was delivered to a collaborator on this project, Dr. Jim Grau of Schlumberger Doll Laboratory. Inspection of the preliminary and qualitative elemental analyses, automatically produced during logging using the oxide-closure model for sedimentary rocks (the default calibration for these tools), shows that geochemical fingerprinting of flows and interbeds in RWMC-MON-A-065 and USGS-009 is possible using the results for Fe, Ti, Al, U, Th and K. Completion of the oxide-closure model and processing routine specific to unsaturated basalts will improve the geochemical fingerprinting capability inherent in these logging data, and will make it possible to confidently correlate flows over long distances in areas of low well density.

Task 3 involved an investigation into augmenting geochemical logging with NMR tools for remnant magnetic correlation of lava flows and characterization of DNAPL-contaminated plumes. The mag-

netic susceptibility and magnetic resonance tools were not deployed for two reasons. First, it was determined that logging any wells in areas under environmental consent decrees or agreements with federal or state regulatory agencies would involve containment and mitigation procedures whose cost would be far beyond the budget of this project. Any valid test of these tools would require logging in areas of known DNAPL contamination. Since all candidate contaminant plumes are in areas already under environmental oversight, deploying these tools would be cost prohibitive. Second, it was decided that the correlation portion of this project could be enhanced if the money budgeted for the magnetic/NMR tools could be used on logging a second well with the geochemical logging suite. In addition to building a valid oxide-closure model, correlating between two wells would be an excellent demonstration of the potential of geochemical logging to solve stratigraphic problems unique to the INEEL.

The fourth task undertaken in this project involved the successful deployment of the Schlumberger suite of geochemical logging tools in the third week of August 2003. Schlumberger delivered preliminary geochemical results in August for Al, Ca, Fe, K, Na, Si, Ti, Th and U based on their oxide-closure model and calibration for sedimentary rocks. These results were sufficient to identify several flows and interbeds, and correlate them between the two wells.

This is a proof-of-principal project, and demonstration of the usefulness will lead to the development of optimum tools for the shallow subsurface, continental basaltic environment. The oilfield and ODP tools are designed for operation at temperatures up to 350°C, and pressures up to 20,000 psi. They are, therefore, expensive to build and use, and not optimized for shallow basaltic environment. Optimizing tools and the data analysis for vadose zone and shallow aquifer conditions is a potential CRADA project with a logging company such as Schlumberger, or could be considered as a direct funding project. Finally, INEEL programs could support such a project for better characterization of the local subsurface environment. Though the oxide-closure model for unsaturated basalt is not yet complete, preliminary results demonstrate the ability of the geochemical logging tools to confidently discriminate basalt flows and interbeds.

This LDRD contributes to environmental quality by providing a more definitive way to correlate lava flow units in the subsurface. Stratigraphic correlation in basaltic volcanic terrains is difficult because of the similarity of physical and chemical properties of lava flows. Increasing the confidence in the correlation of units would be extremely valuable in the subsurface characterization of several DOE sites (INEEL, Hanford, Los Alamos, and perhaps others).

# Fundamental Studies on Gas Contaminant Mobility in the Vadose Zone from Atmospheric Pressure Fluctuations

*Todd Housley*

***The effects of atmospheric pressure on long-term cleanup strategies***

GC101

Subsurface soil-gas concentration data taken from a large vadose-zone contaminant plume at the Radioactive Waste Management Complex (RWMC) at the INEEL have been found to vary at a single point by as much as an order of magnitude 150 feet below land surface. Variations appear to be correlated with atmospheric pressure fluctuations. Preliminary analysis suggests that changes in soil pressure compress and expand the contaminant plume. In addition, results from a vadose zone tracer study indicate that gas-phase transport is significantly influenced by atmospheric pressure changes, and that rates of migration are faster than those indicated by diffusive transport alone. These two findings suggest that current understanding of soil-gas dynamics is incomplete, and that management decisions committing considerable time, effort, and finances to remediation may be based on improper assumptions.

This LDRD is focused on understanding and describing the effect of fluctuations in atmospheric pressure on the shape and dynamics of contaminant vapor plumes in the vadose zone. Laboratory and modeling studies have been initiated to more closely study the influence of pressure fluctuations on soil-gas migration under controlled conditions.

Technical objectives for fiscal year 2003:

- Develop a basic understanding of the propagation of atmospheric pressure changes downward through both homogeneous and heterogeneous porous media and both dense and fractured bedrock.
- Build a mathematical description of the time lag and amplitude suppression of pressure waves through subsurface geologic materials.
- Investigate the kinetics of contaminant partitioning induced by naturally occurring pressure gradients from sequestered phase changes (soil surfaces, organic components, and moisture).
- Develop a computer simulation of the effects of daily and weather cyclic pressure fluctuations on vertical and horizontal soil vapor plume movement in heterogeneous porous media.

A multilevel piezometer containing six ports, each terminating at different depths below land surface, was instrumented to collect soil-gas concentration data and soil pressure data at rotating intervals. The intent was to correlate atmospheric pressure changes and subsequent pressure propagation down through the soil/basalt profile with real-time contaminant concentration changes. Resultant data are the first ever collected describing the influence of atmospheric pressure fluctuations on vadose zone contaminant plumes.

Figure 1 illustrates the type of data observed. Soil pressure and trichloroethylene concentrations were measured at the same point in the subsurface (here 119 feet below land surface). An increase in soil pressure was observed to correlate with a decrease in trichloroethylene concentration. Trichloroethylene concentrations were observed to vary over an order of magnitude at a point. One possible interpretation is that increasing and decreasing pressures compress and expand the contaminant plume. In other words, soil vapor plumes are dynamic in nature, responding to pressure fluctuation. This would make conventional diffusion theory inadequate to completely explain vapor phase transport. That vadose zone plumes are dynamic in position and time is a new concept. A major contribution of this project is that protection of groundwater from vadose zone contaminants should include an evaluation of vadose zone plume dynamics.

Three ports, each in two piezometer wells 25 feet apart, were instrumented to collect both pressure and concentration data. A tracer test was implemented on March 7, 2002. Sulfur hexafluoride ($SF_6$) was injected 112-ft bls in one well until March 24, 2002. Tracer concentration measurements were made at ports in both wells. Results of the tracer test were analyzed to estimate gaseous diffusion parameters for modeling contaminant transport at the RWMC. To fit observed arrival times, diffusion coefficients two to three orders of magnitude higher than conventional air diffusion values were expected, suggesting that other mechanisms play a role in vadose zone contaminant transport (Figure 2).

Tracer breakthrough was observed to correspond to changes in atmospheric pressure, and a plot of atmospheric pressure and tracer arrival showed that tracer concentrations decreased as subsurface pressure at the port depth rose, and increased when pressures decreased. Computer simulation of tracer migration was performed using the model T2VOC. A conventional diffusion approach was unsuccessful until the code was modified to include atmo-

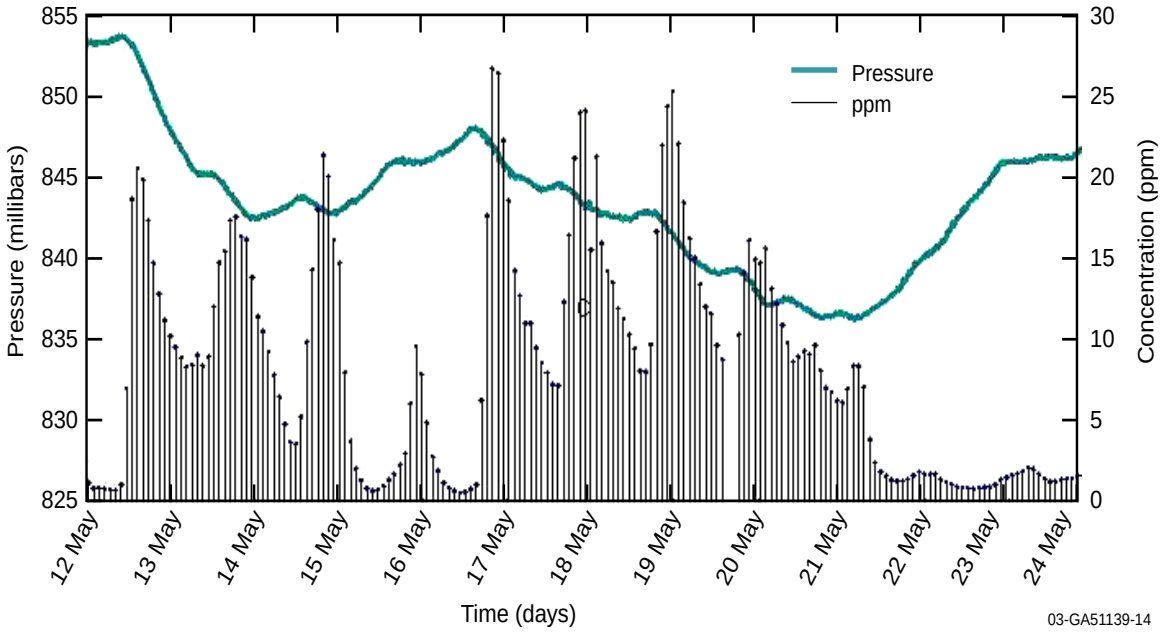


*FIGURE 1. Real-time atmospheric pressure fluctuation and TCE concentration 150 ft below land surface.*

spheric pressure fluctuation (and subsequent propagation through the subsurface) as a boundary condition.

A series of experiments were performed in a 60-cm by 10-cm glass column packed with clean uniform sand. A TCE vapor source was placed in one end of the column with a detector at the other end. Pressures in the column were changed in period and amplitude using a positive-displacement pump. TCE arrival with and without pressure fluctuations was fitted to the Carslaw and Jaegar (1959) analytic solution to the transient diffusion equation. Results showed that fluctuations in pressure enhanced arrival times as much as 20%. A

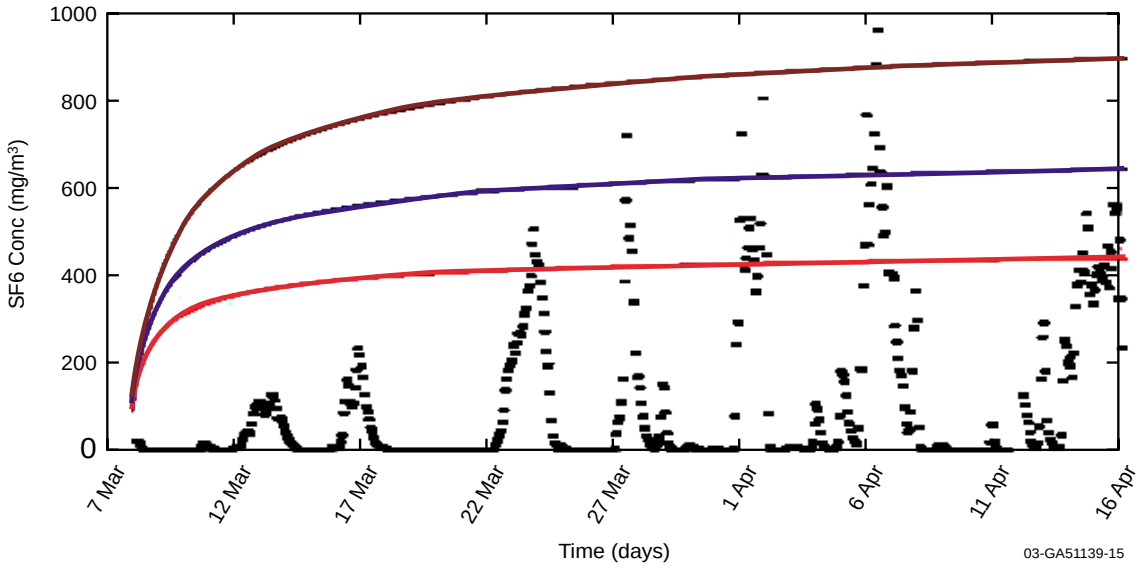


*FIGURE 2. $SF_6$ breakthrough data and Carslaw and Jaeger fitted diffusion expression at Well 77-1, Port 3 (151-ft. bls).*

journal article is in progress describing the addition of a pressure fluctuation component to explain the enhanced transport without relying on inflated parameters to the Fickian diffusion expression.

This LDRD research adds a significant component to understanding of vadose zone contaminant transport, and strengthens the INEEL's position as a DOE leader in subsurface science. At the INEEL, use of atmospheric pressure considerations in evaluating the success of the RWMC soil vapor extraction success will set a much-needed DOE precedent. During this project, significant contributions have been made by Wayne Downs and Vince Wilding (Brigham Young University), Erik Webb and Clifford Ho (Sandia National Laboratory), and John McCray (University of Texas at Austin).

# Estimating Soil Water Flux in the Deep Vadose Zone

*Joel M. Hubbell, James B. Sisson*

***Decreasing uncertainty on contaminant transport at the INEEL***

PH105

Dissolved contaminants in the vadose zone are transported with soil water. Thus, knowing the in situ flux is a crucial variable for predicting contaminant transport in the vadose zone. Soil water flux has been estimated using a variety of indirect techniques (e.g., mass balance, empirical, soil physics approaches) and direct measurement techniques (e.g., lysimeters, tracers). Both the indirect and direct methods have been used almost exclusively in the shallow vadose zone with the exception of tracers.

Soil water data collected throughout the deep vadose zone at the INEEL and other DOE facilities imply that the variation found over time decreases with depth. The reduced variability allows researchers to substantially improve the accuracy and precision of indirect and direct approaches for estimating soil water flux. In addition, the availability of low-cost, high-precision sensors and new instrument installation techniques for placing instrument packages at greater depths in wells below the zone strongly influenced by diurnal fluctuations provides the opportunity to make precise and repeatable measurements.

The objective of this LDRD is to improve estimates of soil water flux in the deep vadose zone. New and improved methodologies to measure soil moisture flux in the deep vadose zone will be developed. Data sets for comparison to other methods will be collected, and improved tools and techniques required to estimate water movement at DOE, NRC, and commercial sites will be provided.

These tools and techniques can be employed to improve risk assessments and estimates of the aquifer recharge rates and quantities. The tools developed in this project also will be useful for validating remediation approaches that involve developing engineered control of soil water flux.

Technical objectives for fiscal year 2003:

- Evaluate data from deep vadose zone instrumentation and in situ sediments to determine the limiting and controlling variables for accurate estimates of moisture movement.
- Complete initial designs for the most promising devices and techniques, and conduct numerical simulations to evaluate the optimum configurations and potential effectiveness of these designs.
- Prepare and submit intellectual invention disclosure reports and patent applications.
- Prepare and submit papers on research.

Data was evaluated from deep vadose zone at semi-arid sites to provide estimates of the spatial and temporal distribution of soil water fluxes using the Darcian approach. Data was evaluated from an existing monitoring system with instruments installed in two, thin, sedimentary interbeds located within volcanic rock at depths of about 30 and 70 m. Soil water flux was calculated using soil water potentials from advanced tensiometer data and hydraulic properties from laboratory analyses of interbed samples. While tensiometer measurements indicated nearly constant conditions over a two-year period in seven locations, the remaining 12 locations showed variations of up to 60 cm in soil water potential. The variation in water potential at these depths indicates precise long-term water potential measurements are a limiting factor for improving flux estimates. Instrumentation and techniques will have to be developed to provide precise measurements over a narrow range of water potentials. This data reflects that the water potential variation over long-time intervals is much smaller than those at shallower depths.

Moisture flux estimates, based on mean water potentials, at all of the sites varied over five orders of magnitude, from 0.2 to about 8000 cm/yr. The in situ water potential measurements provide reasonable data for application of this approach, but the estimation of unsaturated hydraulic properties from sediments at these depths reduced the confidence in the flux estimates. Although preferential recharge and lateral migration of perched water could act to locally enhance flux at this site, the high degree of uncertainty associated with mapping water potential to the unsaturated hydraulic conductivity limits the ability to reach such conclusions from this data.

Small changes in the fitting parameters induced order-of-magnitude changes in the flux estimates. The unsaturated hydraulic conductivity at the in situ conditions controls the flux estimates. This study indicates there is a need for development of accurate techniques to assess flux rates over the range of applicable field conditions to improve the confidence in deep flux estimates. This evaluation of deep soil water flux using the Darcian approach

suggests that laboratory-derived estimates of flux at ambient soil water potential should constrain the fitting parameters over the range of applicable fluxes, thus minimizing errors.

Several instruments for estimating flux in the deep vadose zone, submitted as invention disclosures last year, were modeled to evaluate their designs, potential effectiveness, and optimum configurations. Two of the most promising instruments were chosen for further evaluation. Their overall designs were refined and new prototypes constructed to test the materials and construction in the laboratory. The first instrument will be used for laboratory determination of the flux from undisturbed soil cores at ambient water potential conditions. The design and underlying theory allows the device to be simple to build and operate. Additional laboratory tests will be performed to refine the optimum sizes, materials, and construction, as well as develop standard operational techniques. The second instrument is a modified tension lysimeter for placement at depth in wells. Several designs were evaluated and further laboratory tests will be conducted.

Two patents, relating to this project, were granted in FY03. The first describes an enhancement to tensiometer designs to allow more precise soil water potential measurements for extended periods of time by eliminating the influence of the hanging water column variations within the tensiometer's influence, diminishing the water potential measurement and thus impacting the temporal flux estimates. The second patent is for a technique to allow sampling of soil water fluid or thin saturated zones for chemical analyses. This information can be incorporated into contaminant flux estimates. Three patent applications also were prepared and submitted for direct-push vadose zone monitoring instruments.

The results and instruments developed in this project support the Subsurface Science Initiative and will be utilized at DOE and commercial sites throughout the nation. This project supports the mission of the INEEL and DOE to ensure operations will not adversely impact the environment. This research will decrease uncertainty relating to contaminant transport and long-term waste management practices at the INEEL and other sites. The INEEL is collaborating with researchers from the University of Idaho, Clemson University, and the University of Nevada, Las Vegas, on this project.

# Modeling Solute Partitioning at Interfaces

*Randall LaViolette, John Walter, George Redden, Paul Meakin*

***Improving theories to understand subsurface contaminants***

GC151

The standard theory of adsorption equilibria was devised for single-site binding of adsorbates on a uniform surface. Abundant literature now exists on the deficiencies of that theory for multi-site binding or heterogeneous surfaces, but little has been done to improve the theory. Among these deficiencies is the failure of the Law of Mass Action for multi-dentate organic ligands, which has been noticed both theoretically and via computer simulation.

The goal of this LDRD is to evaluate adsorption equilibrium expressions for organic ligands on heterogeneous and reacting surfaces, such as might be encountered on contaminated surfaces in the vadose zone. The project approach to this problem is to pursue both theory and computer simulation via Monte Carlo (MC). The MC calculations provide equilibrium constants vs. coverage and the structure of adsorbates on a surface, and works for heterogeneous surfaces. Consequently, adsorption equilibria can be obtained for a wide variety of ligands whose binding, in turn, affects the ultimate distribution of contaminants on surfaces.

Technical objectives for fiscal year 2003:

- Develop theory for trimer adsorption on a uniform square lattice.
- Write and test MC simulation code to calculate adsorption of complicated molecules on heterogeneous surfaces.

In the first phase of this study, a theory was developed for 2- vs. 3-site trimer adsorption (vs. coverage) on a uniform square lattice. Figure 1 displays the ratio (as a percent) of 2-site:3-site adsorption of trimers vs. fugacity (i.e., $z_2/z_3 = exp(\mu/RT)$ subject to the constraint $2\rho_2 + 3\rho_3 = \theta$, where $\theta$ is the coverage, $\rho$ is number density, $z$ is fugacity, $\mu$ is chemical potential, R is the gas constant and T is chosen here to be 275K). The dashed curve corresponds to $\mu = 0$, the subsequent curves correspond (left to right) to $\mu = 2$, 3, and 4 *kcal/mol*, respectively.

The theory is limited to uniform surfaces and low coverages of noninteracting (beyond excluded volume) adsorbates, although it is instructive. To pursue the study of surfaces that would likely be encountered in subsurface applications, a general Grand Canonical Monte-Carlo (GCMC) simulation code was written and tested that can be employed to calculate adsorption of complicated molecules on rough, non-uniform, and heterogeneous (structural and chemical) surfaces. It also permits the adsorbates to interact. This effort consumed the majority of this fiscal year's resources.

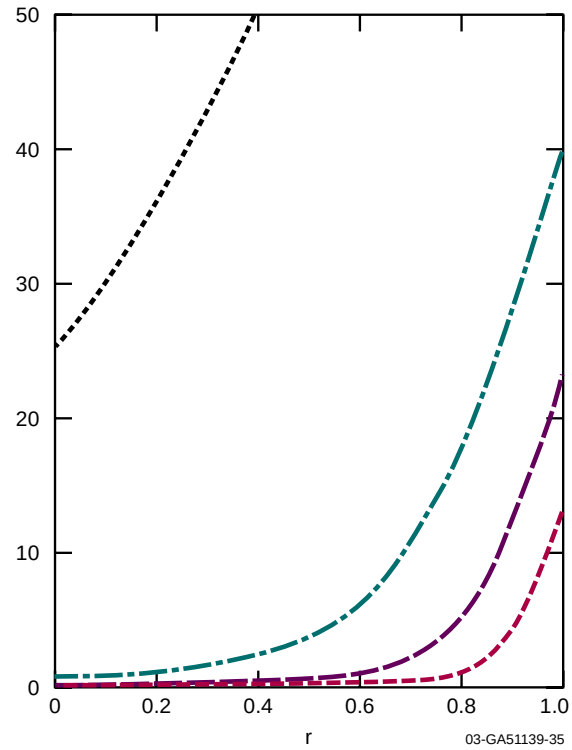


*FIGURE 1. Theory developed for 2- vs. 3-site trimer adsorption.*

It was originally planned to apply the capabilities developed in FY03 to determining the equilibria for the adsorbtion of multi-dentate ligands on heterogeneous surfaces. Part of the work in FY04 will be planning for the best possible application of these new capabilities in view of changes to both funding of the program and the new directions of the INEEL.

This LDRD research should ultimately benefit INEEL programs in Subsurface Contamination, Subsurface Remediation, Separation Technologies, and Detection Technologies (for contaminants in the subsurface).

# Investigation of the Movement and Fate of Chlorinated Hydrocarbons

*Robert Lenhard*

***Using mesoscale experiments to model contaminant behavior***

GC135

The Subsurface Science Initiative at the INEEL emphasizes the need for mesoscale experimental investigations to better understand and predict processes occurring in the field. Too frequently, poor predictions of contaminant flow and transport result when data and parameters from small-scale experiments are used to predict field behavior.

At the INEEL Subsurface Disposal Area (SDA), waste has been buried from DOE's Rocky Flats site that contains carbon tetrachloride ($CCl_4$). This purpose of this LDRD is to help understand and predict $CCl_4$ contamination in groundwater at the SDA. To that end, an experimental cell 3-m long by 2-m wide by 2-m high was constructed for mesoscale investigations. The cell was packed to simulate a fractured porous medium between two unconsolidated sediment layers. Clay and stainless steel tubes were used to represent the fractured porous medium. Sand was used to represent the unconsolidated sediments. Water infiltration and $CCl_4$ gas movement will be measured during experiments, as well as microbial-assisted transformation of $CCl_4$. The data will be used to investigate modeling water and $CCl_4$ movement in spatially variable porous media, including fracture flow.

Technical objectives for fiscal year 2003:

- Pack the mesoscale experimental cell with 17 tons of material.
- Install measurement systems.
- Initiate mesoscale experiments (water infiltration).

Mesoscale experimental investigations may be important for understanding processes at the field scale. From the investigations, researchers can develop approaches for better predicting field-scale phenomena. The investigations also can be used to test both conceptual and mathematical models of fluid movement and contaminant fate. This project focuses on the movement of fluids through fractured porous media and unconsolidated sediments.

In FY02, a mesoscale experimental cell was constructed that is 3-m long by 2-m wide by 2-m high. The cell is designed so that simulated groundwater can flow along the 3-m length in a controlled manner using constant-head reservoirs. This year, the experimental cell was packed with material to yield a sloped, 28-cm thick, fractured porous medium between two layers of unconsolidated sediments. To represent the fractured porous medium, a clay-based mixture was used for the matrix material, and stainless steel tubing was used for the fractures. Sand was used to represent unconsolidated sediments. The total thickness of the packed porous media is approximately 1.8 m, which consisted of 16 tons of sand, 1 ton of clay, and 635 stainless steel tubes with inside diameters ranging from 2 to 28 mm. The stainless steel tubes were inserted in the clay material at known locations that are consistent with a geostatistical realization of a random fracture network with a specified correlation length, which is five times the smallest grid block size that will be used for modeling fluid flow. Figure 1 shows the packing of the sand.

PN04-0004-158b

*FIGURE 1. Sand being packed into the mesoscale experimental cell.*

During packing of the porous media, three measurement systems were installed. One system is for extracting aqueous samples from the water-saturated region to investigate the partitioning of $CCl_4$ gas to water and subsequent mixing. A total of sixteen aqueous samplers were installed. The second system consists of 25 porous sensors that are connected to small-diameter metal tubes that can be periodically flushed to measure the concentration of $CCl_4$ and microbial-assisted transformations of $CCl_4$. The sensors were obtained from Dakota Technologies, Inc. under a subcontract that also included sensor testing for the conditions that will exist in the $CCl_4$ experiment in FY04. The third system is a series of tensiometers connected to

pressure transducers for measuring water pressure. The 86 tensiometers are used to tract how water migrates through the porous media from its water infiltration source. There are two rows of tensiometers, one above and one below the simulated fractured layer, to measure which fractures are dominant in transporting water. Figure 2 shows the network of tensiometers and pressure transducers.

After packing the experimental cell and installing the measurement systems, water infiltration experiments were initiated. Water was applied to a 10-cm by 10-cm source area at the top sand surface by a pump at a rate of 3 L $hr^{-1}$ for 6 days. Thereafter, the water was allowed to become in equilibrium with the water table, and another water infiltration experiment was conducted using an infiltration rate of 9 L $hr^{-1}$. Sampling of the porous media to determine hydraulic properties and data analysis of the water infiltration experiments will not be conducted until FY04.

This research addresses DOE needs for better predicting and understanding fluid flow and chemical transport behavior at it sites. The work will lead to a better understanding of flow through fractured porous media, give insight into a conceptual model of $CCl_4$ contamination at the INEEL, and help evaluate modeling approaches.

The work conducted on this LDRD supports the Subsurface Science Initiative at the INEEL. Efforts are directed at building unique capabilities and expertise to conduct mesoscale experiments that may be important to the Office of Environmental Management and Office of Science in addressing contamination at DOE sites.

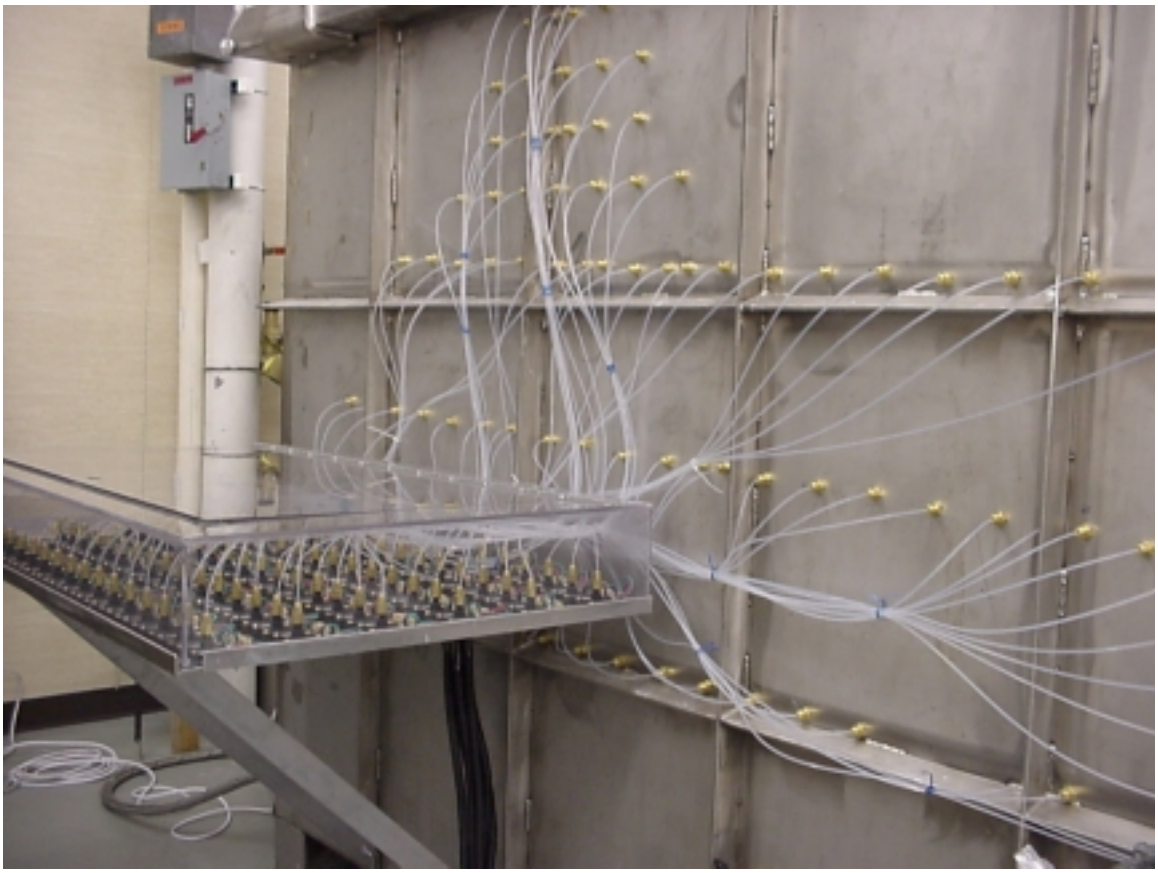

PN04-0004-158aPN04-0004-155g

*FIGURE 2. System of tensiometers connected to pressure transducers to measure water pressure.*

# Regional Setting and Flow Dynamics of the Snake River Plain Aquifer

*Travis L. McLing, Richard P. Smith, Michael J. Rohe*

***Uncovering new insights into contaminant transport***

GC102

Improved understanding of groundwater flow in the Snake River Plain aquifer beneath the INEEL is key to more accurately predicting contaminant transport. Various geophysical, geochemical, and hydrologic data exist for the Snake River Plain, though much of this data was collected for other purposes. This LDRD builds on this data to increase understanding of groundwater flow in the Snake River Plain aquifer. The research focuses on aquifer temperature distribution, water chemistry (both solute and isotopic compositions of strontium and uranium), and water level histories. These sources of data have proven to be a valuable, independent means to characterize groundwater movement as a function of the geologic framework in the Eastern Snake River Plain (ESRP) aquifer.

Aquifer temperature distribution shows areas of major geothermal input from depth, allows determination of aquifer thickness variations, and helps to trace plumes of cold recharge water across the INEEL. Aquifer chemistry and isotopic ratios allow recognition of groundwater flow paths and areas where water is stagnant. The time-histories of water levels in INEEL wells for the past 50 years allow calculation of aquifer gradient variations through time. These tools increase the ability to understand the stresses acting on the aquifer and its response to these stresses. All of the new insights on aquifer geometry and flow dynamics gleaned from analyses of these databases are vital for current and future modeling of contaminant transport.

Technical objectives for fiscal year 2003:

- Use observed temperature distribution to develop parameters and set up simple models to estimate the changes in permeability required to develop aquifer warm zones, given a constant heat input at the base of the aquifer.
- Include additional isotopic data in the chemical flow model for the aquifer beneath INEEL.
- Develop a new methodology for incorporating the effects of matrix diffusion on transport of natural and anthropogenic isotopes in the aquifer.
- Refine aquifer thickness model based on information obtained from 1960's vintage analog (strip chart recorder) temperature logs retrieved from storage in USGS files for 123 wells (many wells have multiple temperature logs), digitize (using summer student help), and add to the INEEL database of temperature logs.
- Separate water level hydrographs for 215 regional aquifer wells into four distinct time-scales (intra-year, seasonal, 4-8 years, near-decadal). Prepare spatial distribution maps of water level variance that occurs at these different time-scales.
- Quantify the magnitude of downward trends in water table elevations as a function of location. Correlate long-term water table changes with precipitation records and evaluated timing differences.
- Confirm that hydrographs for the ESRP aquifer can be grouped into four different characteristic shapes based on the well's location relative to surface water features. Analyze hydraulic gradient variations across the site at different temporal and spatial scales.
- Prepare and present papers on research findings.

The results of this research provide vital data for realistic modeling of contaminant transport in the aquifer and rational explanations for some unexpected observations of contaminant plume migration. Three conceptualizations have been constructed to model the geometry of the flow paths defined by naturally occurring strontium-87/strontium-86 ($^{87/86}$Sr) plumes in the ESRP aquifer. The advection-driven plume is a strong theory but is modeled by assuming a porous media model. Though certain regions may behave as a porous medium, overall the hydraulic conductivity of the aquifer is highly irregular. The diffusion-based model may be responsible for the plume geometries. The Damköhler numbers calculated for the ESRP indicate the diffusion in fracture-bounded blocks is an important process. Geochemical heterogeneity is also a reasonable model for high $^{87/86}$Sr plumes since sediments occur in discontinuous interbeds throughout the region. Sediments yield high $^{87/86}$Sr source material by dissolution and ion exchange but retard plume advancement by sorption. Alternative groundwater sources may also play an important role in the development of such plumes. Upwelling geothermal waters have higher $^{87/86}$Sr ratios. However, the geothermal waters do not represent a large volume relative to the aquifer.

The $^{87/86}Sr$ plumes in the ESRP are not unique. Similar plumes may form by entirely different processes in different geologic settings. These plumes probably result from a combination of conceptual models. $^{87/86}Sr$ plumes alone are not sufficient to identify hydrogeologic features such as fast flow paths.

The elongated, narrow shapes of cold water zones within the aquifer indicate they are preferential flow paths (probably fracture zones or interconnected rubble zones between lava flows) where groundwater velocity is great enough to maintain low temperature, even in areas that are otherwise relatively impermeable and, therefore, warm. The implications of this characteristic of the aquifer are significant; these cold regions may reveal conduits that preferentially transmit contaminants downgradient.

Merging of INEEL aquifer temperature data with that for the entire ESRP provides a more complete understanding of aquifer recharge from adjacent highlands. Local water-level highs are caused by mounds of cold recharge water originating from the drainage basins surrounding the Plain.

A new double-porosity mathematical model was generated that incorporates diffusive processes along with traditional chemical effects in fractured rock media. The new procedure simultaneously models the effects of diffusion and reactions of the individual isotopes in fracture-bounded blocks and advective pathways, and then derives the expected isotopic ratios. This approach differs from other methods because it uses multiple coupled equations to model the system, and provides a better estimate of expected isotope ratios and flow velocities experienced along individual flow paths.

The four different characteristic shapes of INEEL-area hydrographs are related to different recharge/discharge conditions. Irrigation practices and tributary underflow recharge are correlated with the variation of observed aquifer responses at different time-scales. The aquifer responds differently in different locations and the resulting hydraulic gradient is not constant. Figure 1 shows hydrographs for aquifer water table elevation (well USGS-85) and Big Lost River discharge above the Mackey Reservoir. The hydrographs in this figure have been filtered to exclude all signals but those occurring at very low frequencies (periods greater than ten years). Long-term climate effects on snow pack in the Lost River Range and other tributaries feeding the aquifer drive the changes shown in this figure. The bottom set of hydrographs suggests there is a time-lagged correlation between these long-term changes occurring above Mackey and a location in the aquifer central to the INEEL. Such time lags may allow researchers and remediation planners to predict future behavior of the aquifer based on recent precipitation records.

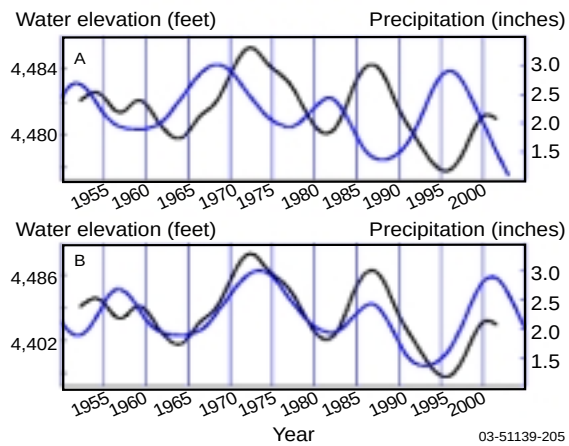


*FIGURE 1. Correlation of aquifer response (well USGS-85) with low-frequency precipitation record (Big Lost River above Mackey Reservoir). Bottom graph shows time lag.*

This LDRD supports DOE prediction of contaminant transport in the aquifer by providing input parameters and uncertainty limits for models and by increasing understanding of aquifer geometry and flow characteristics. It has fostered collaborations with Southern Methodist University, University of Idaho, University of Mississippi, and Los Alamos National Laboratory, each of which provide increased peer acceptance of results. The work is currently supporting development of the Idaho Completion Project's new sub regional-scale numerical groundwater model. The project enables INEEL researchers to apply the techniques and concepts developed at INEEL to other sites where groundwater contamination occurs in complex aquifers.

A number of specific tangible benefits have been realized to date by this LDRD. The data and information generated by this research has had a

direct benefit in the advancement of a new arsenic initiative. This project will enable INEEL scientists to bring technical solutions to communities in the western U.S. that are experiencing difficulties meeting the EPA's new maximum contaminant levels for arsenic. The LDRD has generated an aquifer thickness report and maps for use in WAG-10's sub regional model of aquifer water movement. Additionally, the State of Idaho has incorporated much of the flow information from this work into their ESRP conceptual groundwater model. The investigators participated in WAG-10 planning activities to help site new sampling and monitoring wells at and near INEEL. Knowledge gained from this research helped to site wells in places where maximum information can be obtained, and to develop the logging, sampling, and monitoring methodologies that will optimize benefits of the new wells. In addition, this project has led to participation in a workshop to prioritize uncertainties for the INEEL Water Integration Project and the leading of INEEL Water Integration Field Tours to acquaint interested stakeholders (legislators, regulators, agricultural interests, and the general public) with INEEL aquifer remediation and monitoring activities. Two papers on this research were presented at industry conferences. Three additional manuscripts are in preparation.

# Modeling of Flow and Colloid Behavior in Subsurface Fractures

*Paul Meakin, Daphne Stoner, Alan Stadler, Glenn McCreery*

***Using particle-based methods to model multiphase flows***

GC136

Fractures are omnipresent in the upper part of the Earth's crust. The ability to model the fate and transport of subsurface contaminants with sufficient accuracy and reliability depends on our understanding of fluid flow in fracture apertures and our ability to develop scientifically defensible conceptual models for the long-range flow of fluids in the fractured subsurface. Important contaminants, such as radionuclides, have been found to travel much further and faster than predictions based on the science of a few decades ago. This is usually attributed to the focusing of flow into preferred pathways such as fractures and fracture networks and, in some cases, to the transport of contaminants associated with colloids along similar preferred pathways. If scientists are to reduce the uncertainties in computer-based predictions of subsurface contaminant behavior, computational tools must be developed to model fluid flow in fractured porous media under the wide range of conditions that are encountered in the subsurface. More accurate models would reduce the cost of long-term monitoring and stewardship, and facilitate the development and deployment of more effective remediation technologies.

Despite impressive advances in computational fluid dynamics, the modeling of multiphase flow phenomena remains a formidable challenge. Grid-based methods that perform well for single-phase flow often perform very poorly for multiphase flows because of problems such as artificial front broadening and grid entanglement. These challenges are a consequence of the difficulty of representing sharp interfaces and tracking the dynamics of complex interfaces. These problems become particularly severe for processes that involve the coalescence and fragmentation of bubbles and droplets. Under these conditions, code performance is limited by the front tracking algorithm and complex (error prone) code is required.

The objective of this LDRD is to overcome these hurdles by using a variety of particle-based methods to simulate multiphase flow in the subsurface. When particle-based methods are used, the particles move with the flow, and no front tracking is required. These methods are very flexible (they can be applied to a wide range of multiphase flow and other phenomena) but require very substantial computing resources.

Technical objectives for fiscal year 2003:

- Carry out simulations of multiphase flow in fracture apertures using models identified in FY02.
- Develop computer code for the behavior of colloids in fracture apertures.
- Continue to evaluate new modeling methods for the simulation of multiphase flow in fracture apertures.
- Work with experimentalists to design motivate and interpret experiments.

The original scope of work has been modified in response to budget constraints and new opportunities. Development of computer code for the behavior of colloids has been started, but most of this work has been moved to FY04. A substantial new component (geocentrifuge experiments to study multiphase flow in fracture apertures) has been added. This sub-project was planned to be 50% completed in FY03.

Three different particle-based modeling methods (Lattice Boltzmann Simulations, Dissipative Particle Dynamics Simulations, and Smoothed Particle Hydrodynamics) have been developed to simulate multiphase flow in fracture apertures. These complementary modeling approaches enable simulation of multiphase flow under a wide range of conditions over a wide range of time and length scales. Investigation also has begun of a relatively new and innovative front-tracking method (the level-set method) that can be used in conjunction with grid-based methods. This was not part of the original work plan, but it will enhance the arsenal of methods that are brought to bear on this LDRD's research objectives.

*Lattice Boltzmann Simulations*: In FY02, a single-component, two-phase lattice Boltzmann model for flow in complex fracture apertures was developed. In FY03, the model has been improved to model systems with large liquid/gas density ratios. In addition, a two-component two-phase model has been developed. Hakan Basagoaglu (a postdoctoral associate partially supported by this project) has recently begun developing lattice Boltzmann models for the transport of colloids in fracture apertures.

*Dissipative Particle Dynamics Simulations*: Dissipative particle dynamics simulations are

operationally very similar to molecular dynamics simulations. However, each of the particles in dissipative particle dynamics represents a very small volume of fluid and the particle-particle interaction potential is soft. Both of these characteristics make dissipative particle dynamics much more efficient than molecular dynamics for the purpose of simulating hydrodynamic behavior. In dissipative particle dynamics the effects of thermally driven fluctuations (stochastic particle-particle interactions and dissipative forces) are included. In this respect, dissipative particle dynamics is like Brownian dynamics. This makes dissipative particle dynamics well suited to the modeling of systems such as polymers, colloids, and biofilms in which thermally driven fluctuations play an important role. The investigators have used dissipative particle dynamics to simulate phase separation, fluid injection, fluid-fluid displacement (Fig. 1), and phase separation during injection of a fluid-fluid mixture, all in complex-fracture apertures.

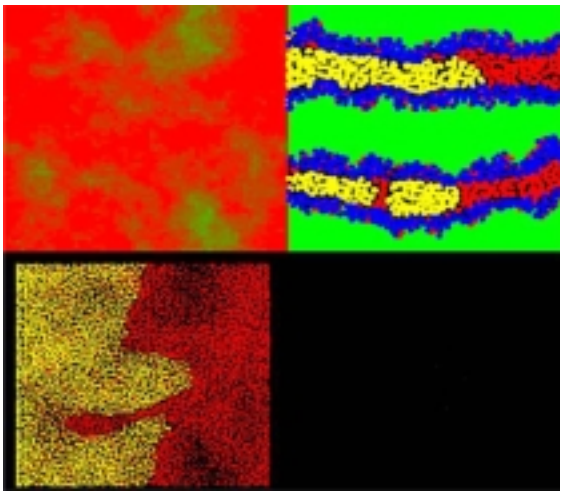

PN04-0004-156a

*FIGURE 1. Simulation of the displacement of a wetting fluid (red) by a non-wetting fluid (yellow) in a complex-fracture aperture. The upper left quadrant shows the aperture field on a color scale that ranges from green (small aperture) to red (large aperture). The lower left quadrant shows a view of the lateral distribution of the fluids and the upper right quadrant shows two mutually perpendicular cross-sections in planes perpendicular to the plane of the aperture.*

*Smoothed Particle Hydrodynamics*: In smoothed particle hydrodynamics the density field is represented by the superposition of weighting functions centered on point particles. The pressure field is calculated from the density field, via an equation of state, and the particles move in response to pressure gradients and external forces. Smoothed particle hydrodynamics was used to simulate the injection of fluids, fluid-fluid displacement, and phase separation during injection of a fluid-fluid mixture, all in complex-fracture apertures.

The objective of the geocentrifuge subproject is to obtain a better understanding of multiphase fluid flow in fracture apertures by using the INEEL geocentrifuge. Transparent flow cells have been fabricated using stereolithography. The design of these cells is based on a self-affine fractal model for fracture surfaces. Simple models for flow in fractured vesicular and granular porous media also have been developed. Since the fracture aperture is based on a computer model, the same aperture can be used in experiments and computer models. Although computer modeling is not part of this subproject, the results will be used in the main project and in future research efforts. In this project, two new technologies are being advanced: the use of stereolithography to fabricate complex flow cells representative of subsurface fractures and pore spaces and; the use of the geocentrifuge to systematically change flow conditions and test scaling concepts. An apparatus for carrying out experiments in the geocentrifuge has been constructed (Fig. 2), and the first geocentrifuge experiment going forward.

This research project is contributing to the build-up of a critical mass of researchers and facilities at INEEL in the area of fluid flow in complex confined geometries. This is an area of considerable scientific and practical importance for applications ranging from the fundamental physics of flow in complex systems to applications in environmental management and fossil fuel extraction.

PN04-0004-156b

*FIGURE 2. An experimental setup for investigating multiphase flow in complex fracture apertures with transparent walls. The cell holder will be used in the geocentrifuge experiments.*

# Multiscale Modeling of Multiphase Flow (Unsaturated)

*Paul Meakin, Alexandre Tartakovsky, Robert Lenhard*

***Enabling scale-dependent prediction of flow behavior***

GC150

The behavior of contaminants in the subsurface depends on physical and chemical heterogeneities that span an enormous range of length scales ranging from the atomic scale (microscopic roughness and diagenetic decoration on individual grain surfaces) to the scale of major geological units. At present, and for the foreseeable future, no geophysical measurement method (or combination of methods) can provide a detailed description of the subsurface over this enormous range of length scales, and no data storage device can contain the required information. In practice, the best current methods use geophysical tools to obtain coarse-grained information over the region of interest (the contaminated site, oil reservoir, etc.) and obtain information on much smaller scales from down-well logging tools and laboratory studies of recovered core samples. This information is used to generate statistically representative models of the spatial distribution of subsurface properties (permeability, porosity, specific mineral surface area, etc.) Prediction of the fate and transport of subsurface contaminants is then based on the results obtained by running a forward model with a sufficiently large number of realizations of the statistical model for subsurface heterogeneity to obtain a reliable estimate of the average behavior of the ensemble and the *statistical* uncertainties.

This LDRD program investigates an alternative approach that uses moment equations. The success of this endeavor depends on determination of the correct statistical model(s) for the spatial variation of physicochemical properties from the limited amount of available geophysical and laboratory data, and the proper application of the statistical model(s) to generate a 3-D map of subsurface heterogeneities.

Technical objectives for fiscal year 2003:

- Develop multiscale relationships describing the correlation of critical porous medium properties such as permeability to account for spatial variability.
- Develop stochastic flow equations in combination with multiscale correlation relationships that enable prediction of flow on different scales.
- Quantify uncertainty in flow predictions using moment equations.

The investigators tested the scale dependent correlation function for a random data field obtained analytically by using wavelet transforms. This function predicts how the variance decreases and the correlation length increase with increasing scale of measurements (the variability of the data decreases and data field becomes smoother as the scale of measurement increases). Qualitatively, these results correspond to field observations. This function was obtained under the assumptions that the underlying field is a self-affine (fractal) field with a power-law correlation function, and that scaling can be applied over a limited range of scales. The field observations showed that hydrological data usually have an exponential correlation structure rather than a power-law correlation structure. The limited number of scales made it inconvenient to use an analytically derived function. By comparing this function with statistics derived from numerically generated data with exponential correlation structure, the new function that describes the correlation structure for a wide range of scales was empirically found. Figure 1 shows the data with an exponential correlation structure numerically generated on the scale 0.2 and upscaled to the scales 0.4, 0.8 and 1.6 using wavelet data transformation.

Figure 2 presents a comparison between variograms calculated from the data and from an empirically obtained correlation function. This figure shows good agreement for all scales from 0.2 to 1.6, and demonstrates that the correlation function allows downscaling of the correlation structure. For the scale s = 0.0015 (after downscaling) the empirical variogram compares well with the variogram obtained analytically by means of wavelet transformation.

The 3-D stochastic moment equations describing two-phase immiscible flow and unsaturated flow in randomly heterogeneous porous media were derived and solved in one spatial dimension. Moment equations that described the uncertainty associated with the above solutions were also derived and solved. The investigators also derived

3-D integral equations describing general immiscible fluid—fluid displacement with arbitrary viscosity ratios and solved them in one and two spatial dimensions. These equations can be used for

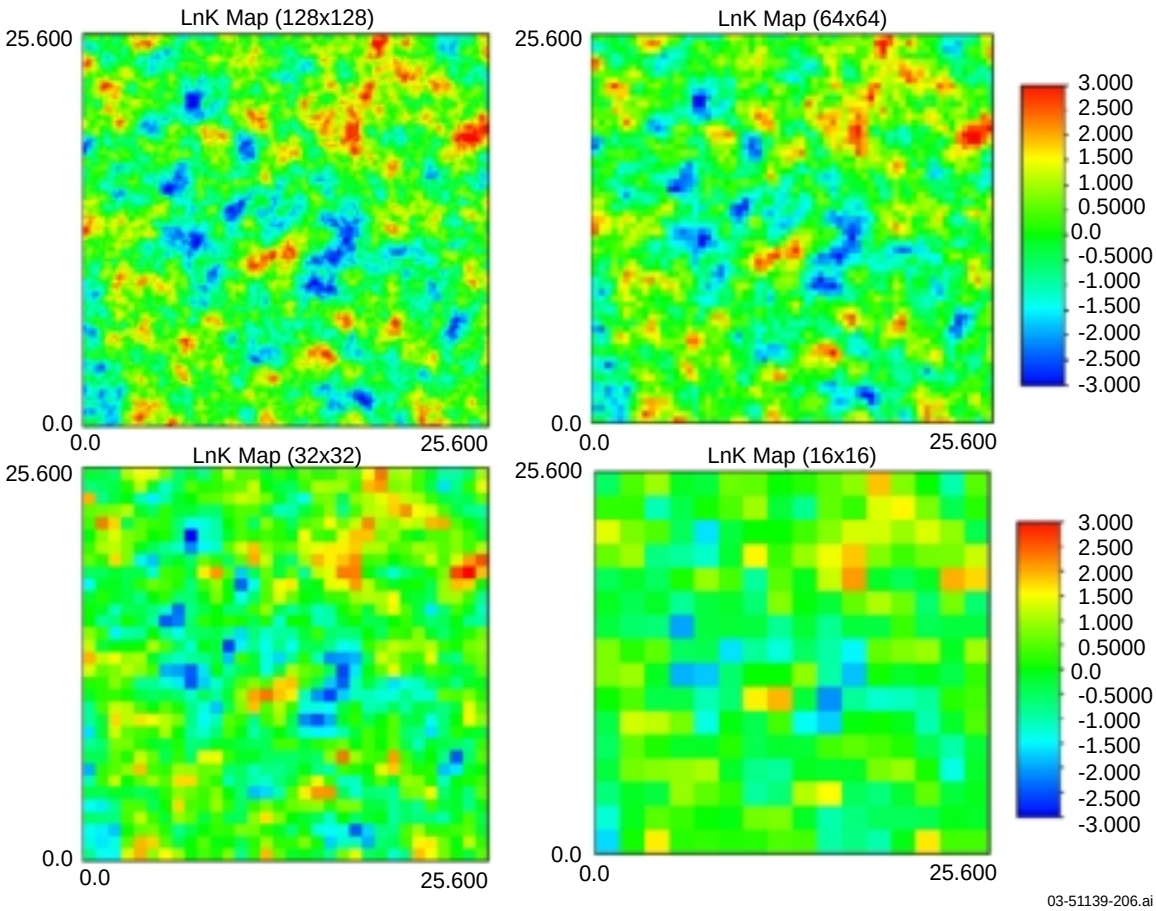


*FIGURE 1. Original field (128 x 128 grids) with grid size corresponding the scale of measurement equals 0.2. Scaled fields with scales of measurements equal to 0.4 (64 x 64 grids), 0.8 (32 x 32) and 1.6 (16 x 16 grids). The data were scaled using wavelet transforms.*

stochastic analysis of immiscible displacement in randomly heterogeneous media. This work was summarized in three papers and was presented at the INRA 2003 meeting in Salt Lake City (October 12-15, 2003).

Combination of these moment equations with empirically derived correlation functions will enable researchers to make scale-dependant predictions of the flow. In FY04, more emphasis will be put on the use of wavelets to obtain better theoretical insight into scaling properties of the correlation functions.

The research resulting from this LDRD will contribute towards the development of computational capabilities and methodologies at the INEEL that can be applied to a wide range of problems.

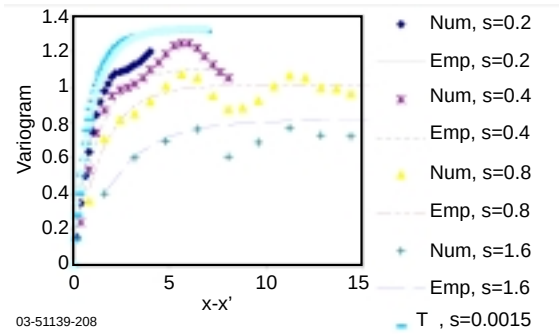


*FIGURE 2. Comparison between correlation structures on different scales obtained from numerically generated data (Num) and empirically derived correlation functions. For the scale s = 0.0015, the variogram was calculated using a wavelet-based theoretical correlation function.*

# Natural and Synthetic Subsurface Colloids

*Glenn A. Moore, George Redden*

***Understanding colloid transport***

GC125

Colloid-facilitated transport is a potential process by which anthropogenic contaminant migration can occur. To effectively model and/or perform mesoscale investigations involving colloid-facilitated contaminant transport, one must first understand the nature of the colloid species present and their dynamic properties.

This LDRD is establishing the requisite capabilities and expertise at the INEEL for collecting and analyzing the natural colloids that are present in vadose zones, perched water zones, and the Eastern Snake River Plain Aquifer. Colloid samples were extracted from Spreading Area B (SAB) soil samples, perch aquifer water/silt samples, and surficial sediment from within the Subsurface Disposal Area (SDA). These samples were characterized for particle size, electrophoretic mobility, morphology, critical coagulation concentration, and mineralogy. Mobility experiments also were conducted using a bench-scale basalt sand column.

A second component of this research involves the synthesis of engineered colloids — man-made colloids that can be made to mimic the mobility characteristics of natural colloids. In FY03, two polymer systems were investigated: poly (bispheoxy) phosphazene (PPOP) and polylactic acid (PLA). Fluorescein-labeled polystyrene was incorporated into the polymer colloids as a tagging agent.

Technical objectives for fiscal year 2003:

- Collect and characterize colloidal matter from INEEL soils.
- Prepare and characterize fluorescent-tagged synthetic colloids tailored to subsurface investigations at the INEEL.

Generally speaking, colloids are particles having a diameter of less than one micrometer. The naturally present inorganic colloidal material in INEEL soil originates from either the parent geologic material or via in situ geochemical processes. These two types of colloidal materials are referred to as detrital and authentic colloidal materials, respectively. Non-native colloidal materials, referred to as man-made or anthropogenic colloidal material can likewise originate from the parent material (e.g., buried materials) directly or be generated in situ via chemical and/or corrosion processes. Colloidal materials can become and remain suspended in groundwater via Brownian motion if sufficient particle-particle and particle-matrix electrostatic repulsion forces are present. Key factors that control colloidal stability in groundwater are particle size, particle surface charge, electrolyte composition and concentration, and pH. However, to realize suspended particles, there also must exist a means for the initial dispersion of the colloidal material in the groundwater present. Such processes include episodic water flow events, dissolution of the binding matrix, geochemical and microbial processes, etc.; otherwise, flocculation, aggregation, and cementation of the colloidal material will likely persist.

Colloidal stability, or lack thereof, in an aqueous suspension is arrived by way of the net particle-particle forces present. Most inorganic “mineral” colloids have a negative surface charge and a gradient charge-interface is established from each particle’s surface into the suspending medium, referred to as the double layer. The first layer of the double layer is the Stern layer, a counter-ion layer sorbed at the particle-liquid interface. The subsequent layer is of graded ionic composition and serves to establish a charge-density transition from the Stern layer to that of the suspending media. The double layer provides a Steric barrier for particle-particle contact. When the particle-particle repulsive forces are dominant, a stable colloidal suspension can be achieved. In this study, the colloidal stability of colloid samples isolated from INEEL soil/sediment was investigated by performing critical coagulation concentration (CCC) experiments. The CCC is a measure of the electrolyte concentration required to promote rapid particle coagulation or flocculation. The method takes advantage of the enhanced settling rate exhibited by flocculated particles in a suspension, a consequence based on hydrodynamic considerations.

A network of 27 Neutron-Probe Access Tubes (NATs) has been established at the Radioactive Waste Management Complex (RWMC). These carbon steel tubes have open bottoms and were installed for monitoring purposes between 1986 and 1993. Installation involved hand-augering through the surficial sediment to the underlying basalt. These bottomless tubes provide a means of accessing residual and/or translocated sediment samples

as well as freestanding water samples when significant rain and snow melt events occur. For this investigation, TPR-1641, Collection of Vadose Zone Water Samples at RWMC, was modified to allow the use of split-spoon samplers, bottom-filling bailers, and suction bailers for obtaining sediment and water samples from the bottom NAT tube holes. In FY03, sediment samples were obtained from thirteen NAT locations: NAT 1, 3, 4, 6, 7, 11, 12, 13, 16, 18, 20, 21, 23. Collected sediment samples from the RWMC were delivered to the INEEL Research Center (IRC), the colloidal material isolated, and characterization experiments were preformed as described below.

Critical Coagulation Concentration (CCC) and colloid mobility experiments were performed. CCC experiments involve the addition of an electrolyte solution to a colloidal suspension, followed by a three-hour settling period in which particle aggregation/flocculation can occur. The concentration and composition of electrolyte solutions used was based on the range of dissolved salt concentration present in INEEL groundwater samples. The ratio of monovalent to divalent cations present in INEEL groundwaters also was taken into consideration. Specifically, the sodium adsorption ratio (SAR) was utilized. The SAR ratio is an empirical measure that takes into consideration the flocculating effectiveness of the cation species present. The SAR ratio is defined as SAR = $[Na^+]/(0.5[Ca^{2+} + Mg^{2+}]^{0.5}$. SAR values are calculated using molar equivalent units, with a SAR of zero representing of a pure divalent solution and a SAR of infinity a pure monovalent solution. In this project's experiments, three SAR ratios were used: 0, 20, and infinity. Sodium chloride and calcium chloride were used as the electrolyte species in the laboratory experiments. The degree of flocculation was quantified by measuring the visible light transmission in the top-most fraction of each sample tube after three hours of settling. The CCC is defined as the electrolyte concentration needed to yield a 97% decrease in absorbance.

Figure 1 shows a graph of the experimental data generated from a CCC series experiment. The data infers that rapid coagulation of the NAT11 colloid sample takes place at electrolyte concentrations between 2.5 and 25 millimolar equivalents per liter (mmolc/L), depending on the electrolyte composition. INEEL groundwaters primarily have electrolyte concentrations of 10-1000 mmolc/L and SAR ratios less than 20. Thus, in most but not all

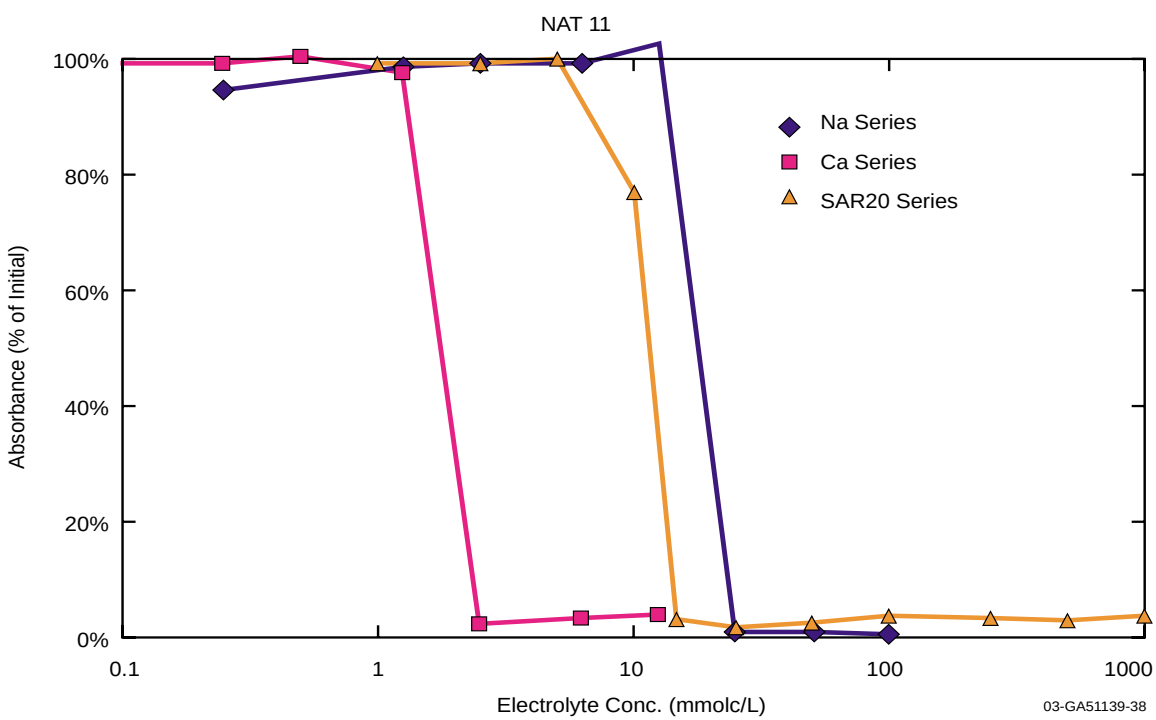


*FIGURE 1. Experimental data generated for determining the Critical Coagulation Concentration (CCC) of a colloidal suspension.*

scenarios the colloidal fraction of NAT11 sample sediment would be prone to rapid coagulation.

Based on the results of the CCC experiments, three electrolyte compositions were selected for subsequent colloid mobility column experiments. The column consisted of a Plexiglas tube (4cm ID and 5cm long) packed with ground INEEL basalt (>0.3mm and <0.6mm in diameter), having a pore volume of 17mL. The column was used under saturated conditions to obtain colloidal break-through curves using dilute colloidal suspensions. Approximately 100-300mg/L of colloidal material was used. This was a concentration that afforded 800,000-1,000,000 counts/sec as measured with a submicron particle size analyzer detector. A flow rate of 168mL/hr, 10-pore volumes/hr, was used to introduce 15 pore volumes of colloidal suspension to the column via an IV pump. This treatment was followed by an infusion of 15 pore volumes of colloid-free electrolyte solution. The electrolyte used in the column experiments was sodium chloride, 0, 10, and 100mmolc/L. An autosampler was used to collect 8ml samples throughout the experiment. Subsequently, the eluted samples were analyzed using the submicron particle size analyzer. Figure 2 shows the colloidal break-through curves generated using NAT13 colloid suspensions.

As expected, colloidal throughput decreased as the electrolyte concentration increased due to the enhanced flocuculation-tendancy of the particles.

Two polymers systems were investigated for colloid synthesis: poly (bispheoxy) phosphazene (PPOP) and polylactic acid (PLA). Fluorescein labeled polystyrene was incorporated into the polymer colloids as a tagging agent. The PPOP and PLA colloids were characterized for particle size, electrophoretic, and fluorescence emission.

The results of this research demonstrate that the INEEL has established the needed laboratory capabilities and expertise for evaluating/comparing stability and mobility of colloids found in the INEEL's surficial sediment. These capabilities and expertise are now being used within the INEEL Completion Project's (ICP) environmental tech-nologies development group in support of filtration process development for sodium-bearing waste sediments. Additionally, the particle characteriza-tion instruments and sample preparation capabilities derived from this LDRD are readily accessible to all INEEL researchers.

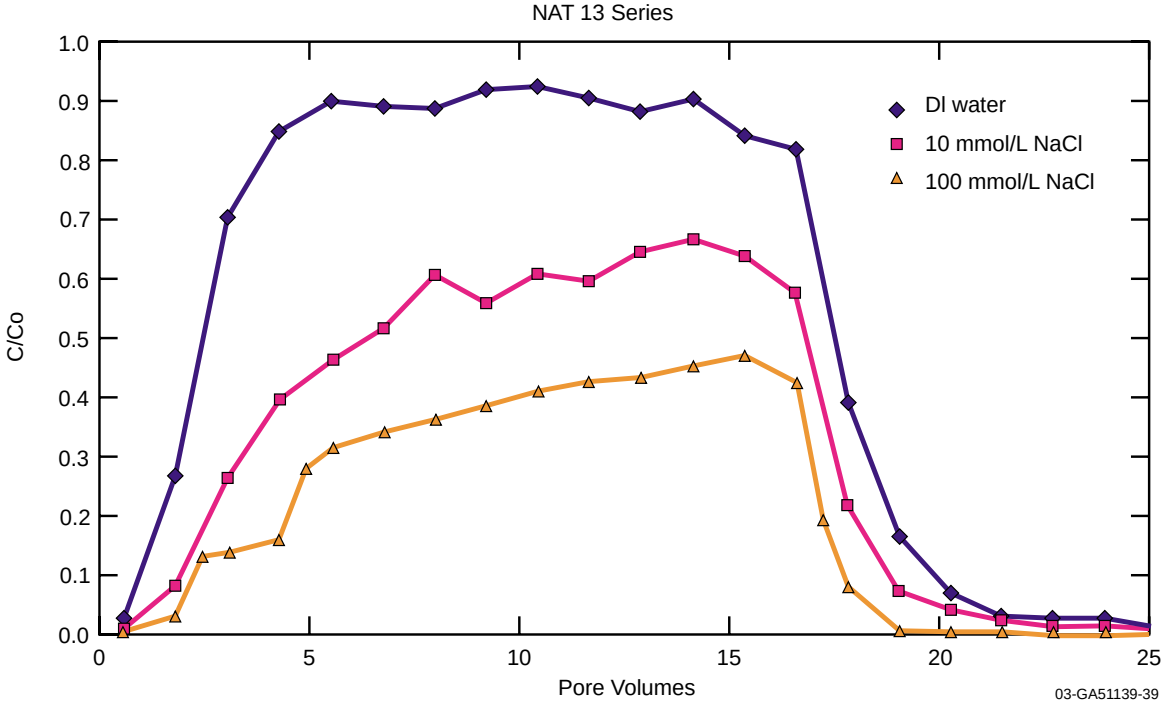


*FIGURE 2. Colloidal breakthrough curves obtained for NAT13 colloids under saturated flow conditions.*

# Modeling an Earth-Borehole System for Physical Property Determination in Shallow Subsurface Environments

*Stephen Novascone, David Weinberg*

***Using orbital vibrators as a physical properties logging tool***

PH104

Porous and fracture properties of subsurface earth materials affect flow and transport of such things as organic pollutants, heavy metals, and radionuclides. Subsurface flow properties are related to subsurface elastic properties. Thus, characterizing elastic properties of the subsurface is important when developing models of subsurface flow and transport.

Early experimental evidence suggests that driving-point impedance measurements can be used to characterize a volume of elastic earth medium surrounding a liquid-filled well (Cole, 1997). Driving-point impedance measurements are obtained by recording the velocity amplitude of a down-hole orbital vibrator (OV) as a function of frequency. An OV is a rotating eccentric mass contained within a closed tube whose frequency of rotation is controllable. When operating in air, the OV displays a circular orbit of constant amplitude throughout its frequency range. Internal cross-polarized geophones (a velocity-measuring device) are sufficiently sensitive to measure the velocity amplitude of that motion. It has been shown experimentally, although qualitatively, that when the OV is placed in a liquid-filled well both orbit amplitude and shape can change because of loading induced by the elastic properties of the well and the medium surrounding the well. This measurable orbit-change phenomenon gives the OV potential for use as a physical-properties-logging tool.

This LDRD is conducting experiments to provide experimental and mathematical modeling evidence that quantifies the sensitivity of the OV to the constitutive properties of the surrounding medium. The mathematical modeling was used to isolate a property of the surrounding medium that affects the steady-state frequency of the OV.

Technical objectives for fiscal year 2003:

- Present results of FY02 experiments and analytical models at SEG conference.
- Create 3-D finite element model (FEM) of OV-liquid-earth.
- Submit technical manuscript regarding 2-D analytical model and OV-lithology experiments to a refereed technical journal.
- Develop analytical model of transverse isotropy in 2-D.
- Create 2-D analytical model that describes observed frequency shift.
- Prepare technical manuscript regarding 3-D FEM, 2-D analytical, and OV-lithology experiments

A 3-D FEM of the OV-liquid-earth has been created using the FEM program ABAQUS. It was hypothesized that a 3-D FEM would capture the physics of the lithology experiments (described in year-end report FY02) better than the 2-D analytical. This hypothesis came from the observation that the small OV was more sensitive to lithology than the large OV. A possible reason for the difference in sensitivity was that the small OV had larger out-of-plane displacements in the surrounding medium because it was shorter than the large OV. The 3-D FEM would capture this behavior. The 3-D FEM was used to show that out-of-plane displacements were indeed larger for the case of the small OV, but did not result in higher sensitivity. It was hypothesized that the small OV was more sensitive because it was lighter than the large OV. Dr. Michael Anderson from the University of Idaho has developed a 2-D analytical model that is capable of modeling a transverse isotropy. This model will be developed further in FY04 to determine if the OV is sensitive to transverse isotropy such as a fracture.

An observation from the lithology experiments was that the frequency of the OV changed when the OV was moved from shale to limestone vertically in the borehole. The frequency shift phenomenon was investigated through analytical modeling and experiment. Two sets of experiments were conducted: one experiment with the OV running in air, and one with the OV running in water. In both sets of experiments, different voltages were applied to the OV motor with geophone signals recorded at each corresponding steady-state frequency. The data from these experiments is presented in Figure 1 as a plot of steady-state frequency vs. applied voltage.

A 2-D model also was developed that shows the energy-absorbing characteristics of the medium surrounding the OV could cause a frequency shift similar to that observed in experiment. This means that the driving-point impedance of the OV is inertial and has a significant damping component. Although this experiment and corresponding model were for a fluid domain, a logical hypothesis is that the damping of the geologic medium can cause a frequency shift. The model calculations for steady-state frequency as a function of voltage also are

plotted in Figure 1. The results of lithology experiments were presented at the 2002 SEG conference in the peer-reviewed Technical Program. The results of the 2-D analytical model of the lithology experiment will be presented at the Acoustical Society of America (ASA) conference in November 2003.

This LDRD has demonstrated that the driving-point impedance of the OV has inertial and energy-dissipating components. Driving-point impedance measurements can be used to distinguish shale and limestone in a cased well by the velocity amplitude and frequency differences of the OV. Further development of analytical and numerical modeling can provide a way to take an OV velocity and frequency measurement and translate that to a geologic elastic property measurement related to energy absorption. The elastic properties can then be used to determine porous and fracture properties. The porous and fracture properties can be used as inputs to subsurface flow models. These models are used to accurately predict contaminant transport, which is a required activity as stated by ER and Site Technology Coordination Group. The new and important FY03 contributions were an explanation of the frequency shift phenomenon and the 2-D transverse isotropy model.

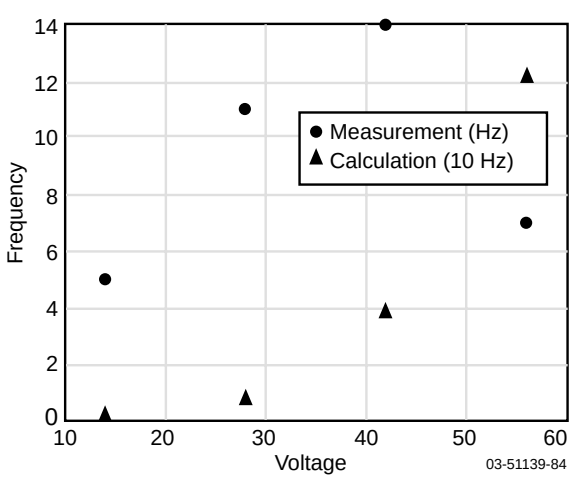


*FIGURE 1. Steady-state frequency in air minus steady-state frequency in water for experimental measurement and analytical model calculation. Note, measurements are in Hz and model calculations are in 10 Hz.*

DOE benefits from this work as it contributes to efforts in meeting DOE obligations to the State of Idaho regarding environmental cleanup. Results of this work can also be applied to other national labs and private industry. This LDRD adds to the sophistication of the region's scientific community in the field of environmental restoration. The INEEL has already benefited by being recognized at international conferences such as the Society of Exploration Geophysicists (SEG) and ASA, and having increased experimental and modeling capabilities that can be considered a national resource to the country.

Further, the implications of this work are important to workers outside of EM, namely, Fossil Energy and National Security. Brief presentations of the OV research results have been provided for Haliburton and Schlumberger. Each company has expressed interest in the application of the OV as a physical properties logger, and CRADAs are a possibility within the next year. An Invention Disclosure Record has been started regarding the use of the OV frequency shift phenomenon for physical properties logging.

# Development of Techniques for In situ Measurement of Groundwater Contaminant Source Strength

*Carl D. Palmer*

***Improving predictability of contaminant transport and fate***

GC130

Plumes of contaminated groundwater are usually generated by stationary sources of contaminants such as non-aqueous-phase organic liquids, ionic contaminants sorbed to mineral surfaces, or mineral phases that dissolve or react to yield contaminants. An important step in designing a remedial response is to measure the rate of mass transfer from the sources into the flowing groundwater. In principle, such rates can be measured in the laboratory; however, the application of such laboratory tests to field-scale problems has not been generally successful. It is better if the rates of mass transfer and the associated biogeochemical parameters are obtained at the field pilot scale, at scale, and under conditions more similar to the actual field conditions.

The purpose of this LDRD is to investigate methods for measuring in situ reaction parameters to improve the design, implementation, and assessment of the performance of groundwater remediation programs. In situ measurement of biogeochemical reactions rates facilitates understanding and manipulation of processes that control the fate of contaminants in the subsurface. The effectiveness of remediation can be monitored by measuring the rate of the relevant reactions and by comparing the pre- and post-treatment rate of dissolved contaminant generation. The parameters can be obtained through single-well push-pull tests (SWPPTs). The mathematical theory, procedures, and equipment for in situ measurement of various biogeochemical processes are being developed. The existing theory for making such measurements with SWPPTs has been extended to more general cases.

Technical objectives for fiscal year 2003:

- Derive mathematical solutions to SWPPT data that can be used to obtain in situ measurement of biogeochemical parameters.
- Test these mathematical models using physical models.

A series of mathematical solutions have been derived to help interpret the data collected from SWPPTs. Most of the analytical solutions derived include reactions occurring during the push, rest, and pull phases for any combination of injection and extraction rates. The rates of decay on the surface, in the well, and in the aquifer can be different. The solutions are more realistic than previously published solutions to similar problems. For first-order decay, the concentration of a reactive tracer declines due to reaction during injection, and the concentration in parcels of solution injected earlier (i.e., those parcels farther from the injection well) is less than that in parcels that were injected later (i.e., those parcels closer to the injection well). Thus, at the end of the injection phase, concentration declines with radial distance from the injection well. This behavior is seen in the solution derived (Fig. 1). In contrast, previously published solutions do not show this behavior. Snodgrass et al. (1998) assume that the solution is injected instantaneously and, therefore, no decay occurs during injection. Haggarty et al. (1998) assume that

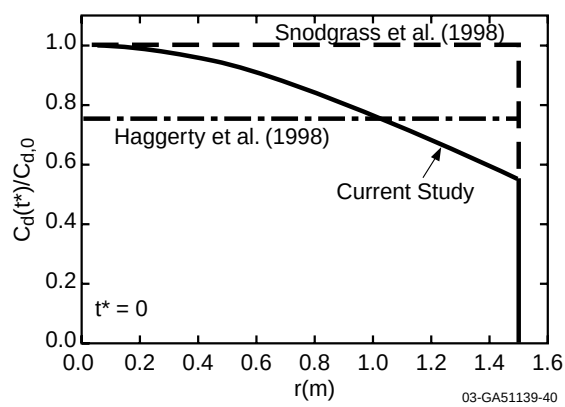


*FIGURE 1. Comparison of model of tracer distributions at end of injection phase.*

decay occurs during a finite injection period, but the injected fluid is completely mixed in the aquifer. Numerical models (PORFLOW) of the concentration distribution at the end of the injection phase (Fig. 2 next page) show good agreement with this project's model with maximum differences between the concentrations calculated with numerical model and those calculated with our model being < 0.01.

Equations also have been derived for a general nth order decay problem. This solution is valid for any value of n not equal to unity. Similar to the first-order decay solution, it accounts for decay on the surface, in the well, and in the aquifer during all phases of the push-pull test. Different flow rates

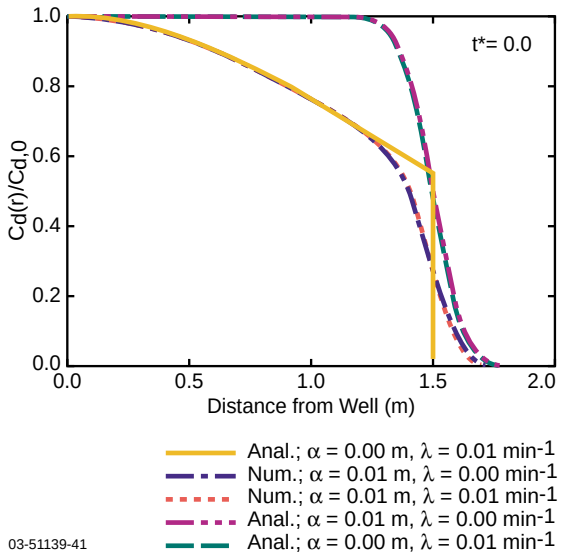


*FIGURE 2. Comparison of numerical and analytical solutions for tracer distributions at the end of injection phase.*

during injection and extraction are included. The only comparable solution is by Snodgrass et al. (1998) for the special case of zeroeth order decay (n = 0) under the assumption of an instantaneous injection. The Snodgrass et al. solution is a special case of the more general solution derived under this LDRD.

In addition to the simple decay processes, comparable equations for dissolution to an equilibrium state have been derived. Such equations are useful in determining the rate of dissolution of nonaqueous liquids or inorganic precipitates within the aquifer.

Most methods for the interpretation of push-pull test data do not include a rest stage, although in practice, there often is one. This research included a rest stage in its method for interpretation of data to obtain first-order and n-th order ($n \neq 1$) rate coefficients; however, it is assumed that advective flow during the rest phase is insignificant. If the background groundwater velocity is relatively large and the injected slug is relatively small, the center of mass of the injected slug will be advected down the gradient and it will no longer be centered on the extraction well. During pumping, water from the injected slug will mix with native groundwater within the extraction well, altering the tracer concentrations and complicating data interpretation. The investigators have derived mathematical equations for a SWPP test using a conservative tracer and a solute undergoing first-order decay that includes the effect of advective transport during the rest phase. These equations will aid in the interpretation of SWPP test data.

There are several limitations to obtaining retardation factors from push-pull test data using commonly used methodologies. To overcome these limitations, Schroth et al. (2001) developed a method for analyzing the data to yield a retardation factor from the dispersion. However, such a second-moment analysis method is likely to have much greater error than methods based on first-moment analysis. This LDRD research proposes that by allowing for a sufficiently long rest period so that the injected slugs of conservative tracer and retarded tracer are not symmetric about the extraction well, there is enough separation of the two tracers to perform a first-moment type analysis to obtain an accurate measure of the retardation factor. The investigators have derived mathematical equations for an asymmetric SWPP test using a conservative tracer and a solute undergoing simple linear partitioning that allows for such first-moment analysis. The general methodology and equations developed under this LDRD will greatly improve the ability to interpret SWPP test data for retarded solutes.

A physical model for testing the mathematical models has been designed and constructed. The model aquifer represents a cylindrical, homogeneous, isotropic, confined, granular aquifer. A well is located at the axis of the cylinder. A constant head boundary is at the circumference of the model. The model is housed in part of a 5-gallon plastic bucket. The model aquifer consists of three sand bodies and an impermeable membrane. The aquifer is simulated by a cylindrical body of finer sand in the bottom of the model. An annular ring of coarser sand is present between the circumference of the

finer sand and the wall of the bucket. This coarser sand ring provides a relatively high hydraulic conductivity zone that is part of the system and maintains a constant hydraulic head at the circumference of the model. Quartz sand (Unimin Corp.) is used as the porous media in the model aquifer. An impermeable membrane comprised of 4-mil polyethylene sheeting is used as a confining layer above the top of the finer sand cylinder and the coarser sand ring.

Two general experiments have been conducted with the physical model. In the first experiment, tritium was used as the conservative tracer and Tc-99m was used as a tracer undergoing first-order decay. In the second experiment, $Br^-$ was used as the conservative tracer and $BaCrO_4$ coated onto quartz sand was used as a precipitate undergoing dissolution. Preliminary interpretation of the SWPPT data from these two tests indicates that calculated porosities (0.45 ±0.06 and 0.38 ±0.02) and dispersivities (0.24 ±0.01 and 0.28 ±0.08 mm) based on the concentrations of the two conservative tracers ($H^3$ and $Br^-$, respectively) are similar. Interpretation of the data from these experiments continues.

The results of this LDRD work will facilitate the interpretation of single-well push-pull data allowing researchers to obtain in situ average biogeochemical parameters. This information is vital in evaluating proposed remedial actions at DOE sites and assessing the long-term stewardship of DOE lands. This project has fostered a relationship with North Wind, Inc., a consulting firm that may be using SWPPT in future work. The work accomplished under this LDRD is also of interest to researchers at two universities who may be interested in future collaborations and potential manuscripts.

# Enhanced Techniques for Evaluating Colloidal Transport Processes

*Judy K. Partin, George D. Redden*

***New sensing technology offers in situ characterization and detection***

GC106

The analysis of colloidal matter, and its role in contaminant mobility, is an important need for DOE sites with significant quantities of buried mixed wastes. In particular, colloidal-facilitated transport may be responsible for the presence of radionuclides occasionally detected in groundwater samples at the INEEL.

Models for contaminant transport processes have typically treated groundwater as a two-phase system in which the contaminants are partitioned between the immobile solid constituents and a mobile aqueous phase. Sub-micron particles, or colloids, may also be mobile in the subsurface environment. These small particles exhibit very high surface area per unit mass, and are often very effective sorbents for metals and other contaminants. Consequently, the association of contamination with colloidal particles may strongly facilitate its transport into groundwater reservoirs. Existing models tend to underestimate, or even ignore, colloidal-transport phenomena due to the limited data available on their composition, concentration, distribution, and affinities for binding with other materials. A better understanding of these transport processes is critical for the accurate assessment of current contamination problems, as well as for the development of cost-effective remediation and containment strategies.

This LDRD is investigating a new sensing technology for the in situ characterization of low-density colloidal suspensions, combining features of laser-induced breakdown spectroscopy and acoustic detection. The technique offers the possibility of not only detecting the presence of sub-micron particles at very low number densities, but also determining their species composition.

Technical objectives for fiscal year 2003:

- Upgrade instrumentation to improve sensitivity and increase spectral range.
- Conduct laboratory testing to validate technology for the characterization of complex mixtures and adsorbed contaminates.

Current monitoring and characterization methods for subsurface colloids rely upon light scattering techniques or the collection of particulate by conventional or ultra-filtration, followed by standard analytical analyses including inductively coupled plasma, scanning electron microscopy, and energy-dispersive spectroscopy. Light scattering techniques are not sensitive enough to detect low concentration suspensions. The filtration techniques are very costly, labor intensive, and may not accurately sample colloidal materials in the very small particle size ranges or at the appropriate times to detect significant events. Most sampling methods are prone to generating artifacts due to physical disturbances, such as pumping, that can remobilize colloids, or collection of fine particles associated with drilling.

This research is investigating a new monitoring capability that is based upon the interaction of small particles with a high-energy laser pulse. When a particle is introduced into the focal volume of such a laser, the particle is vaporized and ionized producing luminous plasma and a pressure wave, or acoustic signal. The spectroscopic analysis of the plasma can be used to determine the elemental composition of the particle, and the amplitude of the acoustic signal, as a function of the laser energy, can be used to determine the particle size. The particle concentration, or number density, is then determined by measuring the number of signals as function of laser shots for a given energy.

In FY01 a series of scoping experiments were performed to establish the ability of the laser-induced breakdown technique to detect various types of sub-micron metallic oxide particulate dispersed into aqueous solutions. During FY02, this testing was expanded to include other colloidal matrices of interest to subsurface applications, including actinide surrogates. These proof-of-concept experiments successfully demonstrated the ability of the technique to detect and characterize the presence of various types of colloids at low number densities. The ability to correlate signals with particle size also was established. Experiments also were conducted to determine if small

amounts of material adsorbed into the colloidal matrix could be detected. The presence of the adsorbates could be detected on colloidal powders but could not always be seen with good signal-to-noise when suspended in aqueous solutions with the existing experimental set-up. Consequently, FY03 work concentrated on upgrading the instrumentation to increase its sensitivity to determine if adsorbed contaminates could be successfully detected and; in addition, to expand the spectral range of detection so that complex mixtures of species could be more readily investigated.

The upgrade involved replacing the18 mm, 760-pixel-format intensified linear array with a 25 mm intensified charge couple device (CCD) array with 1024X256 pixels. The CCD detector increased the spectral range by approximately 30%. It also resulted in improved detection sensitivity by allowing bins of pixels to be averaged, resulting in lower noise and better compensation of pixel-to-pixel variations. The fixed-solution cuvette sample chamber was replaced with a dynamic flow loop and a computer-controllable sample injection system. A second pulsed laser system also was introduced into the experimental configuration and timing circuitry was developed that would allow two separate laser pulses with variable delay to interrogate the sample. This modification allowed the investigation of the impact of the plasma kinetics on the detection sensitivity. A schematic of the upgrade system is presented in Figure 1. Using the upgraded system, the characterization of complex mixtures of goethite, calcite, and kaolinite particulate with sizes ranging from 0.5 –5.0 micron mean diameter was conducted. The results of

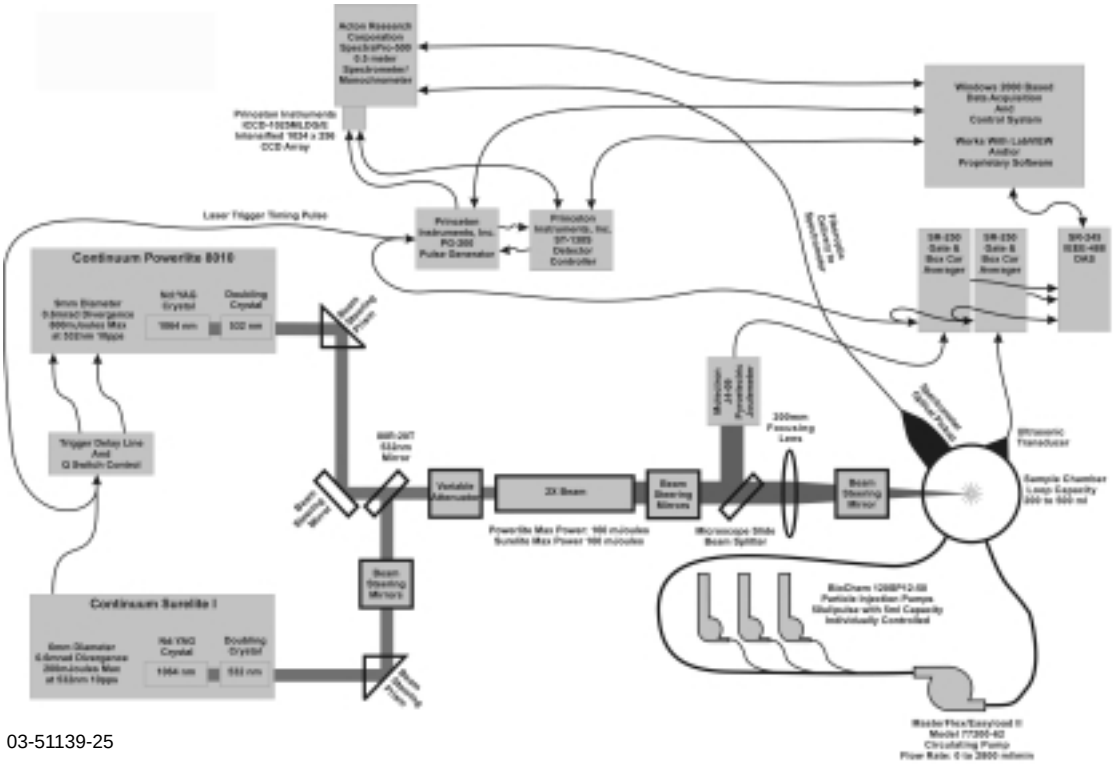


*FIGURE 1. Experimental schematic.*

experiments using a 10 ppm concentration by weight of these materials is presented in Figure 2. Spectral bands corresponding to each of the minerals were identified as they were introduced into the flow loop, as shown. The improved measurement sensitivity also allowed the successful detection of adsorbed contamination on particulate in a liquid medium. In particular, the rare earth element dysprosium was detected when adsorbed on a 0.5 micron particle of goethite.

In addition to providing a unique monitoring capability for predicting and evaluating contaminant transport from buried waste sites throughout the DOE complex, this technology may have a number of other potential applications. The detection and control of suspended fine solids is important to a variety of manufacturing processes, including the semiconductor and biochemical engineering industries. The control of boiler water quality is very important in power production to prevent damage to turbine blades or other critical components. The ability to detect very small levels of various metals could allow an assessment of the health of the plant operation. Mining and mineral recovery operations also could benefit from the technology. Additionally, this work could be valuable to national and homeland security agencies for use in detecting or monitoring for aerosol emissions from biological or dirty bombs.

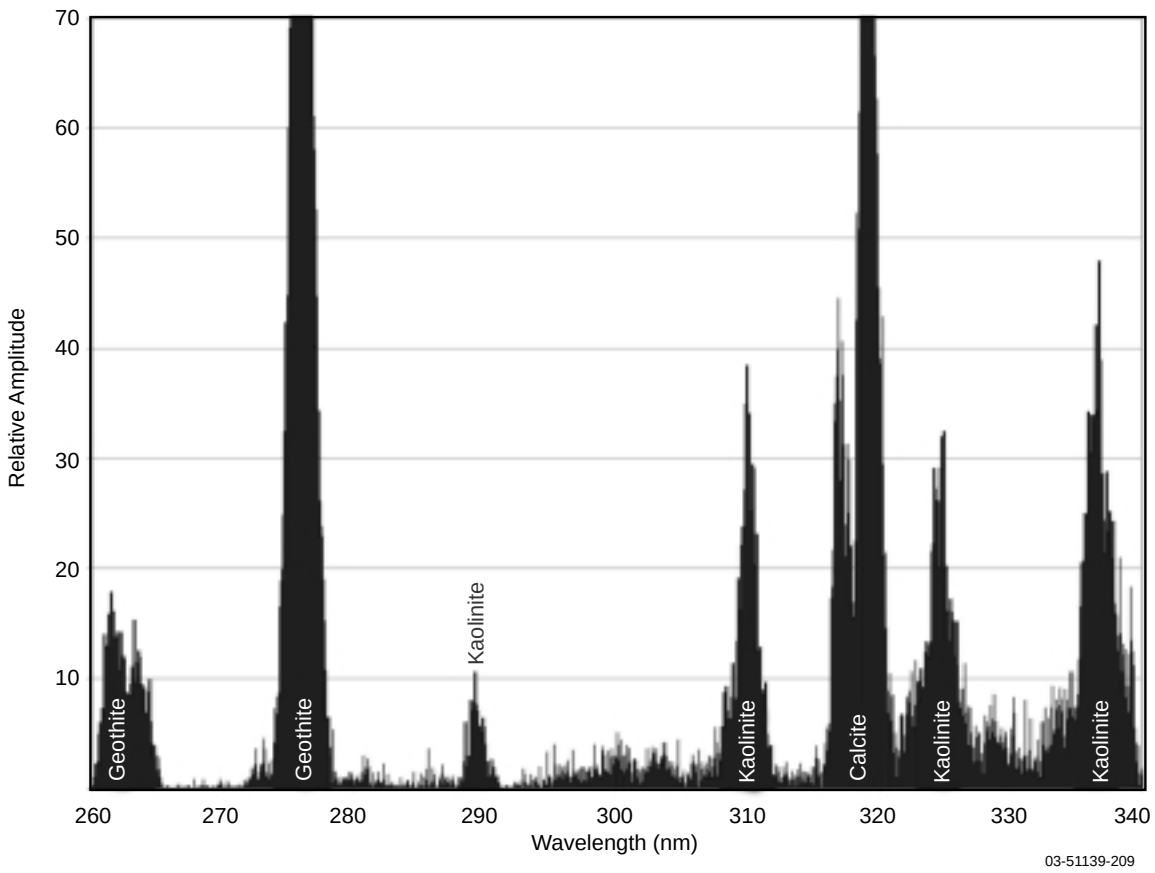


*FIGURE 2. Spectral signatures indicating presence of geothite, kaolinite, and calcite minerals in 10 ppm mixture.*

# Evaluating Microelectrodes and Fiber-Optic Probes for Use in Mesoscale Experiments

*Patrick J. Pinhero, Tedd E. Lister, William F. Bauer, George D. Redden*

***Providing long-term, real-time collection of chemical data***

GC117

The INEEL mission statement includes a directive to improve the understanding of subsurface environments. These environments are notoriously complex as demonstrated by the fact that many systems classified as homogeneous can have heterogeneous transport properties on different scales. To establish links between laboratory observations and the complex systems found in the field, the INEEL has given high priority to mesoscale demonstration projects. Mesoscale projects will be designed on scales necessary to study complex coupled processes. Many of the processes to be studied will largely be influenced by chemical parameters that will be variable due to heterogeneities inherent to or that develop within the system being studied. To derive the most benefit from the mesoscale experiments, it will be necessary to acquire spatially and temporally resolved data using various sensors strategically placed within the experiment.

This LDRD addresses the issues related to in situ measurement of chemical parameters during the course of such a mesoscale experiment. Specifically, available microelectrode and fiber-optic sensor technologies are being evaluated to determine how they may be effectively incorporated into mesoscale experiments to provide long-term, real-time collection of chemical data. When the desired performance is not achieved, adaptations of the sensor technologies are being made to maximize the performance for long-term investigations of the subsurface using mesoscale experiments.

Technical objectives for fiscal year 2003:

- Evaluate fibers and probes for UV applications to directly determine tracers in sand-filled columns.
- Evaluate "microelectrodes" for pH, $O_2$, Na, Ca, etc.
- Program LabView for optimal data collection from the microelectrodes.

The response for the fiber-optic probes was found to be much better than for the microelectrodes. Figure 1A shows a photo of the column assembly. The column was constructed from three individual end-flanged cylinders. Each of these cylinders possesses four ports, oriented 90º to each adjacent port, for positioning each microsensor. The dimension of the assembled column was 9 cm diameter x 25 cm long. The sand column was filled with 23-30 mesh Ottawa sand (Fisher Scientific). The liquid volume of the sand-filled column was estimated at ~660 mL. The target flow rate for the column was adjusted to 4.75 mL/min for the microelectrode experiment. Figure 1B shows a plot of the data from a 20-hour experiment with several microelectrodes. In this particular experiment, a pH microelectrode was positioned in a port in the top section, with another positioned in a port within the bottom section. Oxygen microelectrodes were placed in like positions. In the central section, a potassium (K+) microelectrode was positioned. At 900 s, a 100 mL plug of pH 10 buffer was introduced to the top inlet in the column. This was followed at 2700 s by a rinse cycle with deionized water until 7500 s when the water was deaerated

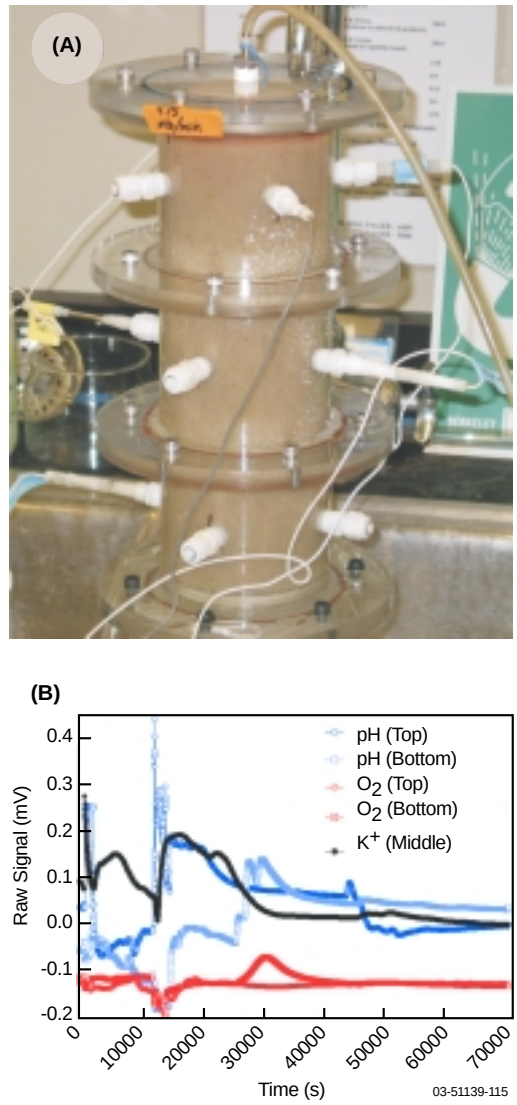


*FIGURE 1. (top) Photo shows the 9 cm x 25 cm test column and arrangement of the microsensors. (bottom) Plot of several microelectrode responses for a 20-hour experiment.*

with nitrogen gas. At 11300 s a 50 mL plug of 1.00 M CaCl2 was introduced, followed at 14200 s by a 100 mL plug oh pH 4 buffer, and finally the column was rinsed with deaerated water from 16000 s to 70000 s. The data track the events quite reliably, but it was found that the robustness of the micro-electrodes was compromised at longer times and their response rapidly deteriorated.

Other than the fiber-optic oxygen sensors offered by Ocean Optics, no commercially available "optodes" for chemical specific sensing have been found other than probes offered for standard transmission, reflectance, or fluorescence spectroscopy. This lack of chemical-specific optodes also has led to the development of a fiber-optic-based direct UV spectroscopic method for determining water quality parameters and common infiltration tracers. The primary problems with this methodology have been the lack of optical transmission of common "solarization-resistant" optical fibers. The optimal optical fibers were the UVM fibers obtained from Polymicro Technologies, LLC, and optimally configured into 1/4" and 1/8" diameter transmission probes with 1 cm pathlengths by C-Technologies, Inc. The probes made with UVM fibers performed consistently and showed very little, if any, degradation at any wavelength with time, even at wavelengths below 250 nm. Conversely, all of the probes with non-UVM fibers rapidly solarized and at less than 250 nm with the relative transmission being <20% after only 6-10 hours of use.

For incorporation into the sand column, the transmission probes were covered with a dialysis membrane to prevent the optical path from being obstructed by the sand, colloidal materials, and microbial growth. A 300,000 Dalton molecular weight cutoff cellulose ester membrane was used (Spectra/Por® CE, Spectrum Laboratories, Inc.). The "breakthrough" time for iodide with this membrane is <3 minutes and equilibrium is reached in ~2 hrs. For mesoscale studies where tracers move only short distances per day, this should be more than adequate.

The 9 cm x 25 cm sand column was filled with 23-30 mesh Ottawa sand (Fisher Scientific) and the fiber-optic transmission and oxygen probes placed within 3 cm of the top and bottom of the column. The liquid volume of the sand-filled column was estimated at ~660 mL. The target flow rate for the column was 1 mL/min. Transients of 1 to 10 mL of 1000 ppm bromide or iodide standards were introduced to the top of the column. Spectra from the four optical channels were collected at 5-minute intervals and typically consisted of an average five scans per channel.

Figure 2 is an example of results that can be obtained with the optical detection methods. Even though the net concentrations of the bromide and iodide tracers were somewhat higher than expected, the results demonstrate the utility of the UV transmission spectroscopic method. Over the period of the ~8 days shown in Figure 2A through 2C, the baseline changed very little indicating the resilience of UVM optical fibers to UV radiation below 210 nm. In fact, even after 21 days the probes appeared to be working with minimal apparent damage. The actual determination of concentrations in Figure 1B with partial least squares (PLS) calibrations is somewhat problematic due to nonlinearities caused by the absorbance values which exceed 3-4 at some wavelengths. However, the concentration determinations at the leading and trailing edges of the transients appear to be good, and are approximately what would be expected. At 1 ml/min, the front requires ~10 hrs to travel from the top to the bottom of the column. While this is probably slightly skewed by the equilibration time for the dialysis membrane, it is more than adequate to see the arrival of the tracer at the probe. Even though some flow problems were encountered, the oxygen-specific fiber-optic probes appeared to be functioning properly after 9 days in the column, and then for the next 13 days.

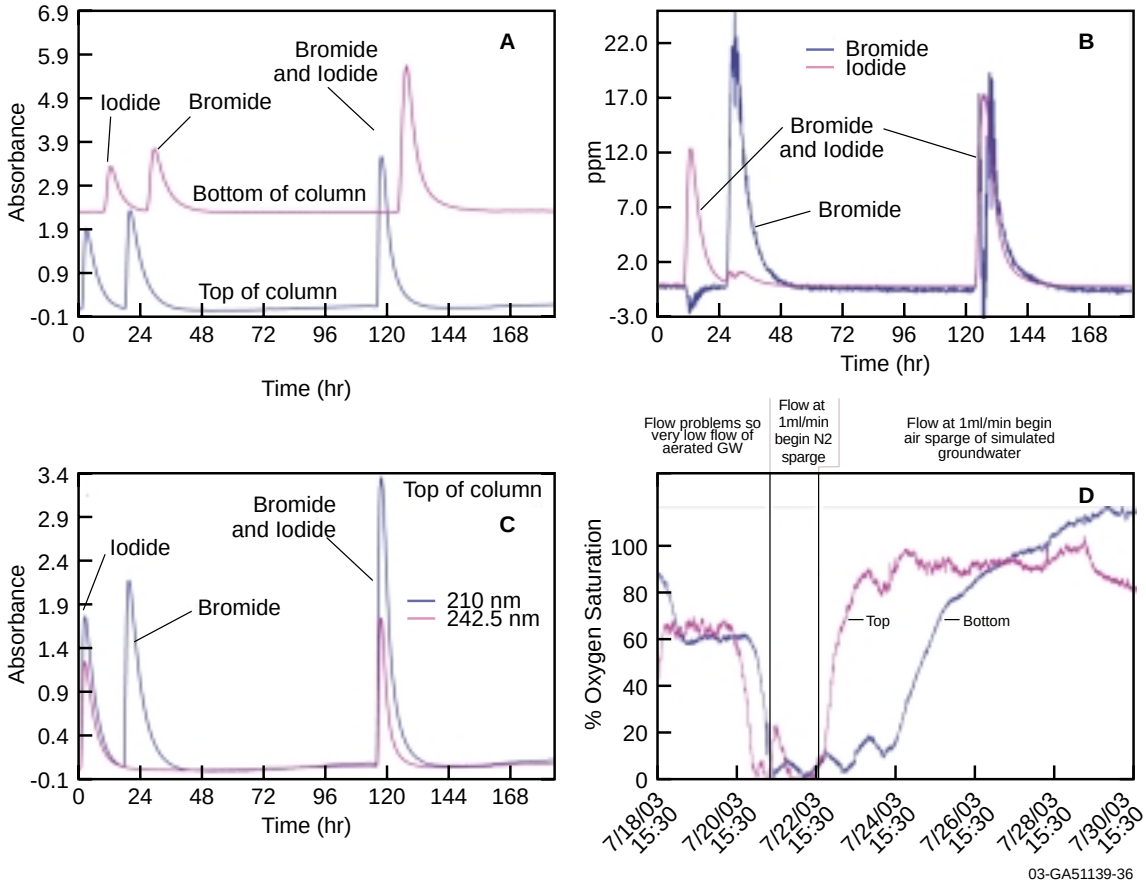


*FIGURE 2. Transients of bromide and iodide tracers and oxygen as detected by UV transmission spectroscopy with fiber-optic probes and oxygen-specific optodes. A) Absorbance at 210 nm of the transients as they pass from the top to bottom of the column. B) Bromide and iodide concentrations determined via PLS calibrations. Absorbance out of linear range causes some error. C) Comparison of the traces at 210 nm and 242.5 nm showing the selectivity for $Br^-$ and $I^-$. D) Oxygen saturation determined with fiber-optic probes over a 13-day period and after the probes had been in the column for ~21 days.*

While the microelectrodes were quite erratic and unreliable in the column, the fiber-optic probes appear to function as expected. Incorporating the fiber-optic techniques into a mesoscale experimental setup would be appropriate.

The INEEL mission statement includes a directive to improve the understanding of subsurface environments. This LDRD work is directly contributing to that objective by improving methods of chemical data collection.

# Estimating the Climatic Sensitivity of Vadose Zone Infiltration Rates Through Paleohydrologic Analyses

*Mitchell A. Plummer*

***Understanding the relationship between recharge and climate***

GC152

Long-term performance of surface landfill covers, sustainable water resources in arid environments, and risk and performance assessments all rely on long-term predictions of water flux rates through the vadose zone. Because that flux varies with climatic conditions, it is important to understand how future climatic shifts may alter moisture flux through the vadose zone. The response of a particular ecosystem to climatic change is complex, as numerous interacting environmental factors control the surface soil-moisture- and energy-balance. The climatic sensitivity of vadose zone moisture flux to even the primary climate variables (temperature and precipitation) is, thus, difficult to predict.

To assess the potential changes in deep percolation that may accompany future climatic change, this LDRD aims to improve understanding of the relationship between recharge and climate by studying how past climatic changes affected recharge. By using relatively undisturbed areas of the remote INEEL site as a natural vadose zone laboratory, this study should also provide important information about natural moisture fluxes in an area where contaminant transport rates through the vadose zone are of critical concern to the DOE.

This study involves two primary efforts: 1) identification and interpretation of a record of changes in deep infiltration, and 2) reconstruction of major temperature and precipitation variations for the same time period.

Technical objectives for fiscal year 2003:

- Examine and identify areas of native vegetation likely to incur low but positive deep percolation rates, and that contain a sufficient depth of sediment to preserve a record of climatically induced changes in that flux.
- Design and implement a field investigation program to obtain soil samples for analyses of soil moisture potential, conservative anion concentration, and stable isotope composition.
- Purchase instrumentation, and develop and test an ion-chromatography method for determination of low concentrations of Cl and Br.
- Develop numerical simulations of the long-term evolution of soil moisture and geochemistry in arid vadose zones (including thermal energy transfers and vapor movement via advection and diffusion).
- Develop a numerical model of the evolution of stable isotopes in an arid vadose zone under a wide range of vertical fluxes.

An important component of this study focuses on conservative tracer accumulation and movement in the vadose zone. In the past, interpretation of the signals of these tracers has been hampered by an incomplete understanding of vadose zone hydrodynamics and resultant discrepancies between predictions and observations of tracer behavior. Recent studies (Walvoord et al. 2003; Scanlon et al. 2003), however, have put forward a new conceptual model of flow in arid-region vadose zones that explains these discrepancies and provides a new interpretation of the tracer signals that are commonly preserved at arid sites. In particular, these studies suggest a new interpretation of the chloride bulges commonly observed in soil moisture profiles obtained from the southwestern U.S. Contrary to previous interpretation, they indicate that chloride bulges represent a long-term state of net upward moisture flux. As a consequence, few studies in the arid and semi-arid western U.S. have examined vadose zone profiles that actually evidence changes in fluxes incurred during the last 10,000 years.

This study focuses on finding areas in which chloride profiles do, in fact, preserve a long-term record of variations in diffuse recharge. The cold semi-arid climate of the Eastern Snake River Plain suggests that the long-protected sagebrush steppe at the INEEL may be such an area, and the FY03 drilling, sampling and analytical program indicates that alluvial deposits in parts of the site preserve a record extending back more than a thousand years. Matric potential profiles obtained during that program also demonstrate that vertical moisture fluxes are at least temporarily upward in the upper ~3 meters of sediment (Fig. 1). This appears to contradict data from tensiometers installed in similar sediments at the site. The investigators will attempt to resolve this discrepancy via installation of additional moisture potential monitoring equipment in FY04.

Previous studies have used chloride as an indicator of net percolation past the root zone. One of the goals of this study is to evaluate the potential of using Cl/Br ratios as another indicator of soil

moisture age. This will be accomplished through examination of Cl/Br ratios along several vertical soil moisture profiles and through analysis of ice samples from an ice core of the Upper Fremont Glacier in the Wind River Range of Wyoming, which dates back to approximately 1850 A.D. In addition, the project will evaluate the potential application of stable isotopes of hydrogen and oxygen as indicators of recharge conditions by numerical simulation of the evolution of the isotopic composition of water under a variety of recharge conditions.

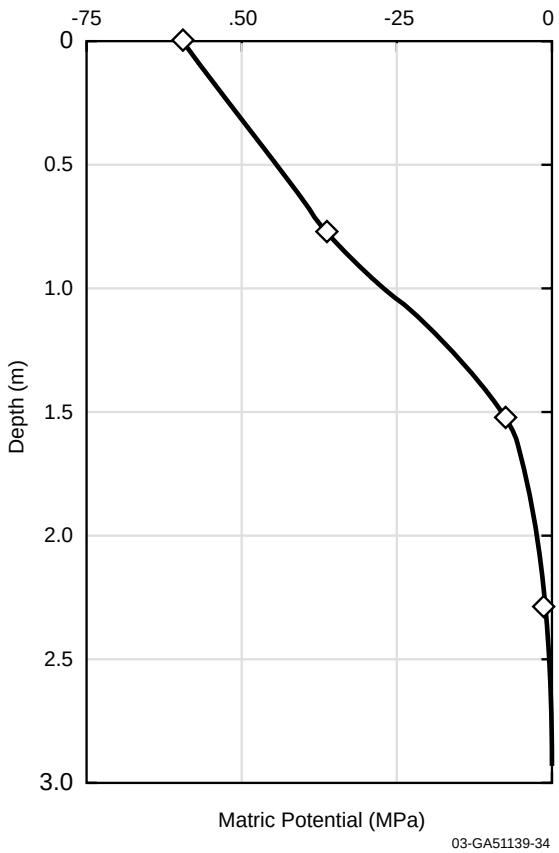


*FIGURE 1. Typical matric potential profile observed in the upper few meters of sediments during this study from test boring performed in August 2003.*

A second task of this project is to refine existing paleoclimate records for the area. As the region contains abundant glacial geomorphic features that were constructed during the latest Quaternary glacial cycles, the investigators first concentrated on paleoclimatic interpretation of those features via application of a 2-D glacier simulator developed specifically for that purpose. The simulator provides detailed maps of the glacial extent and distribution that would result from a wide range of climatic departures from modern conditions, thus enabling the investigators to determine the conditions that could produce observed paleoglacial features. In FY03, minor modifications were made to the model to provide:

- The ability to vary net accumulation/ablation source term with time, thereby allowing simulation of independently reconstructed time-series of climatic variation.
- Tracking of the terminus position along a predetermined flowline.

Subsequent presentation of the model's application to a paleoclimatic record derived from chironomid remains in alpine lakes resulted in several requests for collaborative application of the model to other field areas. In FY04, the investigators will collaborate with researchers in the USGS and National Park Service to apply the model to areas in Yellowstone/Grand Teton National Parks and the Wind River Range of Wyoming, where past climatic changes should be representative of those in southeastern Idaho.

The studies conducted as part of this project, combined with data from previous studies, should provide reasonable estimates of the major changes in temperature, precipitation, and vadose zone fluxes that occurred during the last ~20,000 years. In FY04, the project will examine the climate and infiltration datasets to determine whether there is a consistent relationship that can be used to understand the controls on subsurface infiltration. This relationship will then be used to provide a preliminary assessment of the climatic sensitivity of specific sites at the INEEL (WAG-7, -10). It is anticipated that data, as well as conclusions and questions resulting from this limited study, will provide a strong foundation for a more comprehensive study aimed at examining the relationship between recharge and vegetation, ultimately leading to a remote sensing approach to estimating diffuse recharge rates in arid areas. These capabilities will provide a valuable resource to the INEEL and DOE for long-term stewardship decisions.

# In Situ Degradation of Explosives in the Vadose Zone

*Corey W. Radtke*

***Assessing remediation methods for hazardous waste cleanup***

PH101

Explosives contamination is widespread throughout the DOE complex and includes environmental problems at Pantex, Los Alamos, and the INEEL. This issue also affects over 1200 DOD and private sites in the U.S. and abroad. These sites typically harbor a surface soil or vadose zone source contributing to continuing groundwater contamination. For example, firing ranges are exceedingly difficult to remediate and may contaminate groundwater via vadose-zone leaching.

This LDRD is evaluating the design, optimization and field-testing of an in situ vadose zone explosives remediation system. The treatment system showed very promising laboratory results in batch studies, but column tests revealed less robust degradation, as did an in situ pilot demonstration at the Pantex facility. While several findings of increased explosives degradation due to the added organics are statistically significant, none are estimated to be commercially significant.

As the lab tests were found to imperfectly, and sometimes inadequately, predict the field contaminant metabolism (also found in many other studies throughout the world), the investigators invented a flow-through in situ reactor to bring treatability-study lab work to the field and eliminate many of the shortfalls of lab work. An initial prototype was fabricated and tested, and modifications were made. Then, a second prototype was built and tested using direct-push technology and butane as a vadose zone tracer. The microcosm was successfully installed through 18 inches of soil containing at least 4 inches of tightly packed caliche. The investigators are currently further developing the reactor.

Technical objectives for fiscal year 2003:

- Complete injection of carbon sources into the subsurface at the Pantex facility; sample site to analyze explosives concentration in treated soil after at least six months of treatment.
- Perform a column study to further test the effect of gaseous substrates on explosives degradation in Pantex soil.
- Prepare papers for publication in a peer-reviewed technical journal.

*Batch Studies for Explosives Degradation*. The field site received carbon source augmentation for over one year while being tested for breakthrough of the carbon sources and daughter products as well as explosives concentration in the soil. The batch studies revealed the organic carbon amendments significantly impacted explosives degradation. The carbon source additions themselves degraded to undetectable levels in about 1.5 days (data not shown), while nitrous oxide had a half life of approximately one month. The carbon sources significantly increased the rate of hexahydro-1,3,5-trinitro-1,3,5-triazine (RDX) (Fig. 3) and 1,3,5-Trinitrobenzene (TNB) degradation (Fig. 1 and 2), but had no effect on octahydro-1,3,5,7-tetranitro-1,3,5,7-tetrazocine (HMX) (data not shown). The nitrogen gas control supported limited RDX and TNB degradation. Nitrous oxide control flasks supported TNB but not RDX degradation.

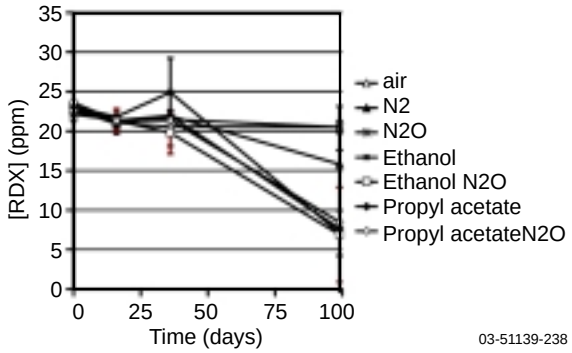


*FIGURE 1. RDX time course in soil under select treatment gases.*

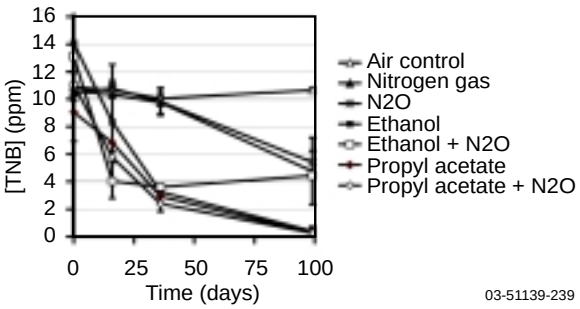


*FIGURE 2. TNB time course in soil under select treatment gases.*

*Column Studies for Explosives Degradation.* The column studies showed less effectiveness than the batch studies in all cases. This was the opposite of what was expected as the columns received overwhelmingly more carbon and energy per unit soil compared to the batch studies. The first round of column studies was carried out for 225 days and revealed that amendments including nitrogen alone, 0.1% oxygen, 1% oxygen, and air did not promote explosives degradation. Ethanol in a nitrogen stream did stimulate degradation, but only in the first 5 inches of the soil. Propyl acetate showed more promise (Fig. 3). Isopropyl acetate showed nearly complete conversion into acetone, which subsequently flowed farther through the soil (Fig. 4). However, in this second column study, it was once again found that only the top portion of soil showed accelerated explosives degradation (Fig. 5).

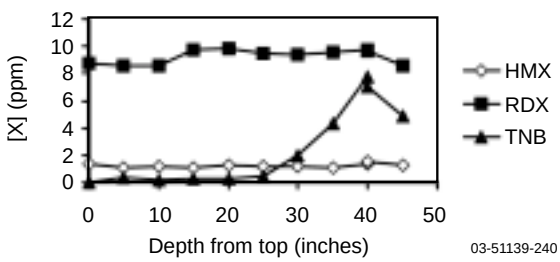


*FIGURE 3. Sectional analysis for trace explosives of a soil column receiving 1000 ppmv n-propyl acetate for 225 days. The gas flow was downward at a linear velocity of 1 cm/min, the same as the flow rate estimated in the field site. Note that 1,3,5-trinitrobenzene (TNB) degraded more quickly toward the source of the gas, while RDX fell to about 8.5 ppm. RDX was initially at 15.1 +/- 1.3 ppm (n=5) in thoroughly homogenized soil.*

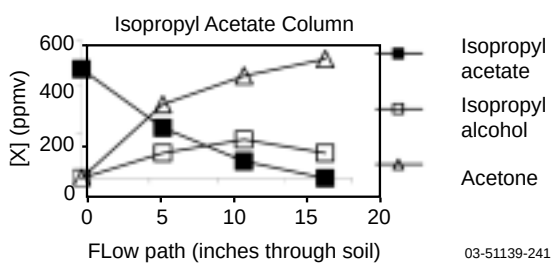


*FIGURE 4. Vapor phase analyses: attenuation of isopropyl acetate with the subsequent increase in daughter products (isopropyl alcohol and acetone) measured on day 62. Note the nearly complete molar conversion to acetone and the relatively slow attenuation of the subsequently produced acetone.*

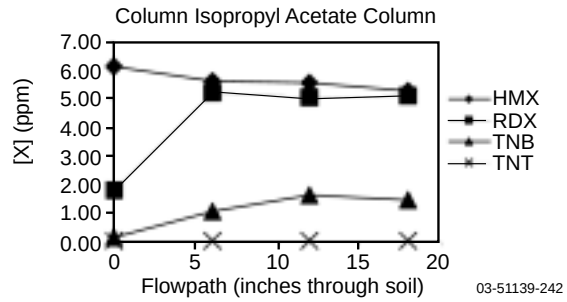


*FIGURE 5. Soil analysis: explosives concentration through a soil column after 62 days of receiving 500 ppmv isopropyl acetate.*

*Field Study for Explosives Degradation*. The field study at the Pantex Plant never plunged to low enough oxygen levels to accommodate true anaerobic organisms. As such, the helium levels were not significantly effected at an effect level robust enough to be commercially significant. The 30'X30'X30' field site received organics for over 45 weeks (Fig. 6), and at one gas sampling point, both the parent and primary daughter compound broke through (Fig. 7).

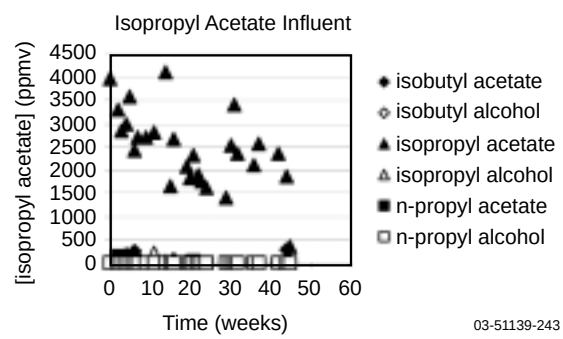


*FIGURE 6. Isopropyl acetate influent vapor at the Pantex site with an injection rate of 17.5 L/min.*

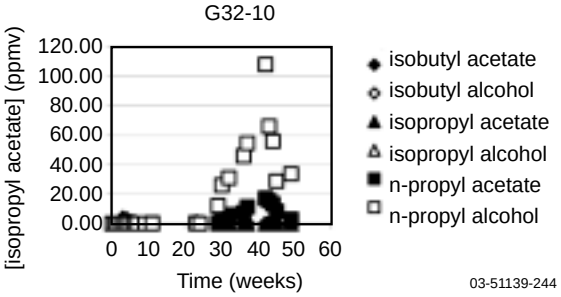


*FIGURE 7. In situ field study at the Pantex site. This gas monitoring point, installed 10 feet below surface and approximately 4 feet from the injection point, shows the breakthrough of the parent propyl acetate and the daughter product propyl alcohol.*

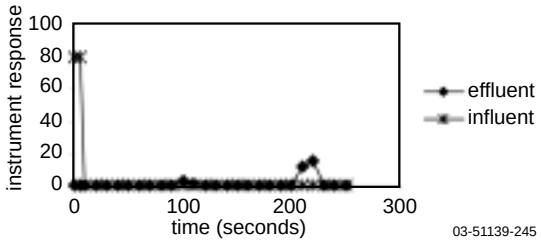


*FIGURE 8. First-ever breakthrough trace of a direct-push-installed, flow-through, in situ reactor (FTISR). The injected pulse was butane, influent flow was 40 mL/min, and outflow was 173 mL/min. The formation interrogated was the upper 20" of the Blackwater Draw in Lubbock, Texas, and included a layer of very hard caliche deposits.*

*Microcosm.* The second prototype of the Flow-Through In Situ Reactor (FTISR) was built and tested in FY03. It was installed through a caliche layer in Lubbock, Texas, allowed to stay for 8 months, then successfully tracer-tested using butane (Fig. 8). This was the first installation of a direct-push, flow-through reactor. Invented in this LDRD, this reactor has received follow-on funding and shows promise across most of the hazardous waste remediation sector.

As a result of this LDRD, DOD has requested a proposal for explosives remediation research. This proposal has been submitted and is currently under review. The Flow Through In Situ Reactor (FTISR), after some revisions, has been resubmitted for patent. The FTISR will be further developed for deployment in the vadose and saturated zones. Many groups are interested in use of the reactors including the EPA, DOD, and DOE, as well as several private companies.

The investigators also have prepared three manuscripts for publication in a peer-reviewed journal.

# Kinetics of Inter-Surface Transfer of Surface-Complexed Metals by Surface-Surface Contact

*George Redden*

***Understanding colloid-facilitated transport of adsorbed contaminants***

GC114

Colloid-facilitated transport of contaminants in the subsurface has proven difficult to predict. Multiple mechanisms control the migration of colloids and the partitioning of sorbed chemical species between the colloid, water, and immobile phases. To model facilitated transport of solutes, it is necessary to understand the rates at which solutes are transferred between the different phases.

The objectives of this LDRD are to measure the kinetics of solute transfer between contacting mineral surfaces, and to interpret the rates in terms of mass transfer limitations (desorption, diffusion, adsorption), thermodynamics (reversibility of sorption, and evolution of surface complexes with time), and surface contact frequency and energy. A computational model for solute transfer has been developed that can be applied to experimental systems using a rotating disk reactor. The experimental goals of this project include synthesis of well-characterized colloid populations, development of methods to separate mixed populations of colloids based on size or magnetic properties, and measurement of the rate of transfer of a model sorbing species (uranyl ion) between colliding surfaces.

Technical objectives for fiscal year 2003:

- Develop a mechanistic, computational model for the transfer of adsorbed chemical species on one solid surface to a second solid surface during surface-surface "contact".
- Synthesize model colloids that can be used in the experimental tasks and are suitable for model testing.
- Develop two experimental approaches for measuring the rate of transfer of model solutes between surfaces. One experimental approach will involve two populations of colloids in a stirred batch reactor. The second experimental approach involves one population of colloids and a flat surface.
- Use the two experimental approaches to measure the transfer of adsorbing solutes between surfaces. Determine whether a simple desorption-diffusion/advection-adsorption model is adequate, or whether transfer is altered by surface-surface interactions.

The model developed for simulating solute transfer accounts for the following processes:

1) Migration of colloids in suspension relative to a hydrodynamic boundary layer adjacent to another surface.

2) Transfer across the hydrodynamic boundary layer.

3) Desorption, diffusion, adsorption of solutes from colloids inside and outside the hydrodynamic boundary layer.

4) Direct contact between colloid-colloid or colloid-stationary phase surfaces.

The model is summarized by the following differential equations and has been implemented in a MathCad program.

$$\frac{dP}{dt} = -K_{EFF}\frac{A_D P}{V}$$

$$\frac{d\hat{C}_C}{dt} = -K_P\left[C_{eq}(\hat{C}_C) - C_B\right] - \frac{K_{m1}A_D}{V}\hat{C}_C + \frac{K_{m1}A_D}{V}K_{EFF}I\hat{C}_{Ci} + \frac{K_{EFF}A_D}{V}\hat{C}_C$$

$$\frac{dC_B}{dt} = K_P\left[C_{eq}(\hat{C}_C) - C_B\right]PA_{SP} + K_{m2}\left[C_{eq}(\hat{C}_D) - C_B\right]\frac{A_D}{V}$$

$$\frac{d\hat{C}_D}{dt} = -K_{m2}\left[C_{eq}(\hat{C}_D) - C_B\right] + \frac{A_{SP}A_D}{A_T}K_{EFF}(\hat{C}_{Ci} - C_D)P + K_\gamma K_{EFF}I\frac{A_D}{A_T}\left[C_{eq}(\hat{C}_{Ci}) - C_{eq}(\hat{C}_D)\right]P$$

$$A_T = A_D + A_{SP}(P_0 - P)V$$

Where P = particle concentration, $K_E$ = effective mass transfer coefficient, $A_D$ = secondary phase surface area, V = volume, $C_C$ = contaminant sorbed to secondary surface, $C_{eq}$ = equilibrium partition concentration, $C_B$ = Bulk concentration of contaminant, $K_{m1}$ = Levich's mass transfer coefficient, $A_{sp}$ = particle surface area, $K_g$ = modified apparent mass transfer coefficient.

The model has been employed to predict the appropriate experimental conditions to study solute transport in colloidal systems with a rotating disk apparatus. Simulations indicate colloid mediated solute transfer dominates mass transfer only for strongly sorbing species, and the rate of transfer is sensitive to the rate of solute transfer from non-

aggregating, close-approach colloid/disk interactions.

A particle-synthesis process for generating near-spherical hematite (iron oxide) colloids was successful at producing particles with sizes and uniformity that would be acceptable for the experimental goals (approximately 50 to 600 nm). Colloid morphology and size distribution were verified using a transmission electron microscope (TEM). Pure hematite colloids were synthesized for both the batch reactor and the rotating disk reactor experiments. In attempts to separate different colloid populations based on size – a requirement for the batch reactor experiments – it was found that filtration, centrifugation, and settling methods were not successful or had certain disadvantages such as time required or excessive sample manipulation. Another approach was developed that involved coating commercially available magnetite particles with hematite. The concept was that the magnetite-hematite particles could then be removed from a mixture of colloids that included pure hematite using a simple bar magnet. This approach was successful although the success occurred late in the project and only preliminary testing was completed.

Experimental procedures were explored to coat glass disks with hematite particles to be used in rotating disk experiments. One procedure involves depositing particles from a colloidal dispersion onto the disk surface by solvent evaporation. The coating structure has been analyzed by optical microscopy and SEM. Optical micrographs of disks show a coating with 65 nm hematite particles. The uniform film of particles deposited is estimated to have a thickness of 1 μm.

A rotating disk reactor was assembled for controlling the collision or contact frequency between suspended colloids and a flat mineral surface. Initial testing was conducted with benzoic acid disks dissolving into aqueous solutions using pH as the analytic indicator. In this system, the dissolution rate is expected to be controlled exclusively by convective mass transfer from the disk into the solution. This problem has been studied previously in the literature. The linear relationship was used to validate the theory of mass transfer from the disk under laminar flow conditions. Subsequently, the deposition of latex particles on the disk was tested to determine whether consistency with Levich's mass transfer model predictions could be observed (Fig. 1). Particle

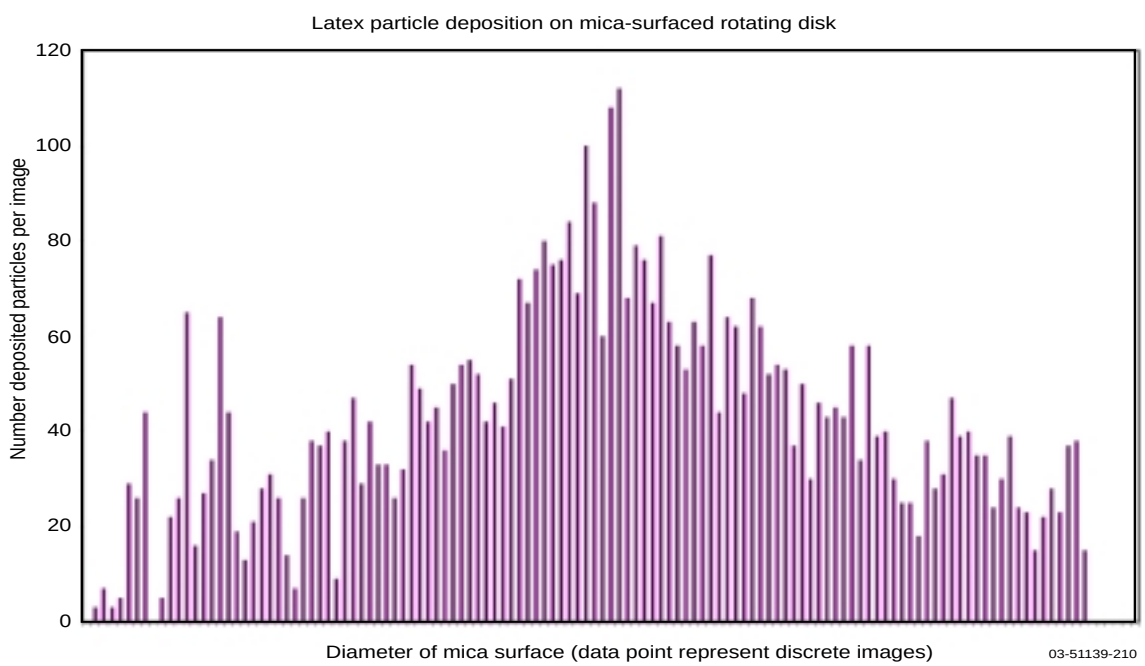


*FIGURE 1. Latex particle deposition density on a rotating disk as a function of radium. The center of the disk is at the center of the x-coordinate.*

deposition rates, determined by optical imaging of the disk face removed from the reactor, were found to be over one order of magnitude greater than predicted by Levich's equations for mass transport with a rotating disk. Possible explanations include lack of opposite charge-enhanced interactions and surface roughness (although unexpected for a molecularly flat mica surface). The distribution of particles also was not uniform across the disk face as expected for a solute. These issues will have to be resolved before proceeding to testing using the synthetic colloids (iron oxides) and adsorbing solute (uranyl ion).

The concept for the batch reactor approach was simple although less amenable to model simulations compared to the rotating disk reactor. Two populations of colloids would be mixed. One population would be pre-equilibrated with a solute, a fraction of one population would be isolated, and the rate of increase or decrease of the sorbing solute would be determined. Attempts to isolate populations of colloids based on size were not successful. However, magnetic separation of colloids with magnetic cores appeared to be successful in preliminary tests. Initial qualitative testing was completed using the following experimental conditions (Table 1).

*TABLE 1. Magnetic separation of colloids test conditions.*

| | |
|---|---|
| Short pre-equilibration, short contact time | Long pre-equilibration, short contact time |
| Short pre-equilibration, long contact time | Long pre-equilibration, long contact time |

03-51139-46a

Pre-equilibration refers to the period for uranyl sorption on one population of colloids. Contact time refers to the period of time the two colloid populations were in contact. Short = 15 minutes, long = 16 hours. The qualitative results were as expected. Longer pre-equilibration periods retarded the transfer of uranyl from one population to the uncontaminated colloids, and long contact time permitted higher degrees of transfer. Additional experimental testing will be required to quantify the rate expressions for solute transfer.

Colloid-facilitated transport continues to occupy a prominent position with respect to explaining "unexpected" transport of contaminants in subsurface environments, and also is being offered as a new approach to subsurface manipulation and remediation. Decisions based on model predictions and risk assessment will rely on defendable models. The kinetics of solute partitioning and transport in the presence of colloids will continue to be a question mark in the near future.

The goals of this project were only partially met. However, there is ample opportunity and sufficient basis for follow-on work. With respect to science or engineering applications, this work points to several potential remediation schemes that are either in situ or part of an extractive methodology (scavenging, subsurface interrogation) in support of INEEL and DOE environmental missions.

# Organic Co-Solvent and Co-Contaminant Effects on Sorption of Uranyl and Cesium to Metal Oxide Surfaces

*George Redden*

***Predicting contaminant behavior in the presence of co-contaminants***

GC116

The manufacture and stockpiling of nuclear weaponry has resulted in large volumes of radioactive waste, currently stored at various DOE facilities around the U.S. These radioactive wastes are often complex mixtures of radionuclides, heavy metals, organic solvents and organic metal-complexing agents. Basic information on the chemical interactions between the various components of the waste mixtures and mineral surfaces is required to develop effective remediation strategies.

This LDRD is determining whether organic co-solvents can alter the sorption behavior of uranyl and cesium on mineral oxide surfaces. The emphasis is on using spectroscopic techniques such as FTIR and Raman Spectroscopy, and x-ray photoelectron spectroscopy (XPS) to examine chemical interactions between complexed and uncomplexed actinide species and mineral surfaces, both in aqueous solutions and in organic solvent-water mixtures. Of particular interest are the mechanisms by which uranium(VI), and cesium(I) adsorb to aluminum and iron oxide minerals, as well as clay minerals, both in the presence and absence of the complexing ligands citric acid and EDTA. The principle product of this LDRD has been the spectroscopic characterization of citric acid-uranyl complexes, both in solution and adsorbed to $Al_2O_3$, as well as characterization of adsorbed uranyl hydroxide complexes.

Technical objectives for fiscal year 2003:

- Use Fourier Transform Infrared Raman Spectroscopy to identify the speciation of uranyl citrate species in water, mixtures of water and organic co-solvents, and as species adsorbed to aluminum oxide.
- Using batch adsorption techniques, determine the effect of organic co-solvents on the sorption behavior of uranyl and cesium on aluminum oxide, iron oxide, and kaolinite.

The primary outcome of this project has been an improved understanding of uranyl citrate speciation using Raman FTIR, and preliminary information about the nature of citrate and uranyl-citrate sorption complexes on Al2O3. Experimental studies of the effects of ethanol and Trichloroethylene (TCE) on uranyl and cesium sorption to iron oxide, aluminum oxide, and kaolinite did not progress to the degree expected due to difficulties encountered when developing a calibration procedure for pH electrodes in the solvent mixtures. However, the tentative results indicate that the co-solvents had very little impact on metal sorption and that the pH scaling probably would not significantly affect the qualitative predictions.

The aqueous chemistry of the $UO_2$-citrate system is complex, involving pH-dependent changes in stoichiometry and $UO_2$ coordination environment. At low pH (pH 2-4), the existence of a 2:2 dimeric $UO_2$:citrate species is well established. Above pH 7, at least two species with $UO_2$:citrate ratios of 3:2 and 3:3 have been reported, although a hexameric $UO_2^{2+}$-citrate complex also has been proposed. While a structure has been reported for the 2:2 species (Fig. 1), and a formation constant determined, only stoichiometric information is available for the 3:2 and 3:3 complexes. This deficiency leads to the neglect of uranyl-citrate complexes formed at environmentally relevant pH values and, as a result, under-prediction of the importance of citrate to the mobility of uranyl in soils. One goal of this study was to characterize the structures of the $UO_2$-citrate complexes formed in aqueous solution and to gain an understanding of their speciation behavior, preliminary to determining formation constants for these species.

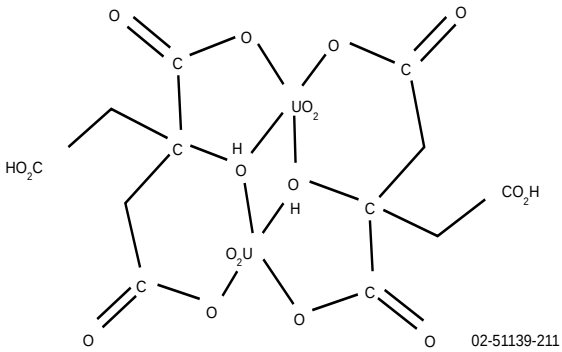


*FIGURE 1. Structure previously proposed for the 2:2 $UO_2$-citrate species.*

In brief, in a solution containing a 3:2 mole ration of $UO_2$:citrate, the relative proportions of $(UO_2)_3Cit_2$ and $(UO_2)_3Cit_3$ at pH > 6.5 were found to be reversed from that described earlier. However, the solution behavior is the same, with $(UO_2)_3Cit_2$

reacting to form $(UO_2)_3Cit_3$ as pH is increased. Even at pH 10, there was no sign of any precipitation, indicating that $UO_2$ is mainly in the form of a citrate complex. Based on these results, the general solution equilibria can be represented as:

$$6UO_2^{2+} + 6Cit^{3-} \rightleftharpoons 3(UO_2)_2Cit_2^{2-}$$

$$\rightleftharpoons 2(UO_2)_3Cit_2$$

$$+ 2Cit^{3-} \rightleftharpoons 2(UO_2)_3Cit_3$$

A tentative structure for the 3:3 uranyl species is shown in Figure 2.

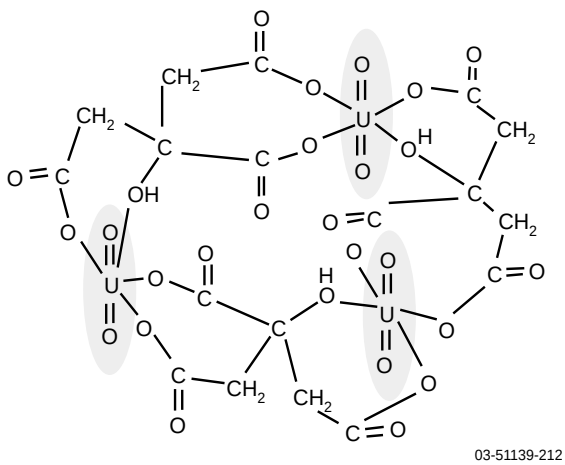


*FIGURE 2. Tentative structure for uranyl-citrate 3:3 complex at pH>7.*

The nature of the citric acid-uranyl complex adsorbed to $\gamma$-$Al_2O_3$ was examined using ATR-FTIR. As a starting point, experiments were carried out at pH 3.5 where the complex shown in Figure 1 is the dominant species in solution. For purposes of comparison, the adsorption of citric acid on $\gamma$-$Al_2O_3$ also was examined. The spectrum of citric acid adsorbed to $\gamma$-$Al_2O_3$ shows marked differences from that of the solution species. Citric acid may coordinate through binding of one or two of the carboxylate groups to surface Al atoms in either a bridging bi-dentate structure or in a mono-dentate configuration. The hydroxyl group of the citrate molecule also is thought to be coordinated to Al(III). In solution, citrate is thought to form a complex with Al(III) by binding the two carboxylate groups and the deprotonated hydroxyl group to Al(III), forming two six-member rings, but it is not known if a similar complex is formed on the surface of aluminum oxides.

The adsorption of hydrolyzed uranyl species on $\alpha$-$Al_2O_3$ powder also was examined using ATR-FTIR. At pH 3.5 the two predominant species in solution are $UO_2^{2+}$, and $(UO_2)_2(OH)_2^{2+}$, with $\nu_2$(O=U=O) (modes at 960 and 945 $cm^{-1}$) respectively. Thus far, the spectral analysis indicates either the formation of a surface complex or surface polymerization.

ATR–FTIR has proven to be a powerful method for examining uranyl surface complexes. Future experiments are planned to examine the pH dependence of surface complex formation on $\gamma$-$Al_2O_3$ and other metal oxides.

Solute complexation on mineral surfaces can be described in multiple ways. A more detailed approach has been to correlate adsorption to surface charge since surface charge will modify the free energy of adsorption for charged solutes or surface complexes that carry charge. The surface charge, in turn, is dependent on a number of factors with pH being a dominant parameter. Therefore, calibration of a pH scale, with pH defined as the negative logarithm of the H+ activity, is necessary. This is a non-trivial exercise since the free energy associated with co-solvent effects are not described by a well-accepted model such as the Debye-Hückel equation. An effort was made to calibrate standard double-junction glass electrodes for a series of solvent mixtures. Several problems were encountered in this effort (primarily the stability of the electrode response), and the experimental component of this project fell behind expectations. Nevertheless, the effect of elevated ethanol and TCE concentrations on uranyl sorption was tested for approximate pH ranges.

The result was that little evidence for co-solvent effects was observed in the case of goethite (iron oxide) as the sorbing phase. This is in contrast to previous reports where sorption and surface charge

were shown to be modified by the presence of co-solvents. One possible explanation is that uranyl sorption is known to form a strong covalent complex and is less affected by either surface charge or competition with proton binding. Ethanol has a relatively minor impact on solvent properties when mixed with water due to similarities in polarizability and hydrogen bonding. TCE has low solubility and is not expected to impact solvent properties, but might have exhibited an impact on surface chemistry if condensation on the mineral surfaces occurred. There is insufficient evidence for TCE-mineral interactions to draw a conclusion at this time.

In the case of cesium sorption, a more pronounced effect of co-solvents was expected since cesium forms relatively weak electrostatic interactions with mineral oxides (unless ion exchange occurs) and the co-solvent effect on surface charge was expected to be significant. However, sorption of Cs was uniform for the system studied (goethite), and no obvious pattern could be detected.

Although the speciation study in this project was highly successful, experimental measurement of the effects of the chosen co-solvents on uranyl and cesium sorption could not be completed according to expectations (due largely to problems with electrode performance problems). However, the topic is important to remediation at disposal sites since mixtures of organic solvents and metal contaminants are relatively common. The impact of strong chemical gradients adjacent to breached waste containers has rarely been accessed due to experimental difficulties and the site-specific nature of the problem. These zones of strong chemical gradients are where some of the more pronounced chemical interactions can occur leading to “anomalous” and transient transport behavior and the precipitation or dissolution of unexpected chemical species – particularly in the form of colloids.

The basic research goals of this project were satisfactorily met although the information that will lead to practical applications lagged. In the future, a greater emphasis will be placed on obtaining data on sorption behavior as the justification for detailed speciation studies.

This LDRD research is generally applicable for waste treatment strategies and for predicting the behavior of contaminant mobility in solids and groundwater.

# Computational Experiments of Hysteretic Chemical and Moisture Migration

*Annette L. Schafer, James B. Sisson*

***Understanding the history dependence of flow transport***

GC140

The processes controlling contaminant migration, bioremediation, in situ flooding for remediation, and the use of partitioning tracers for vadose zone characterization are influenced by the abundance and chemical reactivity of mineral surfaces within the subsurface. Key to enhanced scientific understanding of the processes important for predicting vadose zone transport and remediation, are improved and innovative theories and techniques for describing and incorporating the spatial and temporal distribution of reactive surfaces within the vadose zone.

This LDRD studies the influence of repeated infiltration events on the transport of solutes in variably saturated porous media. The work was motivated by identified sources of uncertainty in contaminant transport predictions conducted in support of environmental management. Specific to this study is the concept that effective geochemical properties are history and flow-direction dependant. This derives from the observation that water flow paths are dictated by spatial variations in hydraulic conductivity, and that they are time dependant because of small-scale variations in grain size. Flow paths determine the specific surfaces available for geochemical reactions. In as much as the movement of water is history dependant, geochemical reactions should be history dependant. In practice, these issues have been neglected, which has been justified by a lack of site-specific information and the ability to collect it, and simulation tools that do not allow incorporation of hysteretic characteristic relationships.

Technical objectives for fiscal year 2003:

- Obtain quantitative characteristics for reactive transport in unsaturated media.
- Select candidate reactive tracers and characterize them.
- Conduct initial transport of reactive tracers through soil columns.

The primary goal of this project was to enable quantification of uncertainty in contaminant transport predictions introduced by neglecting the effects of transient infiltration. Numerical predictions of contaminant transport often form the primary technical basis underlying environmental management decisions. They provide a means of interpreting field data, integrating empirical observations, and testing conceptual models. Historically, predictions supporting environmental decisions are based on simple conceptual models with assumptions made in part because of: a) insufficient empirical data, b) lack of field data and the difficulty in obtaining it, c) computational limitations imposed by stability and CPU requirements when solving the nonlinear governing equations, and d) the simple observation that numerical models commonly employed today do not incorporate more than very simple processes.

This project has begun to address many of these issues for a very specific source of uncertainty, namely that introduced by assuming geochemical homogeneity and temporal property independence during natural precipitation cycles. This is an extremely challenging numerical problem because the governing equations are non-linear, the hydraulic and geochemical parameters are functions of infiltration history as well as being spatially variable, and because there are very few actual transport experiments conducted for the purposes of illucidating the combined effects of geochemical heterogeneity and hysteretic property variation.

In the course of this research, the background was staged to test the following hypotheses:

Hypothesis 1: Reactive surface area is a hysteretic function manifested during transient wetting and drying cycles.

The in situ availability of reactive surfaces is a hysteretic property in vadose zone materials. Based on the relationships between mass-based and surface area-based partition coefficients, and on the dependence of the surface area on grain (and thus, pore) geometry, one would expect that unsaturated systems would exhibit hysteretic adsorption. This hysteretic adsorption should manifest itself as a combination of physical exclusion and chemical adsorption as functions of the pore sizes being filled. What has yet to be shown is the relationship and influence of wetting and drying history on the reactive surface area.

Hypothesis 2: Flux dependent effective available reactive surface area.

The in situ availability of reactive surfaces is a property dependent upon flow magnitude and direction in vadose zone materials. As a function of flow direction and available moisture content, the effective volume-averaged adsorption should be

represented by a flux-weighted tensor. It is this effective adsorption coefficient that should be used for field scale transport predictions.

An experimental campaign was initiated in the laboratory to obtain quatitative characteristics for reactive transport in unsaturated media. Soil has been selected and hydrogeochemical characterization has been conducted. Candidate reactive tracers have been selected and characterized, and initial transport of conservative tracers through the column have been conducted.

Soil characteristics have been obtained for a Jacoby Series soil from the USDA Sheep Experimental Station near Dubois, Idaho, including physical, hydrological, geochemical, and mineralogical properties. As motivated by the idea that chemical properties and fluid contact will depend on wetting history, the geochemical, mineralogical, and surface area analyses were conducted for three distinct categories of particle sizes: 1) medium to coarse grained sands (250-2000 μm), 2) fine grained sands (250-53 μm), and 3) silt and clay sized particles (< 53 μm). Based on the percentage of sand, silt, and clay content, this soil is a sandy loam with a coefficient of uniformity (Cu) that indicates it is poorly sorted with 10% of the particles less than 0.008 mm. Calcium is present in the highest amounts, followed by iron, with soluble calcium highest followed closely by magnesium. Chemical analysis indicates that there should be a measurable difference in transport reactivity as a function of grain size, as indicated by higher cation exchange capacity for medium-coarse grained sands as compared to fine grained sands and silt and clay-sized particles. Mineralogical analysis also suggests differences should occur in transport behavior in that the medium to coarse grained particles consist primarily of quartz silica sands; however, they also are heavily coated with calcium carbonate minerals. In fact, the high surface-area value measured for these particles may be a result of these pitted calcium.

Tracer studies were begun using a conservative (non-reactive) tracer as a function of moisture content. These experiments used the Jacoby Series soil, which was air dried and repacked into a 28 cm long by 5.7 cm inside diameter (ID) polycarbonate column at a bulk density of 1.3 g/cc (~50% porosity). The column was instrumented with three tensiometers to measure soil water matric potential, three water content sensors, and one bar porous ceramic disk at the top and bottom boundaries (Fig. 1). The sensors were installed in the column at 2.5 cm, 12.5 cm, and 22.5 cm vertical distance from the ceramic disk at the top of the column.

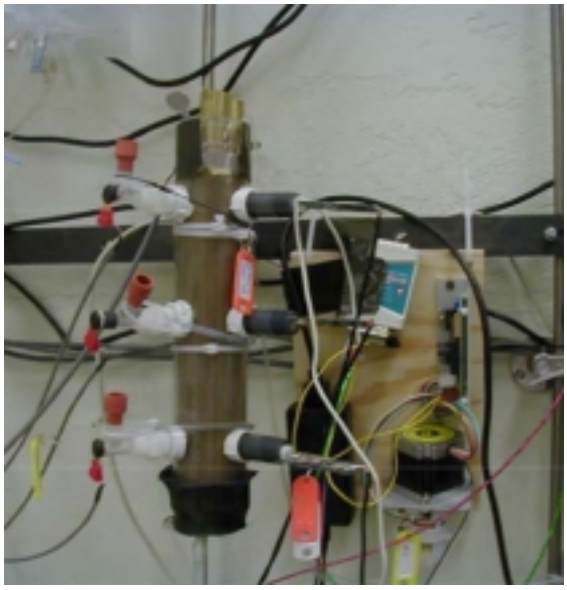

PN04-0004-160a

*FIGURE 1. Instrumented soil column.*

A 0.005 Molar calcium sulfate, 0.003 Molar sodium azide solution was applied at the top of the soil column at a flux rate of 2 cm $day^{-1}$ using a variable speed fluid metering pump, while a tension of approximately 80 cm was applied to the bottom of the column using a vacuum chamber. Sodium azide was introduced to eradicate biomass in the soil column to minimize bioactivity. Once the column reached steady-state conditions, a conservative tracer consisting of 0.007 Molar sodium bromide and 0.005 Molar calcium sulfate solution was introduced to the top of the soil column through the ceramic disk while maintaining previously established constant flux and tension boundary conditions. The soil column effluent was collected using a fraction collector inside the vacuum chamber. The samples were analyzed using

ion chromatography to measure effluent concentrations as plotted in Figure 2.

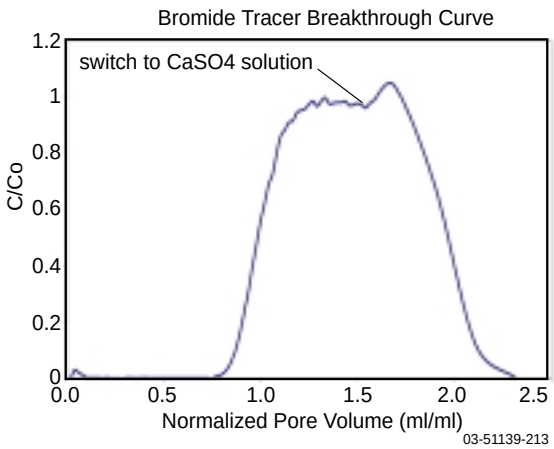


*FIGURE 2. Conservative tracer breakthrough curve.*

One pore volume (PV) is equal to the volume of fluid in the column, which is moisture dependant. Under the 30% moisture conditions in the column, this corresponds to a transport time of 4.8 days. To obtain the data necessary to evaluate the effects of hysteresis on reactive transport, these transport experiments will have to be conducted over many repetitions of the drainage-imbibition cycle, and for each cycle over the full range of moisture content. Transport velocity (and mean residence time) for a reactive tracer scales with the retardation factor ($\nu_r = \nu / R$), where v is the Darcy flux divided by the moisture content, $R = (1 + \rho_b K_d)\theta$, and $K_d$ is the distribution coefficient (sorption isotherm slope). If the bulk density is 1.5, the moisture content is 0.3, and Kd ranges from 1-10, this results in a retardation factor range from 1-51, and travel times on the order of 5-250 days. Clearly the time necessary to conduct these experiments begs a different solution.

To conduct the numerical experiments, a finite difference code was developed to solve a modified Richard's equation

$$\nabla_2 \bullet [K(\theta)\nabla_2 h] = -\left(\frac{d\theta}{d\psi}\right)_\theta \frac{\partial h}{\partial t} = \frac{\partial K}{\partial z} + \frac{\partial \theta}{\partial t}$$

where

$$P_t = \frac{h}{1+\varpi h}.$$

It considered single-phase water flow, heterogeneous properties, and transient boundary conditions in 3-D. The modified form of Richard's equation was modeled after the work of Pan and Wierenga, where the hydraulic head is replaced by a functional ($P_t$) to reduce the nonlinearity in the pressure-saturation relationships. This modification has been implemented in 2-D in commercially available codes, and by the investigators of this project in a 2-D finite difference code. Implementation into a finite difference code (rather than the finite element code) has resulted in a regular matrix structure that lends itself to multigrid and parallel solvers. These faster methods of solution will enable the Monte Carlo simulations necessary to quantify uncertainty. To date, the initial implementation of the code is finished, and the parallelization is in progress. Further, 1-D flow and transport experiments have been conducted using non-reactive tracers, and the laboratory work is nearing completion for the selection of reactive tracers. Due to the long transport times for the reactive tracers, use of the INEEL geocentrifuge is being sought to conduct a greater suite of these transport experiments.

The importance of this project to the INEEL lies in the potential of the developed simulator and proposed experiments to make inroads into quantifying the uncertainty underlying contaminant management and waste disposal decisions at INEEL. In addition, these advances will contribute to the success of the Subsurface Science program. Currently, the INEEL does not claim ownership of computational tools that can be used to simulate vadose zone flow or transport. In developing this tool, the research community will have access to a powerful and stable computational resource that can be modified and adapted to assist in experimental design and evaluation of experimental results. Further, the INEEL has limited expertise in conducting mesoscale transport experiments in geochemically and hydraulically heterogeneous media. This is especially true in transient observation models. The combined experimental- and code-development activities of the second year have greatly expanded the technical capabilities of the INEEL in this area. Application of the code developed in this LDRD will lead to peer-reviewed publications and, thus, will benefit DOE by contributing to the general scientific knowledge base.

# Development of Imaging Fourier Transform Mass Spectrometer Capabilities for Analyses of Complex & Heterogeneous Samples

*Jill R. Scott, Paul L. Tremblay, Timothy R. McJunkin*

***Multipurpose instrument enables 3-in-1 measurement***

GC119

There is significant need at the INEEL and throughout the DOE complex for technology that can analyze complex, heterogeneous, environmental and biological samples.

This LDRD focuses on development of a unique, multipurpose instrument capable of providing both mass spectral and optical imaging of complex, heterogeneous sample surfaces. This new instrument will provide the INEEL with the capability to analyze samples using the high resolution and mass accuracy of the laser desorption Fourier Transform Mass Spectrometer (FTMS), while adding processes for illuminating the structure and environment of chemical species on the samples and retaining the spatial context necessary for imaging. The project has three tasks: 1) enhanced imaging laser desorption FTMS capabilities, 2) integration of surface fluorescence detection within FTMS, and 3) incorporation of Raman detection within FTMS

Under the first task, an individual mass spectrum, obtained by the laser desorption FTMS, will be correlated to its x, y-position; thereby, retaining the contextual relationship among all the spectra obtained from the sample. The second and third tasks will take advantage of the unique laser scanning system to allow incorporation of fluorescence and Raman imaging, respectively. This instrument will be capable of collecting the data equivalent of three separate instruments from the same sample. The optical and mass spectral imaging of complex samples will provide complementary information for complete sample characterization.

Technical objectives for fiscal year 2003:

- Improve chemical imaging and analysis capabilities:
  - Perform collaborative studies for mapping minerals, microbes, soils, etc.
  - Compare the LOCI's capabilities with other instrumentation.
- Integrate Raman detection within FTMS.
- Enhance software intelligence for image data analysis and display.
- Publish and present research results as appropriate.

The research instrument developed in this LDRD is referred to as the laser-based optical and chemical imager (LOCI). The combination of techniques in LOCI provides the opportunity to obtain complementary information from the same sample. The mass spectrometry allows chemical imaging to be acquired. Of the optical spectroscopies, fluorescence provides electronic information for speciation, while Raman provides vibrational information for structure determination. Because the optical detection is non-destructive to the sample, it is performed first. The destructive laser ablation of the sample, to obtain the mass spectra, is performed last. In terms of sensitivity, the mass spectrometry > fluorescence > Raman.

All three techniques utilize the laser-scanning device to raster over the surface of the sample. In the case of the optical spectroscopies, a low fluence laser beam is used. The surface of the sample is excited by the laser beam, and the light is gathered by a custom reflector and fiber optics as illustrated in Figure 1. The fiber optics pass through the 3" probe and are coupled to a multiplexer. The light is then directed into a spectrograph equipped with a CCD camera to obtain either surface fluorescence or Raman spectra.

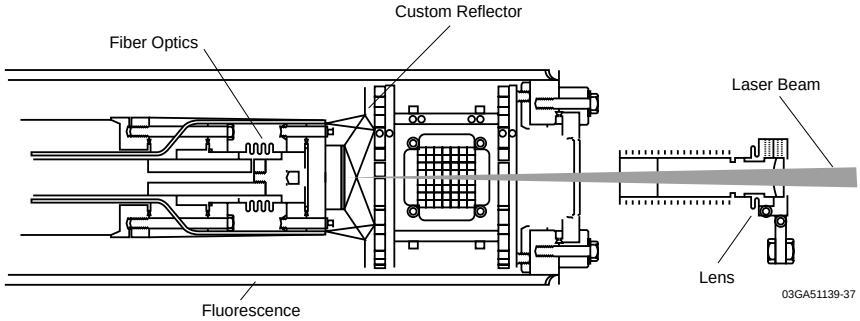


*FIGURE 1. Schematic of surface fluorescence and Raman light-gathering apparatus. Fiber optics embedded in the 3" probe carry light to a multiplexer that is coupled to a spectrograph with a CCD camera.*

Because up to 7200 spectra per hour can be acquired, it would be prohibitive to manually interpret each spectrum. Therefore, a Fuzzy-logic inference engine was designed to assign each spectrum an identity based on the Fuzzy-logic rule base and create the maps (or images) of the surface. Most chemical imaging spectrometers only provide the ability to map a single peak. Several images of single peaks are then overlaid to identify areas of interest. A representative spectrum is then retrieved or reconstructed. While this system also can plot individual peaks, it was decided to utilize all the peaks of interest in the spectra to quickly produce the final image. The Fuzzy-logic inference engine also allows the user to easily interrogate the image to refine the rule based through a graphical user interface (GUI) as illustrated in Figure 2. To help facilitate development of rule bases, a statistical rule-base generator (SRBG) has been added to the software suite. The SRBG analyzes all of the spectra to determine repeating patterns. These patterns are then used to generate the preliminary rule bases. Using the SRBG is not only useful for analyzing homogeneous samples for initial rule bases, but also for analyzing unknowns because it focuses attention on the most important spectral features.

This LDRD addresses several needs of both the INEEL and DOE. Development of this technology will directly support Subsurface Science Initiative projects that need to analyze complex, heterogeneous, environmental and biological samples. This technology could also be employed for materials characterization and for understanding corrosion processes. Although the imaging FTMS is not a field instrument, it can be used to analyze field samples and bolster confidence in field measurements obtained by less-capable, portable instrumentation.

This project has lead to external collaborations with Utah State University, as well as others who have sent samples for analyses. As appropriate, proposals will be submitted to DOE programs, such as EM and SC, as well as outside sources. Proposals have been sent to NASA to support their need to determine methods to identify life or biosignatures for future extraterrestrial missions.

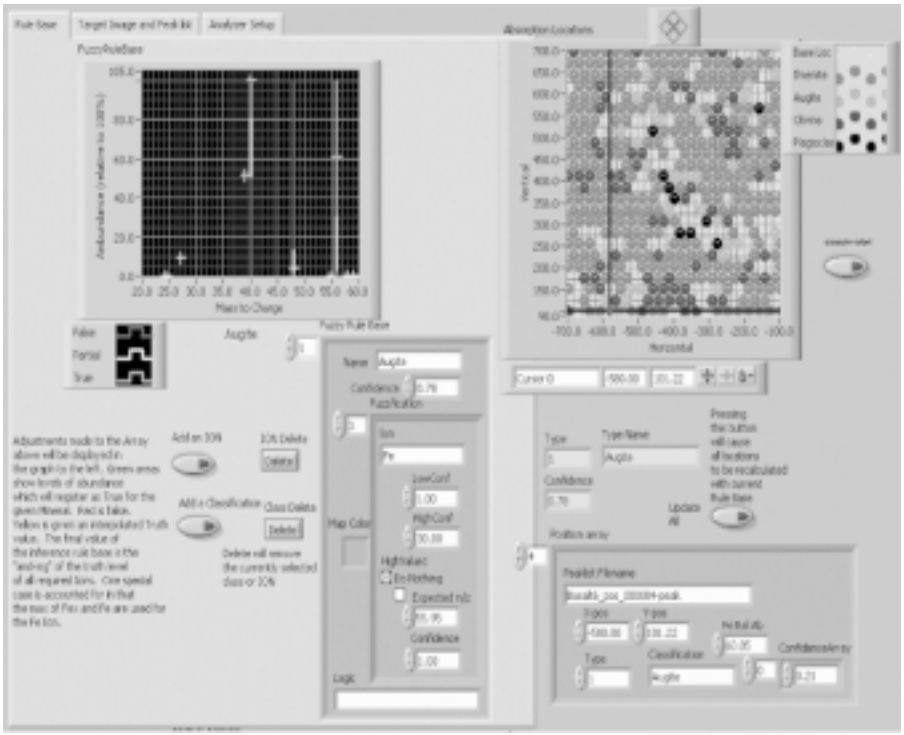

*FIGURE 2. User-friendly Fuzzy-logic inference engine GUI.*

# Dual Electrodes and Defining the Electrically Disturbed Region in Induced Polarization Measurements

*Clark Scott*

***Using electrical behavior to locate contamination***

GC145

With the arrival of the geocentrifuge and the Subsurface Geosciences Laboratory (SGL), methods of imaging and characterization of lab-scale experiments are required. At larger scales, there are continuing needs for characterization technologies in the DOE clean-up process. Of the many physical properties that can be measured, the electrical behavior of the system is one of the most promising for locating the often-subtle signature of contamination.

The current state of the art in sensor development/deployment, data collection/processing, modeling, and interpretation/inversion is technologically inadequate for the range of studies envisioned for the INEEL. Examples of this inadequacy include electrodes that are too invasive and leak contaminants into the experiments, and sensor deployment that minimizes the noise due to electro-chemical disturbance using large spatial separations or time-consuming data collection schemes.

This LDRD addresses these problems by developing at the INEEL a complex resistivity capability for use in contaminant and flow experiments at the lab and field scale. The major issue to be addressed is the necessary separation distances between sensor and source in typical soils to achieve electrochemical independence while satisfying geometric equivalence of the two electrodes at various scales.

Technical objectives for fiscal year 2003:

- Test and characterize laboratory complex resistivity (CR) system.
- Measure and define electrically disturbed zone.
- Develop electrode characteristics and behaviors.
- Evaluate data from disturbed zone.
- Prepare paper describing disturbance zone work.

*Laboratory Complex Resistivity System*. System response of a complex resistivity system is composed of several factors including the capacitive effects of the cabling, the cell factor, inherent charge storage mechanisms in the sample holders, and, in the case of this system, the time-lag factor between the driving signal system and the source amplifier (transmitter). This complicated system response must be derived to accurately retrieve the complex behavior of the material being tested. Characterization of the system response function proceeded by experimentation on three ideal systems: 1) a series of linear resistors to test the zero phase response, 2) a set of Resistive-Capacitive (RC) circuits to test the response to classic and analytical phase responses, 3) specially designed sample cells that are to be used in continuing contamination studies.

Initial results from the resistor tests indicate the fundamental system response comes from a time lag inherent between the driving source and the current amplifier. This lag can be traced to behavior of the primary boards in the transmitting equipment. It is frequency dependent with a primarily quadratic form related to switching architecture, and contains a secondary exponential function created by board circuitry. While this primary response is dominant at higher frequencies, it is stable and can be removed by subtraction of type curves generated from resistor sets. The correction is applied to measurements on the other ideal systems tested and showed that the system can be corrected to a few milli-radians (mR) below 100 Hz and to 8-10 mR below 10 kHz (Fig. 1).

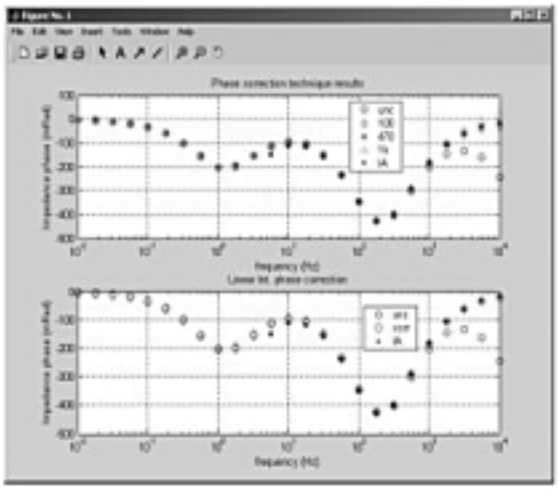

03-GA51139-45

*FIGURE 1. System response curves corrected and uncorrected for an ideal RC circuit. Circuit is shown on the right.*

*Dual-disturbance zone*. The shape of the decay waveform is important to understanding the perturbation of measured voltages on recently transmitted-upon electrodes. The investigators varied the parameters including magnitude and duration of the constant charging current, electrode separations, and immersion media. Of the more

than 250 individual decays observed, waveforms were generally well fit by a double exponential time dependence of the form

$$v(t) = Ae^{-Bt} + C\,e^{-Dt} + F$$

In general, the shorter of the two time constants in Equation 1 is a few tens of seconds, while the longer is a few hundred seconds (Fig. 2). There was no consistent relationship between the total amount of charge delivered and the characteristic decay-time constants as expected. Given the results from this study, the electrode perturbations that have hampered complex resistivity data acquisition when using transmitting electrodes for measurement can be mitigated in several ways: 1) The data can be collected on the same electrodes at frequencies well outside the range of the typical electrode decay waveforms, typically 10-200 Hz, or 2) alternatively, using closely spaced but separate metallic electrodes also appears viable. Separation distances of about 1 cm appear adequate for laboratory and small field-scale monitoring applications.

This LDRD develops the INEEL's capability for the characterization of electrically complex systems. This capability can be applied at the INEEL and at other DOE sites around the country for contaminant studies. Initially, it is envisioned that complex resistivity is applied in lab, mesoscale, and field experiments concerning contaminant flow/characterization and scaling experiments central to Subsurface Science Initiative goals. Beyond these, the capabilities developed through this research in complex resistivity also show promise in areas such as discrimination in unexploded ordinance and mine detection, and in remotely quantifying corrosion in metal drums, tanks, and pipes.

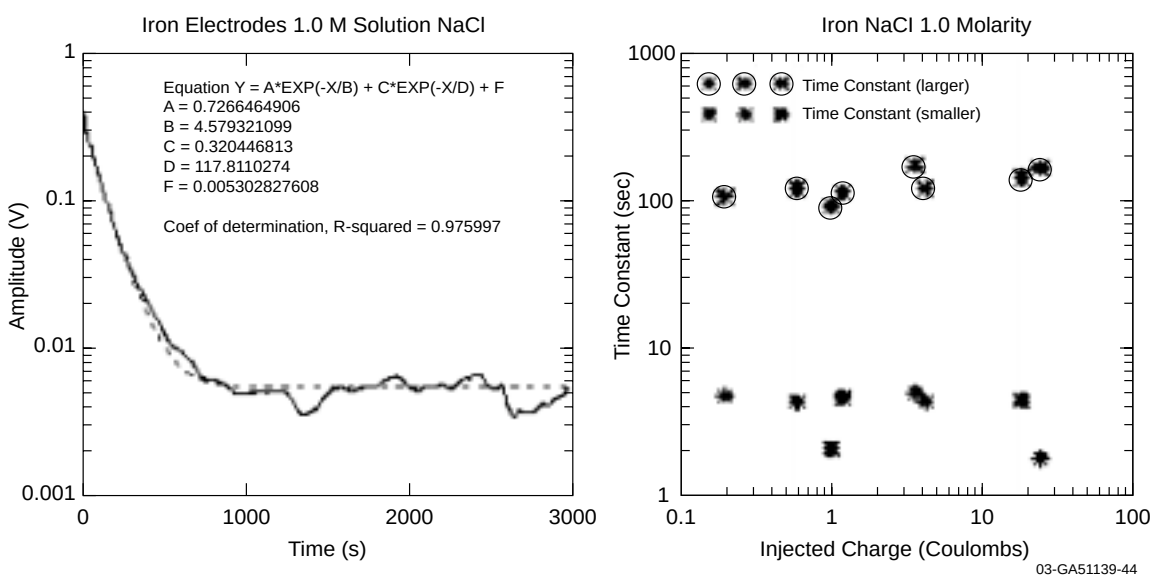


*FIGURE 2. A typical dual exponential decay waveform (left). On the right, is a plot of exponential time constants as a function of injected charge showing the decay is independent of injected charge.*

# Development and Application of Custom Flow Models for Understanding Flow in Porous and Fractured Matrices with Biological Components

*Daphne Stoner, Vance Deason, Paul Meakin*

***Creating repeatable and reliable modeling techniques***

GC134

Key to designing cost-effective, efficient remediation strategies is an understanding of the mechanisms of fluid flow and contaminant transport through porous and fractured matrices, and the impact of microbial activity and growth. Better information will provide the framework for addressing critical issues regarding water resources, materials transport, and the potential use of microorganisms for in situ processes such as enhanced oil recover, mineral dissolution, recovery, and remediation technologies.

The goal of this multidisciplinary LDRD project is to develop methodology and computational modeling techniques for repeatable and reliable determination of the effects of geometry, surface condition, and biofilm growth on flow and materials transport. Stereolithographic methods were used to reliably produce well-characterized structures. These physical models were used to examine localized and system-wide hydrodynamics and the impact that microbial biofilm formation has on these processes. Computational analysis of fluid flow in the physical models was used to evaluate theory and to provide the foundation for the design of future experiments. The project's short-term goal of developing reproducible physical models and experimental systems to examine the impact of microbial biofilm growth on fluid flow behavior is relevant to DOE and INEEL missions. In situ environmental remediation technologies rely on naturally occurring or enhanced microbial communities to degrade organic pollutants and to transform or immobilize inorganic or radioactive contaminants. This research will enhance understanding of biofilm formation and the impact on fluid flow.

Technical objectives for fiscal year 2003:

- Continue the design and fabrication of flow models.
- Present the results of research at a conference.
- Complete experiments examining the impact of biofilm and calcite accumulation on flow.
- Refine the development of computational models.

A number of light-transparent models were designed, fabricated, and tested for examining the impact of biofilm formation on localized and system-wide behavior of fluid flow. These include physical models based on natural fracture surfaces and on computer models for fracture apertures, granular porous media and vesicular porous media. For example, Figure 1 depicts the design and fabricated model for a flow cell based on a natural fracture. Plastic models were designed using 3-D computer-aided drafting programs (CAD), and were fabricated using laser-based stereolithography. Some of the models were fabricated as open-cells models and were fitted with a glass plate and gasket system to allow flow testing and viewing at the macro- and micro-scale. The physical models were integrated with flow delivery and monitoring systems. The flow delivery system consisted of a syringe pump and a pressure control module. Time-lapse images were acquired with a high-resolution digital still camera interfaced with a computer data acquisition system.

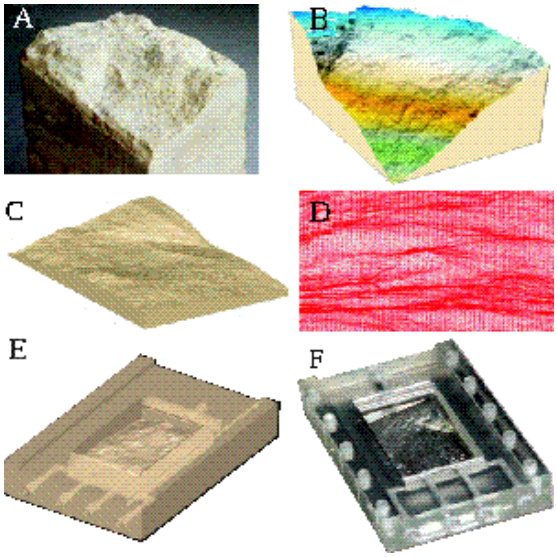


PN04-0004-155k

*FIGURE 1. The design and fabrication of a flow cell containing a replicated fracture surface. A) limestone block that was broken on one edge to form a fracture surface, B) topographical scan of the fracture surface, C) small section of the fracture rendered as a solid, D) meshed design that was imported into the flow cell design, E) transparent CAD drawing of completed flow cell design, and F) fabricated natural fracture model.*

Analysis of system-wide and localized flow effects was accomplished by observation of the time-sequenced movies of the flow and by comparisons of this flow with computational models. A series of time-course studies were conducted to

evaluate localized and system-wide flow of water and low-nutrient media in the physical models with and without accumulated biomass and calcite (Fig. 2).

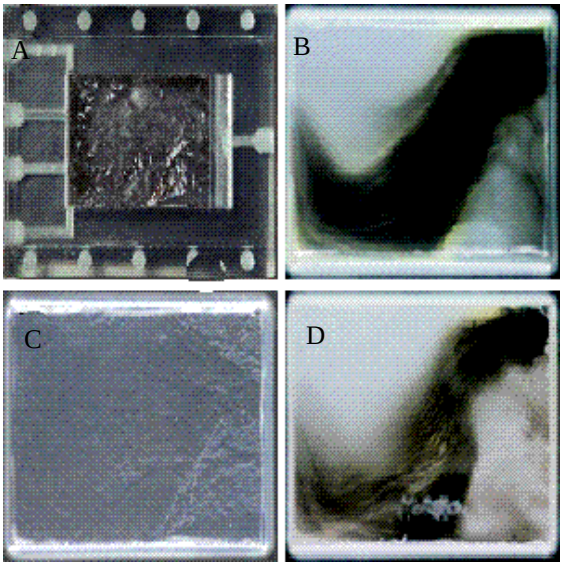


PN04-0004-155k

*FIGURE 2. Impact of calcite precipitation mediated by* Bacillus pasteurii *on liquid flow through the natural fracture flow cell: A) top view of the entire flow cell, B) close-up image of the control flow cell, C) image of the path taken by the colloidal dye as the dye first reached the effluent ports of the flow cell, D) image of dye path through flow cell with precipitate as the dye first reached the effluent port. Flow tests were run at 200 µl/min.*

To address issues relevant to biogeochemistry would require the development of flow models with geochemically relevant surfaces. One approach that is being investigated through this LDRD in collaboration with Alair Emory (Javelin 3D, Salt Lake City, UT) is to fabricate the models from crushed basalt. To achieve such "natural" models involves the fabrication of thin sheets of micron-sized mineral particles bonded by a polymer matrix. A laser cuts this material into a series of horizontal slices of the 3-D model. These are stacked, heated to remove the organic components, and then fired to sinter the particles and fuse the layers into a cohesive form that conforms to the original model. Shrinkage is high, but can be largely compensated for by proper design of the model. Complex internal and external shapes can be fabricated in this manner using any of a variety of ceramic or natural materials. For completely opaque models fabricated out of crushed geological materials or from ceramic, alternative methods of imaging such as nuclear magnetic resonance imaging would be required.

In a separate LDRD program, investigator Paul Meakin has been working on the development of computer models for multiphase flow in complex fracture apertures. As a step towards this goal, lattice Boltzmann models for single phase have been developed and applied to a variety of flow geometries. Results of simulations were compared to results of the dye tracer experiments carried out in this program. These studies demonstrate that the lattice Boltzmann approach can be applied to this project's experiments. Use of this method will be continued.

This LDRD is developing integrated experimental and computation methods for analyzing biofilm formation and its impact on fluid flow. This understanding is significant and will support DOE Basic Energy Sciences, Fossil Energy, Environmental Research, and Environmental Management programs. A proposal for the DOE Basic Energy Sciences, Geosciences, is currently in review by the program office. In addition, technical articles and meeting presentations have resulted from this research, which enhance the INEEL's international reputation in advanced experimental and computational methods.

# Use of Genetic Markers as a Screening Tool for Ecological Risk Assessment

*Angelica I. Stormberg*

***Burrowing animals provide clues to contaminant exposure***

GC147

Radiological and hazardous waste have been disposed of at the INEEL since 1952. Escape of radionuclides and hazardous constituents from uncontained wastes, from deterioration of waste containers, and as a result of waste disposal practices has resulted in contamination of the subsurface soils at the INEEL's Subsurface Disposal Area (SDA) and other facilities. To assess the risks to human and environmental health, the potential impacts of contaminant exposure on identified receptors must be determined.

Burrowing and excavation of the soil by small mammals, including deer mice (*Peromyscus maniculatus*), has been shown to be responsible for some radionuclide transport through the SDA environment; however, the genomic effects of exposure to contaminants at the INEEL are not known. Research was needed to develop new techniques to determine the effects of that exposure to the genome of individuals so that environmental and remedial actions can be properly implemented.

The purpose of this LDRD is to explore the utility of molecular genetic techniques as screening tools for evaluating the risk to natural populations from contaminant exposure. These tools can be used to help evaluate the need for site remediation. If remediation is implemented, genetic characterization of populations can provide insight on the effectiveness of the remediation through long-term monitoring. This report is the culmination of a three-year study wherein radiological and genetic analysis of deer mice collected outside the CERCLA sites of SL-1 and RWMC and two control sites (Burn and Atomic City) was performed. FY03 objectives used samples collected during the first two years of this project.

Technical objectives for fiscal year 2003:

- Re-amplify samples that did not provide initial data using optimization of laboratory techniques.
- Perform comparative analysis of mother/offspring genotypes across the study areas using allelic data compiled from two consecutive field seasons (14 genetic markers, 147 females, 529 embryos, 9,464 PCR reactions).
- Identify mutant alleles in all samples and perform statistical analysis.
- Perform microsatellite genetic analysis for the four study-area populations to determine population structure using a variety of genetic software packages (Genepop, Biosys, and GeneClass).
- Analyze radiological data obtained from all the females collected during FY01 and FY02 and perform statistical analysis.

The null hypothesis to be tested is that there are no significant differences among mammal populations that have been exposed to hazardous or radioactive contaminants and those populations from uncontaminated locations.

Fourteen genetic markers were used to perform microsatellite genetic analysis. Analyses for FY01 (using 14 primers) and part of FY02 (using 8 primers) were subcontracted to Idaho State University (ISU), a collaborator on this project. At the end of FY02, ABI-3100*Avant* genetic analyzer equipment was acquired by the Ecological and Cultural Resources Department at the INEEL. This new equipment allowed the investigators to complete the analysis for FY02 samples for the remaining 6 primers, and thus complete the 14 primer sets in house. Some samples needed to be reanalyzed to check for mutants, as in cases where allele scoring was questionable, or to try to obtain data from previously failed PCR reactions. Data were organized by population and by families; allelic maternal segregation of the offspring was determined, paternal alleles inferred and mutations identified. Only mutations of alleles segregated from the mother were used for this analysis. Not all the families provided useful data and some had to be removed for the genetic analysis (36% of the families were removed). Of those families, both the mother and all of the offspring consistently shared identical genotypes for all of the loci. This is easy to explain since in the majority of the cases, the embryos were too small to be successfully separated from the placental tissue and were probably contaminated during the necropsy. In other cases, alleles were obtained from the offspring but not from the mother and vise versa.

The ratio of microsatellite mutant alleles vs. the non-mutant alleles (m/nm) was used as a direct assessment of mutation using parent-offspring comparison of allele differences. Allele scoring was performed with 14 microsatellite markers for females and offspring from the four study areas. The proportion of mutant alleles from each population was pair-wise compared between populations

and tested for significant differences using the Fisher's exact test. The statistical analysis suggests there is no significant difference when comparing SL-1 (one of the contaminated sites) with the two control sites (Burn and Atomic City); however, there are significant differences when comparing RWMC with all the other populations (Table 1).

*Population Genetic Structure Analysis*. Four different approaches were used to test for population genetic structure. 1) The allele frequency differences among populations were tested using the Fisher's Exact Test where an unbiased estimate of the p-value of the probability test is obtained. The null hypothesis (Ho) "the allelic distribution is uniform across populations" was tested for each locus on a contingency table. 2) The differences in genotype distribution across the populations were based on estimates of Wright's F-statistics. The null hypothesis, $F_{st} = 0$ "the genotypic distribution is uniform across populations" was tested for all loci using a chi-square goodness-of-fit test. 3) The estimate of $Rho_{st}$ statistics is a measure analogous to $F_{st}$ but incorporates allele size estimates and assumes a step-wise mutation model. Calculations of the three estimators were performed using GENEPOP Version 1.2. 4) Finally, an assignment test was performed using GeneClass. This test uses a Bayesian approach to detect immigrants by using multilocus genotypes. The null hypothesis was rejected in the first two methods; that is, the differences in allele frequency distribution and the genotype distribution differences between populations are statistically significant. The third method indicates that some level of gene flow occurs between populations but not enough so that the distributions of alleles or genotypes between them are homogenized. The assignment test also supports population genetic structure since 98.61% of the individuals were correctly assigned to their population of origin.

For radiological analysis, samples from 80 females were used: 43 from Atomic City, 21 from SL-1, and 16 from RWMC. The Burn site was excluded from the analysis due to small available sample size. Female carcasses were processed and analyzed for presence of radiological contaminants. None of the females showed exposure at levels higher than background. Statistical analysis of the radiological data indicates that the differences between the populations are not significant. That is, female mice collected from RWMC and SL-1 had similar levels of radiological (background) contamination compared to the Atomic City control site.

This study shows that there is a difference in the rate of mutation in populations exposed to anthropogenic activities in comparison with populations that have had little or no exposure. The population genetic analysis and the mutation rate data do not support each other. The population genetic analysis suggests that there is a geographical component that plays a role in population differentiation. The populations have different allelic frequency

*TABLE 1. Fisher Exact Test of Independence is presented above the diagonal gray-filled boxes. Number of mutant alleles and non-mutant alleles are summarized for each pair-wise population comparison below the diagonal gray boxes. m = represents the percentage of mutant alleles in each of the populations.*

| | Burn | SL-1 | RWMC | Atomic City |
|---|---|---|---|---|
| Burn<br>*m = 0.59%* | | *p* = 0.281672 | ***p* = 0.000942** | *p* = 0.259213 |
| SL-1<br>*m = 8.36%* | Non-mut Mut<br>Burn 496 2<br>SL-1 615 4 | | ***p* = 0.001769** | *p* = 0.086004 |
| RWMC<br>*m = 6.36%* | Non-mut Mut<br>Burn 496 2<br>RWMC 915 25 | Non-mut Mut<br>SL-1 615 4<br>RWMC 915 25 | | ***p* = 0.000000** |
| Atomic City<br>*m = 1.24%* | Non-mut Mut<br>Burn 496 2<br>AC 1857 4 | Non-mut Mut<br>Burn 615 4<br>AC 1857 4 | Non-mut Mut<br>RWMC 915 25<br>AC 1857 4 | |

03-GA51139-36a

composition, and even though there is evidence that some level of gene flow occurs, and that they are not isolated completely, the migration rate is not strong enough to create a panmictic population (a population with no genetic structure).

It is assumed that natural populations share the same level of mutation rate, since this is an evolutionary force that is stochastic, not affected by any of the evolutionary selective forces, and it occurs at very low frequency. If there are no other contributing factors, it is predicted that in all of the studied populations the mutation rates should be similar. This study indicates that this is true when comparing the two control sites with SL-1; however, this is not the case when comparing SL-1 and the two control sites with the RWMC population. This suggests that some external forces (outside of evolutionary forces) are acting on this population. Mutations can be affected by anthropogenic activities.

The study suggests that some anthropogenic activity is affecting the mutation rate of animals living in the vicinity of RWMC. To test this, deer mice were analyzed for Cesium and Strontium and other gamma emitters. The analysis indicated that the animals collected at the RWMC site have the same level of background exposure as the ones from the other three sites. Based on this study, it cannot be concluded that exposure to radiological contaminants explains why mice from RWMC showed a significantly higher level of mutations within some families. One observation that is important to make, however, is that the two control sites and SL-1 are sites with little or no current human activities, in contrast with RWMC, which is a site that contains a wide variety and quantity of stored chemicals, as well as long-term history of human activity. It is very possible that long exposure (in generation time) to different chemicals has had an impact on the genealogy of a particular family, making it more susceptible to mutation. This study shows that deer mice are genetically sensitive to exposure to anthropogenic contaminants/activity and that further research should be pursued using this species as a biological indicator for environmental monitoring of contaminants, as well as long-term stewardship and ecotoxicological studies.

Developing genetic techniques for application to ecological risk assessment and long-term stewardship builds unique capabilities at the INEEL and puts the laboratory at the forefront of scientific work and the application of genetics to environmental problems. Additionally, recent purchases of Thermocycler instruments and an ABI 3100-*Avant* Fragment Analyzer have significantly increased the INEEL's in-house analytical capabilities. This LDRD also opens numerous new lines of scientific inquiry related to the application of genetics to environmental issues. The experience and capabilities residing at the INEEL will provide future collaborative research opportunities with universities, other government agencies, and other national laboratories.

Long-term stewardship is one of the three proposed initiatives in the Environmental Quality mission area for the DOE. Key elements of the stewardship program include maintenance and environmental monitoring. This research will directly contribute to the key elements by providing a mechanism to assess the long-term impacts of DOE activities on ecosystems and biological processes. This research also spurred collaborative efforts with Idaho State University and Savannah River Ecology Laboratory.

This LDRD research is part of a long-term plan for building a capability at INEEL in the use of genetic markers to address environmental issues. Once the technology is established, numerous applications using other species as environmental monitoring indicators can be explored. For example, an evaluation of the effects of contaminants on mutation rates of local plants would be useful for monitoring effects on crops, such as corn or wheat, which are common near the INEEL. Other applications for this technology include monitoring of mutation rates in birds and other animals that are in potential contact with contaminated soil, such as the marmots and barn swallows, as well as studies of the ecological impacts on threatened and endangered species or candidate species, such as the sage grouse. The technology developed as a result of this research has the potential to determine if mutation rate changes have occurred. This information will help researchers focus resources and efforts on environmental monitoring at sites where there is a high probability of adverse biological impact due to the presence of contaminants.

# Characterization of Nonlinear Complex Resistivity Spectra During Biochemical Reduction of $Cr^{+6}$ to $Cr^{+3}$

*Greg J. Stormberg, Birsen Canan-McGlone, William A. Smith, John Svoboda*

***Exploring minimally or non-invasive monitoring and validation techniques***

GC144

Measurement of direct and indirect geochemical, biochemical, and geophysical properties and processes is among the challenges associated with monitoring and validation of remedial actions. Microbially induced reduction of hexavalent chromium ($Cr^{+6}$) to the less toxic form $Cr^{+3}$ is an alternative to more expensive remedial treatment methods. However, there is a need for a more cost-effective, real-time, continuous, in situ noninvasive or minimally invasive monitoring technique to determine the remediation efficiency.

This LDRD is developing lab measurement capabilities to study a geophysical method for addressing this need. The nonlinear complex resistivity method of geophysics was applied to electrochemically monitor and measure the biological reduction of chromium in quartz sand-packed columns. The results were compared with data from diagnostic biological and chemical analyses to correlate the complex resistivity spectrum associated with the biological reduction processes.

Technical objectives for fiscal year 2003:

- Perform an experiment where $Cr^{+6}$ concentrations are varied with a constant bacterial cell count.
- Evaluate $Cr^{+6}$ reduction in the presence of background processes.
- Perform an experiment where $Cr^{+6}$ concentrations are held constant and evaluate the response to varying bacterial cell counts.

For each of the following sets of experimental parameters, a background matrix of quartz sand and simulated groundwater was used.

Experiment-1 Constant Bacterial Cell Count with Varying $Cr^{+6}$ Concentration: Each of the three columns was filled with quartz sand and simulated groundwater medium (SGM). Overnight measurements established baseline resistivity parameters. The SGM was drained from the columns with pressurized nitrogen gas. After sterilization of the media (autoclaved at 121°C for 25 min), $Cr^{+6}$ was added to the media by adding a concentrated solution of $K_2CrO_4$. Complex resistivity (CR) measurements were made for three concentration levels of $Cr^{+6}$ to form second sets of baseline data over three orders of magnitude: 2.5, 25, and 250 $mgL^{-1}$ $Cr^{+6}$ aqueous phase. The lowest concentration reflects those seen in $Cr^{+6}$-contaminated groundwater at various DOE sites.

The SGM+ $Cr^{+6}$ was again drained from the columns. The columns were then filled with SGM along with the desired concentrations of bacterial cells and $Cr^{+6}$ by pumping the mixture into the columns at a rate of approximately 10 $mLmin^{-1}$. The $Cr^{+6}$ concentration and resistivity data were collected over a period of one week. After the columns were filled, CR data were collected for static columns (no flowing fluids).

Complex Resistivity Results: A key factor in this experiment is the balance between the concentration of the material to be reduced (in this case, $Cr^{+6}$), the reducing bacterial-cell concentration, and the amount of nutrients available for the reduction process referred to here as the MMNB (metal/microbe/nutrient balance). The reduction time appears to be heavily dependant on the MMNB; unfortunately, no studies have looked into the proper relationship of these factors to allow a quantitative estimation of the appropriate experimental parameters and to allow suitable measurement sequences. However, the sample concentrations selected for this experiment gave some degree of insight as explained below.

2.5 $mgL^{-1}$: This concentration was reduced faster than the chemical sampling sequence expected, as shown in Figure 1, 2.5-$mgL^{-1}$ data. Daily analytical chemistry measurements were planned but by the end of day 1, the sample was completely reduced. The analytical chemistry data collected represents the beginning and end of the reduction process. CR data, however, were collected every 45 minutes.

The MMNB used in this experiment reduced the $Cr^{+6}$ concentration faster than analytical chemical samples were taken. Inasmuch as this concentration is similar to that expected in field conditions, a greater level of detailed study is desired in this situation. Although an acceptable balance of MMNB suitable for computer-aided modeling remains unknown, the measurements of the mid-

level concentration used in this experiment indicate a more detailed study should reveal positive results. Not only are the lower experimental concentrations more closely correlated with observed field concentrations, but further experiments at these lower concentrations could be conducted in a shorter time (experimental data for the entire reduction process could be collected within a day or two, rather than the seven days initially allotted for this experiment).

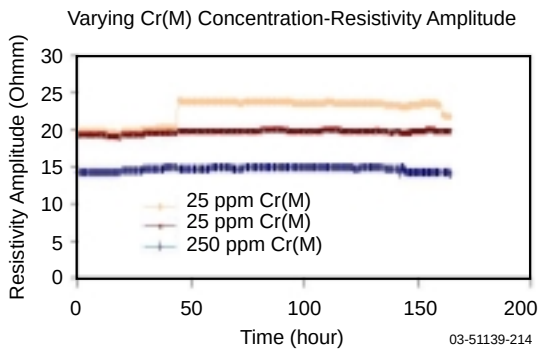


*FIGURE 1. Complex resistivity amplitudes for 2.5, 25 and 250 $Cr^{+6}$ $mgL^{-1}$ samples at 100mHz frequency. Over time, there is no significant change in 25 and 250 $mgL^{-1}$ concentrated samples. The change observed for 2.5 $mgL^{-1}$ samples might be due to metabolic activities of the microorganisms. This has no correlation with reduction time of $Cr^{+6}$.*

25 $mgL^{-1}$: This concentration provided the best $Cr^{+6}$ reduction data within the chosen experimental parameters. The 25-$mgL^{-1}$ concentration was reduced with an appropriate MMNB for the given experimental parameters. The change in concentration is observable via electrical measurements and shows a qualitative correlation to the physical concentration measurements.

250 $mgL^{-1}$: This concentration showed little change over the course of the seven days of the experiment as indicated by the chemical samples.

The MMNB of this measurement was not appropriate for the measurement parameters. Better understanding of the MMNB relationship is needed to determine the experimental parameters necessary to observe reductions at this concentration. However, inasmuch as this concentration did not realistically represent expected field concentrations, further investigation of this concentration was not pursued.

Analytical chemistry data collected at the mid-level concentration show reduction characteristics that readily fit into the experimental parameters used in this experiment. The data suggest that similar observations could be made at other levels of MMNB.

A small but distinct change in electrical parameters was measured throughout the reduction process (Fig.1 and 2). These changes were more pronounced in the phase of CR than in the magnitude spectrum. The decreasing values of phase minimum and its shift to lower frequencies became more clear by displaying phase values at two appropriate frequencies over time and correlating them to the $Cr^{+6}$ concentration change.

The frequency where the phase minimum occurred differs for each column, varying with the ionic concentration of the aqueous phase. For lower concentrations of $Cr^{+6}$, this frequency is lower than the one that corresponds to higher concentrations. To express how reduction of $Cr^{+6}$ changes the frequency where this phase minimum occurs, two frequency points were selected to display the phase change over time. The selection is made for each column depending on the initial phase spectrum's frequency at the phase minimum. The low-frequency point was chosen from the down-slope part of the phase spectrum, the high-frequency point from the up-slope part. The phase minimum resides between these two frequencies.

Figure 2 presents the phase values at 5 and 50-Hz frequencies for the columns with 2.5, 25 and 250 $mgL^{-1}$ concentrations, and at 10 and 50 Hz for the column with the 250-$mgL^{-1}$ $Cr^{+6}$ concentration along with the concentration data for $Cr^{+6}$. As seen, the trend in time of the phase values for the two selected frequencies reversed with respect to each other. While the 5-Hz phase increased, the 50-Hz

phase decreased during the time the $Cr^{+6}$ concentration approached zero for 2.5 and 25 $mgL^{-1}$. This phase trend in time coincides with the chemical concentration data change. The 250-$mgL^{-1}$ concentration was still very high when the experiment was concluded, and the change in phase for the selected frequency was not observed for this column (Fig. 2).

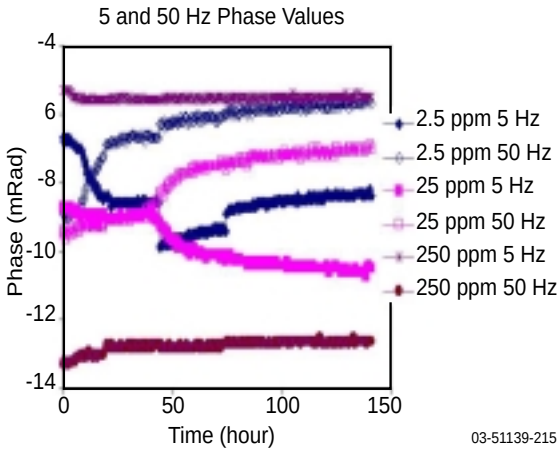


*FIGURE 2. Phase values at 5 and 50 Hz for 2.5, 25 and 250 $Cr^{+6}$ $mgL^{-1}$. Changes in phase values of 2.5 and 25 $mgL^{-1}$ concentrations correspond to completion of the reduction process. However, this change was not observed for 250 $mgL^{-1}$ concentration. This is because the reduction process of $Cr^{+6}$ was not complete.*

Experiment-2 $Cr^{+6}$ Reduction Process in the Presence of the Background Processes:

The same level of SGM plus quartz sand background matrix was used in this experiment. The treatments were:

Column 1: Bacterial cells, but with no $Cr^{+6}$.

Column 2: 25 $mgL^{-1}$ $Cr^{+6}$, but with no bacterial cells.

Column 3: 5 x $10^9$ cfu $mL^{-1}$ bacterial cells with 25-$mgL^{-1}$ $Cr^{+6}$.

Sand and media were mixed before packing the sample columns to ensure uniform distribution of bacterial cells, $Cr^{+6}$, and carbon source within each column. Water samples for chemical analyses were periodically removed from the bottom of the columns.

Experiment-3 Constant $Cr^{+6}$ Concentration with Varying Bacterial Cell Count:

Three levels of bacterial cell concentration were investigated to determine the effects of cell count on the constant 25-$mgL^{-1}$ $Cr^{+6}$ concentration. Each column was filled halfway with the SGM and a bacterial cell plus $Cr^{+6}$. Sand was then added to fill each column. The cell counts for the columns were (a) $10^8$ cells $mL^{-1}$, (b) $10^9$ cells $mL^{-1}$, and (c) $10^{10}$ cells $mL^{-1}$.

This LDRD work is an important first step in positively demonstrating the applicability of the electrochemical geophysical method of complex resistivity to monitor the biological reduction of chromate. The phase component of complex resistivity was found to be more sensitive to the changes of the state of $Cr^{+6}$ than the amplitude. The observed changes occurred in the phase minima, shifting to lower frequency with decreasing $Cr^{+6}$ concentration. The phase minima shift to lower frequency was slow during the reduction process until the $Cr^{+6}$ concentration fell below detection limits (about 0.05 $mgL^{-1}$ in this experiment), at which point the shift became more pronounced. This might be due to the high concentration of ionic species ($Cr^{+6}$) that may cause saturation concentration at which double-layer polarization around the electrode may not change significantly until the concentration reaches a threshold limit.

The reduction time appears to heavily depend on the MMNB. Unfortunately, no study has looked into the proper relationship of these factors to allow a quantitative estimation of the appropriate experimental parameters to allow suitable measurement sequences to be tested. A knowledge of the relationship between MMNB and $Cr^{+6}$ reduction is necessary to properly design an experiment to determine the relationship between CR parameters and $Cr^{+6}$ reduction.

Additional laboratory measurements need to be conducted to determine how the complex resistivity spectra vary as a function of surrounding background matrix, grain size, mineralogical composition, water chemistry, and the presence of other reactions.

# Development of Enzymatic Biosensors for Environmental Applications

*Vicki Thompson, Yoshiko Fujita, Eric Peterson, Tom Luther*

***Testing remediation effectiveness***

GC109

An issue commonly encountered during characterization, remediation, and long-term stewardship of contaminated sites is the lack of comprehensive data regarding contaminant locations and concentrations.

This LDRD is developing capabilities for the design, construction and testing of biosensor technologies based on immobilized enzymes for the determination of chemical species in the subsurface. The first design is a sensor for detection of urea concentrations in groundwater, and complements a pre-existing Environmental Management Science Program (EMSP) project at INEEL. In this project urea will be injected into INEEL groundwater to cause bacterially induced precipitation of calcite with co-precipitation of $Sr^{90}$ and Co contaminants. The urea sensor will enable real-time monitoring of bacterial activity in the subsurface as a measure of remediation effectiveness. In outlying years of this project other types of biological sensors will be examined.

Technical objectives for fiscal year 2003:

- Construct a fieldable urea biosensor.
- Pursue other biosensor concepts.

Initial efforts this year were focused on development of a biosensor where urease enzyme was immobilized via a polymer matrix to the tip of a pH probe. In this design, urea would be hydrolyzed by the urease to produce ammonia and carbon dioxide. The ammonia produced would result in an increase in pH that could be registered by the pH probe. The rate of pH increase could then be related to the concentration of urea present. This approach gave good results; however, difficulties were encountered when multiple samples were measured. After each sample was measured the pH typically increased to approximately 9.0. For measurement of the next sample, it was necessary to return the pH back to the initial value of 7.0. Washing the pH probe with pH 7.0 simulated groundwater or buffer did not result in a reduction in pH even with overnight washing. Eventually a method was developed where low concentrations of hydrochloric acid were used to return the pH to its initial value. This method worked for a few cycles, but the acid caused the enzyme to irreversibly denature over time.

To avoid this problem, an alternative design was developed where the pH probe and the enzyme were physically separated. The resulting flow cell system design for the urea biosensor is shown in Figure 1. The biosensor consists of three components: a pump, a column of immobilized urease, and a pH sensor. To construct the column, urease enzyme was attached to Eupergit beads. These beads have activated surface groups that are reactive with amine groups present on proteins. Enzyme is incubated with the beads for 48 hours for attachment and then any remaining active sites are blocked by a 16-hour incubation with glycine. The beads were then packed into a 1.5 mL plastic column with porous Teflon disks at either end to retain the beads. Bead volumes of 100, 500, 700, and 1000 mL were examined. An ion-select field effect transistor pH probe was used to monitor changes in pH as a result of urea hydrolysis by the urease enzyme. This probe was inserted into a plexiglass block at right angles to an 8 mm-diameter flow channel such that the probe tip was completely in the flow channel. Urea solutions ranging from 0.1 to 10.0 mg/mL were pumped through the immobilized urease column and then past the pH sensor. As the urea solutions passed through the column, the urease converted urea into ammonia and carbon dioxide. The ammonia produced resulted in an increase in pH that was subsequently measured by the pH probe.

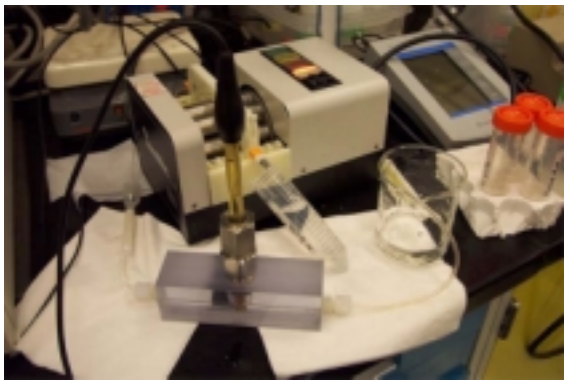

PN04-0004-1560b

*FIGURE 1. Biosensor flow system.*

To increase the sensitivity of the system, urea solution was pumped into the column with the pH probe offline and the flow was stopped for 5-20 minutes. This resulted in a build -up of ammonia

concentration from the hydrolysis of urea. The pH probe then was placed in line and the flow started. Results from one run are shown in Figure 2. After each solution of urea, the column and pH probe were washed with pH 7.0 HEPES buffer until remaining ammonia and carbon dioxide were removed. The column and pH probe were then equilibrated with simulated ground water and a new solution of urea was introduced. The total cycle time for each urea solution was approximately one hour. The major contributor of the cycle time was the time required to wash the ammonia out of the column. Several attempts were made to reduce this cycle time by reducing the size of the immobilized urease column; however, this resulted in a loss of sensitivity. Additional optimization will be necessary to reduce the cycle time to acceptable levels.

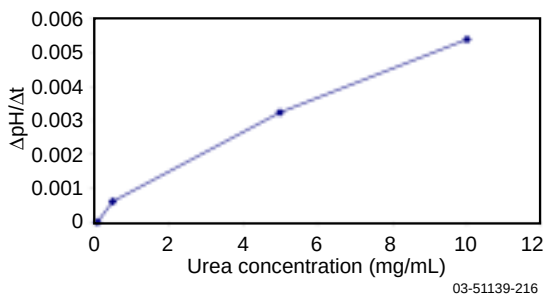


*FIGURE 2. Initial rate of pH increases as a function of urea concentration.*

A biosensor for measurement of phosphate concentrations in groundwater also was examined as part of this LDRD. For this sensor, the enzyme alkaline phosphatase was examined. Alkaline phosphatase catalyzes the cleavage of orthophosphate from orthophosphoric monoesters. This enzyme is widely used as a signaling enzyme in numerous assays, and there are many commercially available substrates that yield colored, fluorescent, or luminescent products upon cleavage. It is known that phosphate ions inhibit the alkaline phosphatase reaction, so an assay based on this inhibition was developed. Alkaline phosphatase was added to solutions of varying phosphate concentrations in a microtiter plate format, and the substrate p-nitrophenyl phosphate (PNPP) was added. The PNPP forms a yellow colored product when cleaved by the enzyme that can be monitored by absorbance at 405 nm. In the presence of phosphate ions the color development was inhibited. The amount of inhibition could be related to the phosphate concentration. This assay could be developed into a microtiter plate format for measurement of phosphate concentrations in contaminated groundwater.

This LDRD is providing the foundation for the development of a new line of innovative, cost-effective monitoring technologies for subsurface investigations, and directly supports the INEEL's mission as a center for environmental technologies. Additionally, this work will provide the basis for development of sensors that can be used for monitoring any contaminated site. This work will constitute a significant milestone in the laboratory's effort to take advantage of its recognized excellence in biologically compatible polymer synthesis for the development of new environmental technologies that can be used by Operations. This contribution is in direct accord with the Environmental Quality Strategic Objectives stated in the INEEL Institutional Plan for improved integration of research and operations, and for the development, demonstration and deployment of innovative technologies that improve program performance. Additionally, it is planned to use the urea sensor to monitor urea concentrations in support of mesoscale studies of ureolytically induced calcite precipitation and ultimately field-scale studies where urea is directly injected into the Snake River Plain Aquifer for stimulation of ureolytic activity by native microorganisms. This activity is part of an ongoing remediation effort to sequester contaminant metals and radionuclides.

# Calibration and Enhancement of Geophysical Imaging Tools in Mesoscale Experiments

*Roelof Versteeg, Russell Hertzog, Cal Christensen, Gail Heath*

***Creating automatic, semi-autonomous systems***

GC141

Effective contaminant remediation and mitigation depends on knowledge of past and future contaminant behavior as well as on insights into the effectiveness of a range of treatment approaches. This knowledge hinges on understanding of subsurface processes, which in turn requires the ability to observe, model, and predict these processes.

Observational data on processes will have to come from large numbers of noninvasive (geophysical) measurements, reinforced with strategically chosen invasive measurements. Interpretation of this data will require the ability to quantitatively integrate geophysical data into hydrological, geochemical, and biological models as well as an infrastructure that allows this integration to occur in a well-defined and traceable manner. This infrastructure should allow a range of users to extract and access information from the data

The fundamental goal of this LDRD is extraction of information on subsurface processes from geophysical data. Developing the ability to observe processes requires both physical and numerical calibration of geophysical imaging tools, and the design and creation of an environment that allows the extraction of information from data collected by these tools. While components of this system can be developed in the laboratory, field-scale implementation of process imaging techniques will require automated semi-autonomous systems. Thus, a core technical component of this research is development of techniques to collect, process, and interpret geophysical and auxiliary data automatically.

Technical objectives for fiscal year 2003:

- Design and implement an integrated structure for data storage, management, and processing.
- Calibrate and enhance electrical resistivity and ground-penetrating radar inversion codes.
- Deploy the system for automated data acquisition and processing of electrical resistivity data in a number of field and laboratory experiments.
- Further the calibration and automation of other geophysical sensors.

In FY02, a conceptual framework was designed to quantify geophysical data in terms of subsurface processes. This framework links the different elements of geophysical data acquisition together. At the end of FY02, an automated system for electrical resistivity data acquisition was constructed. In FY03, the goal was to complete this acquisition system with a structure in which data could be stored, retrieved, and processed. The obvious vehicle for this structure is a relational database. While several relational databases are possible, the choice was made to use an open source database (MySQL) to house the geophysical data, and to use PHP (a server based scripting language) as the interface to this database.

As research progressed, it became clear that this structure could be extended to achieve a fundamental scientific goal – i.e., reproducible and self-documenting research and analysis. The need for this was driven by countless observations that documenting any kind of scientific research is extremely cumbersome, and that reproducing research (or analysis) is virtually impossible. This reality poses a fundamental challenge from a scientific point of view (as research that is not reproducible is by definition not science), from an operational point of view (data analysis results that change when the analysis is repeated create problems), and from an advancement of science point of view (by providing other scientists with access to the ways in which a result was achieved, the ultimate openness of research is achieved).

The challenge of how to perform reproducible research has been approached differently by different researchers, either by distributing a research environment or by requiring the users to use and purchase commercial software. The web-based structure of this research environment led the investigators to choose a third and novel option; a web-based environment for reproducible research. This environment has a large number of advantages. It centralizes the research environment, but distributes the research. Also, it provides instantaneous traceability and authentication of research efforts, allows outside access to research procedures (thus allowing access by duly authorized outside researchers to the assumptions underlying certain analysis results), and provides a suite of tools for research tool validation and verification.

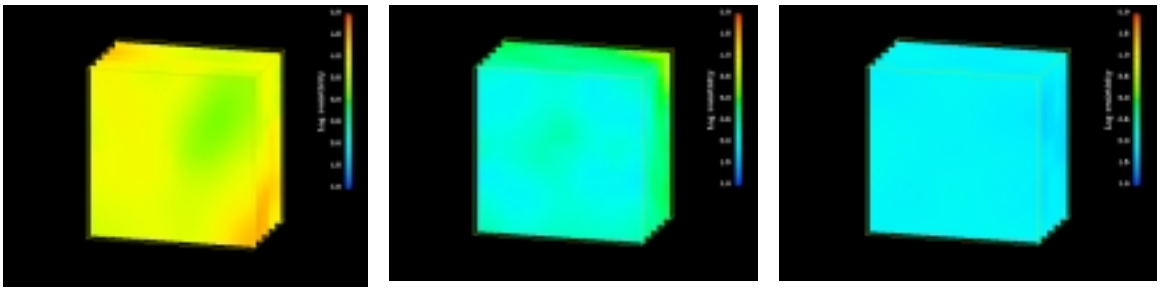

PN04-0004-155o FY03GC141_figure1_c PN04-0004-155n

*FIGURE 1. Comparison of resistivity structure at three different times during the infiltration experiment: (left) at the beginning of experiment, (middle) after 18 days, (right) after 23 days. Yellow indicates high resistivity, blue low resistivity. Blue corresponds to saturated environment. This model demonstrated the ability and benefit of continuous monitoring. The richness of the full data set (390 3-D data sets, each resulting in a 3-D resistivity structure) allows detailed tracking of the flow resulting from the infiltration.*

This structure was mostly implemented in FY03. Some of the elements are fully implemented such as the database structure, PHP front-end, visualization, etc. Other elements, including an environment that allows researchers to create their own research flows, will be completed in FY04.

A second component of the research was the calibration and enhancement of a range of geophysical processing codes. The focus in FY03 was on electrical resistivity codes, as the electrical resistivity method is one of the main methods used in monitoring applications. Electrical resistance tomography (ERT) inversion source code sponsored through prior DOE work was enhanced so that required CPU time was reduced by 90%. Two manuscripts are currently being prepared for submission to technical journals on this work. Also, by integrating data acquisition and analysis, the investigators were able to design an approach that will allow optimal resistivity data acquisition. Efforts to patent this technology will be pursued in FY04. The ERT codes also were compared against a number of commercially available codes, with the results that the current codes now yield detailed information about parameter uncertainty – information that can be integrated in hydrological and geochemical models. Another focus was on Ground Penetrating Radar (GPR) imaging codes. In collaboration with the University of Houston a 3-D GPR migration code was developed and calibrated.

A third component was the deployment of the automated systems in field and laboratory experiments. In addition to a number of smaller experiments, a one-month-long experiment was conducted with the goal of coupling geophysical inversion with hydrological inversions. The investigators collected 390 3-D ERT data sets, as well as continuous directly sensed moisture data from 15 sensors deployed in the model. This experiment ran completely unattended, and served as a proof of concept for the automated acquisition system, the database structure, and for the ability to monitor processes.

A final focus in this LDRD was further calibration and automation of geophysical sensors. This effort included work linked to enhancing the complex resistivity efforts within the laboratory. Specifically, while other related LDRD efforts had focused on development of complex resistivity instrumentation, there was need to design and run a series of relevant experiments using this instrumentation. Through a contract with George Washington University a world-renowned expert on complex resistivity (Professor David Lesmes) was brought in who has assisted in calibrating and enhancing INEEL's complex resistivity systems.

Additional work included an effort to integrate geophysical sensors in robotic platforms. Robotic-acquisition platforms provide significant benefits over manual acquisition of geophysical data for reasons of data quality, lower cost, and reduced risk to the operator. A small effort was pursued to mount two high-precision magnetometers on an Airborne Unmanned Vehicle (AUV). This platform will allow high-quality magnetic data collection over a

range of areas that are currently off limits for geophysical acquisition.

Contaminant remediation and monitoring is an extremely expensive task. DOE spends some $6 billion a year on this task. Other federal and state agencies spend similar amounts. DOD is responsible for many bases that have been contaminated over tens of years of activities. EPA has some 1220 sites on the National Priority List (Superfund), each of which typically will cost tens of millions of dollars to remediate. In addition, there are an estimated 450,000 field sites for which cleanup responsibility and cost are, in most cases, carried by state or local agencies. For all of these sites more precise information on subsurface processes would reduce costs dramatically.

Dynamic and long-term autonomous monitoring systems that provide near real-time, high-quality data on processes would benefit all of these sites. Integration of these monitoring systems with a software environment that both accommodates data from different data streams and provides a web-based environment for access to automatically processed, analyzed and documented data provides the final enhancement to monitoring systems.

# Advanced Borehole Seismic Sources for High-Resolution Subsurface Imaging and Characterization for Environmental Applications

*Phillip West, Stephen Novascone, David Weinberg*

***Improving subsurface characterization for long-term cost savings***

GC105

The INEEL Environmental Restoration (ER) program is concerned with all aspects of investigating and cleaning up contaminated locations on the Site that may pose a threat to human health or the environment. The ER mission is to meet or exceed the cleanup milestones set in the Federal Facility Agreement and Consent Order. Current technologies do not provide large-scale measurements required for modeling. Determination of large-scale properties allows better estimates of risk to groundwater and potential receptors. Assessment of future risk and selection of remedial options for at least two DOE sites (INEEL, Hanford) requires fate and transport modeling through a thick, fractured rock and sedimentary vadose zone. Substantial savings in characterization and long-term monitoring costs can be achieved by the accurate determination of spatial variability of flow of contaminants over large scales in the vadose zone.

The technical problems associated with "seeing" or imaging the subsurface lie within two general areas, namely physical properties of the earth materials through which one wants to image, and the resolution available based on the interrogation technique itself. Subsurface characterization can be performed in a multitude of geophysical ways, but as ever-finer vertical and horizontal resolution is required, acoustic (seismic) techniques have become the overall standard method, especially if detailed 3-D imaging is needed. Substantial savings in characterization and long-term monitoring costs could be achieved by accurately being able to determine spatial variability of flow of contaminants over larger scales of the vadose zone. It is the goal of this LDRD to investigate and design several borehole seismic sources specific to environmental applications.

Technical objectives for fiscal year 2003:

- Test and, if necessary, reconfigure a new AC-motor orbital vibrator (AC OV) and an electromagnetic vertical shear wave (VSH) vibrator.

A total of seven new borehole sources were tested. Four were designed and built at the INEEL. One was reconfigured and two were acquired for comparisons. The INEEL is now in possession of a truly unique set of borehole vibratory seismic sources (Fig. 1).

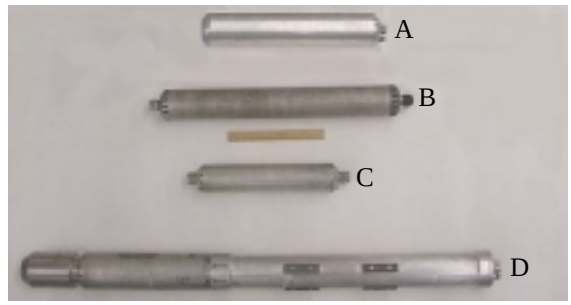


*FIGURE 1. Vibratory borehole seismic sources: (A) INEEL reconfigured AC OV, which measures 23" x 4.5" and weighs 40 lbs. (B) Large dual-motor DC OV, which measures 34" x 4.5" and weighs 25 lbs. (C) Single-motor DC OV, which measures 19.5" x 3.5" and weighs 9 lbs. (D) Electromagnetic vertical shear wave (VSH) source, which measures 54" x 4.5" and weighs 202 lbs.*

During FY03, the INEEL team designed and built three new vibrators to add to the three vibrators provided last year by Cole Engineering. Furthermore, the AC OV was reconfigured to make it into a smaller, lighter, single-body OV. The three vibrators provided last year included a single-motor small-diameter DC OV, an AC-motor OV, and an AC electromagnetic vertical shear wave vibrator. All of the DC vibrators can be run on the INEEL's existing seven-conductor wireline, but the AC vibrators required special provisions. The INEEL addition is a power cable spool and connections. Two of the three new vibrators represent two concepts: resolution is dependent on high frequency, and depth of penetration is dependent on energy/volume. One vibrator is configured to provide an increased frequency (HS) and the other (RAV) offers a novel rotating dipole signature. One of two new vibrators was later reconfigured into yet another OV configuration as a small dual-motor source. The new vibrators demonstrate novelty in design by the way the components are secured within the pressure retaining shell. They also dispose of the flexible coupling between drive and eccentric greatly reducing their length. While this feature might be practical for a prototype design, it could be argued that production devices should not include this feature. Three points can be made:

1) Tolerance stack-up of the components in this type of assembly would not likely amount to more error than bearings and shaft flexure can take indefinitely.

2) Due to the high accuracy of this type of construction the motor's bearing could be eliminated on a production design.

3) Flexure inserts can be used that occupy nearly no space, if flexure is still wanted.

One ongoing problem for modeling is that the motor data does not account for voltages other than maximum and currents other than those at rated power. To accommodate actual data, a dynometer was constructed and the motor was tested at voltages other than rated. Currents were measured to account for the actual power delivered to the earth. This data will augment model performance.

INEEL test sites this fiscal year included TAN and the shallow wells of IRC test area. The TAN well is steel-cased passing through the vadose zone reaching deep into the basalt and the fractured basalt zones. The water level was at about 125' depth. The IRC wells are 75' deep, steel-cased and plugged and filled with tap water. The surrounding earth (during testing) was comprised of dry topsoil ranging in depth from 0 to 7' deep with basalt below that.

TAN tests employed surface geophones for receipt. Sources tested included the large 4.5" dual-motor DCOV the small single-motor DCOV. The IRC tests included the small DCOV, the RAV, the high-speed OV, the small and large dual-motor DC, and the Regenerative Combustion Seismic Source. Various tests were configured using surface geophones, downhole geophones, downhole hydrophones, and downhole hydrophone array. Usual dispositions of equipment did not include a combination of sources. The Physical Properties Logging (PPL) feature of the tools also was tested.

*TAN single-well tests*. A series of tests were performed at a TAN well in the winter of FY03. In this well, the OVs were able to discern fractured vs. unfractured basalt. The large dual-motor DC OV was tested as well as the small single-motor DC (Fig. 2).

*IRC tests (Fig. 3).* Tests were performed through out the summer of 2003 at the IRC. The various tools were operated in the test wells as cross well sources, as PPL tools, and in shallow water tank tests. In all cases, the HSOV and RAV tools were compared to the performance of the small DCOV.

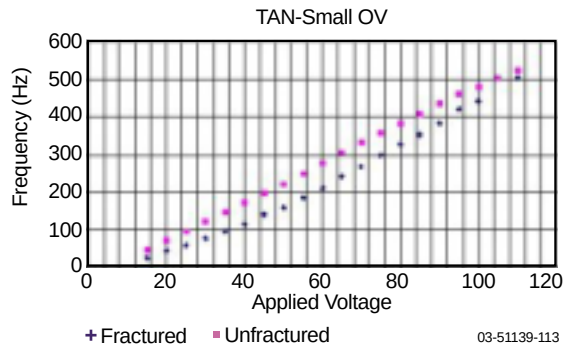


*FIGURE 2. TAN tests.*

The HSOV and the RAV were unable to produce intelligible signals in all cases. The baseline (small DCOV) demonstrated similar inferior performance when operated at low speeds (voltages less than 36v estimated at the tool). But once the DCOV was driven faster, the desired signal became more pronounced and was intelligible over background noise. The parasitic drag imposed by the gearing found in the RAV and HSOV, regardless how efficient it could be configured, was sufficient to prevent the new tools from reaching speeds where signals became discernable above background noise. Another complication in making comparisons between the baseline (DCOV) and these two new sources was that they and the small dual motor DCOV were equipped with accelerometers in place of the geophones used on the DCOV. The accelerometers are more durable but response is highest at higher frequencies. The new sources were unable to reach high frequencies. Replacing the accelerometers in the small dual-motor DC (SDMDC) with geophones improved the PPL capability.

In the best of conditions the DCOV only produced intelligible signals (as a source in the cross well 25' spacing application) when it reached speeds above 200hz (12000 rpm). It is recognized that the small DCOV was not configured with the intent of using it as a source but only as a PPL, and the RAV and HSOV were based on the small DCOV so as to use the latter as a baseline. But the ability of a tool to be a source is not significantly different from being a PPL except for the fact that less power may be required for usefulness in a PPL application. Correspondingly, the HSOV and the RAV may have been a suitable PPL tool had they been equipped with geophones.

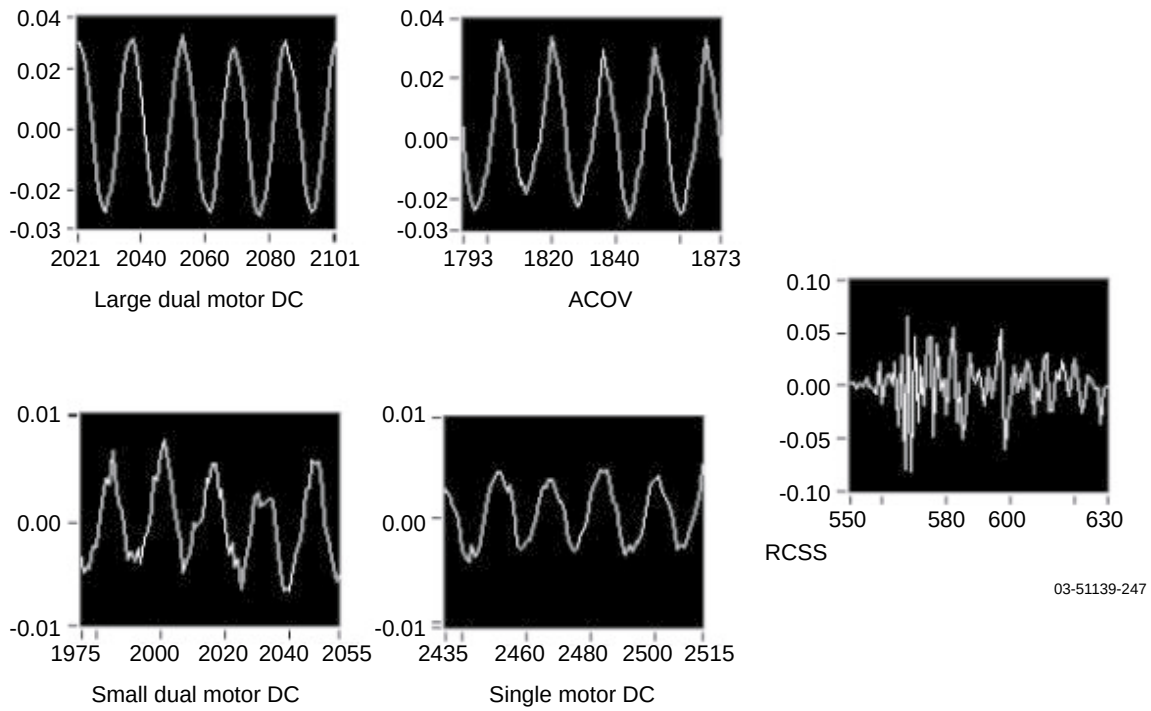


*FIGURE 3: IRC tests.*

Because of the insufficiencies of the RAV as configured, it was dismantled and converted into a dual-motor DC orbital vibrator. Some of the design features incorporated into its design made it an excellent seismic source. Compared to the DCOV, the new dual-motor OV should have provided much better power density. It was twice as powerful with the same size vibrator, only slightly heavier, and with twice the eccentricity. However, its performance was only slightly better at the higher frequencies where the small DCOV provided an intelligible signal. Perhaps the ratio of eccentricity to body mass should have been closer instead of eccentricity to power. On the other hand, it provided a stronger signal at lower frequencies.

Also tested was the INEEL-assembled ACOV. This very powerful source was able to saturate hydrophones placed in the receiver well at the higher frequencies, >300hz. It is rated at nearly 5 hp; where as the DCOV was rated at closer .2 hp. This source uses a 480 v three-phase motor, driven by a variable frequency converter. It was driven to 400hz in the IRC well tests. The graphs in Figure 3 illustrate the hydrophone receipt from the various tools. All vibrators are operating at or near 250hz and the graph is a .02 sec trace. The RCSS also is shown here for comparison.

*Seismic array tests*. A seismic monitoring network was assembled using INEEL seismic equipment. This network included a surface geophone profile employing 24 vertical and horizontal 14 Hz geophones, a borehole array consisting of a 12-channel hydrophone string, and two three-component clamping geophone assemblies. This network was used to monitor different orbital vibrator sources including the ACOV, the small dual-motor DC source and the single-motor DC source. Initial results indicate there is little energy being transmitted in the 100 Hz range. The source well induced resonance in and around the 200 Hz range and increased coupling in the 300-400 Hz range. In this testing sequence, when comparing higher frequency operation, the ACOV source had the greatest

transmitted amplitudes (energy), the single-motor DC source had the next greatest, and the small dual-motor source showed the smallest amount of transmitted energy.

The INEEL design team configured the vertical vibrator for INEEL testing, but all attempts to make it operational failed. On several occasions a single pulse was noted but verification was not possible. Furthermore, the tool was unable to clamp tight enough (even at 200 psi) to transmit the signal even if it had been made operational.

This LDRD research includes collaboration with Dr. Michael Anderson of the University of Idaho and Dr. Jack Cole of the University of Arkansas and Cole Engineering. The project supports development of internal expertise at the INEEL in processing of borehole seismic data, and interpretation of surface seismic and other borehole data. It positions the INEEL to respond to proposals for subsurface-related issues that require acoustic energy sources. Potential customers for this type of technology include those involved with environmental management (EM), fossil energy and national security (NS) applications. Presentations were made on this technology to both Schlumberger and Halliburton.

INEEL

# Appendices

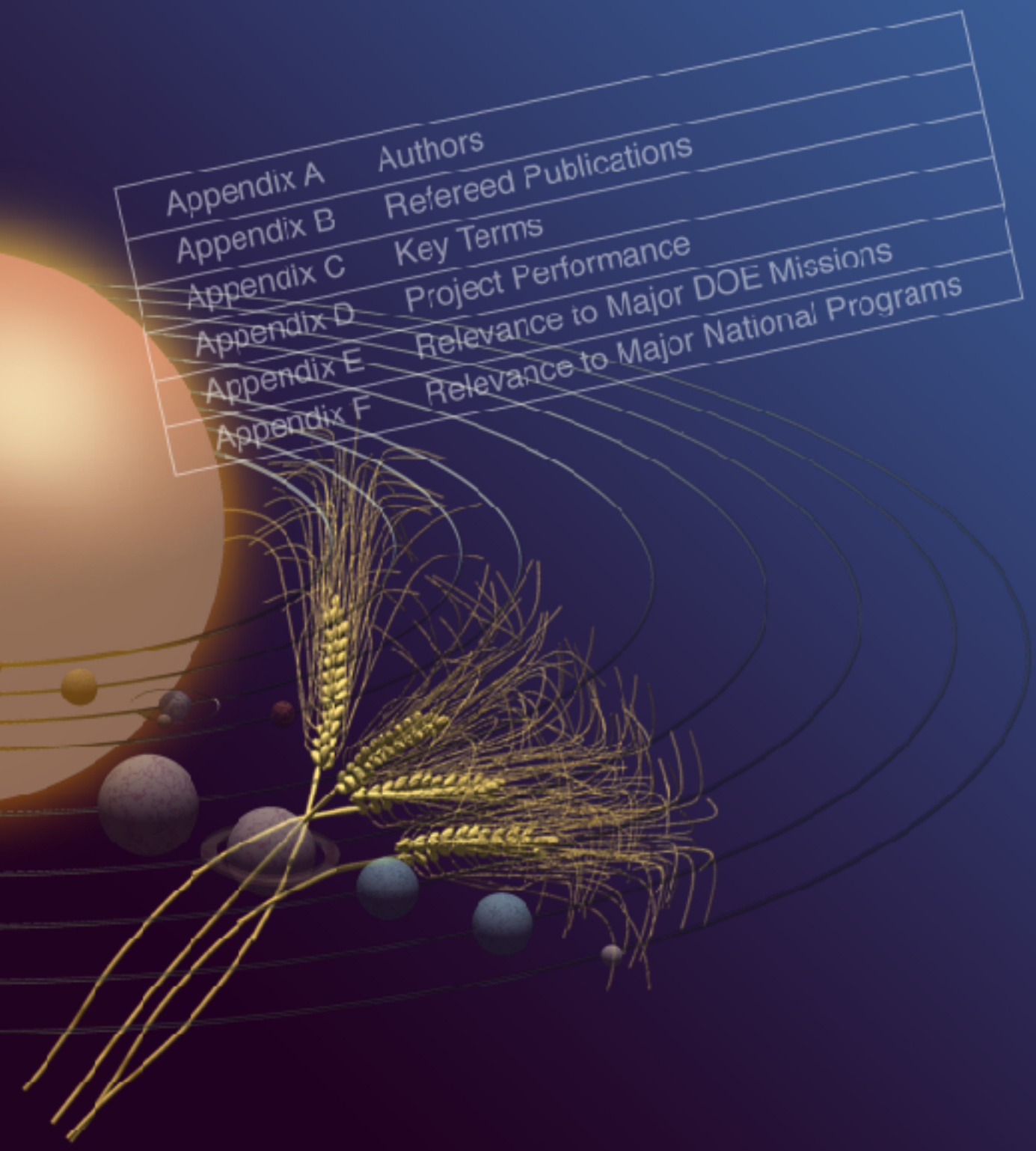

*Appendix A—*

# Authors

# Appendix A—Authors


| Project ID | Principal Investigator | Page # |
|---|---|---|
| | A | |
| ET110 | Abbott, M. L. | 78 |
| ET108 | Alessi, R. S. | 81 |
| ET120 | Anderson, R. P. | 27 |
| ET125 | Anderson, R. P. | 30 |
| ET105 | Apel, W. A. | 84 |
| CE111 | Apel, W. A. | 32 |
| NS134 | Appelhans, A.D. | 149 |
| SC117 | Appelhans, A. D. | 86 |
| NS137 | Austad, W. | 151 |
| NS140 | Austad, W. | 152 |
| | B | |
| NE128 | Baker, J. D. | 34 |
| GC124 | Barnes, J. M. | 255 |
| NS139 | Beitel, G. | 155 |
| ST108 | Berrett, S. | 88 |
| PH106 | Bishop, C. | 257 |
| WT115 | Boardman, R. D. | 203 |
| NE121 | Boardman, R. D. | 36 |
| ET122 | Breckenridge, R. P. | 89 |
| NS135 | Brighton, L. L. | 157 |
| ET116 | Bruemmer, D. | 14 |
| ET116 | Bruemmer, D. | 90 |
| | C | |
| NS132 | Carrington, R. | 160 |
| ET118 | Christensen, C. | 93 |
| NS141 | Chu, H. | 162 |
| NS136 | Corbett, G. | 165 |
| GC131 | Cummings, D. E. | 259 |
| | D | |
| CS114 | Dudenhoeffer , D. | 225 |
| | E | |
| PH102 | Eide, S. A. | 94 |
| NE108 | Evans, R. P. | 37 |
| | F | |
| WT107 | Fox, R. V. | 205 |
| ET114 | Fujita, Y. | 97 |

| Project ID | Principal Investigator | Page # |
|---|---|---|
| | G | |
| SC116 | Ginosar, D. M. | 100 |
| WT101 | Gombert, D. | 207 |
| NE119 | Gougar, H. D. | 39 |
| AC104 | Greenwade, L. E. | 187 |
| | H | |
| ET121 | Hallbert, B. | 102 |
| GC149 | Hamilton, M. A. | 262 |
| CS109 | Hamman, K. D. | 42 |
| ET117 | Harbour, J. L. | 103 |
| ET120 | Harbour, J. L. | 105 |
| GC111 | Harrup, M. K. | 265 |
| NE117 | Hartwell, J. K. | 44 |
| GE108 | Hartwell, J. K. | 235 |
| GE102 | Harvego, E. A. | 238 |
| GC108 | Heath, G. | 268 |
| GC133 | Heath, G. | 271 |
| WT117 | Herbst, R. S. | 210 |
| GE104 | Herring, J. S. | 240 |
| GC138 | Hertzog, R. C. | 273 |
| CE110 | Hoskinson, R. | 47 |
| GC101 | Housley, T. | 276 |
| PH105 | Hubbell, J. M. | 279 |
| NC101 | Hurley, D. | 107 |
| SC118 | Hurley, D. | 109 |
| | J | |
| ST107 | Jacobson, J. J. | 111 |
| CS117 | Jones, J. L. | 228 |
| | K | |
| NS138 | Keener, W. | 167 |
| CE113 | Kenney, K. L. | 49 |
| ES101 | Kong, P. C. | 169 |
| PH103 | Kostelnik, K. M. | 113 |
| NS124 | Kotter, D. | 16 |
| NS124 | Kotter, D. | 172 |
| | L | |
| AC101 | Larson, T. K. | 190 |
| GC151 | LaViolette, R. | 281 |

# Appendix A—Authors


| Project ID | Principal Investigator | Page # |
|---|---|---|
| WT116 | Law, J. D. | 212 |
| GC135 | Lenhard, R. | 282 |
| NC103 | Lessing, P. A. | 114 |
| NS133 | Lillo, T. M. | 174 |
| SC119 | Lister, T. | 116 |
| GE105 | Loewen, E. | 18 |
| GE105 | Loewen, E. | 242 |
| | M | |
| ET119 | Marble, J. L. | 118 |
| GC102 | McLing, T. L. | 284 |
| GC136 | Meakin, P. | 290 |
| GC150 | Meakin, P. | 287 |
| CS118 | Miller, C. J. | 230 |
| NE129 | Mincher, B. J. | 52 |
| GC125 | Moore, G. A. | 292 |
| WT114 | Morton, D. K. | 214 |
| | N | |
| WT111 | Nichols, T. T. | 216 |
| AC103 | Novack, S. D. | 194 |
| PH104 | Novascone, S. | 295 |
| | O | |
| NE127 | Ougouag, A. M. | 54 |
| | P | |
| GC130 | Palmer, C. D. | 297 |
| GC106 | Partin, J. K. | 300 |
| SC115 | Peterson, E. S. | 121 |
| GE101 | Petti, D. | 244 |
| GE101 | Petti, D. | 20 |
| ET106 | Piet, S. J. | 123 |
| GC117 | Pinhero, P. J. | 303 |
| GC152 | Plummer, M. A. | 306 |
| | R | |
| PH101 | Radtke, C. W. | 308 |
| GC114 | Redden, G. | 311 |
| GC116 | Redden, G. | 314 |
| NE114 | Richins, W. | 57 |
| NE114 | Richins, W. | 22 |
| NS118 | Roberto, F. | 178 |
| PH107 | Robertson, E. | 126 |
| NC104 | Rollins, H. | 129 |
| NS121 | Roney, T. | 181 |
| ST105 | Rope, R. | 131 |
| | S | |
| GC140 | Schafer, A. L. | 317 |
| GE103 | Schultz, R. R. | 247 |
| GC145 | Scott, C. | 322 |
| SC111 | Scott, J. R. | 134 |
| GC119 | Scott, J. R. | 320 |
| SC102 | Shook, G. M. | 197 |
| WT112 | Siemer, D. D. | 218 |
| ET107 | Silverman, H. | 137 |
| NE111 | Smartt, H. B. | 60 |
| CE108 | Steffler, E. D. | 62 |
| GC134 | Stoner, D. | 324 |
| GC147 | Stormberg, A. I. | 326 |
| GC144 | Stormberg, G. J. | 329 |
| | T | |
| NE118 | Telschow, K. | 65 |
| NE126 | Telschow, K. | 68 |
| CE112 | Thompson, D. N. | 72 |
| GC109 | Thompson, V. | 332 |
| WT113 | Todd, T. | 221 |
| SC120 | Totemeier, T. C. | 140 |
| | V | |
| SC112 | Van Siclen, C. | 142 |
| GC141 | Versteeg, R. | 334 |
| | W | |
| GE107 | Weaver, K. D. | 249 |
| GC105 | West, P. | 337 |
| ST106 | White, G. J. | 144 |

*Appendix B—*

# Refereed Publications

# Appendix B—Refereed Publications

*Abbott, ET110 – Elemental Tracers and Multi-Variate Receptor Modeling Methods in Assessing Air Pollution*
M. L. Abbott, J. Einerson, P. Schuster, D. Susong, "Trace Elements and Common Ions in Southeastern Idaho Snow: Regional Air Pollutant Tracers for Source Area Emissions," Fuel Processing Technology.

*Apel, ET105 – Biologically Based Catalysts for Processing and Detection in Harsh Service Conditions*
V. Thompson, K. Schaller, W. Apel, "Purification and Characterization of a Novel Thermo-Alkali-Stable Catalase from Thermus brockianus," Biotechnology Progress, Volume 19, pp. 1292-1299.

*Bruemmer, ET116 – Advanced Control Architectures for Human-Robot Synergy in Complex, Multi-Operation Domains*
D. J. Bruemmer, M. C. Walton, "Collaborative Tools for Mixed Teams of Humans and Robot," Multi-Robot Systems, Volume II, Issue 1, pp. 219-231.

*Bruemmer, ET116 – Advanced Control Architectures for Human-Robot Synergy in Complex, Multi-Operation Domains*
D. J. Bruemmer, J. Marble, D. Few, "Intelligent Autonomy for Remote Characterization of Hazardous Environments," Intelligent Controls.

*Bruemmer, ET116 – Advanced Control Architectures for Human-Robot Synergy in Complex, Multi-Operation Domains*
J. L. Marble, D. J. Bruemmer, D. A. Few, "Lessons Learned from Usability Tests with a Collaborative Cognitive Workspace for Human-Robot Teams," Proceedings at the 2003 IEEE International Conference on Systems, Man and Cybernetics."

*Bruemmer, ET116 – Advanced Control Architectures for Human-Robot Synergy in Complex, Multi-Operation Domains*
J. L. Marble, D. J. Bruemmer, D. A. Few, D. D. Dudenhoeffer, "Evaluation of Supervisory vs. Peer-Peer Interaction with Human-Robot Teams," Proceedings at the 2003 IEEE International Conference on Systems Man and Cybernetics.

*Clark, NE111 – Friction Stir Welding of Lightweight Materials for Automotive and Transportation Systems*
D. E. Clark, G. E. Cook, R. Crawford, A. M. Strauss, "Robotic Friction Stir Welding," Industrial Robot.

*Dudenhoeffer, CS114—Critical Infrastructure, Critical Subnetwork*
D. D. Dudenhoeffer, M. Permann, E. Sussman, "A Parallel Simulation Framework for Infrastructure Modeling and Analysis," Proceedings of the 2002 Winter Simulation Conference.

*Evans, NE108 – Two-Phase Mass Flow Measurement for Geothermal Wells*
R. P. Evans, "Mass Flow Measurement Through Flow-Induced Pipe Vibration," Doctoral Dissertation.

*Evans, NE108 – Two-Phase Mass Flow Measurement for Geothermal Wells*
R. P. Evans, J. D. Blotter, A. Stephens, "Flow Rate Measurements Using Flow-Induced Pipe Vibration," ASME Journal of Fluids Engineering.

*Evans, NE108 – Two-Phase Mass Flow Measurement for Geothermal Wells*
R. P. Evans, T. M. Pittard, J. D. Blotter, R. D. Maynes, "Experimental and Numerical Investigation of Turbulent Flow Induced Pipe Vibration in Fully Developed Flow," Journal of the Acoustical Society of America.

*Fox, WT107—Direct Dissolution of Plutonium and Neptunium Species Using Chelated Agents in Carbon Dioxide*
R. V. Fox, B. J. Mincher, "Supercritical Fluid Extraction of Plutonium and Americium from Soil using Thenoyltrifluoroacetone and Tributyl Phosphate Complexation," Radiochimical Acta, August 1, 2003, Volume 89, pp. 613-617.

*Fox, WT107—Direct Dissolution of Plutonium and Neptunium Species Using Chelated Agents in Carbon Dioxide*
R. V. Fox, B. J. Mincher, "Supercritical Fluid Extraction of Plutonium and Americium from Soil using Beta-Diketone and Tributyl Phosphate Complexants," American Chemical Society Symposium Series 860, August 27, 2003, Volume 860, pp. 36-49.

*Fujita, ET114 – Use of Engineered Nano-Particles for Nutrient Delivery and Bioremediation in Subsurface Environments*
M. E. Kauffman, W. Keener, D. W. Reed, Y. Fujita, R. M. Lehman, S. R. Clingenpeel, M. E. Watwood, "Use of 3-Hydroxyphenylacetylene for Activity-Dependent, Fluorescent Labeling of Bacteria that Degrade Toluene via 3-Methylicatechol," Journal of Microbiological Methods.

# Appendix B—Refereed Publications

*Gombert, WT101 – Cold-Crucible Design Parameters for Next Generation High-Level Waste Melters*
G. Hawkes, J. Richardson, J. Morrison, D. Gombert, "Heat Transfer Model for an RF Cold Crucible Induction Heated Melter," ASME Summer Heat Transfer Conference.

*Gougar, NE119 – Advanced Test Reactor Three Dimensional Neutronics Modeling*
H. Gougar, D. .S. Lucas, G. Failla, T. Wareing, J. McGhee, Investigating the Use of 3-D Deterministic Transport for Core Safety Analysis," Proceedings of PHYSOR 2004.

*Harbour, ET117 – Model-Based Decision Making: Conceptual Framework and Environmental-Related Application Development*
H. L. Harbour, H. S. Blackman, "Two Views of Public Participation," Radwaste Solutions, March 2003, Volume 10, Issue 2, pp. 32-39.

*Heath, GC108 – Advanced Technology for Mapping Subsurface Water Conductivity*
G. Heath, J. Svoboda, D. LaBrecque, R. Sharpe, D. Casale, "Combined Electrical and Magnetic Resistivity Tomography: Synthetic Model Study and Inverse Modeling," Journal of Environmental & Engineering Geophysics.

*Heath, GC108 – Advanced Technology for Mapping Subsurface Water Conductivity*
G. Heath, J. Svoboda, D. Alumbaugh, M. A. Ludwig, D. J. LaBrecque, "The Efects of Permeability on Inversion Results of Combined ERT/MMR Data," Geophysics.

*Heath, GC108 – Advanced Technology for Mapping Subsurface Water Conductivity*
G. Heath, J. Svoboda, M. Ludwig, D. Alumbaugh, D. LaBrecque, R. Sharpe, "3D EM Modeling of a New Magnetometric Resistivity System," Third International Symposium on Three-Dimensional Electromagnetics.

*Heath, GC133 – Finding Where Water Moves under Infiltration Ponds Using Remote Sensing Techniques*
G. Heath, R. Versteeg, D. J. LaBrecque, R. Sharpe, "Autonomous Monitoring of Fluid Movement Using Electrical Resistivity Tomography," Environmental and Engineering Geophysical Society (EEGS) – Journal (JEEG).

*Herring, GE104 – Advanced Nuclear Fuels for Enhanced Proliferation Resistance*
J. S. Herring, K. Weaver, P. MacDonald, "Thorium-based Transmuter Fuels for Light Water Reactors," Nuclear Technology.

*Hubbell, PH105 – Improving Soil Water Flux Estimates in the Deep Vadose Zone*
J. M. Hubbell, J. B Sisson, M. J. Nicholl, R. G. Taylor, "Well Design to Reduce Barometric Pressure Effects on Water Level Data in Unconfined Aquifers," Vadose Zone Journal

*Hubbell, PH105 – Improving Soil Water Flux Estimates in the Deep Vadose Zone*
J. M. Hubbell, M. J. Nicholl, "Estimating Flux in a Deep Vadose Zone Using the Darcian Approach," Vadose Zone Journal.

*Hurley, NC101 – Nanostructure Characterization for Sensing*
N. Thantu, "Second Harmonic Generation and Two-Photon Luminescence Upconversion in Glasses Doped with ZnSe Nanocrystalline Quantum Dots," J. Appl. Phys

*Hurley, NC101 – Nanostructure Characterization for Sensing*
D. Hurley, K. Telschow, "Picosecond Surface Acoustic Waves using a Suboptical Wavelength Absorption Grating," Physical Review B, Briefs, 2002, Volume 66, p. 3301.

*Kotter, NS124 – Microantenna Infrared Tags*
D. Kotter, B. Monacelli, G. Boreman, "Design of a Thin-Film Infrared Barcode on a Flexible Substrate," Infrared Physics.

*Lenhard, GC135 – Investigation of the Movement and Fate of Chlorinated Hydrocarbons*
R. J. Lenhard, A. M. Tartakovsky, A. R. Kacimov, H. AbdelRahman, "Modeling Residual NAPL in Water-Wet Porous Media," J. Sci. Res.: Agricultural Sciences, December 1, 2002, Volume 7.

*Lenhard, GC135 – Investigation of the Movement and Fate of Chlorinated Hydrocarbons*
R. J. Lenhard, M. Oostrom, C. Hofstee, T. W. Wietsma, "Flow Behavior and Residual Saturation Formation of Liquid Carbon Tetrachloride in Unsaturated Heterogeneous Porous Media," J. Contaminant Hydrology, January 2003, Volume 64, pp. 93-112.

# Appendix B—Refereed Publications

*Lenhard, GC135 – Investigation of the Movement and Fate of Chlorinated Hydrocarbons*
R. J. Lenhard, M. Oostrom, "Carbon Tetrachloride Flow Behavior in Unsaturated Hanford Caliche Material: An Investigation of Residual NAPL," March 2002, Volume 2, pp. 25-33.

*Lenhard, GC135 – Investigation of the Movement and Fate of Chlorinated Hydrocarbons*
R. J. Lenhard, M. Delshad, M. Oostrom, G. A. Pope, S. Yang, "A Mixed-Wet Hysteretic Relative Permeability and Capillary Pressure Model in a Reservoir Simulator," SPE Reservoir Evaluation and Engineering Journal.

*Lessing, NC103 – Enhanced Transport in Nanocrystalline Ceramic Films*
P. A. Lessing, G. Huestis, "Nanocrystalline NASICON-Type Thin Film Ceramics," Journal of Membrane Science.

*Lillo, NS133 – Novel Fabrication of Blast and Penetration Resistant Materials*
T. Lillo, H. Chu, D. Laughton, D. Bailey, M. Harrison, "Development of a Pressureless Sintered Silicon Carbide Monolith and Special-Shaped Silicon Carbide Whisker Reinforced Silicon Carbide Matrix Composite for Lightweight Armor Application," 2003 Ceramic Engineering and Science Proceedings of the 27th Annual International Conference and Exposition on Advanced Ceramics and Composites.

*Lillo, NS133 – Novel Fabrication of Blast and Penetration Resistant Materials*
T. Lillo, H. Chu, D. Laughton, D. Bailey, M. Harrison, "Development of a Pressureless Sintered Silicon Carbide Monolith and Special-Shaped Silicon Carbide Whisker Reinforced Silicon Carbide Matrix Composite for Lightweight Armor Application," 2003 Proceedings of the 105th Annual Meeting and Exposition to the American Ceramic Society.

*Marble, ET119 – Understanding Societal Issues Associated with Acceptance of Bioremediation Strategies*
J. L. Marble, J. Joe, R. Boring, D. Maiers, M. Kelley, L. Enloe, "Public Perception of Risk Regarding Bioremediation," Risk Analysis.

*Meakin, GC150 – Multiscale Modeling of Multiphase (Unsaturated) Flow*
A. M. Tartakovsky, R. J. Lenhard, S. P. Neuman, "Immiscible Front Evolution in Randomly Heterogeneous Porous Media," Physics of Fluids, November, 2003.

*Miller, CS118 – Advanced Automated Ion Mobility Spectrometer for Explosives Detection*
T. R. McJunkin, J. R. Scott, C. J. Miller, "Toward an Intelligent Ion Mobility Spectrometer (IMS)," The International Journal for Ion Mobility Spectrometry.

*Ougouag, NE127 – Estimation of Neutron Irradiation-Induced Displacements-Per-Atom*
A. M. Ougouag, C. A. Wemple, D. A. Petti, "Displacement Kerma Cross Sections for Neutron Interations in Gas-Cooled Reactor Materials," Global 2003 Conference.

*Peterson, SC115 – Controlled Synthesis, Structural, Electrical, and Optical Properties of One-Dimensional Metals*
E. S. Peterson, B. Anderson, S. Hurst, E. Abbott, B. Keller, L. Spangler, "Solution Equilibria Leading to the Formation of Metal-Metal Bonds in Partially Oxidized Bisoxalatoplatinate(II) Systems," Inorganica Chemica Acta.

*Piet, ET106 – Konvergence Framework for Making Sustainable Cleanup Decisions*
S. J. Piet, P. L. Gibson, J. C Joe, T. A. Kerr, R. L. Nitschke, M. Dakins, "Making Sustainable Decisions Using the KONVERGENCE Framework," Conference Proceedings – Waste Management 2003, Tuscon, Arizona.

*Richins, NE114 – Energy Efficient Building Simulation and Technologies*
W. D. Richins, J. E. Blakeley, M. Lubliner, A. Gordon, A. Persily, N. Moyer, "Building Envelope, Duct Leakage, and HVAC System Performance in HUD-Code Manufactured Homes," AIVC BETEC 2003 (Air Infiltration and Ventilation Center).

*Richins, NE114 – Energy Efficient Building Simulation and Technologies*
W. D. Richins, T. K. Larson, J. M. Lacy, J.E. Blakeley, "Transpired Solar Panel and Ground Source Loop Testing for Residential Housing," American Council for an Energy-Efficient Economy.

# Appendix B—Refereed Publications

*Richins, NE114 – Energy Efficient Building Simulation and Technologies*
J. E. Blakeley, W. D. Richins, T. K. Larson, G. A. Twitchell, "Energy and Air Infiltration Monitoring of Manufactured Homes in Cold Dry Climates," AIVC BETEC 2003 (Air Infiltration and Ventilation Center).

*Richins, NE114 – Energy Efficient Building Simulation and Technologies*
C. C. O'Brien, W. D. Richins, T. K. Larson, "INEEL Severe Weather Test Site in Wyoming," AAWE Newsletter.

*Richins, NE114 – Energy Efficient Building Simulation and Technologies*
C. C. O'Brien, W. D. Richins, T. K. Larson, "INEEL Test Site Hopes to Reveal New Insight into the Performance of Manufactured Homes," Building Safety Journal.

*Rollins, NC104 – Nucleation and Growth of Nanoparticle Materials in Supercritical Fluid Processes*
H. Rollins, "Preparation of Metal and Metal-Sulfide Nanoparticles from Carbon Dioxide Solutions," Encyclopedia of Nanoscience and Nanotechnology.

*Roney, NS121 – Imaging Applications of Photon Beams Produced with Compton Backscatter of Laser Beams*
T. J. Roney, F. Selim, D., Wells, F. Harmon, J. Kwofie, R. Spaulding, G. Erickson, "Bremsstrahlung-Induced Highly Penetrating Probes for Nondestructive Assay and Defect Analysis," Nuclear Instruments and Methods in Physics Research Section A – Accelerators, Spectrometers, Detectors and Associated Equipment, December 2002, Volume 492, Issue 2, pp. 154-160.

*Rope, ST105 – Development of an Integrated-Watershed Information Management Tool for Long-Term Facilities Stewardship*
R. Rope, G. Sehlke, A. Said, D. K. Stevens, "Selection of Remediation Alternatives for Contaminated Water Resources," Journal of Water Resources Planning and Management.

*Rope, ST105 – Development of an Integrated-Watershed Information Management Tool for Long-Term Facilities Stewardship*
G. Sehlke, A. Said, D. K. Stevens, "Estimation of Total Nigrogen/Phosphorous Ratios Using Land Uses," Journal of the American Water Resources Association.

*Rope, ST105 – Development of an Integrated-Watershed Information Management Tool for Long-Term Facilities Stewardship*
G. Sehlke, A. Said, D. K. Stevens, "Exploration of Conversations Schemes and Tmdl Impacts Using Bayesian Networks," Journal of the American Water Resources Association.

*Rope, ST105 – Development of an Integrated-Watershed Information Management Tool for Long-Term Facilities Stewardship*
G. Sehlke, A. Said, D. K. Stevens, "Surface and Ground Water Interaction in the Big Lost River, Idaho," Journal of American Water Resources Association.

*Rope, ST105 – Development of an Integrated-Watershed Information Management Tool for Long-Term Facilities Stewardship*
G. Sehlke, A. Said, D. K. Stevens ,"Towards Sustainable Management of Water Resources – Examining Management Decisions," Journal of American Water Resources Association.

*Rope, ST105 – Development of an Integrated-Watershed Information Management Tool for Long-Term Facilities Stewardship*
G. Sehlke, A. Said, D. K. Stevens, "An Innovative Index for Evaluating Water Quality in Streams," Journal of American Water Resources Association.

*Rope, ST105 – Development of an Integrated-Watershed Information Management Tool for Long-Term Facilities Stewardship*
G. Sehlke, A. Said, D. K. Stevens, D. Sorenson, T. Glover, "Exploring an Innovative Watershed Management Approach: From Feasibility to Sustainability," 2nd Dubrovnik, Conference on Sustainable Development of Energy, Water and Environment Systems, Dubronvik, Croatia, June 15-20, 2003.

*Scott, GC119 – Development of Imaging Fourier Transform Mass Spectrometer Capabilities for Analyses of Complex and Heterogeneous Samples*
J. R. Scott, T. R. McJunkin, P. L. Tremblay, "JClassification of Mass Spectra using Fuzzy Logic Inference Engine," Journal of the Association for Laboratory Automation, April 1, 2003, Volume 8, pp. 61-63.

# Appendix B—Refereed Publications

*Scott, SC111 – Elucidating the Photo-Physics of Complex Metal Ions Trapped in a Fourier Transform Mass Spectrometer*
J. R. Scott, P. L. Tremblay, J. E. Ham, B. Durham, "Ruthenium Trisbipyridine as a Candidate for Gas-Phase Spectrscopic Studies in a Fourier Transform Mass Spectrometer," Spectroscopy: An International Journal.

*Scott, SC111 – Elucidating the Photo-Physics of Complex Metal Ions Trapped in a Fourier Transform Mass Spectrometer*
J. R. Scott, P. L. Tremblay, J. E. Ham, B. Durham, "Comparison of Laser Desorption and Matrix-Assisted Laser Desorption/Ionization for Ruthenium and Osmium Trisbipyridine Complexes using Fourier Transform Mass," Journal of the American Society for Mass Spectrometry, March 18, 2003, Volume 17, pp. 393-400.

*Scott, GC119 – Development of Imaging Fourier Transform Mass Spectrometer Capabilities for Analyses of Complex and Heterogeneous Samples*
T. R. McJunkin, J. R. Scott, P. L. Tremblay, "Fuzzy Logic Classification of Imaging Laser Desorption Fourier Transform Mass Spectrometry Data," IEEE Transaction on Systems, Man and Cybernetics – Part C.

*Silverman, ET107 – Recombinant Adhesive Protein Production and Investigation into Alternate Natural Adhesive Systems in Marine Mussels*
H. Silverman, "Adhesive Proteins from Mussels: Historical Progress and Implications for Materials Applications," Journal of Advanced Materials.

*Stoner, GC134 – Development and Application of Custom Flow Models for Understanding Flow in Porous and Fractured Matrices with Biological Components*
D. L. Stoner, S. M. Watson, P. Meakin, J. M. Barnes, V. A. Deason, R. D. Stedfled, L. Griffel, L. Pegram, "Development and Application of Custom Models for Understanding the Impact of Biofilm Growth and Calcite Precipitation on Fluid Flow," Applied and Environmental Microbiology.

*Van Siclen, SC112 – Mechanical and Flow Properties of Dry Granular Media*
C. Van Siclen, "Force Structure of Frictionless Granular Piles," Physica A.

*Weaver, GE104 – Advanced Nuclear Fuels for Enhanced Proliferation Resistance*
K. Weaver, J. S. Herring, "Performance of Thorium-Based Mixed-Oxide Fuels for the Consumption of Plutonium in Current and Advanced Reactors," Nuclear Technology, July 1, 2003, Volume 143, pp. 22-36.

*White, ST106 – Integrated Environmental Analysis: Development of Collaborative Approaches to Long Term Environmental Stewardship*
W. Keener, M. Lehman, M. E. Kauffman, S. Clingenpeel, M. Watwood, D. Reed, "Activity-Dependent Flourescent Labeling of Bacteria that Degrade Toluene via 3-Methylcatechol," Microbial Methods.

*White, ST106 – Integrated Environmental Analysis: Development of Collaborative Approaches for Long Term Environmental Stewardship*
R. M. Lehman, F. S. Colwell, S. P. O'Connell, O. Snoeyenbos-West, V. D. Winston, D. E. Cummings, M. E. Watwood, "Detection of Archaeal 16S rDNA Sequences from an Oxic Basalt Aquifer," Microbiology Ecology, 2003, Volume 44 pp. 165-173.

*Appendix C—*

# Key Terms

# Appendix C—Key Terms

## *Symbols*


3-D deterministic transport code 39
3-D ion optics 149
93mNb production mechanisms 34


## *A*


AccessGrid node (Agnode). 187
accident management 102
acid hydrolysis pretreatment 32
acoustic detection 300
acoustically induced confinement 107
actinide burning 242
actinide recycle 212
adhesive systems 137
adhesive-related genes 137
adsorbed contaminants 311
adsorption equilibria 281
advanced fuels 240
Advanced Gas Reactor (AGR) 235
advanced lightweight armor systems 174
Advanced Test Reactor (ATR) 39, 54, 68
agricultural biomass 32, 49
air infiltration in residential housing 57
air pathway transport 79
air pollution assessment 79
anaerobic wet storage 72
anthropogenic contaminant migration 292
aquifer temperature distribution 284
armor systems 174
arsenic contamination 221
arsenic initiative 286
ASPEN Plus 216
association-based Pitzer parameters 216
Atmospheric Pressure Surface Analysis Mass Spectrometry (APSAMS) 86
atmospheric transport of pollutants 79
Attila 39
automatic, semi-autonomous systems 334
Autonomous Unmanned Aerial Vehicles 152


## *B*


bagasse 72
ballistic properties 174
beta-diketones 205
bi-material 60
Big Lost River watershed 131
biocatalysts 84
bioenergy 49
biogeochemical processes 297
biological sensors 332
biomass 47, 72
biomass-derived fuels and chemicals 62
biomechanics of stem separation 62
biomimetic glue 137
biorefinery 72
bioremediation 118
biosensor technologies 332
biosensors 84
bioterrorism agents 178
blast- and penetration-resistant materials 174
borehole seismic sources 337
boron neutron capture therapy (BNCT 44
botulinum (BoNT) 167
Bremstrahlung (broadband) x-ray sources 181


## *C*


cancer treatment planning 44
carbon nanotubes 30, 31
catalyst fouling 100
catalytic processes 109
cellulosic stem 62
ceramic oxides 114
ceramics fabrication 174
cereal genotypes 62
cermet filters 169
change detection 105
chaotic mixing 60
chemical & biological weapon agent destruction 169
chemical complexes 134
chemical identification 228
chemical imaging 320
chemical warfare agents 230
chlorinated hydrocarbons 282
chlorocarbon removal 52
classified cluster computing 165
climatic change 306
Cluster File System/Load Balancing Evaluation 191
Cluster Networking Optimization 190
Cluster Parallel Tool 191
cluster technology 190
CO2-sequestration 126
coal bed permeability models 126
coal-fired reactor 36
Cold Crucible Induction Melter 207
colloid-facilitated transport 292, 300, 311
colloidal matter 300
colloids 97
combustion synthesis 169
command and control 102
common cause failure (CCF) 194
complex resistivity 322, 329

# Appendix C—Key Terms

Computational Fluid Dynamics 42, 192, 247
computer simulation and collaboration 187
contaminant migration 317
contaminant remediation 334
contaminant transport 284
contaminant transport and fate 297
contaminant transport predictions 317
contaminant vapor plumes 276
contaminated groundwater 297
contraband 230
core neutronics 242
core/fuel designs 249
corona discharge chemical ionization 86
corrosion processes 116
coupled codes 247
Critical Infrastructure Protection 169, 225
criticality and flux distribution calculations 39
crop residues 49
CYANEX-301 212

*D*

Darcian approach 279
data trace application 160
DC resistivity measurements 268
dechlorination of TCE 259
decision dynamics 123
decision models 103
Decision Support System for Agriculture 47
decision support tools 225
decision-making 81, 118, 123, 194
decision-making models 112
decision-support tools 103
deep vadose zone 279
deer mice 326
detecting bioterrorism agents 178
Diffraction Tag 173
Digital Signal Processing (DSP) Boards 157
displacement kerma cross-sections 54
displacements-per-atom (dpa) 54
distributed computing 190
double scatter neutron spectroscopy 45
down-hole orbital vibrator (OV) 295
driving-point impedance measurements 295
Dual Mode Ion Mobility Spectrometer 230

*E*

Eastern Snake River Plain (ESRP) aquifer 284, 292
ecological health indicators 89
ecological patterns and processes 144
Ecological Risk Assessment 326
elastic properties of the subsurface 295
electric generation station 244
electrical behavior 322
Electrical Resistance Tomography (ERT) 268
electrode characteristics and behaviors 322
electromagnetic energy 68
electrowinning 218
embedded membrane 210
Emergency Response Planning Support Systems 105
end-state planning 111
endoxylanase (EC 3.2.1.8) 32
energetic projectiles 171
energy efficiency 57
enhanced imaging laser desorption FTMS 320
ensiling 72
environmental bacteria 255
environmental management 94
enzymatic hydrolysis 72
enzyme-activity-based assays 167
enzyme-specific probes 144
Enzymes 84
equilibrium isotherms 222
event tree 155
exoxylanase (EC 3.2.1.37) 32
explosives contamination 308
Explosives Degradation 308
extremophilic microbes 32, 84

*F*

fate and transport modeling 337
fate & transport of subsurface contaminants 287, 290
fault tree 155
feedstock harvest/preprocessing 72
Ferritic-martensitic steels 140
Fiber-Optic Probes 303
fiber-optic sensor technologies 303
finite element heat transfer code FIDAP 207
First responders 102
fission product detection systems 235
fluid dynamic processes 42
fluid flow in fracture apertures 287
fluidized-bed reactor 203
fluorescence 134
fluorescence detection 320
fluorescent-tagged synthetic colloids 292
for laser ultrasonic material diagnostics 68
force distribution 142
Fourier transform mass spectrometer 134
Fourier Transform Mass Spectrometer (FTMS 320
fractured basalt sequences 257
Friction Stir Welding 60

# Appendix C—Key Terms

*G*

gamma tube 68
gas mixtures 126
gas-cooled fast reactors 249
gas-phase fluorescence behavior 134
gas-phase ions 134
Generation IV reactor 238, 244
genetically inspired computing 191
genomic effects 326
geochemical logging tools 273
geochemical reactions 317
geologic framework 284
geophysical imaging tools 334
geophysical sensors 335
geothermal well sites 37
granular materials 142
green fluorescent protein (GFP) 255
ground source cooling systems 57
groundwater contamination 255
groundwater flow 284
groundwater remediation 297
GSM 152

*H*

Halomonas campisalis 84
hemicellulose 32
hexavalent chromium (Cr+6) 329
High Level Waste Melters 207
high-performance computing 165, 190
Hollow waveguides 68
Holographic structures 178
hot offgas cleanup sorbent technology 203
hot-cell 68
human safety and health risk models 94
human systems science 81
hybrid glass 178
hydraulic conductivity 317
hydrocarbonaceous compounds 100
hydrodynamics 324
hydrogen absorbing materials 30
hydrogen production 27
hydrogen transport devices 114
hydrogeophysical methodology 257
Hysteretic Chemical and Moisture Migration 317

*I*

imaging for material probing 228
immobilized enzymes 332
Impact Testing Machine (ITM). 214
in situ bioremediation 97
in situ flux 279
In situ measurement 297
in-pile kinetic data 65
induced-emission imaging 181
INEEL waste sites 111
INEELs New Waste Calcination Facility 218
information management 102
infrared (IR) camera 60
Infrared Barcode 172
infrared signatures 172
infrared video scans 57
infrastructure networks 225
Integrated Watershed Information Management Tools WIMT) 131
intelligent robots 90
Intercalated Graphite 30
Internet Protocol (IP)-based cellular 152
Intrusion Detection Systems (IDS) 152
ion exchange/adsorption resin 221
ion lens 149
ion mobility spectrometry 230
ionic transport 114
irradiated supercritical water 52
Irreducible Critical Sub-network 225
isotope ratio mass spectrometry 149
isotope ratio measurements 149
isotopic compositions of strontium 284

*J*

Java 165
Java Management Extensions (JMX), 165

*K*

kinetics of solute transfer 311
Kinetics/catalysis of sulfuric acid decomposition 27

*L*

lactate 97
Land Mobile Radio (LMR) systems 152
landscape ecology 89
Langmuir strain curve 126
lanthanides 205
laser desorption 86
laser ultrasonics 65, 109
laser-based optical and chemical imager (LOCI) 320
Laser-Compton Scattering (LCS) 228
laser-induced breakdown spectroscopy 300
laser-induced fluorescence 52

Lead or Lead-Bismuth Reactor 242
legacy risk 94
Light Water Reactors (LWRs) 238, 240
lignocellulosic residues 72
linear accelerators 181
long-term stewardship 113
loss-of-coolant/loss-of-flow accidents 249

*M*

mass flow measurement system 37
materials characterization 174
mechanical property/corrosion monitoring 65
medical radiation therapy 228
membrane abrasion 210
mental model 123
mercury recovery 218
mesoscale experiments 282, 303, 334
Metal complexation 205
metal nanoparticles 129
metal spray forming process 174
metal-complexation 205
methane recovery 126
methanotrophic bacterial endosymbiont 137
microbial biofilm formation 324
microbially induced reduction 329
microelectrodes 303
modeling of gas-cooled reactors 238
Modular Pebble-Bed Gas-Cooled Reactor 244
molecular genetic techniques 326
molecular markers 62, 255
molecular/nano-wires 121
moment equations 290
multi-axis dynamometer 60
multi-modal interface 90
multielectrode array microscope (MEAM) 116
Multiphase Flow 290
multiphase flow phenomena 287

*N*

N-glycosylases 167
nano-crystalline ceramic thin films 114
nano-pattern recognition strategy (nanosensor) 178
nanocomposite materials 265
nanotrap 178
Narrowband Surface Acoustic Waves 65
National Color-coded Threat Alert 155
natural resource management 89
neutron transport code 39
neutron-based radiotherapy 44
Next Generation IV Fuel Testing 235
non-lattice model 142
normative model 118
nuclear fuel cycle 212
Nuclear Fuels 240
nuclear safety analysis 244
nuclear waste 212
Numerical Model Efficiency 197
Numerical Simulation Laboratory (NSL) 187

*O*

off-normal heat treatment conditions 140
offgas treatment 203
offgas-scrub solution 218
omni-directional 157
organic ligands 281
organic liquid scintillators 45
organic polymers 265
organophosphorus reagents 205
ormogels 178

*P*

Parallel Computing Architecture for Java 165
PIV flow characterization 49
particle-based methods 287
pathogenic microorganisms or toxins 178
Pb or Pb-Bi cooled fast reactor 242
PEBBED 244
perceptions of risk 118
permeable reactive barrier (PRB) 265
Peromyscus maniculatus 326
Phenol 97
photoluminescence 107
Photon Exchange Membrane fuel cell engines 30
phytoextraction 262
picosecond surface acoustic waves 107
pipe damage detection research 160
pitzer model 216
polylactide colloids 97
polymerase chain reaction (PCR) techniques 167
polymeric materials 121
polymerization of the platinum chains 121
polysaccharide degradation 72
Power Burst Facility 112
pressureless sintered (SiC) armor tiles 174
pressurized leakage tests 57
probabilistic risk assessment (PRA) 194
proteases 167
protective caps 144
proteinaceous structures 137
public participation 81

pulse radiolysis 52

*Q*

Quantitative Threat-Risk Index Model (QTRIM) 155
quick-transient TH behavior 247

*R*

radiation chemistry 52
radiation damage 54
Radioactive Waste Management Complex 276
radiochemical purification methods 34
radionuclide transport 326
radionuclides 205, 262, 287
raman detection 320
reactive supercritical fluid regeneration (RSFR) 100
reactor core neutronics 244
reactor physics code 244
real-time CFD-based control 42
receptor modeling 79
red fluorescent protein markers 255
region of interest (ROI) isotherms 222
remediation effectiveness 332
remediation of metals 265
residual hazards management 113
reverse-genetics 137
ricin 167
risk analysis models 155
risk perception 118
robot behavior architecture 90
robotic platforms 335

*S*

SAPHIRE 155
SAPHIRE models 194
SCADA systems 225
Scanning electrochemical microscopy (SECM) 116
supercritical carbon dioxide $scCO_2$ 205
semiconductor nanoparticles 129
sequential implicit scheme 197
silicon (wafer) surfaces 228
single-well push-pull tests (SWPPTs). 297
Smart Antennas 157
Snake River Plain Aquifer 271
sodium-bearing waste 218
soil water flux 279
soil-gas dynamics 276
sorbent particles 36
spatial distribution of subsurface properties 290
spatial element mapping 228
spatial imagery 105
Sr-90 uptake and translocation 262
Stereolithographic methods 324
stochastic flow equations 290
strain rate 214
stratigraphic correlation of subsurface lava flows 273
straw stems 47
stress-strain response models 214
strontium-90 262
structural design 214
subsurface 311
subsurface barriers 265
subsurface bioremediation 97
subsurface characterization 268, 273, 337
subsurface current flow 268
Subsurface Disposal Area (SDA) 282, 326
subsurface environments 303
subsurface flow and transport 295
subsurface heterogeneity 257
subsurface hydrologic processes 271
subsurface Imaging 337
subsurface processes 334
sugar cane bagasse 72
suitable titanium-based structural armor 162
sulfuric acid decomposition 27
Sun Grid Engine 191
supercritical fluid extraction (SFE) 205
supercritical pressure and temperature $CO_2$ 249
superheated drop detectors 44
surface acoustic waves 109
surface magnetic field measurements 268
sustainable environmental protection system 113
Switched Multibeam Antenna/Adaptive Arrays 157
synthetic nano-particles 97

*T*

tagging agents 255
tagging technology 172
temperature effects 214
Test Area North 112, 259
tetanus (TeNT) 167
TETRAD 192, 197
thermal hydraulic design 244
thermal signatures 172
thermal/acid stable hemicellulases 32
thermally sprayed conductive traces 160
thermite combustion synthesis 169
thermo-acidophiles 32
thermochemical cycles 27
*thermus brockian* 84
thorium-based fuels 240
threshold foils 44

time- and probability-modeling tool 103
time-critical operations 103
titanium alloys 162
tracer accumulation 306
tracer gas monitoring 57
transient analyses 247
transient analyses of supercritical-water reactors 238
transient analysis of gas-cooled reactors 238
Transient Bulk Longitudinal Wave Measurement 66
transient infiltration 317
transparent aluminum oxynitride (ALON) 162
transpired solar wall 57
transuranic destruction 249
trichloroethylene (TCE) 259
triple sector isotope ratio mass spectrometer 149
tunable x-ray sources 228
two-phase flow 37

*U*

ultrafiltration membranes 210
ultrasonic measurement 68
Universal Mobile Telecommunication System 152
unsaturated hydraulic conductivity 279
urea concentrations in groundwater 332
urea sensor 332

*V*

vadose zone 265, 271, 276, 281, 306, 308, 317, 337
vadose zones 292
Virtual Reality Reliability, Availability, and Maintainability (VRAM) 194
Visualization Laboratory 187

*W*

Waste Area Groups 111
water flux rates 306
watershed management 131
wet storage systems 72
wireless infrastructure security 152
wireless local area network (WLAN) system 157
Wireless Test Bed (WTB) 152
wormholes in weld roots 60

*X*

x-ray fluorescence (XRF) 181
x-ray fluorescence excitation source 34
x-ray generators 181
XRF tomographic imaging 181

*Z*

zircaloy corrosion in nuclear reactors 65
zircaloy films 65
zirconium 34

*Appendix D—*

# Project Performance

# Appendix D—Project Performance

| Project ID | Principal Investigator | Project Title | FTE | Other Students | Post Docs | Faculty | Crada | WFO | IDR | Patents Awarded | Copyrighting/Trademark | License | Publications | Presentations | Symposia | Awards |
|---|---|---|---|---|---|---|---|---|---|---|---|---|---|---|---|---|
| ET110 | Abbott, M. L. | Elemental Tracers and Multi-Variate Receptor Modeling Methods in Assessing Air Pollution | 0.7 | | | | | | | | | | 1 | 1 | | |
| ET108 | Alessi, R. S. | Improving Stakeholder Interactions: A Stakeholder-based Research Methodology for Reaching Decisions on Polarized Issues | 0.5 | | | 1 | | | | | | | 1 | | | |
| NE120 | Anderson, R. P. | Hydrogen Production from High Temperature Nuclear Reactors | 2.43 | | | | | | | | | | | | 1 | |
| NE125 | Anderson, R. P. | Hydrogen Technologies R&D | 1.13 | | | | 1 | | | | | | | | | |
| CE111 | Apel, W. A. | Stable Enzymes for Hemicellulose Hydrolysis | 0.9 | 2 | | | | | | | | | 1 | | | |
| ET105 | Apel, W. A. | Biologically Based Catalysts for Processing and Detection in Harsh Service Conditions | 1 | 1 | | 1 | | | 1 | | | | 1 | | | |
| NS134 | Appelhans, A. D. | Enhanced Isotope Ratio Measurement Sensitivity | 1 | | | | | | 1 | | | | | | | |
| SC117 | Appelhans, A. D. | Atmospheric Pressure Surface Analysis Mass Spectrometry | 1.1 | | | 1 | | | | | | | | | | |
| NS137 | Austad, W. E. | Security of Cyber Systems | 2.1 | 1 | | | | | | | | | | | | |
| NS140 | Austad, W. E. | Wireless Security Research | 1.58 | 2 | | | | | | | | | | | | |
| NE128 | Baker, J. D. | Nb93m, an Energy-Dispersive, X-Ray Flourescence Excitation Source for the In-Field Analysis of RCRA Elements | 0.3 | 1 | | | 1 | 1 | 1 | | 1 | 1 | 1 | 1 | 1 | 1 |
| GC124 | Barnes, J. M. | Use of Molecular Markers for Detection and Tracking of Environmental Bacteria | 0.75 | | | | | | | | | | | | | |
| NS139 | Beitel, G. A. | Novel Threat-Risk Index Using Probabilistic Risk Assessment and Human Reliability Analysis | 1.17 | 1 | | | | | | | | | | | | 2 |
| ST108 | Berrett, S. | Long Term Record Storage for Long Term Stewardship | 0.05 | | | | | | | | | | | 1 | | |
| PH106 | Bishop, C. W. | A New Hydrogeophysical Method for Characterizing and Monitoring Preferential Flow Paths in Complex Layered and Fractured Basalt | | | | 1 | | | | | | | | | | |
| NE121 | Boardman, R. D. | Contaminants and Improved Energy Production: Laboratory Studies | 2 | 1 | | | | | 1 | | | | | | | |
| WT115 | Boardman, R. D. | Thermally Hot Offgas Cleanup Sorbent Technology Development | 1 | 1 | | | | | | | | | 2 | | | |
| ET122 | Breckenridge, R. P. | Science-Based Landscape Level Management of Resources at Federal Facilities | 1.1 | | | 1 | | | | | | | | | | |
| NS135 | Brighton, L. L. | Smart Antenna Systems in a Wiresless Local Area Network | 1.17 | | | | | | | | | 3 | | | | |

# Appendix D—Project Performance

| Project ID | Principal Investigator | Project Title | FTE | Other Students | Post Docs | Faculty | Crada | WFO | IDR | Patents Awarded | Copyrighting/Trademark | License | Publications | Presentations | Symposia | Awards |
|---|---|---|---|---|---|---|---|---|---|---|---|---|---|---|---|---|
| ET116 | Bruemmer, D. J. | Advanced Multi-Operation Control Architectures for Human-Robot Synergy in Complex, Domains | 1.25 | | | | | 2 | | | | | 4 | 4 | 1 | 1 |
| NS132 | Carrington, R. A. | Automated Control and Electronic Signal Acquisition/Processing Systems for Sprayed Distributed Sensors | 0.6 | 1 | | | | | 1 | | | | | | | |
| ET118 | Christensen, C. D. | Intelligent Control of Multi Nodal Systems | 0.4 | 1 | | 1 | | | | | | | 1 | | | |
| NS141 | Chu, H. S. | Thermomechanical Processing of Titanium 10V-2Al-3Fe | 0.21 | | | | | | | | | | | | | |
| NS136 | Corbett, G. A. | Client/Server Architecture For High-Performance Computing | 1.1 | 1 | | 1 | | | | | | | | | | |
| GC131 | Cummings, D. E. | Characterizing Microbial Population Shifts in Response to Alternative Electron Donors and their Effect on Trichloroethylene Dexhlorination Efficiency | 0.87 | | | | | | | | | | | | | |
| CS114 | Dudenhoeffer, D. D. | Critical Infrastructure Critical Subnetwork | 3 | | | | | | | | | | 1 | | | |
| PH102 | Eide, S. A. | Characterization of Legacy Risk | 0.7 | | | | | | | | | | | | | |
| NE108 | Evans, R. P. | Two-Phase Mass Flow Measurement for Geothermal Wells | 0.11 | 1 | | 2 | | | 1 | 1 | | | 5 | 1 | | |
| WT107 | Fox, R. V. | Direct Dissolution of Plutonium and Neptunium Species Using Chelated Agents in Carbon Dioxide | 0.5 | | | | | | | | | | 2 | 1 | | |
| ET114 | Fujita, Y. | Use of Engineered Nano-Particles for Nutrient Delivery and Bioremediation in Subsurface Environments | 0.97 | | | | | | | | | | 1 | | | |
| SC116 | Ginosar, D. M. | Supercritical Fluid Catalyst Regeneration Chemistry | 1.5 | | | | | | | | | | | | | |
| WT101 | Gombert, D. | Cold-Crucible Design Parameters for Next Generation High Level Waste Melters | 1.1 | | | 3 | | | 1 | | | | 1 | 1 | | |
| NE119 | Gougar, H. D. | Advanced Test Reactor Three Dimensional Neutronics Modeling | 0.473 | | | | | | | | | | 1 | | | |
| AC104 | Greenwade, L. E. | Development and Validation of Advanced Simulation and Collaboration Capability | | | | | | | | | | | | | | |
| ET121 | Hallbert, B. P. | Human Factors for Management of High Consequence Events | | | | | | | | | | | | | | |
| GC149 | Hamilton, M. A. | Uptake and Translocation Patterns of Strontium by Sagebrush Steppe Ecosystem Plants | 0.4 | 1 | | 2 | | | | | | | | | | |
| CE109 | Hamman, K. D. | Computational Fluid Dynamics Model Based Control of Two-Phase Flow | 2 | | | | | | | | | | | | | |
| ET117 | Harbour, G. L. | Model-Based Decision Making: Conceptual Framework and Environmental-Related Application Development | 0.4 | 1 | | | | | | | 1 | | 1 | | | 1 |

# Appendix D—Project Performance

| Project ID | Principal Investigator | Project Title | FTE | Other Students | Post Docs | Faculty | Crada | WFO | IDR | Patents Awarded | Copyrighting/Trademark | License | Publications | Presentations | Symposia | Awards |
|---|---|---|---|---|---|---|---|---|---|---|---|---|---|---|---|---|
| ET120 | Harbour, G. L. | Designing Advanced Emergency Response Planning Support Systems | 0.3 | | | | | | | | | | | | | |
| GC111 | Harrup, M. K. | Hybrid Nanocomposite Materials as Subsurface Permeable Reactive Barriers | 1.85 | 1 | | 1 | | | 1 | | | | 1 | 1 | | |
| GE108 | Hartwell, J. K. | Advanced Fission Product Detection Systems for Generation IV Fuel Testing | 1 | | | | | | | | | | | | | |
| NE117 | Hartwell, J. K. | Active Neutron Spectrometry for Neutron Capture Beam Characterization | 0.3 | 1 | | 1 | | | | | | | | | | |
| GE102 | Harvego, E. A. | Advanced Transient Analysis Capabilities for Generation IV Reactors | 1.4 | | | | | | | | | | | 3 | | |
| GC108 | Heath, G. L. | Advanced Technology for Mapping Subsurface Water Conductivity | 0.4 | 1 | | 1 | | | | | | | 3 | | | |
| GC133 | Heath, G. L. | Electrical Resistivity Imaging to Define Preferred Flow Paths in a Heterogeneous Layered Vadose Zone | 0.25 | | 1 | 1 | | | | | | | 1 | | | |
| WT117 | Herbst, R. S. | Novel Abrasion Resistant, Enhanced Flux Ultrafiltration Membranes | 0.5 | | | | | 1 | | | | | 1 | | | |
| GE104 | Herring, J. S. | Advanced Nuclear Fuels for Enhanced Proliferation Resistance | 0.55 | | | 1 | | | | | | | 2 | | | |
| GC138 | Hertzog, R. C. | Application of New Borehole Geophysical Methods for Stratigraphic Correlation and Identification of Non-Aqueous-Phase Contaminants in INEEL Wells | 15 | | | | | | | | | | | | | |
| CE110 | Hoskinson, R. L. | Development of Analytical Decision-Making Tools for Energy Efficient Agricultural Biomass Production | 0.3 | | | | | | | | | | | | | |
| GC101 | Housley, T. L. | Fundamental Studies on Gas Contaminant Mobility in the Vadose Aone from Atmospheric Pressure Fluctuations | 306 | 3 | | | | | | | | | | 1 | | |
| PH105 | Hubbell, J. M. | Improving Soil Water Flux Estimates in the Deep Vadose Zone | 1 | | | 2 | | | 2 | 1 | | | 3 | | | |
| NC101 | Hurley, D. H. | Nanostructure Characterization for Sensing | 0.7 | | | 1 | | | | | | | 2 | | 1 | |
| SC118 | Hurley, D. H. | Surface-Sensitive Laser Acoustic Studies of Heterogeneous Catalysis | 0.4 | | | 1 | | | | | | | | | | |
| ST107 | Jacobson, J. J. | DOE Complex - Wide Long-term Stewardship Options Analysis System | 1.25 | | | | | | | | | | | 5 | 1 | |
| CS117 | Jones, J. L. | Development of a Compact Laser-Compton X-ray Source | 0.9 | 1 | | | | | | | | | | 3 | | |
| NS138 | Keener, W. K. | Development of Enzyme-Activity-Based Assays for Potential Bioterrorist Agents Designed for use with Current Detection Platforms | 1.35 | | | | | | | | | | | | | |

# Appendix D—Project Performance

| Project ID | Principal Investigator | Project Title | FTE | Other Students | Post Docs | Faculty | Crada | WFO | IDR | Patents Awarded | Copyrighting/Trademark | License | Publications | Presentations | Symposia | Awards |
|---|---|---|---|---|---|---|---|---|---|---|---|---|---|---|---|---|
| CE113 | Kenney, K. L. | Flow Characterization of Complex Biomass Flows for Bioenergy Feedstock Development | 0.33 | | | | | | | | | | | | | |
| ES101 | Kong, P. C. | Cermet Filters for Hazardous Material, Chemical and Biological Weapon Agent Destruction | 3.25 | | | | | | | | | | | | | |
| PH103 | Kostelnik, K. M. | Developing a Predictive Decision Network for Long-Term Stewardship | 0.6 | | | 1 | | | | | | | | 1 | | |
| NS124 | Kotter, D. K. | Microantenna Infrared Tags | 0.55 | 1 | 1 | 1 | | | | | | | 1 | 1 | | |
| AC101 | Larson, T. K. | Parallel Computing with Cluster Technology | 2.1 | 4 | 1 | 3 | | | | | | | 2 | | | |
| GC151 | Laviolette, R. A. | Modeling Solute Partitioning at Interfaces | 1 | | | | | | | | | | | | | |
| WT116 | Law, J. D. | Development of Advanced Aqueous Processing to Support the Nuclear Fuel Cycle | 1 | | | | | | | | | | | | | |
| GC135 | Lenhard, R. J. | Investigation of the Movement and Fate of Chlorinated Hydrocarbons | 0.8 | | | | | | | | | | 5 | 2 | | |
| NC103 | Lessing, P. A. | Enhanced Transport in Nanocrystalline Ceramic Films | 0.85 | | | 1 | | | | | | | 1 | | | |
| NS133 | Lillo, T. M. | Novel Fabrication of Blast and Penetration Resistant Materials | | | | | 1 | | | | | | 2 | 3 | | |
| SC119 | Lister, T. E. | Development of Microelectrode Arrays for In Situ Detection of Localized Corrosion | 0.5 | | | | | | | | | | | | | |
| GE105 | Loewen, E. P. | Design of an Actinide Burning, Lead or Lead-Bismuth Cooled Reactor That Produces Low Cost Electricity | | | | | | | | | | | | | | |
| ET119 | Marble, J. L. | Understanding Societal Issues Associated with Acceptance of Bioremediation Strategies | 0.6 | | | 2 | | | | | | | 1 | | | |
| GC102 | Mc Ling, T. L. | Regional Setting and Flow Dynamics of the Snake River Plain Aquifer | 0.7 | 2 | | | | | | | | | | | | |
| GC136 | Meakin, P. | Modeling of Flow and Colloid Behavior in Subsurface Fractures | 1.5 | | | | | | | | | | | 1 | | |
| GC150 | Meakin, P. | Multiscale Modeling of Multiphase Flow (Unsaturated) | 0.2 | | | | | | | | | | 1 | | | |
| CS118 | Miller, C. J. | Advanced Automated Ion Mobility Spectrometer for Explosives Detection | 1 | | | | | | 1 | | | | 1 | | | |
| NE129 | Mincher, B. J. | Radiation Chemistry of Supercritical Water | 0.2 | | | 1 | | | 1 | | | | 1 | 1 | 1 | 1 |
| GC125 | Moore, G. M. | Natural and Synthetic Subsurface Colloids | 1.25 | | | | | | | | | | | | | |
| WT114 | Morton, D. K. | Investigation and Modeling of Dynamic Strain Rate Effects on Structural Material Response | 0.45 | | | | | | 1 | | | | | | | |

# Appendix D—Project Performance

| Project ID | Principal Investigator | Project Title | FTE | Other Students | Post Docs | Faculty | Crada | WFO | IDR | Patents Awarded | Copyrighting/Trademark | License | Publications | Presentations | Symposia | Awards |
|---|---|---|---|---|---|---|---|---|---|---|---|---|---|---|---|---|
| WT111 | Nichols, T. T. | Thermodynamic Modeling of High-Ionic Non-Ideal Solutions | 1 | | | | | | | | | | | | | |
| AC103 | Novack, S. D. | Aerospace Situation Awareness and Risk Monitor Tool | 0.7 | 1 | | | | | | | | | | 3 | | |
| PH104 | Novascone, S. R. | Modeling an Earth Borehole System for Physical Property Determination in Shallow Subsurface Environments with Emphasis on Vadose Zone Applications. | 1.2 | | | 1 | | | 1 | | | | 2 | 2 | 1 | |
| NE127 | Ougouag, A. M. | Estimation of Neutron-Irradiation Induced Displacements-Per-Atom | 0.5 | | | | | | | | | | 1 | | | |
| GC130 | Palmer, C. D. | Development of Techniques for In Situ Measurement of Groundwater Contaminant Source Strength | | | | 2 | | | | | | | | | | |
| GC106 | Partin, J. K. | Enhanced Techniques for Evaluating Colloidal Transport Processes | 1.25 | | | | | | | | | | | | | |
| SC115 | Peterson, E. S. | The Controlled Synthesis, Structural, Electrical, and Optical Properties of One-dimensional Metals | 0.15 | | | 1 | | | | | | | 1 | 1 | | |
| GE101 | Petti, D. A. | The Modular Pebble-Bed Reactor | 0.86 | | | 1 | | | | | | | | | | |
| ET106 | Piet, S. J. | Konvergence Framework for Making Sustainable Cleanup Decisions | 0.75 | 1 | | | | | | | | | 1 | | | |
| GC117 | Pinhero, P. J. | Evaluating Microelectrodes and Fiber-Optic Probes for use in Meso-Scale Experiments | 1.55 | | | | | | | | | | | | | |
| GC152 | Plummer, M. A. | Estimating the Climatic Sensitivity of Vadose Zone Infiltration Rates through Paleohydrologic Analyses | 0.4 | | | | | | | | | | | | | |
| PH101 | Radtke, C. W. | In-situ Vadose Zone Bioremediation of Explosives | 1.1 | | | 1 | | | 2 | | | | | | | |
| GC114 | Redden, G. D. | Kinetics of Inter-Surface Transfer of Surface-Complexed Metals by Surface-Surface Contact | 0.3 | 1 | | 1 | | | | | | | | | | |
| GC116 | Redden, G. D. | Organic Co-Solvent and Co-Contaminant Effects on Soprtion of Uranyl and Cesium to Metal Oxide Surfaces | 0.8 | 1 | | 1 | | | | | | | 1 | | | |
| NE114 | Richins, W. D. | Energy Efficient Building Simulation and Technologies | 1.65 | 2 | | 2 | | | 1 | | | | 5 | 4 | | |
| NS118 | Roberto, F. F. | Novel Selective Matrix for Collection and Identification of Priority Pathogens | | | | 1 | | | | | | | | | | |
| PH107 | Robertson, E. P. | Dependence of Coal Bed Permeability on Pore Pressure and Adsorbed Gas Content | 0.7 | | | 1 | | | | | | | | 1 | | |
| NC104 | Rollins, H. W. | Nucleation and Growth of Nanoparticle Materials in Supercritical Fluid Processes | 0.75 | | | 1 | | | | | | | 1 | | | |

# Appendix D—Project Performance

| Project ID | Principal Investigator | Project Title | FTE | Other Students | Post Docs | Faculty | Crada | WFO | IDR | Patents Awarded | Copyrighting/Trademark | License | Publications | Presentations | Symposia | Awards |
|---|---|---|---|---|---|---|---|---|---|---|---|---|---|---|---|---|
| NS121 | Roney, T. J. | Imaging of Heavy Metals and Nuclear Materials | 0.5 | | | 1 | | | | | | | 1 | | | |
| ST105 | Rope, R. C. | Development of an Integrated Watershed Information Management Tool for Long-term Facilities Stewardship | 0.8 | 1 | | 1 | | | | | | 1 | 11 | 6 | | |
| GC140 | Schafer, A. L. | Computational Experiments of Hysteretic Chemical and Moisture Migration | 1.5 | | | | | | | | | | | | | |
| GE103 | Schultz, R. R. | Generation IV Gas-Cooled Reactor System Analysis Tools: Defining Their Attributes, Demonstrating Their Capabilities, and Measuring Their Performance | | | | | | | | | | | | | | |
| GC145 | Scott, C. L. | Dual Electrodes and Defining the Electrically Distrubed Region in Induced Polarization (DC/IP) Measurements | 0.5 | | | 1 | | | | | | | 1 | 1 | | |
| GC119 | Scott, J. R. | Development of Imaging Fourier Transform Mass Spectrometer Capabilities for Analyses of Complex & Heterogeneous Samples | 1.7 | | | | | | 1 | | | | 2 | 3 | | |
| SC111 | Scott, J. R. | Elucidating the Photo-Physics of Complex Metal Ions Trapped in a Fourier Transform Mass Spectrometer | 0.4 | 1 | | 1 | | | | | | | 2 | 2 | | |
| AC102 | Shook, G. M. | Improving Numerical Model Efficiency of an Existing In-House Simulation Model | 0.95 | | 1 | | | | | | | | | | | |
| WT112 | Siemer, D. D. | Electrochemical Recovery of Mercury from Nuclear Industry Process Solutions | 0.5 | 1 | | | | | 1 | | | | | | | |
| ET107 | Silverman, H. G. | Recombinant Adhesive Protein Production and Investigation into Alternate Natural Adhesive Systems in Marine Mussels | 1 | 1 | | | | | 1 | | | | 2 | 1 | | 1 |
| NE111 | Smartt, H. B. | Friction Stir Welding of Lightweight Materials | 1 | | | 1 | | | | | | | 1 | | | |
| CE108 | Steffler, E. D. | Genetic Control of Straw Stem Ultrastructure that Affects the Biomechanics of Stem Separation. | 1 | | | | | | | | | | | | | |
| GC134 | Stoner, D. L. | Development and Application of Custom Flow Models for Understanding Flow in Porous and Fractured Matrices with Biological Components | 3.9 | | | | | | | | | | 1 | | | |
| GC147 | Stormberg, A. I. | Use of Genetic Markers as a Screening Tool for Ecological Risk Assessment | 1 | 4 | | 1 | | | | | | | | | | |
| GC144 | Stormberg, G. J. | Characterization of Nonlinear Complex Resistivity Spectra During Biochemical Reduction of Cr+6 to Cr+3 | | | | | | | | | | | | | | |
| NE118 | Telschow, K. L. | Laser Ultrasonic Corrosion Monitor | 2 | | | | | | | | | | | | | |
| NE126 | Telschow, K. L. | Hollow Waveguide Laser Ultrasonics for High Radiation Environments | 1 | | | | | | | | | | | | | |

# Appendix D—Project Performance

| Project ID | Principal Investigator | Project Title | FTE | Other Students | Post Docs | Faculty | Crada | WFO | IDR | Patents Awarded | Copyrighting/Trademark | License | Publications | Presentations | Symposia | Awards |
|---|---|---|---|---|---|---|---|---|---|---|---|---|---|---|---|---|
| CE112 | Thompson, D. N. | Pretreatment Technologies for Cellulosic Biomass | 0.873 | | | | | | | | | | | | | |
| GC109 | Thompson, V. S. | Development of Enzymatic Biosensors for Environmental Applications | 1.04 | | | | | | | | | | | | 1 | |
| WT113 | Todd, T. A. | Highly Selective Sorbents for Removal of Arsenic from Drinking Water | 1 | | | | | | 1 | | | | | | 1 | |
| SC120 | Totemeier, T. C. | Novel Materials for Evaluation of Generation IV Materials | 0.55 | | | | | | | | | | | | | |
| SC112 | Van Siclen, C. D. | Mechanical and Flow Properties of Dry Granular Media | 0.5 | | | | | | | | | | 1 | | | |
| GC141 | Versteeg, R. J. | Calibration and Enhancement of Geophysical Imaging Tools in Mesoscale Experiments | 1.9 | 6 | 1 | 1 | | | | | | | | | | |
| GE107 | Weaver, K. P. | An Innovative Gas-Cooled Fast Reactor | | | | | | | | | | | | | | |
| GC105 | West, P. B. | Advanced Borehole Seismic Sources for High-Resolution Subsurface Imaging and Characterization for Environmental Applications | 1.3 | | | 2 | | | 2 | | 1 | 1 | 1 | 1 | 1 | 1 |
| ST106 | White, G. J. | Developing Collaborative Approaches to Long-Term Environmental Stewardship | 0.75 | | | 3 | | | | | | | 2 | 1 | | |
| | | Totals | 425.2 | 50 | 5 | 57 | 3 | 4 | 23 | 2 | 3 | 6 | 89 | 58 | 10 | 8 |

*Appendix E—*

# Relevance to Major DOE Missions

# Appendix E—Relevance to Major DOE Missions

| Project ID | Principal Investigator | Project Title | Environmental Quality | Energy | Science and Technology | National Defense |
|---|---|---|---|---|---|---|
| ET110 | Abbott, M. L. | Elemental Tracers and Multi-Variate Receptor Modeling Methods in Assessing Air Pollution | X | | X | |
| ET108 | Alessi, R. S. | Improving Stakeholder Interactions: A Stakeholder-based Research Methodology for Reaching Decisions on Polarized Issues | X | X | X | X |
| NE120 | Anderson, R. P. | Hydrogen Production from High Temperature Nuclear Reactors | | X | | |
| NE125 | Anderson, R. P. | Hydrogen Technologies R&D | X | X | | |
| CE111 | Apel, W. A. | Stable Enzymes for Hemicellulose Hydrolysis | | | X | |
| ET105 | Apel, W. A. | Biologically Based Catalysts for Processing and Detection in Harsh Service Conditions | X | X | X | |
| NS134 | Appelhans, A. D. | Enhanced Isotope Ratio Measurement Sensitivity | X | | X | X |
| SC117 | Appelhans, A. D. | Atmospheric Pressure Surface Analysis Mass Spectrometry | X | | X | X |
| NS137 | Austad, W. E. | Security of Cyber Systems | | X | | X |
| NS140 | Austad, W. E. | Wireless Security Research | | X | | X |
| NE128 | Baker, J. D. | Nb93m, an Energy-Dispersive, X-Ray Flourescence Excitation Source for the In-Field Analysis of RCRA Elements | X | | X | |
| GC124 | Barnes, J. M. | Use of Molecular Markers for Detection and Tracking of Environmental Bacteria | | | X | |
| NS139 | Beitel, G. A. | Novel Threat-Risk Index Using Probabilistic Risk Assessment and Human Reliability Analysis | X | X | | X |
| ST108 | Berrett, S. | Long Term Record Storage for Long Term Stewardship | X | X | X | |
| PH106 | Bishop, C. W. | A New Hydrogeophysical Method for Characterizing and Monitoring Preferential Flow Paths in Complex Layered and Fractured Basalt | X | | X | |
| NE121 | Boardman, R. D. | Contaminants and Improved Energy Production: Laboratory Studies | | X | | |
| WT115 | Boardman, R. D. | Thermally Hot Offgas Cleanup Sorbent Technology Development | X | X | X | |
| ET122 | Breckenridge, R. P. | Science-Based Landscape Level Management of Resources at Federal Facilities | X | | | |
| NS135 | Brighton, L. L. | Smart Antenna Systems in a Wireless Local Area Network | | | X | X |
| ET116 | Bruemmer, D J. | Advanced Multi-Operation Control Architectures for Human-Robot Synergy in Complex, Domains | X | X | X | X |
| NS132 | Carrington, R. A. | Automated Control and Electronic Signal Acquisition/Processing Systems for Sprayed Distributed Sensors | | X | | |
| ET118 | Christensen, C. D. | Intelligent Control of Multi Nodal Systems | X | X | X | X |
| NS141 | Chu, H. S. | Thermomechanical Processing of Titanium 10V-2Al-3Fe | | X | X | X |
| NS136 | Corbett, G. A. | Client/Server Architecture For High-Performance Computing | | | X | X |
| GC131 | Cummings, D. E. | Characterizing Microbial Population Shifts in Response to Alternative Electron Donors and their Effect on Trichloroethylene Dechlorination Efficiency | X | | X | |
| CS114 | Dudenhoeffer, D. D. | Critical Infrastructure, Critical Subnetwork | | X | X | X |
| PH102 | Eide, S. A. | Characterization of Legacy Risk | X | X | | X |

# Appendix E—Relevance to Major DOE Missions

| Project ID | Principal Investigator | Project Title | Environmental Quality | Energy | Science and Technology | National Defense |
|---|---|---|---|---|---|---|
| NE108 | Evans, R. P. | Two-Phase Mass Flow Measurement for Geothermal Wells | X | X | X | X |
| WT107 | Fox, R. V. | Direct Dissolution of Plutonium and Neptunium Species Using Chelated Agents in Carbon Dioxide | X | | | |
| ET114 | Fujita, Y. | Use of Engineered Nano-Particles for Nutrient Delivery and Bioremediation in Subsurface Environments | X | | X | |
| SC116 | Ginosar, D. M. | Supercritical Fluid Catalyst Regeneration Chemistry | | X | X | |
| WT101 | Gombert, D. | Cold-Crucible Design Parameters for Next Generation HLW Melters | X | | X | |
| NE119 | Gougar, H. D. | Advanced Test Reactor Three-Dimensional Neutronics Modeling | | X | | |
| AC104 | Greenwade, L. E. | Development and Validation of Advanced Simulation and Collaboration Capability | X | X | X | X |
| ET121 | Hallbert, B. P. | Human Factors for Management of High Consequence Events | | | | X |
| GC149 | Hamilton, M. A. | Uptake and Translocation Patterns of Strontium by Sagebrush Steppe Ecosystem Plants | X | | | |
| CE109 | Hamman, K. D. | Computational Fluid Dynamics Model Based Control of Two-Phase Flow | | X | | |
| ET117 | Harbour, G. L. | Model-Based Decision Making: Conceptual Framework and Environmental-Related Application Development | X | X | X | X |
| ET120 | Harbour, G. L. | Designing Advanced Emergency Response Planning Support Systems | X | X | | |
| GC111 | Harrup, M. K. | Hybrid Nanocomposite Materials as Subsurface Permeable Reactive Barriers | X | | | |
| GE108 | Hartwell, J. K. | Advanced Fission Product Detection Systems for Generation IV Fuel Testing | | | | |
| NE117 | Hartwell, J. K. | Active Neutron Spectrometry for Neutron Capture Beam Characterization | | X | X | |
| GE102 | Harvego, E. A. | Advanced Transient Analysis Capabilities for Generation IV Reactors | X | X | | |
| GC108 | Heath, G. L. | Advanced Technology for Mapping Subsurface Water Conductivity | X | X | | |
| GC133 | Heath, G. L. | Electrical Resistivity Imaging to Define Preferred Flow Paths in a Heterogeneous Layered Vadose Zone | X | | | |
| WT117 | Herbst, R. S. | Novel Abrasion Resistant, Enhanced Flux Ultrafiltration Membranes | X | | | |
| GE104 | Herring, J. S. | Advanced Nuclear Fuels for Enhanced Proliferation Resistance | X | X | X | X |
| GC138 | Hertzog, R. C. | Application of New Borehole Geophysical Methods for Stratigraphic Correlation and Identification of Non-Aqueous-Phase Contaminants in INEEL Wells | X | | X | |
| CE110 | Hoskinson, R. L. | Development of Analytical Decision-Making Tools for Energy Efficient Agricultural Biomass Production | | X | X | |
| GC101 | Housley, T. L. | Fundamental Studies on Gas Contaminant Mobility in the Vadose Zone from Atmospheric Pressure Fluctuations | X | | | |
| PH105 | Hubbell, J. M. | Improving Soil Water Flux Estimates in the Deep Vadose Zone | X | | X | |
| NC101 | Hurley, D. H. | Nanostructure Characterization for Sensing | | | X | |
| SC118 | Hurley, D. H. | Surface-Sensitive Laser Acoustic Studies of Heterogeneous Catalysis | | X | X | |

# Appendix E—Relevance to Major DOE Missions

| Project ID | Principal Investigator | Project Title | Environmental Quality | Energy | Science and Technology | National Defense |
|---|---|---|---|---|---|---|
| ST107 | Jacobson, J. J. | DOE Complex - Wide Long-term Stewardship Options Analysis System | X | X | X | X |
| CS117 | Jones, J. L. | Development of a Compact Laser-Compton X-ray Source | | | X | X |
| NS138 | Keener, W. K. | Development of Enzyme-Activity-Based Assays for Potential Bioterrorist Agents Designed for use with Current Detection Platforms | X | | X | X |
| CE113 | Kenney, K. L. | Flow Characterization of Complex Biomass Flows for Bioenergy Feedstock Development | | X | X | |
| ES101 | Kong, P. C. | Cermet Filters for Hazardous Material, Chemical and Biological Weapon Agent Destruction | | | | X |
| PH103 | Kostelnik, K. M. | Developing a Predictive Decision Network for Long-Term Stewardship | X | | | |
| NS124 | Kotter, D. K. | Microantenna Infrared Tags | | | | X |
| AC101 | Larson, T. K. | Parallel Computing with Cluster Technology | | | X | |
| GC151 | Laviolette, R. A. | Modeling Solute Partitioning at Interfaces | X | X | X | X |
| WT116 | Law, J. D. | Development of Advanced Aqueous Processing to Support the Nuclear Fuel Cycle | | X | | |
| GC135 | Lenhard, R. J. | Investigation of the Movement and Fate of Chlorinated Hydrocarbons | | | X | |
| NC103 | Lessing, P. A. | Enhanced Transport in Nanocrystalline Ceramic Films | X | X | X | X |
| NS133 | Lillo, T. M. | Novel Fabrication of Blast and Penetration Resistant Materials | | X | X | X |
| SC119 | Lister, T. E. | Development of Microelectrode Arrays for In Situ Detection of Localized Corrosion | | | X | |
| GE105 | Loewen, E. P. | Design of an Actinide Burning, Lead or Lead-Bismuth Cooled Reactor That Produces Low Cost Electricity | X | X | X | X |
| ET119 | Marble, J. L. | Understanding Societal Issues Associated with Acceptance of Bioremediation Strategies | X | | X | |
| GC102 | Mc Ling, T. L. | Regional Setting and Flow Dynamics of the Snake River Plain Aquifer | X | | X | |
| GC136 | Meakin, P. | Modeling of Flow and Colloid Behavior in Subsurface Fractures | X | X | X | |
| GC150 | Meakin, P. | Multiscale Modeling of Multiphase Flow (Unsaturated) | X | X | X | |
| CS118 | Miller, C. J. | Advanced Automated Ion Mobility Spectrometer for Explosives Detection | X | | X | X |
| NE129 | Mincher, B. J. | Radiation Chemistry of Supercritical Water | | | | |
| GC125 | Moore, G. M. | Natural and Synthetic Subsurface Colloids | X | | X | |
| WT114 | Morton, D. K. | Investigation and Modeling of Dynamic Strain Rate Effects on Structural Material Response | X | | X | |
| WT111 | Nichols, T. T. | Thermodynamic Modeling of High-Ionic Non-Ideal Solutions | X | | | |
| AC103 | Novack, S. D. | Aerospace Situation Awareness and Risk Monitor Tool | X | X | X | X |
| PH104 | Novascone, S. R. | Modeling an Earth Borehole System for Physical Property Determination in Shallow Subsurface Environments with Emphasis on Vadose Zone Applications | X | X | X | X |
| NE127 | Ougouag, A. M. | Estimation of Neutron Irradiation-Induced Displacements-Per-Atom | | X | | |

# Appendix E—Relevance to Major DOE Missions

| Project ID | Principal Investigator | Project Title | Environmental Quality | Energy | Science and Technology | National Defense |
|---|---|---|---|---|---|---|
| GC130 | Palmer, C. D. | Development of Techniques for In Situ Measurement of Groundwater Contaminant Source Strength | X | | | |
| GC106 | Partin, J. K. | Enhanced Techniques for Evaluating Colloidal Transport Processes | X | | | |
| SC115 | Peterson, E. S. | The Controlled Synthesis, Structural, Electrical, and Optical Properties of One-Dimensional Metals | | X | X | X |
| GE101 | Petti, D. A. | The Modular Pebble-Bed Reactor | X | X | X | X |
| ET106 | Piet, S. J. | Konvergence Framework for Making Sustainable Cleanup Decisions | X | X | | X |
| GC117 | Pinhero, P. J. | Evaluating Microelectrodes and Fiber-Optic Probes for use in Meso-Scale Experiments | X | | X | |
| GC152 | Plummer, M. A. | Estimating the Climatic Sensitivity of Vadose Zone Infiltration Rates through Paleohydrologic Analyses | X | | | |
| PH101 | Radtke, C. W. | In-situ Vadose Zone Bioremediation of Explosives | X | | X | |
| GC114 | Redden, G. D. | Kinetics of Inter-Surface Transfer of Surface-Complexed Metals by Surface-Surface Contact | X | | X | |
| GC116 | Redden, G. D. | Organic Co-Solvent and Co-Contaminant Effects on Soprtion of Uranyl and Cesium to Metal Oxide Surfaces | X | | X | |
| NE114 | Richins, W. D. | Energy Efficient Building Simulation and Technologies | X | X | | |
| NS118 | Roberto, F. F. | Novel Selective Matrix for Collection and Identification of Priority Pathogens | X | | X | X |
| PH107 | Robertson, E. P. | Dependence of Coal Bed Permeability on Pore Pressure and Adsorbed Gas Content | X | X | X | |
| NC104 | Rollins, H. W. | Nucleation and Growth of Nanoparticle Materials in Supercritical Fluid Processes | X | X | X | |
| NS121 | Roney, T. J. | Imaging of Heavy Metals and Nuclear Materials | | | X | X |
| ST105 | Rope, R. C. | Development of an Integrated Watershed Information Management Tool for Long-term Facilities Stewardship | X | | X | |
| GC140 | Schafer, A. L. | Computational Experiments of Hysteretic Chemical and Moisture Migration | | | X | |
| GE103 | Schultz, R. R. | Generation IV Gas-Cooled Reactor System Analysis Tools: Defining Their Attributes, Demonstrating Their Capabilities, and Measuring Their Performance | X | X | X | |
| GC145 | Scott, C. L. | Dual Electrodes and Defining the Electrically Distrubed Region in Induced Polarization (DC/IP) Measurements | X | | X | |
| GC119 | Scott, J. R. | Development of Imaging Fourier Transform Mass Spectrometer Capabilities for Analyses of Complex & Heterogeneous Samples | X | | X | |
| SC111 | Scott, J. R. | Elucidating the Photo-Physics of Complex Metal Ions Trapped in a Fourier Transform Mass Spectrometer | | | X | |
| AC102 | Shook, G. M. | Improving Numerical Model Efficiency of an Existing, In-House Simulation Model | X | X | X | |
| WT112 | Siemer, D. D. | Electrochemical Recovery of Mercury from Nuclear Industry Process Solutions | X | | | |

# Appendix E—Relevance to Major DOE Missions

| Project ID | Principal Investigator | Project Title | Environmental Quality | Energy | Science and Technology | National Defense |
|---|---|---|---|---|---|---|
| ET107 | Silverman, H.G. | Recombinant Adhesive Protein Production and Investigation into Alternate Natural Adhesive Systems in Marine Mussels | X | | X | X |
| NE111 | Smartt, H. B. | Friction Stir Welding of Lightweight Materials | | | X | |
| CE108 | Steffler, E. D. | Genetic Control of Straw Stem Ultrastructure that Affects the Biomechanics of Stem Separation | | | X | |
| GC134 | Stoner, D. L. | Development and Application of Custom Flow Models for Understanding Flow in Porous and Fractured Matrices with Biological Components | X | | X | |
| GC147 | Stormberg, A. I. | Use of Genetic Markers as a Screening Tool for Ecological Risk Assessment | X | | X | |
| GC144 | Stormberg, G. J. | Characterization of Nonlinear Complex Resistivity Spectra During Biochemical Redcuction of Cr+6 to Cr+3 | X | | X | |
| NE118 | Telschow, K. L. | Laser Ultrasonic Corrosion Monitor | | X | | |
| NE126 | Telschow, K. L. | Hollow Waveguide Laser Ultrasonics for High Radiation Environments | | X | | |
| CE112 | Thompson, D. N. | Pretreatment Technologies for Cellulosic Biomass | | | X | |
| GC109 | Thompson, V. S. | Development of Enzymatic Biosensors for Environmental Applications | X | | | |
| WT113 | Todd, T. A. | Highly Selective Sorbents for Removal of Arsenic from Drinking Water | | | | |
| SC120 | Totemeier, T. C. | Novel Materials for Evaluation of Generation IV Materials | X | X | X | |
| SC112 | Van Siclen, C. D. | Mechanical and Flow Properties of Dry Granular Media | X | | X | X |
| GC141 | Versteeg, R. J. | Calibration and Enhancement of Geophysical Imaging Tools in Mesoscale Experiments | | | X | |
| GE107 | Weaver, K. P. | An Innovative Gas Cooled Gas Reactor | | X | | |
| GC105 | West, P. B. | Advanced Borehole Seismic Sources for High-Resolution Subsurface Imaging and Characterization for Environmental Applications | X | X | X | |
| ST106 | White, G. J. | Developing Collaborative Approaches to Long Term Environmental Stewardship | X | | X | |

*Appendix F—*

# Relevance to Major National Programs

# Appendix F—Relevance to Major National Programs

| Project ID | Principal Investigator | Project Title | NNSA - National Nuclear Security Administration | EE - Industrial Technologies | EM - Environmental Management | FE - Fossil Energy | SC - Office of Science | NE - Nuclear Energy | NR - Naval Reactors |
|---|---|---|---|---|---|---|---|---|---|
| ET110 | Abbott, M. L. | Elemental Tracers and Multi-Variate Receptor Modeling Methods in Assessing Air Pollution | S | | P | | | | |
| ET108 | Alessi, R. S. | Improving Stakeholder Interactions: A Stakeholder-based Research Methodology for Reaching Decisions on Polarized Issues | S | S | P | | S | S | |
| NE120 | Anderson, R. P. | Hydrogen Production from High Temperature Nuclear Reactors | | | S | S | | P | |
| NE125 | Anderson, R. P. | Hydrogen Technologies R&D | | P | | S | | | |
| CE111 | Apel, W. A. | Stable Enzymes for Hemicellulose Hydrolysis | | P | | | S | | |
| ET105 | Apel, W. A. | Biologically Based Catalysts for Processing and Detection in Harsh Service Conditions | | S | P | | S | | |
| NS134 | Appelhans, A. M. | Enhanced Isotope Ratio Measurement Sensitivity | P | | S | | | S | S |
| SC117 | Appelhans, A. M. | Atmospheric Pressure Surface Analysis Mass Spectrometry | S | | S | | p | S | |
| NS137 | Austad, W. E. | Security of Cyber Systems | P | | | | | | |
| NS140 | Austad, W. E. | Wireless Security Research | P | | | | | | |
| NE128 | Baker, J. D. | Nb93m, an Energy-Dispersive, X-Ray Flourescence Excitation Source for the In-Field Analysis of RCRA Elements | | | P | | S | S | |
| GC124 | Barnes, J. M. | Use of Molecular Markers for Detection and Tracking of Environmental Bacteria | | | P | | S | | |
| NS139 | Beitel, G. A. | Novel Threat-Risk Index Using Probabilistic Risk Assessment and Human Reliability Analysis | P | S | | | | | |
| ST108 | Berrett, S. | Long Term Record Storage for LTS | | | S | | | | |
| PH106 | Bishop, C. W. | A New Hydrogeophysical Method for Characterizing and Monitoring Preferential Flow Paths in Complex Layered and Fractured Basalt | | | S | | | | |
| NE121 | Boardman, R. D. | Contaminants and Improved Energy Production: Laboratory Studies | | S | S | P | | | |
| WT115 | Boardman, R. D. | Thermally Hot Offgas Cleanup Sorbent Technology Development | | | P | S | | | |
| ET122 | Breckenridge, R. P. | Science Based Landscape Level Management of Resources at Federal Facilities | | | | | | | |
| NS135 | Brighton, L. L. | Smart Antenna Systems in a Wireless Local Area Network | P | | | | S | | |
| ET116 | Bruemmer, D. J. | Advanced Multi-Operation Control Architectures for Human-Robot Synergy in Complex, Domains | S | | P | | S | | |

# Appendix F—Relevance to Major National Programs

| Project ID | Principal Investigator | Project Title | NNSA - National Nuclear Security Administration | EE - Industrial Technologies | EM - Environmental Management | FE - Fossil Energy | SC - Office of Science | NE - Nuclear Energy | NR - Naval Reactors |
|---|---|---|---|---|---|---|---|---|---|
| NS132 | Carrington, R. A. | Automated Control and Electronic Signal Acquisition/Processing Systems for Sprayed Distributed Sensors | P | | | S | | | |
| ET118 | Christensen, C. D. | Intelligent Control of Multi Nodal Systems | P | | S | | S | S | |
| NS141 | Chu, H. S. | Thermomechanical Processing of Titanium 10V-2Al-3Fe | P | S | | S | S | S | |
| NS136 | Corbett, G. A. | Client/Server Architecture For High-Performance Computing | P | | | | | | |
| GC131 | Cummings, D. E. | Characterizing Microbial Population Shifts in Response to Alternative Electron Donors and their Effect on Trichloroethylene Dechlorination Efficiency | | | P | | S | | |
| CS114 | Dudenhoeffer, D. D. | Critical Infrastructure, Critical Subnetwork | P | S | | S | | S | |
| PH102 | Eide, S. A. | Characterization of Legacy Risk | S | | P | | | S | |
| NE108 | Evans, R. P. | Two-Phase Mass Flow Measurement for Geothermal Wells | | P | | | | S | |
| WT107 | Fox, R. V. | Direct Dissolution of Plutonium and Neptunium Species Using Chelated Agents in Carbon Dioxide | | | P | | | | |
| ET114 | Fujita, Y. | Use of Engineered Nano-particles for Nutrient Delivery and Bioremediation in Subsurface Environments | | | P | | | | |
| SC116 | Ginosar, D. M. | Supercritical Fluid Catalyst Regeneration Chemistry | | S | S | | P | | |
| WT101 | Gombert, D. | Cold-Crucible Design Parameters for Next Generation High Level Waste Melters | | | P | | | | |
| NE119 | Gougar, H. D. | Advanced Test Reactor Three Dimensional Neutronics Modeling | | | | | | P | P |
| AC104 | Greenwade, L. E. | Development and Validation of Advanced Simulation and Collaboration Capability | S | S | P | S | S | S | |
| ET121 | Hallbert, B. P. | Human Factors for Management of High Consequence Events | S | | P | | | S | |
| GC149 | Hamilton, M. A. | Uptake and Translocation Patterns of Strontium by Sagebrush Steppe Ecosystem Plants | | | P | | | | |
| CE109 | Hamman, K. D. | Computational Fluid Dynamics Model Based Control of Two-Phase Flow | | P | | | S | S | |
| ET117 | Harbour, G. L. | Model-Based Decision Making: Conceptual Framework and Environmental-Related Application Development | S | S | P | S | | S | |
| ET120 | Harbour, G. L. | Designing Advanced Emergency Response Planning Support Systems | S | | P | | | S | |
| GC111 | Harrup, M. K. | Hybrid Nanocomposite Materials as Subsurface Permeable Reactive Barriers | | | P | | S | | |

# Appendix F—Relevance to Major National Programs

| Project ID | Principal Investigator | Project Title | NNSA - National Nuclear Security Administration | EE - Industrial Technologies | EM - Environmental Management | FE - Fossil Energy | SC - Office of Science | NE - Nuclear Energy | NR - Naval Reactors |
|---|---|---|---|---|---|---|---|---|---|
| GE108 | Hartwell, J. K. | Advanced Fission Product Detection Systems for Generation IV Fuel Testing | | | | | | P | |
| NE117 | Hartwell, J. K. | Active Neutron Spectrometry for Neutron Capture Beam Characterization | | | | | P | | |
| GE102 | Harvego, E. A. | Advanced Transient Analysis Capabilities for Generation IV Reactors | S | | | | | P | |
| GC108 | Heath, G. L. | Advanced Technology for Mapping Subsurface Water Conductivity | | | P | S | | | |
| GC133 | Heath, G. L. | Electrical Resistivity Imaging to Define Preferred Flow Paths in a Heterogeneous Vadose Zone | | | | | | | |
| WT117 | Herbst, R. S. | Novel Abrasion Resistant, Enhanced Flux Ultrafiltration Membranes | | S | P | | | | |
| GE104 | Herring, J. S. | Advanced Nuclear Fuels for Enhanced Proliferation Resistance | S | | | | | P | |
| GC138 | Hertzog, R. C. | Application of New Borehole Geophysical Methods for Stratigraphic Correlation and Identification of Non-Aqueous-Phase Contaminants in INEEL Wells | | | P | | S | | |
| CE110 | Hoskinson, R. L. | Development of Analytical Decision-Making Tools for Energy Efficient Agricultural Biomass Production | | P | | | S | | |
| GC101 | Housley, T. L. | Fundamental Studies on Gas Contaminant Mobility in the Vadose Zone from Atmospheric Pressure Fluctuations | | | P | | S | | |
| PH105 | Hubbell, J. M. | Improving Soil Water Flux Estimates in the Deep Vadose Zone | | | S | | | | |
| NC101 | Hurley, D. H. | Nanostructure Characterization for Sensing | | | S | | P | | |
| SC118 | Hurley, D. H. | Surface-Sensitive Laser Acoustic Studies of Heterogeneous Catalysis | | S | | S | P | | |
| ST107 | Jacobson, J. J. | DOE Complex - Wide Long-term Stewardship Options Analysis System | S | | P | | S | | |
| CS117 | Jones, J. L. | Development of a Compact Laser-Compton X-ray Source | P | | | | S | S | |
| NS138 | Keener, W. K. | Development of Enzyme-Activity-Based Assays for Potential Bioterrorist Agents Designed for use with Current Detection Platforms | P | | S | | S | S | |
| CE113 | Kenney, K. L | Flow Characterization of Complex Biomass Flows for Bioenergy Feedstock Development | | P | | | | | |
| ES101 | Kong, P. C. | Cermet Filters for Hazardous Material, Chemical and Biological Weapon Agent Destruction | P | | | | | | |
| PH103 | Kostelnik, K. M. | Developing a Predictive Decision Network for Long-Term Stewardship | | | P | | | | |

# Appendix F—Relevance to Major National Programs

| Project ID | Principal Investigator | Project Title | NNSA - National Nuclear Security Administration | EE - Industrial Technologies | EM - Environmental Management | FE - Fossil Energy | SC - Office of Science | NE - Nuclear Energy | NR - Naval Reactors |
|---|---|---|---|---|---|---|---|---|---|
| NS124 | Kotter, D. K. | Microantenna Infrared Tags | P | | | | | | |
| AC101 | Larson, T. K. | Parallel Computing with Cluster Technology | S | | S | | P | S | |
| GC151 | Laviolette, R. A. | Modeling Solute Partitioning at Interfaces | | | S | | P | | |
| WT116 | Law, J. D. | Development of Advanced Aqueous Processing to Support the Nuclear Fuel Cycle | | S | | | | P | |
| GC135 | Lenhard, R. J. | Investigation of the Movement and Fate of Chlorinated Hydrocarbons | | | P | | S | | |
| NC103 | Lessing, P. A. | Enhanced Transport in Nanocrystalline Ceramic Films | | S | S | S | P | | |
| NS133 | Lillo, T. M. | Novel Fabrication of Blast and Penetration Resistant Materials | P | S | | | S | S | |
| SC119 | Lister, T. E. | Development of Microelectrode Arrays for In Situ Detection of Localized Corrosion | | | | S | P | S | |
| GE105 | Loewen, E. P. | Design of an Actinide Burning, Lead or Lead-Bismuth Cooled Reactor That Produces Low Cost Electricity | S | | | | | P | |
| ET119 | Marble, J. L. | Understanding Societal Issues Associated with Acceptance of Bioremediation Strategies | | S | P | | S | S | |
| GC102 | Mc Ling, T. L. | Regional Setting and Flow Dynamics of the Snake River Plain Aquifer | | | P | | S | | |
| GC136 | Meakin, P. | Modeling of Flow and Colloid Behavior in Subsurface Fractures | | | P | S | S | | |
| GC150 | Meakin, P. | Multiscale Modeling of Multiphase Flow (Unsaturated) | | | P | S | S | | |
| CS118 | Miller, C. J. | Advanced Automated Ion Mobility Spectrometer for Explosives Detection | P | | S | | S | S | |
| NE129 | Mincher, B. J. | Radiation Chemistry of Supercritical Water | | | S | | S | P | |
| GC125 | Moore, G. A. | Natural and Synthetic Subsurface Colloids | | | P | | S | | |
| WT114 | Morton, D. K. | Investigation and Modeling of Dynamic Strain Rate Effects on Structural Material Response | S | | P | S | S | S | S |
| WT111 | Nichols, T. T. | Thermodynamic Modeling of High-Ionic Non-Ideal Solutions | | | P | | | S | |
| AC103 | Novack, S. D. | Aerospace Situation Awareness and Risk Monitor Tool | P | | | | | S | |
| PH104 | Novascone, S. R. | Modeling an Earth Borehole System for Physical Property Determination in Shallow Subsurface Environments with Emphasis on Vadose Zone Applications | S | | P | S | | | |
| NE127 | Ougouag, A. M. | Estimation of Neutron Irradiation-Induced Displacements-Per-Atom | S | | | | S | P | S |
| GC130 | Palmer, C. D. | Development of Techniques for In Situ Measurement of Groundwater Contaminant Source Strength | | | P | | | | |

# Appendix F—Relevance to Major National Programs

| Project ID | Principal Investigator | Project Title | NNSA - National Nuclear Security Administration | EE - Industrial Technologies | EM - Environmental Management | FE - Fossil Energy | SC - Office of Science | NE - Nuclear Energy | NR - Naval Reactors |
|---|---|---|---|---|---|---|---|---|---|
| GC106 | Partin, J. K. | Enhanced Techniques for Evaluating Colloidal Transport Processes | | | P | | | | |
| SC115 | Peterson, E. S. | The Controlled Synthesis, Structural, Electrical, and Optical Properties of One-Dimensional Metals | S | S | | S | P | | |
| GE101 | Petti, D. A. | The Modular Pebble-Bed Reactor | S | | | | S | P | |
| ET106 | Piet, S. J. | Konvergence Framework for Making Sustainable Cleanup Decisions | | | P | | | | |
| GC117 | Pinhero, P. J. | Evaluating Microelectrodes and Fiber-Optic Probes for use in Meso-Scale Experiments | | | P | | | | |
| GC152 | Plummer, M. A. | Estimating the Climatic Sensitivity of Vadose Zone Infiltration Rates through Paleohydrologic Analyses | | | P | | S | | |
| PH101 | Radtke, C. W. | In-situ Vadose Zone Bioremediation of Explosives | | | P | | S | | |
| GC114 | Redden, G. D. | Kinetics of Inter-Surface Transfer of Surface-Complexed Metals by Surface-Surface Contact | | | P | | S | | |
| GC116 | Redden, G. D. | Organic Co-Solvent and Co-Contaminant Effects on Soprtion of Uranyl and Cesium to Metal Oxide Surfaces | | | P | | | | |
| NE114 | Richins, W. D. | Energy Efficient Building Simulation and Technologies | | P | | | | | |
| NS118 | Roberto, F. F. | Novel Selective Matrix for Collection and Identification of Priority Pathogens | S | | | | X | | |
| PH107 | Robertson, E. P. | Dependence of Coal Bed Permeability on Pore Pressure and Adsorbed Gas Content | | S | S | S | S | | |
| NC104 | Rollins, H. W. | Nucleation and Growth of Nanoparticle Materials in Supercritical Fluid Processes | | S | | S | P | | |
| NS121 | Roney, T. J. | Imaging of Heavy Metals and Nuclear Materials | P | | | | S | | |
| ST105 | Rope, R. C. | Development of an Integrated Watershed Information Management Tool for Long-term Facilities Stewardship | | | P | S | S | | |
| GC140 | Schafer, A. L. | Computational Experiments of Hysteretic Chemical and Moisture Migration | | | P | | S | | |
| GE103 | Schutlz, R. R. | Generation IV Gas-Cooled Reactor System Analysis Tools: Defining Their Attributes, Demonstrating Their Capabilities, and Measuring Their Performance | | S | | | | P | |
| GC145 | Scott, C. L. | Dual Electrodes and Defining the Electrically Distrubed Region in Induced Polarization (DC/IP) Measurements | | | P | | S | | |
| GC119 | Scott, J. R. | Development of Imaging Fourier Transform Mass Spectrometer Capabilities for Analyses of Complex & Heterogeneous Samples | S | | P | | S | | |
| SC111 | Scott, J. R. | Elucidating the Photo-Physics of Complex Metal Ions Trapped in a Fourier Transform Mass Spectrometer | | S | S | | P | | |

# Appendix F—Relevance to Major National Programs

| Project ID | Principal Investigator | Project Title | NNSA - National Nuclear Security Administration | EE - Industrial Technologies | EM - Environmental Management | FE - Fossil Energy | SC - Office of Science | NE - Nuclear Energy | NR - Naval Reactors |
|---|---|---|---|---|---|---|---|---|---|
| AC102 | Shook, G. M. | Improving Numerical Model Efficiency of an Existing, In-House Simulation Model | | S | P | S | | | |
| WT112 | Siemer, D. D. | Electrochemical Recovery of Mercury from Nuclear Industry Process Solutions | | | P | | | S | |
| ET107 | Silverman, H. G. | Recombinant Adhesive Protein Production and Investigation into Alternate Natural Adhesive Systems in Marine Mussels | S | S | | | P | | |
| NE111 | Smartt, H. D. | Friction Stir Welding of Lightweight Materials | | | | | | P | |
| CE108 | Steffler, E. D. | Genetic Control of Straw Stem Ultrastructure that Affects the Biomechanics of Stem Separation. | | P | | | S | | |
| GC134 | Stoner, D. L. | Development and Application of Custom Flow Models for Understanding Flow in Porous and Fractured Matrices with Biological Components | | | P | | S | | |
| GC147 | Stormberg, A. I. | Use of Genetic Markers as a Screening Tool for Ecological Risk Assessment | | | P | | | | |
| GC144 | Stormberg, G. J. | Characterization of Nonlinear Complex Resistivity Spectra During Biochemical Redcuction of Cr+6 to Cr+3 | | | P | | S | | |
| NE118 | Telschow, K. L. | Laser Ultrasonic Corrosion Monitor | S | S | | | S | P | P |
| NE126 | Telschow, K. L. | Hollow Waveguide Laser Ultrasonics for High Radiation Environments | | | | | | S | P |
| CE112 | Thompson, D. N. | Pretreatment Technologies for Cellulosic Biomass | | P | | | | | |
| GC109 | Thompson, V. S. | Development of Enzymatic Biosensors for Environmental Applications | | | P | | S | | |
| WT113 | Todd, T. A. | Highly Selective Sorbents for Removal of Arsenic from Drinking Water | S | | P | | S | | |
| SC120 | Totemeier, T. C. | Novel Materials for Evaluation of Generation IV Materials | | S | | S | | P | S |
| SC112 | Van Siclen, C. D. | Mechanical and Flow Properties of Dry Granular Media | S | S | S | S | S | | |
| GC141 | Versteeg, R. J. | Calibration and Enhancement of Geophysical Imaging Tools in Mesoscale Experiments | | | P | | S | | |
| GE107 | Weaver, K. D. | An Innovative Gas-Cooled Fast Reactor | | | | | | P | |
| GC105 | West, P. B. | Advanced Borehole Seismic Sources for High-Resolution Subsurface Imaging and Characterization for Environmental Applications | | | P | S | | | |
| ST106 | White, G. J. | Integrated Environmental Analysis: Development of Collaborative Approaches to Long Term Environmental Stewardship | | | P | | | | |

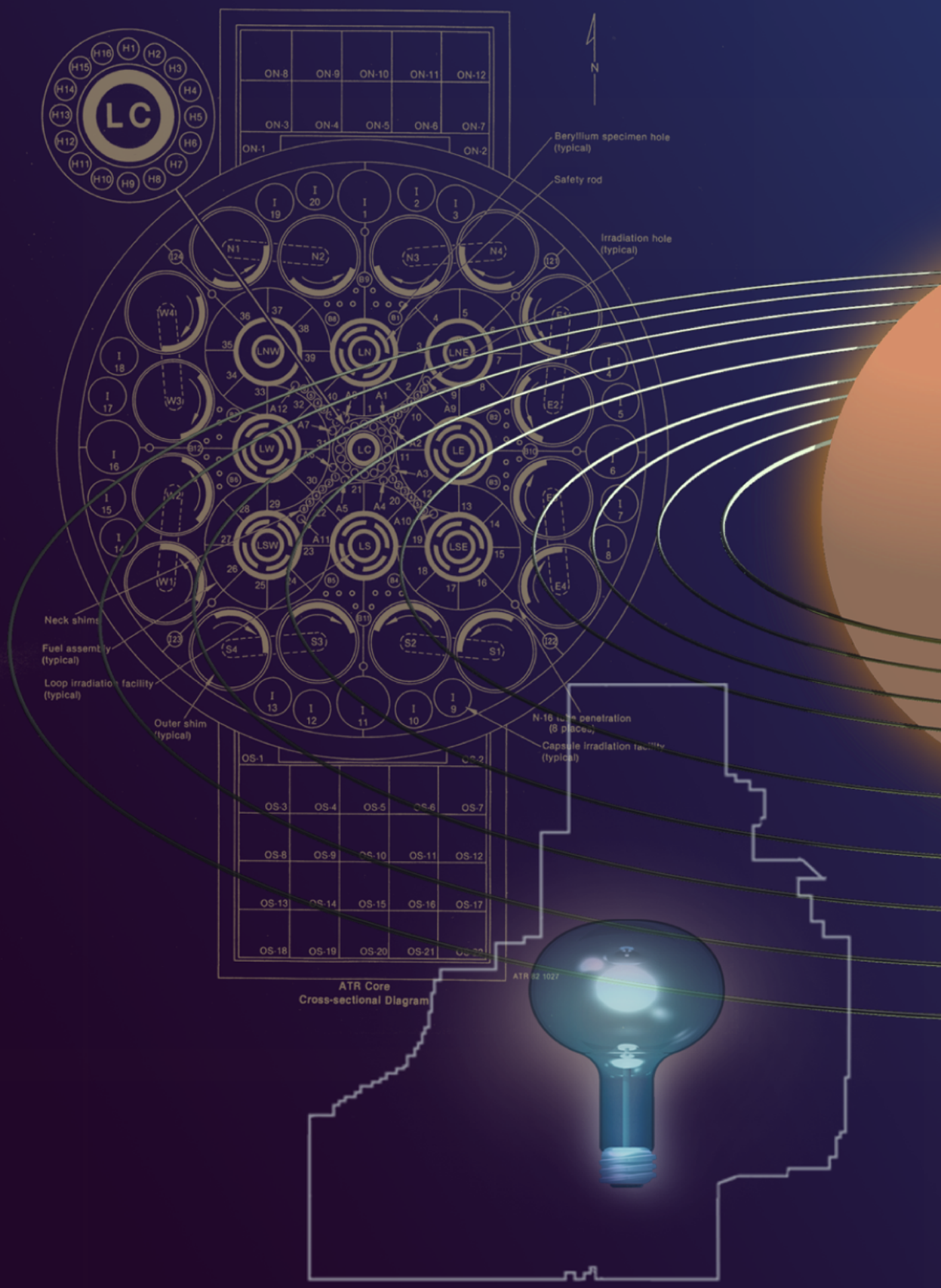


ATR Core
Cross-sectional Diagram